frontiers | Research Topics

Microbial regulation of soil carbon cycling in terrestrial ecosystems

Edited by
Hui Li, Yu Luo, Mikhail Semenov, Ye Deng and Yakov Kuzyakov

Published in
Frontiers in Microbiology

ISSN 1664-8714
ISBN 978-2-8325-3911-8
DOI 10.3389/978-2-8325-3911-8

About Frontiers

Frontiers is more than just an open access publisher of scholarly articles: it is a pioneering approach to the world of academia, radically improving the way scholarly research is managed. The grand vision of Frontiers is a world where all people have an equal opportunity to seek, share and generate knowledge. Frontiers provides immediate and permanent online open access to all its publications, but this alone is not enough to realize our grand goals.

Frontiers journal series

The Frontiers journal series is a multi-tier and interdisciplinary set of open-access, online journals, promising a paradigm shift from the current review, selection and dissemination processes in academic publishing. All Frontiers journals are driven by researchers for researchers; therefore, they constitute a service to the scholarly community. At the same time, the *Frontiers journal series* operates on a revolutionary invention, the tiered publishing system, initially addressing specific communities of scholars, and gradually climbing up to broader public understanding, thus serving the interests of the lay society, too.

Dedication to quality

Each Frontiers article is a landmark of the highest quality, thanks to genuinely collaborative interactions between authors and review editors, who include some of the world's best academicians. Research must be certified by peers before entering a stream of knowledge that may eventually reach the public - and shape society; therefore, Frontiers only applies the most rigorous and unbiased reviews. Frontiers revolutionizes research publishing by freely delivering the most outstanding research, evaluated with no bias from both the academic and social point of view. By applying the most advanced information technologies, Frontiers is catapulting scholarly publishing into a new generation.

What are Frontiers Research Topics?

Frontiers Research Topics are very popular trademarks of the *Frontiers journals series*: they are collections of at least ten articles, all centered on a particular subject. With their unique mix of varied contributions from Original Research to Review Articles, Frontiers Research Topics unify the most influential researchers, the latest key findings and historical advances in a hot research area.

Find out more on how to host your own Frontiers Research Topic or contribute to one as an author by contacting the Frontiers editorial office: frontiersin.org/about/contact

Microbial regulation of soil carbon cycling in terrestrial ecosystems

Topic editors

Hui Li — Institute of Applied Ecology, Chinese Academy of Sciences (CAS), China

Yu Luo — Zhejiang University, China

Mikhail Semenov — V V Dokuchaeva Soil Institute, Russian Academy of Agricultural Sciences, Russia

Ye Deng — Research Center for Eco-environmental Sciences, Chinese Academy of Sciences (CAS), China

Yakov Kuzyakov — University of Göttingen, Germany

Citation

Li, H., Luo, Y., Semenov, M., Deng, Y., Kuzyakov, Y., eds. (2023). *Microbial regulation of soil carbon cycling in terrestrial ecosystems*. Lausanne: Frontiers Media SA.

doi: 10.3389/978-2-8325-3911-8

Table of contents

frontiers | Frontiers in Microbiology

TYPE Editorial
PUBLISHED 30 October 2023
DOI 10.3389/fmicb.2023.1295624

OPEN ACCESS

EDITED AND REVIEWED BY
Paola Grenni,
National Research Council, Italy

*CORRESPONDENCE
Mikhail Semenov
✉ mikhail.v.semenov@gmail.com
Hui Li
✉ huili@iae.ac.cn

RECEIVED 16 September 2023
ACCEPTED 16 October 2023
PUBLISHED 30 October 2023

CITATION
Semenov M, Li H, Luo Y, Deng Y and Kuzyakov Y (2023) Editorial: Microbial regulation of soil carbon cycling in terrestrial ecosystems. *Front. Microbiol.* 14:1295624. doi: 10.3389/fmicb.2023.1295624

Editorial: Microbial regulation of soil carbon cycling in terrestrial ecosystems

Mikhail Semenov[1]*, Hui Li[2]*, Yu Luo[3], Ye Deng[4] and Yakov Kuzyakov[5,6]

[1]Laboratory of Soil Carbon and Microbial Ecology, Dokuchaev Soil Science Institute, Moscow, Russia, [2]CAS Key Laboratory of Forest Ecology and Management, Institute of Applied Ecology, Chinese Academy of Sciences, Shenyang, China, [3]Institute of Soil and Water Resources and Environmental Science, Zhejiang Provincial Key Laboratory of Agricultural Resources and Environment, Zhejiang University, Hangzhou, China, [4]CAS Key Laboratory of Environmental Biotechnology, Research Center for Eco-Environmental Sciences, Chinese Academy of Sciences, Beijing, China, [5]Department of Soil Science of Temperate Ecosystems, Department of Agricultural Soil Science, University of Göttingen, Göttingen, Germany, [6]Agro-Technological Institute, Peoples Friendship University of Russia, Moscow, Russia

KEYWORDS

soil microorganisms, carbon storage and sequestration, organic matter decomposition, carbon-climate feedbacks, metagenomics, ecological modeling, greenhouse gas emission

Editorial on the Research Topic
Microbial regulation of soil carbon cycling in terrestrial ecosystems

The soil organic carbon (SOC) pool is larger than the combined carbon stock in vegetation and in the atmosphere (Davidson et al., 2000; Schmidt et al., 2011; Scharlemann et al., 2014). Carbon (C) exchange between soil and the atmosphere is crucial in the terrestrial C cycle. Soil microbes regulate soil C dynamics through the transformation of plant-derived C, assimilation of C resources to build up their biomass and necromass, decomposition of soil organic matter, and CO_2 release. The intensity and efficiency of these processes are critical determinants of net ecosystem C storage and CO_2 flux (van Bruggen et al., 2017; Wang et al., 2021; Buckeridge et al., 2022; Camenzind et al., 2023; Chen et al., 2023; Tao et al., 2023). Although there is continuing and growing interest in elucidating the underlying microbial mechanisms driving soil C transformation, stabilization, and release processes, many challenges still remain in the manipulation of soil microbial communities for C storage. For example, these challenges include identifying the major players in C storage and decomposition; determining the genetic basis of the mechanisms involved in C sequestration; understanding complex interactions between soil physicochemical properties, plants, and microorganisms over large spatial and temporal scales; and incorporating microbial community patterns and process rates into ecosystem models (Li et al., 2021; Yang et al., 2022; Barnett and Buckley, 2023; Wu et al., 2023).

This Research Topic has aimed to increase our understanding of the role of microorganisms in soil organic C storage and mobilization processes, and also to improve our capacity to develop and evaluate cost-effective microbial strategies for C sequestration and mitigation of anthropogenic CO_2 emissions, ultimately assisting with achievement of the goals of C neutrality and peak CO_2. Altogether, the 11 articles published within the framework of this Research Topic cover a broad range of the processes of C cycling. Most studies have attempted to link plant communities, organic matter properties, and the soil microbiome. Liu et al. examined the characteristics of nutrient release and microbial diversity structure during the decomposition of three types of litter in arid and semi-arid regions. They revealed that the nutrient content and the rate of decomposition of mixed

litter are greatly elevated compared to those of litter of single species. This is because litter mixing raises the richness and diversity of the microbial communities. Based on an original soil microcosm with decomposing corn and soy leaves, as well as soil adjacent to the leaves, Benucci et al. concluded that microbial composition was primarily affected by spatial niches, but also by soil management type and plant species in the fungal microbiome. Moisture content and pore sizes, however, were the most important drivers for bacterial communities. Guo et al. evaluated the impact of natural vegetation restoration on the physical and chemical properties of soil, as well as the diversity and composition of the microbial community, in the alkaline–saline soils of the Songnen Plain, China. *Leymus chinensis* and *Phragmites australis* grown under these harsh conditions increased SOC content and microbial diversity. Analyzing the spatial variability of soil respiration (R_S) and its drivers in the Northwest Caucasus Mountains, Russia, in mixed, fir, and deciduous forests, as well as subalpine and alpine meadows, Sushko et al. concluded that microbial activity plays a crucial role in spatial variability in R_S in forests. Composition of grasses and herbs, however, was found to be the main driver of spatial variability in R_S in grasslands.

Shu et al. collected soils from degraded grasslands that had undergone 14 years of ecological restoration involving planting of shrubs with *Salix cupularis* alone or shrubs with *Salix cupularis* and mixed grasses, and compared these with soil from an extremely degraded grassland as a control. The restoration mode and its interaction with soil depth were crucial for SOC mineralization. Using metagenomics, Zhang et al. analyzed microbial carbohydrate-active enzymes in undisturbed, extensively managed, and intensively managed Moso bamboo plantations. They showed that extensive and intensive management impacts dead plant and microbial biomass decomposition and C turnover, resulting in decreased soil C. They also established that the bacterial community is the main driver of C turnover in soils under bamboo plantations.

Linkages between microbial community, C turnover processes, and potential changes in climate were examined using freeze–thaw and flood–dry cycles. Yang et al. revealed that freeze–thaw cycles in boreal forest soils activated dissolved organic matter (DOM) and increased its biodegradability, hampering C accumulation and sequestration. These findings highlight the potential of DOM molecular composition to regulate the functional states of soil bacterial communities under increased frequency and intensity of freeze–thaw cycles. Zhu et al. highlighted the fact that the shift from flooding to drying in soils collected from a riparian zone of the Three Gorges Reservoir changes keystone taxa and co-occurrence network properties, which was found to regulate soil respiration of soil aggregates.

Wang et al. studied the responses of prokaryotic, fungal, and cercozoan communities following 5 years of inundation treatments in an experimental wetland. The inundation treatments altered microbial communities in coastal wetlands, and the fungal and cercozoan communities played vital roles in regulating methane emission through microbial interactions with the methane-associated community. Jofré-Fernández et al. investigated the role of soil pH in regulating the production and consumption of reactive oxygen species (ROS) during biotic and abiotic SOM decomposition. The activities of lignin peroxidase, manganese peroxidase, and dye-decolorizing peroxidase were linked with the production of superoxide anion ($O_2^{\bullet-}$), hydrogen peroxide (H_2O_2), and hydroxyl radicals (•OH). The mechanisms of SOM oxidation by ROS were found to be extremely sensitive to variations in soil pH and to the stability of oxidant radicals and non-radical compounds. Li et al. investigated the occurrence of horizontal gene transfer (HGT) and established the HGT network of C metabolic genes in 764 soil-borne microbiota genomes. The inter-microbe HGT genetic traits identified in the genetic sequences of the soil-borne microbiota, as well as their involvement in the processes of metabolism and regulation of organic C, suggested the presence of pervasive and substantial effects of HGT on microbial evolution.

Overall, this Research Topic has presented evidence for the pivotal role of soil microorganisms in C cycling processes, the short- and long-term dynamics of microbial community composition, CO_2 flux, and C storage in various ecosystems, including mixed, fir, and deciduous forests, as well as subalpine and alpine meadows, grasses, and intensively managed bamboo plantations. The contributions have expanded our understanding of the complex interplay between soil physicochemical properties, vegetation, and microbial communities at various spatial and temporal scales. These insights hold promise for the development of effective strategies for C sequestration and for the advancement of our goals of C neutrality and mitigation of anthropogenic CO_2 emissions.

Author contributions

MS: Writing—original draft. HL: Writing—review & editing. YL: Writing—review & editing. YD: Writing—review & editing. YK: Writing—review & editing.

Funding

The author(s) declare financial support was received for the research, authorship, and/or publication of this article. This work was funded by the state assignment of the Ministry of Science and Higher Education of the Russian Federation, titled the Study of Microbial Drivers of Sequestration and Storage of Organic Carbon in Soils of Agroecosystems (No. 0439-2022-0018) and the RUDN University Strategic Academic Leadership Program.

Conflict of interest

The authors declare that the research was conducted in the absence of any commercial or financial relationships that could be construed as a potential conflict of interest.

The author(s) declared that they were an editorial board member of Frontiers, at the time of submission. This had no impact on the peer review process and the final decision.

Publisher's note

References

Barnett, S. E., and Buckley, D. H. (2023). Metagenomic stable isotope probing reveals bacteriophage participation in soil carbon cycling. *Environ. Microbiol.* 25, 1785–1795. doi: 10.1111/1462-2920.16395

Buckeridge, K. M., Creamer, C., and Whitaker, J. (2022). Deconstructing the microbial necromass continuum to inform soil carbon sequestration. *Funct. Ecol.* 36, 1396–1410. doi: 10.1111/1365-2435.14014

Camenzind, T., Mason-Jones, K., Mansour, I., Rillig, M. C., and Lehmann, J. (2023). Formation of necromass-derived soil organic carbon determined by microbial death pathways. *Nat. Geosci.* 16, 115–122. doi: 10.1038/s41561-022-01100-3

Chen, Y., Du, Z., Weng, Z., Sun, K., Zhang, Y., Liu, Q., et al. (2023). Formation of soil organic carbon pool is regulated by the structure of dissolved organic matter and microbial carbon pump efficacy: A decadal study comparing different carbon management strategies. *Global Change Biol.* 29, 5445–5459. doi: 10.1111/gcb.16865

Davidson, E., Trumbore, S., and Amundson, R. (2000). Soil warming and organic carbon content. *Nature* 408, 789–790. doi: 10.1038/35048672

Li, H., Yang, S., Semenov, M. V., Yao, F., Ye, J., Bu, R., et al. (2021). Temperature sensitivity of SOM decomposition is linked with a K-selected microbial community. *Global Change Biol.* 27, 2763–2779. doi: 10.1111/gcb.15593

Scharlemann, J. P., Tanner, E. V., Hiederer, R., and Kapos, V. (2014). Global soil carbon: understanding and managing the largest terrestrial carbon pool. *Carbon manag.* 5, 81–91. doi: 10.4155/cmt.13.77

Schmidt, M. W. I., Torn, M. S., Abiven, S., Dittmar, T., Guggenberger, G., Janssens, I. A., and Trumbore, S. E. (2011). Persistence of soil organic matter as an ecosystem property *Nature* 478, 49–56. doi: 10.1038/nature10386

Tao, F., Huang, Y., Hungate, B. A., Manzoni, S., Frey, S. D., Schmidt, M. W., et al. (2023). Microbial carbon use efficiency promotes global soil carbon storage. *Nature* 3, 1–5. doi: 10.1038/s41586-023-06042-3

van Bruggen, A. H., He, M., Zelenev, V. V., Semenov, V. M., Semenov, A. M., Semenova, E. V., et al. (2017). Relationships between greenhouse gas emissions and cultivable bacterial populations in conventional, organic and long-term grass plots as affected by environmental variables and disturbances. *Soil Biol. Biochem.* 114, 145–159. doi: 10.1016/j.soilbio.2017.07.014

Wang, B., An, S., Liang, C., Liu, Y., and Kuzyakov, Y. (2021). Microbial necromass as the source of soil organic carbon in global ecosystems. *Soil Biol. Biochem.* 162, 108422doi: 10.1016/j.soilbio.2021.1084220

Wu, S., Fu, W., Rillig, M. C., Chen, B., Zhu, Y. G., and Huang, L. (2023). Soil organic matter dynamics mediated by arbuscular mycorrhizal fungi–an updated conceptual framework. *New Phytol.* doi: 10.1111/nph.19178

Yang, S., Wu, H., Wang, Z., Semenov, M. V., Ye, J., Yin, L., et al. (2022). Linkages between the temperature sensitivity of soil respiration and microbial life strategy are dependent on sampling season. *Soil Biol. Biochem.* 172, 108758. doi: 10.1016/j.soilbio.2022.108758

frontiers | Frontiers in Microbiology

TYPE Original Research
PUBLISHED 08 November 2022
DOI 10.3389/fmicb.2022.1009091

OPEN ACCESS

EDITED BY
Hui Li,
Institute of Applied Ecology (CAS), China

REVIEWED BY
Xiyang Zhao,
Jilin Agricultural University, China
Benye Xi,
Beijing Forestry University, China

*CORRESPONDENCE
Changjun Ding
changjund@126.com

SPECIALTY SECTION
This article was submitted to Terrestrial Microbiology, a section of the journal Frontiers in Microbiology

RECEIVED 01 August 2022
ACCEPTED 19 October 2022
PUBLISHED 08 November 2022

CITATION
Liu J, Ding C, Zhang W, Wei Y, Zhou Y and Zhu W (2022) Litter mixing promoted decomposition rate through increasing diversities of phyllosphere microbial communities.
Front. Microbiol. 13:1009091.
doi: 10.3389/fmicb.2022.1009091

Litter mixing promoted decomposition rate through increasing diversities of phyllosphere microbial communities

Jiaying Liu[1,2,3], Changjun Ding[2,4]*, Weixi Zhang[2,4], Yawei Wei[1,3], Yongbin Zhou[1,3] and Wenxu Zhu[1,2]

[1]College of Forestry, Shenyang Agriculture University, Shenyang, China, [2]State Key Laboratory of Tree Genetics and Breeding, Research Institute of Forestry, Chinese Academy of Forestry, Beijing, China, [3]Research Station of Liaohe-River Plain Forest Ecosystem, Chinese Forest Ecosystem Research Network (CFERN), Shenyang Agricultural University, Tieling, China, [4]Key Laboratory of Tree Breeding and Cultivation of State Forestry Administration, Research Institute of Forestry, Chinese Academy of Forestry, Beijing, China

Decomposition of forest litter is an essential process for returning nutrients to the soil, which is crucial for preserving soil fertility and fostering the regular biological cycle and nutrient balance of the forest ecosystem. About 70% of the land-based forest litter is made up primarily of leaf litter. However, research on the complex effects and key determinants of leaf litter decomposition is still lacking. In this study, we examined the characteristics of nutrient release and microbial diversity structure during the decomposition of three types of litter in arid and semi-arid regions using 16S rRNA and ITS sequencing technology as well as nutrient content determination. It was revealed that the nutrient content and rate of decomposition of mixed litters were significantly different from those of single species. Following litter mixing, the richness and diversity of the microbial community on leaves significantly increased. It was determined that there was a significant correlation between bacterial diversity and content (Total N, Total P, N/P, and C/P). This study provided a theoretical framework for investigating the decomposition mechanism of mixed litters by revealing the microbial mechanism of mixed decomposition of litters from the microbial community and nutrient levels.

KEYWORDS

litter leaf, mixed decomposition, microbial community, *Populus* × *canadensis* Moench, *Pinus sylvestris* var. *mongolica*

Introduction

Litter, also referred to as organic debris, is a general term for all organic matter in the ecosystem created by the withering of above-ground plant components and returned to the surface as a source of material and energy for decomposers to maintain ecosystem functions (Schlesinger and Lichter, 2001). Leaf litter makes up about 70% of the above-ground forest

litter among them. Leaf litter currently dominates 72% of the research on litter in forest ecosystems (Jia B. R. et al., 2018; Wymore et al., 2018; Nicolas et al., 2019). The primary source of organic matter and nutrients in forest soils is litter decomposition, which also plays a crucial role in the energy flow and nutrient cycling in forest ecosystems (Swift et al., 1979). It also acts as a link between the two carbon pools found in soil and living things (Manzoni et al., 2010). It is the catalyst for biogeochemical cycles and significantly affects climate change (Nevins et al., 2018). The decomposition of leaf litter is a crucial indicator of the functioning of an ecosystem's health because it can return plant carbon, nitrogen and phosphorus to the soil and the atmosphere, as well as other nutrients. This can have an impact on the global element balance, particularly the carbon balance (Cotrufo et al., 2015). Statistics show that every year, 68 GtC of carbon dioxide is released into the atmosphere by the decomposition of litter, making up roughly 70% of the annual carbon flux worldwide (Raich and Schlesinger, 1992). It also serves as a rich source of nutrients for microorganisms, and is crucial for maintaining soil fertility, promoting the regular biological cycle, and maintaining the nutrient balance in forest ecosystems (Manzoni et al., 2008; Jiang et al., 2013), all of which have long been of great concerned to researchers (Gui et al., 2017; Tan et al., 2020).

The nature of the litter, the composition and diversity of the decomposer community, soil conditions, and the climate all have an impact on how quickly litter decomposes (Handa et al., 2014; Stefano, 2017; Han et al., 2019; Sébastien et al., 2021). Climate has a significant impact on the rate at which litter decomposes both globally and locally. On a smaller scale, the type of the litter itself has the greatest impact on how quickly it decomposes. Litter leaf quality largely determines the decomposition of litter and the release of nutrients and minerals to the soil (Lucas-Borja et al., 2018), especially the carbon-nitrogen ratio of the litter (Bradford et al., 2016). The quality of this litter substrate will reduce its decomposition rate (Xiao et al., 2019), and higher C/N and C/P will inhibit the decomposition of leaf litter and its release of nutrients (Lucas-Borja et al., 2018). Coniferous litter typically has a higher C/N than broad-leaved litter. In view of this, understanding the nutrient cycle of leaf litter depends on understanding the stoichiometric characteristics of different shelterbelt species' leaf litter.

The qualities of leaf litter (N and C/N) vary greatly between different plants, and the properties of leaf litter and the chemical structure of organic carbon are significant factors affecting the decomposition of the litter (Cotrufo et al., 2015). The primary source of leaf litter decomposition and the primary force driving the decomposition occurs when plant leaves fall to the ground (Davidson and Janssens, 2006; Cornelissen et al., 2007). The quality of the litter and its specialized microorganisms work together to cause litter to decompose. Uncertainty persists regarding the microbial community changes that occur as various plant leaf litter decomposes.

Leaf microbes are microorganisms that live as epiphytes or parasites on the leaves of plants (Jia T. et al., 2018; Yao et al., 2019). Phyllosphere microbial communities have different makeups depending on the type of plant and the environment it lives in. Although different species' phyllosphere microbial communities differ significantly from one another (Bao et al., 2019), they all share a similar structure (Wallace et al., 2018). As plants progressively wither, variability of phyllosphere microbes gradually increases (Ferreira et al., 2016), and changes in phyllosphere microbial communities during decomposition (Whipps et al., 2010; Kembel et al., 2014) are influenced by leaves' strong influence on physicochemical properties. The abundance of microbial communities significantly increased along with the degree of physical and biological fragmentation of litter (Guerreiro et al., 2017). Fungi are thought to play a significant role in the biogeochemical cycles and the decomposition of leaf litter (Osono et al., 2004). Saprophytic basidiomycetes are the primary decomposers of litter and have the ability to break down materials that are difficult to decompose, like the cellulose found in woody litter (Eichlerová et al., 2015; Urbanová et al., 2015; Baldrian, 2017). Bacteria, which can break down cellulose and hemicellulose, are also necessary for the decomposition of leaf litter. It is not yet clear, though, whether the succession of fungi during the decomposition of litter is consistent with bacterial succession. Additionally, and There is no information on the dynamic changes in phyllosphere microbial composition over time involving multiple decomposition stages, and most studies only concentrate on one stage of plant leaf decomposition or associated leaf litter surface microbes. A though understanding of the connection between the microbial community and litter decomposition over time can be gained by studying the phyllosphere's microbial community.

Early research concentrated on the decomposition of a single leaf litter, but the majority of leaf litter in forest ecosystems was mixed, which had an impact on the nutrient release law during the decomposition process (Lu et al., 2020). Coniferous and broad-leaved litter's physicochemical differences can have an impact on the structure and operation of the litter microbial community (Lin et al., 2021). In general, mixed litter has higher fungal and bacterial abundances and microbial community diversity than single litter, and they have significantly different microbial community compositions (Sun et al., 2018; Pereira et al., 2019; Zhang et al., 2019). This could cause variations in the metabolic functions of microbial communities (Li et al., 2015).

Microorganisms are the primary actors in the decomposition of litter, according to previous research (Muscolo et al., 2014; Lin et al., 2015; Scheibe et al., 2015), and they decompose more quickly in the decomposition of mixed litter than in the decomposition of asingle litter (Patoine et al., 2017; Tonin et al., 2017). According to some studies, the structure and operation of microbial communities can be affected in specific ways by the mixing of litter (Wang et al., 2019). This is due to the mixed litter's higher levels of carbon sources and nutrients, which increase the nutrient supply to microorganisms and accelerate decomposition

through complementary effects (Cline and Zak, 2015; Xiao et al., 2019). Evidently, there is currently a dearth of knowledge regarding the impact of microbial composition on litter decomposition. In addition, research on the structure of the microbial community involved in the decomposition of litter focuses less on that process and instead primarily on the structure of the microbial community in the soil (Sun et al., 2017). Therefore, it is useful to understand the mechanism of litter decomposition to study the changes in microbial community composition during decomposition.

"Three-North" Shelter Forest Program was launched by the Chinese government in 1978 in Northwest China, North China and Northeast China (collectively referred to as the "Three-North" Regions) in an effort to improve the ecological environment. Important tree species for afforestation in the "Three-North" Shelter Forest Program include *Populus* × *canadensis* Moench and *Pinus sylvestris* var. *mongolica*, both of which have straight trunks, a love of light, and a resistance to cold. In order to study the mixed decomposition characteristics of litter, *Populus* × *canadensis* Moench and *Pinus sylvestris* var. *mongolica* plantation litter in arid and semi-arid regions was chosen as the research object. The following hypotheses were put forth: (1) mixed litter decomposition altered the physicochemical characteristics of leaves in comparison to pure *Pinus sylvestris* var. *mongolica* forests; (2) conifer litter's microbial community structure and diversity were affected by the addition of *Populus*×*canadensis* Moench litter; (3) the decomposition of *Pinus sylvestris* var. *mongolica* litter is accelerated by a mixture of withered leaves from coniferous and broad-leaved species. To provide a theoretical foundation for the decomposition of leaf litter, it's necessary to reveal the interactions in mixed decomposition of *Populus*×*canadensis* Moench and *Pinus sylvestris* var. *mongolica*.

Materials and methods

Site description

The study site was established in the Liaohe Plain Forest Ecological Station of the National Forestry and Grassland Administration which is Fujia Forest Farm in Changtu County, Tieling City, Liaoning Province (43°21′143″–42°53′623″N, 123°53′623″–123°53′623″E). It is located in the southeastern part of Horqin Sandy Land, at the junction of Liaoning Province, Jilin Province, and Inner Mongolia Autonomous Region. The topography is flat, and there are a small number of sand dunes in the Liaohe throttle. It is a temperate semi-humid and semi-arid continental climate with an average annual precipitation of 400–550 mm, mainly concentrated in July and August, and evaporates 1,843 mm per year. The maximum temperature was 35.6°C, the lowest temperature was −31.5°C, and the average daily temperature was 6.3°C. The soil type contains low levels of organic substances and other nutrients.

Litter sampling

A litter collector of 1 m × 1 m was set up at the study site, and fresh litter samples of *Populus*×*canadensis* Moench and *Pinus sylvestris* var. *mongolica* were collected in October 2020. Litter samples were then mixed and stored in ice boxes for immediate shipment back to the lab. The leaves of *Populus*×*canadensis* Moench and *Pinus sylvestris* var. *mongolica* were air-dried and put into drop bags. The collected litter was packed into a nylon mesh decomposition bag with a size of 20 cm×20 cm (the aperture was 1 mm×1 mm, i.e., 16 mesh). The total weight of each bag was 8 g, and the mass ratios of litter leaves of *Populus*×*canadensis* Moench and *Pinus sylvestris* var. *mongolica* were 1:0, 1:1, and 0:1 (YS, YZ, and ZS in subsequent analysis). The litter bags were kept in a dehumidified, air-conditioned room. A decomposition test was set up under a *Pinus sylvestris* var. *mongolica* stand in April 2021. Eight litter decomposition bags of different proportions were set in each plot, and a total of four plots were repeated. In July 2021, bags' surface waste was carefully removed, the litter bag retrieved and stored in an ice box for immediate transport back to the laboratory. Then 8 litter bags from the same plot were mixed, weighed and divided into 2 parts. A piece of the litter was dried at 65°C to a constant weight, then weighed to calculate its moisture content and total dry weight. The dried litter samples were crushed and pulverized through a 0.15 mm sieve (100 mesh). The chemical properties of dried litter samples were determined after crushing, including total carbon (total C), total nitrogen (total N), and total phosphorus (total P). The other part was put into a sterilization bag and stored in a −80°C refrigerator for the determination of microbial diversity.

Determination of litter characteristics

An elemental analyzer (Elementar Vario EL III, Germany) was used to measure total C and total N in litter (Song et al., 2015). The total P in litter was determined by the molybdenum-antimony anti-spectrophotometric method (Ba et al., 2020). The weight loss rate of litter (Dw) was determined by the drying method.

$$Dw = \frac{Mo - Mt}{Mo} \times 100\%$$

In the formula: Dw is the weight loss rate of litter (%), Mo is the dry weight (g) of the sample in the decomposition bag at the time of delivery, and Mt. is dry weight (g) of litter after sample decomposition.

DNA extraction and amplification sequencing

Total DNA extraction was carried out according to the MoBio PowerSoil DNA Isolation Kit (MP Biomedicals, Santa Ana, CA, United States) Kit procedure of OMEGA, and each sample was weighed at about 0.5 g. A NanoDrop ND-1000 spectrophotometer

(Thermo Fisher Scientific, Waltham, MA, United States) determined the quantity and quality of the extracted DNA. Primers 338F (5′-ACTCCTACGGGAGGCAGCA-3′) and 806R (5′-GGACTACHVGGGTWTCTAAT-3′) were used to amplify the V3-V4 region of the bacterial 16S rRNA gene (Claesson et al., 2009). The fungal ITS region was amplified with primers ITS5 (5′-GGAAGTAAAAGTCGTAACAAGG-3′) and ITS2 (5′-GCTGCGTTCTTCATCGATGC-3′; White, 1994). The PCR amplification system has a total of 25 μl, including: DNA template 2 μl, each 1 μl upstream and downstream primers (10 μmol·L^{-1}), buffer 5 μl, Q5 high-fidelity buffer 5 μl, 0.25 μl high-fidelity DNA polymerase (5 U·μl^{-1}), dNTP (2.5 mmol·L^{-1}) 2 μl, ultrapure water (dd H_2O) 8.75 μl. PCR amplification conditions were first pre-denatured at 98°C for 2 min, then repeated 25 times in a cycle of 98°C for 15 s, 55°C for 30 s, and 72°C for 30 s, and finally extended at 72°C for 5 min. The PCR amplicons were purified by using Agincourt AM-Pure Beads (Beckman Coulter, Indianapolis, IN), and quantified by using the Pico Green dsDNA detection kit (Invitrogen, Carlsbad, CA, United States). The PCR products were sequenced by using the Illumina NovaSeq 6000 sequencing platform by Shanghai Personal Biotechnology Co., Ltd.

Microbial bioinformatics analysis

QIIME2 (2019.4) and UPARSE Pipeline were used to carry out correlation calculation and analysis on the original data sequences of high-throughput sequencing, and the sequence length was screened (Caporaso et al., 2010). QIIME2's UCLUST, a sequence alignment tool, was used to merge the effective sequences with more than 97% similarity to OTU, and the sequence with the highest abundance of each OTU was selected as the representative sequence of OTU (Edgar, 2010), and compared with the template sequence of Silva database (Release123)[1] to obtain the classification information of each OTU (Quast et al., 2012). Then, according to the number of sequences contained in each sample, a matrix file of OTU abundance in each sample is constructed, namely, OTU table. The richness indices of OTUs and diversity index, including Shannon index, Simpson index, and Chao1 index, were analyzed.

Statistical analysis

For data processing, Microsoft Excel (2019) was used, and the data in the table were all repeated Average ± Standard Error. SPSS 26.0 was used for statistical analysis. One-way analysis of variance was used to analyze the differences in physicochemical properties of different litter leaves, and two-way correlation analysis was used to compare the relationship between physicochemical properties of litter leaves and microbial diversity. Ecologists use alpha diversity and beta diversity indices to characterize the diversity of species within and between habitats, respectively, to comprehensively evaluate their overall diversity (Whittaker, 1960; Whittaker, 1972). In order to comprehensively assess the alpha diversity of microbial communities, Chao1 (Chao, 1984) and Observed species indices were used to characterize richness, and Shannon (Chiani, 1948; Shannon, 1948) and Simpson (Simpson, 1949) indices were used to characterize diversity. Evenness was characterized by Pielou's evenness index (Pielou, 1966), and coverage by Good's coverage index (Good, 1953). And the ggplot2 package of R (R v.3.4.4) was used to draw a boxplot. Principal coordinates analysis (PCoA) is one of the most classic unconstrained sorting (Classical Multidimensional Scaling, cMDScale) analysis methods (Alban, 2010). The differences in the β-diversity of litter leaves were analyzed and compared according to the OTU table and the ape package of R (R v.3.4.4). Among the samples, shared and unique OTUs of litter microbial communities were used in R (R v.3.4.4) and the "Venn Diagram" package to create Venn diagrams. Heatmaps for the top 50 taxonomic genera in each sample were constructed using R (R v.3.4.4) and the pheatmap package. The linear discriminant analysis (LDA) effect size (LEfSe) method was used to detect potentially biomarker-rich taxa based on a cross-group normalized relative abundance matrix using default parameters. The CoHeatmap analysis was carried out by the genescloud tool[2] utilizing the Spearman rank correlation coefficient algorithm, $R = 0.5$. The matrix was constructed using Galaxy, an online interactive analysis of microbial community data.

Results

Characterization of physicochemical properties of different species of litter

There were extremely significant differences in Dw ($p < 0.01$, $F = 3296.941$), total C ($p < 0.01$, $F = 20.538$), total P ($p < 0.05$, $F = 7.668$), C/N ($p < 0.01$, $F = 68.247$), N/P ($p < 0.01$, $F = 21.415$), and C/P ($p < 0.01$, $F = 26.931$) among the three types of leaf litter, but there was no significant difference in the content of total N ($p > 0.05$, $F = 4.355$), as shown in Table 1. The total C content of YS was 679.25 g·kg^{-1}, which was significantly lower than that of YZ and ZS, while the total P content (2.31 g·kg^{-1}) was significantly higher than that of YZ and ZS ($p < 0.01$). The total C, total N and total P contents of YZ were 879.00 g·kg^{-1}, 57.75 g·kg^{-1} and 1.69 g·kg^{-1}, respectively, which were higher than those of ZS. The significance rules of N/P and C/P of the three types of litter were consistent, and ZS was extremely significantly higher than YS and YZ ($p < 0.01$). The C/N of YZ was significantly different from that of YS ($p < 0.01$), but not significantly different from that of ZS ($p > 0.05$). Dw intuitively represents the rate at which litter decomposes. As can be seen from Table 1, YS had the highest decomposition rate, followed by YZ, and ZS was the lowest.

1 http://www.arb-silva.de

2 https://www.genescloud.cn

TABLE 1 Differences in physicochemical properties of three types of litter.

Different samples	Total C/g·kg^{-1}	Total N/g·kg^{-1}	Total P/g·kg^{-1}	C/N	N/P	C/P	Dw/%
YS	679.25 ± 59.28B	54.00 ± 3.16A	2.31 ± 0.85A	12.56 ± 0.36B	25.21 ± 7.06B	315.89 ± 86.75B	20.91 ± 0.09A
ZS	824.50 ± 12.87A	54.00 ± 0.82A	0.78 ± 0.15B	15.27 ± 0.10A	71.75 ± 14.37A	1094.78 ± 214.60A	17.44 ± 0.05C
YZ	879.00 ± 50.50A	57.75 ± 1.50A	1.69 ± 0.43AB	15.21 ± 0.53A	35.79 ± 8.78B	544.44 ± 133.58B	20.20 ± 0.02B
F test	20.538	4.355	7.668	68.247	21.415	26.931	3296.941

Data were means ± standard error ($n = 4$). Degrees of freedom = 11. Different capital letters meant significant difference at 0.01 level. YS: *Populus* × *canadensis Moench*; YZ: *Populus* × *canadensis Moench* – *Pinus sylvestris var. mongolica*; ZS: *Pinus sylvestris var. mongolica*.

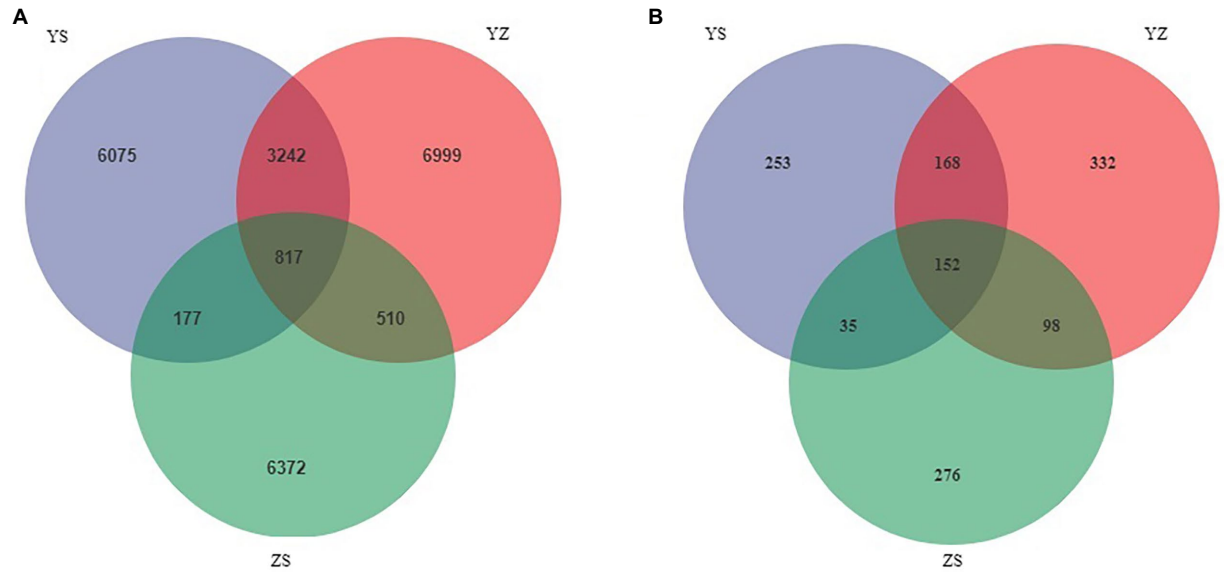

FIGURE 1
Venn diagrams showed the unique and shared OTU of litter microorganisms from three different samples. **(A)** unique and shared OTUs of leaf litter bacteria in three different samples; **(B)** unique and shared OTUs of leaf litter fungal in three different samples. YS: *Populus* × *canadensis* Moench; YZ: *Populus*×*canadensis* Moench-*Pinus sylvestris* var. *mongolica*; ZS: *Pinus sylvestris* var. *mongolica*.

Characteristics of microbial community composition In different types of litter leaves

Venn plots were used to compare OTUs common to and unique to bacterial and fungal communities across all samples. At the bacterial level, a total of 24,192 OTUs were detected. Among them, the OTUs of YS, YZ and ZS were 10,311, 11,586, and 7,876, respectively. The total OTU of the three samples was 817. The OTUs specific to YS, YZ and ZS were 6,075, 6,999, and 6,372, respectively (Figure 1A). At the fungal level, however, the number of detected OTUs was only 1,314. Among them, the OTUs of YS, YZ and ZS are 608, 750, and 561. The common OTU among them was 152. The OTUs specific to YS, YZ, and ZS were 253, 332, and 276, respectively (Figure 1B). Principal coordinates analysis (PCoA) based on Bray-Curtis distance analysis of the different samples showed that the composition of bacterial and fungal communities between YS, YZ, and ZS were all different, forming three disjoint confidence ellipses, and all split along the PCo1 axis (Figure 2).

Alpha diversity refers to an index in ecology to estimate the richness, diversity and evenness of species and flora. Regarding the bacterial alpha-diversity, there was a distinction between the alpha diversity of the three litter types, including Chao1 index ($F = 20.99$; $p = 0.0073$), Goods_coverage ($F = 22.77$; $p = 0.012$), Shannon index ($F = 25.98$; $p = 0.0073$), Simpson index ($F = 83.11$; $p = 0.0073$), Pielou_e index ($F = 43.12$; $p = 0.0073$) and Observed_species ($F = 14.18$; $p = 0.012$). The six indexes of YZ were significantly different from those of ZS ($p < 0.01$), but the indexes of YZ and YS were not significantly different ($p > 0.05$). From Figure 3A, it could be seen intuitively that the Chao1 index, Pielou_e index, Shannon index, Simpson index and Observed_species index of YZ are the highest, followed by YS and ZS the lowest. And the Goods_coverage index showed the opposite law, namely ZS > YS > YZ. At the fungal level, only YS and YZ had significant differences between Pielou_e index ($F = 97.84$;

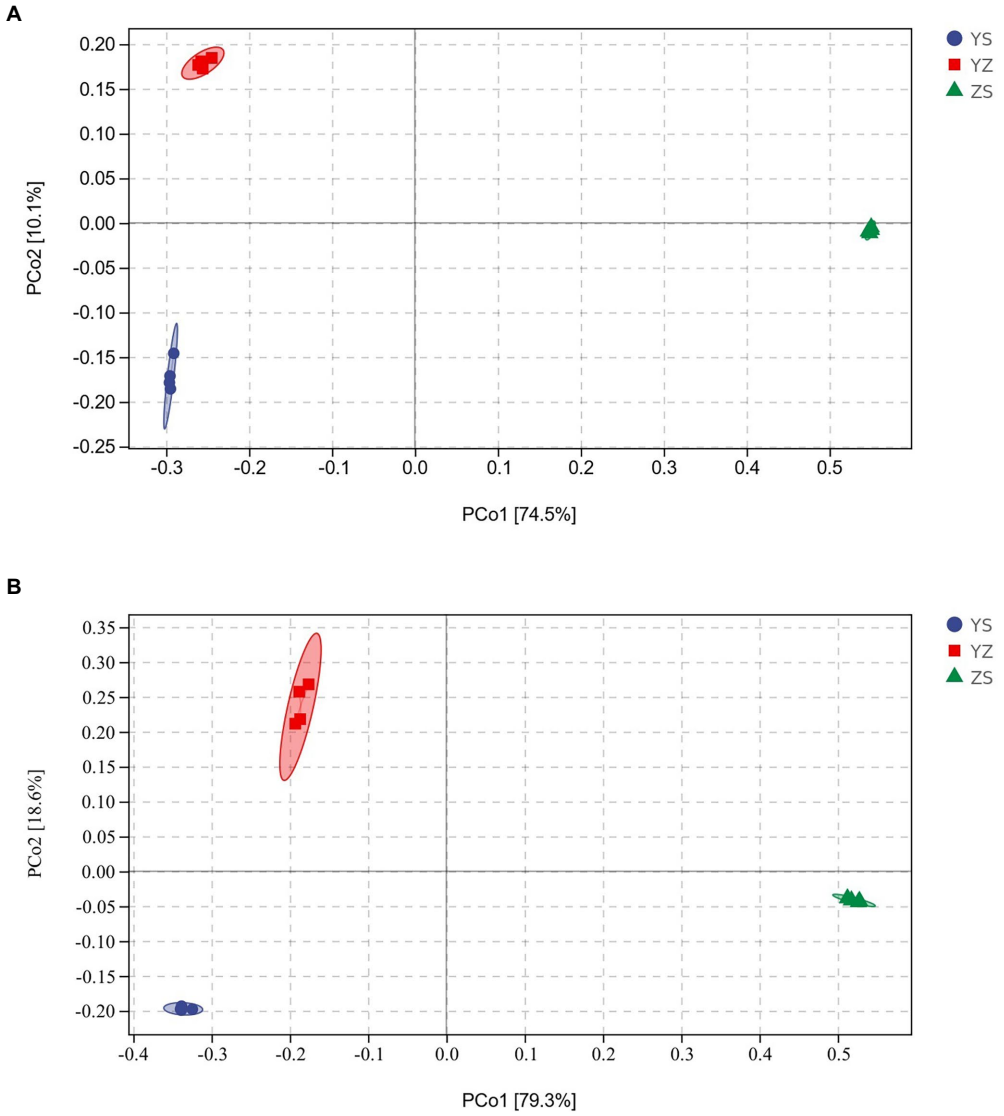

FIGURE 2
Priniciple coordinate analysis (PCoA) of Bray-Curtis' diatance from all samples. **(A)** PCoA of bacteria communities in different samples; **(B)** PCoA of fungal communities in different samples. YS: *Populus*×*canadensis* Moench; YZ: *Populus*×*canadensis* Moench-*Pinus sylvestris* var. *mongolica*; ZS: *Pinus sylvestris* var. *mongolica*.

$p = 0.0073$), Shannon index ($F = 126.27$; $p = 0.0073$), and Simpson index ($F = 118.38$; $p = 0.0073$), and there were no significant differences between the other indicators and samples ($p > 0.05$). The same as bacteria, YZ had the highest Chao1 index, Pielou_e index, Shannon index, Simpson index, and Observed_species index. In the above index, except that the Chao1 index of YS was higher than ZS, the rest were ZS higher than YS (Figure 3B).

The relative abundance of microorganisms in the samples of the three litter types was counted, and the top 10 relative abundances were drawn at the phylum level (others are shown) and genus level (others not shown), respectively, as shown in Figure 4. At the bacterial phylum level, the top 10 relative abundances were Proteobacteria, Actinobacteria, Bacteroidetes, Acidobacteria, Patescibacteria, Firmicutes, Chloroflexi, Cyanobacteria, Verrucomicrobia, Armatimonadetes. The relative abundance of Proteobacteria was the highest in ZS at 71.65%, followed by YZ (41.32%) and YS (41.00%). On the contrary, Actinobacteria had the highest relative abundance in YS at 47.6%, followed by YZ (46.23%) and ZS (19.05%). The relative abundance of Bacteroidetes was YZ > YS > ZS (Figure 4A). At the fungal phylum level, Ascomycota, Basidiomycota, Chytridiomycota, Mortierellomycota, Mucoromycota and Olpidiomycota were relatively abundant. Among them, only Ascomycota and Basidiomycota have relative abundance higher than 1%. The relative abundance of Ascomycota is the highest in YS at 82.75%, followed by YZ (70.70%) and the lowest in ZS (63.39%); the relative abundance of Basidiomycota is just the opposite, that is, ZS (33.29%) > YZ (3.38%) > YS (2.08%; Figure 4C).

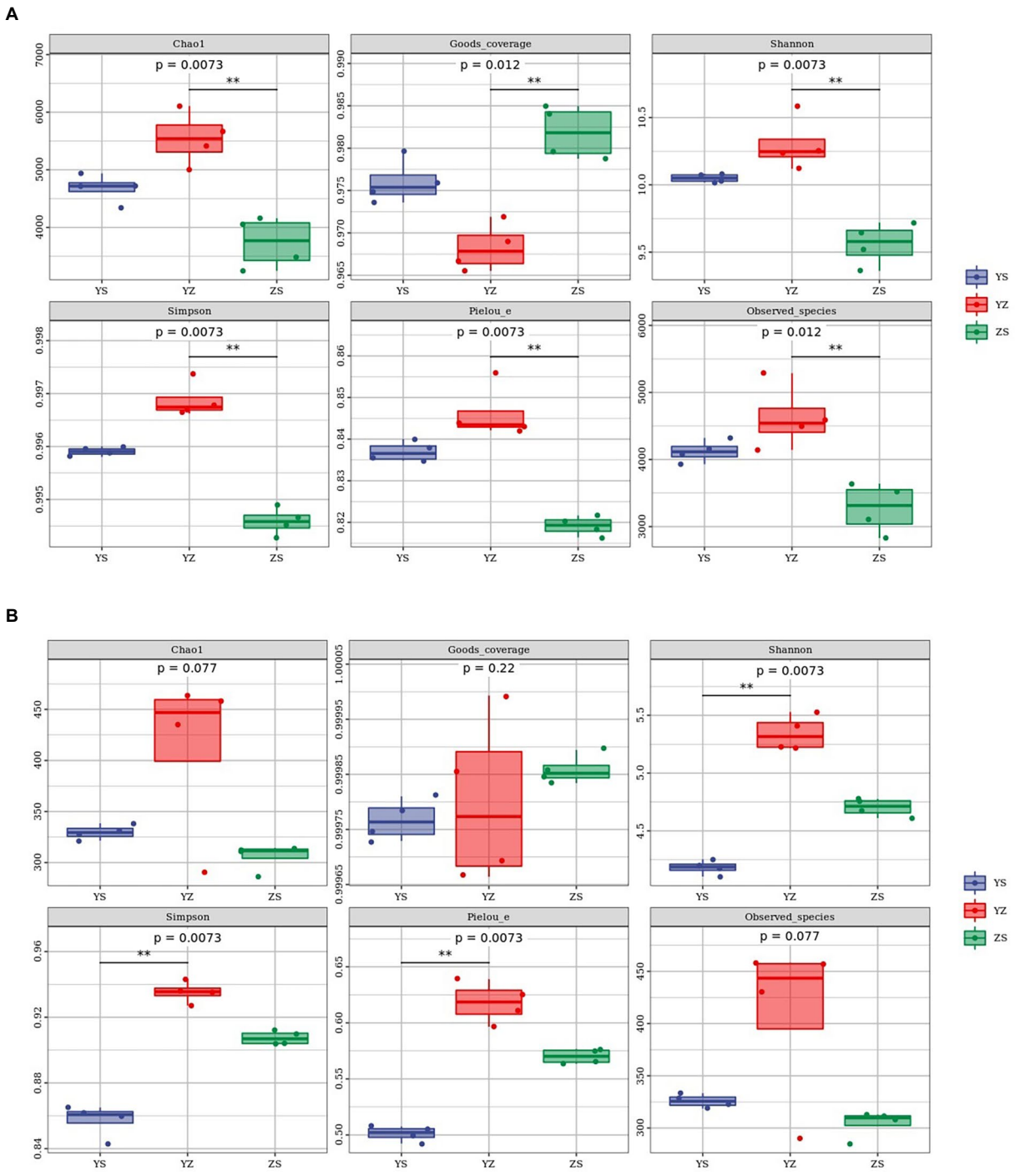

FIGURE 3
Litter microbial diversity index in YS, YZ and ZS. **(A)** Alpha diversity analysis of leaf litter bacterial community. **(B)** Alpha diversity analysis of leaf litter fungal community. YS: *Populus*×*canadensis* Moench; YZ: *Populus*×*canadensis* Moench-*Pinus sylvestris* var. *mongolica*; ZS: *Pinus sylvestris* var. *mongolica*. ** meant significant difference at 0.01 level.

At the bacterial genus level, the top 10 relative abundances were *Sphingomonas*, *Massilia*, *Allorhizobium-Neorhizobium-Pararhizobium-Rhizobium*, *Methylobacterium*, *Actinoplanes*, *Pseudomonas*, *Devosia*, *Flavobacterium*, *Burkholderia-Caballeronia-Paraburkholderia*, and *Microbacterium* (Figure 4B).

It is evident from Figure 5A that there was a correlation between the physicochemical characteristics of the litter and these 10 genera. *Sphingomonas*, *Methylobacterium*, *Pseudomonas*, *Burkholderia-Caballeronia-Paraburkholderia* were significantly positively correlated with litter N/P, C/P ($p < 0.01$), and negatively

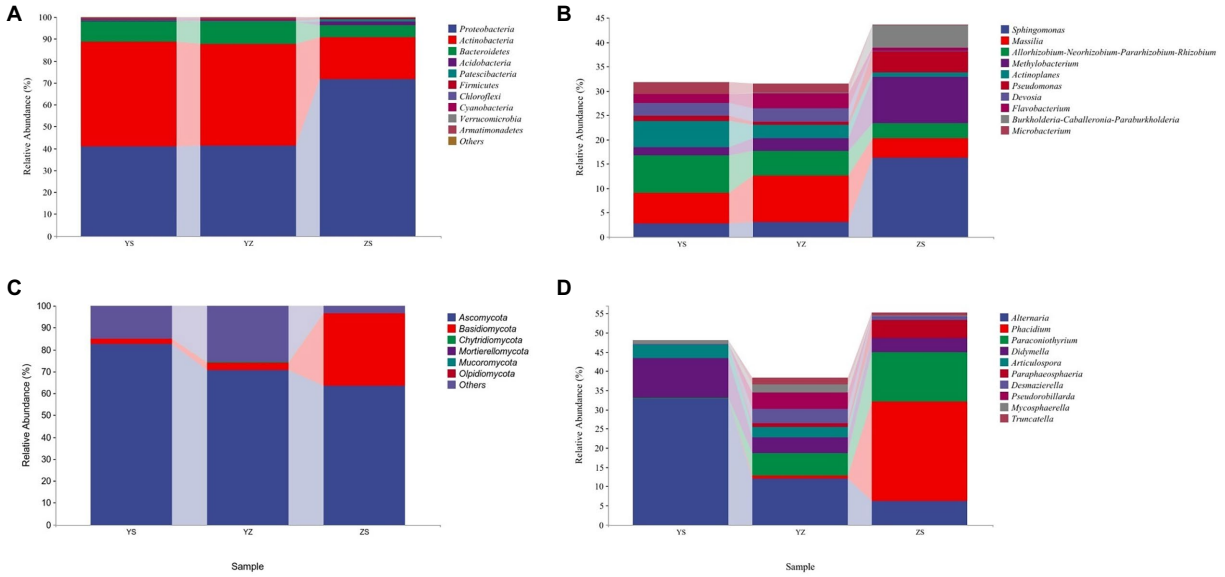

FIGURE 4
The relative abundance of microorganisms at pyhlum and genus levels in litter from different samples. **(A)** The relative abundance of dominant bacterial community at the phylum level; **(B)** The relative abundance of dominant bacterial community at the genus level (not showing others); **(C)** The relative abundance of dominant fungal community at the phylum level; **(D)** The relative abundance of dominant fungal community at the genus level (not showing others). YS: *Populus*×*canadensis* Moench; YZ: *Populus*×*canadensis* Moench-*Pinus sylvestris* var. *mongolica*; ZS: *Pinus sylvestris* var. *mongolica*.

correlated with Dw ($p < 0.01$). *Allorhizobium-Neorhizobium-Pararhizobium-Rhizobium*, *Actinoplanes*, *Devosia*, *Flavobacterium*, and *Microbacterium* were significantly negatively correlated with litter N/P, C/P (*Flavobacterium*, $p < 0.05$; other else, $p < 0.01$) was significantly negatively correlated with N/P and positively correlated with TN, Dw ($p < 0.05$).

At the fungal genus level, the top 10 relative abundances were *Alternaria*, *Phacidium*, *Paraconiothyrium*, *Didymella*, *Articulospora*, *Paraphaeosphaeria*, *Desmazierella*, *Pseudorobillarda*, *Mycosphaerella*, and *Truncatella* (Figure 4D). Similarly, as can be seen from Figure 5B, *Alternaria*, *Didymella*, and *Articulospora* were significantly negatively correlated with litter N/P, C/P (Didymella, $p < 0.05$; other else, $p < 0.01$), and positively correlated with Dw ($p < 0.01$). *Phacidium*, *Paraconiothyrium*, and *Paraphaeosphaeria* were significantly positively correlated with litter N/P, C/P ($p < 0.01$), and negatively correlated with Dw ($p < 0.01$). Nevertheless, the relatively low levels of *Desmazierella*, *Pseudorobillarda*, *Mycosphaerella*, and *Truncatella* was not significantly correlated with Dw ($p > 0.05$).

Lefse is a recent analysis method based on Linear discriminant analysis (LDA) effect size. Its essence is to combine linear discriminant analysis with nonparametric Kruskal-Wallis and Wilcoxon rank sum tests to screen for key biomarkers (i.e., key community members; Segata et al., 2011). With LDA effect size scores >4.5, 16 bacterial taxa were significantly different across treatments (Figure 6A). When LDA effect size scores were > 5, 3 bacterial taxa were significantly different in litter from ZS and YS. Among them, at the bacterial phylum level, the main enriched bacterial taxa in YS leaf litter were Actinobacteria, ZS was mainly enriched by Proteobacteria, and YZ was Bacteroidetes (Figure 7A). As shown in Figure 6B, when the LDA effect size score was >4, the relative abundances of 19 fungal taxa were significantly different among different treatments ($p < 0.05$). Regarding the fungal alpha-diversity, Ascomycota was mainly enriched in YS litter, while Basidiomycota was mainly enriched in ZS (Figure 7B).

The Bray-Curtis-based heatmap showed that the litter bacterial communities of YS and YZ were clustered together, indicating that the litter leaf communities from ZS were clearly distinct from those of YS and YZ (Supplementary Figure S1). The fungal community of the litter also showed the same conclusion (Supplementary Figure S2).

Correlation between physicochemical properties of litter and microbial community diversity in litter

Regarding the bacterial alpha-diversity, total N of leaf litter was significantly positively correlated with Pielou_e ($r = 0.595$, $p < 0.05$) and Simpson index ($r = 0.588$, $p < 0.05$); total P was significantly positively correlated with Pielou_e ($r = 0.642$, $p < 0.05$) and Shannon index ($r = 0.587$, $p < 0.05$); N/P was significantly positively correlated with Goods_coverage ($r = 0.581$, $p < 0.05$); N/P and C/P were significantly negatively correlated with Chao 1 index ($r = -0.651$, $p < 0.05$; $r = -0.626$, $p < 0.05$), Observed_species index ($r = -0.704$, $p < 0.05$; $r = -0.683$, $p < 0.05$), Pielou_e index ($r = -0.760$, $p < 0.01$; $r = -0.735$, $p < 0.01$), Shannon index ($r = -0.751$, $p < 0.01$; $r = -0.730$, $p < 0.01$) and Simpson index

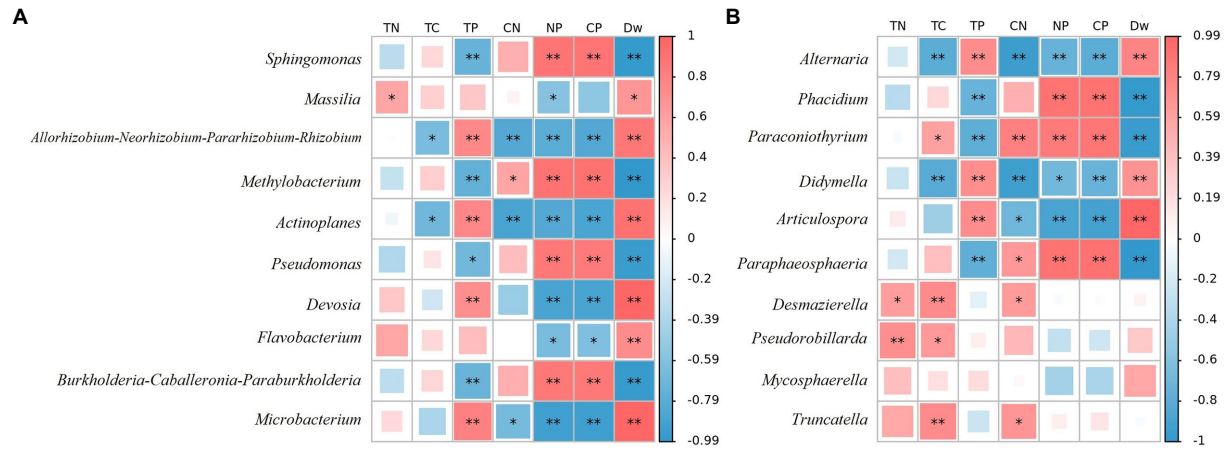

FIGURE 5
CoHeatmap shows the 10 genera relative abundance and chemical composition in various samples of litter. **(A)** Bacteria; **(B)** Fungi. The legend shows the correlation coefficient values, with red representing positive correlations and blue representing negative correlations. Shades of color indicate the strength of the correlation. *represents $p<0.05$; **represents $p<0.01$. TN: Total N; TC: Total C; TP: Total P; CN: C/N; NP: N/P; CP: C/P.

($r=-0.729$, $p<0.01$; $r=-0.699$, $p<0.05$). Dw was significantly positively correlated with Chao 1 index ($r=0.693$, $p<0.05$), Goods_coverage ($r=0.623$, $p<0.05$), Pielou_e index ($r=0.728$, $p<0.01$), Shannon index ($r=0.819$, $p<0.01$) and Simpson index ($r=0.794$, $p<0.01$). Dw was significantly negatively correlated with Observed_species index ($r=-0.632$, $p<0.05$). There was no significant relationship between litter total C and bacterial community diversity index (Table 2).

Regarding the fungal alpha-diversity, total N of leaf litter was significantly positively correlated with Shannon index ($r=0.602$, $p<0.05$); total C and C/N were significantly positively correlated with Pielou_e index ($r=0.841$, $p<0.01$; $r=0.835$, $p<0.05$), Shannon index ($r=0.846$, $p<0.01$; $r=0.791$, $p<0.01$) and Simpson index ($r=0.888$, $p<0.01$; $r=0.886$, $p<0.01$). There was no significant relationship between total P, N/P, C/P, Dw and microbial diversity index of litter (Table 3).

Discussions

"Litter mass," according to Swift et al., (1989), refers to the physicochemical composition of litter. It is the nutrient composition and structure, which includes easily degradable parts (N, P) and resistant organic parts (lignin, cellulose, etc.). The primary controlling factor influencing the rate of litter decomposition is thought to be litter quality (Cornwell et al., 2008). The three elements C, N, and P are currently the primary physicochemical elements involved in research on litter decomposition in my country, and the majority of these studies concentrate on the quality of the litter matrix and the release dynamics of physicochemical elements (Jia et al., 2016). Given the strict stoichiometric requirements for microbial decomposer growth, it is possible that the scarcity of a particular nutrient will slow down the decomposition of litter (Ni et al., 2021). Numerous studies have discovered a strong correlation between the rate of litter decomposition and the initial N content of the litter as well as N-related substrate quality indicators. Indicators of C/N and C/P are frequently used to forecast the rate at which litter will decompose. The decomposition rate decreases as C/N and C/P values rise (Aber and Melillo, 1982; Magill et al., 2000; Sariyildiz and Anderson, 2003). It is consistent with the findings of this research (Table 1). The same pattern was shown in Figure 5. The decomposition rate of mixed litter was found in this study to be significantly higher than that of coniferous forest, but lower than that of pure broad–leaved forest. This is consistent with the findings of Pastor et al. (1984) who conducted experiments on nitrogen mineralization and litter decomposition in pine forests on Blackhawk Island in the United States. Sariyildiz also came to the same conclusion in his simulated experiments on beech and oak trees (Sariyildiz, 2015).

The primary factor influencing nutrient release is plant litter quality, and its C/N value is frequently regarded as an important attribute for measuring litter quality (Silver and Miya, 2001; Hu et al., 2006). For instance, Brady and Weil (1996) discovered that nitrogen release occurs when C/N values in the remaining litter are lower than 25 and nitrogen fixation occurs when C/N values are >25 (Killham, 1994). The rate of decomposition can be regulated by early litter decomposition C/N (Cotrufo and Ineson, 1995; Berg, 2000). Litter C/P has a threshold between 200 and 480, and this threshold affects how much litter P content is released. The litter P content is a net release when the litter C/P is <480 (Gosz et al., 1973; Dziadowiec, 1987; Manzoni et al., 2010). Furthermore, Liu's research made the case that litter N/P can be used as a gauge for determining nutrient limitation. P limit how much litter can decompose if N/P is >25 (Liu et al., 2016). The results of this experiment demonstrated that the phenomenon that P limited the decomposition of coniferous species could very well be improved by the addition

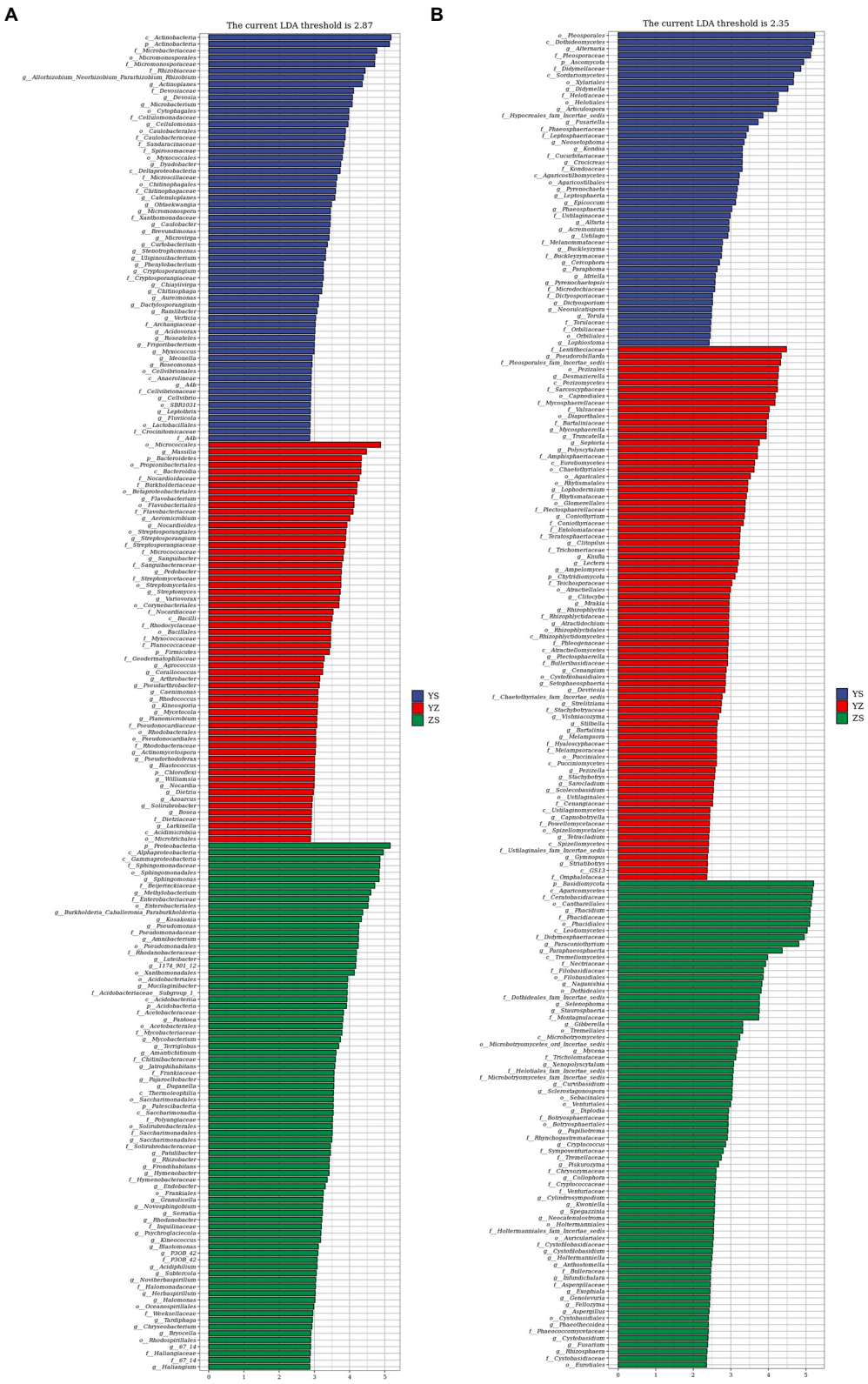

FIGURE 6
Microbial community of different leaf litter ratios with significantly different taxa. **(A)** litter bacterial communities; **(B)** litter fungal communities. YS: *Populus*×*canadensis* Moench; YZ: *Populus*×*canadensis* Moench-*Pinus sylvestris* var. *mongolica*; ZS: *Pinus sylvestris* var. *mongolica*. The longer the length, the more significant the difference between the taxon units, and the different color of the bar chart indicates the higher abundance sample group corresponding to the taxon.

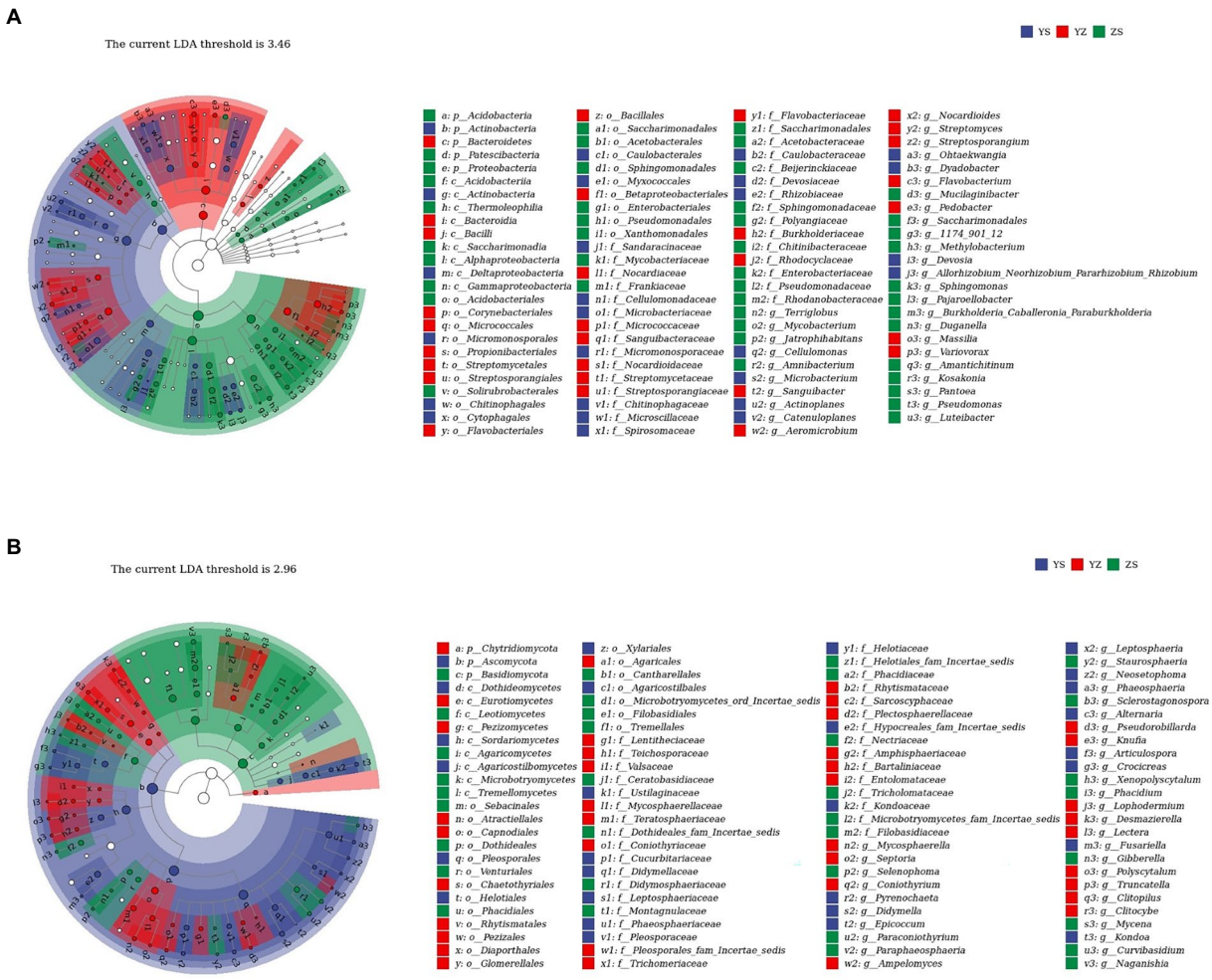

FIGURE 7
(A) Lefse with an LDA of 3.46 indicates that the 100 groups are significantly different between litter bacterial communities of YS, YZ, and ZS. **(B)** Lefse with an LDA of 2.96 indicates that the 100 groups are significantly different between litter fungal communities of YS, YZ, and ZS. YS: *Populus*×*canadensis* Moench; YZ: *Populus*×*canadensis* Moench-*Pinus sylvestris* var. *mongolica*; ZS: *Pinus sylvestris* var. *mongolica*. Circle radiation from inner to outer of evolutionary branch figure represents the classification of the level from phylum door genus; every small circle represents the level of a classification in different classification level. The diameter of the circle is prportional to the relative abundance.

TABLE 2 Correlation between litter physicochemical properties and bacterial community diversity.

	Chao1	Goods_coverage	Observed_species	Pielou_e	Shannon	Simpson
Total N	0.423	−0.404	0.406	0.595*	0.478	0.588*
Total C	0.124	−0.180	0.046	0.113	0.053	0.168
Total P	0.421	−0.314	0.515	0.642*	0.587*	0.567
C/N	−0.074	−0.007	−0.165	−0.172	−0.192	−0.098
N/P	−0.651*	0.581*	−0.704*	−0.760**	−0.751**	−0.729**
C/P	−0.626*	0.553	−0.683*	−0.735**	−0.730**	−0.699*
Dw	0.693*	0.623*	−0.632*	0.728**	0.819**	0.794**

$n = 12$, ** means significant correlation at $p < 0.01$level; * means significant correlation at $p < 0.05$ level.

of broad–leaved species. In conclusion, adding broad–leaved litter can increase the rate at which coniferous litter decomposes, this is because mixed litter decomposes more quickly than litter from a single tree species.

Previous research has shown that single-species litter and mixed litter have significantly different community compositions and structures (Aneja et al., 2006; Chapman and Newman, 2010; Prescott and Grayston, 2013; Santonja et al., 2017). Microbial

TABLE 3 Correlation between litter physicochemical properties and fungal community diversity.

	Chao1	Goods_coverage	Observed_species	Pielou_e	Shannon	Simpson
Total N	0.563	−0.168	0.567	0.517	0.602*	0.538
Total C	0.461	0.068	0.472	0.841**	0.846**	0.888**
Total P	0.143	−0.407	0.130	−0.417	−0.313	−0.454
C/N	0.293	0.204	0.307	0.835**	0.791**	0.886**
N/P	−0.280	0.446	−0.267	0.282	0.159	0.343
C/P	−0.236	0.435	−0.222	0.344	0.224	0.406
Dw	0.378	−0.414	0.368	−0.288	−0.134	−0.345

$n = 12$, ** means significant correlation at $p < 0.01$level; * means significant correlation at $p < 0.05$ level.

biomass and community composition can vary depending on the microenvironment or chemical makeup of the litter (Malosso et al., 2004; Das et al., 2007; Xu et al., 2013). The current study discovered differences between the alpha diversity of single-species litter and mixed litter microbial communities. Mixed litter made up of *Populus* × *canadensis* and *Pinus sylvestris* var. *mongolica* differed significantly from *Pinus sylvestris* var. *mongolica* litter in terms of bacterial richness, diversity, uniformity and coverage, but not from *Populus* × *canadensis* litter. However, the coverage and richness of mixed litter and *Populus* × *canadensis* litter were not significantly different, and the fungal community diversity and homogeneity of the *Populus* × *canadensis* – *Pinus sylvestris* var. *mongolica* litter were only significantly higher than those of *Populus* × *canadensis*. This has also been supported by earlier researches (Aneja et al., 2006; Chapman and Newman, 2010; Prescott and Grayston, 2013; Santonja et al., 2017). Proteobacteria and Ascomycetes are the most abundant taxa in the early stage of litter decomposition and are the main decomposers (Voříšková and Baldrian, 2012; Zhang et al., 2017). This study also found that Proteobacteria dominated the bacterial community and Ascomycota dominated the fungal community. According to research, fungi and bacteria work together to speed up the decomposition of litter (Wright and Covich, 2005). Fungi are primarily responsible for the decomposition of carbonaceous organic matter (Frey et al., 1999; Guggenberger et al., 1999; Pascoa and Cássio, 2004), while bacteria primarily consume nitrogenous organic matter (Six et al., 2002). Ascomycetes, the predominant decomposing bacteria in the three types of litter, are primarily in charge of breaking down cellulose and hemicellulose (Pointing and Hyde, 2000; Sánchez, 2009; Zhang et al., 2016), and Proteobacteria are in charge of breaking down proteins (Schweitzer et al., 2001; Kazakov et al., 2009).

In the breakdown of apoplast, various genera also play various roles. For instance, the top 10 species in terms of relative abundance in this study, *Massilia*, *Allorhizobium-Neorhizobium-Pararhizobium-Rhizobium*, *Actinoplanes*, *Devosia*, *Flavobacterium*, and *Microbacterium*, all have the job of breaking down organic acids, polyols, aromatic compounds, and other substances in the environment (Du et al., 2011; Feng et al., 2019; Menon et al., 2019). Both simple carbohydrates and refractory materials are thought to be capable of being broken down by *Alternaria* (Jatav et al., 2020). An endophytic fungus called *Paraconiothyrium* degrades lignin (Gao et al., 2011). They all play a role in the breakdown of *apoplastic* matter, which is consistent with the study's findings.

The structure and operation of the litter microbial community are also impacted by the differences between coniferous and broad-leaved litter's physical and chemical characteristics. Previous researches have also demonstrated a connection between the chemical properties of decomposed substrates and the diversity of the microbial community (Hawke and Vallance, 2015; Zeng et al., 2017). The two main microbial taxa involved in decomposition litter are fungi and bacteria, and depending on the ecosystem and type of litter, their functional characteristics and carbon requirements may vary (Lin et al., 2018). Although fungi are thought to decompose more quickly than bacteria, bacteria are more effective at using labile carbon compounds (Hunt et al., 1987). This may account for the stronger relationship between apomictic Dw and bacterial community alpha diversity as well as the lack of a relationship with fungal communities. When compared to coniferous pure forest litter, mixed forest litter has different carbon and mineral nutrient contents, offering a wider substrate for microbes that break down organic matter (Hooper and Vitousek, 1998; Hättenschwiler et al., 2011).

Conclusion

In this study, it was discovered that the decomposition effect of mixed litter was different from that of a species of tree by simulating the mixed decomposition of *Populus* × *canadensis* Moench and *Pinus sylvestris* var. *mongolica* litter. (1) Compared to leaf litter from a single tree species, mixed leaf litter had different nutrients. However, the contents of total P, C/N, N/P and C/P were as YZ was between YS and ZS. The total C and total N of YZ were higher than those of single tree species. (2) There were variations in the organization and composition of the microbial communities in mixed leaf litter compared to of single tree species, but the difference was not very significant. (3) The investigation revealed that leaf nutritional variables had an impact on the variety of the microbial community composition and organization in leaf litter. (4) The decomposition of *Populus* × *canadensis* Moench litter was significantly aided by the addition of *Pinus sylvestris* var. *mongolica* litter. N/P, C/P, total N, and total P had a substantial impact on the

bacterial community, while C/N, total C, and total N had a large impact on the fungal community. Consequently, this research provided a theoretical framework for the investigation of the decomposition mechanism of mixed litter from the nutritional level and microbial community.

Data availability statement

The datasets presented in this study can be found in online repositories. The names of the repository/repositories and accession number(s) can be found at: https://www.ncbi.nlm.nih.gov/, PRJNA832892.

Author contributions

WZu designed the research. JL, CD, and WZa performed the research. JL, CD, YW, and YZ analyzed the data. WZu, CD, and JL wrote the manuscript. All authors contributed to the article and approved the submitted version.

Funding

This work was supported by the National Key Research and Development Program of China (grant number 2021YFD2201205), the Basic Research Fund of RIF (grant no. CAFYBB2020SZ002), the National Natural Science Foundation of China (grant nos. 31870662 and 32271843), and Liaoning Province Scientific Research Funding Project (LSNQN202012).

Conflict of interest

The authors declare that the research was conducted in the absence of any commercial or financial relationships that could be construed as a potential conflict of interest.

Publisher's note

All claims expressed in this article are solely those of the authors and do not necessarily represent those of their affiliated organizations, or those of the publisher, the editors and the reviewers. Any product that may be evaluated in this article, or claim that may be made by its manufacturer, is not guaranteed or endorsed by the publisher.

Supplementary material

The Supplementary material for this article can be found online at: https://www.frontiersin.org/articles/10.3389/fmicb.2022.1009091/full#supplementary-material

References

Aber, J. D., and Melillo, J. M. (1982). Nitrogen immobilization in decaying hardwood leaf litter as a function of initial nitrogen and lignin content. *Can. J. Bot.* 60, 2263–2269. doi: 10.1139/b82-277

Alban, R. (2010). Multivariate analyses in microbial ecology. *FEMS Microbiol. Ecol.* 62, 142–160. doi: 10.1111/j.1574-6941.2007.00375.x

Aneja, M. K., Sharma, S., Fleischmann, F., Stich, S., Heller, W., Bahnweg, G., et al. (2006). Microbial colonization of beech and spruce litter-influence of decomposition site and plant litter species on the diversity of microbial community. *Microb. Ecol.* 52, 127–135. doi: 10.1007/s00248-006-9006-3

Ba, H., Jiang, H., Shen, P., Cao, Y., and Li, L. (2020). Screening of phosphate-resolving bacteria in rhizosphere of cold sunflower and physiological and biochemical study. *IOP Conf. Series Earth Environ. Sci.* 526:012038. doi: 10.1088/1755-1315/526/1/012038

Baldrian, P. (2017). Forest microbiome: diversity, complexity and dynamics. *FEMS Microbiol. Rev.* 41, 109–130. doi: 10.1093/femsre/fuw040

Bao, L., Cai, W., Zhang, X., Liu, J., Chen, H., Wei, Y., et al. (2019). Distinct microbial community of phyllosphere associated with five tropical plants on Yongxing Island, South China Sea. *Microorganisms* 7:525. doi: 10.3390/microorganisms7110525

Berg, B. (2000). Litter decomposition and organic matter turnover in northern forest soils. *Forest Ecol. Manag.* 133, 13–22. doi: 10.1016/S0378-1127(99)00294-7

Bradford, M. A., Berg, B., Maynard, D. S., Wieder, W. R., and Wood, S. A. (2016). Understanding the dominant controls on litter decomposition. *J. Ecol.* 104, 229–238. doi: 10.1111/1365-2745.12507

Brady, N. C., and Weil, R. R.. (1996). *The Nature and Properties of Soil. 11th ed.* Englewood Cliffs: Prentice-Hall *740*.

Caporaso, J. G., Kuczynski, J., Stombaugh, J., Bittinger, K., Bushman, F. D., Costello, E. K., et al. (2010). QIIME allows analysis of high-throughput community sequencing data. *Nat. Methods* 7, 335–336. doi: 10.1038/nmeth.f.303

Chao, A. (1984). Nonparametric estimation of the number of classes in a population. *Scand. J. Stat.* 11, 265–270. doi: 10.2307/4615964

Chapman, S. K., and Newman, G. S. (2010). Biodiversity at the plant-soil interface: microbial abundance and community structure respond to litter mixing. *Oecologia* 162, 763–769. doi: 10.1007/s00442-009-1498-3

Chiani, M. (1948). A mathematical theory of communication. *Bell Labs Tech. J.* 27, 623–656. doi: 10.1002/j.1538-7305.1948.tb00917.x

Claesson, M. J., O'Sullivan, O., Wang, Q., Nikkilä, J., Marchesi, J. R., Smidt, H., et al. (2009). Comparative analysis of pyrosequencing and a phylogenetic microarray for exploring microbial community structures in the human distal intestine. *PLoS One* 4:e6669. doi: 10.1371/journal.pone.0006669

Cline, L. C., and Zak, D. R. (2015). Initial colonization, community assembly and ecosystem function: fungal colonist traits and litter biochemistry mediate decay rate. *Mol. Ecol.* 24, 5045–5058. doi: 10.1111/mec.13361

Cornelissen, J. H., Van Bodegom, P. M., Aerts, R., Callaghan, T., Longtestijn, R., Alatalo, J., et al. (2007). Global negative vegetation feedback to climate warming responses of leaf litter decomposition rates in cold biomes. *Ecol. Lett.* 10, 619–627. doi: 10.1111/j.1461-0248.2007.01051.x

Cornwell, W. K., Cornelissen, J. H. C., Amatangelo, K., Dorrepaal, E., Eviner, V. T., Godoy, O., et al. (2008). Plant species traits are the predominant control on litter decomposition rates within biomes worldwide. *Ecol. Lett.* 11, 1065–1071. doi: 10.1111/j.1461-0248.2008.01219.x

Cotrufo, M. F., and Ineson, P. (1995). Effects of enhanced atmospheric CO_2 and nutrient supply on the quality and subsequent decomposition of fine roots of Betula pendula Roth. And Picea sitchensis (bong.) Carr. *Plant Soil* 170, 267–277. doi: 10.1007/bf00010479

Cotrufo, M. F., Soong, J. L., Horton, A. J., Campbell, E. E., Haddix, M. L., Wall, D. H., et al. (2015). Formation of soil organic matter *via* biochemical and physical pathways of litter mass loss. *Nat. Geosci.* 8, 776–779. doi: 10.1038/ngeo2520

Das, M., Royer, T. V., and Leff, L. G. (2007). Diversity of fungi, bacteria, and actinomycetes on leaves decomposing in a stream. *Appl. Environ. Microb.* 73, 756–767. doi: 10.1128/AEM.01170-06

Davidson, E. A., and Janssens, I. A. (2006). Temperature sensitivity of soil carbon decomposition and feedbacks to climate change. *Nature* 440, 165–173. doi: 10.1038/nature04514

Du, Y., Yu, X., and Wang, G. (2011). *Massilia tieshanensis* sp. nov. isolated from mining soil. *Int. J. Syst. Evol. Microbiol.* 62, 2356–2362. doi: 10.1099/ijs.0.034306-0

Dziadowiec, H. (1987). The decomposition of plant litterfall in an oak-linden-hornbeam forest and an oak-pine mixed forest of the Bialoweza national park. *Acta Soc. Bot. Pol.* 56, 169–185. doi: 10.5586/asbp.1987.019

Edgar, R. C. (2010). Search and clustering orders of magnitude faster than BLAST. *Bioinformatics* 26, 2460–2461. doi: 10.1093/bioinformatics/btq461

Eichlerová, I., Homolka, L., Žifčáková, L., Lisá, L., Dobiášová, P., and Baldrian, P. (2015). Enzymatic systems involved in decomposition reflects the ecology and taxonomy of saprotrophic fungi. *Fungal Ecol.* 13, 10–22. doi: 10.1016/j.funeco.2014.08.002

Feng, Y., Yuan, Q., Yang, Z., Zhang, T., Liu, X., Li, C., et al. (2019). Effect of *Sphingomonas* sp. strain on degradation of polyphenols in redried tobacco leaves. *Acta Tabacaria Sinica* 25, 19–24. doi: 10.16472/j.chinatobacco.2018.038

Ferreira, V., Raposeiro, P. M., Pereira, A., Cruz, A. M., Costa, A. C., Graca, M., et al. (2016). Leaf litter decomposition in remote oceanic island streams is driven by microbes and depends on litter quality and environmental conditions. *Freshw. Biol.* 61, 783–799. doi: 10.1111/fwb.12749

Frey, S. D., Elliott, E. T., and Paustian, K. (1999). Bacterial and fungal abundance and biomass in conventional and no-tillage agroecosystems along two climatic gradients. *Soil Biol. Biochem.* 31, 573–585. doi: 10.1016/S0038-0717(98)00161-8

Gao, H., Wang, Y., Zhang, W., Wang, W., and Mu, Z. (2011). Isolation, identification and application in lignin degradation of an ascomycete GHJ-4. *Afr. J. Biotechnol.* 10, 4166–4174. doi: 10.4314/AJB.V10I20

Good, I. J. (1953). The population frequency of species and the estimation of the population parameters. *Biometrics* 40, 237–264. doi: 10.2307/2333344

Gosz, J. R., Likens, G. E., and Bormann, F. H. (1973). Nutrient release from decomposition leaf and branch litter in the Hubbard Brool Forest, New Hampshire. *Ecolog. Monog.* 43, 173–191. doi: 10.2307/1942193

Guerreiro, M. A., Brachmann, A., Begerow, D., and Peršoh, D. (2017). Transient leaf endophytes are the most active fungi in 1-year-old beech leaf litter. *Fungal Divers.* 89, 237–251. doi: 10.1007/s13225-017-0390-4

Guggenberger, G., Frey, S. D., Six, J., Paustian, K., and Elliott, E. T. (1999). Bacterial and fungal cell-wall residues in conventional and no-tillage agroecosystems. *Soil Sci. Soc. Am. J.* 63, 1188–1198. doi: 10.2136/sssaj1999.6351188x

Gui, H., Purahong, W., Hyde, K. D., Xu, J. C., and Mortimer, P. E. (2017). The arbuscular mycorrhizal fungus *Funneliformis mosseae* alters bacterial communities in subtropical forest soils during litter decomposition. *Front. Microbiol.* 8:1120. doi: 10.3389/fmicb.2017.01120

Han, C., Liu, T., Lu, X., Duan, L., Singh, V., and Ma, L. (2019). Effect of litter on soil respiration in a man-made *Populus* L. forest in a dune-meadow transitional region in China's Horqin sandy land. *Ecol. Eng.* 127, 276–284. doi: 10.1016/j.ecoleng.2018.12.005

Handa, I. T., Aerts, R., Berendse, F., Berg, M. P., Bruder, A., Butenschoer, O., et al. (2014). Consequences of biodiversity loss for litter decomposition across biomes. *Nature* 509, 218–221. doi: 10.1038/nature13247

Hättenschwiler, S., Fromin, N., and Barantal, S. (2011). Functional diversity of terrestrial microbial decomposers and their substrates. *C. R. Biol.* 334, 393–402. doi: 10.1016/j.crvi.2011.03.001

Hawke, D. J., and Vallance, J. R. (2015). Microbial carbon concentration in samples of seabird and non-seabird forest soil: implications for leaf litter cycling. *Pedobiologia* 58, 33–39. doi: 10.1016/j.pedobi.2015.01.002

Hooper, D. U., and Vitousek, P. M. (1998). Effects of plant composition and diversity on nutrient cycling. *Ecol. Monogr.* 68, 121–149. doi: 10.2307/2657146

Hu, Y. L., Wang, S. L., and Zeng, D. H. (2006). Effects of single Chinese fir and mixed leaf litters on soil chemical, microbial properties and soil enzyme activities. *Plant Soil* 282, 379–386. doi: 10.1007/s11104-006-0004-5

Hunt, H. W., Coleman, D. C., and Ingham, E. R. (1987). The detrital food web in a short grass prairie. *Biol. Fertil. Soils* 3-3, 57–68. doi: 10.1007/BF00260580

Jatav, B. K., Sharma, T., and Dassani, S. (2020). Succession of microfungi on leaf litter of Acacia catechu in Datia, Madhya Pradesh, India. *J. Pure Appl. Microbiol.* 14, 581–590. doi: 10.22207/JPAM.14.1.60

Jia, T., Wang, R., Fan, X., and Chai, B. (2018). A comparative study of fungal community structure, diversity and richness between the soil and the Phyllosphere of native grass species in a copper tailings dam in Shanxi Province, China. *Appl. Sci.* 8:1297. doi: 10.3390/app8081297

Jia, B. R., Xu, Z. Z., Zhou, G. S., and Yin, X. J. (2018). Statistical characteristics of forest litter fall in China. *Sci. China Life Sci.* 61, 358–360. doi: 10.1007/s11427-016-9143-x

Jia, B., Zhou, G., and Xu, Z. (2016). Forest litterfall and its composition: a new data set of observational data from China. *Ecology* 97:1365. doi: 10.1890/15-1604.1

Jiang, Y. F., Yin, X. Q., and Wang, F. B. (2013). The influence of litter mixing on decomposition and soil fauna assemblages in a Pinus koraiensis mixed broad-leaved forest of the Changbai Mountains, China. *Eur. J. Soil Biol.* 55, 28–39. doi: 10.1016/j.ejsobi.2012.11.004

Kazakov, A. E., Rodionov, D. A., Alm, E., Arkin, A. P., Dubchak, I., and GelFaNd, M. S. (2009). Comparative genomics of regulation of fatty acid and branched-chain amino acid utilization in Proteobacteria. *J. Bacteriol.* 191, 52–64. doi: 10.1128/JB.01175-08

Kembel, S. W., O'Connor, T. K., Arnold, H. K., Hubbell, S. P., Wright, S. J., and Green, J. L. (2014). Relationships between phyllosphere bacterial communities and plant functional traits in a neotropical forest. *Proc. Natl. Acad. Sci. U. S. A.* 111, 13715–13720. doi: 10.1073/pnas.1216057111

Killham, K. (1994). *Soil Ecology*. Cambridge: Cambridge University Press.

Li, T. Y., Kang, F. F., Han, H. R., Gao, J., Song, X., and Yu, S. (2015). Responses of soil microbial carbon metabolism to the leaf litter composition in Liaohe River nature reserve of northern Hebei Province, China. *J. Appl. Ecol.* 26, 715–722. doi: 10.13287/j.1001-9332.20150506.004

Lin, N., Bartsch, N., Heinrichs, S., and Vor, T. (2015). Long-term effects of canopy opening and liming on leaf litter production, and onleaf litter and fine-root decomposition in a European beech (*Fagus sylvatica*, L.) forest. *Forest Ecol. Manag.* 338, 183–190. doi: 10.1016/j.foreco.2014.11.029

Lin, H., Li, Y., Bruelheide, H., Zhang, S., Ren, H., Zhang, N., et al. (2021). What drives leaf litter decomposition and the decomposer community in subtropical forests – the richness of the above-ground tree community or that of the leaf litter? *Soil Biol. Biochem.* 160:108314. doi: 10.1016/j.soilbio.2021.108314

Lin, D., Pang, M., Fanin, N., Wang, H., Qian, S., Zhao, L., et al. (2018). Fungi participate in driving home-field advantage of litter decomposition in a subtropical forest. *Plant Soil* 434, 467–480. doi: 10.1007/s11104-018-3865-5

Liu, D., Keiblinger, K. M., Leitner, S., Mentler, A., and Zechmeister-Boltenstern, S. (2016). Is there a convergence of deciduous leaf litter stoichiometry, biochemistry and microbial population during decay? *Geoderma* 272, 93–100. doi: 10.1016/j.geoderma.2016.03.005

Lu, S., Xu, E., Wu, D., Lu, Y., Guo, J., and Yang, Y. (2020). Response of soil microbial community composition on litterfall input in a Castanopsis carlesii plantation. *J. For. Environ.* 40, 16–23. doi: 10.13324/j.cnki.jfcf.2020.01.00

Lucas-Borja, M. E., Hedod, S. J., Yang, Y., Shen, Y., and Candel-Pérez, D. (2018). Nutrient, metal contents and microbiological properties of litter and soil along a tree age gradient in Mediterranean forest ecosystems. *Sci. Total Environ.* 650, 749–758. doi: 10.1016/j.scitotenv.2018.09.079

Magill, A. H., Aber, J. D., Berntson, G. M., McDowell, W. H., Nadelhoffer, K. J., Melillo, J. M., et al. (2000). Long-term nitrogen additions and nitrogen saturation in two temperate forests. *Ecosystems* 3, 238–253. doi: 10.1007/s100210000023

Malosso, E., English, L., Hopkins, D. W., and O'Donnell, A. G. (2004). Use of 13 C-labelled plant materials and ergosterol, PLFA and NLFA analyses to investigate organic matter decomposition in Antarctic soil. *Soil Biol. Biochem.* 36, 165–175. doi: 10.1016/j.soilbio.2003.09.004

Manzoni, S., Jackson, R. B., Trofymow, J. A., and Porporato, A. (2008). The global stoichiometry of litter nitrogen mineralization. *Science* 321, 684–686. doi: 10.1126/science.1159792

Manzoni, S., Trofymow, J. A., Jackson, R. B., and Porporato, A. (2010). Stoichiometric controls on carbon, nitrogen, and phosphorus dynamics in decomposing litter. *Ecol. Monogr.* 80, 89–106. doi: 10.1890/09-0179.1

Menon, R. R., Kumari, S., Kumar, P., Verma, A., Krishnamurthi, S., and Rameshbumar, N. (2019). Sphingomonas pokkalii sp. nov., a novel plant associated rhizobacterium isolated from a saline tolerant pokkali rice and its draft genome analysis. *Syst. Appl. Microbiol.* 42, 334–342. doi: 10.1016/j.syapm.2019.02.003

Muscolo, A., Bagnato, S., Sidari, M., and Mercurio, R. (2014). A review of the roles of forest canopy gaps. *J. Forestry Res.* 25, 725–736. doi: 10.1007/s11676-014-0521-7

Nevins, C. J., Nakatsu, C., and Armstrong, S. (2018). Characterization of microbial community response to cover crop residue decomposition. *Soil Biol. Biochem.* 127, 39–49. doi: 10.1016/j.soilbio.2018.09.015

Ni, X., Lin, C., Chen, G., Xie, J., and Yang, Y. (2021). Decline in nutrient inputs from litterfall following forest plantation in subtropical China. *Forest Ecol. Manag.* 496:119445. doi: 10.1016/j.foreco.2021.119445

Nicolas, B., Alexandre, C., Jacinthe, R., Steven, W. K., and David, R. (2019). Microsite conditions influence leaf litter decomposition in sugar maple bioclimatic domain of Quebec. *Biogeochemistry* 145, 107–126. doi: 10.1007/s10533-019-00594-1

Osono, T., Bhatta, B. K., and Takeda, H. (2004). Phyllosphere fungi on living and decomposing leaves of giant dogwood. *Mycoscience* 45, 35–41. doi: 10.1007/S10267-003-0155-7

Pascoal, C., and Cássio, F. (2004). Contribution of fungi and bacteria to leaf litter decomposition in a polluted river. *Appl. Environ. Microbiol.* 70, 5266–5273. doi: 10.1128/AEM.70.9.5266-5273.2004

Pastor, J., Aber, J. D., Mc Claugherty, C. A., and Jerry, M. M. (1984). Aboveground production and N and P cycling along a nitrogen mineralization gradient on Blackhawk Island, Wisconsin. *Ecology* 65, 256–268. doi: 10.2307/1939478

Patoine, G., Thakur, M. P., Friese, J., Nock, C., Honig, L., Haase, J., et al. (2017). Plant litter functional diversity effects on litter mass loss depend on the macro-detritivore community. *Pedobiologia* 65, 29–42. doi: 10.1016/j.pedobi.2017.07.003

Pereira, A. P. A., Durrer, A., Gumiere, T., Robin, A., Wang, J., Verma, J. P., et al. (2019). Mixed eucalyptus plantations induce changes in microbial communities and increase biological functions in the soil and litter layers. *Forest Ecol. Manag.* 433, 332–342. doi: 10.1016/j.foreco.2018.11.018

Pielou, E. C. (1966). The measurement of diversity in different types of biological collections. *J. Theor. Biol.* 13, 131–144. doi: 10.1016/0022-5193(66)90013-0

Pointing, S. B., and Hyde, K. D. (2000). Lignocellulose-degrading marine fungi. *Biofouling* 15, 221–229. doi: 10.1080/08927010009386312

Prescott, C. E., and Grayston, S. J. (2013). Tree species influence on microbial communities in litter and soil: current knowledge and research needs. *For. Ecol. Manag.* 309, 19–27. doi: 10.1016/j.foreco.2013.02.034

Quast, C., Pruesse, E., Yilmaz, P., Gerken, J., Schweer, T., Yarza, P., et al. (2012). The SILVA ribosomal RNA gene database project: improved data processing and web-based tools. *Nucleic Acids Res.* 41, D590–D596. doi: 10.1093/nar/gks1219

Raich, J. W., and Schlesinger, W. H. (1992). The global carbon dioxide flux in soil respiration and its relationship to vegetation and climate. *Tellus* 44, 81–99. doi: 10.1034/j.1600-0889.1992.t01-1-00001.x

Sánchez, C. (2009). Lignocellulosic residues: biodegradation and bioconversion by fungi. *Biotechnol. Adv.* 27, 185–194. doi: 10.1016/j.biotechadv.2008.11.001

Santonja, M., Rancon, A., Fromin, N., Baldy, V., Hättenschwilerc, S., Fernandez, C., et al. (2017). Plant litter diversity increases microbial abundance, fungal diversity, and carbon and nitrogen cycling in a Mediterranean shrubland. *Soil Biol. Biochem.* 111, 124–134. doi: 10.1016/j.soilbio.2017.04.006

Sariyildiz, T. (2015). Effects of tree species and topography on fine and small root decomposition rates of three common tree species (*Alnus glutinosa*, *Picea orientalis*, and *Pinus sylvestris*) in Turkey. *Forest Ecol. Manag.* 335, 71–86. doi: 10.1016/j.foreco.2014.09.030

Sariyildiz, T., and Anderson, J. M. (2003). Interactions between litter quality, decomposition and soil fertility: a laboratory study. *Soil Biol. Biochem.* 35, 391–399. doi: 10.1016/S0038-0717(02)00290-0

Scheibe, A., Steffens, C., Seven, J., Jacob, A., Hertel, D., Leuschner, C., et al. (2015). Effects of tree identity dominate over tree diversity on the soil microbial community structure. *Soil Biol. Biochem.* 81, 219–227. doi: 10.1016/j.soilbio.2014.11.020

Schlesinger, W. H., and Lichter, J. (2001). Limited carbon storage in soil and litter of experimental forest plots under increased atmospheric CO_2. *Nature* 411, 466–469. doi: 10.1038/35078060

Schweitzer, B., Huber, I., Amann, R., Ludwig, W., and Simon, M. (2001). α-And β-Proteobacteria control the consumption and release of amino acids on lake snow aggregates. *Appl. Environ. Microb.* 67, 632–645. doi: 10.1128/AEM.67.2.632-645.2001

Sébastien, I., Brun, C., Millery, A., Piton, G., and Jean-Christophe, C. (2021). Litter and soil characteristics mediate the buffering effect of snow cover on litter decomposition. *Plant Soil* 460, 511–525. doi: 10.1007/s11104-020-04803-x

Segata, N., Izard, J., Waldron, L., Gevers, D., Miropolsky, L., Garrett, W. S., et al. (2011). Metagenomic biomarker discovery and explanation. *Genome Biol.* 12:R60. doi: 10.1186/gb-2011-12-6-r60

Shannon, C. E. (1948). A mathematical theory of communication. *Bell Syst. Tech. J.* 27, 623–656. doi: 10.1002/j.1538-7305.1948.tb01338.x

Silver, W. L., and Miya, R. K. (2001). Global patterns in root decomposition: comparisons of climate and litter quality effects. *Oecologia* 129, 407–419. doi: 10.1007/s004420100740

Simpson, E. H. (1949). Measurement of diversity. *Nature* 163:688. doi: 10.1136/thx.27.2.261

Six, J., Feller, C., Denef, K., Ogle, S. M., and Albrecht, A. (2002). Soil organic matter, biota and aggregation in temperate and tropical soils-effects of no-tillage. *Agronomie* 22, 755–775. doi: 10.1051/agro:2002043

Song, P., Ren, H. B., Jia, Q., Guo, J. X., Zhang, N. L., and Ma, K. P. (2015). Effects of historical logging on soil microbial communities in a subtropical forest in southern China. *Plant Soil* 397, 115–126. doi: 10.1007/s11104-015-2553-y

Stefano, M. (2017). Flexible carbon-use efficiency across litter types and during decomposition partly compensates nutrient imbalances-results from analytical stoichiometric models. *Front. Microbiol.* 8:661. doi: 10.3389/fmicb.2017.00661

Sun, H., Wang, Q. X., Liu, N., Li, L., Zhang, C. G., Liu, Z. B., et al. (2017). Effects of different leaf litters on the physicochemical properties and bacterial communities in *Panax ginseng*-growing soil. *Appl. Soil Ecol.* 111, 17–24. doi: 10.1016/j.apsoil.2016.11.008

Sun, H., Wang, Q., Zhang, C., Li, L., Liu, Z., Liu, N., et al. (2018). Effects of different leaf litter on ginseng soil physicochemical properties and microbial community structure. *Acta Ecol. Sin.* 38, 3603–3615. doi: 10.5846/stxb201704180697

Swift, M. J., and Anderson, J. M. (1989). "Decomposition," in *Ecosystems of the World, 14B. Tropical Rain Forest Ecosystems: Biogeographical and Ecological Studies*. eds. H. Lieth and M. J. A. Werger (Amsterdam: Elsevier), 547–569.

Swift, M. J., Heal, O. W., and Anderson, J. M.. (1979). *Decomposition in Terrestrial Ecosystems*. California: University of California Press.

Tan, X., Megan, B., Machmuller, M., Francesca, C., and Shen, W. (2020). Shifts in fungal biomass and activities of hydrolase and oxidative enzymes explain different responses of litter decomposition to nitrogen addition. *Biol. Fert. Soils* 56, 423–438. doi: 10.1007/s00374-020-01434-3

Tonin, A. M., Boyero, L., Monroy, S., Basaguren, A., Pérez, J., Pearson, R. G., et al. (2017). Stream nitrogen concentration, but not plant N-fixing capacity, modulates litter diversity effects on decomposition. *Funct. Ecol.* 31, 1471–1481. doi: 10.1111/1365-2435.12837

Urbanová, M., Šnajdr, J., and Baldrian, P. (2015). Composition of fungal and bacterial communities in forest litter and soil is largely determined by dominant trees. *Soil Biol. Biochem.* 84, 53–64. doi: 10.1016/j.soilbio.2015.02.011

Voříšková, J., and Baldrian, P. (2012). Fungal community on decomposing leaf litter undergoes rapid successional changes. *ISME J.* 7, 477–486. doi: 10.1038/ismej.2012.116

Wallace, J., Laforest-Lapointe, I., and Kembel, S. W. (2018). Variation in the leaf and root microbiome of sugar maple (*Acer saccharum*) at an elevational range limit. *PeerJ* 6:e5293. doi: 10.7717/peerj.5293

Wang, W., Chen, D., Sun, X., Zhang, Q., and Zhang, S. (2019). Impacts of mixed litter on the structure and functional pathway of microbial community in litter decomposition. *Appl. Soil Ecol.* 144, 72–82. doi: 10.1016/j.apsoil.2019.07.006

Whipps, J. M., Hand, P., Pink, D., and Bending, G. D. (2010). Phyllosphere microbiology with special reference to diversity and plant genotype. *J. Appl. Microbiol.* 105, 1744–1755. doi: 10.1111/j.1365-2672.2008.03906.x

White, T. J. (1994). *Amplification and Direct Sequencing of Fungal Ribosomal RNA Genes for Phylogenetics*, *Vol. 38*. Pittsburgh, Pennsylvania, USA: Academic Press, 315–322.

Whittaker, R. H. (1960). Vegetation of the siskiyou mountains, Oregon and California. *Ecol. Monogr.* 30, 279–338. doi: 10.2307/1948435

Whittaker, R. H. (1972). Evolution and measurement of species diversity. *Taxon* 21, 213–251. doi: 10.2307/1218190

Wright, M. S., and Covich, A. P. (2005). Relative importance of bacteria and fungi in a tropical headwater stream: leaf decomposition and invertebrate feeding preference. *Microb. Ecol.* 49, 536–546. doi: 10.1007/s00248-004-0052-4

Wymore, A. S., Salpas, E., Casaburi, G., Liu, C. M., Price, L. B., Hungate, B. A., et al. (2018). Effects of plant species on stream bacterial communities *via* leachate from leaf litter. *Hydrobiologia* 807, 131–144. doi: 10.1007/s10750-017-3386-x

Xiao, W., Chen, H., Kumar, P., Chen, C., and Guan, Q. (2019). Multiple interactions between tree composition and diversity and microbial diversity underly litter decomposition. *Geoderma* 341, 161–171. doi: 10.1016/j.geoderma.2019.01.045

Xu, W., Shi, L., and Chan, O. (2013). Assessing the effect of litter species on the dynamic of bacteria and fungi communities during leaf decomposition in microcosm by molecular techniques. *PLoS One* 8:e84613. doi: 10.1371/journal.pone.0084613

Yao, H., Sun, X., He, C., Maitra, P., Li, X., and Guo, L. (2019). Phyllosphere epiphytic and endophytic fungal community and network structures differ in a tropical mangrove ecosystem. *Microbiome* 7:57. doi: 10.1186/s40168-019-0671-0

Zeng, Q., Yang, L., and An, S. (2017). Impact of litter quantity on the soil bacteria community during the decomposition of quercus wutaishanica litter. *PeerJ* 5:e3777. doi: 10.7717/peerj.3777

Zhang, L., Jia, Y., Zhang, X., Feng, X., Wu, J., Wang, L., et al. (2016). Wheat straw: an inefficient substrate for rapid natural lignocellulosic composting. *Bioresour. Technol.* 209, 402–406. doi: 10.1016/j.biortech.2016.03.004

Zhang, W., Lu, Z., Yang, K., and Zhu, J. (2017). Impacts of conversion from secondary forests to larch plantations on the structure and function of microbial communities. *Appl. Soil Ecol.* 111, 73–83. doi: 10.1016/j.apsoil.2016.11.019

Zhang, W., Yang, K., Lyu, Z., and Zhu, J. (2019). Microbial groups and their functions control the decomposition of coniferous litter: a comparison with broadleaved tree litters. *Soil Biol. Biochem.* 133, 196–207. doi: 10.1016/j.soilbio.2019.03.009

frontiers | Frontiers in Microbiology

TYPE Original Research
PUBLISHED 15 December 2022
DOI 10.3389/fmicb.2022.1051721

OPEN ACCESS

EDITED BY
Yu Luo,
Zhejiang University,
China

REVIEWED BY
Rongxiao Che,
Yunnan University,
China
Kai Feng,
Research Center for Eco-environmental Sciences (CAS), China

*CORRESPONDENCE
Zheke Zhong
zhekez@163.com

SPECIALTY SECTION
This article was submitted to Terrestrial Microbiology, a section of the journal Frontiers in Microbiology

RECEIVED 23 September 2022
ACCEPTED 22 November 2022
PUBLISHED 15 December 2022

CITATION
Zhang X, Huang Z, Zhong Z, Li Q, Bian F and Yang C (2022) Metagenomic insights into the characteristics of soil microbial communities in the decomposing biomass of Moso bamboo forests under different management practices. *Front. Microbiol.* 13:1051721. doi: 10.3389/fmicb.2022.1051721

Metagenomic insights into the characteristics of soil microbial communities in the decomposing biomass of Moso bamboo forests under different management practices

Xiaoping Zhang[1,2,3], Zhiyuan Huang[1,2], Zheke Zhong[1,2]*, Qiaoling Li[1,2], Fangyuan Bian[1,2] and Chuanbao Yang[1,2]

[1]Key Laboratory of Bamboo Forest Ecology and Resource Utilization of National Forestry and Grassland Administration, China National Bamboo Research Center, Zhejiang, China, [2]National Long-term Observation and Research Station for Forest Ecosystem in Hangzhou-Jiaxing-Huzhou Plain, Zhejiang, China, [3]Engineering Research Center of Biochar of Zhejiang Province, Zhejiang, China

Introduction: Considering the rapid growth and high biomass productivity, Moso bamboo (*Phyllostachys edulis*) has high carbon (C) sequestration potential, and different management practices can strongly modify its C pools. Soil microorganisms play an important role in C turnover through dead plant and microbial biomass degradation. To date, little is known about how different management practices affect microbial carbohydrate-active enzymes (CAZymes) and their responses to dead biomass degradation.

Methods: Based on metagenomics analysis, this study analyzed CAZymes in three comparable stands from each Moso bamboo plantation: undisturbed (M0), extensively managed (M1), and intensively managed (M2).

Results: The results showed that the number of CAZymes encoding plant-derived component degradation was higher than that encoding microbe-derived component degradation. Compared with the M0, the CAZyme families encoding plant-derived cellulose were significantly ($p < 0.05$) high in M2 and significantly ($p < 0.05$) low in M1. For microbe-derived components, the abundance of CAZymes involved in the bacterial-derived peptidoglycan was higher than that in fungal-derived components (chitin and glucans). Furthermore, M2 significantly increased the fungal-derived chitin and bacterial-derived peptidoglycan compared to M0, whereas M1 significantly decreased the fungal-derived glucans and significantly increased the bacterial-derived peptidoglycan. Four bacterial phyla (Acidobacteria, Actinobacteria, Proteobacteria, and Chloroflexi) mainly contributed to the degradation of C sources from the plant and microbial biomass. Redundancy analysis (RDA) and mantel test suggested the abundance of CAZyme encoding genes for plant and microbial biomass degradation are significantly correlated with soil pH, total P, and available K. Least Squares Path Modeling (PLS-PM) showed that management practices indirectly affect the CAZyme encoding genes associated with plant and microbial biomass degradation by regulating the soil pH and nutrients (total N and P), respectively.

Discussion: Our study established that M2 and M1 impact dead biomass decomposition and C turnover, contributing to decreased C accumulation and establishing that the bacterial community plays the main role in C turnover in bamboo plantations.

KEYWORDS

CAZyme, plant-derived components, microbial-derived components, forest management, carbon sequestration

Introduction

Forest ecosystems are the most important carbon (C) pools and sinks in terrestrial ecosystems (Ameray et al., 2021), and store approximately two-thirds of the soil organic C (SOC) in terrestrial ecosystems (Canadell Josep et al., 2007). The forest soil C pool mainly comprises C allocated to the soil by tree roots and C contained in dead plant biomass (López-Mondéjar et al., 2020; Feng et al., 2022). Plant residues mainly consist of cellulose, hemicelluloses, and lignin, which form a complex and recalcitrant matrix (Mansora et al., 2019). Microbial biomass (e.g., bacterial and fungal cell walls) represents another important organic C pool (Wang et al., 2021; Patoine et al., 2022). The biomass of fungal residues mainly contains polysaccharides, which account for 80–90% of the total cell wall (Baldrian et al., 2013; Gow and Lenardon, 2022). Although bacterial cell wall composition can vary substantially (Silhavy et al., 2010), peptidoglycan is typically the main component (Egan et al., 2017; Apostolos and Pires, 2022).

Soil microorganisms are an important link between soil C input and output (Liang et al., 2017; Bhattacharyya et al., 2022), playing a critical role in C balance through dead biomass decomposition (López-Mondéjar et al., 2018). Žifčáková et al. (2017) suggested that the dead biomass turnover can be traced by studying the microbial carbohydrate-active enzymes (CAZymes) that mediate their C cycle. Among the CAZymes, glycoside hydrolases (GHs) and auxiliary activities (AAs) are associated with the decomposition of polysaccharides and lignin, respectively (López-Mondéjar et al., 2018; Lladó et al., 2019). Cellulases, β-glucosidases, and hemicellulases from GH families have been reported as the main enzymes degrading plant biomass (Bomble et al., 2017), whereas lysozymes and chitinases from GH families are linked to dead biomass degradation from microbial communities (Žifčáková et al., 2017). Ren et al. (2021) showed that the bacterial phyla Actinobacteria, Proteobacteria, and Acidobacteria dominated plant and microbial dead biomass decomposition through their corresponding CAZyme families. Members of Chloroflexi taxa are related to the degradation of plant compounds, such as cellulose, starch, and long-chain sugars (Li et al., 2020). Although CAZymes have been previously studied in forest soils, the mechanisms of C degradation driven by microbial communities are yet to be elucidated.

Moso bamboo (*Phyllostachys edulis*) is a typical representative forest resource in China, occupying 4.68 million hectares and accounting for approximately 72.96% of all the bamboo forests in the forested areas of China (Li and Feng, 2019). This bamboo species is an important non-wood forest product in China (Fei, 2021) due to its rapid growth, strong regeneration ability (Song et al., 2016), and C sequestration potential (Yen and Lee, 2011). A previous study confirmed that Moso bamboo forests are characterized by a higher C sequestration rate (8.13 Mg ha^{-1} year^{-1}) than Chinese fir forests (3.35 Mg ha^{-1} year^{-1}). Two management practices are used in Moso bamboo plantations: intensive management (such as fertilizer application, tillage, and removal of understory vegetation) and extensive management (including selective and regular harvesting of bamboo stems and shoots) (Yang et al., 2019). Previous studies have also found a relationship between different management approaches and soil C dynamics in Moso bamboo plantations (Li et al., 2013; Yang et al., 2019; Zhang et al., 2022). Specifically, Li et al. (2013) indicated that long-term intensive management practice decreases SOC storage and alters SOC chemical compositions, such as increased alkyl C and carbonyl C contents and decreased O-alkyl C and aromatic C contents. In contrast, extensive management can promote the accumulation of recalcitrant organic materials while decreasing C mineralization rates (Yang et al., 2019). However, the characteristics of the CAZymes in bamboo forests remain unclear.

This study describes an enzymatic toolbox that aids in the microbial decomposition of various biomass types. Soil samples from three different management practices were collected, and metagenomics was used to analyze the enzymatic tools of microbial decomposers. Moreover, we hypothesized that there were categories of CAZyme families involved in plant- and microbial-derived biomass decomposition and that the bacterial community contributes more to the dead biomass degradation in the Moso bamboo plantations. This study aimed to: (i) elucidate the distribution of the microbial CAZyme pool, (ii) characterize microbial taxa contribution to CAZyme genes related to the degradation of plant- and microbe-derived components, and (iii) examine the relationships between environmental parameters and specific CAZyme families.

Materials and methods

Experimental site and sample collection

The soil samples and their physiochemical properties used in this study were recently published (Zhang et al., 2022).

The study area was Anji County (30°31′–30°14′N, 119°37–119°15′ E) in Zhejiang Province, China. A previous study presented meteorological data for the study area (Yang et al., 2019). Moso bamboo plantations under three different management strategies were selected: unmanaged (M0), extensively managed (M1), and intensively managed (M2). The M0 bamboo plantation had not been managed for >60 years (recoded by the Anji County Forestry Bureau), and had gradually developed into a mixed forest; the M1 bamboo plantation had been subjected to some management practices including selective and regular harvest of bamboo trunks, and shoots every 2 years; the M2 practices included selective harvesting, understory vegetation removal, and annual fertilization (nitrogen [N], 300–500 kg·ha^{-1}; phosphorus [P], 50–200 kg·ha^{-1}; and potassium [K], 100–250 kg·ha^{-1}) during mid-to-late June. More information regarding the Moso bamboo plantations can be found in a study by Yang et al. (2019).

Three sites in the study area (3 × 2 km) were chosen for investigation in May 2021 based on similarities to the initial site conditions found in previous studies (Yang et al., 2019; Zhang et al., 2022). At each site, three comparable stands (M0, M1, and M2) with similar forest-land characteristics, such as soil type, elevation, slope gradient, and other features, were chosen. Three 20 × 20 m plots were established in each selected bamboo stand for sampling. A composite sample within each plot was obtained from five different points at depths of 0–20 cm. Fresh soil samples were sieved (mesh size of 2 mm) to remove stones, roots, and large organic residues. Subsequently, they were divided into two parts: one part was stored at −80°C for metagenomics, and the other was air-dried to analyze physicochemical properties.

Soil chemical analysis

A glass electrode was used to measure the soil pH at a soil/water ratio of 1:2.5. SOC was determined using a total organic C (TOC) analyzer (Multi N/C 3100; Analytik Jena, Germany). Soil total N (TN, the Kjeldahl method), total P (TP, ammonium molybdate method), and available K (AK, extracted using 1 mol·L^{-1} ammonium acetate acid); were determined according to Lu (2000). Detailed information on the soil factors at these sampling sites is shown in Supplementary Table S1.

DNA extraction and sequencing

Soil DNA was extracted using the FastDNA SPIN kit (MP Biomedical, Santa Anna, CA, United States), according to the manufacturer's instructions. The quality and concentration of the DNA extracts were assessed using a NanoDrop 2000. Library construction and Illumina NovaSeq 6,000 sequencing were conducted at the Shanghai Majorbio Bio-Pharm Technology Co., Ltd.

Metagenome sequencing and analysis

Raw reads (about 12 Gb nucleotides for each sample) from the metagenome sequencing were processed to obtain quality-filtered reads for further analysis. The adaptor sequences and low-quality reads were removed using fastp version 0.20.0 (Chen et al., 2018) on the online platform of Majorbio Cloud Platform[1] (Ren et al., 2022). Subsequently, contigs were assembled using the MEGAHIT assembler (Li et al., 2015) (parameters: kmer_min = 47, kmer_max = 97, step = 10), which uses succinct de Bruijn graphs. Contigs with a minimum size of 300 base pairs (bp) were selected for the final assembly. The open reading frames (ORFs) were identified using MetaGene (Noguchi et al., 2006), and the predicted ORFs over 100 bp in length were translated into amino acid sequences using the National Center for Biotechnology Information (NCBI) translation table. All predicted genes with an identity and coverage ≥0.9 were clustered using the CD-HIT program (Fu et al., 2012). SOAPaligner (Li et al., 2008) was utilized to map the reads after quality control to non-redundant gene sets with 95% identity, and to calculate gene abundance. Representative sequences of non-redundant gene catalogs were annotated based on the NCBI NR database using the Basic Local Alignment Search Tool for Proteins (BLASTP), as implemented in DIAMOND v0.9.19, with an e-value cutoff of 1e^{-5} using Diamond (Buchfink et al., 2015) for taxonomic annotations. Carbohydrate-active enzyme annotation was conducted using hmmscan[2] against the CAZyme database[3] with an e-value cut-off of 1e^{-5}.

Statistical analyses

The abundance values in metagenomes normalized by transcripts per kilobase per million mapped reads (TPM). Non-metric multidimensional scaling (NMDS), permutational multivariate analysis of variance (PERMANOVA) and redundancy analysis (RDA) were performed in the 'Vegan' (Dixon, 2003) package based on Bray-Curtis distance. The circos plots were generated using the 'circlize' package (Gu et al., 2014). The R package'ggcor'was used for Spearman's correlation test and the Mantel test (Huang et al., 2020). Least Squares Path Modeling (PLS-PM) were performed with the R package 'plspm' (Sanchez et al., 2017). Contribution analysis was conducted on the Majorbio Cloud Platform[4] (Ren et al., 2022). The significance of differences among soil samples was tested by One-way ANOVA followed by least significant difference (LSD) *post hoc* test.

1 https://cloud.majorbio.com/
2 http://hmmer.janelia.org/search/hmmscan
3 http://www.cazy.org/
4 http://www.majorbio.com

Results

Changes in glycoside hydrolases and auxiliary enzyme families

In total, 7,759,044 CAZymes were identified from 13,509,440 predicted proteins in the metagenome. Of these, > 98% was assigned to bacteria (Supplementary Table S2). Moreover, of the total CAZyme pools, GHs and AAs represented average values of 29.38 and 10.69%, respectively (Supplementary Table S3). Most GHs were mainly attributed to Proteobacteria (56.95%), Acidobacteria (19.72%), Actinobacteria (12.30%), Chloroflexi (3.90%), and Verrucomicrobia (1.42%; Figure 1A), whereas AAs were largely attributed to Proteobacteria (36.48%), Acidobacteria (29.75%), Actinobacteria (13.84%), Chloroflexi (6.50%), Verrucomicrobia (3.71%), Candidatus Rokubacteria (1.69%), and Gemmatimonadetes (1.55%; Figure 1B). Compared to M0 and M1, M2 significantly increased GHs abundance, whereas there was no significant difference between M1 and M0 (Supplementary Table S3). In addition, no differences in AAs among the three groups were identified (Supplementary Table S3).

The NMDS further revealed significant differences in GHs (PERMANOVA: $R^2 = 0.859$, $p = 0.005$) and AA (PERMANOVA: $R^2 = 0.826$, $p = 0.01$) families among the different management approaches (Figures 1C,D).

Changes in specific CAZyme families involved in the degradation of plant, fungal, and bacterial biomass

The genes were assigned to the enzymatic activities involved in the degradation of plant- and microbial- compounds according to Ren et al. (2021). For plant biomass (Figure 2; Supplementary Table S4), M2 significantly increased the abundance of CAZyme families involved in plant-derived cellulose than M0 ($p < 0.05$), whereas it significantly decreased in M1 ($p < 0.05$); Among the three groups, no significant differences ($p > 0.05$) were observed in the CAZyme families involved in plant-derived hemicellulose and lignin. Additionally, M2 exhibited a significantly ($p < 0.05$) higher abundance of CAZyme families involved in fungi-derived chitin within fungal biomass than M0

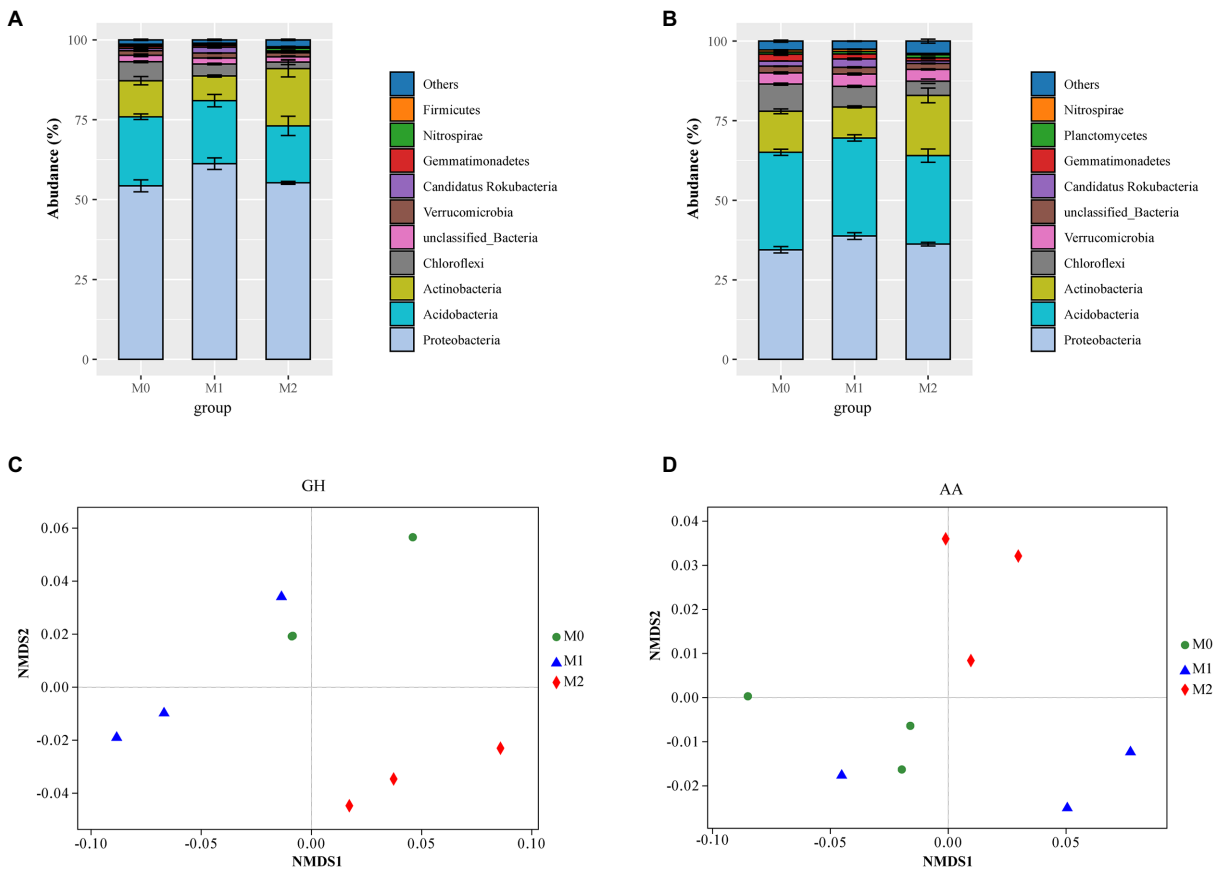

FIGURE 1
The abundance of microbial glycoside hydrolases (GHs) and auxiliary activities (AAs) in the bamboo plantations under different management practices. **(A,B)** contribution of microbial phyla to the GHs and AAs families; **(C,D)** Non-metric multidimensional scaling (NMDS) of the GH and AA families. M0, M1, and M2 indicates undisturbed, extensively managed, and intensively managed bamboo plantations, respectively.

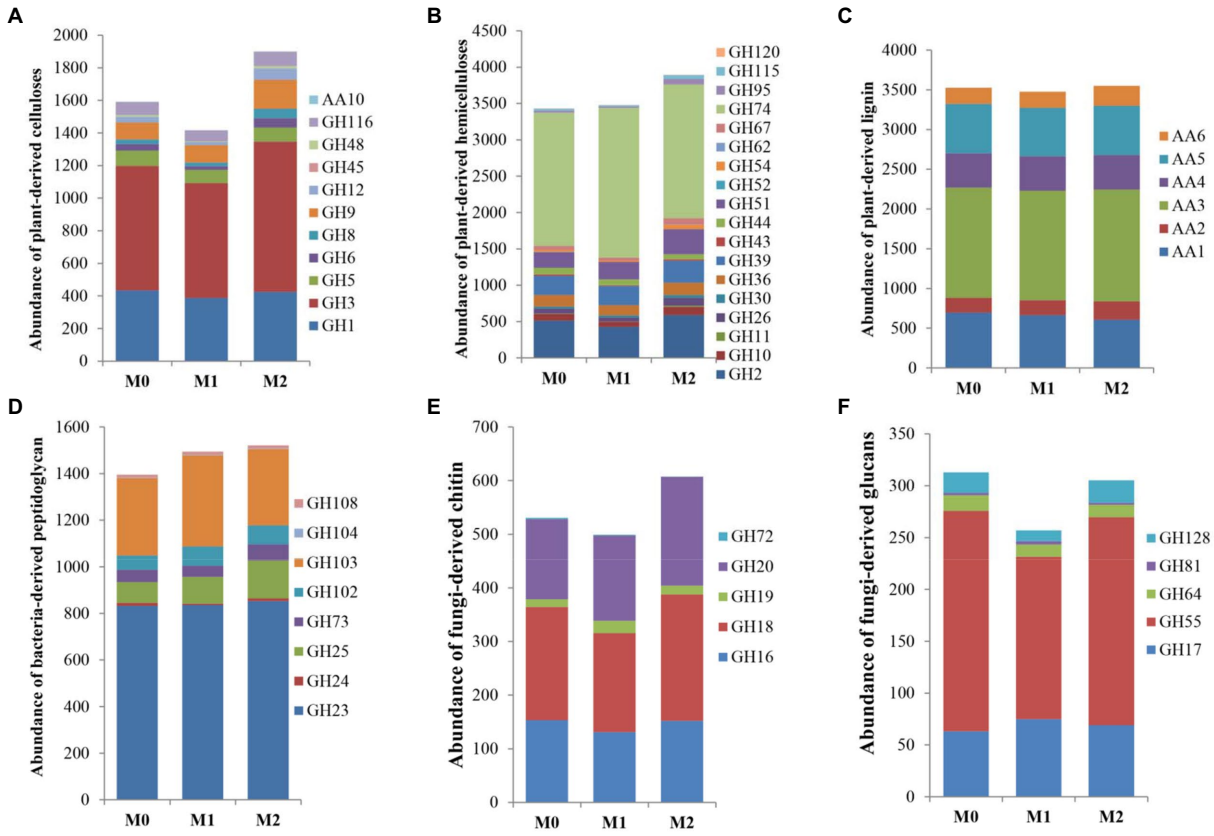

FIGURE 2
The abundance of selected GHs and AAs related to the degradation of the plant- and microbial- derived biomass in the bamboo plantations under different management practices. **(A–C)** plant-derived biomass decomposotion; **(D)** bacteria-derived biomass decomposition; **(E,F)** fungi-derived biomass decomposition.

and M1 (Figure 2; Supplementary Table S4). No significant difference ($p > 0.05$) was observed between M0 and M1. Moreover, M1 exhibited a significantly ($p < 0.05$) lower abundance of CAZyme families involved in fungi-derived glucans than M0 and M2 (Figure 2; Supplementary Table S4). There was no significant difference ($p > 0.05$) between M0 and M2 (Figure 2; Supplementary Table S4). Furthermore, M2 and M1 significantly increased ($p < 0.05$) the abundance of CAZyme families involved in bacteria-derived peptidoglycan than M0 (Figure 2; Supplementary Table S4).

The CAZyme families associated with the degradation of plant- and microbe-derived components were mainly assigned to four bacterial phyla: Acidobacteria, Actinobacteria, Proteobacteria, and Chloroflexi (Figure 3). In particular, Actinobacteria, Chloroflexi, and Proteobacteria exhibited significant differences among the three groups (Supplementary Table S5). The analysis of microbial phyla contribution to plant-derived biomass decomposition revealed that Actinobacteria was significantly increased in M2 than in M0 and significantly decreased in M1 (Supplementary Table S5). Chloroflexi exhibited a lower number of transcripts per million (TPM) in M1 and M2 than in M0, whereas Proteobacteria exhibited a significant difference among the three groups (plant-derived cellulose, $M1 > M2 \approx M0$; plant-derived hemicellulose, $M2 > M0$; plant-derived lignin, $M2 \approx M1 > M0$) (Supplementary Table S5). The three phyla were identified according to the contribution of microbial phyla to fungi-derived biomass decomposition in the following order: fungi-derived chitin (Actinobacteria, $M2 > M0 > M1$; Chloroflexi, $M0 \approx M1 > M2$; and Proteobacteria, $M2 > M0 \approx M1$) and fungi-derived glucans (Actinobacteria, $M2 \approx M0 > M1$; Chloroflexi, $M0 > M1 > M2$; and Proteobacteria, $M2 \approx M1 \approx M0$) (Supplementary Table S5). Regarding the contribution of microbial phyla to bacteria-derived peptidoglycan decomposition, Actinobacteria was significantly higher in M2 than in M0 and M1, and Chloroflexi ($M0 > M1 > M2$) and Proteobacteria ($M1 > M2 > M0$) exhibited significant differences among the three groups (Supplementary Table S5).

Management practices altered specific families related to the degradation of plant- and microbe-derived components (Supplementary Table S6). For the plant-derived components, GH3 (β-glucosidase, 797.31 TMP, $M2 > M0 > M1$), GH74 (xyloglucanase, 1910.99 TMP, $M1 > M2 \approx M0$), and AA3 (oxidase, 1390.84 TMP, $M2 \approx M1 \approx M0$) were the most abundant families involved in plant-derived cellulose, hemicellulose, and lignin

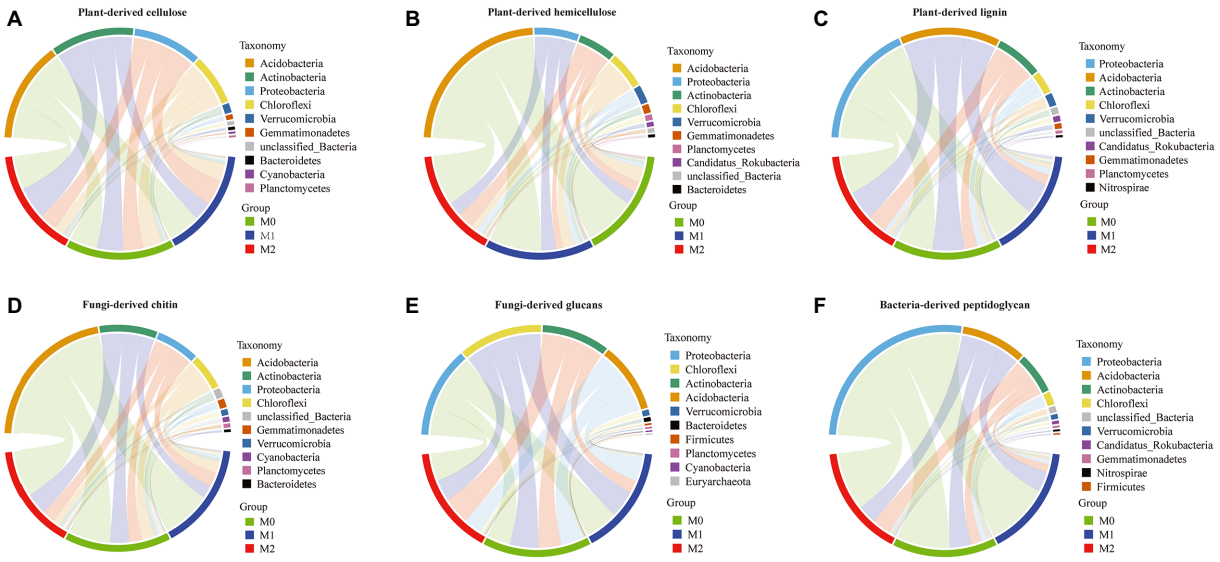

FIGURE 3
Contribution of the microbial phyla to microbial CAZyme genes for the dead biomass decomposing in the bamboo plantations. **(A–C)** plant-derived biomass decomposotion; **(D,E)** fungi-derived biomass decomposition; **(E,F)** bacteria-derived biomass decomposition.

decomposition, respectively (Supplementary Table S6). For the microbe-derived components, GH18 (chitinase, 210.26 TMP, M2 > M1), GH55 (exo-β-1, 3-glucanase/endo-1, 3-β-glucanase, 190.05 TMP, M0 ≈ M2 > M1), and GH23 (lysozyme, 840.24 TMP, M0 ≈ M1 ≈ M2) were the most abundant families involved in fungi-derived chitin and glucans, and bacteria-derived peptidoglycan decomposition, respectively (Supplementary Table S6).

Relationship between the CAZymes involved in the degradation of dead biomass and soil properties

RDA showed that the first two RDA axes accounted for 83.70 and 79.66%, respectively, of the total variation of CAZyme families related to plant and microbial biomass degradation (Figure 4). Soil pH, TOC, TN, TP, AK significantly affected the CAZyme families associated with plant and microbial biomass degradation (Figure 4). Furthermore, the Mantel test revealed that soil pH, TP, and AK were significantly correlated with the CAZyme families involved in the decomposition of plant and microbial biomass; soil TOC and TN were also significantly correlated with CAZyme families involved in the decomposition of microbial biomass (Table 1).

PLS-PM was implemented to assess the direct and indirect effects of management practices and soil properties on the CAZyme families (Figure 5). PLS-PM with a Goodness-of-Fit (GoF) index of 0.833 explained 82.2 and 73.5% of the variation for CAZyme families in plant and microbial biomass decomposition, respectively. The PLS-PM analysis indicated that the management practices had an indirect positive effect on the plant and microbial biomass degradation by changing soil nutrients (TN and TP) (path coefficient = −0.881) and pH (path coefficient = −0.993), respectively. Management practices also indirectly affected the soil nutrients (TN and TP) *via* altering soil TOC (path coefficient = −8.129).

Discussion

Effects of management practices on microbial CAZyme genes in the bamboo plantations

Our findings suggest that soil microbes contain numerous CAZymes which are involved in plant and microbial biomass degradation, and facilitates C utilization in bamboo plantations. This result supports previous findings on soil microbes as the primary consumers of simple and recalcitrant substrates (Kramer et al., 2016; López-Mondéjar et al., 2018). Furthermore, the number of CAZymes associated with plant-derived component degradation was greater than that associated with microbe-derived components (Figure 2). This indicates that dead plant biomass contributes more to the soil C pool in bamboo plantations. This finding is consistent with previous findings that plant biomass is rich in C and can enrich the soil through above- and underground litter, which is the primary source of soil organic matter (SOM) (Castellano et al., 2015). Our findings also showed that the forest management practices influenced soil microbial CAZyme families involved in plant-derived cellulose but not plant-derived hemicellulose and lignin. These results suggest that

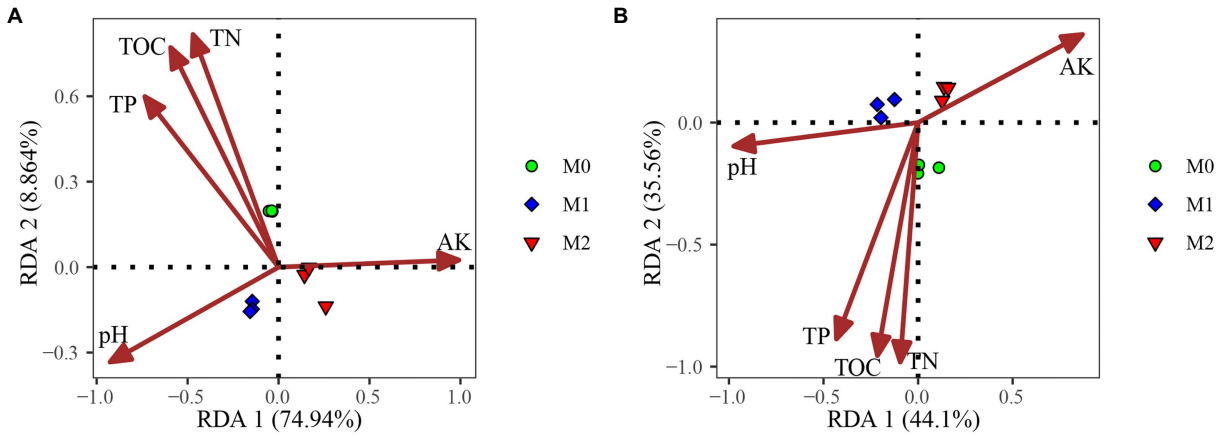

FIGURE 4
Redundancy analysis of soil properties and microbial CAZyme genes for the plant- **(A)** and microbial-derived **(B)** biomass decomposing in the bamboo plantations under different management practices.

TABLE 1 Spearman's correlation analysis and Mantel tests for microbial CAZyme families involved in the decomposition of the plant- and microbial-derived components against soil properties (9,999 permutations).

	Plant-derived components		Microbial-derived components	
	r	*p*-value	*r*	*p*-value
pH	0.552	0.015	0.78	0.0002
TOC	0.281	0.0583	0.366	0.0329
TN	0.237	0.0843	0.331	0.0384
TP	0.654	0.0081	0.477	0.0188
AK	0.876	0.0002	0.748	0.0009

plant-derived cellulose is a key factor determining SOC accumulation in bamboo plantations. Moreover, microbial CAZyme families involved in plant-derived cellulose were significantly increased in M2 than in M0 but decreased in M1, indicating that more disturbance promotes the degradation of plant-derived cellulose. A significant correlation was discovered between soil pH and AK in CAZyme families associated with plant-derived cellulose degradation. Therefore, the soil pH and AK variations partially contributed to the changes in the CAZyme families associated with plant-derived cellulose degradation.

Our results revealed that the abundance of genes involved in the decomposition of bacteria-derived biomass was greater than that of fungi-derived biomass. This indicates that bacteria-derived biomass degradation for C cycling is more important than fungi-derived biomass. Our findings are consistent with Gunina et al. (2017), who reported that dead bacterial biomass had a higher turnover rate than fungal biomass. Egan et al. (2017) also demonstrated that bacterial-derived peptidoglycan is the main and universal component of the cell wall that changes rapidly. This study found that M2 and M1 significantly increased the abundance of soil microbial CAZyme families involved in bacterial-derived peptidoglycan, indicating that forest management can increase the decomposition rate of bacterial-derived peptidoglycan. Ren et al. (2021) suggested that the soil environment and substrates influence the decomposition of microbe-derived components in forest soils. In this study, CAZyme families involved in bacteria-derived peptidoglycan degradation were negatively correlated with soil TOC, TN, and TP. Thus, the changes in soil properties (especially TOC, TN, and TP) contributed to the variations in the CAZyme families involved in bacteria-derived peptidoglycan degradation.

M1 exhibited a lower abundance in the CAZyme families involved in fungi-derived biomass than M2. According to Clemmensen et al. (2013), some fungal biomass fractions are highly recalcitrant and are likely a major source of recalcitrant SOM. Combined with the results for the CAZyme families involved in plant-derived cellulose, M1 can alleviate the degradation of SOC relative to M2. Similar to the results of Yang et al. (2019), who found that the rate of C mineralization was highest in M2 and lowest in M1, indicating M0 and M1 had much higher potential in terms of soil C sequestration than M2.

Microbial CAZymes for metabolic activity in bamboo plantations under different management practices

This study found that bacterial communities accounted for >98% of the microbial community in the bamboo soils studied. This result suggests that the bacterial community plays important roles in the degradation of dead plants and microbial biomass, partly because bacteria produce enzymes and participate in the degradation of cellulose, hemicellulose, and chitin (Eichorst and Kuske, 2012; López-Mondéjar et al., 2016). The microbial CAZyme families associated with the degradation of dead plants and microbial biomass were mainly assigned to four bacterial

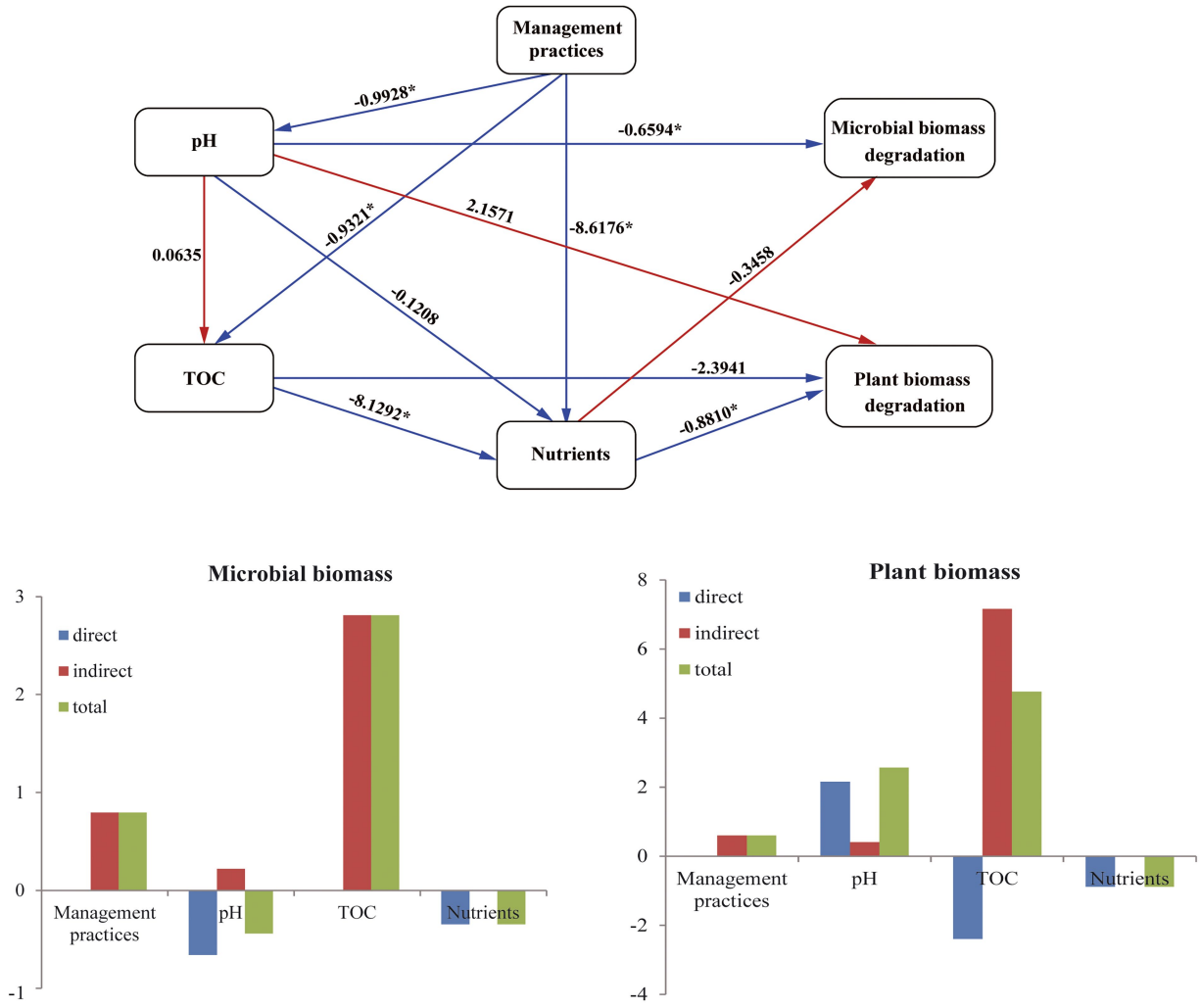

FIGURE 5
PLS-PM shows the effects of management practices on the microbial CAZyme genes for the plant- and microbial-derived biomass decomposing.

phyla: Acidobacteria, Actinobacteria, Proteobacteria, and Chloroflexi. Members of the Actinobacteria produce extracellular enzymes and play a role in the degradation of plant polysaccharides and phenolic compounds (Mccarthy, 1987; Warren, 1996). Notably, the analysis of the contribution of microbial phyla to plant-derived cellulose degradation revealed that these four phyla were significantly altered. Actinobacteria and some Acidobacteria are oligotrophic bacteria (Kielak et al., 2016; Liu et al., 2018), affecting the decomposition of organic matter under limited nutrient conditions (Fierer et al., 2007; Banerjee et al., 2016). Therefore, the increased Actinobacteria and Acidobacteria indicated low nutrient levels in M2. Members of Proteobacteria were related to N fixation, organic matter degradation, and plant growth improvement (Yarwood et al., 2009; Delmont et al., 2018). Several studies reported that Proteobacteria are rich in higher pH soils (Christian et al., 2009; Chu et al., 2010). The increased pH can clarify the higher abundance of Proteobacteria in M1 than in M0 and M2. The phylum Chloroflexi plays a role in cycling C and N (Hug et al., 2013). Thus, the increased abundance of Chloroflexi was related to the higher TOC and TN contents in M0 than in M1 and M2.

Factors driving the CAZyme families involved in plant and microbial biomass degradation

Several studies have found that soil properties are one of the most important factors influencing soil microbial diversity and function (Zhang et al., 2021; Wang et al., 2022). According to Cardenas et al. (2015), soil properties can exert selective pressure on soil microorganisms, shaping changes in CAZyme coding genes. In our study, RDA and mantel tests showed that soil pH, TP, and AK content significantly affected the abundance of CAZyme encoding genes. Results of PLS-PM suggested that management practices altered the CAZyme families during the decomposition

of plant and microbial biomass by changing the soil nutrients (TN and TP) and pH, respectively. These results indicated soil pH and TP were the major factors shaping the specific CAZyme families. Studies have shown that pH is the vital factor shaping soil microbial communities (Qi et al., 2018; Lopes et al., 2021). Conversely, soil pH indirectly affects microbial communities due to its close relationship with other soil factors, such as fertility and nutrient availability (Christian et al., 2009; Penn and Camberato, 2019). Phosphorus is an important macronutrient for all biota on Earth, and changes therein affect the microbial community (Bergkemper et al., 2016; Samaddar et al., 2019).

Conclusion

This study elucidated the trends of microbial CAZymes in Moso bamboo stands. The abundance of CAZymes targeting dead plant biomass was higher than that of dead microbial biomass, indicating that dead plant biomass was the major source of the soil C pool in the bamboo plantations. Management practices alter the abundance of microbial CAZymes encoding plant- and microbial-derived biomass degradation, further affecting the C accumulation. The dominant microorganisms for microbial C degradation were bacterial communities, suggesting that the bacterial community contributes more to the degradation of microbial C in the bamboo soil and that Acidobacteria, Actinobacteria, Proteobacteria, and Chloroflexi, in particular, are essential for microbial C decomposition. Overall, our findings expand the understanding of the relationship between microbial CAZyme families and C decomposition, establishing the importance of the bacterial community for C cycling in bamboo plantations.

Data availability statement

The data presented in the study are deposited in the National Center for Biotechnology Information (NCBI) BioProject repository, accession number PRJNA883525. https://www.ncbi.nlm.nih.gov/bioproject/PRJNA883525.

Author contributions

XZ and ZZ: conceptualization and methodology. XZ, ZH, QL, FB, and CY: investigation. XZ: writing—original draft preparation. ZZ: writing—review and editing. XZ and ZZ: funding acquisition. All authors contributed to the article and approved the submitted version.

Funding

This research was supported by the People's Government of Zhejiang Province–Chinese Academy of Forestry cooperative project (2020SY01), and the Fundamental Research Funds of CAF (CAFYBB2021QB007).

Conflict of interest

The authors declare that the research was conducted in the absence of any commercial or financial relationships that could be construed as a potential conflict of interest.

Publisher's note

Supplementary material

The Supplementary material for this article can be found online at: https://www.frontiersin.org/articles/10.3389/fmicb.2022.1051721/full#supplementary-material

References

Ameray, A., Bergeron, Y., Valeria, O., Montoro Girona, M., and Cavard, X. (2021). Forest carbon management: a review of silvicultural practices and management strategies across boreal, temperate and tropical forests. *Curr. For. Rep.* 7, 245–266. doi: 10.1007/s40725-021-00151-w

Apostolos, A., and Pires, M. M. (2022). Impact of crossbridge structure on peptidoglycan crosslinking: a synthetic stem peptide approach. *Method Enzymol.* 665:259. doi: 10.1016/bs.mie.2021.11.019

Baldrian, P., Šnajdr, J., Merhautová, V., Dobiášová, P., Cajthaml, T., and Valášková, V. (2013). Responses of the extracellular enzyme activities in hardwood forest to soil temperature and seasonality and the potential effects of climate change. *Soil Biol. Biochem.* 56, 60–68. doi: 10.1016/j.soilbio.2012.01.020

Banerjee, S., Kirkby, C. A., Schmutter, D., Bissett, A., Kirkegaard, J. A., and Richardson, A. E. (2016). Network analysis reveals functional redundancy and keystone taxa amongst bacterial and fungal communities during organic matter decomposition in an arable soil. *Soil Biol. Biochem.* 97, 188–198. doi: 10.1016/j.soilbio.2016.03.017

Bergkemper, F., Schöler, A., Engel, M., Lang, F., Krüger, J., Schloter, M., et al. (2016). Phosphorus depletion in forest soils shapes bacterial communities towards phosphorus recycling systems. *Environ. Microbiol.* 18, 1988–2000. doi: 10.1111/1462-2920.13188

Bhattacharyya, S. S., Ros, G. H., Furtak, K., Iqbal, H. M., and Parra-Saldívar, R. (2022). Soil carbon sequestration–an interplay between soil microbial community and soil organic matter dynamics. *Sci. Total Environ.* 815:152928. doi: 10.1016/j.scitotenv.2022.152928

Bomble, Y. J., Lin, C., Amore, A., Wei, H., Evert, K. H., Ciesielski, P. N., et al. (2017). Lignocellulose deconstruction in the biosphere. *Curr. Opin. Chem. Biol.* 41, 61–70.

Buchfink, B., Xie, C., and Huson, D. H. (2015). Fast and sensitive protein alignment using DIAMOND. *Nat. Methods* 12, 59–60. doi: 10.1038/nmeth.3176

Canadell Josep, G., Le Quéré, C., Raupach Michael, R., Field Christopher, B., Buitenhuis Erik, T., Ciais, P., et al. (2007). Contributions to accelerating

atmospheric CO_2 growth from economic activity, carbon intensity, and efficiency of natural sinks. *Proc. Natl. Acad. Sci. U. S. A.* 104, 18866–18870. doi: 10.1073/pnas.0702737104

Cardenas, E., Kranabetter, J. M., Hope, G., Maas, K. R., Hallam, S., and Mohn, W. W. (2015). Forest harvesting reduces the soil metagenomic potential for biomass decomposition. *ISME J.* 9, 2465–2476. doi: 10.1038/ismej.2015.57

Castellano, M. J., Mueller, K. E., Olk, D. C., Sawyer, J. E., and Six, J. (2015). Integrating plant litter quality, soil organic matter stabilization, and the carbon saturation concept. *Glob. Chang. Biol.* 21, 3200–3209. doi: 10.1111/gcb.12982

Chen, S., Zhou, Y., Chen, Y., and Gu, J. (2018). Fastp: an ultra-fast all-in-one FASTQ preprocessor. *Bioinformatics* 34, i884–i890. doi: 10.1093/bioinformatics/bty560

Christian, L., Hamady, M., Knight, R., and Fierer, N. (2009). Pyrosequencing-based assessment of soil pH as a predictor of soil bacterial community structure at the continental scale. *Appl. Environ. Microbiol.* 75, 5111–5120. doi: 10.1128/AEM.00335-09

Chu, H., Fierer, N., Lauber, C. L., Caporaso, J. G., Knight, R., and Grogan, P. (2010). Soil bacterial diversity in the Arctic is not fundamentally different from that found in other biomes. *Environ. Microbiol.* 12, 2998–3006. doi: 10.1111/j.1462-2920.2010.02277.x

Clemmensen, K. E., Bahr, A., Ovaskainen, O., Dahlberg, A., Ekblad, A., Wallander, H., et al. (2013). Roots and associated fungi drive long-term carbon sequestration in boreal Forest. *Science* 339, 1615–1618. doi: 10.1126/science.1231923

Delmont, T. O., Quince, C., Shaiber, A., Esen, C., Lee, S. T. M., Rappé, M. S., et al. (2018). Nitrogen-fixing populations of Planctomycetes and Proteobacteria are abundant in surface ocean metagenomes. *Nat. Microbiol.* 3, 804–813. doi: 10.1038/s41564-018-0176-9

Dixon, P. (2003). VEGAN, a package of R functions for community ecology. *J. Veg. Sci.* 14, 927–930. doi: 10.1111/j.1654-1103.2003.tb02228.x

Egan, A. J. F., Cleverley, R. M., Peters, K., Lewis, R. J., and Vollmer, W. (2017). Regulation of bacterial cell wall growth. *FEBS J.* 284, 851–867. doi: 10.1111/febs.13959

Eichorst, S. A., and Kuske, C. R. (2012). Identification of cellulose-responsive bacterial and fungal communities in geographically and edaphically different soils by using stable isotope probing. *Appl. Environ. Microbiol.* 78, 2316–2327. doi: 10.1128/AEM.07313-11

Fei, B. (2021). "Economic value and research significance of Moso bamboo," in *The Moso Bamboo Genome*. ed. J. Gao (Cham: Springer), 1–12.

Feng, J., He, K., Zhang, Q., Han, M., and Zhu, B. (2022). Changes in plant inputs alter soil carbon and microbial communities in forest ecosystems. *Glob. Chang. Biol.* 28, 3426–3440. doi: 10.1111/gcb.16107

Fierer, N., Bradford, M. A., and Jackson, R. B. (2007). Toward an ecological classification of soil bacteria. *Ecology* 88, 1354–1364. doi: 10.1890/05-1839

Fu, L., Niu, B., Zhu, Z., Wu, S., and Li, W. (2012). CD-HIT: accelerated for clustering the next-generation sequencing data. *Bioinformatics* 28, 3150–3152. doi: 10.1093/bioinformatics/bts565

Gow, N. A., and Lenardon, M. D. (2022). Architecture of the dynamic fungal cell wall. *Nat. Rev. Microbiol.* 1-12. doi: 10.1038/s41579-022-00796-9

Gu, Z., Gu, L., Eils, R., Schlesner, M., and Brors, B. (2014). Circlize implements and enhances circular visualization in R. *Bioinformatics* 30, 2811–2812. doi: 10.1093/bioinformatics/btu393

Gunina, A., Dippold, M., Glaser, B., and Kuzyakov, Y. (2017). Turnover of microbial groups and cell components in soil: ^{13}C analysis of cellular biomarkers. *Biogeosciences* 14, 271–283. doi: 10.5194/bg-14-271-2017

Huang, H., Zhou, L., Chen, J., and Wei, T. (2020). *ggcor: Extended Tools for Correlation Analysis and Visualization. R package version 0.9.7.*

Hug, L. A., Castelle, C. J., Wrighton, K. C., Thomas, B. C., Sharon, I., Frischkorn, K. R., et al. (2013). Community genomic analyses constrain the distribution of metabolic traits across the Chloroflexi phylum and indicate roles in sediment carbon cycling. *Microbiome* 1:22. doi: 10.1186/2049-2618-1-22

Kielak, A. M., Barreto, C. C., Kowalchuk, G. A., Van Veen, J. A., and Kuramae, E. E. (2016). The ecology of Acidobacteria: moving beyond genes and genomes. *Front. Microbiol.* 7:744. doi: 10.3389/fmicb.2016.00744

Kramer, S., Dibbern, D., Moll, J., Huenninghaus, M., Koller, R., Krueger, D., et al. (2016). Resource partitioning between bacteria, fungi, and Protists in the Detritusphere of an agricultural soil. *Front. Microbiol.* 7:1524. doi: 10.3389/fmicb.2016.01524

Li, Y., and Feng, P. (2019). Bamboo resources in China based on the ninth national forest inventory data. *World Bamboo Ratt.* 17, 45–48. doi: 10.12168/sjzttx.2019.06.010

Li, R., Li, Y., Kristiansen, K., and Wang, J. (2008). SOAP: short oligonucleotide alignment program. *Bioinformatics* 24, 713–714. doi: 10.1093/bioinformatics/btn025

Li, D., Liu, C.-M., Luo, R., Sadakane, K., and Lam, T.-W. (2015). MEGAHIT: an ultra-fast single-node solution for large and complex metagenomics assembly via succinct de Bruijn graph. *Bioinformatics* 31, 1674–1676. doi: 10.1093/bioinformatics/btv033

Li, S., Wang, S., Fan, M., Wu, Y., and Shangguan, Z. (2020). Interactions between biochar and nitrogen impact soil carbon mineralization and the microbial community. *Soil Till. Res.* 196:104437. doi: 10.1016/j.still.2019.104437

Li, Y., Zhang, J., Chang, S. X., Jiang, P., Zhou, G., Fu, S., et al. (2013). Long-term intensive management effects on soil organic carbon pools and chemical composition in Moso bamboo (Phyllostachys pubescens) forests in subtropical China. *For. Ecol. Manag.* 303, 121–130. doi: 10.1016/j.foreco.2013.04.021

Liang, C., Schimel, J. P., and Jastrow, J. D. (2017). The importance of anabolism in microbial control over soil carbon storage. *Nat. Microbiol.* 2:17105. doi: 10.1038/nmicrobiol.2017.105

Liu, Y. R., Delgado-Baquerizo, M., Wang, J. T., Hu, H. W., Yang, Z., and He, J. Z. (2018). New insights into the role of microbial community composition in driving soil respiration rates. *Soil Biol. Biochem.* 118, 35–41. doi: 10.1016/j.soilbio.2017.12.003

Lladó, S., Větrovský, T., and Baldrian, P. (2019). Tracking of the activity of individual bacteria in temperate forest soils shows guild-specific responses to seasonality. *Soil Biol. Biochem.* 135, 275–282. doi: 10.1016/j.soilbio.2019.05.010

Lopes, L. D., Hao, J., and Schachtman, D. P. (2021). Alkaline soil pH affects bulk soil, rhizosphere and root endosphere microbiomes of plants growing in a Sandhills ecosystem. *FEMS Microbiol. Ecol.* 97:fiab 028. doi: 10.1093/femsec/fiab028

López-Mondéjar, R., Brabcová, V., Štursová, M., Davidová, A., Jansa, J., Cajthaml, T., et al. (2018). Decomposer food web in a deciduous forest shows high share of generalist microorganisms and importance of microbial biomass recycling. *ISME J.* 12, 1768–1778. doi: 10.1038/s41396-018-0084-2

López-Mondéjar, R., Tláskal, V., Větrovský, T., Štursová, M., Toscan, R., Da, N., et al. (2020). Metagenomics and stable isotope probing reveal the complementary contribution of fungal and bacterial communities in the recycling of dead biomass in forest soil. *Soil Biol. Biochem.* 148:107875. doi: 10.1016/j.soilbio.2020.107875

López-Mondéjar, R., Zühlke, D., Becher, D., Riedel, K., and Baldrian, P. (2016). Cellulose and hemicellulose decomposition by forest soil bacteria proceeds by the action of structurally variable enzymatic systems. *Sci. Rep.* 6:25279. doi: 10.1038/srep25279

Lu, R. K. (2000). *Analysis Method of Soil Agricultural Chemistry*. Beijing: China Agricultural Science and Technology Press.

Mansora, A. M., Lima, J. S., Anib, F. N., Hashima, H., and Hoa, W. S. (2019). Characteristics of cellulose, hemicellulose and lignin of MD2 pineapple biomass. *Chem. Eng.* 72, 79–84. doi: 10.3303/CET1972014

Mccarthy, A. J. (1987). Lignocellulose-degrading actinomycetes. *FEMS Microbiol. Rev.* 46, 145–163. doi: 10.1111/j.1574-6968.1987.tb02456.x

Noguchi, H., Park, J., and Takagi, T. (2006). MetaGene: prokaryotic gene finding from environmental genome shotgun sequences. *Nucleic Acids Res.* 34, 5623–5630. doi: 10.1093/nar/gkl723

Patoine, G., Eisenhauer, N., Cesarz, S., Phillips, H. R., Xu, X., Zhang, L., et al. (2022). Drivers and trends of global soil microbial carbon over two decades. *Nat. Commun.* 13:4195. doi: 10.1038/s41467-022-31833-z

Penn, C. J., and Camberato, J. J. (2019). A critical review on soil chemical processes that control how soil pH affects phosphorus availability to plants. *Agriculture* 9:120. doi: 10.3390/agriculture9060120

Qi, D., Wieneke, X., Tao, J., Zhou, X., and Desilva, U. (2018). Soil pH is the primary factor correlating with soil microbiome in karst rocky desertification regions in the Wushan County, Chongqing. *China. Front. Microbiol.* 9:1027. doi: 10.3389/fmicb.2018.01027

Ren, Y., Yu, G., Shi, C., Liu, L., Guo, Q., Han, C., et al. (2022). Majorbio cloud: a one-stop, comprehensive bioinformatic platform for multiomics analyses. *iMeta* 1:e12. doi: 10.1002/imt2.12

Ren, C., Zhang, X., Zhang, S., Wang, J., Xu, M., Guo, Y., et al. (2021). Altered microbial CAZyme families indicated dead biomass decomposition following afforestation. *Soil Biol. Biochem.* 160:108362. doi: 10.1016/j.soilbio.2021.108362

Samaddar, S., Chatterjee, P., Truu, J., Anandham, R., Kim, S., and Sa, T. (2019). Long-term phosphorus limitation changes the bacterial community structure and functioning in paddy soils. *Appl. Soil Ecol.* 134, 111–115. doi: 10.1016/j.apsoil.2018.10.016

Sanchez, G., Trinchera, L., and Russolillo, G. (2017). *plspm: tools for partial least squares path modeling (PLS-PM). R package version 0.4.9.*

Silhavy, T. J., Kahne, D., and Walker, S. (2010). The bacterial cell envelope. *Cold Spring Harb. Perspect. Biol.* 2:a000414. doi: 10.1101/cshperspect.a000414

Song, X., Peng, C., Zhou, G., Gu, H., Li, Q., and Zhang, C. (2016). Dynamic allocation and transfer of non-structural carbohydrates, a possible mechanism for

the explosive growth of Moso bamboo (Phyllostachys heterocycla). *Sci. Rep.* 6:25908. doi: 10.1038/srep25908

Wang, Z., Liu, X., Zhou, W., Sinclair, F., Shi, L., Xu, J., et al. (2022). Land use intensification in a dry-hot valley reduced the constraints of water content on soil microbial diversity and multifunctionality but increased CO_2 production. *Sci. Total Environ.* 852:158397. doi: 10.1016/j.scitotenv.2022.158397

Wang, C., Qu, L., Yang, L., Liu, D., Morrissey, E., Miao, R., et al. (2021). Large-scale importance of microbial carbon use efficiency and necromass to soil organic carbon. *Glob. Change Boil.* 27, 2039–2048. doi: 10.1111/gcb.15550

Warren, R. A. J. (1996). Microbial hydrolysis of polysaccharides. *Annu. Rev. Microbiol.* 50, 183–212. doi: 10.1146/annurev.micro.50.1.183

Yang, C., Ni, H., Zhong, Z., Zhang, X., and Bian, F. (2019). Changes in soil carbon pools and components induced by replacing secondary evergreen broadleaf forest with Moso bamboo plantations in subtropical China. *Catena* 180, 309–319. doi: 10.1016/j.catena.2019.02.024

Yarwood, S. A., Myrold, D. D., and Högberg, M. N. (2009). Termination of belowground C allocation by trees alters soil fungal and bacterial communities in a boreal forest. *FEMS Microbiol. Ecol.* 70, 151–162. doi: 10.1111/j.1574-6941.2009.00733.x

Yen, T.-M., and Lee, J.-S. (2011). Comparing aboveground carbon sequestration between moso bamboo (Phyllostachys heterocycla) and China fir (Cunninghamia lanceolata) forests based on the allometric model. *For. Ecol. Manag.* 261, 995–1002. doi: 10.1016/j.foreco.2010.12.015

Zhang, X., Gai, X., Zhong, Z., Bian, F., Yang, C., Li, Y., et al. (2021). Understanding variations in soil properties and microbial communities in bamboo plantation soils along a chromium pollution gradient. *Ecotox. Environ. Safe* 222:112507. doi: 10.1016/j.ecoenv.2021.112507

Zhang, X. P., Li, Q. L., Zhong, Z. K., Huang, Z. Y., Bian, F. Y., Yang, C. B., et al. (2022). Changes in soil organic carbon fractions and fungal communities, subsequent to different management practices in Moso bamboo plantations. *J. Fungi* 8:640. doi: 10.3390/jof8060640

Žifčáková, L., Větrovský, T., Lombard, V., Henrissat, B., Howe, A., and Baldrian, P. (2017). Feed in summer, rest in winter: microbial carbon utilization in forest topsoil. *Microbiome* 5:122. doi: 10.1186/s40168-017-0340-0

frontiers | Frontiers in Microbiology

TYPE Original Research
PUBLISHED 06 January 2023
DOI 10.3389/fmicb.2022.1076610

OPEN ACCESS

EDITED BY
Lidong Shen,
Nanjing University of Information Science and Technology, China

REVIEWED BY
Dong Wang,
Henan University, China
Weidong Kong,
Institute of Tibetan Plateau Research (CAS), China

*CORRESPONDENCE
Ye Deng
✉ yedeng@rcees.ac.cn

†These authors have contributed equally to this work and share first authorship

SPECIALTY SECTION
This article was submitted to Terrestrial Microbiology, a section of the journal Frontiers in Microbiology

RECEIVED 21 October 2022
ACCEPTED 05 December 2022
PUBLISHED 06 January 2023

CITATION
Wang L, Zhao M, Du X, Feng K, Gu S, Zhou Y, Yang X, Zhang Z, Wang Y, Zhang Z, Zhang Q, Xie B, Han G and Deng Y (2023) Fungi and cercozoa regulate methane-associated prokaryotes in wetland methane emissions.
Front. Microbiol. 13:1076610.
doi: 10.3389/fmicb.2022.1076610

Fungi and cercozoa regulate methane-associated prokaryotes in wetland methane emissions

Linlin Wang[1†], Mingliang Zhao[2†], Xiongfeng Du[3,4], Kai Feng[3,4], Songsong Gu[3], Yuqi Zhou[5,6], Xingsheng Yang[3,4], Zhaojing Zhang[1], Yingcheng Wang[7], Zheng Zhang[1], Qi Zhang[1], Baohua Xie[8,9], Guangxuan Han[8,9] and Ye Deng[1,3,4]*

[1]Institute of Marine Science and Technology, Shandong University, Qingdao, China, [2]CAS Key Laboratory of Coastal Environmental Processes and Ecological Remediation, Yantai Institute of Coastal Zone Research, Chinese Academy of Sciences, Yantai, China, [3]CAS Key Laboratory for Environmental Biotechnology, Research Center for Eco-Environmental Sciences, Chinese Academy of Sciences (CAS), Beijing, China, [4]College of Resources and Environment, University of Chinese Academy of Sciences, Beijing, China, [5]Institute of Soil and Water Resources and Environmental Science, College of Environmental and Resource Sciences, Zhejiang University, Hangzhou, China, [6]Zhejiang Provincial Key Laboratory of Agricultural Resources and Environment, Zhejiang University, Hangzhou, China, [7]Collage of Agriculture and Animal Husbandry, Qinghai University, Xining, China, [8]Yellow River Delta Field Observation and Research Station of Coastal Wetland Ecosystem, Chinese Academy of Sciences, Yantai, China, [9]Key Laboratory of Coastal Zone Environmental Processes and Ecological Remediation, Yantai Institute of Coastal Zone Research, Chinese Academy of Sciences, Yantai, China

Wetlands are natural sources of methane (CH_4) emissions, providing the largest contribution to the atmospheric CH_4 pool. Changes in the ecohydrological environment of coastal salt marshes, especially the surface inundation level, cause instability in the CH_4 emission levels of coastal ecosystems. Although soil methane-associated microorganisms play key roles in both CH_4 generation and metabolism, how other microorganisms regulate methane emission and their responses to inundation has not been investigated. Here, we studied the responses of prokaryotic, fungal and cercozoan communities following 5 years of inundation treatments in a wetland experimental site, and molecular ecological networks analysis (MENs) was constructed to characterize the interdomain relationship. The result showed that the degree of inundation significantly altered the CH_4 emissions, and the abundance of the *pmoA* gene for methanotrophs shifted more significantly than the *mcrA* gene for methanogens, and they both showed significant positive correlations to methane flux. Additionally, we found inundation significantly altered the diversity of the prokaryotic and fungal communities, as well as the composition of key species in interactions within prokaryotic, fungal, and cercozoan communities. Mantel tests indicated that the structure of the three communities showed significant correlations to methane emissions ($p<0.05$), suggesting that all three microbial communities directly or indirectly contributed to the methane emissions of this ecosystem. Correspondingly, the interdomain networks among microbial communities revealed that methane-associated prokaryotic and cercozoan OTUs were all keystone taxa. Methane-associated OTUs were more likely to interact in pairs and correlated negatively with the fungal and cercozoan communities. In addition, the modules significantly positively correlated with methane flux were affected

by environmental stress (i.e., pH) and soil nutrients (i.e., total nitrogen, total phosphorus and organic matter), suggesting that these factors tend to positively regulate methane flux by regulating microbial relationships under inundation. Our findings demonstrated that the inundation altered microbial communities in coastal wetlands, and the fungal and cercozoan communities played vital roles in regulating methane emission through microbial interactions with the methane-associated community.

KEYWORDS

wetland, inundation level, CH_4 flux, sediment microbiota, interdomain network

1. Introduction

Methane (CH_4) has accounted for roughly 30% of global warming since pre-industrial times (Saunois et al., 2016) and, as such, it is generally considered a nonnegligible factor in climate change discussions (Ocko et al., 2021). Wetlands are the largest natural source of CH_4 emissions, contributing 150–225 Tg CH_4 per year, and accounting for one-third of total global CH_4 emissions (Bridgham et al., 2013; Kirschke et al., 2013; Saunois et al., 2016; Dean et al., 2018). In wetlands, water table level controls biogeochemical cycles and has a profound impact on wetland functions (Paschalis et al., 2017). A higher water level can provide a direct barrier to the release of gases from soil or the water column, most likely *via* oxidation as gasses passes through the latter (Peacock et al., 2017), or the inundation level provides an anaerobic environment to inhibit methane aerobic oxidation in the root zone (Li et al., 2018). The process of CH_4 emission into the atmosphere is ultimately a coordination between CH_4 production, transportation, and oxidation through the soil-water-plant continuum. Initially, the remains of plant detritus from sedimentary organic matter, a part of this organic matter is released into the atmosphere in the form of CO_2 again after decomposition by microorganisms, while another part of the organic matter, and inorganic carbon, accumulates in the wetland (Friborg et al., 2003; Fiore-Donno et al., 2020), however, due to the anaerobic environment of wetland water and a large number of microorganisms, fixed carbon in wetland environments will be released into the atmosphere again through respiration or microbial decomposition, mainly as CO_2 and CH_4. Hence, CH_4 fluxes from soils are biologically mediated processes (Shiau et al., 2018). Consequently, focusing on the microbial mechanism behind methane emission under inundation conditions is of great importance.

Microorganisms are linked by strong ecological interactions, and shifts in those interactions could greatly affect ecosystem functioning (de Vries et al., 2013). Previous studies indicated that altering hydrological fluctuation also can reshape soil microbial composition and diversity (Ye et al., 2013; Garssen et al., 2015). Different microbial taxa have displayed divergent responses to inundation across different types of soils or sediments. For example, the structure of the bacterial communities is driven by the hydric dynamics of the infiltration basin, but no such trend was found for fungal communities (Badin et al., 2011). The relative abundance and diversity of methanogenic taxa were much greater in frequently flooded soil than in soil by other means of flooding in the Amazonian floodplain (Hernandez et al., 2019). Unger et al. (2009) found that increased flooding reduced the soil bacteria-fungi ratio by up to 10% in the wetland. Inundation also increased the complexity of prokaryotic communities (Gao et al., 2021), with higher moisture leading to decreased complexity of methanotrophic communities in the Qinghai-Tibetan Plateau (Zhang et al., 2019). Together these studies revealed the diversity and interactions within each soil microbial kingdom responding to water flooding, but far less attention has been paid to interactions among the prokaryotic, fungal, and protist communities under inundation conditions. Therefore, understanding the microbial interactions among different groups or trophic levels along a continuous gradient of inundation is important to assess the functions within coastal wetlands.

Methane flux results from complex interactions between microbes and the environment (le Mer and Roger, 2001). Generally, as the executors for methanogenesis, methanogens can drive the final step of decomposition of anaerobic fermentation end products (i.e., H_2/CO_2 and acetate; Bridgham et al., 2013). At present, the extensively studied methanogens belong to the Euryarchaeota, including Methanopyrales, Methanococcales, Methanobacteriales, Methanomicrobiales, Methanosarcinales (Sakai et al., 2011), and Methanocellales (Borrel et al., 2013)/ Methanomassiliicoccales (Borrel et al., 2014). The key enzyme of methanogenesis is Methyl Coenzyme M Reductase (MCR), and its encoding gene, *mcrA*, is widely used as a functional gene marker to identify methanogens (Kim et al., 2008). On the other side, aerobic methanotrophs are the most important natural absorbers of CH_4 emissions from the ecosystem, and the *pmoA* gene encoding the β subunit of the pMMO enzyme is widely used to detect aerobiotic methanotrophs (Freitag et al., 2010; Liebner et al., 2012). Fungi are also vital to many ecosystem processes such as nutrient cycling and decomposition, and they can form direct connections to primary producers (Oliver and Schilling, 2018), while protists can act as a dynamic bond among sediment microorganisms (Xiong et al., 2018), especially with top-down effects on bacterial communities (Zhou et al., 2021). Hence, microbial communities, including prokaryotes, fungi and protists might interact with methane-associated communities to execute

disproportionate characteristics in CH_4 emission processes. Exploration of these interactions may improve our estimates of CH_4 budgets, resolve CH_4 dynamics in these environments and improve the predictions of their responses to climate change.

The Yellow River Delta is one of the most active regions of land-ocean interaction in the world (Zhao et al., 2013). As a blue carbon reservoir, it harbors great value in supporting wildlife and is important for climate regulation (Osland et al., 2018). We collected samples from a five-year inundation site experiment in a typical nontidal coastal soil from the Yellow River Delta (Dongying, Shandong, China), which is known for its vital significance in carbon sequestration and climate change (Osland et al., 2016; Feher et al., 2017). Integration of high-throughput DNA sequencing together with multivariate statistical methods can help us understand the divergence among microbial communities in their response to inundation. Three hypotheses were proposed in this study: (i) inundation would tend to alter microbial community compositions and reshape within group microbial interaction networks in this long-term inundation ecosystem; (ii) the changes of fungal and protist communities by inundation, as well as prokaryotes, would lead to the changes of methane emissions; and (iii) changes in sediment properties caused by inundation may contribute to the interactions among these three microbial kingdoms that positively regulate methane emissions.

2. Materials and methods

2.1. Study site

The study site was located at the Yellow River Delta Ecological Station of Coastal Wetlands (37°45′50″ N, 118°59′24″ E), Chinese Academy of Sciences, Dongying City, in the northeast of Shandong, China. The elevation of the study site was 2.5 m above sea level. The mean annual temperature (MAT) was about 12.9°C and the mean annual precipitation (MAP) was 550–640 mm. The highest percentage of precipitation occurs from June to September. The soil texture is mainly a sandy clay loam with 6.54 g kg^{-1} soil organic matter content at 0–20 cm depth (Zhao M. et al., 2020). At the sampling site, inundation treatment was applied from April to October of each year beginning in 2017. The study area was dominated by common reeds (*Phragmites australis*; Yang et al., 2017). Specifically, the whole surface inundation control test platform included seven inundation level treatments, such as control (no treatment, only natural precipitation), 0 (inundation to soil saturation), 5, 10, 20, 30, and 40 cm (specified surface inundation treatment continued based on soil water saturation) inundation height, respectively. Each treatment had 4 replicate plots, except for the 0 cm inundation treatment which had 3 replicate samples, because one of the samples was missing. Every replicate plot (2 m length × 2 m width × 0.5 m height) was separated by cement barriers at a 40 cm spacing. The height of the cement barriers is 50 cm above and 20 cm underground. The filtered water for each plot was obtained from a nearby lake (originally from the Yellow River which runs into the Bohai Sea). The inundation level was controlled by a tube connected to an opaque plastic water tank located 1.5 meters above the ground surface. When the surface inundation water level falls, water would flow from the tank into the plot until the inundation level reached the original specified level.

2.2. Sediment sampling and sediment properties measurement

Sediment cores were collected from each plot from 0 to 20 cm depths on 20th September 2019. After the removal of roots, the roots-removed sediment was gently mixed for homogenization, and then stored at −80°C. Sediment samples were dried using a vacuum freeze-drying machine (18 N; SCIENTZ) for 48 h to prepare for the subsequent experiments. The physical and chemical properties of the sediment were assessed. Sediment pH was measured by mixing dry sediment and distilled water in a 1:2.5 (w/v) ratio. The remaining sediment properties such as organic matter (potassium dichromate oxidation iron salt titration method), total nitrogen (alkaline potassium persulfate oxidation-UV spectrophotometric method), total phosphorus (ammonium molybdate spectrophotometric method), ammonia nitrogen (Nessler's Reagent Colorimetric Method) and nitrate nitrogen (spectrophotometric method) were all measured at the Institute of Soil Science, Chinese Academy of Sciences (Nanjing, China). CH_4 flux was measured in a static cylindrical transparent chamber connected to LGR Ultraportable Greenhouse Gas Analyzer (UGGA, Los Gatos Research, Inc., San Jose, USA; Wei et al., 2020). Transparent acrylic plastic base frames (30 cm in diameter, 10, 10, 15, 20, 30, 40 and 50 cm in height) for the seven treatments were installed into the sediment to a 5 cm depth, with 5 cm of the frame emerging above the water surface, a removable middlebox (30 cm in diameter, 100 cm in height) and a removable top box (30 cm in diameter, 100 cm in height) was hermetically placed on the top of the base frame. Two battery-driven fans (8 cm in diameter, 12v) were installed inside the top of each chamber to mix the air in the chamber during sampling. The gas flux was measured from 8 a.m. to 11a.m once a day. For each measurement, chambers were sealed for 3 min.

2.3. Sediment DNA extraction amplifications and high-throughput sequencing

After sediment was freeze-dried for at least 48 h (18 N; SCIENTZ), DNA was extracted from 0.5 g of the freeze-dried sediment to extract using the Qiagen DNeasy Power Soil kit. The extracted DNA concentration and quality were assessed with a NanoDrop One Spectrophotometer (Thermo Scientific), then all DNA was stored at −80°C. The primer sets 515F (5′-GTGCC AGCMGCCGCGGTAA-3′) and 806R (5′-GGACTACHVGGG TWTCTAAT-3′) with unique barcodes for each sample were used

for amplification of the V4 region of the prokaryotic 16S rRNA gene (Caporaso et al., 2011). The polymerase chain reaction (PCR) amplifications were carried out in a 50 μl of reaction volume, containing 1 μl Phanta Max Super-Fidelity DNA Polymerase (Vazyme, China), 25 μl 2 × Phanta Max Buffer, 1 μl dNTP Mix (10 μM each), 2 μl forward primer, 2 μl reverse primer, 1 μl template DNA (20–30 ng/μL) and 18 μl ddH_2O. The PCR reaction conditions were as follows: 95°C for 3 min, 30 cycles of 95°C for 10 s, 60°C for 10 s, 72°C for 45 s, and a final extension at 72°C for 5 min. The fungal ITS2 region was amplified using primer sets 5.8S-Fun (5′AACTTTYRRCAAYGGATCWCT-3′) and ITS4-Fun (5′-AGCCTCCGCTTATTGATATGCTTAART-3′; Taylor et al., 2016). The PCRs reactions were carried out in a 50 μl of reaction volumes with 1 μl Phanta Max Super-Fidelity DNA Polymerase (Vazyme, China), 25 μl 2 × Phanta Max Buffer, 1 μl dNTP Mix (10 μM each), 2 μl forward primer, 2 μl reverse primer, 1 μl template DNA (20–30 ng/μl) and ddH_2O. The reaction conditions were as follows: 95°C for 3 min, 35 cycles of 95°C for 10 s, 52°C for 10 s, 72°C for 45 s, and a final extension at 72°C for 5 min. The V4 hypervariable region of 18S rRNA gene was amplified using a two-step PCR (Fiore-Donno et al., 2018), in the first reaction, the forward primer was a 1:1 mixture of C_615F_Cerco (5′-GTTAAAAAGCTCGTAGTTG-3′) and C_615F_Phyt (5′-GTTAAAARGCTCGTAGTCG-3′), while the reverse primer was C_S963R_Phyt_1st (5′-CAACTTTCGTTCTTGATYAAA-3′), the PCR amplification was carried out in a 10 μl reaction volume containing 0.2 μl Phanta Max Super-Fidelity DNA Polymerase, 5 μl 2 × Phanta Max Buffer, 0.2 μl dNTP Mix (10 μM each), 0.6 μl forward primer, 0.6 μl reverse primer, 1 μl template DNA (20–30 ng/μL) and ddH_2O (fill the system to 10 μl). The reaction conditions were as follows: 95°C for 3 min, 24 cycles of 95°C for 15 s, 55°C for 15 s, 72°C for 40 s, and a final extension at 72°C for 5 min. The product of the first reaction served as the template of the second reaction after 100-times dilution, the primer set of the second amplification step was C_615F_Cerco_2nd (5'-GTTAAAARGCTCGTAGTYG-3′) and C_S947R_Phyt_2nd (5'-AAGARGAYATCCTTGGTG-3′) with unique barcode sequences, the PCR amplification was carried out in a 50 μl reaction volume containing 1 μl Phanta Max Super-Fidelity DNA Polymerase, 25 μl 2 × Phanta Max Buffer, 1 μl dNTP Mix (10 μM each), 3 μl forward primer, 3 μl reverse primer, 2 μl template DNA (10–20 ng/μL) and ddH_2O (fill the system to 50 μl). The reaction conditions were as follows: 95°C for 3 min, 10 cycles of 95°C for 15 s, 60 to 50°C for 15 s (decrease 1°C in each cycle), 72°C for 40 s, 25 cycles of 95°C for 15 s, 50°C for 15 s, 72°C for 40 s and a final extension at 72°C for 5 min. All PCR products were purified by gel electrophoresis, and their concentration and quality were measured by NanoDrop spectrophotometer (D2500-02, OMEGA BioTek). Then equal molar amounts of DNA were pooled for library construction and quantified with a Qubit fluorimeter (Invitrogen, Carlsbad, CA). The NovaSeq 6000 platform (Illumina), located at Guangdong Magigene Biotechnology Co. Ltd. (Guangzhou, China), was used to sequence each amplification library. The Illumina sequence reads were deposited in China National Genomics Data Center (CNCB) with accession numbers (PRJCA013006).

2.4. Quantification of *mcrA* gene and *pmoA* gene for prokaryotes

To assess the gene copy abundances of *mcrA* and *pmoA* present at different surface inundation levels, real-time quantitative PCR detecting system (qPCR) experiments were performed. The primer sets mlas (GGTGGTGTMGGDTT CACMCARTA) and mcrA-rev1 (CGTTCATBGCRTAGTT NGGRTAGT; Steinberg and Regan, 2008) were used to amplify a fragment of *mcrA* gene and about 469 bps in length. The primers set A189F (GGNGACTGGGACTTCTGG) and mb661r (CCGGMGCAACGTCYTTACC; Knief, 2015) were used to amplify an approximately 470 bps fragment of the *pmoA* gene. Both qPCR experiments were conducted in 20 μl volumes containing 10 μl MonAmp™ SYBR Green qPCR Mix, 0.4 μl forward and reverse primers (10 μM each), 2 μl DNA (5–30 ng), and 7.2 μl ddH_2O. Three replicates were performed for each sample. The two genes' cycling conditions were set as follows: 95°C for 30 s, 40 cycles of 95°C for 10 s, 56°C for 10 s and 72°C for 30 s. All reactions were performed in triplicate on a CFX96 Touch Real-Time PCR Detection System (BioRad, California, USA).

2.5. Bioinformatics processing and statistical analysis

The raw sequences were processed *via* a public pipeline[1] (Feng et al., 2017; Zhang et al., 2017). The raw sequence data were sorted after barcode identification, allowing a maximum of one mismatch, and the primers at the ends of sequences were removed. Then pair-end fragments were combined by FLASH (Magoč and Salzberg, 2011). The Btrim program was used to filter out unqualified sequences with a threshold Quality Score > 20 (Kong, 2011). Operational taxonomic units (OTUs) were estimated with a 97% similarity cut-off using UPARSE after chimera filtering and OTU clustering (Edgar, 2013). Taxonomic annotation was conducted using the RDP training set NO.18 (prokaryotes; Wang et al., 2007), UNITE 8.2 (fungi; Nilsson et al., 2019), and PR2 4.14.0 (cercozoa; Guillou et al., 2013; del Campo et al., 2018) databases, respectively. To account for the effects of uneven sequencing depth among samples. we resampled reads in the OTU tables to 50,000, 51,591 and 33,548 sequences for prokaryotes, fungi, and cercozoa, respectively. As the rarefaction curves indicated that the sequencing depth was sufficient, they were then used for the following biodiversity analyses.

We combined control and 0 cm as the low inundation (IL) group, 5, 10, and 20 cm as the moderate inundation (IM) group, while the high inundation (IH) group contained 30, 40 cm, respectively. SPSS Statistics 23.0 (IBM Corporation, Armonk, NY, USA) was used to perform one-way ANOVA analysis to evaluate differences in sediment physiochemical properties, gene copies,

1 http://mem.rcees.ac.cn:8080

and α diversities among different inundation states. In this study, the Shannon index, Pielou evenness, Chao1 and Richness, of prokaryotic, fungal, and cercozoan communities were calculated. Then, for the prokaryotic community, the OTUs belonging to the methanogenic and methanotrophic communities were identified and annotated using the Functional Annotation of the Prokaryotic Taxa (FAPROTAX) database (Louca et al., 2016), and these OTUs were used together in several following analyses. The divergence of community structure was shown using Principal component analysis (PCA) plots. Based on relative abundance, the dominant species of prokaryotic, fungal, and cercozoan communities, methanogenic and methanotrophic OTUs were calculated at the phylum, class, class, order, and order level, respectively. Mantel tests were used to estimate the effect of environmental factors on community structure. Spearman correlation analysis was executed between sediment properties and gene copies while linear regression was performed for the relationships between CH_4 flux and gene copies. Figures were drawn in R (version 4.0.1) using the ggplot2 package (Murrell, 2009; Wickham, 2011).

2.6. Construction of molecular ecological networks under different inundation levels

To investigate the molecular interaction of three microbial communities under different inundation levels, molecular ecological networks (MENs) were constructed. To ensure the reliability of network comparison, according to the PCA analysis results of prokaryotes, we removed the 4 samples that display a large divergence from the other 8 samples in the IM group for the prokaryotic community. Therefore, the sample numbers of the three groups are 7 (IL), 8 (IM), and 8 (IH), respectively. OTUs that were shared by more than 80% of samples were retained to construct the MENs using Spearman's correlation for prokaryotes, fungi and cercozoa, respectively. For a fair comparison, the correlation thresholds for each group species were kept consistent (prokaryotes = 0.960, fungi = 0.840, cercozoa = 0.890). Finally, the networks were visualized in Cytoscape 3.8.0 and the R package igraph. Then the network topology and global network properties were explored (Deng et al., 2012). Network vulnerability was calculated by the R code provided by Yuan et al. (2021). Robustness calculated the proportion of species remaining in the network after removing random or target nodes (Deng et al., 2012; Montesinos-Navarro et al., 2017).

We further analyzed the networks containing all three microbial communities and methane-associated OTUs to identify their potential functions related to methane emissions. Firstly, we eliminate methanotrophic and methanogenic OTUs from the prokaryotic OTUs. Then the majority of prokaryotes (25), fungi (9), methanotrophs (3), methanogens (3), and cercozoa (9) was performed, and used to calculate the appropriate threshold (0.85) based on the RMT method. In each network, the roles of individual nodes were estimated by two topological parameters: the within-module connectivity *Zi*, which quantified to what extent a node connected to other nodes in its own module, another is the among module connectivity *Pi*, which quantified how well the node connected to different modules. The nodes with either a high value of *Zi* or *Pi* were defined as keystone taxa, including module hubs ($Zi > 0.25$, $Pi \geq 0.62$; critical to its own module coherence), connector hubs ($Zi < 0.25$, $Pi > 0.62$; connect modules together and important to network coherence), network hubs ($Zi > 0.25$, $Pi > 0.62$; vital to both network and its own module coherence), all other nodes are peripherals nodes (le Mer and Roger, 2001). The network modules detection was performed using fast greedy modularity optimization (Deng et al., 2012). For network modules, the module eigengene could summarize the closely connected members within a module (de Menezes et al., 2015). The singular value decomposition of the module expression matrix was used to represent the module eigengene networks (Alter et al., 2000). The module eigengene of the module was defined as the first principal component of the standardized module expression data (Langfelder and Horvath, 2007). In addition, the correlations between module-based eigenvalues and sediment properties were calculated based on Pearson algorithm (Deng et al., 2012; Feng et al., 2019). Both networks and modules were visualized in Cytoscape 3.8.0. All of the above methods and statistical tools for the networks were executed on the Inter-Domain Ecological Network Analysis Pipeline (iNAP)[2] (Feng et al., 2022).

3. Result

3.1. Physicochemical properties and CH_4 flux shifted under different levels of inundation

Sediment CH_4 flux and physicochemical properties were altered by long-term inundation. As the inundation level rose, CH_4 flux also gradually rose initially, reaching a maximum at 10 cm inundation, but then decreased as the inundation level continued to rise (Figure 1). On average, the values of CH_4 flux increased by 188 and 195% under the moderate inundation (IM) and the high inundation (IH) groups, respectively, than in the low inundation group (IL; $p < 0.05$; Supplementary Table S1). Among the physicochemical properties, dissolved oxygen and sediment pH were significantly lower in IM than in IL ($p < 0.05$). In addition, total sediment phosphate was 33% higher in IH than in IL ($p < 0.05$). Nitrate nitrogen decreased with inundation levels ($p < 0.05$). However, there were no detectable variations for total nitrate, ammonia nitrogen, organic matter, or salinity among the different inundation groups (Supplementary Table S1). These results suggested that inundation significantly altered the CH_4 flux and several physicochemical properties.

2 http://mem.rcees.ac.cn:8081

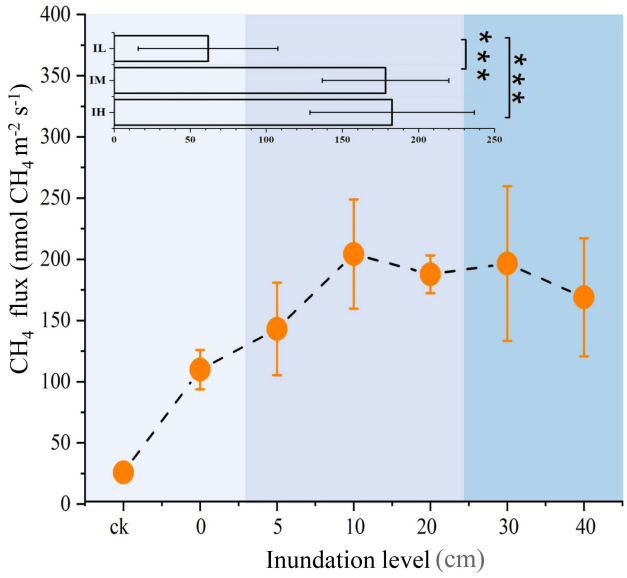

FIGURE 1
Variations in CH_4 fluxes at different inundation depths (means ± SE, n=27). In insets, inundation depths in soil were subjected to three treatments: Soils were exposed to low inundation (IL, n=7), moderate inundation (IM, n=12) and high inundation (IH, n=8). One-way analysis of variance (ANOVA) of three groups was performed. For all panels, the extent of blue backgrounds indicates the three groups. ***p<0.001.

3.2. Inundation changed the abundance of *mcrA* and *pmoA* genes in soil

Functional genes of the two methane-associated cycles, i.e., *pmoA* and *mcrA* showed distinct tendencies with inundation levels (Figure 2). *pmoA* gene copies increased slightly, peaking at the inundation level of 20 cm, subsequently decreasing sharply ($5.3 \pm 0.9 \times 10^7$ g^{-1} to $1.3 \pm 0.9 \times 10^7$ g^{-1}), showing a significant difference under 30 cm and 40 cm inundations ($p < 0.01$) compared to 20 cm inundation (Figure 2A). However, the *mcrA* gene copies displayed no distinct trend under different inundation levels (Figure 2C). A significant linear relationship was found between CH_4 flux and *pmoA* gene copies ($R^2 = 0.136$, $p = 0.032$; Figure 2B) and *mcrA* gene copies ($R^2 = 0.172$, $p = 0.018$; Figure 2D). Additionally, the *pmoA* gene quantity in soil was significantly positively correlated with oxygen content (Supplementary Table S2). The above results indicated that the inundation level could change the abundance of *pmoA* genes more significantly than *mcrA* genes, and the greater inundation levels may accelerate methane utilization rather than methane generation.

3.3. Inundation shifted the composition and structure of soil microbial communities

To estimate the α diversity of microbial communities under different levels of inundation, several indexes were calculated, including the Shannon index, Pielou evenness, Chao1 and Richness index. In the prokaryotic community, the Shannon ($p = 0.046$) and Pielou evenness ($p = 0.044$) indices significantly decreased in the IM group compared with the IL, while the shift of these two indices between the IL and IH groups was not significant (Supplementary Figures S1a–d), no significant variation among these indices was found in the fungal community (Supplementary Figures S1b–h). In the cercozoan community, Chao 1 increased in the IH group compared with IM group (Supplementary Figures S1i–l). Next, using FARPROTAX, 67 methanogenic OTUs and 23 methanotrophic OTUs were identified from the prokaryotic community. Accordingly, we also performed α diversity analysis on these OTUs. Chao 1 and observed richness were significantly increased in the methanotrophic group from IL to IM, and Chao 1 was significantly decreased from IM to IH (Supplementary Figures S1m–p), however, α diversity indices of methanogens did not show any significant difference among the three inundation groups (Supplementary Figures S1q–t).

The β diversity of prokaryotes and fungi was remarkably divergent among the three groups based on the multiple dissimilarity tests, but for the cercozoan community, there was only a significant difference between the IL and IH groups. In the methanogenic community, there was a significant difference between the IL and IM groups, while no significant differences were observed in the methanotrophic community (Supplementary Table S3). Moreover, PCA analysis of the microbial communities showed a distinct separation between the IL and IH groups, while the IM community was only partially separated from the others (Supplementary Figures S2a–e). The composition of microbial communities also shifted under inundation (Supplementary Figures S2f–j). Additionally, to discern the associations between soil variables and the structure

of all microbial communities. Mantel tests based on Jaccard distance were performed. The results indicated that the CH_4 flux was significantly correlated with the prokaryotic ($p = 0.002$), fungal ($p = 0.001$), and cercozoan ($p = 0.001$) communities (Table 1).

The functional divergence observed in the prokaryotic community, especially, the abundances of methanogenic and methanotrophic microorganisms, increased with inundation depth (Supplementary Figure S3a). Among methanogens, the

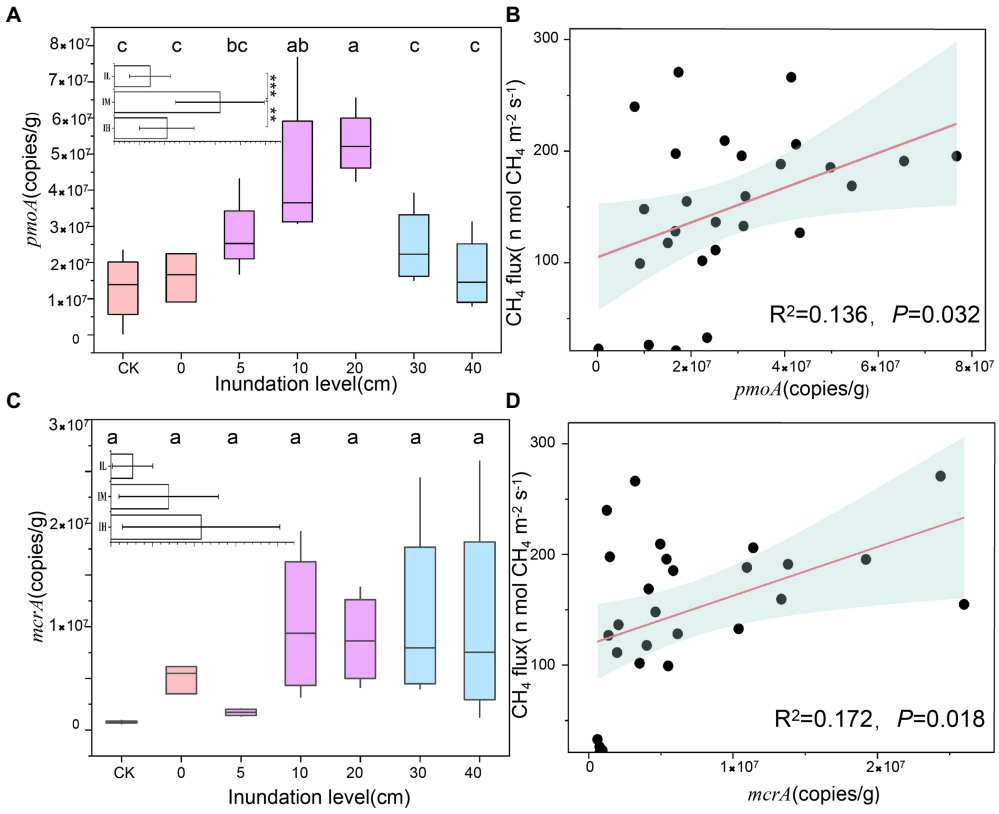

FIGURE 2
Variations in gene copies at different inundation depth and its relationship with CH_4. **(A)** Variations in *pmoA* gene copies at different inundation depths (means ± SE, n=27). In insets, inundation levels in soil were subjected to the three treatments: Soils were exposed to low inundation (IL), moderate inundation (IM) and high inundation (IH), IL (n=7), IM (n=12), IH (n=8), one-way analysis of variance (ANOVA) of the three groups was performed. **(B)** Relationships between *pmoA* gene copies and CH_4, The pink lines are fitted regressions, and the light blue-shaded areas around the regression lines are 95% confidence. **(C)** Variations in *mcrA* gene copies at different inundation levels (means ± SE, n=27). **(D)** Relationships between *mcrA* gene copies and CH_4 flux. Values with superscript letters a, b, c and are significantly different across columns (p<0.05).

TABLE 1 Mantel tests for the correlation between environmental variables and community structure in prokaryotic, fungal, cercozoan communities based on Jaccard distance.

		TN (mg/kg)	TP (mg/kg)	Ammonium (mg/kg)	Nitrate (mg/kg)	DOM (%)	pH	Salinity (ppt)	Oxygen (vol%)	CH_4 flux (n mol CH_4 m^{-2} s^{-1})
Prokaryotes	*r*	−0.1704	−0.1295	0.004	0.0535	0.057	0.0811	0.0085	0.2299	0.5425
	p	0.963	0.874	0.444	0.285	0.255	0.187	0.431	**0.006**	**0.001**
Fungi	*r*	−0.0942	−0.1401	0.101	0.1992	0.0999	0.0933	0.0317	0.1414	0.3909
	p	0.81	0.908	0.056	**0.013**	0.114	0.129	0.335	**0.025**	**0.001**
Cercozoa	*r*	−0.0935	−0.0451	0.0333	0.0423	−0.0205	0.0705	0.0646	0.2218	0.4418
	p	0.771	0.648	0.286	0.338	0.604	0.222	0.22	**0.003**	**0.001**

Significantly ($p < 0.05$) related environment variables are shown in bold.

hydrogenotrophic methanogenesis pathway dominated, especially the hydrogenotrophic pathway *via* the CO_2-reducing pathways, while relative abundances of the acetoclastic and methylotrophic methanogenesis pathways were lower (Supplementary Figure S3b). These results suggested that inundation played an important role in shaping the microbial communities, and that there were significantly positive correlations between microbial communities and methane flux.

3.4. The shift of co-occurrence networks under different levels of inundation

Co-occurrence networks for each microbial group (prokaryotic, fungal and cercozoan communities) were explored to characterize the shift of potential interactions along the inundation gradient (Supplementary Figure S4), and their global topological properties were measured (Supplementary Table S4). For the prokaryotic community, the number of nodes decreased in IM and then increased sharply in IH, with similar patterns observed for the fungal and cercozoan communities. The number of edges within the networks showed a similar trend as the nodes. Network complexity decreased according to changes in average path distance (GD) and clustering coefficient (avgCC). The vulnerability of prokaryotes and cercozoa decreased at first before increasing with the increase of inundation levels, while the vulnerability of the fungal community increased initially and then decreased with the increase of inundation levels (Supplementary Table S4). The keystone taxa including modules hubs ($Zi > 0.25$, $Pi \leq 0.62$), and connectors ($Zi \leq 0.25$, $Pi > 0.62$) were identified (Supplementary Figure S4). For prokaryotic networks, the module hubs changed from Planctomycetes and Proteobacteria to Actinobacteria, Acidobacteria, Planctomycetes, Chloroflexi and Proteobacteria, while the connector hubs shifted from many different taxa to Rhodothermaeota, Actinobacteria, Acidobacteria, and Chloroflexi. Initially, there were no module hubs in the fungal networks, and then taxa such as Sordariomycetes, Pezizomycetes, Dothideomycetes became module hubs, and Saccharomycetes and Sordariomycetes became the connectors. For cercozoan networks, only the connectors shifted from Endomyxa to Filosa-Sarcomonadea and Endomyxa-Phytomyxea (Supplementary Figure S4). Therefore, these results indicated that the vulnerability of the microbiome changed in different ways, and the keystone species in co-occurrence networks for prokaryotic, fungal and cercozoan communities shifted with increasing inundation levels.

3.5. Intra-kingdom ecological association networks under inundation

Due to all prokaryotic, fungal and cercozoan communities being significantly correlated with methane flux (Table 1), we constructed an intra-kingdom ecological network to discern the potential contributions of fungi and cercozoa to methane-associated cycles. The integrated network contained 478 nodes, including 100 cercozoa, 269 prokaryotes, 84 fungi, 11 methanotrophs, and 14 methanogens (Figure 3A). Interestingly, methanogenic and methanotrophic taxa displayed negative relationships to fungal and cercozoan OTUs, but no connections with other prokaryotic taxa. Numerous positive relationships were observed among the prokaryotic taxa not involved in methanogens or methanotrophs (Figure 3A). More nodes were connected to methanogenic taxa (Figure 3B) than to methanotrophic taxa (Figure 3C). Only seven module hubs were identified as keystone nodes in this network, i.e., two nodes from prokaryotic taxa (Proteobacteria), three from methanogenic taxa (two nodes annotated Methanomassiliicoccales, one node annotated Methanomicrobiales), one from methanotrophic taxa (Methylococcales), one from cercozoan taxa, which was annotated Unclassified at class level. In methanogenic taxa, two of the three module hubs annotated Methanomassiliicoccales were closely related to the methanotrophic taxa and cercozoan taxa, while the taxa closely related toward the Methanomicrobiales were methanotrophic taxa and fungal taxa (Figures 3A,B). For methanotrophic taxa, the module hub Methylococcales was connected intimately with methanogenic taxa and cercozoan taxa (Figures 3A,C).

In addition to the discovery of key nodes in the network, the specific clustering modules were examined to find significant module-trait related to CH_4 flux. Modules I-III showed significant negative correlations with CH_4 flux, whereas Modules IV, V, VIII, and X showed an inconsistent trend (Figure 4A; Supplementary Table S5), among these modules, modules I, III and IV only contain prokaryotic OTUs (Supplementary Table S5). Four subnetworks, consisting of modules II, V, VIII, and X, respectively, were further extracted due to the presence of module hubs. The modules negatively correlated with methane were all composed of prokaryotic OTUs (Supplementary Table S5). Of these modules, module II had a module hub annotated as Proteobacteria (Methyloceanibacter at the order level) that had many positive correlations (Figure 4B). In modules that were positively correlated with methane fluxes, there were 4 module hubs in module V (Figure 4C), two from methanogenic taxa (Methanomassiliicoccales), one from methanotrophic taxa (Methylococcales), and one from cercozoan taxa. Methanomassiliicoccales possessed more connections with methanotrophic taxa (mainly annotated as Methylococcales) and cercozoan taxa (mainly annotated Filosa-Sarcomonadea; Supplementary Figures S5b,c). The Methylococcales module hub was related more to cercozoan taxa (Fliso-Sarcomonade; Supplementary Figure S5a). The cercozoan module hub was not connected to any methanogenic taxa, but it is noteworthy that it was significantly related to the module hubs annotated Methylococcales (Supplementary Figure S5d). Module VIII had one module hub, Methanomicrobiales, which was from the methanogens, and it was more tightly bound to fungi than cercozoa

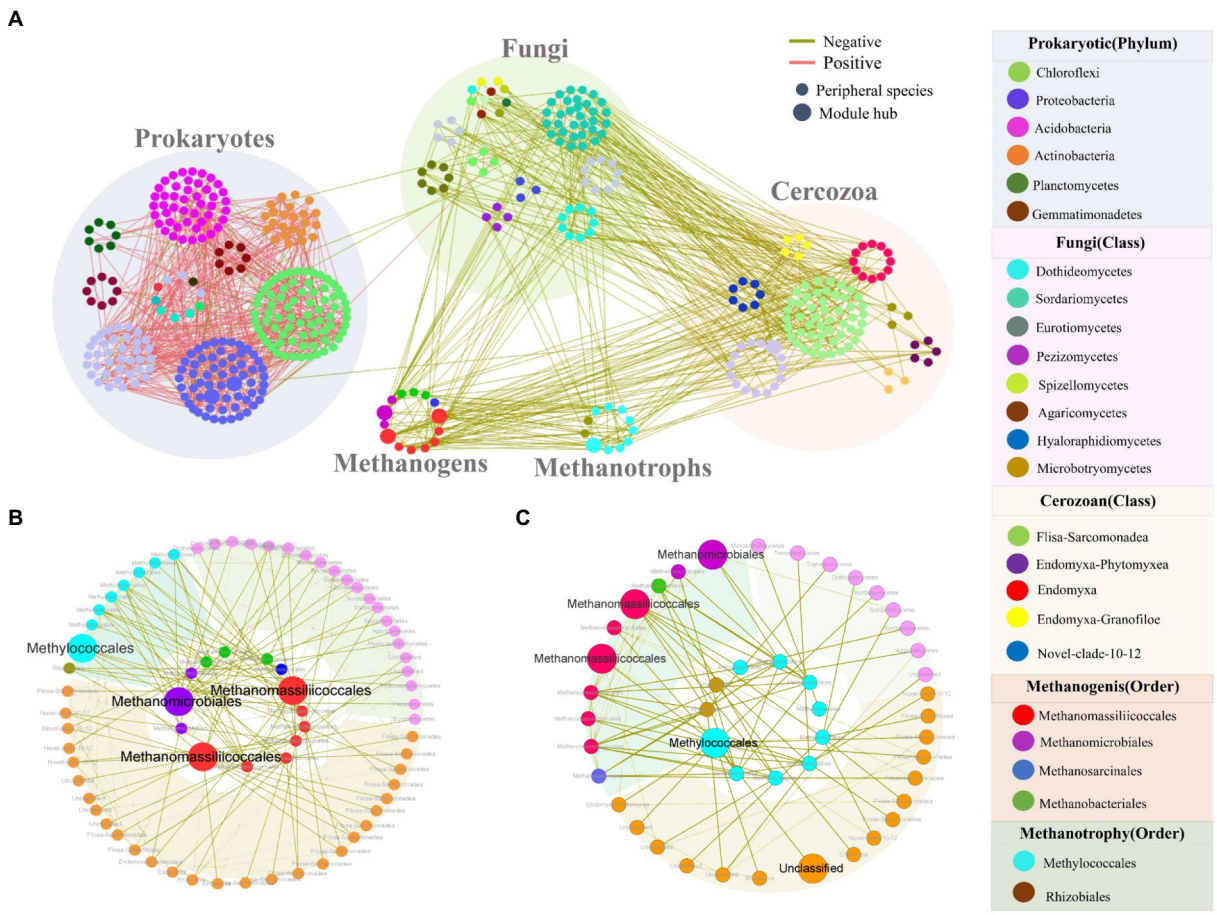

FIGURE 3
Intertrophic networks among five communities and two subnetworks relative to methanotrophic OTUs and methanogenic OTUs. **(A)** Intertrophic networks of prokaryotic, fungal, cercozoan communities, methanotrophic OTUs and methanogenic OTUs under inundation. Node color indicates different taxonomic. Node size is proportional to network role, with larger nodes being module hubs. Red and green links represent positive and negative interactions, respectively. **(B)** Subnetworks showing the OTUs related to methanogenic OTUs, inner circle are methanogenic OTUs while outer circles are their connected OTUs. **(C)** Subnetworks showing the OTUs relative to methanotrophic OTUs, inner circle are methanotrophic OTUs while outer circles are the connected OTUs. The background colors represent different communities: fungi (purple), cercozoa (pink), methanotrophic OTUs and methanogenic OTUs (green).

(Figure 4D). In module X, the module hub belonged to the Proteobacteria, and the module contained positive relationships (Figure 4E). These results suggested that cercozoa and fungi had close associations with methane-associated prokaryotes.

4. Discussion

Atmospheric methane is an important topic in climate change discussions, and its most significant source is all kinds of wetland ecosystems (Saunois et al., 2016). Microorganisms act as both the generators (methanogens) and consumers (methanotrophs) of methane, and thus they make a significant contribution to climate change. Some non-methanogenic/methanotrophic microorganisms may play important roles in the process of methane emission. For example, several unicellular protists participate in the flow of carbon mediated by food chains and microbial loops as consumers (Adl et al., 2019). Based on the respiration of their massive amounts of hyphal material, several fungi are a driving force in the biological component of the terrestrial carbon cycle (Barron, 2003). However, fungi and protists associated with methane emissions have previously only been studied in rumen studies of cattle (Lopez-Garcia et al., 2022), and less attention has been paid to their role in natural ecosystems. In a natural ecosystem, microorganisms associate with each other through complex interactions (Zhang et al., 2018; Zhao Y. et al., 2020; Qian et al., 2021), and exploring these interactions through co-occurrence networks (Fan et al., 2018) could help us to better understand ecosystem function and maintenance mechanisms (Kobayashi and Crouch, 2009; van Overbeek and Saikkonen, 2016; Deveau et al., 2018). Here, we systematically investigated the cross-trophic networks among prokaryotes, fungi, protists and

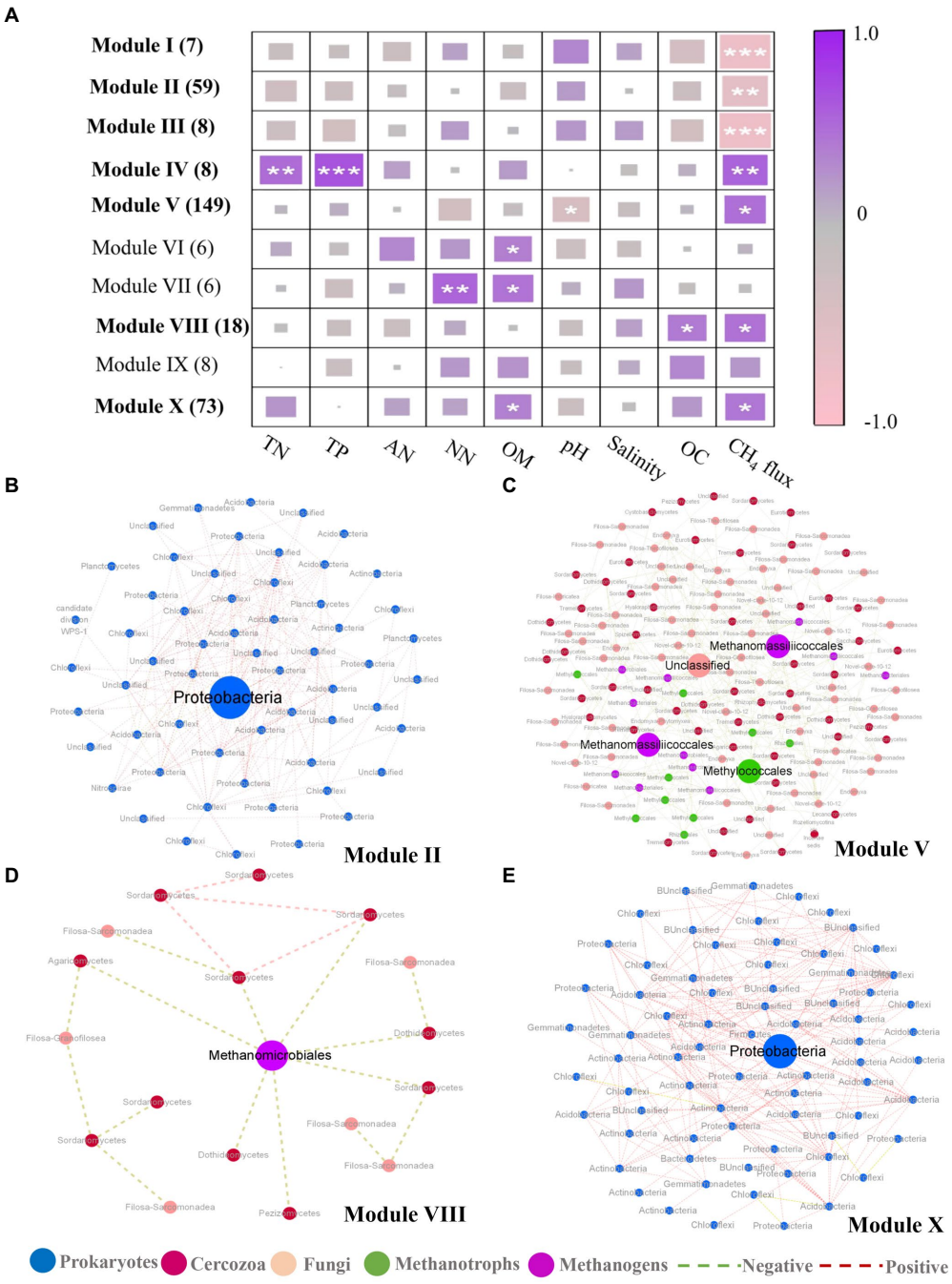

FIGURE 4
Correlation between module eigengenes and soil properties and display of related modules. **(A)** Correlation coefficients between module eigengenes and soil properties together with ecosystem methane (CH_4) under inundation treatments. The numbers in parentheses indicate the number of nodes observed in each module. Module eigengenes significantly related to CH_4 are in bold. Asterisks denote the significant relationships (*p<0.05, **p<0.01 and ***p<0.001). TN, total nitrogen; TP, total phosphorus; AN, Ammonia nitrogen; NN, Nitrate nitrogen; OC, Oxygen content. **(B–E)** Representative modules that were significantly related to CH_4 under inundation. In each module, node size is proportional to the network role, with larger nodes representing module hubs. Node color represents taxonomic groups. Prokaryotes (blue), cercozoa (red), fungi (pink), methanotrophic OTUs (green) and methanogenic OTUs (purple).

methane-associated communities in a gradient of simulated inundation conditions.

The shift in microbial community diversity, structure, and composition showed an inconsistent tendency along divergent inundation levels among different microbial groups. Previous studies have proposed that inundation can adjust the diversity and composition of microbial communities (Rinklebe and Langer, 2006; Goldman et al., 2017; Shiau et al., 2018; Yang et al., 2019; de

Jong et al., 2020). Here we compared the microbial diversity (Shannon index, Pelious evenness, Chao1 index, Richness), structure, and composition among IL (CK, 0 cm), IM (5–20 cm), IH (30–40 cm) groups (Supplementary Figures S1, S2). Our results demonstrated that prokaryotic Pelious evenness decreased in IM as compared to IL, which was inconsistent with observations from mangrove peat soil under inundation (Chambers et al., 2016). Badin et al. (2011) observed the fungal biomass was less driven by moisture content, similar to the observations in this study, while previous studies in three kinds of the floodplain showed that fungi had low survival rates in chronically submerged soil (Rinklebe and Langer, 2006). The cercozoan diversity in IH was higher than IM. The methanotrophic community showed a parallel tendency with the whole prokaryotic community. Methanogenic diversity showed no divergence, even though previous studies indicated that methanogenic community would be affected by flooding (Hernández et al., 2019; Shen et al., 2022). Except for these changes in methane-related microbes, methane-related genes (*mcrA* and *pmoA*) showed a significant positive correlation with methane flux under inundation conditions. First, the substrate of methane generation was produced, then the *mcrA* gene could express to produce methane based on this substrate, therefore, the copy numbers of *mcrA* gene are consistent with the methane flux (Steinberg and Regan, 2008). The positive correlation between *pmoA* gene copies (Knief, 2015) and methane flux may be due to that methane generation may directly affect the expression of the *pmoA* gene in an inundation environment, as soon as methane is created, it is rapidly utilized. These consistent or inconsistent tendencies in prokaryotic, fungal, and protistan diversity indicated that coastal soils could be susceptible and the divergence in microbial diversity did not linearly correlate with the inundation level gradient. In addition, the changes of methane-related microbes and methane-related gene expression showed a unique pattern under inundation condition.

Except for biodiversity, the co-occurrence networks within each microbial community along the inundation gradient were altered. Within the intradomain networks (Supplementary Figure S4; Supplementary Table S4), the number of edges and nodes first decreased and then increased along the gradient of inundation level, and this trend is consistent with the change in richness values and Chao 1. The phenomenon may be due to a partial plant stomatal closure under water with lower photosynthesis activity in the submerged leaves, when the inundation reaches a certain level (Schedlbauer et al., 2010; Han et al., 2015). Thus, an anaerobic environment is formed, resulting in the extinction of aerobic microorganisms. However, if the inundation level rises again to a higher level, more plant shoots and leaves are submerged, and the increase in organic residues provides resources for microorganisms, which may buffer the adverse effects of the anaerobic environment on the microbes. Inundation resulted in a slight increase in the vulnerability of the prokaryotic community, but a more pronounced change in the fungal and cercozoan communities, possibly due to their inherently low diversity. Inundation causes water to infiltrate into the soil pore space, altering the distribution of nutrient content. Also, the flowing water bodies create difficulties for microbial colonization, further leading to heterogeneity and irregularity in the distribution of these microorganisms in the soil. As a result, their species interactions become more susceptible to external influences under the stressful environments of inundation. Except for it, the robustness of the network was calculated (Supplementary Figure S6), as for prokaryotic communities, the robustness increased significantly at high inundation levels, but the robustness of fungal communities and cercozoan communities did not change significantly (Deng et al., 2012; Montesinos-Navarro et al., 2017). The result suggested that prokaryotic communities are more likely to remain stable under high inundation conditions. In addition, keystone species also shifted greatly in the co-occurrence network along different inundation levels. Similar results were reported in Gao's study, which revealed that increasing water content can significantly decrease the relative abundance of keystone species (Gao et al., 2021). Keystone species such as connectors or module hubs are considered to play critical roles in network structure maintenance (Deng et al., 2012; Ma et al., 2016), and this shift also demonstrated the sensitivity of molecular interactions to inundation as well. Taken together, inundation can make the interaction between microorganisms fragile, especially in fungal and cercozoan communities.

In this study, the methane-associated communities may show a preference for interaction under inundation, as they may be more likely to negatively interact with the cercozoan and fungal communities (Figure 3). This inverse correlation was inconsistent with previous studies in the rumen of animals, where the metabolites of anaerobic fungi can be used by methanogens to co-exist (Wood et al., 1986; Nakashimada et al., 2000). A possible explanation for this divergence may be due to microorganisms from different sources showing a diversity of birth environment preference and metabolic mode. Hydrogen generated by ciliated protozoa can be utilized by methanogens to synthesize methane for methanogenic taxa, but it is important to note that not all protozoa are the same (Newbold et al., 1995; Ranilla et al., 2007). For example, holotrich protozoa play a disproportionate role in supporting methanogenesis by competing with methanogens for nutrients (Newbold et al., 2015). Cercozoa is known to feed on bacteria, fungi, and even some eukaryotes (Dumack et al., 2020), and thus another factor may be that the predation effect of cercozoa on microbiota is much stronger than its synergistic effect on methanogens in an inundation environment. The negative correlation between methanogenic communities and fungi, cercozoa may result from resource competition and predation. But for methanotrophic taxa, it is likely due to apparent competition (Holt, 1977) and predation, respectively.

Because of the priority effects provided by negative correlation, late-arriving species could not grow because of the effects of early arriving species, the competition or predation can stabilize the fluctuation of community with disturbance and promote the stability of the network (Coyte et al., 2015; de Vries et al., 2018). Conventionally, methanogens could cooperate with the fermenting bacteria and syntrophic bacteria to finish the typical anaerobic syntrophic oxidation (McInerney et al., 1979), however, in this study, methane-related microbes were more likely to interact with the cercozoa and fungi, the reasons may as follows: the function and composition of syntrophic bacteria and fermenting bacteria may become fragile due to the influence of water osmotic pressure (Badin et al., 2011), and their potential ability to degrade substrates became weakened. In addition, hydrological changes may affect the interactions among microorganisms (Unger et al., 2009), to stabilize the whole community, methane-related microbes tend to reinforce negative interactions with cercozoa and fungi among many microorganisms rather than the positive interactions with prokaryotes (Coyte et al., 2015; de Vries et al., 2018). Therefore, the preference and negative correlation of methane-associated microorganisms with cercozoa and fungi may be a special way to maintain a stable species interaction state in an inundation environment.

Among several methane-related modules, environmental factors tend to affect the modules positively correlated with CH_4 flux, and pH may be an important environmental factor in regulating modules. Among the modules negatively correlated with methane, the Alphaproteobacterial OTU annotated as Methyloceanibacter (genus) was one of the module hubs in module II (Figure 4B). Marine methylotrophs are vitally important in the global carbon cycle as they metabolize one-carbon compounds. One of the newly isolated Methyloceanibacter species from the North Sea was found to be capable of oxidizing methane as the sole source of carbon and energy by solely using a soluble methane monooxygenase (Takeuchi et al., 2014; Vekeman et al., 2016). Therefore, Methyloceanibacter is crucial for suppressing methane production under inundation. In module V (Figure 4B), one of the four module hubs was a cercozoan OTU (Figure 4C), which indicated that cercozoa may be a nonnegligible component of the soil microbiome under inundation. Previous studies show that protists can act as dynamic bonds among soil microorganisms (Xiong et al., 2018; Asiloglu et al., 2021). It was interesting that there was a significant negative correlation between this cercozoan OTU and a Methylococcales module hub, the negative correlation may contribute to the positive association of the whole module with methane emissions. The other two module hubs were Methanomassiliicoccales and Methanomicrobiales, the form of which is a new methanogenic archaea order, belonging to the Euryarchaeota, present in marine and lake habitats (Söllinger et al., 2016), and can use external H_2 to reduce methyl compounds for the production of methane (Borrel et al., 2014). Methanomicrobiales are widely found in mangrove sediments, which is one of the more abundant Euryarchaeotal methanogenic orders (Li et al., 2012; Zhou et al., 2014). In modules significantly correlated with CH_4 (Figure 4A), environmental factors such as total nitrogen, total phosphate, organic matter and pH are more likely to drive species interactions among modules that are positively correlated with CH_4. In addition, Module V was correlated significantly with pH. In previous studies, pH is one of the key factors driving the prokaryotic community in offshore sediments (Yu et al., 2022). This environmental factor mainly affects the prokaryotic community through affecting the structure of microbial cell membrane and availability of soil nutrients (Gabler et al., 2017; Wang et al., 2020). Thus, pH may be an important factor in regulating species interaction to contribute to CH_4 emission positively. Therefore, under inundation conditions, several environmental factors, especially pH, may tend to contribute positively to methane production and by influencing species interaction.

5. Conclusion

The present study revealed the feedback of microbial communities driving methane emissions in coastal soils. Our results indicated that the methane flux increased first and then decreased with the increase of inundation level, and the diversity, community composition and co-occurrence networks of soil prokaryotic, fungal, and cercozoan communities were significantly shifted with different inundation levels. In addition, during the inundation state, methane-associated species and cercozoan community OTUs dominated the species interactions. Environmental factors mainly affected the interaction between species that could promote methane emissions. Overall, simulated inundation triggered some negative correlations between methane-associated species and other microorganisms, and the fungal and cercozoan communities may both play a leading role in regulating methane emission. Moreover, the environmental variables, especially pH, tend to regulate network modules significantly positively related to CH_4. This study provides a new perspective on microbial cross-trophic relationships for the budget of wetland CH_4 emissions.

Data availability statement

The datasets presented in this study can be found in online repositories. The names of the repository/repositories and accession number(s) can be found at: accession number: PRJCA013006 (https://ngdc.cncb.ac.cn/search/?dbId=gsa&q=PRJCA013006).

Author contributions

LW, MZ, and YD conceived and designed the experiments. LW, YZ, SG, ZhaZ, YW, ZheZ, XD, and XY collected the soil samples and performed the experiments. LW analyzed the data. LW and YD wrote the paper. LW, MZ, XD, KF, SG, YZ, XY, ZhaZ, YW, ZheZ, QZ, BX, GH, and YD contributed substantially to this paper. All authors contributed to the article and approved the submitted version.

Funding

This project was supported by the National Natural Science Foundation of China (U1906223, 42071126, and 42107136).

Acknowledgments

We thank James Walter Voordeckers for carefully editing the grammar of the manuscript and for some valuable suggestions for this manuscript.

Conflict of interest

The authors declare that the research was conducted in the absence of any commercial or financial relationships that could be construed as a potential conflict of interest.

Publisher's note

Supplementary material

The Supplementary material for this article can be found online at: https://www.frontiersin.org/articles/10.3389/fmicb.2022.1076610/full#supplementary-material

References

Adl, S. M., Bass, D., Lane, C. E., Lukeš, J., Schoch, C. L., Smirnov, A., et al. (2019). Revisions to the classification, nomenclature, and diversity of eukaryotes. *J. Eukaryot. Microbiol.* 66, 4–119. doi: 10.1111/jeu.12691

Alter, O., Brown, P. O., and Botstein, D. (2000). Singular value decomposition for genome-wide expression data processing and modeling. *Proc. Natl. Acad. Sci. U. S. A.* 97, 10101–10106. doi: 10.1073/pnas.97.18.10101

Asiloglu, R., Kenya, K., Samuel, S. O., Sevilir, B., Murase, J., Suzuki, K., et al. (2021). Top-down effects of protists are greater than bottom-up effects of fertilisers on the formation of bacterial communities in a paddy field soil. *Soil Biol. Biochem.* 156:108186. doi: 10.1016/j.soilbio.2021.108186

Badin, A. L., Monier, A., Volatier, L., Geremia, R. A., Delolme, C., and Bedell, J. P. (2011). Structural stability, microbial biomass and community composition of sediments affected by the hydric dynamics of an urban Stormwater Infiltration Basin: dynamics of physical and microbial characteristics of Stormwater sediment. *Microb. Ecol.* 61, 885–897. doi: 10.1007/s00248-011-9829-4

Barron, G. L. (2003). Predatory fungi, wood decay, and the carbon cycle. *Biodiversity* 4, 3–9. doi: 10.1080/14888386.2003.9712621

Borrel, G., O'Toole, P. W., Harris, H. M. B., Peyret, P., Brugère, J. F., and Gribaldo, S. (2013). Phylogenomic data support a seventh order of methylotrophic methanogens and provide insights into the evolution of methanogenesis. *Genome Biol. Evol.* 5, 1769–1780. doi: 10.1093/gbe/evt128

Borrel, G., Parisot, N., Harris, H. M. B., Peyretaillade, E., Gaci, N., Tottey, W., et al. (2014). Comparative genomics highlights the unique biology of Methanomassiliicoccales, a Thermoplasmatales-related seventh order of methanogenic archaea that encodes pyrrolysine. *BMC Genomics* 15:679. doi: 10.1186/1471-2164-15-679

Bridgham, S. D., Cadillo-Quiroz, H., Keller, J. K., and Zhuang, Q. (2013). Methane emissions from wetlands: biogeochemical, microbial, and modeling perspectives from local to global scales. *Glob. Chang. Biol.* 19, 1325–1346. doi: 10.1111/gcb.12131

Caporaso, J. G., Lauber, C. L., Walters, W. A., Berg-Lyons, D., Lozupone, C. A., Turnbaugh, P. J., et al. (2011). Global patterns of 16S rRNA diversity at a depth of millions of sequences per sample. *Proc. Natl. Acad. Sci. U. S. A.* 108, 4516–4522. doi: 10.1073/pnas.1000080107

Chambers, L. G., Guevara, R., Boyer, J. N., Troxler, T. G., and Davis, S. E. (2016). Effects of salinity and inundation on microbial community structure and function in a mangrove peat soil. *Wetlands* 36, 361–371. doi: 10.1007/s13157-016-0745-8

Coyte, K. Z., Schluter, J., and Foster, K. R. (2015). The ecology of the microbiome: networks, competition, and stability. *Micobiome.* 350, 663–666. doi: 10.1126/science.aad2602

de Jong, A. E. E., Guererro-Cruz, S., van Diggelen, J. M. H., Vaksmaa, A., Lamers, L. P. M., Jetten, M. S. M., et al. (2020). Changes in microbial community composition, activity, and greenhouse gas production upon inundation of drained iron-rich peat soils. *Soil Biol. Biochem.* 149:107862. doi: 10.1016/j.soilbio.2020.107862

de Menezes, A. B., Prendergast-Miller, M. T., Richardson, A. E., Toscas, P., Farrell, M., Macdonald, L. M., et al. (2015). Network analysis reveals that bacteria and fungi form modules that correlate independently with soil parameters. *Environ. Microbiol.* 17, 2677–2689. doi: 10.1111/1462-2920.12559

de Vries, F. T., Griffiths, R. I., Bailey, M., Craig, H., Girlanda, M., Gweon, H. S., et al. (2018). Soil bacterial networks are less stable under drought than fungal networks. *Nat. Commun.* 9:3033. doi: 10.1038/s41467-018-05516-7

de Vries, F. T., Thébault, E., Liiri, M., Birkhofer, K., Tsiafouli, M. A., Bjørnlund, L., et al. (2013). Soil food web properties explain ecosystem services across European land use systems. *Proc. Natl. Acad. Sci. U. S. A.* 110, 14296–14301. doi: 10.1073/pnas.1305198110

Dean, J. F., Middelburg, J. J., Röckmann, T., Aerts, R., Blauw, L. G., Egger, M., et al. (2018). Methane feedbacks to the global climate system in a warmer world. *Rev. Geophys.* 56, 207–250. doi: 10.1002/2017RG000559

del Campo, J., Kolisko, M., Boscaro, V., Santoferrara, L. F., Nenarokov, S., Massana, R., et al. (2018). EukRef: phylogenetic curation of ribosomal RNA to enhance understanding of eukaryotic diversity and distribution. *PLoS Biol.* 16:e2005849. doi: 10.1371/journal.pbio.2005849

Deng, Y., Jiang, Y.-H., Yang, Y., He, Z., Luo, F., and Zhou, J. (2012). Molecular ecological network analyses. *BMC Bioinformatics* 13:113. doi: 10.1186/1471-2105-13-113

Deveau, A., Bonito, G., Uehling, J., Paoletti, M., Becker, M., Bindschedler, S., et al. (2018). Bacterial-fungal interactions: ecology, mechanisms and challenges. *FEMS Microbiol. Rev.* 42, 335–352. doi: 10.1093/femsre/fuy008

Dumack, K., Fiore-Donno, A. M., Bass, D., and Bonkowski, M. (2020). Making sense of environmental sequencing data: ecologically important functional traits of the protistan groups Cercozoa and Endomyxa (Rhizaria). *Mol. Ecol. Resour.* 20, 398–403. doi: 10.1111/1755-0998.13112

Edgar, R. C. (2013). UPARSE: highly accurate OTU sequences from microbial amplicon reads. *Nat. Methods* 10, 996–998. doi: 10.1038/nmeth.2604

Fan, K., Weisenhorn, P., Gilbert, J. A., and Chu, H. (2018). Wheat rhizosphere harbors a less complex and more stable microbial co-occurrence pattern than bulk soil. *Soil Biol. Biochem.* 125, 251–260. doi: 10.1016/j.soilbio.2018.07.022

Feher, L. C., Osland, M. J., Griffith, K. T., Grace, J. B., Howard, R. J., Stagg, C. L., et al. (2017). Linear and nonlinear effects of temperature and precipitation on ecosystem properties in tidal saline wetlands. *Ecosphere* 8. doi: 10.1002/ecs2.1956

Feng, K., Peng, X., Zhang, Z., Gu, S., He, Q., Shen, W., et al. (2022). iNAP: an integrated network analysis pipeline for microbiome studies. *iMeta* 1. doi: 10.1002/imt2.13

Feng, K., Zhang, Z., Cai, W., Liu, W., Xu, M., Yin, H., et al. (2017). Biodiversity and species competition regulate the resilience of microbial biofilm community. *Mol. Ecol.* 26, 6170–6182. doi: 10.1111/mec.14356

Feng, K., Zhang, Y., He, Z., Ning, D., and Deng, Y. (2019). Interdomain ecological networks between plants and microbes. *Mol. Ecol. Resour.* 19, 1565–1577. doi: 10.1111/1755-0998.13081

Fiore-Donno, A. M., Richter-Heitmann, T., and Bonkowski, M. (2020). Contrasting responses of Protistan plant parasites and Phagotrophs to ecosystems, land management and soil properties. *Front. Microbiol.* 11:1823. doi: 10.3389/fmicb.2020.01823

Fiore-Donno, A. M., Rixen, C., Rippin, M., Glaser, K., Samolov, E., Karsten, U., et al. (2018). New barcoded primers for efficient retrieval of cercozoan sequences in high-throughput environmental diversity surveys, with emphasis on worldwide biological soil crusts. *Mol. Ecol. Resour.* 18, 229–239. doi: 10.1111/1755-0998.12729

Freitag, T. E., Toet, S., Ineson, P., and Prosser, J. I. (2010). Links between methane flux and transcriptional activities of methanogens and methane oxidizers in a blanket peat bog. *FEMS Microbiol. Ecol.* 73, 157–165. doi: 10.1111/j.1574-6941.2010.00871.x

Friborg, T., Soegaard, H., Christensen, T. R., Lloyd, C. R., and Panikov, N. S. (2003). Siberian wetlands: where a sink is a source. *Geophys. Res. Lett.* 30, 2129–2133. doi: 10.1029/2003GL017797

Gabler, C. A., Osland, M. J., Grace, J. B., Stagg, C. L., Day, R. H., Hartley, S. B., et al. (2017). Macroclimatic change expected to transform coastal wetland ecosystems this century. *Nat. Clim. Chang.* 7, 142–147. doi: 10.1038/nclimate3203

Gao, G. F., Peng, D., Zhang, Y., Li, Y., Fan, K., Tripathi, B. M., et al. (2021). Dramatic change of bacterial assembly process and co-occurrence pattern in Spartina alterniflora salt marsh along an inundation frequency gradient. *Sci. Total Environ.* 755:142546. doi: 10.1016/j.scitotenv.2020.142546

Garssen, A. G., Baattrup-Pedersen, A., Voesenek, L. A. C. J., Verhoeven, J. T. A., and Soons, M. B. (2015). Riparian plant community responses to increased flooding: a meta-analysis. *Glob. Chang. Biol.* 21, 2881–2890. doi: 10.1111/gcb.12921

Goldman, A. E., Graham, E. B., Crump, A. R., Kennedy, D. W., Romero, E. B., Anderson, C. G., et al. (2017). Biogeochemical cycling at the aquatic-terrestrial interface is linked to parafluvial hyporheic zone inundation history. *Biogeosciences* 14, 4229–4241. doi: 10.5194/bg-14-4229-2017

Guillou, L., Bachar, D., Audic, S., Bass, D., Berney, C., Bittner, L., et al. (2013). The Protist ribosomal reference database (PR2): a catalog of unicellular eukaryote small sub-unit rRNA sequences with curated taxonomy. *Nucleic Acids Res.* 41, D597–D604. doi: 10.1093/nar/gks1160

Han, G., Chu, X., Xing, Q., Li, D., Yu, J., Luo, Y., et al. (2015). Effects of episodic flooding on the net ecosystem CO2 exchange of a supratidal wetland in the Yellow River Delta. *J. Geophys. Res. Biogeosci.* 120, 1506–1520. doi: 10.1002/2015JG002923

Hernández, M., Klose, M., Claus, P., Bastviken, D., Marotta, H., Figueiredo, V., et al. (2019). Structure, function and resilience to desiccation of methanogenic microbial communities in temporarily inundated soils of the Amazon rainforest (Cunia reserve, Rondonia). *Environ. Microbiol.* 21, 1702–1717. doi: 10.1111/1462-2920.14535

Holt, R. D. (1977). Predation, apparent competition, and the structure of prey communities. *Theor. Popul. Biol.* 12, 197–229. doi: 10.1016/0040-5809(77)90042-9

Kim, S. Y., Lee, S. H., Freeman, C., Fenner, N., and Kang, H. (2008). Comparative analysis of soil microbial communities and their responses to the short-term drought in bog, fen, and riparian wetlands. *Soil Biol. Biochem.* 40, 2874–2880. doi: 10.1016/j.soilbio.2008.08.004

Kirschke, S., Bousquet, P., Ciais, P., Saunois, M., Canadell, J. G., Dlugokencky, E. J., et al. (2013). Three decades of global methane sources and sinks. *Nat. Geosci.* 6, 813–823. doi: 10.1038/ngeo1955

Knief, C. (2015). Diversity and habitat preferences of cultivated and uncultivated aerobic methanotrophic bacteria evaluated based on pmoA as molecular marker. *Front. Microbiol.* 6:1346. doi: 10.3389/fmicb.2015.01346

Kobayashi, D. Y., and Crouch, J. A. (2009). Bacterial/fungal interactions: from pathogenes to mutualistic endosymbionts. *Annu. Rev. Phytopathol.* 47, 63–82. doi: 10.1146/annurev-phyto-080508-081729

Kong, Y. (2011). Btrim: a fast, lightweight adapter and quality trimming program for next-generation sequencing technologies. *Genomics* 98, 152–153. doi: 10.1016/j.ygeno.2011.05.009

Langfelder, P., and Horvath, S. (2007). Eigengene networks for studying the relationships between co-expression modules. *BMC Syst. Biol.* 1:54. doi: 10.1186/1752-0509-1-54

le Mer, J., and Roger, P. (2001). Production, oxidation, emission and consumption. *Soil Biol. Biochem.* 37, 25–50. doi: 10.1016/S1164-5563(01)01067-6

Li, H., Dai, S., Ouyang, Z., Xie, X., Guo, H., Gu, C., et al. (2018). Multi-scale temporal variation of methane flux and its controls in a subtropical tidal salt marsh in eastern China. *Biogeochemistry* 137, 163–179. doi: 10.1007/s10533-017-0413-y

Li, Q., Wang, F., Chen, Z., Yin, X., and Xiao, X. (2012). Stratified active archaeal communities in the sediments of Jiulong River estuary. *China. Front Microbiol* 3:311. doi: 10.3389/fmicb.2012.00311

Liebner, S., Schwarzenbach, S. P., and Zeyer, J. (2012). Methane emissions from an alpine fen in Central Switzerland. *Biogeochemistry* 109, 287–299. doi: 10.1007/s10533-011-9629-4

Lopez-Garcia, A., Saborio-Montero, A., Gutierrez-Rivas, M., Atxaerandio, R., Goiri, I., Garcia-Rodriguez, A., et al. (2022). Fungal and ciliate protozoa are the main rumen microbes associated with methane emissions in dairy cattle. *Gigascience* 11:giab088. doi: 10.1093/gigascience/giab088

Louca, S., Parfrey, L. W., and Doebeli, M. (2016). Decoupling function and taxonomy in the global ocean microbiome. *Science* 11, 1272–1277. doi: 10.1126/science.aaf4507

Ma, B., Wang, H., Dsouza, M., Lou, J., He, Y., Dai, Z., et al. (2016). Geographic patterns of co-occurrence network topological features for soil microbiota at continental scale in eastern China. *ISME J.* 10, 1891–1901. doi: 10.1038/ismej.2015.261

Magoč, T., and Salzberg, S. L. (2011). FLASH: fast length adjustment of short reads to improve genome assemblies. *Bioinformatics* 27, 2957–2963. doi: 10.1093/bioinformatics/btr507

McInerney, M. J., Bryant, M. P., and Pfennig, N. (1979). Anaerobic bacterium that degrades fatty acids in syntrophic association with methanogens. *Arch. Microbiol.* 122, 129–135. doi: 10.1007/BF00411351

Montesinos-Navarro, A., Hiraldo, F., Tella, J. L., and Blanco, G. (2017). Network structure embracing mutualism-antagonism continuums increases community robustness. *Nat. Ecol. Evol.* 1, 1661–1669. doi: 10.1038/s41559-017-0320-6

Murrell, P. (2009). R Graphics. *Wiley Interdiscip. Rev. Comput. Stat.* 1, 216–220. doi: 10.1002/wics.022

Nakashimada, Y., Srinivasan, K., Murakami, M., and Nishio, N. (2000). Direct conversion of cellulose to methane by anaerobic fungus Neocallimastix frontalis and defined methanogens. *Biotechnol. Lett.* 22, 223–227. doi: 10.1023/A:1005666428494

Newbold, C. J., de la Fuente, G., Belanche, A., Ramos-Morales, E., and McEwan, N. R. (2015). The role of ciliate protozoa in the rumen. *Front. Microbiol.* 6:1313. doi: 10.3389/fmicb.2015.01313

Newbold, C. J., Jouany, J. P., and Jouany, J. P. (1995). The importance of methanogens associated with ciliate protozoa in ruminal methane production in vifro. *Lett. Appl. Microbiol.* 21, 230–234. doi: 10.1111/j.1472-765X.1995.tb01048.x

Nilsson, R. H., Larsson, K. H., Taylor, A. F. S., Bengtsson-Palme, J., Jeppesen, T. S., Schigel, D., et al. (2019). The UNITE database for molecular identification of fungi: handling dark taxa and parallel taxonomic classifications. *Nucleic Acids Res.* 47, D259–D264. doi: 10.1093/nar/gky1022

Ocko, I. B., Sun, T., Shindell, D., Oppenheimer, M., Hristov, A. N., Pacala, S. W., et al. (2021). Acting rapidly to deploy readily available methane mitigation measures by sector can immediately slow global warming. *Environ. Res. Lett.* 16:054042. doi: 10.1088/1748-9326/abf9c8

Oliver, J. P., and Schilling, J. S. (2018). Harnessing fungi to mitigate CH4 in natural and engineered systems. *Appl. Microbiol. Biotechnol.* 102, 7365–7375. doi: 10.1007/s00253-018-9203-2

Osland, M. J., Enwright, N. M., Day, R. H., Gabler, C. A., Stagg, C. L., and Grace, J. B. (2016). Beyond just sea-level rise: considering macroclimatic drivers within coastal wetland vulnerability assessments to climate change. *Glob. Chang. Biol.* 22, 1–11. doi: 10.1111/gcb.13084

Osland, M. J., Gabler, C. A., Grace, J. B., Day, R. H., McCoy, M. L., McLeod, J. L., et al. (2018). Climate and plant controls on soil organic matter in coastal wetlands. *Glob. Chang. Biol.* 24, 5361–5379. doi: 10.1111/gcb.14376

Paschalis, A., Katul, G. G., Fatichi, S., Palmroth, S., and Way, D. (2017). On the variability of the ecosystem response to elevated atmospheric CO2 across spatial and temporal scales at the Duke Forest FACE experiment. *Agric. For. Meteorol.* 232, 367–383. doi: 10.1016/j.agrformet.2016.09.003

Peacock, M., Ridley, L. M., Evans, C. D., and Gauci, V. (2017). Management effects on greenhouse gas dynamics in fen ditches. *Sci. Total Environ.* 578, 601–612. doi: 10.1016/j.scitotenv.2016.11.005

Qian, X., Li, X., Li, H., and Zhang, D. (2021). Floral fungal-bacterial community structure and co-occurrence patterns in four sympatric island plant species. *Fungal Biol.* 125, 49–61. doi: 10.1016/j.funbio.2020.10.004

Ranilla, M. J., Jouany, J. P., and Morgavi, D. P. (2007). Methane production and substrate degradation by rumen microbial communities containing single protozoal species in vitro. *Lett. Appl. Microbiol.* 45, 675–680. doi: 10.1111/j.1472-765X.2007.02251.x

Rinklebe, J., and Langer, U. (2006). Microbial diversity in three floodplain soils at the Elbe River (Germany). *Soil Biol. Biochem.* 38, 2144–2151. doi: 10.1016/j.soilbio.2006.01.018

Sakai, S., Takaki, Y., Shimamura, S., Sekine, M., Tajima, T., Kosugi, H., et al. (2011). Genome sequence of a mesophilic hydrogenotrophic methanogen Methanocella paludicola, the first cultivated representative of the order Methanocellales. *PLoS One* 6:e22898. doi: 10.1371/journal.pone.0022898

Saunois, M., Bousquet, P., Poulter, B., Peregon, A., Ciais, P., Canadell, J. G., et al. (2016). The global methane budget 2000-2012. *Earth Syst. Sci. Data* 8, 697–751. doi: 10.5194/essd-8-697-2016

Schedlbauer, J. L., Oberbauer, S. F., Starr, G., and Jimenez, K. L. (2010). Seasonal differences in the CO2 exchange of a short-hydroperiod Florida Everglades marsh. *Agric. For. Meteorol.* 150, 994–1006. doi: 10.1016/j.agrformet.2010.03.005

Shen, L., Dong Geng, C., Yu Ren, B., Jie Jin, J., Hao Huang, H., Chen Liu, X., et al. (2022). Detection and quantification of Candidatus Methanoperedens-like Archaea in freshwater wetland soils. *Microb. Ecol.* doi: 10.1007/s00248-022-01968-z

Shiau, Y. J., Cai, Y., Te Lin, Y., Jia, Z., and Chiu, C. Y. (2018). Community structure of active aerobic Methanotrophs in red mangrove (Kandelia obovata) soils under different frequency of tides. *Microb. Ecol.* 75, 761–770. doi: 10.1007/s00248-017-1080-1

Söllinger, A., Schwab, C., Weinmaier, T., Loy, A., Schleper, C., and Urich, T. (2016). Phylogenetic and genomic analysis of Methanomassiliicoccales in wetlands and animal intestinal tracts reveals clade-specific habitat preferences. *FEMS Microbiol. Ecol.* 92:fiv149. doi: 10.1093/femsec/fiv149

Steinberg, L. M., and Regan, J. M. (2008). Phylogenetic comparison of the methanogenic communities from an acidic, oligotrophic fen and an anaerobic digester treating municipal wastewater sludge. *Appl. Environ. Microbiol.* 74, 6663–6671. doi: 10.1128/AEM.00553-08

Takeuchi, M., Katayama, T., Yamagishi, T., Hanada, S., Tamaki, H., Kamagata, Y., et al. (2014). Methyloceanibacter caenitepidi gen. Nov., sp. nov., a facultatively methylotrophic bacterium isolated from marine sediments near a hydrothermal vent. *Int. J. Syst. Evol. Microbiol.* 64, 462–468. doi: 10.1099/ijs.0.053397-0

Taylor, D. L., Walters, W. A., Lennon, N. J., Bochicchio, J., Krohn, A., Caporaso, J. G., et al. (2016). Accurate estimation of fungal diversity and abundance through improved lineage-specific primers optimized for Illumina amplicon sequencing. *Appl. Environ. Microbiol.* 82, 7217–7226. doi: 10.1128/AEM.02576-16

Unger, I. M., Kennedy, A. C., and Muzika, R. M. (2009). Flooding effects on soil microbial communities. *Appl. Soil Ecol.* 42, 1–8. doi: 10.1016/j.apsoil.2009.01.007

van Overbeek, L. S., and Saikkonen, K. (2016). Impact of bacterial-fungal interactions on the colonization of the Endosphere. *Trends Plant Sci.* 21, 230–242. doi: 10.1016/j.tplants.2016.01.003

Vekeman, B., Kerckhof, F. M., Cremers, G., de Vos, P., Vandamme, P., Boon, N., et al. (2016). New Methyloceanibacter diversity from North Sea sediments includes methanotroph containing solely the soluble methane monooxygenase. *Environ. Microbiol.* 18, 4523–4536. doi: 10.1111/1462-2920.13485

Wang, Q., Garrity, G. M., Tiedje, J. M., and Cole, J. R. (2007). Naïve Bayesian classifier for rapid assignment of rRNA sequences into the new bacterial taxonomy. *Appl. Environ. Microbiol.* 73, 5261–5267. doi: 10.1128/AEM.00062-07

Wang, Y., Wang, K., Huang, L., Dong, P., Wang, S., Chen, H., et al. (2020). Fine-scale succession patterns and assembly mechanisms of bacterial community of Litopenaeus vannamei larvae across the developmental cycle. *Microbiome* 8:106. doi: 10.1186/s40168-020-00879-w

Wei, S., Han, G., Chu, X., Song, W., He, W., Xia, J., et al. (2020). Effect of tidal flooding on ecosystem CO2 and CH4 fluxes in a salt marsh in the Yellow River Delta. *Estuar. Coast. Shelf Sci.* 232:106512. doi: 10.1016/j.ecss.2019.106512

Wickham, H. (2011). ggplot2. *Wiley Interdiscip. Rev. Comput. Stat.* 3, 180–185. doi: 10.1002/wics.147

Wood, T. M., Wilson, C. A., McCrae, S. I., and Joblin, K. N. (1986). A highly active extracellular cellulase from the anaerobic rumen fungus *Neocallimastix frontalis*. *FEMS Microbiol. Lett.* 34, 37–40. doi: 10.1111/j.1574-6968.1986.tb01344.x

Xiong, W., Jousset, A., Guo, S., Karlsson, I., Zhao, Q., Wu, H., et al. (2018). Soil protist communities form a dynamic hub in the soil microbiome. *ISME J.* 12, 634–638. doi: 10.1038/ismej.2017.171

Yang, W., Li, X., Sun, T., Yang, Z., and Li, M. (2017). Habitat heterogeneity affects the efficacy of ecological restoration by freshwater releases in a recovering freshwater coastal wetland in China's Yellow River Delta. *Ecol. Eng.* 104, 1–12. doi: 10.1016/j.ecoleng.2017.04.007

Yang, F., Zhang, D., Wu, J., Chen, Q., Long, C., Li, Y., et al. (2019). Anti-seasonal submergence dominates the structure and composition of prokaryotic communities in the riparian zone of the three gorges reservoir, China. *Sci. Total Environ.* 663, 662–672. doi: 10.1016/j.scitotenv.2019.01.357

Ye, C., Zhang, K., Deng, Q., and Zhang, Q. (2013). Plant communities in relation to 'flooding and soil characteristics in the water level fluctuation zone of the three gorges reservoir, China. *Environ. Sci. Pollut. Res.* 20, 1794–1802. doi: 10.1007/s11356-012-1148-x

Yu, H., Zhong, Q., Peng, Y., Zheng, X., Xiao, F., Wu, B., et al. (2022). Environmental filtering by pH and salinity jointly drives prokaryotic community assembly in coastal wetland sediments. *Front. Mar. Sci.* 8. doi: 10.3389/fmars.2021.792294

Yuan, M. M., Guo, X., Wu, L., Zhang, Y., Xiao, N., Ning, D., et al. (2021). Climate warming enhances microbial network complexity and stability. *Nat. Clim. Chang.* 11, 343–348. doi: 10.1038/s41558-021-00989-9

Zhang, L., Adams, J. M., Dumont, M. G., Li, Y., Shi, Y., He, D., et al. (2019). Distinct methanotrophic communities exist in habitats with different soil water contents. *Soil Biol. Biochem.* 132, 143–152. doi: 10.1016/j.soilbio.2019.02.007

Zhang, X., Zhang, R., Gao, J., Wang, X., Fan, F., Ma, X., et al. (2017). Thirty-one years of rice-rice-green manure rotations shape the rhizosphere microbial community and enrich beneficial bacteria. *Soil Biol. Biochem.* 104, 208–217. doi: 10.1016/j.soilbio.2016.10.023

Zhang, B., Zhang, J., Liu, Y., Shi, P., and Wei, G. (2018). Co-occurrence patterns of soybean rhizosphere microbiome at a continental scale. *Soil Biol. Biochem.* 118, 178–186. doi: 10.1016/j.soilbio.2017.12.011

Zhao, Y., Bu, C., Yang, H., Qiao, Z., Ding, S., and Ni, S. Q. (2020). Survey of dissimilatory nitrate reduction to ammonium microbial community at national wetland of Shanghai, China. *Chemosphere* 250:126195. doi: 10.1016/j.chemosphere.2020.126195

Zhao, M., Han, G., Wu, H., Song, W., Chu, X., Li, J., et al. (2020). Inundation depth affects ecosystem CO_2 and CH_4 exchange by changing plant productivity in a freshwater wetland in the Yellow River estuary. *Plant Soil* 454, 87–102. doi: 10.1007/s11104-020-04612-2

Zhao, F., Xu, K., and Zhang, D. (2013). Spatio-temporal variations in the molecular diversity of microeukaryotes in particular ciliates in soil of the Yellow River delta, China. *J. Eukaryot. Microbiol.* 60, 282–290. doi: 10.1111/jeu.12035

Zhou, Z., Chen, J., Cao, H., Han, P., and Gu, J. D. (2014). Comparison of communities of both methane-producing and metabolizing archaea and bacteria in sediments between the northern South China Sea and coastal Mai Po nature reserve revealed by PCR amplification of mcrA and pmoA genes. *Front. Microbiol.* 5:789. doi: 10.3389/fmicb.2014.00789

Zhou, Y., Sun, B., Xie, B., Feng, K., Zhang, Z., Zhang, Z., et al. (2021). Warming reshaped the microbial hierarchical interactions. *Glob. Chang. Biol.* 27, 6331–6347. doi: 10.1111/gcb.15891

frontiers | Frontiers in Microbiology

TYPE Original Research
PUBLISHED 09 January 2023
DOI 10.3389/fmicb.2022.1012512

OPEN ACCESS

EDITED BY
Yu Luo,
Zhejiang University,
China

REVIEWED BY
Pengfa Li,
Nanjing Agricultural University,
China
Yuan Liu,
Michigan State University,
United States

*CORRESPONDENCE
Huajun Fang
✉ fanghj@igsnrr.ac.cn
Shulan Cheng
✉ slcheng@ucas.ac.cn

SPECIALTY SECTION
This article was submitted to Terrestrial Microbiology, a section of the journal Frontiers in Microbiology

RECEIVED 05 August 2022
ACCEPTED 19 December 2022
PUBLISHED 09 January 2023

CITATION
Yang Y, Cheng S, Fang H, Guo Y, Li Y, Zhou Y, Shi F and Vancampenhout K (2023) Linkages between the molecular composition of dissolved organic matter and soil microbial community in a boreal forest during freeze–thaw cycles. *Front. Microbiol.* 13:1012512. doi: 10.3389/fmicb.2022.1012512

Linkages between the molecular composition of dissolved organic matter and soil microbial community in a boreal forest during freeze–thaw cycles

Yan Yang[1,2], Shulan Cheng[2]*, Huajun Fang[1,2,3,4]*, Yifan Guo[1], Yuna Li[2], Yi Zhou[2], Fangying Shi[1] and Karen Vancampenhout[5]

[1]Key Laboratory of Ecosystem Network Observation and Modeling, Institute of Geographic Sciences and Natural Resources Research, Chinese Academy of Sciences, Beijing, China, [2]College of Resources and Environment, University of Chinese Academy of Sciences, Beijing, China, [3]Northwest Plateau Institute of Biology, Chinese Academy of Sciences, Xining, China, [4]The Zhongke-Ji'an Institute for Eco-Environmental Sciences, Ji'an, China, [5]Division of Forest, Nature and Landscape, Department of Earth and Environmental Sciences, Faculty of Sciences, KU Leuven, Leuven, Belgium

Soil dissolved organic matter (DOM) plays a vital role in biogeochemical processes. Global warming leads to increased freeze–thaw cycles (FTCs) in boreal forest soils, which can change DOM production and consumption. However, the interactions between the chemical composition of DOM molecules and the microbial communities that drive C decomposition in the context of freeze–thaw are poorly understood. Here, a FTCs incubation experiment was conducted. Combined with pyrolysis gas chromatography–mass spectrometry and high-throughput sequencing techniques, the relationships between DOM chemodiversity and microbial community structure were assessed. Results indicated that both low-frequency (2FTCs) and high-frequency freeze–thaw cycles (6FTCs) significantly increased soil dissolved organic carbon (DOC) contents in the surface (0–10 cm) and subsurface (50–60 cm) soil layers. In the topsoil, FTCs significantly reduced the relative abundance of aromatic compounds, but increased the relative proportions of alkanes, phenols, fatty acid methyl esters (Me) and polysaccharides in the DOM. In the subsuface soil layer, only the relative abundance of Me in the 6FTCs treatment increased significantly. The response of bacterial communities to FTCs was more sensitive than that of fungi, among which only the relative abundance of *Gammaproteobacteria* increased by FTCs. Moreover, the relative abundance of these taxa was positively correlated with the increment of DOC. Co-occurrence networks confirmed DOM-bacterial interactions, implying that specific microorganisms degrade specific substrates. At class level, *Gammaproteobacteria* were significantly positively correlated with labile C (polysaccharides and alkanes), whereas other bacterial classes such as *Actinobacteria*, *Alphaproteobacteria*, and *Thermoleophilia* were significantly positively correlated with aromatic compounds in the topsoil. Collectively, FTCs tended to activate DOM and enhance its biodegradability of DOM, potentially hampering DOC accumulation and C sequestration. These findings highlight the potential of DOM molecular mechanisms to

regulate the functional states of soil bacterial communities under increased FTCs.

KEYWORDS

freeze–thaw cycles, dissolved organic matter, pyrolysis gas chromatography–mass spectrometry, high-throughput sequencing, boreal forest

Highlights

- Freeze–thaw cycles (FTCs) increase DOC release and change the chemical structure of DOM in the surface and deep soils in the boreal forest.
- The improvement of DOM bioavailability is detrimental to DOC accumulation.
- *Gammaproteobacteria* play a dominant role in DOC production under the scenarios of intensified freezing–thawing.

1. Introduction

Dissolved organic matter (DOM) is the most active and bioavailable component of organic matter in soil. It is defined as a heterogeneous continuum of organic molecules of various sizes, that are soluble in water and can pass through a 0.45 um pore size filter (Rombolà et al., 2022). Soil DOM is mainly composed of amino acids, polysaccharides, organic acids, and low molecular weight components (Caricasole et al., 2010). Although accounting for only 2% of total soil organic matter (SOM), DOM plays a central role as a microbial substrate source, in soil aggregation, in carbon storage, and in the supply of plant nutrients (Nebbioso and Piccolo, 2013). The composition and quantity of DOM in soils is susceptible to many natural and anthropogenic factors, microbial processes and soil properties (e.g., soil pH, C/N ratio). It is likely that the complex chemical composition of soil DOM is stongly affected by environmental variations and soil composition. The release of DOM due to these environmental factors may chemically alter soil nutrient cycles, as well as transport carbon with pore water through leaching and surface run-off, leading to carbon losses. Soil freeze–thaw cycles (FTCs) are a prominent aspect of global change in high-latitude ecosystems, and have a significant effect on soil DOM release and chemical changes (Gao et al., 2021).

Reduced snow cover at high latitudes leads to an increase in the frequency and severity of soil FTCs (Gao et al., 2021). FTCs cause repeated fluctuations in the soil water phase and in soil temperature. These changes lead to microbial cell death, soil aggregate disruption and exposure of exchange sites, which in turn leads to increases in soil DOM concentration, thus affecting sequestration and stability of SOC (Oztas and Fayetorbay, 2003; Tan et al., 2014). In the past decade, most of the research on DOM in the context of freeze–thaw was limited to the amount of DOM (Hentschel et al., 2008; Watanabe et al., 2019). Only a few studies have reported that freeze –thaw changed the chemical composition of DOM. They found that FTC reduced the polysaccharide content and increased the lignin content of DOM in forest soils (Schmitt et al., 2008; Wu et al., 2017).

Laboratory incubation studies furthermore indicated that 4–93% of soil derived DOM can be decomposed by microorganisms (Kalbitz et al., 2003). So, a more comprehensive understanding of DOM chemical composition is necessary to identify the organic compounds that control the susceptibility of DOM to microbial degradation (Ward and Cory, 2015). Among analytical techniques for determining DOM chemistry, pyrolysis–gas chromatography/mass spectrometry (Py-GC/MS) is an effective tool that can directly offer information on molecular structures (Rombolà et al., 2022). This technique adopts a thermal pulse method to break macromolecules into fragments which are suitable for GC. The technique is semiquantitative. Due to selectivity of the GC column and the large number of compounds after pyrolysis, it is difficult to use specific internal standards for quantitative analysis. Nevertheless, it can be used for assessing changes in the relative abundance of different macromolecular components in DOM (Kaal et al., 2017).

Soil microorganisms, in particular, are vital mediators of degrading organic matter and together with DOM biodegradability partly determine biogeochemical fluxes (Ward and Cory, 2015). Furthermore, specific compound metabolism has been linked to specific microbial groups (e.g., lignin decomposition, nitrogen fixation; Cottrell and Kirchman, 2000). That linkage implies that the microbiota in the natural environment have the ability to selectively use different carbon substrates (Judd et al., 2006). For instance, *copiotrophic* bacteria (e.g., *Proteobacteria*, *Acidobacteria*) tend to favor decomposition of protein components in DOM (Yang et al., 2020), whereas soil bacterial activity can be inhibited by high concentrations of organic acids (Lehmann et al., 2020). Fungi also play an important role in DOM degradation due to their broad enzymatic capabilities and substrate preferences (Glassman et al., 2018). Fungi are regarded as the main organisms producing DOM, because their activity results in an incomplete degradation of SOM (Zsolnay, 2003). FTCs improve C and N availability, i.e., they cause significant increase in dissolved organic carbon (DOC) and dissolved organic nitrogen (DON) contents, thereby affecting the composition and function of the soil microbial community (Feng et al., 2007). Preferential utilization

of labile C and N by surviving microorganisms can alter decomposition and substrate preferences, enabling a shift from complex plant polymers to low molecular weight compounds found in necromass (Perez-Mon et al., 2020). The fate of DOM-microbe interactions in freeze–thaw environments has not been elucidated. Except for the physical release of DOM, it is necessary to know which particular microbial assemblages dominate DOM production and which microbiota are reduced.

The objectives of this study are to explore the changes in DOM chemical composition under FTCs treatments, as well as the microbial degradation mechanism and their controlling factors. We hypothesize that: (1) FTCs can increase the bioavailability of DOM and can promote the conversion of aromatic compounds into polysaccharides; (2) FTCs increase the activity of dominant species and thus increase mineralization, while eliminating sensitive microorganisms, both of which jointly dominate DOC production.

2. Materials and methods

2.1. Study area

The Greater Khingan Mountains in Inner Mongolia (Northeast China), are located at the southern edge of the Eurasian permafrost region. This region is characterized by a cold temperate continental monsoon climate with long cold winters and short warm summers, and a fragile permafrost that is sensitivity to global warming. The annual average air temperature is −5.4°C and the mean annual precipitation is 580 mm. The annual average temperature has been increasing 0.32°C/ 10a over the past 60 year (1960–2020; Liu et al., 2020). Compared with the daily average temperature during the spring freeze–thaw period in the past 20 years (2000–2020), the frequency of FTCs increased significantly (Supplementary Figure S1a). The study sites were selected in the Greater Khingan Mountains Forest Ecosystem Research Station (121°30′-121°31′ E, 50°49′-50°51′ N, altitude 800–1,000 m). The zonal vegetation is mainly composed of Dahurian larch (*Larix gmelinii*) mixed with a number of White birches (*Betula platyphylla*) in the arbor layer, with dense *Rhododendron dauricum* and *Ledum palustre* in the herbaceous layer (Gao et al., 2019). The dominant soil types are Cambic and Leptic Umbrisols (WRB; Lützow et al., 2006). The average thickness of the organic layer is 10 cm and the average thickness of the active layer is about 60 cm. The soil is slightly acidic, with a pH in the range 6.10–6.52 (Table 1).

2.2. Soil sampling and FTCs experimental design

In September 2020, three 20 m × 20 m square plots were established in mixed forests dominated by White birch and Dahurian larch. Plot were separated by a buffer zone of 20 m wide. In each plot, after removing the litter layer, the soils were sampled at 10 points along the diagonal line at the depths of 0–10 cm and 50–60 cm using a soil auger (Φ = 4 cm). The sample soils from each plot at the same depth were mixed uniformly into a composite sample. Those samples were sieved with a 2-mm mesh to remove roots, gravels, etc. and subsamples were air-dried at 40°C to determine pH, soil moisture, total nitrogen (TN), and total carbon (TC). The remaining subsamples were used to conduct a simulation FTCs experiment.

The daily air temperature measured at the Forest Ecosystem Research Station in the Greater Khingan Mountains showed that freeze–thaw mostly occurs from mid-March to mid-April. The average temperature during that period range from −10°C to 5°C, and the number of freeze–thaw cycles in that period varies between 2 and 6 (Supplementary Figure S1b). Accordingly, the simulation FTCs experiment was designed with three treatments: (i) constant culture at 5°C (CK), (ii) two freeze–thaw cycles (2FTCs), and (iii) six freeze–thaw cycles (6FTCs). The incubation temperature was

TABLE 1 Soil properties under freeze–thaw treatment at different depths.

Soil layer	Treatment†	TC (gkg^{-1})	TN (gkg^{-1})	C/N	NH_4^+-N ($mgkg^{-1}$)	NO_3^--N ($mgkg^{-1}$)	pH
0–10 cm	CK	130.67 ± 1.69	7.04 ± 0.06	18.57 ± 0.11	10.22 ± 0.70	0.42 ± 0.05	6.52 ± 0.25
	2FTC	128.49 ± 0.22	6.93 ± 0.22	18.58 ± 0.59	9.54 ± 1.53	0.22 ± 0.05	6.25 ± 0.10
	6FTC	127.37 ± 1.07	7.37 ± 0.17	18.18 ± 0.84	11.95 ± 0.56	0.44 ± 0.14	6.11 ± 0.05
	F	2.09	1.89	0.15	1.47	1.77	1.74
	P	0.2	0.23	0.86	0.3	0.25	0.25
50–60 cm	CK	164.88 ± 2.79	8.00 ± 0.08	20.61 ± 0.17	10.25 ± 0.47	0.36 ± 0.04a	6.10 ± 0.02
	2FTC	161.42 ± 3.00	7.42 ± 0.03	21.74 ± 0.45	6.51 ± 0.75	0.05 ± 0.02b	6.18 ± 0.03
	6FTC	166.21 ± 0.99	7.78 ± 0.21	21.39 ± 0.53	9.64 ± 2.55	0.08 ± 0.03b	6.15 ± 0.05
	F	1.03	4.86	1.98	1.66	10.64	1.21
	P	0.41	0.06	0.22	0.27	0.01	0.36

†CK, 2FTC, 6FTC are cultured at 5°C, freeze–thaw treatment of 2 cycles and 6 cycles, respectively. TC, total carbon; TN, total nitrogen. Lowercase letters represent significant difference among freeze–thaw treatments at each soil depth in one-way ANOVA ($p < 0.05$).

set to −10°C, −5°C, 2°C, and 5°C in sequence for one freeze–thaw cycle (Supplementary Figure S1c). Each temperature was cultured for 6 days and 2 days under the scenarios of 2FTCs and 6FTCs, respectively. Homogenized soil samples of 100 g each were put into 250 mL glass Mason jars with the moisture adjusted to 60% of water filled pore space (WFPS). All samples were pre-incubated at 5°C for 7 days to allow microorganisms to acclimatize. All samples were incubated for 55 days.

2.3. Measurement of soil chemical properties

A subsample of each air-dried soil sample was milled with a ball mill (MM400, Retsch GmbH, Haan, Germany) and then analyzed for soil TC and TN concentrations using an elemental analyzer (Vario EL III, Elementar, Hanau, Germany). Fresh soil samples were extracted with 2.0 M KCl (soil: solution = 1:10 w/v) and inorganic nitrogen (NH_4^+-N, NO_3^--N) concentrations were measured using a continuous flow autoanalyzer (AA3, SEAL, Germany). Water-extractable DOC was determined using a TOC analyzer (Liqui TOCII, Elementar, Germany). Soil pH (soil: water = 1:2.5 w/v) was determined using a portable pH meter (Mettler Toledo FE28, Switzerland).

2.4. Molecular characterization of DOM by analytical pyrolysis

Pyrolysis-gas chromatography–mass spectrometry analysis was conducted for DOM characterization using a multi-shot pyrolyzer (PY-3030D, Frontier Laboratories, Fukushima, Japan) attached to an Agilent 7,890 N gas chromatograph (GC) connected to an Agilent 7000B mass spectrometer (MS). The GC was equipped with an elastic Quartz Capillary Column (HP-5MS, 30 m × 0.25 mm × 0.25 μm inner diameter). DOM-containing extracts were lyophilized using a freeze-dryer (ALPHA1-4/Ldplus, Germany). Lyophilized samples (10 mg) were weighted into a small stainless-steel cup and inserted into a pre-heated furnace. The pyrolysis temperature was set as follows: 50°C for 1 min then rose to 600°C, from 50°C to 250°C at a rate of 50°C min^{-1} and 250°C to 600°C at 30°C min^{-1}. The GC oven was heated from 40°C to 290°C at 4°C min^{-1}. The MS was operated in electron ionization mode (70 eV, scanning 50–550 m/z) with GC injector at 230°C and ion source temperature at 280°C. The carrier gas was helium (1.2 mL min^{-1}). The relative proportion of each compound was equal to the percentage of the peak area of each product to the total peak area.

2.5. DNA extraction, amplification, and Miseq sequencing

Genomic DNA was extracted from 0.25 g of homogenized soil sample, using a PowerSoil DNA Isolation Kit (MoBio Laboratories, Inc., Carlsbad, CA, USA) according to the manufacturer's recommendation. The V3-V4 regions of bacterial 16S rRNA were amplified using the primer sets 515F (5′-GTGCCAGCM GCCGCGG-3′) and 907R (5′-CCGTCAATTCMTTTRAGTTT-3′; Gao et al., 2015). The primers ITS1F (5′-CTTGGTCATTT AGAGGAAGTAA-3′) and ITS2R (5′-GCTGCGTTCTTC ATCGATGC-3′) were used to amplify fungal ITS genes (Orgiazzi et al., 2012). A qPCR was performed in a TransGen AP221-02 reaction system containing 4 μL (2×) FastPfu Buffer, 0.8 μL Primer (5 μM), 2 μL dNTPs (2.5 mM), 0.4 μL FastPfu Polymerase, 10 ng template DNA, 0.2 μL BSA, and mixed 20 μL ultra-pure water. The purified PCR products were subjected to paired-end sequencing using a Miseq Illumina platform (Majorbio Bio-Pharm Technolggy Co., Ltd., Shanghai, China). The raw sequences were analyzed using a Trimmomatic v.0.32 (Bolger et al., 2014). We used FLASH to assemble paired-end clean reads which were merged as original tags, and the sequences with quality scores below 20 and/or lengths less than 150 bp were removed (Magoč and Salzberg, 2011). The denoised and sorted raw sequences were clustered into operational taxonomic units (OTUs) by using the UPARSE method with 97% identity threshold (Caporaso et al., 2010; Edgar, 2013). The taxonomic identities of the fungi and bacteria were assigned using RDP Classifier 2.2 (Wang et al., 2007) based on comparison with the UNITE 7.2 (Kõljalg et al., 2013) database and SILVA 128 (Quast et al., 2012), respectively. To compensate for different sequencing depths, samples were rarefied to an even depth of 69,041 reads for 16S and 45,955 for ITS sequences.

2.6. Data analysis

All analyses were conducted in R software (version 4.1.1). Before statistical analysis, the normality of the data was checked by a Shapior–Wilk's test and the homogeneity of variance was test by a Levene's test. One-way analysis of variance (ANOVA) combined with a Turkey's HSD test were used to compare the means in test parameters between FTCs treatments. A Student's t-test was performed to analyze the differences in abiotic and biotic properties at two soil depths (0–10 cm and 50–60 cm). Principal component analysis (PCA) was performed to evaluate changes in the DOM chemical compositions under different FTCs treatments with the 'factoextra' package. After calculating the Bray-Curtis distances, principal coordinates analysis (PCoA) was used to analyze the dissimilarity of soil microbial composition at the OTU level. Differences in the microbial communities between FTC treatments were further tested by analysis of similarities (ANOSIM) and non-parametric multivariate analysis (ADONIS) using the 'vegan' package. Mantel tests were implemented to interpret the significance of soil properties on the microbial compositions. The relationships between response variables and explanatory variables under FTCs treatments were tested using ordinary least squares (OLS). Co-occurrence networks were inferred for each soil layer (9 samples per layer) between the bacteria OTUs (abundance >0.05%) and DOM molecules based

on the Spearman correlation matrix using the 'psych' package. To reduce network complexity, only individual DOM molecules with their abundance >0.01%, a correlation coefficient $|R| > 0.8$, and $p < 0.001$ were retained for further analysis. The co-occurrence networks were visualized by the Cytoscape 3.9.0 software. Redundancy analysis (RDA), following a Monte Carlo permutation test (999 permutations) was conducted to evaluate the influence of soil chemical parameters on bacterial community composition under FTCs treatment. The soil chemical parameters were first examined to reduce the collinearity by eliminating predictors with VIF > 10. A forward selection procedure on environmental variables were performed by the 'ordiR2step' function in the vegan package to select the descriptors that affect bacterial community composition. Forward selection is a type of stepwise regression that starts with an empty model and adds variables one by one. In each forward step, it adds the one variable that gives the single best improvement to the regression model and this process is carried out by an automatic procedure.

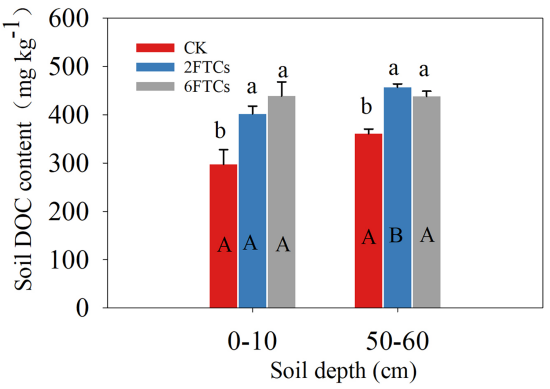

FIGURE 1
DOC contents in the 0–10 cm and 50–60 cm soil layer under different freeze–thaw cycles. CK was cultured at 5°C, while 2FTC, and 6FTC represent freeze–thaw treatment of 2 cycles and 6 cycles, respectively. Different lowercase letters indicate significant differences within each freeze–thaw treatment (p<0.05). Different capital letters showed significant differences between the two soil dephts (p<0.05).

3. Results

3.1. Soil chemical properties

Soil TC, TN, C/N, pH and NH_4^+-N were not significantly different among the FTCs treatments. However, FTCs significantly decreased the subsurface soil NO_3^-N content (Table 1). FTCs significantly increased the soil DOC content in the surface and subsurface layers from 35.04 to 47.57% and from 26.73 to 21.44%, respectively (Figure 1).

3.2. DOM chemical properties

A total of 121 pyrolytic compounds were identified from DOM extracts (Table S1). The pyrolytic compounds were grouped according to their chemical similarity and probable origin in the following categories: alkanes, alkenes, aromatics, polyaromatics (PAH), nitrogen compounds (N-comps), phenols, polysaccharides (Polysac), and fatty acid methyl esters (Me; Figure 2). In both surface (0–10 cm) and subsuface soils (50–60 cm), the relative abundance of polysaccharides (41.94%) was the highest, followed by that of aromatics (29.32%). The relative abundances of PAH, N-comps, and phenols were less than 10%. The relative abundances of alkanes and alkenes were less than 1.6% (Figure 2). The relative abundance of Me was two orders of magnitude lower than that of other compounds (Figure 2). In topsoil, the 6FTCs treatment significantly increased the relative abundance of polysaccharides by 40.76%, and increased the relative abundance of Me by 1.35-folds (Figure 2A). Similarly, the 2FTCs treatment significantly increased the relative abundance of alkanes by 2.32-folds and increased the relative abundance of phenols by 61.94% (Figure 2A). On the contrary, the relative abundance of aromatics significantly decreased from 30.53 to 17.04% under the 6FTCs treatment (Figure 2A). In the deeper soil layer, only Me showed a significant difference under FTCs treatments (Figure 2B), i.e., increased by 2.25-folds under the 6FTCs treatment.

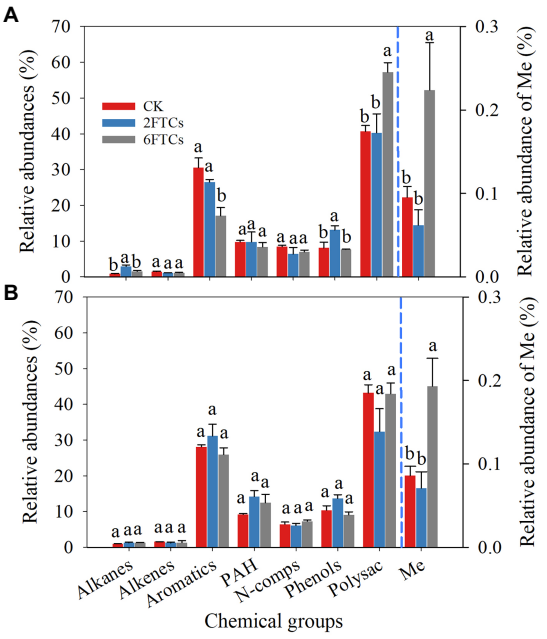

FIGURE 2
Relative abundances of 8 chemicals groups of DOM in different freeze–thaw cycles. **(A)** 0–10 cm; **(B)** 50–60 cm. PAH, Polyaromatics; N-comps, N-compounds; Polysac, Polysaccharide compounds; Me, Fatty acid methy esters. CK, 2FTC, and 6FTC represent cultured at 5°C, freeze–thaw treatment of 2 cycles and 6 cycles, respectively. The relative abundances of Me are represented on the right axis. Different lowercase letters indicate significant differences within each freeze–thaw treatment (p<0.05).

In the topsoil, 2FTCs significantly increased the relative abundance of long-chain alkanes (C25-C32), while 6FTCs only significantly increased C23 and C25 (Figure 3A). In the deeper soil, 2FTCs tended to significantly increase long-chain alkanes (C26–C30), but 6FTCs significantly increased short-chain alkanes (C13–C19; Figure 3B). The n-alkane series exhibited even-to-odd predominance, which was not affected by FTCs treatments (Figures 3C, D). A homolog series of n-fatty acids (C16–C22) was found in all DOM extracts samples with a maximum at C16 (Figures 3E, F). C18 was increased significantly in surface soil under 6FTCs treatment, and C16 and C18 also increased considerably in deep soil (Figures 3E, F).

The PCA of DOM chemical components for each soil layer is presented in Supplementary Figure S2. The first two axes of the PCA explained 37.16 and 22.37% of the overall variation for the topsoil (Supplementary Figure S2a). For deep soils, the first two axes explained 65.76% of the variation (PC1 = 44.53%; PC2 = 21.23%) in DOM chemical composition (Supplementary Figure S2c). PCA sample scores showed that 6FTCs had a greater impact on DOM chemical compositions in both surface and deep soils (Supplementary Figures S2b, d) than 2FTCs.

3.3. Microbial community structure and diversity

PCoA analysis indicated that FTCs had significant effects on bacterial community but not fungal community in the two soil layers (Figure 4). The dominant phyla of bacteria were *Proteobacteria* (48.60%) and *Actinobancteria* (24.55%; Supplementary Figures S3a, b). At class level, *Gemmaproteobacteria*, *Actinobacteria, and Alphaproteobacteria,* accounted for 71.89% of the total bacterial abundance (Figures 5A, B). In the topsoil, FTCs significantly increased the relative abundance of

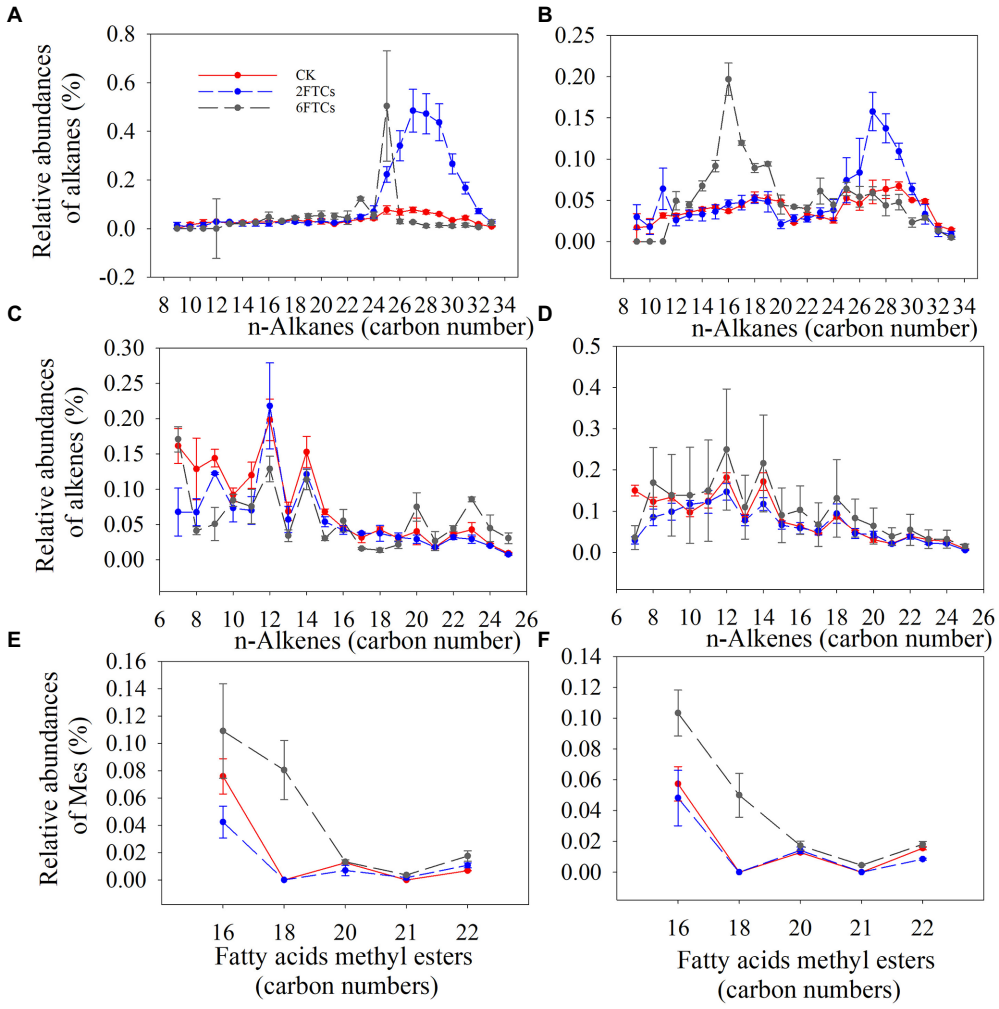

FIGURE 3
Distribution and relative abundance of Alkane in **(A)** 0–10 cm; **(B)** 50–60 cm. Alkene in **(C)** 0–10 cm; **(D)** 50–60 cm. Fatty acid methyl esters in **(E)** 0–10 cm; **(F)** 50–60 cm. CK, 2FTCs, and 6FTCs represent culture at 5°C, two freeze–thaw cycles, and six freeze–thaw cycles, respectively.

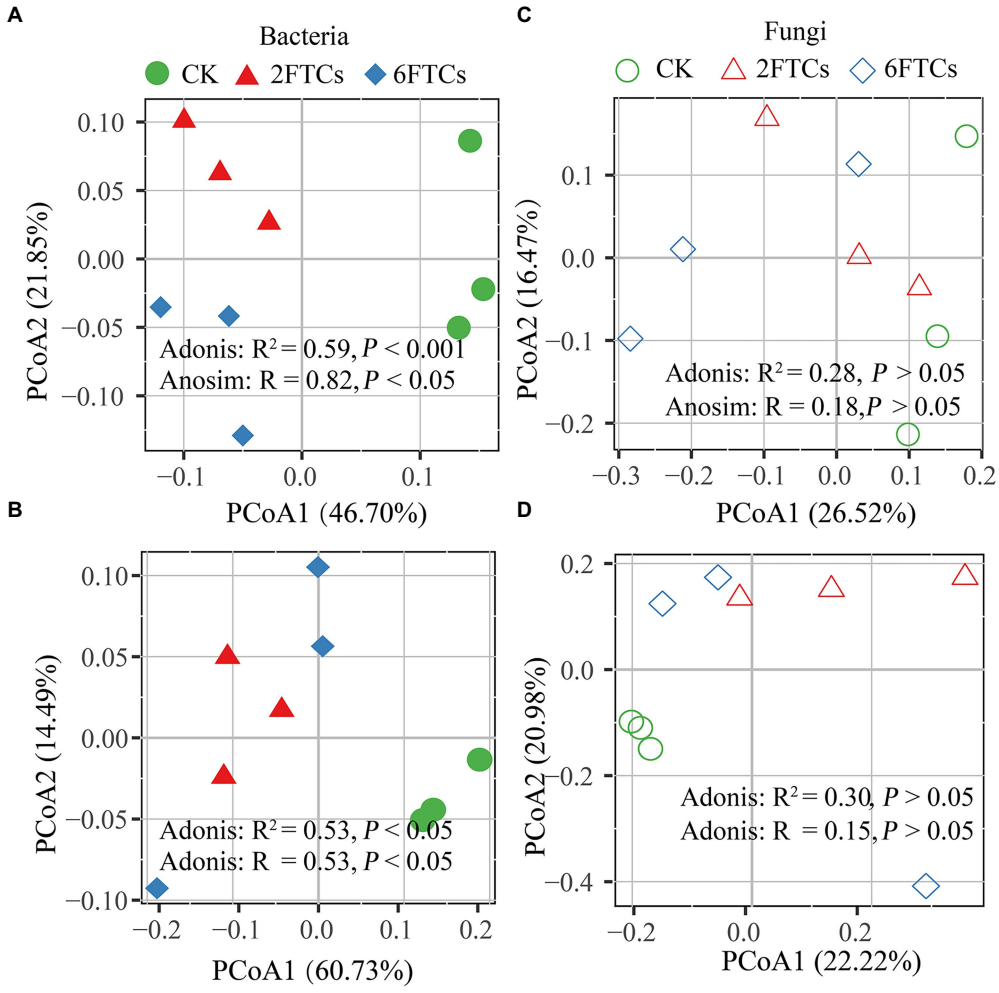

FIGURE 4
PCoA analysis of the bacterial community composition in **(A)** 0–10 cm; **(B)** 50–60 cm, and the fungal community composition in **(C)** 0–10 cm; **(D)** 50–60 cm based on the Bray-Curtis distance in different freeze–thaw treatments. CK, 2FTCs, and 6FTCs represent culture at 5°C, two freeze–thaw cycles, and six freeze–thaw cycles, respectively.

Gemmaproteobacteria, but clearly decreased the relative abundances of *Alphaproteobacteria*, *Thermoleophilia*, *Acidobacteriae*, *Gemmatimonadetes*, and *Planctomycetes* (Figure 5A). Similarly, in addition to the decreased bacterial classes listed above, FTCs also significantly reduced the relative abundances of *Bacilli* and *KD4-96* in deep soil (Figure 5B). FTCs significantly changed the Shannon index of bacterial alpha diversity regardless of the soil layer (Supplementary Figure S4). For soil fungi community, the dominant fungal phyla in the control soils were *Ascomycota* (87.01%) and *Basidiomycota* (5.55%; Supplementary Figures S3c, d), and the dominant classes were *Leotiomycetes* (45.66%), followed by *Dothideomycetes* (17.58%; Figures 5C, D). Fungal community composition did not respond sensitively to FTCs, either at the phylum or class level (Figures 5C, D, Supplementary Figures S3c, d). Furthermore, the Shannon index of fungi did not change significantly under FTCs treatment (Supplementary Figure S4).

3.4. Association between soil chemical properties and microbial community

In the topsoil, aromatic compounds were positively correlated with *Actinobacteria*, *Alphaproteobacteria* and *Thermoleophilia*, but were negatively correlated with *Gammaproteobacteria*. Alkenes were positively associated with *Alphaproteobacteria* and *Acidobacteriae*, whereas Alkanes showed a negative correlation with *Acidobacteriae*. At OTU level, OTU7008, which belonged to members of *KD4-96, Chloroflexi*, showed strong positive (blue lines) correlation with recalcitrant compounds (Aromatics and PAH; Figure 6B). OTU9140 affiliated to members of *Solibacterales*, *Acidobacteriae*, and was significantly negatively correlated with long-chain alkanes (A26–A32; Figure 6B). Pyridine (N2), as a small nitrogen-containing compound, showed a significant positive association with *Acidobacteriae* (OTU8237, OTU9421, OTU8187, OTU7455, and OTU7472; Figure 6B). A Mantel test revealed that

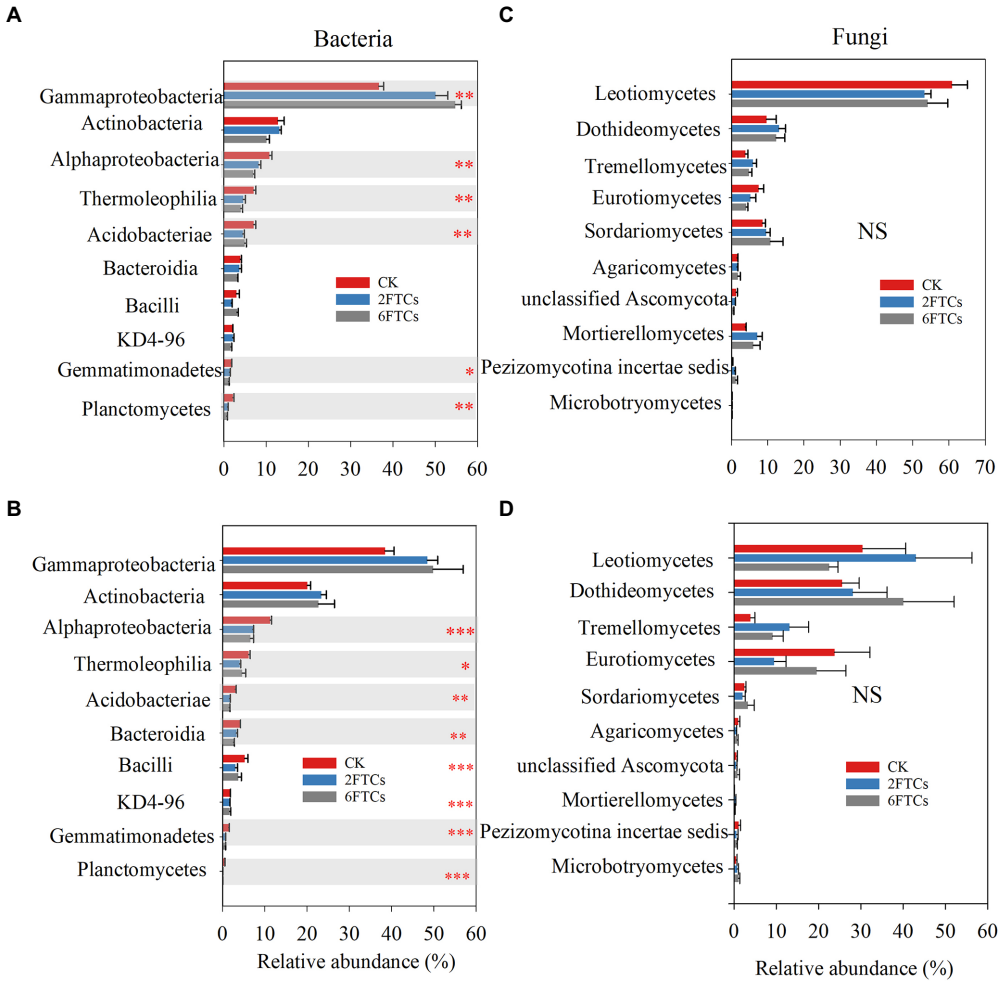

FIGURE 5
The relative abundance of dominant bacterial class in **(A)** 0–10 cm; **(B)** 50–60 cm, and fungal class in **(C)** 0–10 cm; **(D)** 50–60cm in response to different freeze–thaw cycles. CK, 2FTCs, and 6FTCs represent culture at 5°C, two freeze–thaw cycles, and six freeze–thaw cycles, respectively. *, **, *** indicate significant differences at $p<0.05$, < 0.01, and <0.001, respectively. NS means no significant difference between the two soil depths.

soil DOC, alkenes and aromatics were the dominant factors which independently affected the bacterial community structure (Table S2). In deep soil, *Bacteroidia* were negatively related to Me. *Actinobacteria* had a positive correlation with PAH (Figure 6C). Specifically, OTU9000 affiliated to *Actinobacteria*, was significantly positively correlated with PAH (Figure 6D). OTU10619, belonging to *Gammaproteobacteria*, was a keystone member with the highest degree of connectivity. It was significantly negatively correlated with short-chain alkanes and aromatics (Figure 6D). A Mantel test further indicated that DOC and Me were the most important factors affecting the bacterial community composition (Supplementary Table S2). RDA analysis revealed that DOM chemical compounds explained 92.51% of the bacterial community changes in the topsoil among FTCs treatments (Figure 7A). But in deep soil the DOC quantity, combined with soil pH, explained 63.50% of bacterial community variation (Figure 7B). Furthermore, bivariate regression showed that DOC increments were significantly positively correlated with *Gammaproteobacteria* increments under FTCs treatment (Figure 8).

4. Discussion

4.1. The effects of FTCs on soil dissolved C and N concentrations

FTCs notably increased soil DOC contents in the top and deep soil layers. Increased DOC contents are largely attributed to disruption of soil aggregates, lysis of microbial cells, and the reduction of microbial immobilization capacity (Gao et al., 2021). It was reported that about half of the microbial populations died when the temperature drops below −10°C during the first FTCs (Sawicka et al., 2010). That lysis of soil microbial cells directly leads to the spillover of micro-molecules such as phosphate, amino acids, and polysaccharides (Larsen et al., 2002; Meisner et al., 2021). Also, repeated expansion and contraction of soil aggregates causes disintegration of soil macroaggregates, resulting in the release of dissolved C and N (Gao et al., 2018). Furthermore, the decreased of immobilization ability of microorganisms to

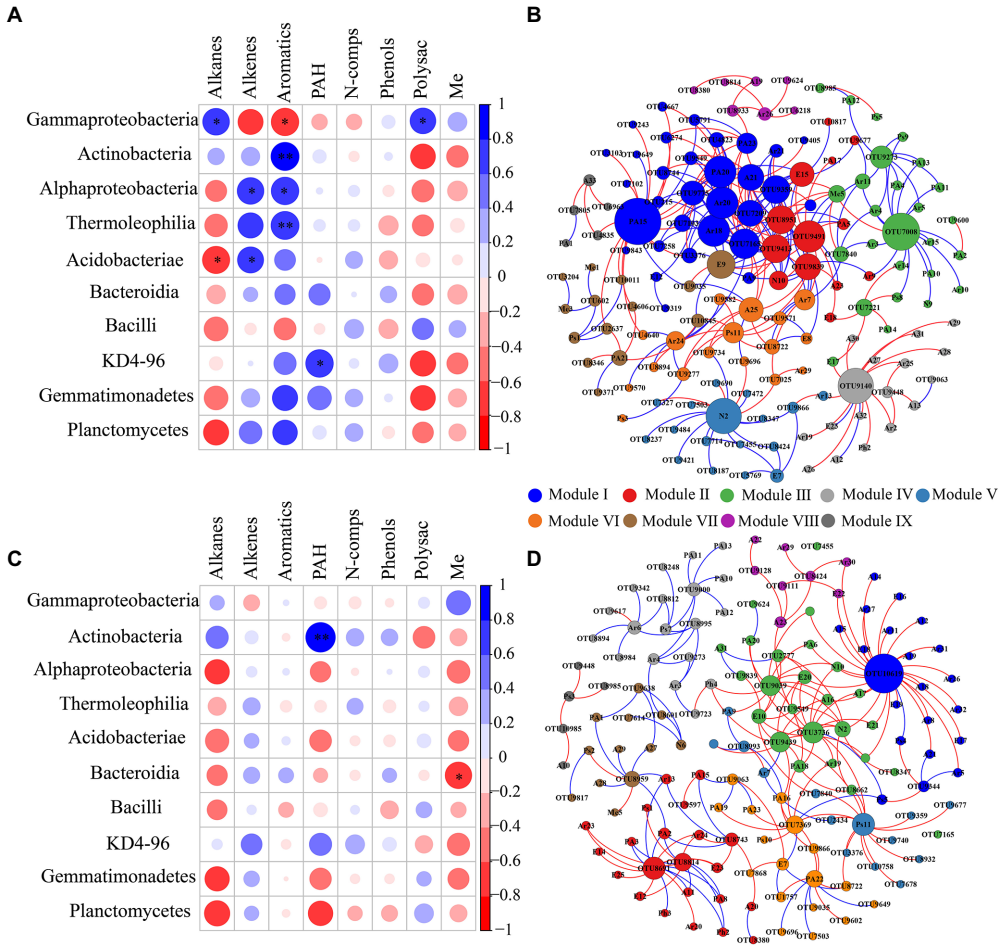

FIGURE 6
Spearman correlation analysis of the relative abundance of DOM chemical composition with the relative abundance of dominant bacterial class in **(A)** 0–10 cm; **(C)** 50–60 cm; *, **, *** indicate significant differences at $p<0.05$, < 0.01, and <0.001, respectively. The occurrence network between total DOM molecules and microbial OTUs based on Spearman correlation ($|r|>0.8$, $p<0.001$) in **(B)** 0–10 cm; **(D)** 50–60 cm. Positive and negative correlations are represented in blue and red lines, respectively. The size of each node is proportional to the number of connections. The color of the node indicates the module of the cluster. Abbreviations for DOM molecules are as in Supplementary Table S1.

unstable substrates in FTCs environments indirectly led to DOC increase. Surviving soil microorganisms may utilize these active substrates triggered by FTCs, thereby enhancing soil C mineralization ability (Nielsen et al., 2001). The significant reduction in soil NO_3^--N found in deep soils can be related to the finding that soil denitrifying bacteria are more tolerant to freezing temperatures than nitrobacteria (Smith et al., 2010). Denitrification recovers rapidly once the soil starts to thaw, resulting in NO_3^--N consumption (Müller et al., 2003).

4.2. Effects of FTCs on the chemical composition of DOM

FTCs significantly decreased the relative abundance of aromatic compounds, but increased the relative abundance of polysaccharides, phenols and Me in the topsoil layer. FTCs thus tended to increase the biodegradability of DOM, which confirmed the first hypothesis. Indeed, the hydrophilic neutral fraction of DOM, represented by high contents of organic acids, carbohydrates, and proteins typically enhances biodegradability. In contrast, hydrophobic and aromatic structures reduce DOM biodegradability possibly due to their recalcitrance or inhibition of enzymatic activity (Marschner and Kalbitz, 2003).

The alkanes (A8–A33) and alkenes (E7–E25) made up only a small fraction of the pyrolysis products. Long-chain (A25–A33) alkanes and alkenes are typically derived from microbial lipids and plant biopolymers (e.g., cutin, suberin), while mid-chain and short-chain aliphatics can be attribute to microbial polymers (Buurman et al., 2007a; Vancampenhout et al., 2010). The latter may also represent parts of longer chains, that were degraded by microorganisms (chain-length shortening; Buurman et al., 2007b; Yassir and Buurman, 2012). So the release of long-chain alkanes by FTCs in our experiment may be attributed to the rupture of

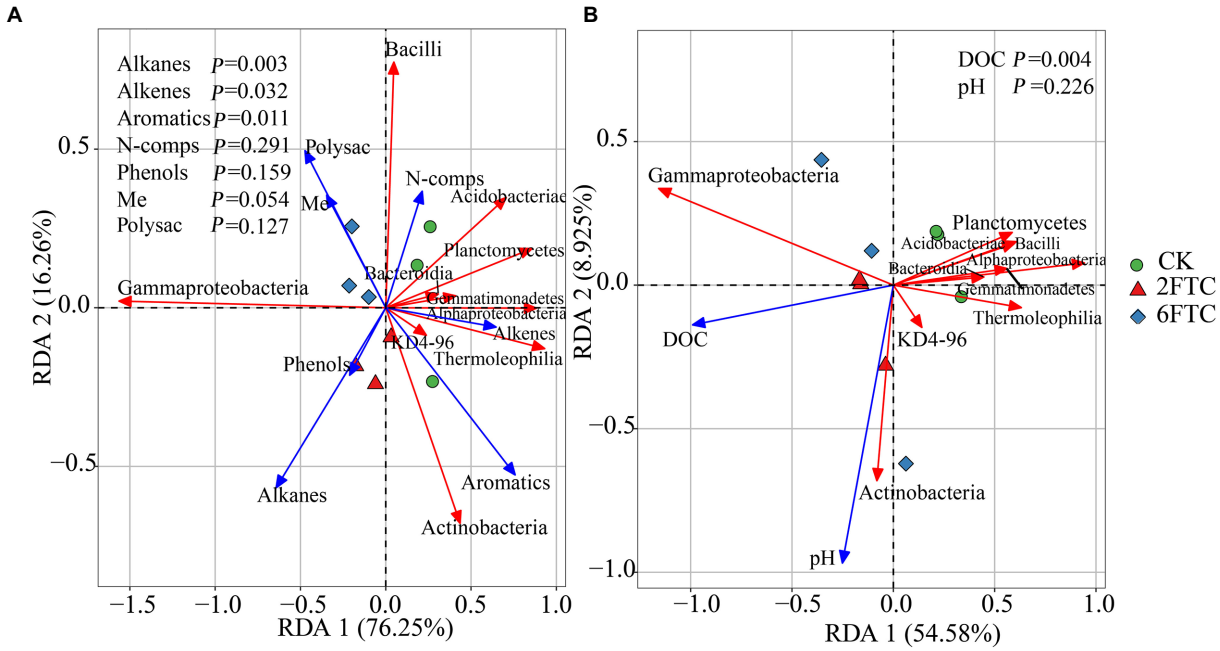

FIGURE 7
Redundancy analysis (RDA) of soil bacterial community composition at the class level as a function of soil chemical properties in **(A)** 0–10 cm and **(B)** 50–60 cm. Blue vectors represent trajectories of soil chemical properties; Red vectors represent dominant bacterial classes. Soil chemical parameters with significant effects on major bacterial classes were assessed at the 0.05 level (Monte Carlo tests with 999 permutations).

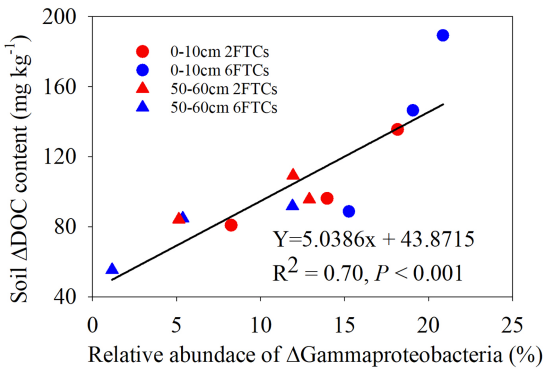

FIGURE 8
The bivariate relationship between relative abundance of △*Gammaproteobacteria* and soil △DOC contents in freeze–thaw cycles.

microbial cell membranes, while the variation of short chains might be attributed to variation in microbial decomposition. Fatty acid methyl esters (Me) can be generated by the cyclization of fatty acids (FAs) and phenolic hydroxyl groups (Musadji and Geffroy-Rodier, 2020). Generally, long-chain FAs ascribe to microbial degradation or microbial lipid fragments (Sousa et al., 2007), and FAs are typically combined with long-chain fatty alcohols or sterols to form esters (Chiavari et al., 1994). Me dominated by C16 and C18, are indicative for autochthonous (bacterial) origin (Kaal et al., 2017). Therefore, the increase in Me abundance particularly C16 and C18 caused by FTCs in our experiment could be related to microbial degradation or the accumulation of microbial lipid biomacromolecules (Figure 3). The interaction of aliphatic compounds and microorganisms is detailed in Section 4.3.

Aromatic compounds formed during the pyrolysis process mainly originate from proteins, lignin, carbohydrates and charcoal (Yassir and Buurman, 2012). Benzene (Ar1) and toluene (Ar2) were the most abundant products in our pyrograms (≈21% of total relative abundance). The potential source of benzene is mainly condensed aromatic structures, while possible sources of toluene and other alkylbenzenes (Ar19–Ar32) are proteins, tyrosine-containing peptide, lignin, and polysaccharides (De la Rosa et al., 2012). The increase of benzene content in SOM may be a caused by accelerated aliphatic cyclization or humification of organic matter (Ayuso et al., 1996). Thus, the decrease of benzene content in DOM extracts under FTCs treatment may be due to the reduced DOM humification, suggesting that the DOC released by FTCs was more conducive to microbial mining rather than C sequestration.

Some pyrolytic compounds were phenol and alkyl phenols, which can be derived from any phenolic precursor such as tannin, lignin, proteinaceous biomass, and carbohydrates (Vancampenhout et al., 2009). However, since phenols are less fractions of the pyrograms of polycarboxylic acids and proteins, the high proportion of phenols in DOM pyrolysis products may be related to degraded lignin (Rombolà et al., 2022). High methoxyphenol contents have been reported in DOM, which were considered to be the degradation products of lignin-derived DOM

(Neff et al., 2006). Degradation of lignin is an important factor controlling DOM production in litter decomposition (Kalbitz et al., 2006). So we suggest that the increase in phenol yields by FTCs may be related to lignin degradation.

FTCs increased the relative proportion of polysaccharides in the topsoil layer. Polysaccharides that can be derived from microorganisms include benzofuran, furfural, and methylfuran while residuals from plant material include levoglucosan and levomannosan (Verde et al., 2008; Vancampenhout et al., 2010). Only microbial derived polysaccharide compounds were found in our study. These compounds are characterized by long residence times due to their recycling in SOM decomposition and humification (Gleixner et al., 2002).

N-compounds identified upon pyrolysis in soils generally originate from peptides, amino acids, and proteins. Pyridine (N2) and its derivatives (N6) can be formed by microbial degradation of plant lignin and other phenolic substances under NH_3-enriched conditions (Buurman et al., 2007b). Because of the ubiquity of peptides and amino acids, N-compounds cannot be specifically attributed to plant and microbial sources, with the exception of chitin (De la Rosa et al., 2012). Peptides tend to adsorb on the surface of soil minerals, thereby improving their stability (Lützow Lützow et al., 2006). PAH are generally considered to be products of charred materials (e.g., charcoal), or the result of cyclization reactions during pyrolysis (Rumpel et al., 2007; Rombolà et al., 2022). However, PAH represented by methylnaphthalene (PA8) and phenanthrene (PA18) are produced by the cleavage of unsaturated fatty acids (Wagner et al., 2018). FTCs had no significant effect on their relative abundance, which may be related to their recalcitrance.

4.3. Association between DOM composition and bacterial community

To date, several researches have aimed to elucidate the link between DOM chemical diversity and bacterial community diversity (Underwood et al., 2019; Ling et al., 2022). The interactions between them can be bidirectional. Specifically, (i) DOM chemical composition has been shown to drive the composition of the microbial community, and in general more complex DOM molecules correspond to relatively high microbial abundance and diversity (Li et al., 2018). It has been demonstrated that a diversity of DOM molecules trigger an increase in bacterial diversity, especially the abundance of *Betaproteobacteria*, *Gammaproteobacteria* and *Flavobacteria* has been related to complex DOM profiles (Zhao et al., 2019) (ii) Specific microbial communities moreover have been reported to exclusively decompose specific DOM substrates (Ling et al., 2022). e.g., *Nitrospira* was negatively associated with DOM recalcitrant components, revealing that *Nitrospira* specialized in decomposing this type of DOM components (Li et al., 2018). The latter can be interpreted by the affinities of soil microorganisms for individual organic matter molecules. Considering the utilization of DOM by soil microorganisms, higher microbial biomass resulted in less C substrates remaining after consumption, especially in closed systems without substrate replenishment. A negative correlation has been used in the literature to represent the affinity of microorganisms for C compounds in a closed system without continuous substrates supplied (Ling et al., 2022). Although the FTCs treatment lead to a continuous release of DOM, which can be considered equivalent to providing a semi-continuous substrates for microorganisms, we propose that a positive correlation between soil microorganisms and DOM molecules in our experiments also indicates that microorganisms preferentially utilize individual DOM compounds.

The phylum *Proteobacteria* have been identified as *copiotrophic* groups (r-strategy), which are not only significantly positively correlated with labile DOM components (particularly polysaccharide compounds), but also with recalcitrant DOM compounds (Ho et al., 2017; Li et al., 2019). *Gammaproteobacteria* have been reported to play a crucial role in the degradation of alkanes and labile carbohydrates under aerobic conditions (Martirani-Von Abercron et al., 2016). This contradiction needs detailed taxonomy at lower phylogenetic levels. For example, *Gammaprotepbacteria* (i.e., *Pseudomonadales*, *Enterobacteriales*) and *Betaproteobacteria* (i.e., *Burkholderiales*) responded quickly to unstable C (Di Lonardo et al., 2017), whereas the class of *Alphaproteobacteria* (i.e., *Sphingomonadalaes*) is inclined to utilize both labile sucrose and recalcitrant compounds (Goldfarb et al., 2011). *Microvirga* (*Alphaproteobacteria*) aggregated in heavy metal contaminated and nutrient-deficient soils (Igwe and Vannette, 2019). Thus, the changes in the corresponding C components associated with *Proteobacteria* suggested that this group can adapt to C substrates with diverse chemical recalcitrance (Goldfarb et al., 2011). It was also confirmed by the results of the utilization of different DOM components by *Gammaproteobacteria* and *Alphaprobacteria* in our study. In addition, *Gammaproteobacteria* were observed to have a strong positive correlation with DOC increment under FTCs treatment (Figure 8). The release of active components (e.g., DOC, DON) after each freeze–thaw is comparable to a repeated addition of multiple substrates in soil priming experiments. We proposed that repeated multiple substrates release under FTCs treatments may increase the living microbial activity and SOM mineralization rate when the substrate input of each repeated addition exceeds the threshold amount required for soil priming effects (Fontaine et al., 2003).

The phylum *Actinobacteria*, which is a representative of *oligotrophic* bacteria (K- strategy), could grow slowly in low-nutrient soils and tolerate harsh conditions. The relative proportion of *Actinobacteria* did not change significantly after FTCs treatment. Classes of *Actinobacteria* and *Thermoleophilia* both belonged to the phylum *Actinobacteria*, and *Actinobacteria* were not affected by freeze–thaw, while the relative abundance of *Thermoleophilia* was significantly reduced under FTC treatment. One possible reason is that *Thermoleophilia* are

known to be moderately thermophilic and oil-loving (Foesel et al., 2016). Recent studies have indicated *Actinobacteria* and *Thermoleophilia* correlated to both unstable components (particularly carbohydrates) and recalcitrant compounds *via* co-metabolism (Ling et al., 2022). Our findings only support the idea that these two classes could decompose aromatic DOM compounds. *Actinobacteria* are vital saprophytes capable of using a range of enzymes (protease, xylanase, β-glucosidase, celluases, and other ligninolytic enzymes) to decompose rhizodeposits and litter (Kabuyah et al., 2012; Manivasagan et al., 2013). These enzymes can act on amino sugars, polysaccharides, cellulose, and lignin, so that both small molecules and complex substances can be degraded (Lladó et al., 2016; Zhang et al., 2017). Moreover, the hyphal-like morphology of *Actinobacteria* facilitate their contact with organic matter and promote C mineralization. *Actinobacteria* are considered as one of the key contributors to SOC mineralization in biochar-amended soils (Jeewani et al., 2020).

Several *oligotrophic* species in the phylum *Acidobacteria* function to decompose relatively stable and recalcitrant SOM (Hale et al., 2019). *Acidobacteriae* were observed to be negatively associated with alkanes. Lipids, including alkanes and alkenes, represent a varied group of amphiphilic and hydrophobic biomolecules whose physicochemical attributes allow them to present diverse cellular functions. They can be act as components of cell membranes and membrane proteins, and can also be active intercellular and intracellular signaling molecules in energy homeostasis. Under FTCs treatment, the relative abundance of *Acidobacteriae* significantly decreased but the relative proportion of long-chain alkanes increased remarkably. Therefore, we suggest that the release of long-chain alkanes may be related to the lysis of cell membranes of *Acidobacteriae*. This was also confirmed by the results of OTU9140 (affiliated to *Solibacterales*, *Acidobacteria*) and long-chain alkanes (A26-A32) in the co-occurrence network (Figure 6B). *Acidobacteriae* were closely associated with alkenes, particularly the short-chain alkenes (E9, E12; Figures 6A, B). Short-chain aliphatic compounds generally originate from microbial polymers or from microbial degradation of longer chains (Yassir and Buurman, 2012; Nam et al., 2021). Thus, *Acidobacteriae* may play a role in degrading alkenes. *Bacilli* (*Firmicutes*), KD4-96 (*Chloroflexi*), *Gemmatimonadetes*, and *Planctomycetes* were not correlated with the DOM chemical compositions, except that KD4-96 was positively correlated with PAH in topsoil. This might be due to the reduction of microbial activity of low-abundance microorganisms under freeze–thaw environments. Another possible reason is that the DOM bioavailability has not changed significantly under the freeze–thaw treatment. Thus, in topsoil, the chemical composition of DOM is one of the major drivers of bacterial community variability under FTCs treatment, while in deeper soil, DOC content is the main factor shaping the bacterial community.

The co-occurrence network pattern reflected that taxa of the same class, or even same genus, presented diverse correlations with DOM components of distinct chemical characteristics. Specifically, there are the same associations for different categories of DOM compounds, or opposite associations for the same class of molecules. For instance, *Acidobacteriae* showed negative and positive correlations with alkanes and alkenes, respectively. *Alphaproteobacteria* presented positive correlations with alkenes and aromatic compounds. A module in the co-occurrence network corresponds to a functional cluster, indicating that microorganisms in that cluster utilize similar DOM molecules (Deng et al., 2012). OTUs in the same module may indicate that these microorganisms occupy similar ecological niches (Zhou et al., 2010). The network modules thus support the finding that specific microorganisms degrade specific substrates (Li et al., 2018).

5. Conclusion

This study demonstrated that freeze and thaw increased DOC contents in the surface and deep soils of a boreal forest, and changed the chemical composition of DOM. In particular, the decrease of aromatic compounds and the increase of alkanes, phenols, polysaccharides, and Me in the topsoil indicated an improvement of DOM bioavailability. Soil bacteria were more sensitive to FTCs as compared to fungi, manifesting as a decrease in relative abundance of bacterial classes (e.g., *Alphaproteobacteria*, *Thermoleophilia*, and *Acidobacteriae*) and a decrease in Shannon index. Furthermore, *Gammaproteobacteria* were dominant in freeze and thaw cycled soils and most likely induced the largest contribution to DOC release. The interactions between DOM molecules and bacterial communities showed that specific microorganisms can degrade specific substrates. In the topsoil, DOM chemical composition shaped bacterial communities, with labile C correlated to *Gammaproteobacteria*, and more recalcitrant C associated with other bacteria (e.g., *Actinobacteria*, *Alphaproteobacteria*, and *Thermoleophilia*). In comparison, DOC contents were more likely to explain the variation of bacterial communities in the deeper soil layers. This study thus provides new insights into DOC accumulation, transformation, and stability in boreal forest soils under scenarios of intensified freezing–thawing.

Data availability statement

The datasets presented in this study can be found in online repositories. The names of the repository/repositories and accession number(s) can be found at: https://www.ncbi.nlm.nih.gov/, PRJNA899719 and PRJNA900157.

Author contributions

YY, HF, and SC: conceptualization, methodology, data curation, and writing—review and editing. YY: software and writing—original draft preparation. YY, YG, YL, YZ, and FS:

formal analysis. HF: investigation and project administration. HF and SC: resources and supervision. KV: visualization. HF and KV: funding acquisition. All authors contributed to the article and approved the submitted version.

Funding

This research was funded by the Second Tibetan Plateau Scientific Expedition and Research Program (STEP) (No. 2019QZKK1003), the Strategic Priority Research Program of the Chinese Academy of Sciences (Nos. XDA28130100, XDA200204020, and XDA23060401), National Natural Science Foundation of China (Nos. 41977041 and 31770558), the "Thousand Talents Plan" Project of High-End Innovative Talents of Qinghai Province (No. TTPPHEITQP-2019), and Key research and development projects of Ji'an Science and Technology Bureau (20111ZDF04022). KV received an FWO sabbatical bench fee (number VWH-E1313-SAB/22/016).

Conflict of interest

The authors declare that the research was conducted in the absence of any commercial or financial relationships that could be construed as a potential conflict of interest.

Publisher's note

Supplementary material

The Supplementary material for this article can be found online at: https://www.frontiersin.org/articles/10.3389/fmicb.2022.1012512/full#supplementary-material

References

Ayuso, M., Hernandez, T., Garcia, C., and Pascual, J. (1996). Biochemical and chemical-structural characterization of different organic materials used as manures. *Bioresour. Technol.* 57, 201–207. doi: 10.1016/0960-8524(96)00070-3

Bolger, A. M., Lohse, M., and Usadel, B. (2014). Trimmomatic: a flexible trimmer for Illumina sequence data. *Bioinformatics* 30, 2114–2120. doi: 10. 1093/bioinformatics/btu170, doi: 10.1093/bioinformatics/btu170

Buurman, P., Peterse, F., and Almendros Martin, G. (2007a). Soil organic matter chemistry in allophanic soils: a pyrolysis-GC/MS study of a costa Rican andosol catena. *Eur. J. Soil Sci.* 58, 1330–1347. doi: 10.1111/j.1365-2389.2007.00925.x

Buurman, P., Schellekens, J., Fritze, H., and Nierop, K. (2007b). Selective depletion of organic matter in mottled podzol horizons. *Soil Biol. Biochem.* 39, 607–621. doi: 10.1016/j.soilbio.2006.09.012

Caporaso, J. G., Kuczynski, J., Stombaugh, J., Bittinger, K., Bushman, F. D., Costello, E. K., et al. (2010). QIIME allows analysis of high-throughput community sequencing data. *Nat. Methods* 7, 335–336. doi: 10.1038/nmeth.f.303

Caricasole, P., Provenzano, M., Hatcher, P., and Senesi, N. (2010). Chemical characteristics of dissolved organic matter during composting of different organic wastes assessed by ^{13}C CPMAS NMR spectroscopy. *Bioresour. Technol.* 101, 8232–8236. doi: 10.1016/j.biortech.2010.05.095

Chiavari, G., Torsi, G., Fabbri, D., and Galleti, G. (1994). Comparative study of humic substances in soil using pyrolytic techniques and other conventional chromatographic methods. *Analyst* 119, 1141–1150. doi: 10.1039/AN9941901141

Cottrell, M. T., and Kirchman, D. L. (2000). Natural assemblages of marine proteobacteria and members of the Cytophaga-Flavobacter cluster consuming low- and high-molecular-weight dissolved organic matter. *Appl. Environ. Microbiol.* 66, 1692–1697. doi: 10.1128/AEM.66.4.1692-1697.2000

De la Rosa, J. M., Faria, S. R., Varela, M. E., Knicker, H., González-Vila, F. J., González-Pérez, J. A., et al. (2012). Characterization of wildfire effects on soil organic matter using analytical pyrolysis. *Geoderma* 191, 24–30. doi: 10.1016/j.geoderma.2012.01.032

Deng, Y., Jiang, Y.-H., Yang, Y., He, Z., Luo, F., and Zhou, J. (2012). Molecular ecological network analyses. *BMC Bioinformatics* 13, 1–20. doi: 10.1186/1471-2105-13-113

Di Lonardo, D., De Boer, W., Gunnewiek, P. K., Hannula, S., and Van der Wal, A. (2017). Priming of soil organic matter: chemical structure of added compounds is more important than the energy content. *Soil Biol. Biochem.* 108, 41–54. doi: 10.1016/j.soilbio.2017.01.017

Edgar, R. C. (2013). UPARSE: highly accurate OTU sequences from microbial amplicon reads. *Nat. Methods* 10, 996–998. doi: 10.1038/nmeth.2604

Feng, X., Nielsen, L. L., and Simpson, M. J. (2007). Responses of soil organic matter and microorganisms to freeze–thaw cycles. *Soil Biol. Biochem.* 39, 2027–2037. doi: 10.1016/j.soilbio.2007.03.003

Foesel, B. U., Geppert, A., Rohde, M., and Overmann, J. (2016). Parviterribacter kavangonensis gen. Nov., sp. nov. and Parviterribacter multiflagellatus sp. nov., novel members of Parviterribacteraceae fam. Nov. within the order Solirubrobacterales, and emended descriptions of the classes Thermoleophilia and Rubrobacteria and their orders and families. *Int. J. Syst. Evol. Microbiol.* 66, 652–665. doi: 10.1099/ijsem.0.000770

Fontaine, S., Mariotti, A., and Abbadie, L. (2003). The priming effect of organic matter: a question of microbial competition? Soil biol. *Biochemist* 35, 837–843. doi: 10.1016/S0038-0717(03)00123-8

Gao, D., Bai, E., Yang, Y., Zong, S., and Hagedorn, F. (2021). A global meta-analysis on freeze-thaw effects on soil carbon and phosphorus cycling. *Soil Biol. Biochem.* 159:108283. doi: 10.1016/j.soilbio.2021.108283

Gao, W., Yao, Y., Gao, D., Wang, H., Song, L., Sheng, H., et al. (2019). Responses of N_2O emissions to spring thaw period in a typical continuous permafrost region of the Daxing'an mountains, Northeast China. *Atmos. Environ.* 214:116822. doi: 10.1016/j.atmosenv.2019.116822

Gao, D., Zhang, L., Liu, J., Peng, B., Fan, Z., Dai, W., et al. (2018). Responses of terrestrial nitrogen pools and dynamics to different patterns of freeze-thaw cycle: a meta-analysis. *Glob. Chang. Biol.* 24, 2377–2389. doi: 10.1111/gcb.14010

Gao, W., Zhao, W., Yang, H., Yang, H., Chen, G., Luo, Y., et al. (2015). Effects of nitrogen addition on soil inorganic N content and soil N mineralization of a cold-temperate coniferous forest in great Xing'an mountains. *Acta Ecol. Sin.* 35, 130–136. doi: 10.1016/j.chnaes.2015.07.003

Glassman, S. I., Weihe, C., Li, J., Albright, M. B., Looby, C. I., Martiny, A. C., et al. (2018). Decomposition responses to climate depend on microbial community composition. *Proc. Natl. Acad. Sci. U. S. A.* 115, 11994–11999. doi: 10.1073/pnas.1811269115

Gleixner, G., Poirier, N., Bol, R., and Balesdent, J. (2002). Molecular dynamics of organic matter in a cultivated soil. *Org. Geochem.* 33, 357–366. doi: 10.1016/S0146-6380(01)00166-8

Goldfarb, K. C., Karaoz, U., Hanson, C. A., Santee, C. A., Bradford, M. A., Treseder, K. K., et al. (2011). Differential growth responses of soil bacterial taxa to carbon substrates of varying chemical recalcitrance. *Front. Microbiol.* 2:94. doi: 10.3389/fmicb.2011.00094

Hale, L., Feng, W., Yin, H., Guo, X., Zhou, X., Bracho, R., et al. (2019). Tundra microbial community taxa and traits predict decomposition parameters of stable, old soil organic carbon. *ISME J.* 13, 2901–2915. doi: 10.1038/s41396-019-0485-x

Hentschel, K., Borken, W., and Matzner, E. (2008). Repeated freeze–thaw events affect leaching losses of nitrogen and dissolved organic matter in a forest soil. *J. Plant Nutr. Soil Sci.* 171, 699–706. doi: 10.1002/jpln.200700154

Ho, A., Di Lonardo, D. P., and Bodelier, P. L. (2017). Revisiting life strategy concepts in environmental microbial ecology. *FEMS Microbiol. Ecol.* 93:fix006. doi: 10.1093/femsec/fix006

Igwe, A. N., and Vannette, R. L. (2019). Bacterial communities differ between plant species and soil type, and differentially influence seedling establishment on serpentine soils. *Plant Soil* 441, 423–437. doi: 10.1007/s11104-019-04135-5

Jeewani, P. H., Gunina, A., Tao, L., Zhu, Z., Kuzyakov, Y., Van Zwieten, L., et al. (2020). Rusty sink of rhizodeposits and associated keystone microbiomes. *Soil Biol. Biochem.* 147:107840. doi: 10.1016/j.soilbio.2020.107840

Judd, K. E., Crump, B. C., and Kling, G. W. (2006). Variation in dissolved organic matter controls bacterial production and community composition. *Ecology* 87, 2068–2079. doi: 10.1890/0012-9658(2006)87[2068:VIDOMC]2.0.CO;2

Kaal, J., Cortizas, A. M., and Biester, H. (2017). Downstream changes in molecular composition of DOM along a headwater stream in the Harz mountains (Central Germany) as determined by FTIR, pyrolysis-GC–MS and THM-GC–MS. *J. Anal. Appl. Pyrolysis* 126, 50–61. doi: 10.1016/j.jaap.2017.06.025

Kabuyah, R. N., van Dongen, B. E., Bewsher, A. D., and Robinson, C. H. (2012). Decomposition of lignin in wheat straw in a sand-dune grassland. *Soil Biol. Biochem.* 45, 128–131. doi: 10.1016/j.soilbio.2011.10.014

Kalbitz, K., Kaiser, K., Bargholz, J., and Dardenne, P. (2006). Lignin degradation controls the production of dissolved organic matter in decomposing foliar litter. *Eur. J. Soil Sci.* 57, 504–516. doi: 10.1111/j.1365-2389.2006.00797.x

Kalbitz, K., Schmerwitz, J., Schwesig, D., and Matzner, E. (2003). Biodegradation of soil-derived dissolved organic matter as related to its properties. *Geoderma* 113, 273–291. doi: 10.1016/S0016-7061(02)00365-8

Kõljalg, U., Nilsson, R. H., Abarenkov, K., Tedersoo, L., Taylor, A. F., Bahram, M., et al. (2013). Towards a unified paradigm for sequence-based identification of fungi. *Mol. Ecol.* 22, 5271–5277. doi: 10.1111/mec.12481

Larsen, K. S., Jonasson, S., and Michelsen, A. (2002). Repeated freeze–thaw cycles and their effects on biological processes in two arctic ecosystem types. *Appl. Soil Ecol.* 21, 187–195. doi: 10.1016/S0929-1393(02)00093-8

Lehmann, J., Hansel, C. M., Kaiser, C., Kleber, M., Maher, K., Manzoni, S., et al. (2020). Persistence of soil organic carbon caused by functional complexity. *Nat. Geosci.* 13, 529–534. doi: 10.1038/s41561-020-0612-3

Li, Y., Nie, C., Liu, Y., Du, W., and He, P. (2019). Soil microbial community composition closely associates with specific enzyme activities and soil carbon chemistry in a long-term nitrogen fertilized grassland. *Sci. Total Environ.* 654, 264–274. doi: 10.1016/j.scitotenv.2018.11.031

Li, X.-M., Sun, G.-X., Chen, S.-C., Fang, Z., Yuan, H.-Y., Shi, Q., et al. (2018). Molecular chemodiversity of dissolved organic matter in paddy soils. *Environ. Sci. Technol.* 52, 963–971. doi: 10.1021/acs.est.7b00377

Ling, L., Luo, Y., Jiang, B., Lv, J., Meng, C., Liao, Y., et al. (2022). Biochar induces mineralization of soil recalcitrant components by activation of biochar responsive bacteria groups. *Soil Biol. Biochem.* 172:108778. doi: 10.1016/j.soilbio.2022.108778

Liu, M., Feng, F., Cai, T., and Tang, S. (2020). Soil microbial community response differently to the frequency and strength of freeze–thaw events in a *Larix gmelinii* Forest in the Daxing'an mountains, China. *Front. Microbiol.* 11:1164. doi: 10.3389/fmicb.2020.01164

Lladó, S., Žifčáková, L., Větrovský, T., Eichlerová, I., and Baldrian, P. (2016). Functional screening of abundant bacteria from acidic forest soil indicates the metabolic potential of Acidobacteria subdivision 1 for polysaccharide decomposition. *Biol. Fertil. Soils* 52, 251–260. doi: 10.1007/s00374-015-1072-6

Lützow, M. V., Kögel-Knabner, I., Ekschmitt, K., Matzner, E., Guggenberger, G., Marschner, B., et al. (2006). Stabilization of organic matter in temperate soils: mechanisms and their relevance under different soil conditions–a review. *Eur. J. Soil Sci.* 57, 426–445. doi: 10.1111/j.1365-2389.2006.00809.x

Magoč, T., and Salzberg, S. L. (2011). FLASH: fast length adjustment of short reads to improve genome assemblies. *Bioinformatics* 27, 2957–2963. doi: 10.1093/bioinformatics/btr507

Manivasagan, P., Venkatesan, J., Sivakumar, K., and Kim, S.-K. (2013). Production, characterization and antioxidant potential of protease from Streptomyces sp. MAB18 using poultry wastes. *BioMed Res. Int.* 2013, 2013:496586. doi: 10.1155/2013/496586

Marschner, B., and Kalbitz, K. (2003). Controls of bioavailability and biodegradability of dissolved organic matter in soils. *Geoderma* 113, 211–235. doi: 10.1016/S0016-7061(02)00362-2

Martirani-Von Abercron, S.-M., Pacheco, D., Benito-Santano, P., Marín, P., and Marqués, S. (2016). Polycyclic aromatic hydrocarbon-induced changes in bacterial community structure under anoxic nitrate reducing conditions. *Front. Microbiol.* 7:1775. doi: 10.3389/fmicb.2016.01775

Meisner, A., Snoek, B. L., Nesme, J., Dent, E., Jacquiod, S., Classen, A. T., et al. (2021). Soil microbial legacies differ following drying-rewetting and freezing-thawing cycles. *ISME J.* 15, 1207–1221. doi: 10.1038/s41396-020-00844-3

Müller, C., Kammann, C., Ottow, J., and Jäger, H. J. (2003). Nitrous oxide emission from frozen grassland soil and during thawing periods. *J. Plant Nutr. Soil Sci.* 166, 46–53. doi: 10.1002/jpln.200390011

Musadji, N. Y., and Geffroy-Rodier, C. (2020). Simple derivatization–gas chromatography–mass spectrometry for fatty acids profiling in soil dissolved organic matter. *Molecules* 25:5278. doi: 10.3390/molecules25225278

Nam, S., Alday, J. G., Kim, M., Kim, H., Kim, Y., Park, T., et al. (2021). The relationships of present vegetation, bacteria, and soil properties with soil organic matter characteristics in moist acidic tundra in Alaska. *Sci. Total Environ.* 772:145386. doi: 10.1016/j.scitotenv.2021.145386

Nebbioso, A., and Piccolo, A. (2013). Molecular characterization of dissolved organic matter (DOM): a critical review. *Anal. Bioanal. Chem.* 405, 109–124. doi: 10.1007/s00216-012-6363-2

Neff, J., Finlay, J., Zimov, S., Davydov, S., Carrasco, J., Schuur, E., et al. (2006). Seasonal changes in the age and structure of dissolved organic carbon in Siberian rivers and streams. *Geophys. Res. Lett.* 33:L23401. doi: 10.1029/2006GL028222

Nielsen, C. B., Groffman, P. M., Hamburg, S. P., Driscoll, C. T., Fahey, T. J., and Hardy, J. P. (2001). Freezing effects on carbon and nitrogen cycling in northern hardwood forest soils. *Soil Sci. Soc. Am. J.* 65, 1723–1730. doi: 10.2136/sssaj2001.1723

Orgiazzi, A., Lumini, E., Nilsson, R. H., Girlanda, M., Vizzini, A., Bonfante, P., et al. (2012). Unravelling soil fungal communities from different Mediterranean land-use backgrounds. *PLoS One* 7:e34847. doi: 10.1371/journal.pone.0034847

Oztas, T., and Fayetorbay, F. (2003). Effect of freezing and thawing processes on soil aggregate stability. *Catena* 52, 1–8. doi: 10.1016/S0341-8162(02)00177-7

Perez-Mon, C., Frey, B., and Frossard, A. (2020). Functional and structural responses of arctic and alpine soil prokaryotic and fungal communities under freeze-thaw cycles of different frequencies. *Front. Microbiol.* 11:982. doi: 10.3389/fmicb.2020.0098

Quast, C., Pruesse, E., Yilmaz, P., Gerken, J., Schweer, T., Yarza, P., et al. (2012). The SILVA ribosomal RNA gene database project: improved data processing and web-based tools. *Nucleic Acids Res.* 41, D590–D596. doi: 10.1093/nar/gks1219

Rombolà, A. G., Torri, C., Vassura, I., Venturini, E., Reggiani, R., and Fabbri, D. (2022). Effect of biochar amendment on organic matter and dissolved organic matter composition of agricultural soils from a two-year field experiment. *Sci. Total Environ.* 812:151422. doi: 10.1016/j.scitotenv.2021.151422

Rumpel, C., González-Pérez, J. A., Bardoux, G., Largeau, C., Gonzalez-Vila, F. J., and Valentin, C. (2007). Composition and reactivity of morphologically distinct charred materials left after slash-and-burn practices in agricultural tropical soils. *Org. Geochem.* 38, 911–920. doi: 10.1016/j.orggeochem.2006.12.014

Sawicka, J. E., Robador, A., Hubert, C., Jørgensen, B. B., and Brüchert, V. (2010). Effects of freeze–thaw cycles on anaerobic microbial processes in an Arctic intertidal mud flat. *ISME J.* 4, 585–594. doi: 10.1038/ismej.2009.140

Schmitt, A., Glaser, B., Borken, W., and Matzner, E. (2008). Repeated freeze–thaw cycles changed organic matter quality in a temperate forest soil. *J. Plant Nutr. Soil Sci.* 171, 707–718. doi: 10.1002/jpln.200700334

Smith, J., Wagner-Riddle, C., and Dunfield, K. (2010). Season and management related changes in the diversity of nitrifying and denitrifying bacteria over winter and spring. *Appl. Soil Ecol.* 44, 138–146. doi: 10.1016/j.apsoil.2009.11.004

Sousa, D. Z., Pereira, M. A., Stams, A. J., Alves, M. M., and Smidt, H. (2007). Microbial communities involved in anaerobic degradation of unsaturated or saturated long-chain fatty acids. *Appl. Environ. Microbiol.* 73, 1054–1064. doi: 10.1128/AEM.01723-06

Tan, B., Wu, F.-Z., Yang, W.-Q., and He, X.-H. (2014). Snow removal alters soil microbial biomass and enzyme activity in a Tibetan alpine forest. *Appl. Soil Ecol.* 76, 34–41. doi: 10.1016/j.apsoil.2013.11.015

Underwood, G. J., Michel, C., Meisterhans, G., Niemi, A., Belzile, C., Witt, M., et al. (2019). Organic matter from Arctic Sea-ice loss alters bacterial community structure and function. *Nat. Clim. Chang.* 9, 170–176. doi: 10.1038/s41558-018-0391-7

Vancampenhout, K., De Vos, B., Wouters, K., Van Calster, H., Swennen, R., Buurman, P., et al. (2010). Determinants of soil organic matter chemistry in maritime temperate forest ecosystems. *Soil Biol. Biochem.* 42, 220–233. doi: 10.1016/j.soilbio.2009.10.020

Vancampenhout, K., Wouters, K., De Vos, B., Buurman, P., Swennen, R., and Deckers, J. (2009). Differences in chemical composition of soil organic matter in natural ecosystems from different climatic regions–a pyrolysis–GC/MS study. *Soil Biol. Biochem.* 41, 568–579. doi: 10.1016/j.soilbio.2008.12.023

Verde, J., Buurman, P., Martínez-Cortizas, A., Macías, F., and Camps Arbestain, M. (2008). NaOH-extractable organic matter of andic soils from Galicia (NW Spain) under different land use regimes: a pyrolysis GC/MS study. *Eur. J. Soil Sci.* 59, 1096–1110. doi: 10.1111/j.1365-2389.2008.01082.x

Wagner, T. V., Mouter, A. K., Parsons, J. R., Sevink, J., van der Plicht, J., and Jansen, B. (2018). Molecular characterization of charcoal to identify adsorbed SOM and assess the effectiveness of common SOM-removing pretreatments prior to radiocarbon dating. *Quat. Geochronol.* 45, 74–84. doi: 10.1016/j.quageo.2017.10.006

Wang, Q., Garrity, G. M., Tiedje, J. M., and Cole, J. R. (2007). Naive Bayesian classifier for rapid assignment of rRNA sequences into the new bacterial taxonomy. *Appl. Environ. Microbiol.* 73, 5261–5267. doi: 10.1128/AEM.00062-07

Ward, C. P., and Cory, R. M. (2015). Chemical composition of dissolved organic matter draining permafrost soils. *Geochim. Cosmochim. Acta* 167, 63–79. doi: 10.1016/j.gca.2015.07.001

Watanabe, T., Tateno, R., Imada, S., Fukuzawa, K., Isobe, K., Urakawa, R., et al. (2019). The effect of a freeze–thaw cycle on dissolved nitrogen dynamics and its relation to dissolved organic matter and soil microbial biomass in the soil of a northern hardwood forest. *Biogeochemistry* 142, 319–338. doi: 10.1007/s10533-019-00537-w

Wu, H., Xu, X., Cheng, W., Fu, P., and Li, F. (2017). Antecedent soil moisture prior to freezing can affect quantity, composition and stability of soil dissolved organic matter during thaw. *Sci. Rep.* 7, 6380–6312. doi: 10.1038/s41598-017-06563-8

Yang, J., Duan, Y., Zhang, R., Liu, C., Wang, Y., Li, M., et al. (2020). Connecting soil dissolved organic matter to soil bacterial community structure in a long-term grass-mulching apple orchard. *Ind. Crop. Prod.* 149:112344. doi: 10.1016/j.indcrop.2020.112344

Yassir, I., and Buurman, P. (2012). Soil organic matter chemistry changes upon secondary succession in Imperata grasslands, Indonesia: a pyrolysis–GC/MS study. *Geoderma* 173-174, 94–103. doi: 10.1016/j.geoderma.2011.12.024

Zhang, Q., Liang, G., Guo, T., He, P., Wang, X., and Zhou, W. (2017). Evident variations of fungal and actinobacterial cellulolytic communities associated with different humified particle-size fractions in a long-term fertilizer experiment. *Soil Biol. Biochem.* 113, 1–13. doi: 10.1016/j.soilbio.2017.05.022

Zhao, Z., Gonsior, M., Schmitt-Kopplin, P., Zhan, Y., Zhang, R., Jiao, N., et al. (2019). Microbial transformation of virus-induced dissolved organic matter from picocyanobacteria: coupling of bacterial diversity and DOM chemodiversity. *ISME J.* 13, 2551–2565. doi: 10.1038/s41396-019-0449-1

Zhou, J., Deng, Y., Luo, F., He, Z., Tu, Q., and Zhi, X. (2010). Functional molecular ecological networks. *MBio* 1, e00169–e00110. doi: 10.1128/mBio.00169-10, Functional molecular ecological networks

Zsolnay, A. (2003). Dissolved organic matter: artefacts, definitions, and functions. *Geoderma* 113, 187–209. doi: 10.1016/S0016-7061(02)00361-0

frontiers | Frontiers in Microbiology

TYPE Original Research
PUBLISHED 06 April 2023
DOI 10.3389/fmicb.2023.1131836

OPEN ACCESS

EDITED BY
Yu Luo,
Zhejiang University, China

REVIEWED BY
Dong Wang,
Henan University, China
Muhammad Auwal,
Kano University of Science and Technology, Nigeria

*CORRESPONDENCE
Yufu Hu
✉ huyufu@sicau.edu.cn

†These authors have contributed equally to this work

SPECIALTY SECTION
This article was submitted to Terrestrial Microbiology, a section of the journal Frontiers in Microbiology

RECEIVED 26 December 2022
ACCEPTED 17 March 2023
PUBLISHED 06 April 2023

CITATION
Shu X, Hu Y, Liu W, Xia L, Zhang Y, Zhou W, Liu W and Zhang Y (2023) Linking between soil properties, bacterial communities, enzyme activities, and soil organic carbon mineralization under ecological restoration in an alpine degraded grassland. *Front. Microbiol.* 14:1131836. doi: 10.3389/fmicb.2023.1131836

Linking between soil properties, bacterial communities, enzyme activities, and soil organic carbon mineralization under ecological restoration in an alpine degraded grassland

Xiangyang Shu[1†], Yufu Hu[1*†], Weijia Liu[1,2†], Longlong Xia[3], Yanyan Zhang[1], Wei Zhou[1], Wanling Liu[1] and Yulin Zhang[4]

[1]College of Resources, Sichuan Agricultural University, Chengdu, China, [2]Chengdu Academy of Agriculture and Forestry Sciences, Chengdu, China, [3]Institute for Meteorology and Climate Research (IMK-IFU), Karlsruhe Institute of Technology, Karlsruhe, Baden-Wurttemberg, Germany, [4]Department of Civil Engineering, The University of Hong Kong, Pokfulam, Hong Kong SAR, China

Soil organic carbon (SOC) mineralization is affected by ecological restoration and plays an important role in the soil C cycle. However, the mechanism of ecological restoration on SOC mineralization remains unclear. Here, we collected soils from the degraded grassland that have undergone 14years of ecological restoration by planting shrubs with *Salix cupularis* alone (SA) and, planting shrubs with *Salix cupularis* plus planting mixed grasses (SG), with the extremely degraded grassland underwent natural restoration as control (CK). We aimed to investigate the effect of ecological restoration on SOC mineralization at different soil depths, and to address the relative importance of biotic and abiotic drivers of SOC mineralization. Our results documented the statistically significant impacts of restoration mode and its interaction with soil depth on SOC mineralization. Compared with CK, the SA and SG increased the cumulative SOC mineralization but decreased C mineralization efficiency at the 0–20 and 20–40cm soil depths. Random Forest analyses showed that soil depth, microbial biomass C (MBC), hot-water extractable organic C (HWEOC), and bacterial community composition were important indicators that predicted SOC mineralization. Structural equal modeling indicated that MBC, SOC, and C-cycling enzymes had positive effects on SOC mineralization. Bacterial community composition regulated SOC mineralization *via* controlling microbial biomass production and C-cycling enzyme activities. Overall, our study provides insights into soil biotic and abiotic factors in association with SOC mineralization, and contributes to understanding the effect and mechanism of ecological restoration on SOC mineralization in a degraded grassland in an alpine region.

KEYWORDS

ecological restoration, enzyme activity, soil microorganisms, carbon mineralization and storage, alpine grassland

Introduction

The alpine grasslands on the Qinghai-Tibetan Plateau, which cover roughly 40% of China's grassland area, serve as an essential ecological barrier and carbon sink (Chen et al., 2022; Wang Y. et al., 2022). However, due to human disturbances and climate changes, degradation of alpine grasslands is widespread and has accelerated in the past decades, resulting in a significant loss of biodiversity and soil C stocks (Bardgett et al., 2021). Ecological restoration is one of several actions that can ameliorate degraded and disturbed soils, with the goal of rebuilding, initiating, or accelerating recovery of disturbed ecosystems (Martin, 2017). Restoration activities can reverse soil degradation, mitigate climate change, and combat the loss of biodiversity and ecosystem services (Dong et al., 2020). It is known that the effect of ecological restoration on the soil C pool depends on the balance between C input from plants and C effluxes *via* microbial mineralization (Jackson et al., 2017; Dynarski et al., 2020). Meanwhile, carbon dioxide (CO_2) mitigation and soil fertility maintenance can both be achieved through reducing the process of SOC mineralization (Zhang B. et al., 2021; Zhang S. et al., 2021; Dong et al., 2022). By slowing down the rate of SOC mineralization and increasing SOC content, it is possible to reduce the release of CO_2 into the atmosphere and maintain soil health. To date, our understanding of how ecological restoration affects SOC mineralization and its mechanism in alpine grasslands lags considerably behind that of SOC storage (Zhou et al., 2022). These knowledge gaps undermine our predictions of ecological restoration effects on soil C processes and constrain the improvement of restoration management practices to resist land degradation.

Soil physiochemical properties are essential factors affecting SOC mineralization (Zhao et al., 2008; Ahn et al., 2009). For instance, soil pH affects SOC mineralization by altering microbial communities and enzyme activities (Zhang et al., 2022; Zhuang et al., 2022). Soil nutrient availability, such as nitrogen and phosphorus, can also impact SOC mineralization by impacting microbial activities (Jing et al., 2017; Wei et al., 2020; Peixoto et al., 2021). For instance, when nitrogen or phosphorus is limiting, microbes may switch from using organic carbon to using other sources of carbon, reducing the rate of SOC mineralization. Meanwhile, the labile C fractions, such as microbial biomass carbon (MBC), easily oxidized carbon (EOC), and hot-water extractable carbon (HWEOC), serve as the main C sources for microorganisms that determine SOC mineralization (Rousk et al., 2016). Therefore, understanding the variation in soil physiochemical properties and carbon fractions and their relations to SOC mineralization under ecological restoration could improve our ability to make accurate predictions.

Soil microbiota constitute a large part of the earth's biodiversity and are involved in C sequestration, SOM decomposition, and nutrient cycling and availability (Liang et al., 2017; Banerjee et al., 2018; Yang et al., 2018; Crowther et al., 2019; Shu et al., 2022). Therefore, any changes in the diversity, composition, and potential functions of microbial communities may alter the direction and magnitude of SOC mineralization (Schimel and Schaeffer, 2012; Juarez et al., 2013; Tardy et al., 2015; Zhang et al., 2019; Ibrahim et al., 2021). Microbial extracellular enzymes, especially C-cycling enzymes (e.g., β-1,4-glucosidase, β-D-cellobiosidase, peroxidase, polyphenol oxidase), play an essential role in the decomposition of SOC and the regulation of C fractions (Chen et al., 2018a; Yang et al., 2019; Chen J. et al., 2020). Ecological restoration may affect microbial community structure and enzyme activities through a direct effect of *via* regulating the quantity and quality of litter inputs, and through an indirect effect of modifying soil physiochemical properties (Deng et al., 2010; Raiesi and Salek-Gilani, 2018; Xu et al., 2021; Yang et al., 2022). Therefore, soils under different ecological restoration modes may differ in microbial community structure and enzyme activities and consequently the SOC mineralization. However, limited data are available regarding the comprehensive influences of soil physiochemical properties, microbial community composition, and enzyme activities on SOC mineralization.

Here, we explored how ecological restoration may influence SOC mineralization and its relation to soil physiochemical properties, labile carbon fractions, enzyme activities and bacterial communities in degraded grasslands on the Tibetan Plateau. The primary aims of this study were: (1) to explore changes in soil physiochemical properties, labile carbon fractions, bacterial communities, and enzyme activities after 14-year restoration treatments; (2) to determine the influence of ecological restoration on SOC mineralization; and (3) to identify the relative importance of biotic and abiotic factors in determining SOC mineralization under ecological restoration.

Materials and methods

Site description

The study area is located in the Restoration Demonstration region of a degraded grassland in Hongyuan County (33°1' N and 102°37′ E), China, at the eastern margin of the Tibetan Plateau (Supplementary Figure S1). The average elevation of this region is over 3,400 m. The mean annual precipitation in this region is 791.95 mm. The mean annual temperature is 1.1°C, and the mean temperatures are −10.3 and 10.9°C for the coldest and warmest months, respectively. The soil is classified as cambic arenosol (FAO Classification, 2006). The dominant vegetation species in the recovery area are mainly *Salix cupularis*, *Carex peaeclara*, *Kobresia pygmaea*, *Artemisia wellbyi*, and *Heracleum souliei*. Since 2007, the extremely degraded grassland at this site has undergone natural restoration with the dominant species being *Cyperus stoloniferus*; this was the control (CK) for the study. Two artificial restoration actions were started as well to restore the degraded grassland. The artificial restoration actions included: (1) planting shrubs with *Salix cupularis* alone (SA), and (2) planting shrubs with *Salix cupularis* plus mixed grasses (SG). The primary species in SA were *Salix cupularis*, *Lancea tibetica*, and *Leymus secalinus*. The primary species in SG were *Salix cupularis*, *Euphrasia regelii subsp. Kangtienensis*, *Anaphalis lacteal*, *Peucedanum praeruptorum*, *Potentilla discolor*, and *Elymus nutans*. At the time of our study, the natural and artificial restoration actions had been ongoing for 14 years.

Experimental design

In August 2021, soil samples were taken from three areas in an extremely degraded grassland; one that underwent natural restoration (CK), one that was planted with shrubs and *Salix cupularis* alone (SA), and one that was planted with shrubs and *Salix cupularis* plus grasses

(SG). Four independent plots were selected for each treatment, where four quadrats, each 1 m × 1 m were set up. The characteristics of the vegetation community were examined in the field before collecting soil samples (Supplementary Table S1). We randomly sampled 1 kg of soil from the 0–20 cm and 20–40 cm soil layers in each plot using a 5-cm diameter soil auger. Then, we pooled and thoroughly mixed the samples to produce a composite soil sample. In total, 24 samples (3 treatments × 4 replicates × 2 depths) were collected. After transporting these samples to the laboratory on ice, one-tenth of each soil sample was stored at −80°C for the soil bacterial community analysis. Two-tenths of each soil sample was stored at 4°C for testing soil microbial biomass carbon and enzyme activities. The remaining soil was air-dried and sieved for pH, soil organic carbon (SOC), and soil nutrients analysis. Moreover, a cutting ring with a capacity of 100 cm^3 was used to collect undisturbed soil before performing soil bulk density analysis.

Soil physicochemical characterization

Soil physicochemical characteristics were analyzed as previously described by Carter and Gregorich (2007). Soil pH was determined by a glass electrode with a soil-to-water ratio of 1:2.5 (weight/volume) (Mettler Toledo MP220, Mettler-Toledo, Switzerland). SOC content was analyzed using the $K_2Cr_2O_7$ oxidation method. Soil total nitrogen (TN) content was measured using a flow injection autoanalyzer (AutoAnalyzer 3, Bran+ Luebbe, Germany). Soil total phosphorus (TP) content was analyzed calorimetrically using the H_2SO_4-$HClO_4$ method. Bulk density was examined by the cutting ring method, undisturbed soil samples were dried at 105°C to reach a constant weight.

Soil labile carbon fractions and C-cycling enzymes

Microbial biomass carbon (MBC) was measured by the chloroform fumigation-extraction method (Vance et al., 1987). Hot-water extractable organic carbon (HWEOC) was determined using a TOC analyzer (Elementer Analysensysteme, Germany) (Hou et al., 2021). Easily oxidized carbon (EOC) was measured according to the 333 mol L^{-1} $KMnO_4$ method as described by Dong et al. (2022). Additionally, we analyzed the potential activities of four C-cycling enzymes, including β-glucosidase (BG), β-D-cellubiosidase (CBH), peroxidase (POD), and polyphenol oxidase (PPO). All enzymes were measured using commercial enzyme kits following the manufacturer's protocol (Solarbio Science and Technology Co., Ltd., Beijing, China).

Soil C mineralization

Cumulative SOC mineralization was determined according to the method described by Hou et al. (2021). First, two 25 ml glass beakers filled with 10 g fresh soil and 15 ml 1 M NaOH solution, respectively, were put side by side in an airtight plastic 250 ml jar. Deionized water was spread on the bottom of the jar and surrounded the breakers to keep constant soil moisture. Then, these 250 ml jars were placed in a thermostatic incubator at 25°C for 28 days. During the incubation, the CO_2 gas generated was absorbed in the NaOH solution, and the remaining NaOH was measured by titrating with 0.1 M HCl to quantify SOC mineralization.

DNA extraction and Illumina MiSeq sequencing

For each sample, total DNA was extracted from 0.5 g soil using the PowerSoil® DNA Isolation Kit (MoBio Laboratories Inc., Carlsbad, CA, United States) following the manufacturer's instructions. The concentration and quality of DNA were measured by Nanodrop 2000 (Thermo Scientific, Wilmington, DE, United States). Before performing PCR amplification, the DNA sample was diluted to 10 ng/μL. The 16S rRNA V4–V5 regions were sequenced for bacterial communities with the primer pair 515F (5′-GTGCCAGCMG CCGCGGTAA-3′) and 909R (5′-CCCCGYCAATTCMTTTRAGT-3′). Sequencing was conducted on an Illumina MiSeq2500 platform by Novogene (Beijing, China). The raw sequence data of the 16S rRNA were analyzed using the Quantitative Insights into Microbial Ecology (QIIME) pipeline. Using a dissimilarity level of 3%, the unique sequence set clustered operational taxonomic units (OTUs) into the UPARSE pipeline.

Functional analysis of the bacterial community using PICRUSt2

Changes in functional genes involved in C cycling (including C degradation and C fixation) were predicted by phylogenetic investigation of bacterial communities by reconstruction of unobserved states 2 (PICRUSt2) according to the Kyoto Encyclopedia of Genes and Genomes (KEGG) database and 16S rRNA bacterial community data (Li et al., 2022). The KEGG orthologues of each gene generated by PICRUSt2 were obtained from the table of absolute abundance for the KEGG pathway, which then was converted into the relative abundance of the corresponding genes.

Calculation of indices

Stocks of SOC were calculated using Equation 1 (Hu et al., 2018):

$$\text{SOC stock}\left(\text{Mg ha}^{-1}\right) = \text{SOC}\left(\text{g kg}^{-1}\right) \times \text{bulk density}\left(\text{g cm}^{-3}\right) \times \text{soil depth}\left(\text{cm}\right)/10 \quad (1)$$

where SOC stock indicates the soil organic carbon stock, and SOC indicates the soil organic carbon content.

The following Equation 2 was adopted to calculate carbon mineralization efficiency (Dong et al., 2022):

$$\text{CME}\left(\text{mg CO}_2 - \text{C g}^{-1}\text{SOC}\right) = \text{Cumulative SOC mineralization}\left(\text{mg CO}_2 - \text{C kg}^{-1}\right)/\text{SOC}\left(\text{g kg}^{-1}\right) \quad (2)$$

where CME indicates the carbon mineralization efficiency and SOC indicates the soil organic carbon content.

Statistical analyses

Statistical analyses were conducted using the R statistical software (R version 4.0.2, R Core Team, Vienna, Austria). Unless otherwise stated, statistical significance was set at $p < 0.05$. Difference in soil physiochemical properties, labile C fractions, enzyme activity, and SOC mineralization between different treatments at two different soil depths were tested using a two-way analysis of variance (ANOVA). When two-way ANOVA revealed differences, a Tukey's honestly significant difference (Tukey HSD) test was used to compare the average value of variables among the different treatments. Linear regression analysis was used to evaluate the relationships between soil physiochemical properties, labile C fractions, the diversity and composition of bacterial communities, enzyme activities and SOC mineralization. Principal coordinates analysis (PCoA) was used to determine significant differences in microbial communities for the various restoration modes and soil depths. Redundancy analysis (RDA) was performed with a Monte Carlo permutation test (999 permutation) to identify soil properties that influence the bacterial community structure. The Mantel test was performed to identify soil variables that influence the microbial community structure. We performed random forest analysis to evaluate important predictors of SOC mineralization among soil depth, physiochemical properties, labile C fractions, enzyme activities, bacterial Shannon index, bacterial Chao1 index, and bacterial composition. Bacterial community composition was estimated based on Bray–Curtis distances between samples. Random forest analysis was performed using the "randomForest" package, with the significance of the model and each predictor was evaluated using the "rfPermute" packages. Furthermore, we constructed structural equation modeling (SEM) to evaluate the direct and indirect effect of various variables on SOC mineralization under ecological restoration. Bacterial composition was represented by scaling 1, the first component of principal coordinates analysis. The goodness of fit of the SEM was evaluated using the Chi-square test, the whole-model p value, Akaike information criterion (AIC), and the goodness-of -fit (GFI) statistic. The SEM was conducted using AMOS software (IBM SPSS Amos 24.0.0).

Results

Soil physiochemical properties and labile C fractions

The two-way ANOVA demonstrated that soil pH significantly differed in restoration mode ($F = 67.58$, $p < 0.001$), soil depth ($F = 6.36$, $p < 0.05$), and by the interaction of restoration mode and soil depth ($F = 4.00$, $p < 0.05$) (Supplementary Table S2). Compared with CK, SA significantly decreased soil pH at the 0–20 and 20–40 cm soil depths ($p < 0.05$). Restoration mode had a significant effect on SOC ($F = 18.07$, $p < 0.001$), TN ($F = 91.85$, $p < 0.001$), and SOC stock ($F = 17.97$, $p < 0.001$), but had no significant effect on soil BD and TP. On average, the SOC content, TN content and SOC stock followed the order of SG > SA > CK (Table 1). Restoration mode had a significant effect on MBC ($F = 6.94$, $p < 0.01$), EOC ($F = 60.20$, $p < 0.001$), HWEOC ($F = 93.34$, $p < 0.001$), and HWEOC/SOC ($F = 8.43$, $p < 0.001$). Soil depth had a significant effect on HWOEC ($F = 6.20$, $p < 0.05$). Moreover, MBC ($F = 4.26$, $p < 0.05$) and EOC ($F = 4.05$, $p < 0.05$) significantly varied with the interaction of restoration mode and soil depth (Supplementary Table S2 and Figure 1).

TABLE 1 Effects of different restoration modes on soil physiochemical properties in different soil depths.

Soil depth	Variable	CK	SA	SG
0–20 cm	pH	6.81 ± 0.08 a	6.27 ± 0.18 b	6.68 ± 0.04 a
	BD ($g\,cm^{-3}$)	1.42 ± 0.04 a	1.35 ± 0.05 a	1.41 ± 0.07 a
	TN ($g\,kg^{-1}$)	0.11 ± 0.02 b	0.17 ± 0.02 b	0.39 ± 0.08 a
	TP ($g\,kg^{-1}$)	0.16 ± 0.00 a	0.17 ± 0.01 a	0.18 ± 0.01 a
	SOC ($g\,kg^{-1}$)	2.05 ± 0.78 b	3.39 ± 1.26 ab	5.39 ± 1.33 a
	SOC stock ($Mg\,ha^{-1}$)	5.82 ± 2.29 b	9.15 ± 3.56 ab	15.01 ± 2.91 a
20–40 cm	pH	6.85 ± 0.03 a	5.95 ± 0.18 c	6.57 ± 0.15 b
	BD ($g\,cm^{-3}$)	1.39 ± 0.13 a	1.38 ± 0.06 a	1.39 ± 0.09 a
	TN ($g\,kg^{-1}$)	0.12 ± 0.02 b	0.18 ± 0.05 b	0.36 ± 0.03 a
	TP ($g\,kg^{-1}$)	0.17 ± 0.01 a	0.17 ± 0.00 a	0.17 ± 0.00 a
	SOC ($g\,kg^{-1}$)	2.30 ± 0.35 a	3.05 ± 0.27 a	4.31 ± 0.82 a
	SOC stock ($Mg\,ha^{-1}$)	6.46 ± 1.38 a	8.40 ± 0.87 a	12.03 ± 2.88 a

Values are represented as the mean followed by a standard deviation in parentheses ($n = 3$). Different lowercase letters indicate a significant different ($p < 0.05$) among different modes, based on the analysis of variance, and Tukey's honest significance difference (HSD) test. BD, bulk density, SOC, soil organic carbon; TN, total nitrogen; TP, total phosphorus; SOC stock, soil organic carbon stock.

Bacterial community diversity and composition

Restoration mode had a significant effect on the Shannon index for bacteria in 0–20 cm soil layer ($p < 0.05$). The highest average value of the Shannon index at the 0–20 cm and 20–40 cm soil depths were observed in SG (Figure 2A). The Chao1 index for bacteria varied significantly with restoration mode ($p < 0.05$). Compared with CK, modes SA and SG significantly increased theChao1 index in the 0–20 cm and 20–40 cm soil depths ($p < 0.05$) (Figure 2B). SOC, TN, HWEOC, and EOC were positively correlated with the Chao1 and Shannon indices ($p < 0.05$). MBC was positively correlated with the Chao1 index ($p < 0.05$) (Supplementary Figure S2).

The most abundant bacterial phyla were *Proteobacteria*, *Actinobacteria*, *Acidobacteria*, and *Chloroflexi*. Compared with CK, modes SA and SG increased the relative abundance of *Proteobacteria*, *Acidobacteria*, and *Bacteroidetes*, but decreased the relative abundance of *Actinobacteria*, *Chloroflexi*, and *Thaumarchaeota* at the 0–20 cm and 20–40 cm soil depths (Figure 3). The PCoA analyses showed that the soil bacterial community in CK was separated from the soil bacterial community of soils in SA and SG (Figure 4A). RDA was used to identify the major soil properties controlling the soil bacterial

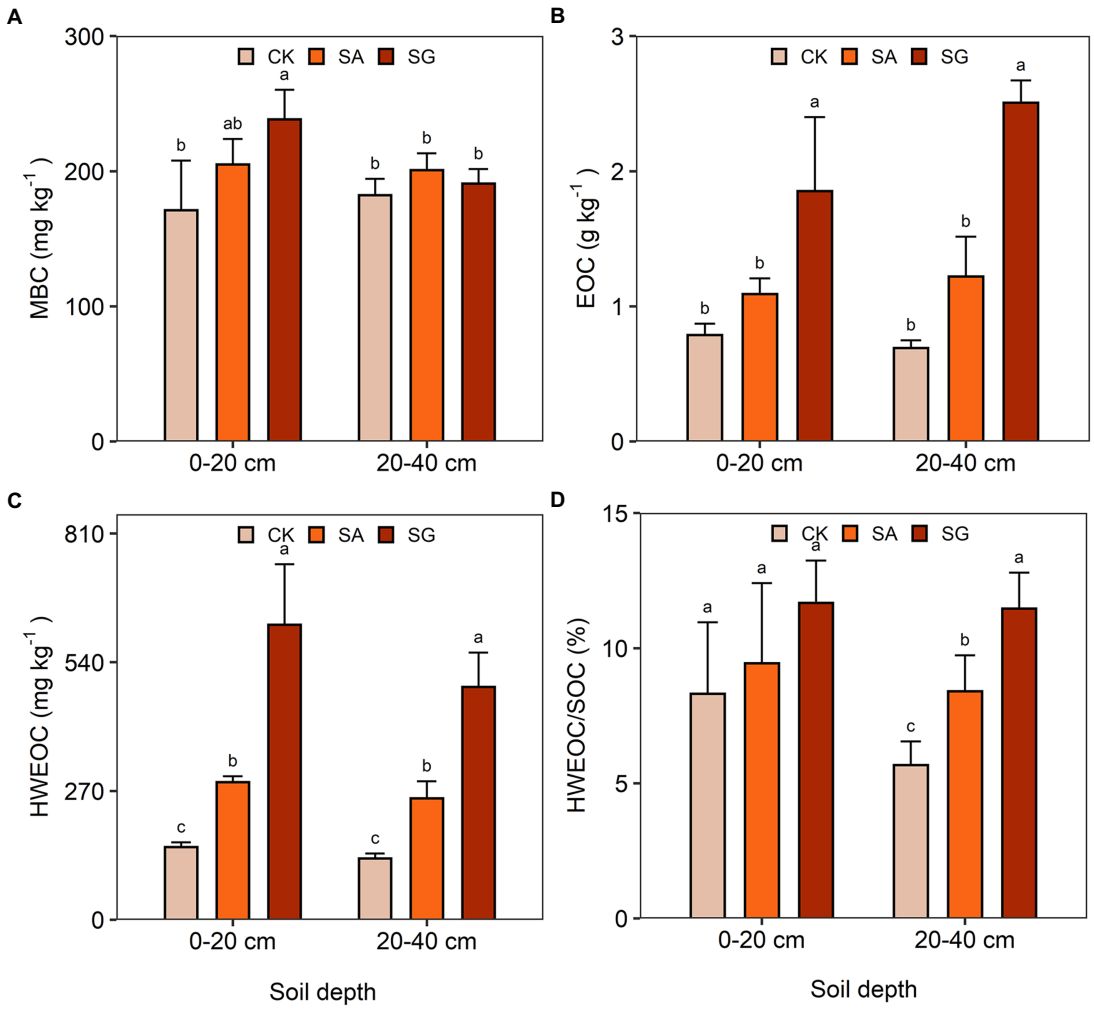

FIGURE 1
Effects of different restoration modes on soil labile carbon fractions. **(A)** Microbial biomass carbon (MBC), **(B)** easily oxidized carbon (EOC), **(C)** hot-water extractable organic carbon (HWEOC), **(D)** the ratio of hot-water extractable organic carbon to soil organic carbon (HWEOC/SOC). Error bars indicate standard deviation; Different lowercase letters indicate significant differences at $p<0.05$ among treatments, based on the Tukey's honest significance difference (HSD) test.

community structure. The first two components explained 49.5% of the total variability for bacterial community structure. Soil pH, TN, EOC, and HWEOC were the important soil properties controlling the bacterial community structure (Supplementary Figure S3). The Mantel test indicated that soil pH, TN, EOC, HWEOC, and the ratio of HWEOC to SOC were the critical soil parameters affecting the bacterial community composition (Figure 4B). The PICRUST2 analysis indicated that ecological restoration significantly improved the role of microbes in C-fixation and decomposition. The relative abundance of C-fixation genes (*rbcL*, *meh*, *mct*, *ppc*, *IDH1*, and *frdA*) and C-degradation genes (*csxA*, *glgX*, *malQ*, and *PYG*) were higher in SA and SG than in CK (Figure 5).

C-cycling enzyme activities

Restoration mode had a significant effect on the activities of BG ($F = 10.37$, $p < 0.01$) and CBH ($F = 4.88$, $p < 0.05$), but had no significant effect on the activities of PPO and POD (Supplementary Table S4). Compared with CK, modes SA and SG increased the activities of BG and CBH in the 0–20 and 20–40 cm soil depths (Figure 6A). Modes SA and SG decreased the ratio of ligninase to cellulase by 40.6 and 66.0% in the 0–20 cm soil depth, and by 29.3 and 58.9% in 20–40 cm soil depth, respectively, relative to CK (Figure 6B). Both BG and CBH were positively correlated with TN, MBC, and HWEOC ($p < 0.05$) (Supplementary Figure S4). The ratio of ligninase to cellulase was negatively associated with SOC content and SOC stocks ($p < 0.05$) (Supplementary Figure S5).

SOC mineralization

Restoration mode had a significant effect on cumulative C mineralization ($F = 59.22$, $p < 0.001$) (Supplementary Table S5). Compared with CK, the cumulative C mineralization at the 0–20 and 20–40 cm soil depth increased by 15.7 and 76.8% in the SA mode, and by 94.0 and 83.1% in the SG mode, respectively. The CME in the SG mode was lower than in CK (Figure 7). Soil depth had a significant

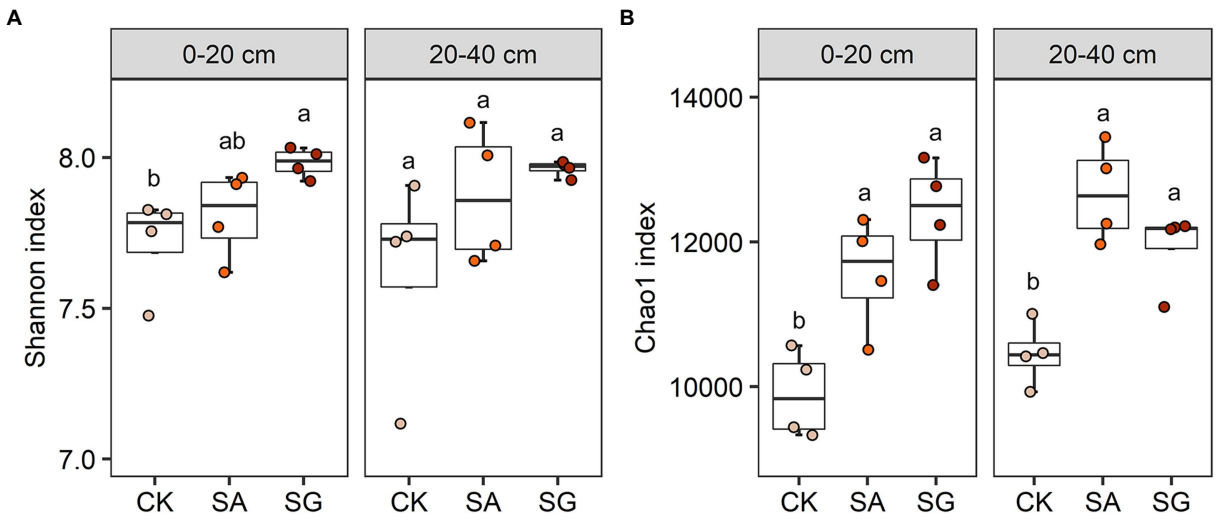

FIGURE 2
Effects of different restoration modes on bacterial alpha diversity. **(A)** Bacterial Shannon index and **(B)** bacterial Chao1 index. Error bars indicate standard deviation; different lowercase letters indicate significant differences at $p<0.05$ among treatments, based on the Tukey's honest significance difference (HSD) test.

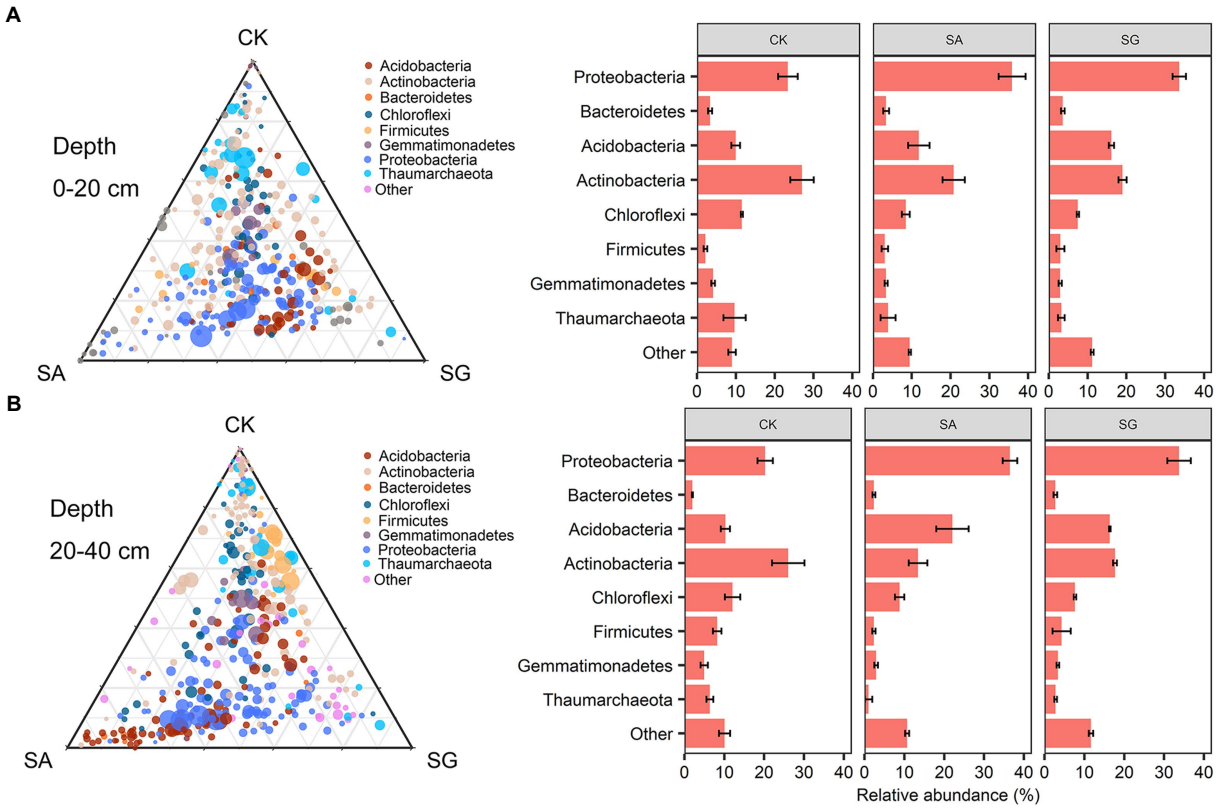

FIGURE 3
Taxonomic distribution of bacterial taxa responsible for community different among different restoration modes at 0–20 cm **(A)** and 20–40 cm **(B)** soil depth.

effect on cumulative C mineralization ($F = 166.07$, $p < 0.001$) and CME ($F = 15.78$, $p < 0.001$). The cumulative C mineralization significantly varied with the interaction of restoration mode and soil depth ($F = 20.06$, $p < 0.001$) (Supplementary Table S5).

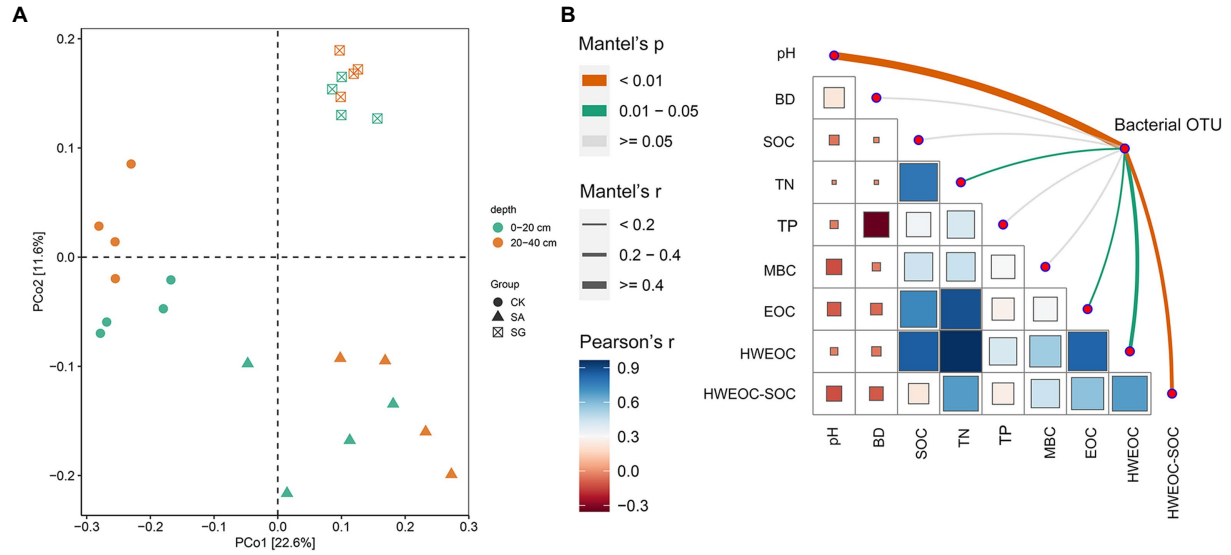

FIGURE 4
(A) Principial coordinates analysis (PCoA) of bacterial community composition based on Bray–Curtis distances. **(B)** Mantel test analysis of bacterial community changes with soil properties.

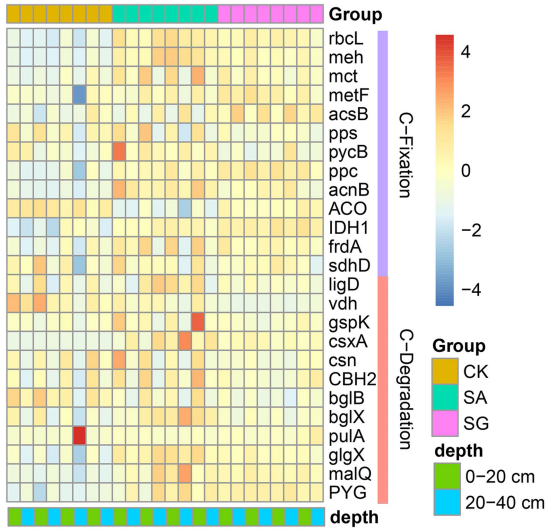

FIGURE 5
Effects of ecological restoration on the relative abundance of functional genes involved in C-cycling according to PICRUST2.

Contribution of abiotic and biotic factors to SOC mineralization

Random forest modeling indicated that the top six most important factors were soil depth, MBC, HWEOC, bacterial composition, and SOC (Figure 8A). SEM analysis showed that both SOC, MBC and C-cycling enzymes had a positive effect on the cumulative C mineralization, but soil depth had a negative effect on cumulative C mineralization ($p < 0.05$). Soil pH and SOC had a significant effect on bacterial composition ($p < 0.05$). Bacterial community composition had a significant positive effect on MBC and C-cycling enzymes ($p < 0.05$) (Figure 8B).

Discussion

Effects of ecological restoration on soil physiochemical characteristics and C fractions

Ecological restoration plays a critical role in maintaining soil quality *via* increasing nutrient contents, improving soil physical properties (e.g., aggregate stability and water holding capacity), and promoting soil C sequestration. In this study, restoration modes SA and SG decreased soil pH relative to CK. For example, the SA mode had the lowest pH value at the 0–20 cm soil depth. This is presumably due to restoration-induced changes in plant residue decomposition and root processes (Hong et al., 2018). Meanwhile, restoration mode had a significant effect on SOC stocks, and the highest value of SOC stock was observed in the SG mode. This result has two explanations. First, compared with CK and SA, higher plant richness in the SG mode increased plant productivity through niche complementary effects, and consequently, improved plant C inputs into the soil and enhanced SOC accumulation (Chen S. et al., 2018; Chen X. et al., 2019; Li et al., 2019; Jia et al., 2021). Second, SG enhanced soil N and P content more effectively, which played an important role in SOC accumulation by affecting primary productivity and SOC decomposition (Averill and Waring, 2018; Chen et al., 2018a,bChen S. et al., 2018; Wang et al., 2020; Ding et al., 2021). Moreover, we found that ecological restoration significantly increased soil TN, but had no significant effect on TP, in line with a recent meta-analysis (Tian et al., 2021). This could be mainly because, unlike nitrogen, the external source of phosphorus is limited. For instance, diazotrophic microbes can enhance soil N content because of their immense N-fixation ability (Hsu and Buckley, 2009; Xu et al., 2019). Furthermore, SOC mineralization can produce soil nitrogen, hence, a high SOC increases the TN (Tan et al., 2021).

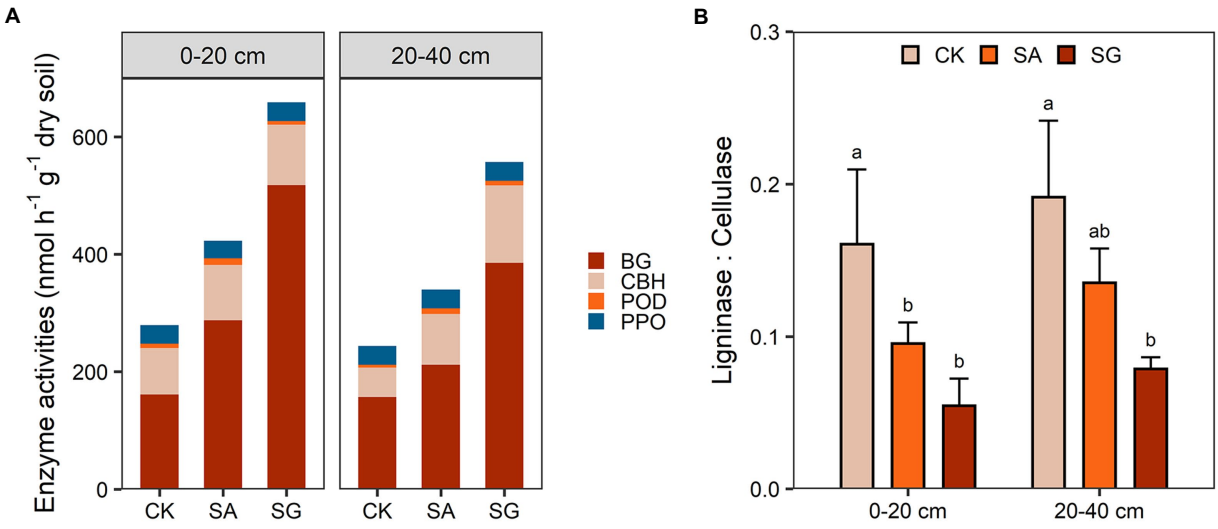

FIGURE 6
Effects of different restoration modes on soil carbon-cycling enzyme activities **(A)** and the ratio of ligninase to cellulase **(B)**. CK, extremely degraded grassland. SA, planting shrub with *Salix cupularis* alone (SA). SG, planting shrub with *Salix cupularis* plus mixed grasses. Error bars indicate standard deviation; different lowercase letters indicate significant differences at $p<0.05$ among treatments, based on the Tukey's honest significance difference (HSD) test.

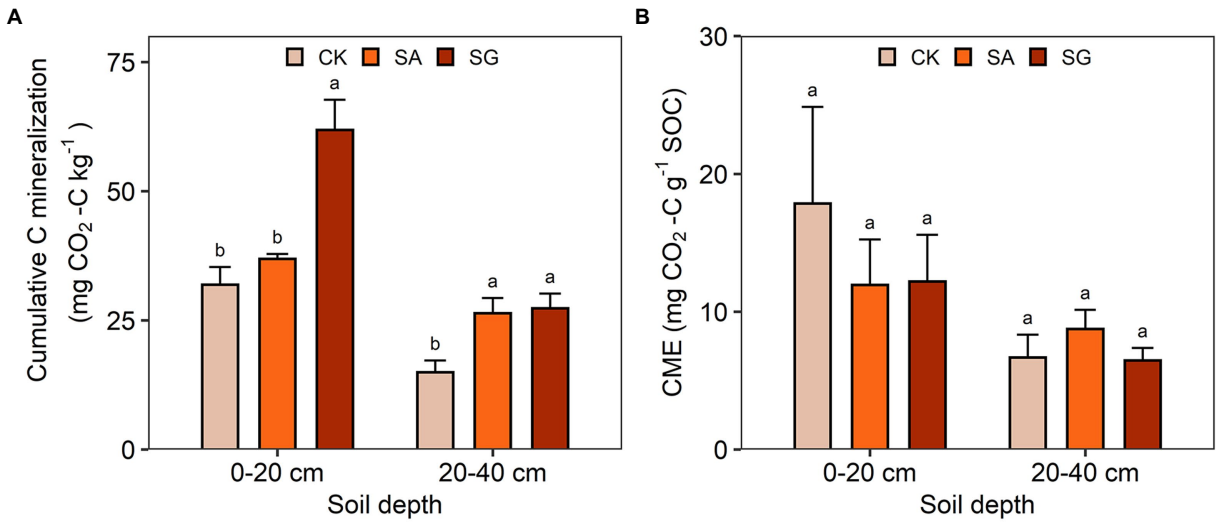

FIGURE 7
Effects of ecological restoration on **(A)** the cumulative carbon mineralization and **(B)** carbon mineralization efficiency (CME). Error bars indicate standard deviation; different lowercase letters indicate significant differences at $p<0.05$ among treatments, based on the Tukey's honest significance difference (HSD) test.

It is generally accepted that MBC, EOC, and HWEOC are the most labile fractions of SOC, which is easily decomposed and mineralized by soil microorganisms (Liang et al., 2021; Xiao et al., 2022). Here, we found that ecological restoration positively affected MBC, EOC, and HWEOC content. Meanwhile, the variation trend of these labile C fractions under ecological restoration was basically similar to that of SOC with a good positive correlation, suggesting that the concentration of these labile C fractions was mainly determined by the plant carbon input. Recently, the ratio of HWEOC to SOC (HWEOC/SOC) was chosen as a chemical index to describe SOC stability (Plante et al., 2011; Hou et al., 2021). The higher HWEOC/SOC, the faster the nutrient cycling rate, which is not conducive to the accumulation of SOC, so the chemical stability is worse and SOC decomposes more easily (Wang et al., 2021). Our result indicated that HWEOC/SOC in the SG mode was higher than in the CK and SA modes, suggesting that SOC in SG easily decomposed and transformed.

Effects of ecological restoration on the bacterial community and its potential function

Our results revealed that bacterial alpha diversity in SA and SG modes was higher than in CK. Furthermore, bacterial alpha diversity

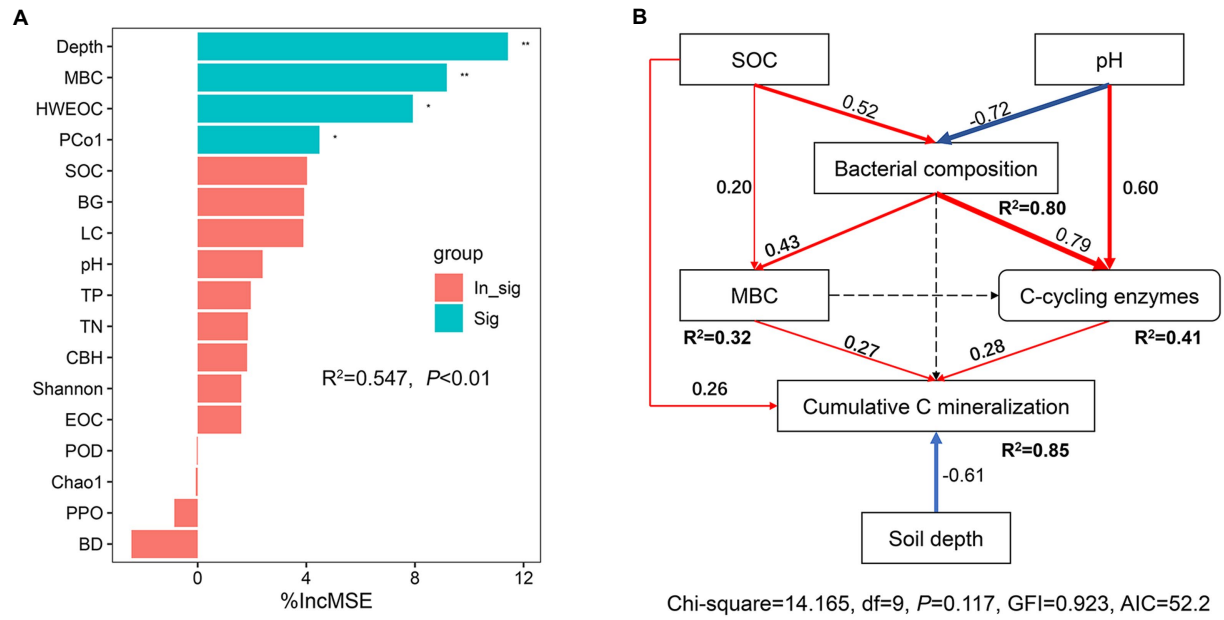

FIGURE 8
(A) Random Forest regression model shows the main factors of SOC mineralization. MSE, is the mean square error. *p<0.05, **p<0.01 on the bar indicated that the associated factor had a significant effect on SOC mineralization. **(B)** Structural equal model (SEM) analysis of the direct and indirect effects on the response of SOC mineralization to ecological restoration. Red and blue solid arrows indicate positive and negative relationships, respectively. Black arrows represent tested, but not significant paths. The arrow width is proportional to the strength of the relationship. Goodness-of-fit statistics for the model are shown below the model. *p<0.05, **p<0.01.

was positively correlated with SOC, TN, TP, HWEOC, and EOC. The evidence suggests that higher labile C and available nutrients in the SA and SG modes can create a more suitable microenvironment for bacterial communities to survive, and thus enhance bacterial alpha diversity. In addition, higher plant richness in the SA and SG modes may provide the bacteria with greater accessibility to a variety of root exudates, which results in more niches to support higher bacterial diversity.

According to the oligotrophic-copiotrophic theory, *Proteobacteria* and *Bacteroidetes* are generally classified as copiotrophic microbes, whereas *Choroflexi* is classified as oligotrophic microbes (Ho et al., 2017; Yao et al., 2017). Our results indicated that modes SA and SG increased the relative abundance of *Proteobacteria* and *Bacteroidetes* but decreased the relative abundance of *Choroflexi*. Correlation analysis indicated that TN, TP, HWEOC, and MBC were positively correlated with *Proteobacteria* and *Bacteroidetes* but negatively correlated with *Choroflexi*, suggesting that copiotrophic taxa gain more advantages in competition due to ecological restoration-induced increasing labile C pools and to nutrient availability. The relative abundance of *Actinobacteria* in SA and SG modes was lower than in CK. Meanwhile, we found a significant positive relationship between pH and *Actinobacteria* under ecological restoration (Supplementary Figure S2). This indicated that the restoration-mediated decrease of pH may decrease their ability to compete with other bacteria taxa (Fu et al., 2022). The negative relationship between *Actinobacteria* and HWOEC and EOC under ecological restoration may be due to some taxa of *Actinobacteria* being oligotrophic groups (Zhong et al., 2019). Additionally, SA and SG increased the relative abundance of *Acidobacteria* relative to CK. Recent studies have found that *Acidobacteria* is a keystone taxon in soil and is involved in the decomposition of soil organic matter (Costa et al., 2020), nitrogen cycling, and plant growth promotion (Eichorst et al., 2018; Kalam et al., 2020). A positive relationship was observed between TN and *Acidobacteria* (Supplementary Figure S2), indicating that the changes in *Acidobacteria* may be tightly linked to soil nitrogen content.

In our study, the Mantel test revealed that soil pH was a major driver of bacterial community composition, which was in line with previous studies on regional studies and large scales (Maestre et al., 2015; Cheng et al., 2020; Hermans et al., 2020). This may be due to the relatively narrow optimal pH for bacterial growth. Many previous studies have demonstrated the important role of soil labile C fractions in shaping soil bacterial communities (Delgado-Baquerizo et al., 2016; Ren et al., 2018; Ramírez et al., 2020). Fundamentally, ecological restoration considerably affected the amount and quality of soil C fractions, which in turn altered microbial community composition (Hu et al., 2022). Our results showed that bacterial community composition was more sensitive to labile C fractions (particularly EOC and HWEOC) than SOC. This suggested that soil labile C fractions could be a critical predictor for bacterial community composition changes in ecological restoration.

Recent evidence has indicated that ecological restoration provides favorable environments for soil carbon functional microbes and stimulates soil C turnover (Guo et al., 2018; Sun and Badgley, 2019; Hu et al., 2022; Li et al., 2022). In our study, the relative abundance of C-fixation genes (*rbcL*, *meh*, *mct*, *ppc*, *IDH1*, and *frdA*) in SA and SG were higher than in CK, suggesting that soil microbes in SA and SG have a strong ability to fix carbon and thus increase the accumulation of SOC. Meanwhile, the relative abundance of *csxA*, *glgX*, *malQ*, and

PYG genes increased dramatically under SA and SG. This indicated that ecological restoration also improved the microbial decomposition of C sources, and consequently increased CO_2 production.

Effects of ecological restoration on C-cycling enzyme activities

Typically, cellulases, *β*-1,4-glucosidase (BG), and *β*-D-cellobiohydrolase (CBH), are related to the degradation of labile C pools, while ligninases, polyphenol oxidase (PPO) and peroxidase (POD) are associated with degradation of recalcitrant C pools (Zhang B. et al., 2021; Zhang S. et al., 2021). Our results showed that ecological restoration had a stronger positive effect on cellulase activity rather than ligninase activity. On the one hand, increasing plant richness under ecological restoration may exhibit stronger niche partition and consequently improve primary productivity as well as soil labile and recalcitrant C pools (Mahaut et al., 2019; Michalet et al., 2021). In this situation, microbes may preferentially invest energy in cellulase production to acquire labile resources over ligninase production since cellulase synthesis requires less energy than ligninase synthesis (Wang et al., 2012; Chen et al., 2018a,b; Chen S. et al., 2018). Our results found positive relationships between labile C fractions and cellulase activity (Supplementary Figure S4), indicating that ecological restoration could enhance cellulase activity *via* increasing labile C substrates. On the other hand, ecological restoration-induced changes in microbial biomass and community composition may also impact enzyme activities (Wu et al., 2021). Positive relationships between cellulase activities, MBC, and SOC (Supplementary Figure S4), indicated that faster microbial degradation and transformation of labile C substrates mediate the accumulation of SOC in SA and SG modes. Moreover, ecological restoration enhanced the relative abundance of copiotrophic microbes (Zeng et al., 2017; Yao et al., 2018; Wang S. et al., 2022; Wang Y. et al., 2022). These microbes had a higher investment in extracellular enzymes to decompose the labile C substrates (Ramin and Allison, 2019). Our results indicated that the cellulase activity was positively correlated to the relative abundance of copiotrophic taxa (*Proteobacteria* and *Bacteroidetes*) (Supplementary Figure S2), which provided evidence that ecological restoration-induced changes in bacterial community composition could affect the response of cellulase activity. Notably, we observed that the ratio of ligninase to cellulase was negatively correlated with SOC content and stocks under ecological restoration (Supplementary Figure S5). This finding indicated that the decreased ratio of ligninase to cellulase under ecological restoration could be benefitical to the accumulation of SOC under ecological restoration, which was consistent with a recent meta-analysis (Wu et al., 2022).

Effects and mechanisms of ecological restoration on SOC mineralization

Determining the underlying mechanisms controlling SOC mineralization under ecological restoration is challenging since SOC mineralization is regulated by complex factors, including soil physiochemical properties, SOC quality and availability, enzyme activities and soil microbiota. Here, we observed that ecological restoration had a significant effect on the cumulative C mineralization and C mineralization efficiency. The cumulative C mineralization in SA and SG was higher than in CK. The fundamental explanation for the increased C release is that SOC stock was elevated by ecological restoration, which is supported by the substantial positive relationship between cumulative C mineralization and SOC content and stocks. Meanwhile, structural equal modeling revealed that SOC was the main factor driving C mineralization under ecological restoration. In addition to SOC stock, soil N and P content also mediate SOC mineralization by altering microbial activity and community composition (Meyer et al., 2018), which is supported by the positive association between TN and TP and cumulative SOC mineralization.

This study indicated that MBC and HWEOC could better predict the variation in the cumulative C mineralization than SOC. Indeed, higher labile C contents can boost microbial activity and thus stimulate soil C mineralization (Dong et al., 2022). Our SEM showed that MBC had a direct and positive effect on C mineralization. MBC is the C content of live and dead microorganisms, which has a faster turnover and is often used to define soil microbial biomass (Chen C. et al., 2019; Chen X. et al., 2019). When HWEOC is abundant, microbial biomass becomes a major factor limiting C mineralization, thereby playing a critical role in C mineralization (Dong et al., 2022).

Microbial enzymes are "sensors" of microbial function and can provide useful links between microbes and C cycling (Ashraf et al., 2021; Hu et al., 2023). In our study, we observed that BG was significantly and positively associated with cumulative C mineralization, which is in line with previous studies (Zhu et al., 2014; Zhang B. et al., 2021; Zhang S. et al., 2021). SEM results further indicated that C-cycling enzyme activities had a direct and positive effect on C mineralization. This suggested a limitation of enzyme activities on substrate conversion and consumption in degraded grassland soils.

The diversity and composition of the soil microbial community play essential roles in regulating SOC decomposition in terrestrial ecosystems (Qin et al., 2021; Chen et al., 2023). In this study, the Shannon index for bacteria was positively correlated to cumulative C mineralization. In general, soils with higher bacterial diversity may boost the levels of soil microbial functions due to the high functional redundancy of the soil bacterial community (Philippot et al., 2013; Louca et al., 2018; Maron et al., 2018), corroborating the positive correlations between bacterial diversity and enzyme activities, MBC, TN, and TP. Meanwhile, higher bacterial diversity may also sustain plant richness and plant C inputs (van der Heijden et al., 2008; Chen J. et al., 2020; Chen Q. et al., 2020), and finally promote SOC mineralization. Random forest analysis revealed that bacterial community composition played a critical role in controlling SOC mineralization. SEM results showed that bacterial community composition had no significant effect on SOC mineralization but had a significant effect on MBC and C-cycling enzyme activities. This highlighted that bacterial community composition was a crucial underlying factor controlling SOC mineralization *via* mediating microbial production and microbial functionality.

Additionally, soil depth was a key factor that predicted the variation in SOC mineralization. The interpretation was that the SOC pool, labile C content, enzyme activities, and the diversity and activities of soil microorganisms decreased with increasing soil depth, resulting in a decreased SOC mineralization rate (Qin et al., 2021). Overall, our findings suggested that soil physiochemical characteristics, labile C fractions, and the diversity and composition

and function of the bacterial community jointly determined the response of SOC mineralization to ecological restoration.

Effects of ecological restoration on SOC mineralization efficiency

Soil organic carbon mineralization efficiency is crucial in regulating the C cycle and determining the magnitude of soil CO_2 emissions, thus playing an important role in mitigating climate change. A low SOC mineralization efficiency can result in more C accumulated in the soil, thereby benefiting soil fertility and plant growth. In this study, we found that ecological restoration significantly decreased the SOC mineralization efficiency. Ecological restoration increased large soil aggregates to make inner SOC physically stable and protect it from microbial decomposition. In addition, ecological restoration can change soil physiochemical properties (e.g., pH and texture), which may affect the compositions and activities of soil microbial communities, thereby impacting SOC mineralization efficiency (Dong et al., 2022).

Conclusion

Ecological restoration had a positive effect on SOC content and stocks, TN, the contents of labile C fractions, cellulase activity, and microbial diversity, whereas decreased soil pH and the ratio of ligninase to cellulase. Soil pH, TN, EOC, and HWOEC were major factors that determining bacterial community composition. Ecological restoration increased the SOC mineralization, but decreased the SOC mineralization efficiency. SOC, MBC and C-cycling enzyme activities had a positive effect on SOC mineralization. Bacterial community composition can regulate SOC mineralization *via* boosting microbial biomass and C-cycling enzyme activities. Our results indicate that shrub with *Salix cupularis* plus grasses had a better SOC accumulation, microbial diversity and functions, which was an optimum mode for restoring alpine degraded grassland.

Data availability statement

The datasets presented in this study can be found in online repositories. The names of the repository/repositories and accession number(s) can be found at: https://www.ncbi.nlm.nih.gov/, PRJNA915791.

Author contributions

YH: conceptualization, supervision, funding acquisition, and reviewing and editing. XS and WJL: data collection, data analysis, and writing – original draft. LX, YYZ, WZ, YLZ, and WLL: writing – review and editing. All authors contributed to the article and approved the submitted version.

Funding

This research was supported by the National Natural Science Foundation of China (41771552) and the Sichuan Science and Technology Program (2020JDRC0074, 2021JDRC0082 and 2022YFS0469).

Conflict of interest

The authors declare that the research was conducted in the absence of any commercial or financial relationships that could be construed as a potential conflict of interest.

Publisher's note

Supplementary material

The Supplementary material for this article can be found online at: https://www.frontiersin.org/articles/10.3389/fmicb.2023.1131836/full#supplementary-material

References

Ahn, M., Zimmerman, A. R., Comerford, N. B., Sickman, J. O., and Grunwald, S. (2009). Carbon mineralization and labile organic carbon pools in the sandy soils of a North Florida watershed. *Ecosystems* 12, 672–685. doi: 10.1007/s10021-009-9250-8

Ashraf, M. N., Jusheng, G., Lei, W., Mustafa, A., Waqas, A., Aziz, T., et al. (2021). Soil microbial biomass and extracellular enzyme–mediated mineralization potentials of carbon and nitrogen under long-term fertilization (>30 years) in a rice–rice cropping system. *J. Soils Sediments* 21, 3789–3800. doi: 10.1007/s11368-021-03048-0

Averill, C., and Waring, B. (2018). Nitrogen limitation of decomposition and decay: how can it occur? *Glob. Change Biol.* 24, 1417–1427. doi: 10.1111/gcb.13980

Banerjee, S., Schlaeppi, K., and van der Heijden, M. (2018). Keystone taxa as drivers of microbiome structure and functioning. *Nat. Rev. Microbiol.* 16, 567–576. doi: 10.1038/s41579-018-0024-1

Bardgett, R. D., Bullock, J. M., Lavorel, S., Manning, P., Schaffner, U., Ostle, N., et al. (2021). Combatting global grassland degradation. *Nat. Rev. Earth Env.* 2, 720–735. doi: 10.1038/s43017-021-00207-2

Carter, M. R., and Gregorich, E. G. (2007). *Soil sampling and methods of analysis* CRC press.

Chen, C., Chen, H., Chen, X., and Huang, Z. (2019). Meta-analysis shows positive effects of plant diversity on microbial biomass and respiration. *Nat. Commun.* 10:1332. doi: 10.1038/s41467-019-09258-y

Chen, X., Chen, H. Y. H., Chen, C., Ma, Z., Searle, E. B., Yu, Z., et al. (2019). Effects of plant diversity on soil carbon in diverse ecosystems: a global meta-analysis. *Biol. Rev.* 95, 167–183. doi: 10.1111/brv.12554

Chen, Q., Ding, J., Zhu, Y., He, J., and Hu, H. (2020). Soil bacterial taxonomic diversity is critical to maintaining the plant productivity. *Environ. Int.* 140:105766. doi: 10.1016/j.envint.2020.105766

Chen, J., Elsgaard, L., van Groenigen, K. J., Olesen, J. E., Liang, Z., Jiang, Y., et al. (2020). Soil carbon loss with warming: new evidence from carbon-degrading enzymes. *Glob. Change Biol.* 26, 1944–1952. doi: 10.1111/gcb.14986

Chen, H., Ju, P., Zhu, Q., Xu, X., Wu, N., Gao, Y., et al. (2022). Carbon and nitrogen cycling on the Qinghai–Tibetan plateau. *Nat. Rev. Earth Env.* 3, 701–716. doi: 10.1038/s43017-022-00344-2

Chen, J., Luo, Y., García Palacios, P., Cao, J., Dacal, M., Zhou, X., et al. (2018a). Differential responses of carbon-degrading enzyme activities to warming: implications for soil respiration. *Glob. Change Biol.* 24, 4816–4826. doi: 10.1111/gcb.14394

Chen, J., Luo, Y., van Groenigen, K. J., Hungate, B. A., Cao, J., Zhou, X., et al. (2018b). A keystone microbial enzyme for nitrogen control of soil carbon storage. *Sci. Adv.* 4:q1689. doi: 10.1126/sciadv.aaq1689

Chen, S., Wang, W., Xu, W., Wang, Y., Wan, H., Chen, D., et al. (2018). Plant diversity enhances productivity and soil carbon storage. *P. Natl. Acad. Sci. U. S. A.* 115, 4027–4032. doi: 10.1073/pnas.1700298114

Chen, J., Zhang, Y., Kuzyakov, Y., Wang, D., and Olesen, J. E. (2023). Challenges in upscaling laboratory studies to ecosystems in soil microbiology research. *Glob. Change Biol.* 29, 569–574. doi: 10.1111/gcb.16537

Cheng, J., Zhao, M., Cong, J., Qi, Q., Xiao, Y., Cong, W., et al. (2020). Soil ph exerts stronger impacts than vegetation type and plant diversity on soil bacterial community composition in subtropical broad-leaved forests. *Plant Soil* 450, 273–286. doi: 10.1007/s11104-020-04507-2

Costa, O., Pijl, A., and Kuramae, E. E. (2020). Dynamics of active potential bacterial and fungal interactions in the assimilation of acidobacterial EPS in soil. *Soil Biol. Biochem.* 148:107916. doi: 10.1016/j.soilbio.2020.107916

Crowther, T. W., van den Hoogen, J., Wan, J., Mayes, M. A., Keiser, A. D., Mo, L., et al. (2019). The global soil community and its influence on biogeochemistry. *Science* 365:eaav0550. doi: 10.1126/science.aav0550

Delgado-Baquerizo, M., Maestre, F. T., Reich, P. B., Trivedi, P., Osanai, Y., Liu, Y. R., et al. (2016). Carbon content and climate variability drive global soil bacterial diversity patterns. *Ecol. Monogr.* 86, 373–390. doi: 10.1002/ecm.1216

Deng, H., Zhang, B., Yin, R., Wang, H., Mitchell, S. M., Griffiths, B. S., et al. (2010). Long-term effect of re-vegetation on the microbial community of a severely eroded soil in sub-tropical China. *Plant Soil* 328, 447–458. doi: 10.1007/s11104-009-0124-9

Ding, W., Cong, W., and Lambers, H. (2021). Plant phosphorus-acquisition and -use strategies affect soil carbon cycling. *Trends Ecol. Evol.* 36, 899–906. doi: 10.1016/j.tree.2021.06.005

Dong, L., Fan, J., Li, J., Zhang, Y., Liu, Y., Wu, J., et al. (2022). Forests have a higher soil C sequestration benefit due to lower C mineralization efficiency: evidence from the central loess plateau case. *Agr. Ecosys. Environ.* 339:108144. doi: 10.1016/j.agee.2022.108144

Dong, S., Shang, Z., Gao, J., and Boone, R. B. (2020). Enhancing sustainability of grassland ecosystems through ecological restoration and grazing management in an era of climate change on Qinghai-Tibetan plateau. *Agr. Ecosys. Environ.* 287:106684. doi: 10.1016/j.agee.2019.106684

Dynarski, K. A., Bossio, D. A., and Scow, K. M. (2020). Dynamic stability of soil carbon: reassessing the "permanence" of soil carbon sequestration. *Front. Envi. Sci.* 8:514701. doi: 10.3389/fenvs.2020.514701

Eichorst, S. A., Trojan, D., Roux, S., Herbold, C., Rattei, T., and Woebken, D. (2018). Genomic insights into the *Acidobacteria* reveal strategies for their success in terrestrial environments. *Environ. Microbiol.* 20, 1041–1063. doi: 10.1111/1462-2920.14043

FAO Classification (2006). *Guidelines for soil description*. 4th Edition. Rome, Italy: Food and Agriculture Organization of the United Nations.

Fu, Y., Luo, Y., Auwal, M., Singh, B. P., Van Zwieten, L., and Xu, J. (2022). Biochar accelerates soil organic carbon mineralization via rhizodeposit-activated Actinobacteria. *Biol. Fert. Soils* 58, 565–577. doi: 10.1007/s00374-022-01643-y

Guo, Y., Chen, X., Wu, Y., Zhang, L., Cheng, J., Wei, G., et al. (2018). Natural revegetation of a semiarid habitat alters taxonomic and functional diversity of soil microbial communities. *Sci. Total Environ.* 635, 598–606. doi: 10.1016/j.scitotenv.2018.04.171

Hermans, S. M., Buckley, H. L., Case, B. S., Curran-Cournane, F., Taylor, M., and Lear, G. (2020). Using soil bacterial communities to predict physico-chemical variables and soil quality. *Microbiome* 8:79. doi: 10.1186/s40168-020-00858-1

Ho, A., Lonardo, D. P. D., and Bodelier, P. L. E. (2017). Revisiting life strategy concepts in environmental microbial ecology. *FEMS Microbiol. Ecol.* 93:fix006. doi: 10.1093/femsec/fix006

Hong, S., Piao, S., Chen, A., Liu, Y., Liu, L., Peng, S., et al. (2018). Afforestation neutralizes soil pH. *Nat. Commun.* 9:520. doi: 10.1038/s41467-018-02970-1

Hou, Y., He, K., Chen, Y., Zhao, J., Hu, H., and Zhu, B. (2021). Changes of soil organic matter stability along altitudinal gradients in Tibetan alpine grassland. *Plant Soil* 458, 21–40. doi: 10.1007/s11104-019-04351-z

Hsu, S. F., and Buckley, D. H. (2009). Evidence for the functional significance of diazotroph community structure in soil. *ISME J.* 3, 124–136. doi: 10.1038/ismej.2008.82

Hu, L., Li, Q., Yan, J., Liu, C., and Zhong, J. (2022). Vegetation restoration facilitates belowground microbial network complexity and recalcitrant soil organic carbon storage in Southwest China karst region. *Sci. Total Environ.* 820:153137. doi: 10.1016/j.scitotenv.2022.153137

Hu, Y., Shu, X., He, J., Zhang, Y., Xiao, H., Tang, X., et al. (2018). Storage of C, N, and P affected by afforestation with *Salix cupularis* in an alpine semiarid desert ecosystem. *Land Degrad. Dev.* 29, 188–198. doi: 10.1002/ldr.2862

Hu, M. J., Wang, J. L., Lu, L. L., Shao, P. S., Zhou, Z. X., Wang, D., et al. (2023). Post-fire soil extracellular enzyme activities in subtropical-warm temperate climate transitional forests. *Land Degrad. Dev.*, 1–11. doi: 10.1002/ldr.4582

Ibrahim, M. M., Zhang, H., Guo, L., Chen, Y., Heiling, M., Zhou, B., et al. (2021). Biochar interaction with chemical fertilizer regulates soil organic carbon mineralization and the abundance of key c-cycling-related bacteria in rhizosphere soil. *Eur. J. Soil Biol.* 106:103350. doi: 10.1016/j.ejsobi.2021.103350

Jackson, R. B., Lajtha, K., Crow, S. E., Hugelius, G., Kramer, M. G., and Piñeiro, G. (2017). The ecology of soil carbon: pools, vulnerabilities, and biotic and abiotic controls. *Annu. Rev. Ecol. Evol. S.* 48, 419–445. doi: 10.1146/annurev-ecolsys-112414-054234

Jia, Y., Zhai, G., Zhu, S., Liu, X., Schmid, B., Wang, Z., et al. (2021). Plant and microbial pathways driving plant diversity effects on soil carbon accumulation in subtropical forest. *Soil Biol. Biochem.* 161:108375. doi: 10.1016/j.soilbio.2021.108375

Jing, Z., Chen, R., Wei, S., Feng, Y., Zhang, J., and Lin, X. (2017). Response and feedback of C mineralization to P availability driven by soil microorganisms. *Soil Biol. Biochem.* 105, 111–120. doi: 10.1016/j.soilbio.2016.11.014

Juarez, S., Nunan, N., Duday, A., Pouteau, V., and Chenu, C. (2013). Soil carbon mineralisation responses to alterations of microbial diversity and soil structure. *Biol. Fert. Soils* 49, 939–948. doi: 10.1007/s00374-013-0784-8

Kalam, S., Basu, A., Ahmad, I., Sayyed, R. Z., El-Enshasy, H. A., Dailin, D. J., et al. (2020). Recent understanding of soil Acidobacteria and their ecological significance: a critical review. *Front. Microbiol.* 11:580024. doi: 10.3389/fmicb.2020.580024

Li, Y., Bruelheide, H., Scholten, T., Schmid, B., Sun, Z., Zhang, N., et al. (2019). Early positive effects of tree species richness on soil organic carbon accumulation in a large-scale forest biodiversity experiment. *J. Plant Ecol.* 12, 882–893. doi: 10.1093/jpe/rtz026

Li, N., Wang, B., Huang, Y., Huang, Q., Jiao, F., and An, S. (2022). Response of *cbbL*-harboring microorganisms to precipitation changes in a naturally-restored grassland. *Sci. Total Environ.* 838:156191. doi: 10.1016/j.scitotenv.2022.156191

Li, J., Yang, Y., Wen, J., Mo, F., and Liu, Y. (2022). Continuous manure application strengthens the associations between soil microbial function and crop production: evidence from a 7-year multisite field experiment on the Guanzhong plain. *Agr. Ecosys. Environ.* 338:108082. doi: 10.1016/j.agee.2022.108082

Liang, Y., Li, X., Zha, T., and Zhang, X. (2021). Vegetation restoration alleviated the soil surface organic carbon redistribution in the hillslope scale on the loess plateau, China. *Front. Envi. Sci.* 8:614761. doi: 10.3389/fenvs.2020.614761

Liang, C., Schimel, J. P., and Jastrow, J. D. (2017). The importance of anabolism in microbial control over soil carbon storage. *Nat. Microbiol.* 2:17105. doi: 10.1038/nmicrobiol.2017.105

Louca, S., Polz, M. F., Mazel, F., Albright, M. B. N., Huber, J. A., Connor, O., et al. (2018). Function and functional redundancy in microbial systems. *Nat. Ecol. Evol.* 2, 936–943. doi: 10.1038/s41559-018-0519-1

Maestre, F. T., Delgado-Baquerizo, M., Jeffries, T. C., Eldridge, D. J., Ochoa, V., Gozalo, B., et al. (2015). Increasing aridity reduces soil microbial diversity and abundance in global drylands. *P. Natl. Acad. Sci. U. S. A.* 112, 15684–15689. doi: 10.1073/pnas.1516684112

Mahaut, L., Fort, F., Violle, C., and Freschet, G. T. (2019). Multiple facets of diversity effects on plant productivity: species richness, functional diversity, species identity and intraspecific competition. *Funct. Ecol.* 34, 287–298. doi: 10.1111/1365-2435.13473

Maron, P., Sarr, A., Kaisermann, A., Lévêque, J., Mathieu, O., Guigue, J., et al. (2018). High microbial diversity promotes soil ecosystem functioning. *Appl. Environ. Microb.* 84, e02738–e02717. doi: 10.1128/AEM.02738-17

Martin, D. M. (2017). Ecological restoration should be redefined for the twenty-first century. *Restor. Ecol.* 25, 668–673. doi: 10.1111/rec.12554

Meyer, N., Welp, G., Rodionov, A., Borchard, N., Martius, C., and Amelung, W. (2018). Nitrogen and phosphorus supply controls soil organic carbon mineralization in tropical topsoil and subsoil. *Soil Biol. Biochem.* 119, 152–161. doi: 10.1016/j.soilbio.2018.01.024

Michalet, R., Delerue, F., Liancourt, P., and Pugnaire, F. I. (2021). Are complementarity effects of species richness on productivity the strongest in species-rich communities? *J. Ecol.* 109, 2038–2046. doi: 10.1111/1365-2745.13658

Peixoto, L., Elsgaard, L., Rasmussen, J., and Olesen, J. E. (2021). Nitrogen and phosphorus co-limit mineralization of labile carbon in deep subsoil. *Eur. J. Soil Sci.* 72, 1879–1884. doi: 10.1111/ejss.13083

Philippot, L., Spor, A., Henault, C., Bru, D., Bizouard, F., Jones, C. M., et al. (2013). Loss in microbial diversity affects nitrogen cycling in soil. *ISME J.* 7, 1609–1619. doi: 10.1038/ismej.2013.34

Plante, A. F., Fernández, J. M., Haddix, M. L., Steinweg, J. M., and Conant, R. T. (2011). Biological, chemical and thermal indices of soil organic matter stability in four grassland soils. *Soil Biol. Biochem.* 43, 1051–1058. doi: 10.1016/j.soilbio.2011.01.024

Qin, S., Kou, D., Mao, C., Chen, Y., Chen, L., and Yang, Y. (2021). Temperature sensitivity of permafrost carbon release mediated by mineral and microbial properties. *Sci. Adv.* 7:abe3596. doi: 10.1126/sciadv.abe3596

Raiesi, F., and Salek-Gilani, S. (2018). The potential activity of soil extracellular enzymes as an indicator for ecological restoration of rangeland soils after agricultural abandonment. *Appl. Soil Ecol.* 126, 140–147. doi: 10.1016/j.apsoil.2018.02.022

Ramin, K. I., and Allison, S. D. (2019). Bacterial tradeoffs in growth rate and extracellular enzymes. *Front. Microbiol.* 10:2956. doi: 10.3389/fmicb.2019.02956

Ramírez, P. B., Fuentes-Alburquenque, S., Díez, B., Vargas, I., and Bonilla, C. A. (2020). Soil microbial community responses to labile organic carbon fractions in relation to soil type and land use along a climate gradient. *Soil Biol. Biochem.* 141:107692. doi: 10.1016/j.soilbio.2019.107692

Ren, C., Wang, T., Xu, Y., Deng, J., Zhao, F., Yang, G., et al. (2018). Differential soil microbial community responses to the linkage of soil organic carbon fractions with respiration across land-use changes. *Forest Ecol. Manag.* 409, 170–178. doi: 10.1016/j.foreco.2017.11.011

Rousk, K., Michelsen, A., and Rousk, J. (2016). Microbial control of soil organic matter mineralization responses to labile carbon in subarctic climate change treatments. *Glob. Change Biol.* 22, 4150–4161. doi: 10.1111/gcb.13296

Schimel, J. P., and Schaeffer, S. M. (2012). Microbial control over carbon cycling in soil. *Front. Microbiol.* 3:348. doi: 10.3389/fmicb.2012.00348

Shu, X., He, J., Zhou, Z., Xia, L., Hu, Y., Zhang, Y., et al. (2022). Organic amendments enhance soil microbial diversity, microbial functionality and crop yields: a meta-analysis. *Sci. Total Environ.* 829:154627. doi: 10.1016/j.scitotenv.2022.154627

Sun, S., and Badgley, B. D. (2019). Changes in microbial functional genes within the soil metagenome during forest ecosystem restoration. *Soil Biol. Biochem.* 135, 163–172. doi: 10.1016/j.soilbio.2019.05.004

Tan, Q., Jia, Y., and Wang, G. (2021). Decoupling of soil nitrogen and phosphorus dynamics along a temperature gradient on the Qinghai-Tibetan plateau. *Geoderma* 396:115084. doi: 10.1016/j.geoderma.2021.115084

Tardy, V., Spor, A., Mathieu, O., Lévèque, J., Terrat, S., Plassart, P., et al. (2015). Shifts in microbial diversity through land use intensity as drivers of carbon mineralization in soil. *Soil Biol. Biochem.* 90, 204–213. doi: 10.1016/j.soilbio.2015.08.010

Tian, D. S., Xiang, Y. Z., Seabloom, E., Chen, H., Wang, J. S., Yu, G. R., et al. (2021). Ecosystem restoration and belowground multifunctionality: a network view. *Ecol. Appl.* 32:e2575. doi: 10.1002/eap.2575

van der Heijden, M. G. A., Bardgett, R. D., and van Straalen, N. M. (2008). The unseen majority: soil microbes as drivers of plant diversity and productivity in terrestrial ecosystems. *Ecol. Lett.* 11, 296–310. doi: 10.1111/j.1461-0248.2007.01139.x

Vance, E. D., Brookes, P. C., and Jenkinson, D. S. (1987). An extraction method for measuring soil microbial biomass C. *Soil Biol. Biochem.* 19, 703–707. doi: 10.1016/0038-0717(87)90052-6

Wang, D., Chi, Z. S., Yue, B. J., Huang, X. D., Zhao, J., Song, H. Q., et al. (2020). Effects of mowing and nitrogen addition on the ecosystem c and n pools in a temperate steppe: a case study from northern China. *Catena* 185:104332. doi: 10.1016/j.catena.2019.104332

Wang, Y., Lv, W., Xue, K., Wang, S., Zhang, L., Hu, R., et al. (2022). Grassland changes and adaptive management on the Qinghai–Tibetan plateau. *Nat. Rev. Earth Env.* 3, 668–683. doi: 10.1038/s43017-022-00330-8

Wang, G., Post, W. M., Mayes, M. A., Frerichs, J. T., and Sindhu, J. (2012). Parameter estimation for models of ligninolytic and cellulolytic enzyme kinetics. *Soil Biol. Biochem.* 48, 28–38. doi: 10.1016/j.soilbio.2012.01.011

Wang, Z., Ren, J., Xu, C., Geng, Z., Du, X., and Li, Y. (2021). Characteristics of water extractable organic carbon fractions in the soil profiles of *Picea asperata* and *Betula albosinensis* forests. *J. Soils Sediments* 21, 3580–3589. doi: 10.1007/s11368-021-03034-6

Wang, S., Zhao, S., Yang, B., Zhang, K., Fan, Y., Zhang, L., et al. (2022). The carbon and nitrogen stoichiometry in litter-soil-microbe continuum rather than plant diversity primarily shapes the changes in bacterial communities along a tropical forest restoration chronosequence. *Catena* 213:106202. doi: 10.1016/j.catena.2022.106202

Wei, X., Zhu, Z., Liu, Y., Luo, Y., Deng, Y., Xu, X., et al. (2020). C:N:P stoichiometry regulates soil organic carbon mineralization and concomitant shifts in microbial community composition in paddy soil. *Biol. Fert. Soils* 56, 1093–1107. doi: 10.1007/s00374-020-01468-7

Wu, J., Cheng, X., Luo, Y., Liu, W., and Liu, G. (2021). Identifying carbon-degrading enzyme activities in association with soil organic carbon accumulation under land-use changes. *Ecosystems.* 25, 1219–1233. doi: 10.1007/s10021-021-00711-y

Wu, J., Zhang, Q., Zhang, D., Jia, W., Chen, J., Liu, G., et al. (2022). The ratio of ligninase to cellulase increased with the reduction of plant detritus input in a coniferous forest in subtropical China. *Appl. Soil Ecol.* 170:104269. doi: 10.1016/j.apsoil.2021.104269

Xiao, Y., Huang, Z., Ling, Y., Cai, S., Zeng, B., Liang, S., et al. (2022). Effects of forest vegetation restoration on soil organic carbon and its labile fractions in the Danxia landform of China. *Sustainability-Basel.* 14:12283. doi: 10.3390/su141912283

Xu, Y., Dong, S., Gao, X., Yang, M., Li, S., Shen, H., et al. (2021). Aboveground community composition and soil moisture play determining roles in restoring ecosystem multifunctionality of alpine steppe on Qinghai-Tibetan plateau. *Agr. Ecosys. Environ.* 305:107163. doi: 10.1016/j.agee.2020.107163

Xu, Y., Zhang, W., Zhong, Z., Guo, S., Han, X., Yang, G., et al. (2019). Vegetation restoration alters the diversity and community composition of soil nitrogen-fixing microorganisms in the loess hilly region of China. *Soil Sci. Soc. Am. J.* 83, 1378–1386. doi: 10.2136/sssaj2019.03.0066

Yang, T., Chen, Q., Yang, M., Wang, G., Zheng, C., Zhou, J., et al. (2022). Soil microbial community under bryophytes in different substrates and its potential to degraded karst ecosystem restoration. *Int. Biodeterior. Biodegradation* 175:105493. doi: 10.1016/j.ibiod.2022.105493

Yang, Y., Dou, Y., and An, S. (2018). Testing association between soil bacterial diversity and soil carbon storage on the loess plateau. *Sci. Total Environ.* 626, 48–58. doi: 10.1016/j.scitotenv.2018.01.081

Yang, S., Yao, F., Ye, J., Fang, S., Wang, Z., Wang, R., et al. (2019). Latitudinal pattern of soil lignin/cellulose content and the activity of their degrading enzymes across a temperate forest ecosystem. *Ecol. Indic.* 102, 557–568. doi: 10.1016/j.ecolind.2019.03.009

Yao, M., Rui, J., Li, J., Wang, J., Cao, W., and Li, X. (2018). Soil bacterial community shifts driven by restoration time and steppe types in the degraded steppe of Inner Mongolia. *Catena* 165, 228–236. doi: 10.1016/j.catena.2018.02.006

Yao, F., Yang, S., Wang, Z., Wang, X., Ye, J., Wang, X., et al. (2017). Microbial taxa distribution is associated with ecological trophic cascades along an elevation gradient. *Front. Microbiol.* 8:2071. doi: 10.3389/fmicb.2017.02071

Zeng, Q., An, S., and Liu, Y. (2017). Soil bacterial community response to vegetation succession after fencing in the grassland of China. *Sci. Total Environ.* 609, 2–10. doi: 10.1016/j.scitotenv.2017.07.102

Zhang, B., Cai, Y., Hu, S., and Chang, S. X. (2021). Plant mixture effects on carbon-degrading enzymes promote soil organic carbon accumulation. *Soil Biol. Biochem.* 163:108457. doi: 10.1016/j.soilbio.2021.108457

Zhang, S., Fang, Y., Luo, Y., Li, Y., Ge, T., Wang, Y., et al. (2021). Linking soil carbon availability, microbial community composition and enzyme activities to organic carbon mineralization of a bamboo forest soil amended with pyrogenic and fresh organic matter. *Sci. Total Environ.* 801:149717. doi: 10.1016/j.scitotenv.2021.149717

Zhang, K., Li, X., Cheng, X., Zhang, Z., and Zhang, Q. (2019). Changes in soil properties rather than functional gene abundance control carbon and nitrogen mineralization rates during long-term natural revegetation. *Plant Soil* 443, 293–306. doi: 10.1007/s11104-019-04212-9

Zhang, H., Zheng, X., Cai, Y., and Chang, S. X. (2022). Land-use change enhanced soc mineralization but did not significantly affect its storage in the surface layer. *Int. J. Env. Res. Pub. He.* 19:3020. doi: 10.3390/ijerph19053020

Zhao, M., Zhou, J., and Kalbitz, K. (2008). Carbon mineralization and properties of water-extractable organic carbon in soils of the south loess plateau in China. *Eur. J. Soil Biol.* 44, 158–165. doi: 10.1016/j.ejsobi.2007.09.007

Zhong, Z., Wang, X., Zhang, X., Zhang, W., Xu, Y., Ren, C., et al. (2019). Edaphic factors but not plant characteristics mainly alter soil microbial properties along a restoration chronosequence of *Pinus tabulaeformis* stands on Mt Ziwuling, China. *Forest Ecol. Manag.* 453:117625. doi: 10.1016/j.foreco.2019.117625

Zhou, G., Zhou, X., Eldridge, D. J., Han, X., Song, Y., Liu, R., et al. (2022). Temperature and rainfall patterns constrain the multidimensional rewilding of global forests. *Adv. Sci.* 9:2201144. doi: 10.1002/advs.202201144

Zhu, B., Gutknecht, J. L. M., Herman, D. J., Keck, D. C., Firestone, M. K., and Cheng, W. (2014). Rhizosphere priming effects on soil carbon and nitrogen mineralization. *Soil Biol. Biochem.* 76, 183–192. doi: 10.1016/j.soilbio.2014.04.033

Zhuang, Y., Zhu, J., Shi, L., Fu, Q., Hu, H., and Huang, Q. (2022). Influence mechanisms of iron, aluminum and manganese oxides on the mineralization of organic matter in paddy soil. *J. Environ. Manag.* 301:113916. doi: 10.1016/j.jenvman.2021.113916

frontiers | Frontiers in Microbiology

TYPE Original Research
PUBLISHED 12 May 2023
DOI 10.3389/fmicb.2023.1167353

OPEN ACCESS

EDITED BY
Yu Luo,
Zhejiang University, China

REVIEWED BY
Dong Wang,
Henan University, China
Yuji Jiang,
Institute of Soil Science,
Chinese Academy of Sciences (CAS), China

*CORRESPONDENCE
Ping Huang
✉ huangping@cigit.ac.cn

RECEIVED 16 February 2023
ACCEPTED 19 April 2023
PUBLISHED 12 May 2023

CITATION
Zhu K, Jia W, Mei Y, Wu S and Huang P (2023) Shift from flooding to drying enhances the respiration of soil aggregates by changing microbial community composition and keystone taxa.
Front. Microbiol. 14:1167353.
doi: 10.3389/fmicb.2023.1167353

Shift from flooding to drying enhances the respiration of soil aggregates by changing microbial community composition and keystone taxa

Kai Zhu, Weitao Jia, Yu Mei, Shengjun Wu and Ping Huang*

Key Laboratory of Reservoir Aquatic Environment, Chongqing Institute of Green and Intelligent Technology, Chinese Academy of Sciences, Chongqing, China

Changes in the water regime are among the crucial factors controlling soil carbon dynamics. However, at the aggregate scale, the microbial mechanisms that regulate soil respiration under flooding and drying conditions are obscure. In this research, we investigated how the shift from flooding to drying changes the microbial respiration of soil aggregates by affecting microbial community composition and their co-occurrence patterns. Soils collected from a riparian zone of the Three Gorges Reservoir, China, were subjected to a wet-and-dry incubation experiment. Our data illustrated that the shift from flooding to drying substantially enhanced soil respiration for all sizes of aggregate fractions. Moreover, soil respiration declined with aggregate size in both flooding and drying treatments. The keystone taxa in bacterial networks were found to be *Acidobacteriales*, *Gemmatimonadales*, *Anaerolineales*, and *Cytophagales* during the flooding treatment, and *Rhizobiales*, *Gemmatimonadales*, *Sphingomonadales*, and *Solirubrobacterales* during the drying treatment. For fungal networks, *Hypocreales* and *Agaricalesin* were the keystone taxa in the flooding and drying treatments, respectively. Furthermore, the shift from flooding to drying enhanced the microbial respiration of soil aggregates by changing keystone taxa. Notably, fungal community composition and network properties dominated the changes in the microbial respiration of soil aggregates during the shift from flooding to drying. Thus, our study highlighted that the shift from flooding to drying changes keystone taxa, hence increasing aggregate-scale soil respiration.

KEYWORDS

soil respiration, soil aggregates, water regime changes, microbial community, co-occurrence network, keystone taxa

1. Introduction

Soil aggregates, the fundamental building blocks of soil structure, perform a vital function in SOC turnover and nutrient cycling by providing different habitats for microbial activity (Six et al., 2004; Wang et al., 2021). According to the hierarchical model, aggregates are classified as macroaggregates (> 0.25 mm) and microaggregates (< 0.25 mm; Tisdall and Oades, 1982). Different aggregate size classes have distinct roles in soil nutrient supply and retention by influencing soil biological processes and pore characteristics (Mangalassery et al., 2013; Chen et al., 2023), thereby leading to small-scale heterogeneity in SOC mineralization (i.e., soil

respiration) (Wang et al., 2019). Macroaggregates generally comprise labile young SOC, predominantly originating from fresh SOC inputs, fungal hyphae, and plant residues (Six et al., 2004). However, the most recalcitrant SOC formed by microbial-induced bonding of clay particles and organometallic complexes is stored in microaggregates (Zhang et al., 2018). Although macroaggregates are considered to have higher soil respiration than microaggregates (Noellemeyer et al., 2008; Fernández et al., 2010; Bandyopadhyay and Lal, 2014), macroaggregates have been shown to reduce soil respiration in contrast to microaggregates in various studies (Drury et al., 2004; Sey et al., 2008) or the same among aggregate size fractions (Razafimbelo et al., 2008; Rabbi et al., 2014). These conflicting results suggest that further research is required on the regulatory mechanisms of aggregate-scale soil respiration.

Soil respiration is profoundly affected by soil water regimes (Luo and Zhou, 2006; Zhu et al., 2020, 2022a). The changes in water regimes, such as intensive rain after a long drought or drying after intensive flooding, are dominant factor regulating biogeochemical processes in soils (Bodner et al., 2013; Evans and Wallenstein, 2014). These changes have a vital impact on soil aggregate stability, nutrient cycling, and microbial community composition and activity (Denef et al., 2001; Jansson and Hofmockel, 2020). Various microbial communities may colonize a given environment because varied sizes of aggregates provide unique niches for them to thrive in (including aerobic and anaerobic environments, for example) (Trivedi et al., 2017). Microaggregates have a high fungal abundance and a low bacterial abundance (Gupta and Germida, 1988; Jiang et al., 2018; Wang et al., 2021). Microaggregates amass more recalcitrant carbon, which is more favorable to oligotrophs, while macroaggregates contain comparatively much labile carbon, which favors copiotrophs (Trivedi et al., 2017). Increased soil water content generally promotes bacterial abundance, whereas drought decreases bacterial activity (Johan et al., 1986; Meisner et al., 2013). Owing to their thick cell walls, fungi are insufficiently sensitive to changes in soil moisture (Holland and Coleman, 1987; Umair et al., 2020; Dacal et al., 2022). Therefore, soil bacteria and fungi may respond differently to water regime changes at the aggregate scale (Navas et al., 2021), thereby affecting soil respiration. However, at the aggregate scale, our knowledge of how soil microbe communities respond to changes in water availability is still rather restricted.

Riparian zones, or the transition zones between aquatic and terrestrial ecosystems, facilitate critical ecological functions, such as supplying corridors for species migration and improving biodiversity (Jones et al., 2010; de Sosa et al., 2018). Water-level fluctuations have a significant impact on riparian ecosystems' functions (Leira and Cantonati, 2008). These fluctuations are the major drivers of water regime changes (the shift from aerobic to anaerobic environments), which substantially affects soil respiration, soil aggregates and soil microbial community structure (Fierer et al., 2003; Zhu et al., 2022a). Nevertheless, it is not clear how microbial community changes at the aggregate scale due to water regime changes and how these changes affect respiration.

To date, research on the impacts of water regime changes on soil respiration and its mechanisms have primarily focused on wet–dry cycles (Jarvis et al., 2007), rewetting (i.e., rainfall) after long-term drought (De Nijs et al., 2019), peatland drainage, and water level decline (Silvola et al., 1996; Danevčič et al., 2010). Among these studies, the focus has been on bulk soil. However, little is known about the impact of soil microbes on aggregate-scale soil respiration under water regime changes in the riparian zone. Filling this knowledge gap will improve our understanding of the SOC dynamics in water regime changes, which thus contributing to the realization of riparian ecosystem carbon sequestration and emission reduction targets.

The riparian zones of the Three Gorges Reservoir (TGR) are an excellent location for investigating the influence of soil microbes in soil respiration in the face of extreme shifts in the water regime. The water level of the TGR in China varies from 145 m to 175 m during summer and winter, respectively, due to dam activities, which results in the formation of a new riparian zone that is 349 km^2 (Zhu et al., 2020). In the TGR riparian zone, yearly disruption from fluctuating water levels, soil erosion and deposition caused by periodical draining and flooding, and the presence of microorganisms all have the potential to significantly alter soil aggregation (Xiang et al., 2018; Zhu et al., 2022a). She et al. (2022) recently reported that water regime changes result in distinct microbial community compositions and functions between the drainage and flooding periods, thereby controlling CH_4 and CO_2 emissions in the TGR. Zhu et al. (2022a) reported that in the riparian zone of the TGR, intense wet–dry oscillations reduce the soil's aggregate stability while simultaneously increasing soil respiration. However, in this zone, the microbial mechanisms of aggregate-scale soil respiration under water regime changes remain unclear.

This research sought to examine how aggregate-scale soil respiration is regulated by microbial community structure in response to changes in the water regime (i.e., from flooding to drying), with a specific focus on microbiota population, microbial co-occurrence tendencies, and their keystone taxa in networks. Specifically, this study investigates (1) how varying aggregate sizes influence soil respiration, bacterial and fungal community composition, and co-occurrence networks during flooding and drying; (2) how the microbial keystone taxa change during the flooding and drying periods and whether soil respiration is regulated by keystone taxa at the aggregate scale; and (3) how to reveal the regulatory mechanisms of aggregate-scale soil respiration for different flooding and drying treatments. Considering that soil respiration and microbial communities are susceptible to disturbance due to water regime changes, we hypothesized that (1) soil respiration rate and microbial community richness would decline with the decrease in soil aggregate size, and their respiration would increase with the shift from flooding to drying, and (2) the microbial keystone taxa would predominantly regulate soil respiration in both flooding and drying treatments.

2. Materials and methods

2.1. Experimental sites and soil sampling

In June 2018, soil samples for this research were taken from the Wuyangwan riparian zone (31°11′20″N, 108°27′40″E), which is representative of the riparian zones along the Pengxi River. As a result of the activities of the Three Gorges Dam, the water level of the Pengxi River, which is a secondary branch in the TGR of the Yangtze River, varies between 145 and 175 meters above sea level (m.a.s.l) in the summer and winter, respectively (Figure 1) since the TGR was fully impounded in 2010 (Zhu et al., 2020). With average annual temperatures of 18.2 ° C and average annual precipitation of 1,200 mm, the climate of this region may be described as a humid and

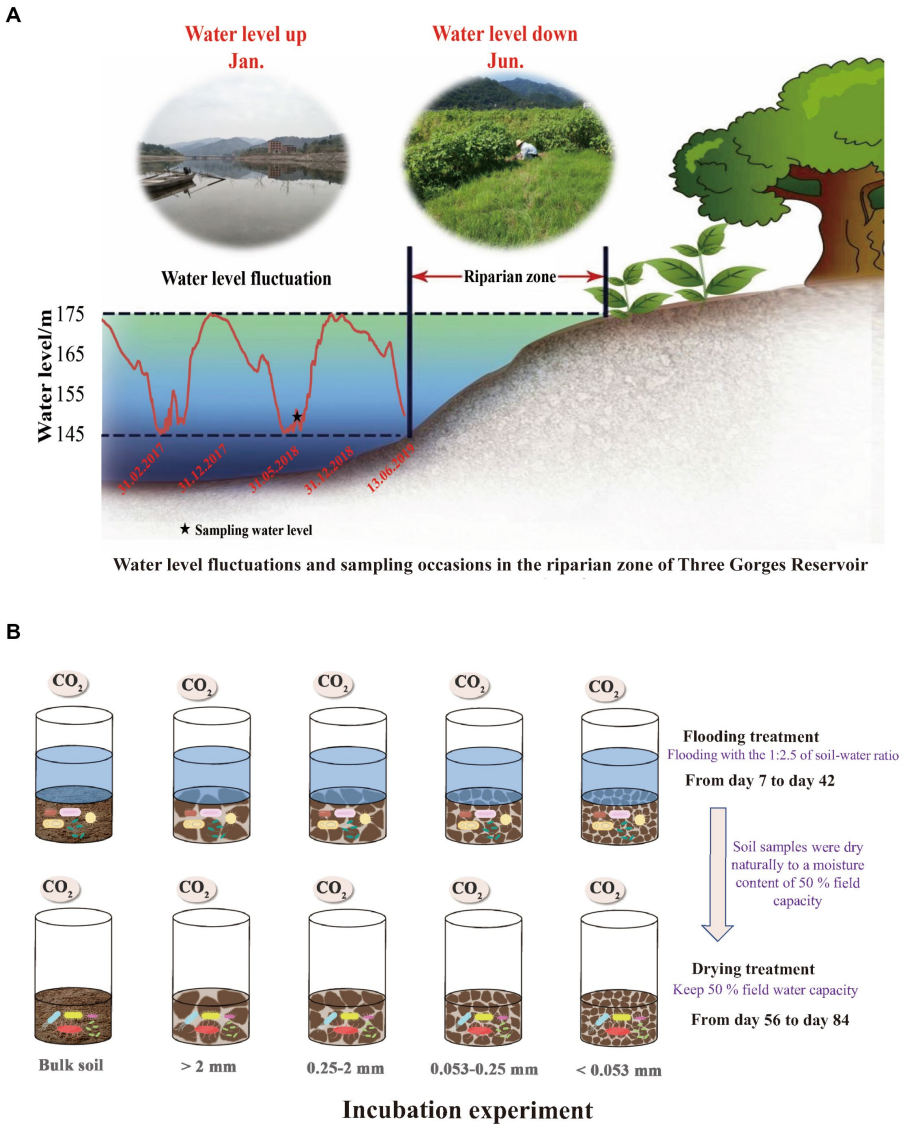

Water level fluctuations and sampling occasions in the riparian zone of Three Gorges Reservoir

FIGURE 1
Water level changes in the Three Gorges Reservoir and sampling frequency in the riparian zone **(A)**; Schematic design and flow chart of the lab incubation experiment **(B)**.

mid-subtropical monsoon. The period from April through September, which is considered to be the plant growth season, receives over 60% of the total yearly precipitation (Zhu et al., 2020). Purple soil, formed from purple sandstone, is the dominant zonal soil type (Entisols in the World Reference Base) (Chen et al., 2014) with a texture dominated by silt loam (2.50% clay, 65.41% silt, and 30.09% sand) (Zhu et al., 2022b). Most native trees have died because of periodic flooding. Moreover, tillage is not allowed in the TGR riparian zone owing to environmental concerns. Thus, grasslands are the dominant land-use type, comprising flood-tolerant grasses such as *Xanthium sibiricum, Paspalum thunbergii*, and *Cynodon dactylon* (Ye et al., 2019). Since 2010, corn fields have been converted to selected grasslands, which were used as the study sites.

Based on an S-shaped sampling strategy and using a soil corer (5.7 cm diameter), nine soil samples, weighing approximately 1.5 kg were obtained at random from the grasslands from 0 to 10 cm depths. To avoid any impacts that might break the macroaggregates, we used a wooden mallet to carefully drive the corer into the soil.

2.2. Soil physicochemical properties

The soil that had been dried in an oven was used in the calculation of the soil bulk density (SBD). After mixing the sample with distilled water at a ratio of 1:2.5 soil to water, the pH of the soil was determined. SOC and TN were determined by the dry combustion method with a CN elemental analyzer (Vario Max CN Macro Elemental Analyzer, Elementar Analysensysteme GmbH, Hanau, Germany) (Nelson and Sommers, 1996).

2.3. Sieving of soil aggregates

Bulk soil (BS) samples were broken by hand along the fractures of the peds (> 8 mm). Plant residues, stones, visible fauna, and roots were excluded from the samples. Aggregate fractions were measured using wet sieving as described by Márquez et al. (2004). Briefly, a stack of sieves (2-, 0.25-and 0.053-mm) was used to manually fractionate air-dried samples of soil into four size classes in distilled water for 2 min at a rate of 30 times/min. The bulk soil was broken down into 4 aggregate fractions: > 2 mm (large macroaggregates, LM), 0.25–2 mm (small macroaggregates, SM), 0.053–0.25 mm (microaggregates, MI), and < 0.053 mm (silt and clay, SC). As soon as wet sieving was complete, the aggregates were given a gentle rinse in sterile water.

2.4. Incubation experiment

The prepared soils were introduced into 1,000 ml incubation jars (equivalent to 200 g of oven-dried soil in each), with three replicate jars of each treatment. In total, 15 glass jars were used for the incubation experiments, including three jars each for BS, LM, SM, MI, and SC. To accomplish soil microbial stability, we pre-incubated all soil samples at 15°C for 7 days with 50% water-filled pore space (Butterly et al., 2010; Jiang et al., 2021).

To simulate the soil moisture changes in the TGR riparian zone, the experiment was conducted at 15°C with two treatments: (a) flooding at a ratio of 1:2.5 soil to water and (b) drying with a moisture content of 50% field capacity. All incubated samples were placed in a constant-temperature incubator at 15°C, and in case it was deemed essential, deionized water was introduced into the mixture. Following the pre-incubation period, gas samples were withdrawn from the flooding incubation using a syringe on days 7, 14, 21, 28, 35, and 42. Subsequently, the flooding incubation experiment was terminated, and the soil samples were naturally dried to a moisture content of 50% field capacity on the 55th day. Gas samples were extracted on days 56, 63, 70, 77, and 84 of the drying incubation. Twice weekly, the jars were weighed, and water was replenished to prevent excessive evaporation and keep the humidity level consistent. Following the removal of the polyethylene film from the jars, their headspaces were purged with fresh air for approximately 15 min. Gas was collected in the jars after they were hermetically sealed with rubber septum covers. At 0 and 1 h after the jar had been sealed, a gas-tight syringe was used to extract about 30 ml of gas from the headspace. The levels of carbon dioxide in the samples were determined by the use of Gas chromatography (GC-2014, Shimadzu, Japan).

2.5. Microbial community analysis

Following the guidelines provided by the manufacturer of the MoBio PowerSoil DNA extraction kit, total DNA was extracted from 0.25 g of soil. Following amplification with fungal primers, ITS1F/ITS2R (Adams et al., 2013) and bacterial primers, 338\u00B0F/806R (Lee et al., 2012), samples were sent to the Novogene Biotechnology Co., Ltd. (Beijing, China) for sequencing via Illumina® MiSeq. To extract the valid data (clean data) after sequencing, the raw data were first demultiplexed and then subjected to quality filtering using the Trimmomatic program (Magoč and Salzberg, 2011). A table of operational taxonomic units (OTUs) was created by clustering the sequences. Using the UPARSE program (UPARSE v7.0.1001[1]; Edgar, 2013) Sequences from bacteria and fungi with a similarity of ≥97% were placed in the same OTU. BLAST was employed to search the UNITE (fungi) and RDP (bacteria) databases for matching sequences, and then representatives of each OTU were chosen for taxonomic annotation (Wang et al., 2007; Kõljalg et al., 2013). There were a total of 17,115 16S OTUs and 5,033 ITS OTUs discovered across all samples. Bacterial and fungal raw sequencing data were jointly submitted to the National Center for Biotechnology Information (NCBI) Sequence Read Archive (SRA) database under BioProject accession number PRJNA844584.

2.6. Calculations and statistical analysis

The soil microbial respiration was calculated according to the following formula (Wang et al., 2014):

$$F = \rho \cdot \frac{v}{a} \cdot \frac{p}{p_0} \cdot \frac{t_0}{t} \cdot \frac{dC_t}{d_t} \quad (1)$$

Whereby, F denotes the CO_2 flux (mg m^{-2} h^{-1}); ρ (kg m^{-3}) represents the CO_2 density under normal circumstances; the effective volume is denoted by v (m^3) while the bottom of the incubation jar is denoted by (m^2); t_0 represents the absolute temperature when circumstances are normalized; t signifies the absolute temperature within the jar; and $\frac{dC_t}{d_t}$ is the shift in the level of CO_2 (m^3 m^{-3}) that occurred within the jar throughout the sampling duration (h).

R software (version 4.1.0) was used for every computation along with the data analyzes. The Levene's and Kolmogorov–Smirnov tests were completed to correspondingly ensure the homogeneity of variances and the normality of the data before proceeding with the analysis. If the conditions were not met, a log or square-root transformation was applied. Soil aggregate fractions were separated into four groups, and their individual attributes were compared via analysis of variance (ANOVA). Soil respiration variations between aggregate fractions were analyzed through repeated-measure ANOVA. Also, an independent sample t-test was conducted to contrast the impacts of flooding and drying treatments on the aforementioned characteristics at the same aggregate scale. Two-way ANOVA was executed to determine the different moisture treatments, soil aggregate sizes, and their interactions with soil respiration.

Using the cmdscale function in the *vegan* package, principal coordinate analysis (PCoA) was utilized to investigate the differences in bacterial and fungal community architectures across the various treatments and aggregate fractions. To show the connections between microbial populations and to compute their topological features, we adopted the co-occurrence network inference (CoNet) in Gephi 0.9.2. Keystone species were identified as OTUs exhibiting a high degree, high eigenvector centrality, and high closeness/betweenness centrality (Wang et al., 2021). The highest average degree was considered a complex microbial network (Wagg et al., 2019). Soil

1 http://drive5.com/uparse

respiration and keystone species abundance were also subjected to regression analyzes (Banerjee et al., 2016).

To determine how various predictor factors may be influencing soil respiration, partial least squares path modeling (PLS-PM) was carried out using the *plspm* program (Sanchez, 2013). Fourteen manifest variables [SOC, C/N ratio, pH, soil respiration, positive to negative edges (P/N) of the overall network (BPN), bacterial P/N related to keystone taxa (BKPN), bacterial average clustering coefficients (BACC), bacterial richness (BR), bacterial first dominant eigengenes BFDE, fungi richness (FR), fungal first dominant eigengenes (FFDE), fungal P/N of the overall network (FPN), fungal P/N related to keystone taxa (FKPN), and fungal average clustering coefficients (FACC)] and four latent variables (bacterial network, bacterial community composition, fungal network, and fungal community composition) were condensed for use in the PLS-PM. There were two or three manifest variables associated with each latent variable. The bacterial networks encompassed BPN, BKPN, and BACC. The bacterial community composition comprised BR and BFDE. Fungal networks included FR, FFDE, and FPN. The fungal community composition included FR and FFDE. We then computed the models' path coefficients, which describe the direction and intensity of the linear correlations between the variables, as well as the explained variability (R^2). Based on this information, we determined the overall influence (both direct and indirect) that each variable had on soil respiration. The path coefficients represent the direct impacts, while the indirect effects may be calculated by multiplying the direct effects by the indirect path's path coefficients. The model's overall prediction accuracy was measured by calculating its goodness of fit. Before running PLS-PM, we used a *car* package to ensure there wasn't any multicollinearity between our chosen independent variables. In this investigation, we conducted regression random forest analysis with the *rfPermute* program to determine the most important soil variables for soil respiration. Variables with low levels of intercorrelation, a variance inflation factor of <10, significance levels of <0.05, and greater levels of mean squared error (MSE percent) were retained (Liaw and Wiener, 2002). Consequently, the proportion of soil aggregates, TN, and SBD was excluded (Supplementary Figure S1).

3. Results

3.1. Soil characteristics and microbial respiration

Flooding and drying influenced soil properties (Table 1). Flooding to drying generally decreased SOC and TN contents but slightly increased soil pH in all aggregate fractions. The SOC and TN contents of >2 mm aggregate fractions were substantially elevated relative to those of the other aggregate fractions in both the flooding and drying treatments. The SBD decreased as the aggregate size increased in both the flooding and drying treatments (i.e., LM < SM < MI < SC).

The soil CO_2 flux (i.e., soil respiration) slightly increased with incubation time during the flooding phase (Figure 2). In contrast, soil respiration slightly decreased with increasing incubation time during the drying phase (Figure 2). Mean soil respiration dropped as the aggregate size became smaller in both the flooding and drying treatments (i.e., LM > SM > MI > SC). Notably, flooding to drying substantially enhanced the mean soil respiration ($p < 0.05$; Figure 3).

3.2. Abundance and composition of the microbial population

The soil microbial community richness is presented in Supplementary Table S1. The bacterial richness considerably decreased in response to the shift from flooding to drying. In contrast, the fungal richness substantially increased in response to the shift from flooding to drying. The maximum bacterial richness among the aggregate fractions in the flooding and drying conditions were MI (i.e., 5139.00 ± 38.73) and SC (i.e., 4290.67 ± 152.78), respectively. The minimum bacterial richness among the aggregate fractions in the flooding and drying conditions were SC (i.e., 4617.00 ± 107.41) and MI (i.e., 3671.33 ± 93.38), respectively. The maximum fungal richness among the aggregate fractions in the flooding and drying conditions were SM (i.e., 611.00 ± 22.15) and SC (i.e., 723.33 ± 86.33), respectively. The minimum fungal richness among the aggregate fractions in the flooding and drying conditions were MI (i.e., 512.67 ± 61.06) and SM (i.e., 663.67 ± 27.28), respectively. Nevertheless, no significant variance in fungal richness was discovered among the aggregate fractions under the drying treatment. Moreover, the shift from flooding to drying reduced the bacteria-to-fungi ratio in all the aggregate fractions.

The relative abundance of the dominant bacterial and fungal phyla in soil aggregates under flooding and drying treatments are shown in Figure 4. The bacterial communities in soil aggregates predominately comprised *Proteobacteria* (34.6–43.3%), *Acidobacteria* (11.4–16.3%), *Actinobacteria* (6.8–12.1%), *Firmicutes* (3.6–7.7%), and *Planctomycetes* (1.9–2.2%). Compared with the flooding, the drying treatment resulted in an increase of 38.4–57.5% in the relative abundance of *actinobacteria*. The bacterial communities primarily included Ascomycota (9.3–36.5%), *Basidiomycota* (1.9–26.5%), *Rozellomycota* (0.1–5.2%), and *Chytridiomycota* (0.1–4.1%). Compared with the flooding treatment, the drying treatment generally enhanced the relative abundance of *Basidiomycota* and *Ascomycota* in soil aggregates.

The PCoA revealed that both bacterial and fungal community compositions were distinct among the aggregate fractions and treatments (Figure 5). Three samples from the same moisture conditions were grouped, regardless of the aggregate size. Moreover, the samples from different moisture conditions were completely separated from each other. The first two principal coordinates together explained 34.29 and 29.24% of the differences in soil bacteria and fungi community compositions, correspondingly.

3.3. Soil microbial co-occurrence networks

To evaluate differences in network features between individual treatments and for every aggregate fraction, we generated 20 subnetworks from the bacterial and fungal populations. Supplementary Table S3 displays the results of the ANOVA. Both bacteria and fungi community compositions exhibited modified co-occurrence patterns in response to the varying soil moisture treatments (Figure 6). The changes in the soil moisture conditions

10.3389/fmicb.2023.1167353

TABLE 1 Main soil properties under drying and drying treatments.

	SOC (gkg^{-1})		TN (gkg^{-1})		C:N (–)		pH		SBD		PSA
	Flooding	Drying	Flooding	Drying	Flooding	Drying	Flooding	Drying	Flooding	Drying	
BS	21.1bA	16.2bB	1.9aA	1.5bB	11.11bA	10.80bA	6.41aA	7.01aA	1.16abA	1.17abA	-
LM	27aA	24.2aA	1.6bA	1.6aA	16.88aA	15.13aA	6.53aA	6.92aA	1.07cA	1.09cA	38.97a
SM	17.3bA	16.3bA	1.4bA	1.3bA	12.36bA	12.54bA	6.75aA	6.92aA	1.13bA	1.13bA	30.56a
MI	12.1cA	10.4cA	1cA	0.9cA	12.10bA	11.56bA	6.88aA	6.99aA	1.18aA	1.19aA	14.33b
SC	12.1cA	11.7cA	1.3bA	1.2bA	9.31bA	9.75bA	6.94aA	6.79aA	1.21aA	1.23aA	16.33b

BS, bulk soil; LM, >2 mm aggregate fractions; SM, 0.25–2 mm aggregate fractions; MI, 0.053–0.25 mm aggregate fractions; SC, <0.053 mm aggregate fractions; SOC, soil organic carbon; TN, soil total nitrogen; C:N, soil carbon to nitrogen ratio; SBD, soil bulk density; PSA, percentage of the aggregate size fractions. Significant deviations among various aggregate size fractions within the same column are denoted by small letters; Significant variations ($p < 0.05$) between soil moisture treatments within the same row are denoted by capital letters.

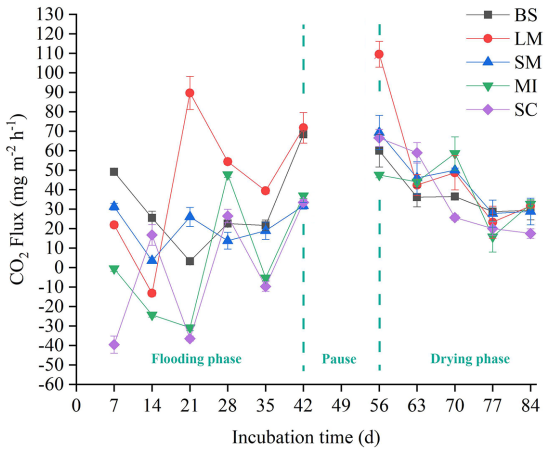

FIGURE 2
Flux of CO_2 among soil aggregates in flooding and drying status. BS, bulk soil; LM, large macroaggregate, > 2mm; SM, small macroaggregate, 0.25–2mm; MI, microaggregate, 0.053–0.25mm; SC, silt and clay, < 0.053mm.

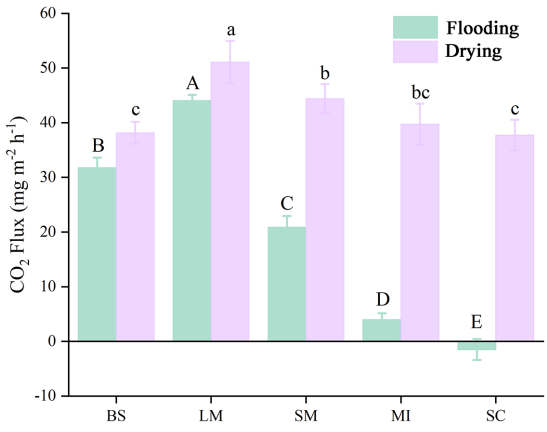

FIGURE 3
Mean soil respiration of different aggregate sizes in flooding and drying treatments during the incubation period. BS, bulk soil; LM, large macroaggregate, > 2mm; SM, small macroaggregate, 0.25–2mm; MI, microaggregate, 0.053–0.25mm; SC, silt and clay, < 0.053mm. A significant difference in soil respiration across aggregate sizes (p 0.05) in both the flooded and dried conditions is shown by the bars designated with capital letters and lowercase letters, correspondingly.

substantially affected the dynamics of the microbial and fungal populations' interplay. The shift from flooding to drying increased the ratio of positive to negative edges (P/N), average degree, and average clustering coefficient in all bacteria and fungi networks and most subnetworks (Table 2; Supplementary Tables S2, S3).

The changes in soil moisture conditions changed the keystone taxa (Table 3). For bacterial networks, *Acidobacteria* (*unclassified Acidobacteria* at the order level), *Acidobacteria* (*Acidobacteriales*), *Gemmatimonadetes* (*Gemmatimonadales*), *Chloroflexi* (*Anaerolineales*), and *Bacteroidetes* (*Cytophagales*) were the keystone taxa in the flooding treatment, whereas, in the drying treatment, the keystone taxa were *Proteobacteria* (unclassified), *Proteobacteria* (*Rhizobiales*), *Gemmatimonadetes* (*Gemmatimonadales*), *Proteobacteria* (*Sphingomonadales*), and *Actinobacteria* (*Solirubrobacterales*). For fungal networks, the keystone taxa in the flooding and drying treatments were *Ascomycota* (*Hypocreales*) and *Basidiomycota* (*Agaricales*), respectively.

Variation in the keystone taxa was observed across soil moisture manipulations (Supplementary Table S3). Bacterial subnetworks showed changes in their keystone taxa in response to manipulations of soil moisture and particle size distributions. P/N was solely influenced by soil moisture treatments for fungal subnetworks, whereas the average clustering coefficient was influenced by the interplay of aggregate sizes and soil moisture treatments.

3.4. Keystone taxa regulated soil respiration

The keystone taxa abundance was shown to have a strong correlation with soil respiration in regression analyzes (Figure 7). For bacteria, soil respiration was positively influenced by OTU88 (*Proteobacteria*; $R^2 = 0.75$, $p < 0.01$) under flooding treatment. Under drying treatment, soil respiration was positively influenced by OTU88 (i.e., *Proteobacteria*; $R^2 = 0.32$, $p < 0.01$), OTU89 (*Gemmatimonadetes*; $R^2 = 0.88$, $p < 0.01$), OUT144 (*Actinobacteria*; $R^2 = 0.95$, $p < 0.01$), OTU162 (*Actinobacteria*; $R^2 = 0.60$, $p < 0.01$), and OTU13562 (*Actinobacteria*; $R^2 = 0.21$, $p < 0.05$). For fungi, soil respiration was positively influenced by OTU2732 (*Ascomycota*; $R^2 = 0.29$, $p < 0.05$) under flooding treatment. Under flooding treatment, soil respiration was negatively influenced by OTU13 (*unclassified fungus*; $R^2 = 0.68$, $p < 0.01$). Moreover, under drying treatment soil respiration was positively influenced by OTU11 (*Basidiomycota*; $R^2 = 0.32$, $p < 0.01$), OTU12 (*Ascomycota*; $R^2 = 0.88$, $p < 0.01$), OTU3 (*Basidiomycota*; $R^2 = 0.95$, $p < 0.01$), OTU222 (*Basidiomycota*; $R^2 = 0.60$, $p < 0.01$), and OTU477 (*unclassified fungus*; $R^2 = 0.21$, $p < 0.05$).

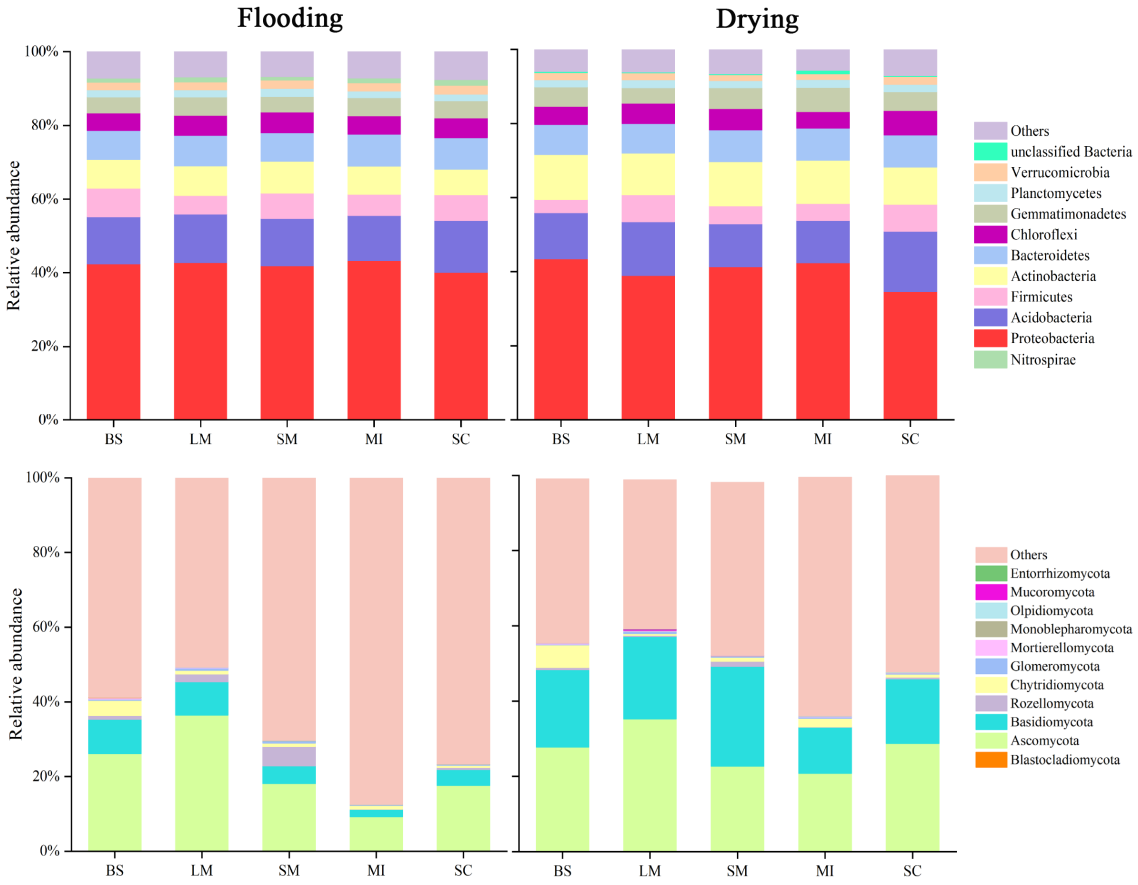

FIGURE 4
Aggregate size fractions during flooding and drying conditions and the relative abundance of key phyla within fungi and bacteria communities.

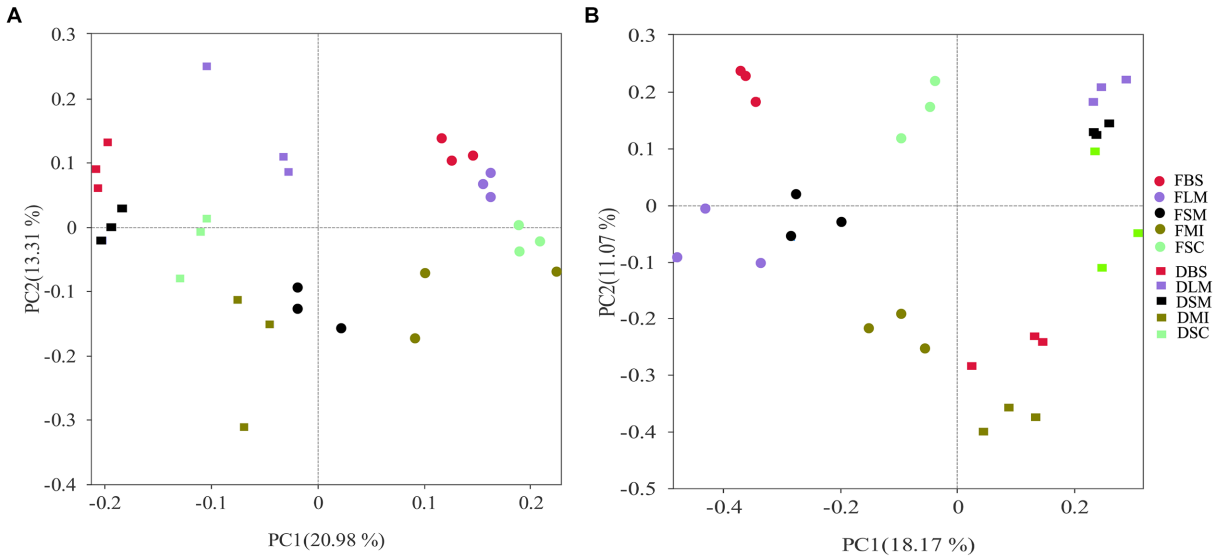

FIGURE 5
The impacts of moisture status and aggregate fractions on bacterial **(A)** and fungal **(B)** populations are shown using principal coordinate analysis predicated on the Bray-Curtis distances. Symbols of varying hues depict various aggregate fractions, each corresponding to a certain treatment of soil moisture. FBS, bulk soil in the flooding treatment; FLM, large macroaggregates in the flooding treatment; FSM, small macroaggregates in the flooding treatment; FMI, microaggregates in the flooding treatment; FSC, silt and clay in the flooding treatment; DBS, bulk soil in the drying treatment; DLM, large macroaggregates in the drying treatment; DSM, small macroaggregates in the drying treatment; DMI, microaggregates in the drying treatment; DSC, silt, and clay in the drying treatment.

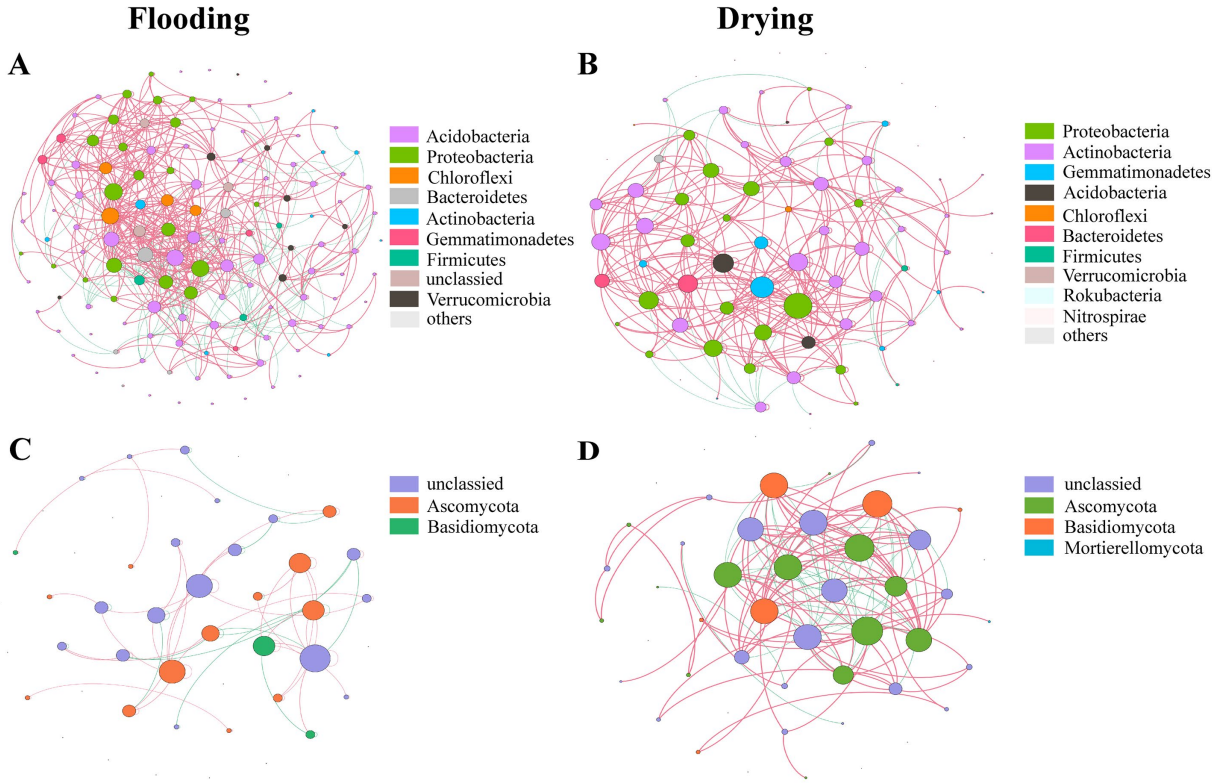

FIGURE 6
Networks showing the co-occurrence of bacterial **(A,B)** and fungal **(C,D)** populations under flooding and drying, respectively. A connection represents a statistically significant (p<0.005) relationship between two OTUs. In a network, a node's size is equivalent to the number of its connections (i.e., degree), and the Pearson correlation coefficients are used to determine the thickness of the edges connecting the nodes. Positive and negative interactions are denoted by the red and green edges, correspondingly.

3.5. The influence of soil characteristics and microbial community on soil respiration

A regression random forest analysis was showed that the key soil parameters that were linked to soil respiration were SOC, C/N ratio, and pH (Supplementary Figure S1). Soil respiration was also significantly influenced by the make-up of the microbial population (as measured by the first dominant eigengenes, FDE) and the features of the microbial network (as measured by the P/N ratio related to keystone taxa and the mean cluster coefficients).

In both the flooded and dried soils, PLS-PM analysis showed causative links between soil respiration, soil microbial network, soil microbial community composition, and environmental factors (Figure 8). In the flooding treatment, SOC, bacterial network, and fungal community composition exhibited a remarkable direct effect on soil respiration, with path coefficients of 0.71, 0.21, and 0.26, correspondingly ($p < 0.05$). Additionally, the SOC and C/N ratios both exhibited substantial indirect effects on soil respiration through fungal community composition, with path coefficients of 0.15 and-0.20, correspondingly ($p < 0.05$). Consequently, SOC had a strong beneficial effect on soil respiration, as measured by a path coefficient of 0.86. Bacterial networks predominantly and significantly relied on BPN and BACC with loading coefficients of 0.40 and 0.56, correspondingly ($p < 0.05$). Fungal community composition dominantly relied on their FFDE with a loading coefficient of 0.85 ($p < 0.05$).

In the drying treatment, SOC, bacterial network, fungal community composition, and the fungal network exhibited substantial direct effects on soil respiration, as indicated by path coefficients of 0.57, 0.32, 0.25, and 0.56, correspondingly ($p < 0.05$). Moreover, the SOC and pH exhibited substantial indirect effects on soil respiration through fungal community composition, as illustrated by coefficients of 0.14 and 0.11, correspondingly ($p < 0.05$). By way of the microbial community, the C/N ratio strongly influenced soil respiration (path coefficient = −0.19) ($p < 0.05$). Furthermore, SOC had a path coefficient of 0.71, indicating that it considerably and positively influenced soil respiration. The bacterial network dominantly and significantly relied on BKPN with a loading coefficient of 0.61 ($p < 0.05$). Moreover, fungal community composition predominantly relied on FR with a loading coefficient of 0.94 ($p < 0.05$). The fungal network predominantly relied on FACC with a loading coefficient of 0.79 ($p < 0.05$).

4. Discussion

4.1. Soil respiration impacted by flooding and drying conditions at the aggregate scale

Soil respiration reflects short-term dynamics of SOC, which are primarily affected by several biotic and abiotic factors, like

TABLE 2 Topological properties of bacterial and fungal subnetworks.

	Bulk/Aggregate soil	Treatments	P/N of the whole network	P/N associated with keystone taxa	Average degree	Average clustering coefficient
Bacterial networks	Bulk soil	Flooding	1.891	9.000	2.220	0.234
		Drying	2.616	4.000	3.359	0.301
	>2 mm	Flooding	0.127	0.095	2.987	0.213
		Drying	1.459	0.125	3.488	0.322
	0.25–2 mm	Flooding	0.134	0.167	2.920	0.224
		Drying	1.462	3.000	4.014	0.276
	0.053–0.25 mm	Flooding	0.186	0.170	3.593	0.247
		Drying	1.531	1.750	3.754	0.300
	<0.053 mm	Flooding	2.262	4.167	3.618	0.324
		Drying	3.718	13.500	5.531	0.320
Fungal networks	Bulk soil	Flooding	0.495	0.100	8.179	0.288
		Drying	0.300	15.000	5.337	0.264
	>2 mm	Flooding	0.530	1.375	6.248	0.342
		Drying	0.712	15.500	7.538	0.381
	0.25–2 mm	Flooding	0.722	0.444	4.656	0.303
		Drying	0.793	3.714	8.803	0.336
	0.053–0.25 mm	Flooding	0.526	1.500	4.360	0.258
		Drying	0.713	2.000	5.930	0.299
	<0.053 mm	Flooding	0.946	13.000	8.041	0.335
		Drying	1.002	1.000	10.271	0.362

microorganisms, substrate availability, and water content (Luo and Zhou, 2006; Wang et al., 2020). In this study, the respiration of different-sized soil aggregates slightly increased with the incubation time during the flooding phase, whereas it slightly decreased with incubation time during the drying phase (Figure 2). These differences may be caused by the discrepancy between the labile and recalcitrant carbon fractions used by microbes (Rusalimova and Barsukov, 2006). Generally, labile organic carbon is preferentially decomposed by soil microorganisms during the early stages of incubation. However, microorganisms began to use the recalcitrant organic carbon fraction which is more difficult to decompose in the late stage of incubation (Hao et al., 2008; Rabbi et al., 2014; Bimüller et al., 2016). In addition, the soil respiration rate fluctuated during the incubation process, which was likely because of soil disturbance caused by the pretreatment process, such as the collection of soil samples (Hao et al., 2008).

The variations in soil respiration at different aggregate sizes reflect the dominant roles of carbon and nitrogen contents and microbial activity within the aggregates under relatively uniform incubation conditions (Gupta and Germida, 1988; Kan et al., 2020). Our results showed that significant differences in the respiration of different size fractions of soil aggregates were observed under the same incubation conditions, and the mean soil respiration rate generally increased with the soil aggregate size-classes. These results support our first hypothesis, conforming to the conclusions drawn by Noellemeyer et al. (2008). The reasons for this are as follows. First, in the absence of plant roots, soil respiration is primarily derived from the decomposition of organic carbon by soil microorganisms (Ontl and Schulte, 2012). Further, the activities of microorganisms responded to the discrepancy in the amount and stability of organic carbon in different soil aggregate sizes, thereby leading to variations in soil respiration among different aggregate size-classes (Trivedi et al., 2017). Second, macroaggregate-associated carbon primarily derives from labile organic carbon (e.g., fresh plant residues) that easily decomposes, whereas microaggregate-associated carbon primarily comprises humus that is difficult to decompose and use (Six et al., 1999). Moreover, because the pore necks in microaggregates are <0.2 μm in width, the pores in these structures are impenetrable to bacteria, thereby inhibiting biological activity (Erktan et al., 2020; Zhu et al., 2022b).

The mean soil respiration of all aggregate size fractions in the drying treatment was substantially elevated in contrast to the flooding treatment under a constant temperature (Figure 3). The results primarily showed the inhibition of organic matter decomposition, as soil pore spaces are occupied by water in the flooding treatment (Gorham, 1995); Additionally, during the drying treatment, 50% field water retention capacity was maintained in the soil samples since it is suitable for microbial activity, particularly in the early stage of measurement (Manzoni et al., 2012).

4.2. Microorganisms in soil aggregates under flooding and drying treatments

Soil aggregates act as heterogeneous microhabitats for highly spatially organized microorganism communities (Upton et al., 2019).

10.3389/fmicb.2023.1167353

TABLE 3 The keystone taxa in the bacterial and fungal networks in flooding and drying treatments.

ID	Phylum	Order	Degree	Eigen centrality	Closeness centrality	Betweeness centrality	Treatment
OTU326	*Acidobacteria*	*Unclassified*	32	0.97	0.50	621.44	
OTU110	*Acidobacteria*	*Acidobacteriales*	37	1	0.38	448.98	
OTU88	*Proteobacteria*	*Unclassified*	31	0.96	0.40	215.48	Flooding
OTU1276	*Chloroflexi*	*Anaerolineales*	37	0.92	0.38	525.64	
OTU714	*Bacteroidetes*	*Cytophagales*	32	0.74	0.38	411.07	
OTU89	*Gemmatimonadetes*	*Gemmatimonadales*	36	1	0.42	353.45	
OTU162	*Proteobacteria*	*Rhizobiales*	34	0.98	0.41	386.78	
OTU88	*Proteobacteria*	*Unclassified*	32	0.96	0.41	341.53	Drying
OTU13562	*Proteobacteria*	*Sphingomonadales*	37	0.91	0.42	386.78	
OTU144	*Actinobacteria*	*Solirubrobacterales*	34	0.90	0.40	370.63	
OTU13	*Unclassified*	*NA*	9	1	0.71	37	
OTU12	*Ascomycota*	*Hypocreales*	8	0.73	0.57	16	
OTU21	*Ascomycota*	*NA*	8	0.72	0.63	31.5	Flooding
OTU2732	*Ascomycota*	*Hypocreales*	7	0.75	0.38	15	
OTU15	*Unclassified*	*Unclassified*	7	0.80	0.57	7	
OTU12	*Ascomycota*	*Hypocreales*	17	0.92	0.49	134.65	
OTU11	*Basidiomycota*	*Agaricales*	16	1	0.48	16.07	
OTU222	*Basidiomycota*	*Agaricales*	15	0.96	0.52	121.19	Drying
OTU3	*Basidiomycota*	*Agaricales*	15	0.99	0.47	41.81	
OTU477	*Unclassified*	*Unclassified*	15	0.89	0.47	786.78	

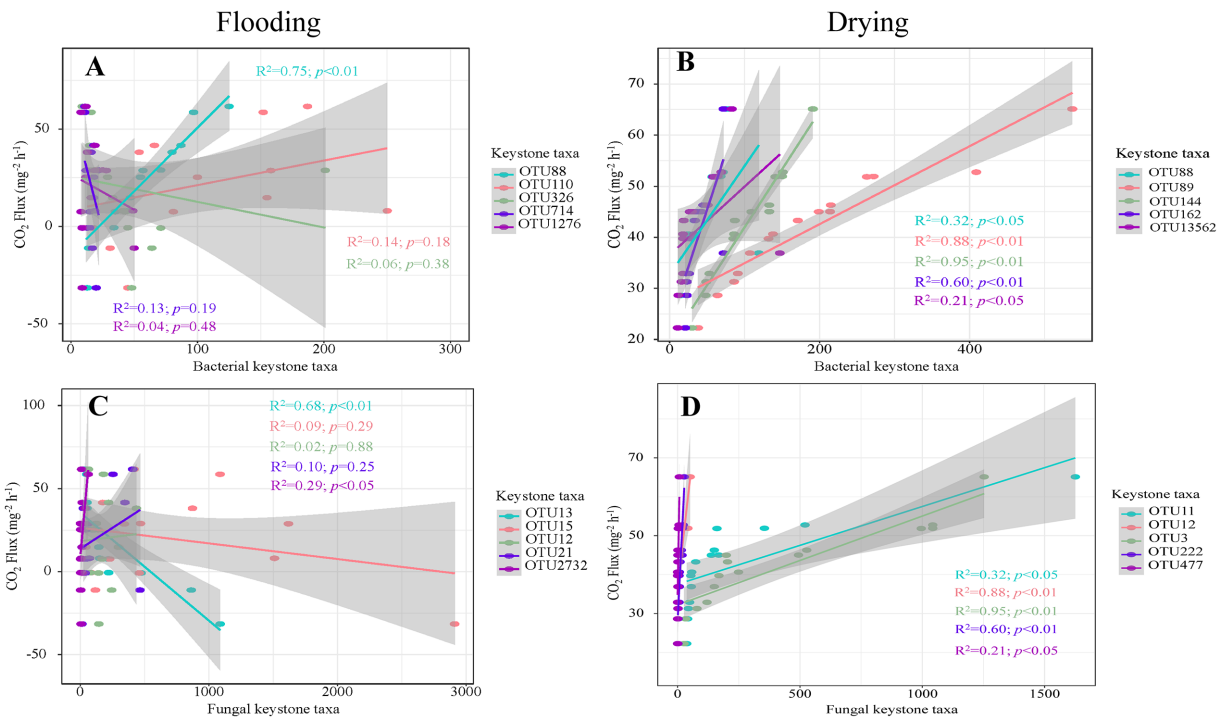

FIGURE 7
The relationships of soil respiration with the richness of key bacterial **(A,C)** and fungal members **(B,D)**.

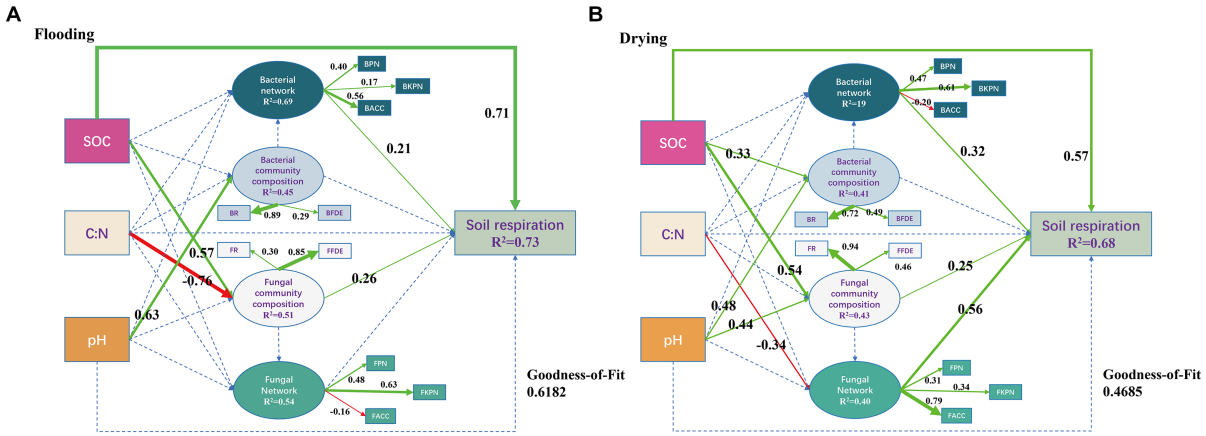

FIGURE 8
Soil respiration derived from different sizes of aggregates after exposure to flooding **(A)** and drying **(B)** treatments were modeled using a partial least squares path model of the impacts of soil characteristics, microbial population structure, and microbial network topological parameters **(B)**. Positive paths ($p<0.05$) are denoted by solid arrows, while insignificant paths ($p>0.05$) are illustrated by the dotted arrows. The goodness-of-fit (GoF) statistic was employed to evaluate the model. SOC, soil organic carbon; C:N, the ratios of total carbon and nitrogen; BPN, P/N of the entire network; BKPN, P/N of the bacterial network related to keystone taxa; BACC, average clustering coefficients of the whole network; BR, the relative abundance of bacteria; BFDE, first dominant eigengenes of the bacterial community composition; FPN, P/N of the entire network; FKPN, P/N of the bacterial network related to keystone taxa; FACC, average clustering coefficients of the fungal network; FR, the relative abundance of fungi; FFDE, first dominant eigengenes of fungal community composition.

In this study, the maximum bacterial abundances among the aggregate fractions under flooding and drying conditions were MI and SC, respectively. SM had the maximum fungal abundance under flooded conditions. These findings were comparable to those obtained in earlier investigations which revealed that the bacterial and fungal abundances are maximum in <0.25 mm and >0.25 mm aggregates, correspondingly (Zhang et al., 2014; Bach et al., 2018; Wilpiszeski et al., 2019). The presence of protected habitats in microaggregates may facilitate niche creation for bacteria by excluding their predators (protozoa) and competing with fungi, since predation serves as a crucial structuring force for bacterial communities (Zhang et al., 2014). Additionally, due to the narrow gaps that exist between microaggregates, silt, and clay fractions, it is physically impossible for fungi to penetrate the interior of these habitats (Zhang et al., 2014; Erktan et al., 2020).

Soil water regimes, which are associated with most soil properties and processes, have a profound influence on the structure and function of the soil microbial population in the soil (Brockett et al., 2012; Schimel, 2018). In this study, the shift from flooding to drying decreased the bacteria–fungi ratio in all aggregate size fractions. Notably, fungi are heterotrophic and essentially aerobic with limited anaerobic capabilities (McGinnis and Tyring, 1996). The shift from flooding to drying changed the soil microenvironment and improved the exchange of air and heat, which was conducive to soil fungal aeration. Fungal communities are generally more resistant to environmental alterations than bacterial communities (Lin et al., 2019). Consequently, fungi rapidly reproduce, thereby improving their diversity (Zhang, 2010). In addition, soil bacteria might adjust their expression of certain metabolic processes (e.g., resulting in the synthesis of compounds with osmoprotective properties) in response to the stress environment and maintain their growth during flooding (Chowdhury et al., 2019). For bacteria, *Proteobacteria* were the dominant taxa in both flooding and drying treatments. *Acidobacteria* and *Bacteroidetes* were the subdominant groups in the flooding and drying treatments, respectively. Among fungi, the dominant taxa were *Ascomycetes* and *Basidiomycetes*. However, the shift from flooding to drying considerably increased the relative abundance of Basidiomycetes. These results were in line with those found in earlier investigations, which revealed that the microbial communities *Proteobacteria*, *Acidobacteria*, *Bacteroidetes*, *Ascomycetes*, and *Basidiomycetes* are abundant in wetland soils which are frequently anaerobic (Tait et al., 2007; Peralta et al., 2013). Moreover, the relative abundance of dominant microbial taxa generally decreased with an increase in aggregate size, which might be related to the nutrient strategy of the microbial community (Fierer et al., 2007; Zhang et al., 2016) where macroaggregates tend to be nutrient-rich, whereas microaggregates are relatively barren (Fonte et al., 2014).

The co-occurrence patterns of soil microbes could be revealed by using network analysis, which is conducive to acquiring a more comprehensive knowledge of the structure of microbial communities and the biological principles that guide community formation (Barberán et al., 2012). Herein, in both the flooding and drying conditions, *Proteobacteria* and *Actinobacteria* predominated in the bacterial network, while *Ascomycota* predominated in the fungus network, indicating that these phyla could be the most influential in determining the overall architecture of microbiomes. This is likely because *Proteobacteria*, *Actinobacteria*, and *Ascomycota* can resist external pressure and disturbances (Zhou et al., 2020; Faitová, 2021). This finding aligns with the conclusions drawn by Ye et al. (2021) in their study of co-occurrence patterns in the soil microbial network within the riparian zone of the TGR. In addition, the fungal network exhibited higher average degrees, and more nodes and edges in the drying treatment than in the flooding treatment, suggesting that the shift from flooding to drying enhanced the connectivity and complexity of the fungal network (Wagg et al., 2019; Ye et al., 2021). These results are in agreement with those of earlier research showing that flooding drastically decreases the complexity of co-occurrence networks (Zhang et al., 2019; Gao et al., 2021) owing to resource

limitations and environmental stresses, such as severe flooding stress, reduced water, and availability of nutrients (Malik et al., 2020; Qiu et al., 2021). In addition, positive linkages in the bacterial network, especially those linked to keystone taxa, rose as flooding duration reduced, whereas negative ones dropped as a result of the shift from flooding to drying (i.e., the P/N of the overall network and that related to keystone taxa) (Table 2). This indicates that the shift from flooding to drying increased niche breadths by eliminating flooding stress and reactivating aerobic microbes to enhance the availability of organic materials (Malik et al., 2020), thereby mitigating competition (Banerjee et al., 2016) and exhibiting favorable co-occurrence patterns with selected copiotrophic keystone taxa (Wang et al., 2021).

4.3. Soil respiration regulated by keystone taxa at the aggregate scale

Soil respiration is determined by the richness of certain taxa (Banerjee et al., 2016). Confirming our second hypothesis, both bacterial and fungal keystone taxa were found using the network analysis, and they were shown to have substantial ties to soil respiration (Figure 7). The abundance of *Proteobacteria* in bacteria and *Ascomycota* (*Hypocreales*) in fungi exhibited remarkably favorable impact on soil respiration during flooding treatment. *Proteobacteria*, *Proteobacteria* (*Rhizobiales*), *Gemmatimonadetes* (*Gemmatimonadales*), *Proteobacteria* (*Sphingomonadales*), and *Actinobacteria* (*Solirubrobacterales*) in bacteria and *Ascomycota* (*Hypocreales*), *Basidiomycota* (*Agaricales*), an unclassified taxon, in fungi, exhibited strong positive effects on soil respiration in the drying treatment. *Proteobacteria*, *Firmicutes*, and *Actinobacteria* have been found to decompose plant polymers by releasing soil enzymes like xylanases and β-glucosidase (Wang et al., 2010; Tiwari et al., 2016; Zheng et al., 2018). Earlier literature has shown that the families of α-*Proteobacteria* are decomposers of both fresh and soil organic matter (Bernard et al., 2012; Liu et al., 2021). Herein, both *Rhizobiales* and *Sphingomonadales* belong to *α-Proteobacteria*, which positively affected soil respiration. Actinobacteria are an essential bacterium class that participates in many activities throughout ecosystems, including the breakdown of organic molecules, which can mineralize fused aromatic C-ring structures (Faitová, 2021). *Gemmatimonadetes* are typically abundant and active in low-moisture soils, playing a vital role in driving soil carbon cycling processes (He et al., 2020; Fan et al., 2021). Thus, our findings illustrated that *Gemmatimonadetes* positively affected soil respiration during the drying treatment rather than during the flooding treatment. In addition, an unclassified keystone fungus exhibited a considerable negative impact on soil respiration in the flooding treatment, which could explain why negative rates of soil respiration were detected during the drying treatment. *Agaricales*, an order of *Basidiomycota*, is an extremely common soft-rot fungus that aids in decomposing dead wood and litter and may generate a spectrum of hydrolytic enzymes capable of breaking down humic and lignin acids (Voříšková and Baldrian, 2013). During decomposition, the prevalent and persistent ascomycetous fungi (*Hypocreales*) are the endophytes of a wide variety of plants and also include extracellular fungi that produce enzymes (Voříšková and Baldrian, 2013; Herzog et al., 2019). However, the keystone taxa *Rhizobiales*, *Gemmatimonadales*, *Sphingomonadales*, and *Solirubrobacterales*, *Hypocreales*, *Agaricales* are uncultured bacterial or fungal orders. Therefore, further studies are required to determine how they affect the composition and function of soil microbes (Wang et al., 2021). Additionally, keystone taxa should be selectively excluded in future studies to verify the changes in species interactions affecting soil respiration (Zheng et al., 2021).

4.4. Regulating mechanisms of soil respiration at the aggregate scale in flooding and drying treatments

Microbial community structure and network properties assume critical roles in the dynamics of SOC (Banerjee et al., 2016; Zheng et al., 2021). In both flooding and drying treatments, aggregate fractions remarkably modified the composition of microbial communities and microbial networks, primarily by altering their associated SOC levels (Cookson et al., 2005). In addition, SOC was the dominant regulator of soil respiration, with a path coefficient of 0.86 in the flooding treatment and 0.71 in the drying treatment (Figure 8), suggesting that substrate supply was the major factor affecting CO_2 release in this study (Luo and Zhou, 2006). Furthermore, the mechanisms regulating soil respiration were distinct between the flooding and drying treatments (Figure 8).

In the flooding treatment, except for SOC, soil respiration was principally modulated by the ACC and P/N of the entire network and FFDE. However, in the drying treatment, soil respiration was predominantly modulated by FR, FACC, and P/N associated with the bacterial keystone taxa. These results show that the shift from flooding to drying changed the regulatory mechanisms of soil respiration, particularly the fungal network. Archived literatures illustrates that decreasing competitive interactions with keystone taxa enhances soil respiration (Wang et al., 2021), whereas soil respiration diminishes when competitive interactions increase among keystone taxa (Chen et al., 2019). The shift from flooding to drying relieved water stress, thereby alleviating interactions that are competitive with the co-occurrence networks' keystone taxa. Moreover, C mineralization is less energy-efficient during anaerobic degradation (Wang et al., 2021). Therefore, the shift from flooding to drying increased the average soil respiration rate (Figure 3). Notably, the relieved water stress increases oxygen availability, which creates copiotrophic environments for fungi that prefer aerobic conditions (McGinnis and Tyring, 1996) and interacts with other species by using both labile and recalcitrant carbon fractions (Bian et al., 2022). Also, the effect of the bacterial network on soil respiration increased from a path coefficient of 0.21 to 0.32 (Figure 8), which revealed that the dominant bacterial network with positive interaction in aerobic conditions facilitated the utilization of carbon sources by microorganisms, thereby stimulating soil respiration (Wang et al., 2021).

5. Conclusion

Our study reveals that the shift from flooding to drying changes the microbial community composition and keystone taxa, thereby enhancing the microbial respiration of soil aggregates. Specifically, soil respiration decreases with a decrease in aggregate size in both flooding and drying treatments. Additionally, the microbial respiration of soil aggregates is substantially higher in the drying treatments than in the flooding treatment as a result of the changes in keystone taxa. Notably, the fungal community composition and network properties dominate the changes in microbial respiration of soil aggregates during the flooding to the drying process. This study reveals the crucial roles of

fungal community composition and co-occurrence network properties in regulating soil respiration during the shift from flooding to drying conditions. Moreover, this analysis offers valuable knowledge of the mechanisms of soil respiration changes at the aggregate scale under different water regimes.

Data availability statement

The original contributions presented in the study are included in the article/Supplementary material, further inquiries can be directed to the corresponding authors.

Author contributions

KZ: conceptualization, methodology, validation, formal analysis, investigation, writing–original draft, visualization, and funding acquisition. WJ: writing–review and editing. YM: investigation and data curation. SW: methodology and funding acquisition. PH: conceptualization, resources, writing–review and editing, supervision, and project administration. All authors contributed to the article and approved the submitted version.

Funding

This study was sponsored by Natural Science Foundation of Chongqing, China (2022NSCQ-MSX1111), "Through Train" for Doctors in Chongqing (sl202100000124), the National Natural Science Foundation of China (41771266), the Three Gorges' follow-up scientific research project from Chongqing Municipal Bureau of Water Resources (No. 5000002021BF40001). PH is also supported by the "Light of West China" Program funded by the Chinese Academy of Sciences. China Postdoctoral Science Foundation (2021M703137), Chongqing Postdoctoral Science Foundation (cstc2021jcyj-bsh0080).

Conflict of interest

The authors declare that the research was conducted in the absence of any commercial or financial relationships that could be construed as a potential conflict of interest.

Publisher's note

All claims expressed in this article are solely those of the authors and do not necessarily represent those of their affiliated organizations, or those of the publisher, the editors and the reviewers. Any product that may be evaluated in this article, or claim that may be made by its manufacturer, is not guaranteed or endorsed by the publisher.

Supplementary material

The Supplementary material for this article can be found online at: https://www.frontiersin.org/articles/10.3389/fmicb.2023.1167353/full#supplementary-material

References

Adams, R. I., Miletto, M., Taylor, J. W., and Bruns, T. D. (2013). Dispersal in microbes: fungi in indoor air are dominated by outdoor air and show dispersal limitation at short distances. *ISME J.* 7, 1262–1273. doi: 10.1038/ismej.2013.28

Bach, E. M., Williams, R. J., Hargreaves, S. K., Yang, F., and Hofmockel, K. S. (2018). Greatest soil microbial diversity found in micro-habitats. *Soil Biol. Biochem.* 118, 217–226. doi: 10.1016/j.soilbio.2017.12.018

Bandyopadhyay, K. K., and Lal, R. (2014). Effect of land use management on greenhouse gas emissions from water stable aggregates. *Geoderma* 232-234, 363–372. doi: 10.1016/j.geoderma.2014.05.025

Banerjee, S., Kirkby, C. A., Schmutter, D., Bissett, A., Kirkegaard, J. A., and Richardson, A. E. (2016). Network analysis reveals functional redundancy and keystone taxa amongst bacterial and fungal communities during organic matter decomposition in an arable soil. *Soil Biol. Biochem.* 97, 188–198. doi: 10.1016/j.soilbio.2016.03.017

Barberán, A., Bates, S. T., Casamayor, E. O., and Fierer, N. (2012). Using network analysis to explore co-occurrence patterns in soil microbial communities. *ISME J.* 6, 343–351. doi: 10.1038/ismej.2011.119

Bernard, L., Chapuis-Lardy, L., Razafimbelo, T., Razafindrakoto, M., Pablo, A.-L., Legname, E., et al. (2012). Endogeic earthworms shape bacterial functional communities and affect organic matter mineralization in a tropical soil. *ISME J.* 6, 213–222. doi: 10.1038/ismej.2011.87

Bian, Q., Wang, X., Bao, X., Zhu, L., Xie, Z., Che, Z., et al. (2022). Exogenous substrate quality determines the dominant keystone taxa linked to carbon mineralization: evidence from a 30-year experiment. *Soil Biol. Biochem.* 169:108683. doi: 10.1016/j.soilbio.2022.108683

Bimüller, C., Kreyling, O., Kölbl, A., von Lützow, M., and Kögel-Knabner, I. (2016). Carbon and nitrogen mineralization in hierarchically structured aggregates of different size. *Soil Tillage Res.* 160, 23–33. doi: 10.1016/j.still.2015.12.011

Bodner, G., Scholl, P., and Kaul, H. P. (2013). Field quantification of wetting-drying cycles to predict temporal changes of soil pore size distribution. *Soil Tillage Res.* 133, 1–9. doi: 10.1016/j.still.2013.05.006

Brockett, B. F. T., Prescott, C. E., and Grayston, S. J. (2012). Soil moisture is the major factor influencing microbial community structure and enzyme activities across seven biogeoclimatic zones in western Canada. *Soil Biol. Biochem.* 44, 9–20. doi: 10.1016/j.soilbio.2011.09.003

Butterly, C. R., Marschner, P., McNeill, A. M., and Baldock, J. A. (2010). Rewetting CO2 pulses in Australian agricultural soils and the influence of soil properties. *Biol. Fertil. Soils* 46, 739–753. doi: 10.1007/s00374-010-0481-9

Chen, L., Jiang, Y., Liang, C., Luo, Y., Xu, Q., Han, C., et al. (2019). Competitive interaction with keystone taxa induced negative priming under biochar amendments. *Microbiome* 7:77. doi: 10.1186/s40168-019-0693-7

Chen, C., Meurk, C., Chen, J., Lv, M., Wen, Z., Jiang, Y., et al. (2014). Restoration design for three gorges reservoir shorelands, combining Chinese traditional agro-ecological knowledge with landscape ecological analysis. *Ecol. Eng.* 71, 584–597. doi: 10.1016/j.ecoleng.2014.07.008

Chen, J., Zhang, Y., Kuzyakov, Y., Wang, D., and Olesen, J. E. (2023). Challenges in upscaling laboratory studies to ecosystems in soil microbiology research. *Glob. Chang. Biol.* 29, 569–574. doi: 10.1111/gcb.16537

Chowdhury, T. R., Lee, J.-Y., Bottos, E. M., Brislawn, C. J., White, R. A., Bramer, L. M., et al. (2019). Metaphenomic responses of a native prairie soil microbiome to moisture perturbations. *mSystems* 4, e00061–e00019. doi: 10.1128/mSystems.00061-19

Cookson, W. R., Abaye, D. A., Marschner, P., Murphy, D. V., Stockdale, E. A., and Goulding, K. W. T. (2005). The contribution of soil organic matter fractions to carbon and nitrogen mineralization and microbial community size and structure. *Soil Biol. Biochem.* 37, 1726–1737. doi: 10.1016/j.soilbio.2005.02.007

Dacal, M., García-Palacios, P., Asensio, S., Wang, J., Singh, B. K., and Maestre, F. T. (2022). Climate change legacies contrastingly affect the resistance and resilience of soil microbial communities and multifunctionality to extreme drought. *Funct. Ecol.* 36, 908–920. doi: 10.1111/1365-2435.14000

Danevčič, T., Mandic-Mulec, I., Stres, B., Stopar, D., and Hacin, J. (2010). Emissions of CO_2, CH_4 and N_2O from southern European peatlands. *Soil Biol. Biochem.* 42, 1437–1446. doi: 10.1016/j.soilbio.2010.05.004

De Nijs, E. A., Hicks, L. C., Leizeaga, A., Tietema, A., and Rousk, J. (2019). Soil microbial moisture dependences and responses to drying–rewetting: the legacy of 18 years drought. *Glob. Chang. Biol.* 25, 1005–1015. doi: 10.1111/gcb.14508

de Sosa, L. L., Glanville, H. C., Marshall, M. R., Prysor Williams, A., and Jones, D. L. (2018). Quantifying the contribution of riparian soils to the provision of ecosystem services. *Sci. Total Environ.* 624, 807–819. doi: 10.1016/j.scitotenv.2017.12.179

Denef, K., Six, J., Bossuyt, H., Frey, S. D., Elliott, E. T., Merckx, R., et al. (2001). Influence of dry–wet cycles on the interrelationship between aggregate, particulate organic matter, and microbial community dynamics. *Soil Biol. Biochem.* 33, 1599–1611. doi: 10.1016/S0038-0717(01)00076-1

Drury, C. F., Yang, X. M., Reynolds, W. D., and Tan, C. S. (2004). Influence of crop rotation and aggregate size on carbon dioxide production and denitrification. *Soil Tillage Res.* 79, 87–100. doi: 10.1016/j.still.2004.03.020

Edgar, R. C. (2013). UPARSE: highly accurate OTU sequences from microbial amplicon reads. *Nat. Methods* 10, 996–998. doi: 10.1038/nmeth.2604

Erktan, A., Or, D., and Scheu, S. (2020). The physical structure of soil: determinant and consequence of trophic interactions. *Soil Biol. Biochem.* 148:107876. doi: 10.1016/j.soilbio.2020.107876

Evans, S. E., and Wallenstein, M. D. (2014). Climate change alters ecological strategies of soil bacteria. *Ecol. Lett.* 17, 155–164. doi: 10.1111/ele.12206

Faitová, A.. (2021). *Actinobacteria communities in natural and anthropogenic environments*. Univerzita Karlova, Prague.

Fan, J., Jin, H., Zhang, C., Zheng, J., Zhang, J., and Han, G. (2021). Grazing intensity induced alternations of soil microbial community composition in aggregates drive soil organic carbon turnover in a desert steppe. *Agric. Ecosyst. Environ.* 313:107387. doi: 10.1016/j.agee.2021.107387

Fernández, R., Quiroga, A., Zorati, C., and Noellemeyer, E. (2010). Carbon contents and respiration rates of aggregate size fractions under no-till and conventional tillage. *Soil Tillage Res.* 109, 103–109. doi: 10.1016/j.still.2010.05.002

Fierer, N., Bradford, M. A., and Jackson, R. B. (2007). Toward an ecological classification of soil bacteria. *Ecology* 88, 1354–1364. doi: 10.1890/05-1839

Fierer, N., Schimel, J. P., and Holden, P. A. (2003). Influence of drying–rewetting frequency on soil bacterial community structure. *Microb. Ecol.* 45, 63–71. doi: 10.1007/s00248-002-1007-2

Fonte, S. J., Nesper, M., Hegglin, D., Velásquez, J. E., Ramirez, B., Rao, I. M., et al. (2014). Pasture degradation impacts soil phosphorus storage via changes to aggregate-associated soil organic matter in highly weathered tropical soils. *Soil Biol. Biochem.* 68, 150–157. doi: 10.1016/j.soilbio.2013.09.025

Gao, G.-F., Peng, D., Zhang, Y., Li, Y., Fan, K., Tripathi, B. M., et al. (2021). Dramatic change of bacterial assembly process and co-occurrence pattern in *Spartina alterniflora* salt marsh along an inundation frequency gradient. *Sci. Total Environ.* 755:142546. doi: 10.1016/j.scitotenv.2020.142546

Gorham, E. (1995). "The biogeochemistry of northern peatlands and its possible responses to global warming" in *Biotic feedbacks in the global climate system: will the warming feed the warming*. eds. G. M. Woodwell and F. T. MacKenzie (New York: Oxford University), 169–187.

Gupta, V. V. S. R., and Germida, J. J. (1988). Distribution of microbial biomass and its activity in different soil aggregate size classes as affected by cultivation. *Soil Biol. Biochem.* 20, 777–786. doi: 10.1016/0038-0717(88)90082-X

Hao, R. J., Li, Z. P., Che, Y. P., and Fang, H. L. (2008). Organic carbon mineralization in various size aggregates of paddy soil under aerobic and submerged conditions. *Ying. Yong. Sheng. Xue Bao* 19, 1944–1950.

He, H., Miao, Y., Gan, Y., Wei, S., Tan, S., Rask, K. A., et al. (2020). Soil bacterial community response to long-term land use conversion in Yellow River Delta. *Appl. Soil Ecol.* 156:103709. doi: 10.1016/j.apsoil.2020.103709

Herzog, C., Hartmann, M., Frey, B., Stierli, B., Rumpel, C., Buchmann, N., et al. (2019). Microbial succession on decomposing root litter in a drought-prone scots pine forest. *ISME J.* 13, 2346–2362. doi: 10.1038/s41396-019-0436-6

Holland, E. A., and Coleman, D. C. (1987). Litter placement effects on microbial and organic matter dynamics in an agroecosystem. *Ecology* 68, 425–433. doi: 10.2307/1939274

Jansson, J. K., and Hofmockel, K. S. (2020). Soil microbiomes and climate change. *Nat. Rev. Microbiol.* 18, 35–46. doi: 10.1038/s41579-019-0265-7

Jarvis, P., Rey, A., Petsikos, C., Wingate, L., Rayment, M., Pereira, J., et al. (2007). Drying and wetting of Mediterranean soils stimulates decomposition and carbon dioxide emission: the birch effect†. *Tree Physiol.* 27, 929–940. doi: 10.1093/treephys/27.7.929

Jiang, Y., Qian, H., Wang, X., Chen, L., Liu, M., Li, H., et al. (2018). Nematodes and microbial community affect the sizes and turnover rates of organic carbon pools in soil aggregates. *Soil Biol. Biochem.* 119, 22–31. doi: 10.1016/j.soilbio.2018.01.001

Jiang, M., Yang, N., Zhao, J., Shaaban, M., and Hu, R. (2021). Crop straw incorporation mediates the impacts of soil aggregate size on greenhouse gas emissions. *Geoderma* 401:115342. doi: 10.1016/j.geoderma.2021.115342

Johan, S., Clarholm, M., Sven, B., and Rosswall, T. (1986). Effects of moisture on soil microorganisms and nematodes: a field experiment. *Microb. Ecol.* 12, 217–230. doi: 10.1007/BF02011206

Jones, K. B., Slonecker, E. T., Nash, M. S., Neale, A. C., Wade, T. G., and Hamann, S. (2010). Riparian habitat changes across the continental United States (1972–2003) and potential implications for sustaining ecosystem services. *Landsc. Ecol.* 25, 1261–1275. doi: 10.1007/s10980-010-9510-1

Kan, Z. R., Ma, S. T., Liu, Q. Y., Liu, B. Y., Virk, A. L., Qi, J. Y., et al. (2020). Carbon sequestration and mineralization in soil aggregates under long-term conservation tillage in the North China plain. *Catena* 188:104428. doi: 10.1016/j.catena.2019.104428

Kõljalg, U., Nilsson, R. H., Abarenkov, K., Tedersoo, L., Taylor, A. F. S., Bahram, M., et al. (2013). Towards a unified paradigm for sequence-based identification of fungi. *Mol. Ecol.* 22, 5271–5277. doi: 10.1111/mec.12481

Lee, C. K., Barbier, B. A., Bottos, E. M., McDonald, I. R., and Cary, S. C. (2012). The inter-valley soil comparative survey: the ecology of dry valley edaphic microbial communities. *ISME J.* 6, 1046–1057. doi: 10.1038/ismej.2011.170

Leira, M., and Cantonati, M. (2008). Effects of water-level fluctuations on lakes: an annotated bibliography. *Hydrobiologia* 613, 171–184. doi: 10.1007/s10750-008-9465-2

Liaw, A., and Wiener, M. (2002). Classification and regression by random Forest. *R News* 2, 18–22.

Lin, Y., Ye, G., Kuzyakov, Y., Liu, D., Fan, J., and Ding, W. (2019). Long-term manure application increases soil organic matter and aggregation, and alters microbial community structure and keystone taxa. *Soil Biol. Biochem.* 134, 187–196. doi: 10.1016/j.soilbio.2019.03.030

Liu, X. J. A., Hayer, M., Mau, R. L., Schwartz, E., Dijkstra, P., and Hungate, B. A. (2021). Substrate stoichiometric regulation of microbial respiration and community dynamics across four different ecosystems. *Soil Biol. Biochem.* 163:108458. doi: 10.1016/j.soilbio.2021.108458

Luo, Y., and Zhou, X.. (2006). *Soil respiration and the environment*. Elsevier, San Diego.

Magoč, T., and Salzberg, S. L. (2011). FLASH: fast length adjustment of short reads to improve genome assemblies. *Bioinformatics* 27, 2957–2963. doi: 10.1093/bioinformatics/btr507

Malik, A. A., Martiny, J. B. H., Brodie, E. L., Martiny, A. C., Treseder, K. K., and Allison, S. D. (2020). Defining trait-based microbial strategies with consequences for soil carbon cycling under climate change. *ISME J.* 14, 1–9. doi: 10.1038/s41396-019-0510-0

Mangalassery, S., Sjögersten, S., Sparkes, D. L., Sturrock, C. J., and Mooney, S. J. (2013). The effect of soil aggregate size on pore structure and its consequence on emission of greenhouse gases. *Soil Tillage Res.* 132, 39–46. doi: 10.1016/j.still.2013.05.003

Manzoni, S., Schimel, J. P., and Porporato, A. (2012). Responses of soil microbial communities to water stress: results from a meta-analysis. *Ecology* 93, 930–938. doi: 10.1890/11-0026.1

Márquez, C. O., Garcia, V. J., Cambardella, C. A., Schultz, R. C., and Isenhart, T. M. (2004). Aggregate-size stability distribution and soil stability. *Soil Sci. Soc. Am. J.* 68, 725–735. doi: 10.2136/sssaj2004.7250

McGinnis, M. R., and Tyring, S. K.. (1996). *Introduction to mycology. Medical microbiology. 4th Edn*. Galveston, TX: University of Texas Medical Branch at Galveston.

Meisner, A., Bååth, E., and Rousk, J. (2013). Microbial growth responses upon rewetting soil dried for four days or one year. *Soil Biol. Biochem.* 66, 188–192. doi: 10.1016/j.soilbio.2013.07.014

Navas, M., Martín-Lammerding, D., Hontoria, C., Ulcuango, K., and Mariscal-Sancho, I. (2021). The distinct responses of bacteria and fungi in different-sized soil aggregates under different management practices. *Eur. J. Soil Sci.* 72, 1177–1189. doi: 10.1111/ejss.12997

Nelson, D. W., and Sommers, L. E. (1996). "Total carbon, organic carbon, and organic matter" in *Methods of soil analysis*. eds. D. L. Sparks, A. L. Page, P. A. Helmke, R. H. Loeppert, P. N. Soltanpour and M. A. Tabatabai (Madison: SSSA Book Series), 961–1010.

Noellemeyer, E., Frank, F., Alvarez, C., Morazzo, G., and Quiroga, A. (2008). Carbon contents and aggregation related to soil physical and biological properties under a land-use sequence in the semiarid region of Central Argentina. *Soil Tillage Res.* 99, 179–190. doi: 10.1016/j.still.2008.02.003

Ontl, T. A., and Schulte, L. A. (2012). Soil carbon storage. *Nat. Educ. Knowl.* 3:35.

Peralta, R. M., Ahn, C., and Gillevet, P. M. (2013). Characterization of soil bacterial community structure and physicochemical properties in created and natural wetlands. *Sci. Total Environ.* 443, 725–732. doi: 10.1016/j.scitotenv.2012.11.052

Qiu, L., Zhang, Q., Zhu, H., Reich, P. B., Banerjee, S., van der Heijden, M. G. A., et al. (2021). Erosion reduces soil microbial diversity, network complexity and multifunctionality. *ISME J.* 15, 2474–2489. doi: 10.1038/s41396-021-00913-1

Rabbi, S. M. F., Wilson, B. R., Lockwood, P. V., Daniel, H., and Young, I. M. (2014). Soil organic carbon mineralization rates in aggregates under contrasting land uses. *Geoderma* 216, 10–18. doi: 10.1016/j.geoderma.2013.10.023

Razafimbelo, T. M., Albrecht, A., Oliver, R., Chevallier, T., Chapuis-Lardy, L., and Feller, C. (2008). Aggregate associated-C and physical protection in a tropical clayey soil under Malagasy conventional and no-tillage systems. *Soil Tillage Res.* 98, 140–149. doi: 10.1016/j.still.2007.10.012

Rusalimova, O., and Barsukov, P. (2006). "Decomposition of labile and recalcitrant soil organic matter of Gleyic Cryosols in permafrost region of Siberia" in *Symptom of*

environmental change in Siberian permafrost region. eds. R. Hatano and G. Guggenberger (Sapporo: Hokkaido University Press), 93–102.

Sanchez, G.. (2013). *PLS path modeling with R*. Berkeley: Trowchez Editions *383*, 551.

Schimel, J. P. (2018). Life in dry soils: effects of drought on soil microbial communities and processes. *Annu. Rev. Ecol. Evol. Syst.* 49, 409–432. doi: 10.1146/annurev-ecolsys-110617-062614

Sey, B. K., Manceur, A. M., Whalen, J. K., Gregorich, E. G., and Rochette, P. (2008). Small-scale heterogeneity in carbon dioxide, nitrous oxide and methane production from aggregates of a cultivated sandy-loam soil. *Soil Biol. Biochem.* 40, 2468–2473. doi: 10.1016/j.soilbio.2008.05.012

She, W., Yang, J., Wu, G., and Jiang, H. (2022). The synergy of environmental and microbial variations caused by hydrologic management affects the carbon emission in the three gorges reservoir. *Sci. Total Environ.* 821:153446. doi: 10.1016/j.scitotenv.2022.153446

Silvola, J., Alm, J., Ahlholm, U., Nykanen, H., and Martikainen, P. J. (1996). CO_2 fluxes from peat in boreal mires under varying temperature and moisture conditions. *J. Ecol.* 84, 219–228. doi: 10.2307/2261357

Six, J., Bossuyt, H., Degryze, S., and Denef, K. (2004). A history of research on the link between (micro)aggregates, soil biota, and soil organic matter dynamics. *Soil Tillage Res.* 79, 7–31. doi: 10.1016/j.still.2004.03.008

Six, J., Elliott, E. T., and Paustian, K. (1999). Aggregate and soil organic matter dynamics under conventional and no-tillage systems. *Soil Sci. Soc. Am. J.* 63, 1350–1358. doi: 10.2136/sssaj1999.6351350x

Tait, E., Carman, M., and Sievert, S. M. (2007). Phylogenetic diversity of bacteria associated with ascidians in eel pond (woods hole, Massachusetts, USA). *J. Exp. Mar. Biol. Ecol.* 342, 138–146. doi: 10.1016/j.jembe.2006.10.024

Tisdall, J. M., and Oades, J. M. (1982). Organic matter and water-stable aggregates in soils. *J. Soil Sci.* 33, 141–163. doi: 10.1111/j.1365-2389.1982.tb01755.x

Tiwari, R., Kumar, K., Singh, S., Nain, L., and Shukla, P. (2016). Molecular detection and environment-specific diversity of Glycosyl hydrolase family 1 β-Glucosidase in different habitats. *Front. Microbiol.* 7:1597. doi: 10.3389/fmicb.2016.01597

Trivedi, P., Delgado-Baquerizo, M., Jeffries, T. C., Trivedi, C., Anderson, I. C., Lai, K., et al. (2017). Soil aggregation and associated microbial communities modify the impact of agricultural management on carbon content. *Environ. Microbiol.* 19, 3070–3086. doi: 10.1111/1462-2920.13779

Umair, M., Sun, N., Du, H., Hui, N., Altaf, M., Du, B., et al. (2020). Bacterial communities are more sensitive to water addition than fungal communities due to higher soil K and Na in a degraded karst ecosystem of southwestern China. *Front. Microbiol.* 11:562546. doi: 10.3389/fmicb.2020.562546

Upton, R. N., Bach, E. M., and Hofmockel, K. S. (2019). Spatio-temporal microbial community dynamics within soil aggregates. *Soil Biol. Biochem.* 132, 58–68. doi: 10.1016/j.soilbio.2019.01.016

Voříšková, J., and Baldrian, P. (2013). Fungal community on decomposing leaf litter undergoes rapid successional changes. *ISME J.* 7, 477–486. doi: 10.1038/ismej.2012.116

Wagg, C., Schlaeppi, K., Banerjee, S., Kuramae, E. E., and van der Heijden, M. G. A. (2019). Fungal-bacterial diversity and microbiome complexity predict ecosystem functioning. *Nat. Commun.* 10:4841. doi: 10.1038/s41467-019-12798-y

Wang, X., Bian, Q., Jiang, Y., Zhu, L., Chen, Y., Liang, Y., et al. (2021). Organic amendments drive shifts in microbial community structure and keystone taxa which increase C mineralization across aggregate size classes. *Soil Biol. Biochem.* 153:108062. doi: 10.1016/j.soilbio.2020.108062

Wang, B., Brewer, P. E., Shugart, H. H., Lerdau, M. T., and Allison, S. D. (2019). Soil aggregates as biogeochemical reactors and implications for soil–atmosphere exchange of greenhouse gases–a concept. *Glob. Chang. Biol.* 25, 373–385. doi: 10.1111/gcb.14515

Wang, D., Chi, Z., Yue, B., Huang, X., Zhao, J., Song, H., et al. (2020). Effects of mowing and nitrogen addition on the ecosystem C and N pools in a temperate steppe: a case study from northern China. *Catena* 185:104332. doi: 10.1016/j.catena.2019.104332

Wang, Q., Garrity, G. M., Tiedje, J. M., and Cole, J. R. (2007). Naïve Bayesian classifier for rapid assignment of rRNA sequences into the new bacterial taxonomy. *Appl. Environ. Microbiol.* 73, 5261–5267. doi: 10.1128/AEM.00062-07

Wang, Z., Li, Y., Chang, S. X., Zhang, J., Jiang, P., Zhou, G., et al. (2014). Contrasting effects of bamboo leaf and its biochar on soil CO_2 efflux and labile organic carbon in an intensively managed Chinese chestnut plantation. *Biol. Fertil. Soils* 50, 1109–1119. doi: 10.1007/s00374-014-0933-8

Wang, G., Wang, Y., Yang, P., Luo, H., Huang, H., Shi, P., et al. (2010). Molecular detection and diversity of xylanase genes in alpine tundra soil. *Appl. Microbiol. Biotechnol.* 87, 1383–1393. doi: 10.1007/s00253-010-2564-9

Wilpiszeski, R. L., Aufrecht, J. A., Retterer, S. T., Sullivan, M. B., Graham, D. E., Pierce, E. M., et al. (2019). Soil aggregate microbial communities: towards understanding microbiome interactions at biologically relevant scales. *Appl. Environ. Microbiol.* 85, e00324–e00319. doi: 10.1128/AEM.00324-19

Xiang, Y., Wang, Y., Zhang, C., Shen, H., and Wang, D. (2018). Water level fluctuations influence microbial communities and mercury methylation in soils in the three gorges reservoir, China. *J. Environ. Sci.* 68, 206–217. doi: 10.1016/j.jes.2018.03.009

Ye, F., Ma, M. H., Wu, S. J., Jiang, Y., Zhu, G. B., Zhang, H., et al. (2019). Soil properties and distribution in the riparian zone: the effects of fluctuations in water and anthropogenic disturbances. *Eur. J. Soil Sci.* 70, 664–673. doi: 10.1111/ejss.12756

Ye, F., Wang, X., Wang, Y., Wu, S., Wu, J., and Hong, Y. (2021). Different pioneer plant species have similar rhizosphere microbial communities. *Plant Soil* 464, 165–181. doi: 10.1007/s11104-021-04952-7

Zhang, G. (2010). Changes of soil labile organic carbon in different land uses in Sanjiang plain, Heilongjiang Province. *Chin. Geogr. Sci.* 20, 139–143. doi: 10.1007/s11769-010-0139-4

Zhang, L., Adams, J. M., Dumont, M. G., Li, Y., Shi, Y., He, D., et al. (2019). Distinct methanotrophic communities exist in habitats with different soil water contents. *Soil Biol. Biochem.* 132, 143–152. doi: 10.1016/j.soilbio.2019.02.007

Zhang, H., Ding, W., He, X., Yu, H., Fan, J., and Liu, D. (2014). Influence of 20–year organic and inorganic fertilization on organic carbon accumulation and microbial community structure of aggregates in an intensively cultivated sandy loam soil. *PLoS One* 9:e92733. doi: 10.1371/journal.pone.0092733

Zhang, C., Liu, G., Xue, S., and Wang, G. (2016). Soil bacterial community dynamics reflect changes in plant community and soil properties during the secondary succession of abandoned farmland in the loess plateau. *Soil Biol. Biochem.* 97, 40–49. doi: 10.1016/j.soilbio.2016.02.013

Zhang, Q., Shao, M. A., Jia, X., and Zhang, C. (2018). Understory vegetation and drought effects on soil aggregate stability and aggregate-associated carbon on the loess plateau in China. *Soil Sci. Soc. Am. J.* 82, 106–114. doi: 10.2136/sssaj2017.05.0145

Zheng, H., Yang, T., Bao, Y., He, P., Yang, K., Mei, X., et al. (2021). Network analysis and subsequent culturing reveal keystone taxa involved in microbial litter decomposition dynamics. *Soil Biol. Biochem.* 157:108230. doi: 10.1016/j.soilbio.2021.108230

Zheng, W., Zhao, Z., Gong, Q., Zhai, B., and Li, Z. (2018). Effects of cover crop in an apple orchard on microbial community composition, networks, and potential genes involved with degradation of crop residues in soil. *Biol. Fertil. Soils* 54, 743–759. doi: 10.1007/s00374-018-1298-1

Zhou, H., Gao, Y., Jia, X., Wang, M., Ding, J., Cheng, L., et al. (2020). Network analysis reveals the strengthening of microbial interaction in biological soil crust development in the mu us Sandy land, northwestern China. *Soil Biol. Biochem.* 144:107782. doi: 10.1016/j.soilbio.2020.107782

Zhu, K., Li, W., Yang, S., Ran, Y., Lei, X., Ma, M., et al. (2022a). Intense wet-dry cycles weakened the carbon sequestration of soil aggregates in the riparian zone. *Catena* 212:106117. doi: 10.1016/j.catena.2022.106117

Zhu, K., Ma, M., Ran, Y., Liu, Z., Wu, S., and Huang, P. (2020). In mitigating CO_2 emission in the reservoir riparian: the influences of land use and the dam-triggered flooding on soil respiration. *Soil Tillage Res.* 197:104522. doi: 10.1016/j.still.2019.104522

Zhu, K., Ran, Y., Ma, M., Li, W., Mir, Y., Ran, J., et al. (2022b). Ameliorating soil structure for the reservoir riparian: the influences of land use and dam-triggered flooding on soil aggregates. *Soil Tillage Res.* 216:105263. doi: 10.1016/j.still.2021.105263

frontiers | Frontiers in Microbiology

TYPE Original Research
PUBLISHED 08 June 2023
DOI 10.3389/fmicb.2023.1148750

OPEN ACCESS

EDITED BY
Mikhail Semenov,
Russian Academy of Agricultural Sciences, Russia

REVIEWED BY
Ilya Yevdokimov,
Russian Academy of Sciences, Russia
Rakesh Kumar Sharma,
Manipal University Jaipur, India

*CORRESPONDENCE
Carolina Merino-Guzmán
✉ carolina.merino@ufrontera.cl

RECEIVED 20 January 2023
ACCEPTED 20 April 2023
PUBLISHED 08 June 2023

CITATION
Jofré-Fernández I, Matus-Baeza F and Merino-Guzmán C (2023) White-rot fungi scavenge reactive oxygen species, which drives pH-dependent exo-enzymatic mechanisms and promotes CO_2 efflux.
Front. Microbiol. 14:1148750.
doi: 10.3389/fmicb.2023.1148750

White-rot fungi scavenge reactive oxygen species, which drives pH-dependent exo-enzymatic mechanisms and promotes CO_2 efflux

Ignacio Jofré-Fernández[1,2,3], Francisco Matus-Baeza[3,4] and Carolina Merino-Guzmán[2]*

[1]Scientific and Technological Bioresource Nucleus (BIOREN), Universidad de La Frontera, Temuco, Chile, [2]Laboratory of Geomicrobiology, Department of Chemical Sciences and Natural Resources, Universidad de La Frontera, Temuco, Chile, [3]Laboratory of Conservation and Dynamics of Volcanic Soils, Department of Chemical Sciences and Natural Resources, Universidad de La Frontera, Temuco, Chile, [4]Network for Extreme Environmental Research (NEXER), Universidad de La Frontera, Temuco, Chile

Soil organic matter (SOM) decomposition mechanisms in rainforest ecosystems are governed by biotic and abiotic procedures which depend on available oxygen in the soil. White-rot fungi (WRF) play an important role in the primary decomposition of SOM via enzymatic mechanisms (biotic mechanism), which are linked to abiotic oxidative reactions (e.g., Fenton reaction), where both processes are dependent on reactive oxygen species (ROS) and soil pH variation, which has yet been studied. In humid temperate forest soils, we hypothesize that soil pH is a determining factor that regulates the production and consumption of ROS during biotic and abiotic SOM decomposition. Three soils from different parent materials and WRF inoculum were considered for this study: granitic (Nahuelbuta, *Schizophyllum commune*), metamorphic (Alerce Costero, *Stereum hirsutum*), and volcanic-allophanic (Puyehue, *Galerina patagonica*). CO_2 fluxes, lignin peroxidase, manganese peroxidase, and dye-decolorizing peroxidase levels were all determined. Likewise, the production of superoxide anion (O_2•-), hydrogen peroxide (H_2O_2), and hydroxyl radicals (•OH) were assessed in soils microcosms after 36days of anaerobic incubation with WRF inoculum and induced Fenton reaction under pH variations ranging from 2.5 to 5.1. ROS significantly increased biotic and abiotic CO_2 emissions in all tested soils, according to the findings. The highest values (217.45 mg C kg^{-1}) were found during the anaerobic incubation of sterilized and inoculated soils with WRF at a natural pH of 4.5. At pH 4.0, the lowest levels of C mineralization (82 mg C kg^{-1}) were found in Nahuelbuta soil. Enzyme activities showed different trends as pH changed. The Fenton reaction consumed more H_2O_2 between pH 3 and 4, but less between pH 4.5 and 2.5. The mechanisms that oxidized SOM are extremely sensitive to variations in soil pH and the stability of oxidant radical and non-radical compounds, according to our findings.

KEYWORDS

white-rot fungi, SOM decomposition, greenhouse gasses, reactive oxygen species, enzymatic activity

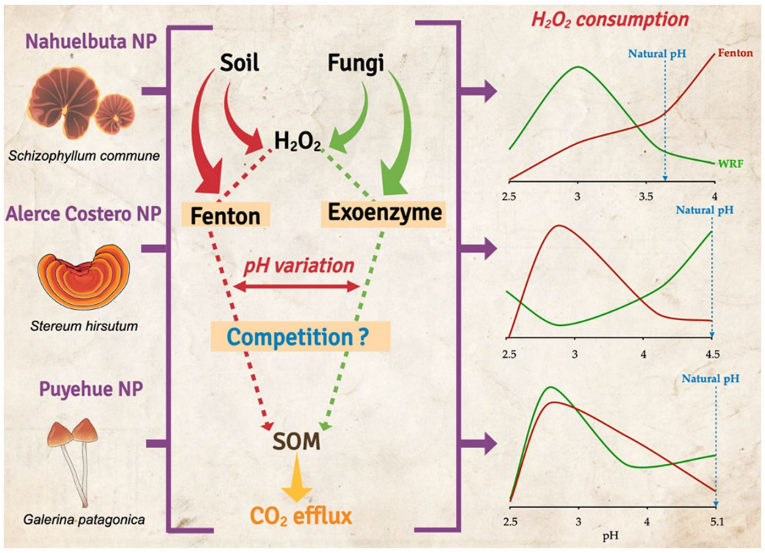

GRAPHICAL ABSTRACT

1. Introduction

The rate of industrialization has accelerated changes in carbon dioxide (CO_2), methane (CH_4), and reactive nitrogen oxides (NxO) emissions from human activities over the last 150 years (Köster et al., 2017; Walsh et al., 2017). Furthermore, the geological and natural sources from which they are released frequently contribute to the current climate change problem. After photosynthesis, soils are the second largest source of CO_2 fluxes in terrestrial ecosystems (Raich and Schlesinger, 1992; Dixon et al., 1994; Schlesinger and Andrews, 2000). The sources of emissions are well understood, such as rhizosphere basal microbial respiration and the decomposition of plant residues and soil organic matter (SOM) (Kuzyakov, 2006). As a result, microbial communities play an important role in GHG emissions (Xu et al., 2013). Fungi have a significant function in the forest soil biome because they recycle and decompose both labile and recalcitrant materials like wood lignin under aerobic and anaerobic conditions (Lin et al., 2021; Naylor et al., 2022). This allows fungi to deal with changes in soil redox state resulting from rainfall in the winter and drying in the summer. This means that factors like soluble O_2, pH, and oxidation–reduction processes in iron-rich soils in temperate rain forests may have a significant impact on SOM stability under a warming scenario.

The most common type of fungi in these rainforest soils that can efficiently convert lignin into CO_2 are white-rot fungi (WRF). This fungus produces a diverse family of hemoperoxidases, including lignin peroxidases (LiP), manganese peroxidase (MnP), and dye peroxidase (DyP), all of which catalyze the decomposition of recalcitrant SOM via a step-by-step reaction catalyzed by hydrogen peroxide (H_2O_2) as acceptor, and resulting in CO_2 efflux (Lenhart et al., 2012). The primary abiotic source of H_2O_2 in the soil is rainfall deposition (Willey et al., 1996; Kakeshpour et al., 2022). This occurs as a result of a photochemical or electrochemical reaction, such as water photolysis or an electrical storm (electro-Fenton). Furthermore, volatile terpene compounds can produce reactive oxygen species (ROS) in forest ecosystems via indirect biotic processes, reacting with ozone to produce hydroxyl radicals (•OH) and hydrogen peroxide (H_2O_2), both of which are then deposited in soil by precipitation (Becker et al., 1990). Furthermore, some aerobic soil bacteria produce biotic sources of ROS as a byproduct of respiration by releasing superoxide anion (O_2•-), which is rapidly converted into H_2O_2 by the activity of different rhizosphere isoforms of extracellular superoxide dismutase enzymes (Takahashi et al., 2003; Jofré et al., 2021). Furthermore, ROS stability has been measured over a wide pH range (i.e., 2–10), whereas the maximum rate for metal oxidation occurs only at pH 3 (Garrido-Ramírez et al., 2010; Du et al., 2019).

Although SOM decomposition stimulates GHG release (Merino et al., 2020, 2021a), it is unclear whether biotic (exoenzymes) and abiotic (e.g., Fenton reaction) ROS production can be correlated with soil carbon emission, and whether this mechanism is transversal to the forest with similar structure on a not local scale. This hypothesis appears to be dependent on optimal pH values for biotic GHG production, which is dependent on enzymatic activity and abiotic pathways (Merino et al., 2021a). The optimal soil pH for methanogenesis, according to some reports, is between 4 and 7, but higher CO_2 emissions were recorded at circumneutral pH (Dalal and Allen, 2008). As a result, soil pH affects all chemical, physical, and biological soil properties, affecting C fluxes.

Under pH variation, factors such as the availability and consumption of oxidant and radical species (H_2O_2, •OH, and O_2•-) in biotic and abiotic redox reactions should be considered to determine the potential of GHG emissions in temperate rainforest soils. According to changes in soil pH, we hypothesize that the stability and consumption of reactive oxygen species (ROS) from biotic and abiotic reactions can significantly drive the CO_2 emission rate from temperate rainforest soils. We investigated the dynamics of ROS under oxygen-limiting conditions, with and without white-rot fungal inoculum, and the Fenton reaction in long-term incubations in this study.

2. Materials and methods

2.1. Study sites and sampling

Three temperate forest soil types with mean annual precipitation ranging from 1,500 to >5,000 mm were chosen. The first soil sampled was a loamy Inceptisol (Soil Survey Staff, 2014) which was derived from intrusive granodiorite rocks in Nahuelbuta National Park (37°47′S, 72°12′W) (Bernhard et al., 2018). This soil was formed by ancient *Araucaria araucana* and Nothofagus pumilio forests. The second soil sampled in Alerce Costero National Park in the Coastal range under Nothofagus spp. and *Fitzroya cupressoides* (40°22′S 73°38′W) was a loamy clay Ultisol derived from metamorphic mica-schist materials with illite-kaolinite as dominant clays (Luzio et al., 2003). The final soil was collected in the Andes Cordillera from a primary temperate rainforest of Nothofagus betuloides in Puyehue National Park (40°47′S, 72°12′W) as Andisol derived from recent volcanic ash and basaltic scoria deposits with a high content of allophane, imogolite, and ferrihydrite (Neculman et al., 2013).

Four composite soil samples were extracted from the top Ah mineral horizon (0–15 cm) at each site after the litter layer was removed. The samples were cleaned in the laboratory to remove coarse organic debris and separated into two parts: one was stored at 4°C for a microcosm experiment and microbial analyses, and the other was air-dried for further physico-chemical analyses.

2.2. Analytical soil procedures

The pH and electrical conductivity were measured in an aliquot of soil in a 1:2.5 suspension of soil:water. TOC-VCSH (Shimadzu, Kyoto, Japan) was used to determine soil organic C, and total N was determined using Kjeldahl distillation (VELP, Usmate, Italy). The aluminum, iron and manganese were extracted by oxalate; Al_o, Fe_o and Mn_o respectively, using 0.2 M ammonium oxalate at pH 3 (Sadzawka et al., 2006). The aluminium, iron and Mn complexed with SOM, extracted by pyrophosphate, Al_p, Fe_p and Mn_p, respectively were obtained using a solution of 0.1 M sodium pyrophosphate (Van Reeuwijk, 2002). To identify exchangeable, crystalline, and complexed-SOM metals in soil samples, dithionite-citrate-bicarbonate (Fe_d) was used. Atomic absorption spectroscopy (Perkin Elmer 3110, Waltham, Massachusetts, United States) was used to determine Fe and Mn concentrations at 248.3 nm for Fe and 279.5 nm for Mn using a nitrous oxide acetylene flame. Cation exchange capacity (CEC) and nutrient characterization were carried out as Sadzawka et al. (2006) suggested. The total Fe concentration in 100 mg of dry soil was determined by adding 0.9 mL 0.28 M hydroxylamine hydrochloride and 1 mL 0.28 M HCl (Stookey, 1970). Approximately 100 µL of the extract was added to 4 mL of ferrozine color reagent (1 g ferrozine in 6.5 M ammonium acetate solution). Iron (II) concentration was determined in 100 mg of soil by adding 1 mL of 0.5 M HCl and vigorously shaking. Ferrozine reagent was added as previously described, and absorbance at 562 nm (ferrozine-Fe(II) complex standard) was measured in a UV spectrophotometer (Lovley and Phillips, 1987). The difference between total Fe and extractable Fe(II)-HCl forms was used to calculate the Fe(III) (oxyhydr) oxide content.

2.3. Culture conditions and fungal identification

In the same areas where soil samples were taken, white rot fungi were isolated from small fragments of decayed wood or fruiting body pieces. The fragments were placed in sterile tubes and stored at 4°C until they were analyzed. Small fragments of fungi fruiting bodies or decayed wood colonized by fungi were incubated on acidified glucose malt extract agar plates (15 g/L agar, 3.5 g/L malt extract, 10 g/L glucose, pH 5.5). Under aseptic conditions, pure mycelial cultures were obtained, and strains were identified using ITS sequencing. The DNA from each strain was extracted using the E.Z.N.A.® SP Fungal DNA Mini Kit D5524-01 (Omega, Bio-Tek, Norcross, GA, United States). The ITS1-5.8S—ITS2 rDNA was amplified using ITS1 and ITS4 primers (White et al., 1990). PCR was carried out in a total volume of 25 µL with 0.1 mM dNTPs, 0.1 mM of each primer, 5 U of Taq DNA polymerase, and the supplied reaction buffer (Promega Inc., Seoul, Korea). An ABI PRISM 3730l DNA Analyzer System was used to sequence the PCR products (Macrogen, Seoul, Korea). The nucleotide sequences were compared in the GenBank database (Horisawa et al., 2013). Schizophyllum commune was identified in Nahuebuta soil, Stereum hirsutum in Alerce Costero soil, and Galerina patagonica in Puyehue soil (see Supplementary Table S1, for more information). In each microcosm, the isolates were inoculated at a final concentration of 3×10^8 CFU gr soil^{-1} in 100 µL of sterilized water.

2.4. Microcosm anaerobic experiments

Under anaerobic conditions, the contribution of and ROS production and consumption from soils at different pH levels was determined in a sterilized portion of soil at field capacity (80%) from each soil (oxygen-free by N_2 purge). In a destructive sampling design, soil samples were incubated in 120 mL serum bottles for 36 h at 12°C to monitor CO_2 evolution, ROS production, and enzymatic activity. To remove the microbial resistant structures, the soil samples were sterilized for 20 min at 121°C (in an autoclave) on four consecutive days. The soils were then fumigated with chloroform vapor for 24 h in a vacuum chamber (Trevors, 1996). Autoclaving was chosen because it has little effect on the structure of SOM, primarily causing changes in the carbohydrate and N-alkyl domains (Berns et al., 2008). Because it causes Fe reduction and oxidation, gamma radiation was avoided (Bank et al., 2008; Abedini et al., 2014; Sutherland et al., 2017). Gamma radiation also increased the bioavailability of Fe(III) (oxyhydr)oxide minerals, which helped in Fe(III) reduction (Brown et al., 2012). There were three treatments (WRF, Fenton reaction, and WRF + Fenton) and four replicates with four induced pH in each soil; 2.5, 3, 4, and the natural pH of each soil (3.6, 4.5, and 5.1 for Nahuelbuta, Alerce Costero, and Puyehue, respectively). A H_2O_2:Fe(II) ratio was also added to induce the Fenton reaction, as previously reported by Merino et al. (2020). This was achieved by adding 120–143 mL of H_2O_2 (0.1 M) and 1.29 g Fe(II) kg^{-1} soil as $FeCl_2$ to the soil (Sigma Aldrich, United States). A total of 144 serum bottles with septums for gas sampling were used. CO_2 was collected at 0.5, 4, 8, 12, 24, and 36 days of incubation. Approximately 10 mL of CO_2 gas sample was extracted and injected into a gas chromatograph with Flame Ionization Detector (GC/FID) (Thermo Fisher ScientificTM, Austin, TX) with a 30 mm DB1-MS column and selected ion mode at each

sampling time. At the end of the incubation period, 72 microcosm bottles were harvested, and soil was homogenized and quickly subsampled for ROS analysis and enzymatic activity at each sampling.

2.5. Reactive oxygen species (ROS) detection

Superoxide anion (O_2•-) production was measured in 0.5 g of soil, which was extracted with 12 mL of potassium phosphate buffer (PPB, 65 mM, pH = 7.8) and centrifuged at 10,000×*g* for 15 min at 4°C. The supernatant (5 mL) was combined with 0.9 mL of PPB, 1 mL of sulfanilamide (17 mM), 1 mL of hydroxylamine hydrochloride (10 mM), and 1 mL of naphthylamine (7 mM) and incubated in the dark for 20 min at 25°C. At 530 nm, the absorbance of the samples was measured (Greenwald, 2018). Hydrogen peroxide (H_2O_2) was determined using the iodometric titration method (Velikova et al., 2000). The concentration of H_2O_2 in mg L^{-1} was determined using a calibration curve as the standard. Although iodometric titration is less precise than permanganate titration, it produces fewer interferences with SOM (Liang and He, 2018; Merino et al., 2020). Page et al. (2013) previously used terephthalic acid (TPA) in soil to measure •OH production. Approximately 200 l of soil water (1:2.5 soil:water suspension) was injected into 3 mL aliquots of deoxygenated water for the blank (in triplicate) and 3 mL of TPA for the test (in triplicate) (1.5 mM, in triplicate). TPA-treated soil suspension was incubated for 24 h in the dark to oxidize into hydroxyterephthalic acid (hTPA). Finally, the sample was filtered at 0.22 m and the fluorescence was measured in a microplate reader at λex = 310 nm, λem = 425 nm (Synergy HT, Biotek). The fluorescence intensity was compared to a standard curve with 2-hydroxyterephthalic acid (0, 2, 20, 40, and 80 nM) (hTPA, Sigma Aldrich).

2.6. Enzyme activity

Exoenzymatic activities were spectrophotometrically measured under pH variations after 36 h of incubation. The formation of Mn(III)-tartrate complex during the oxidation of 0.1 mM $MnSO_4$ in 100 mM tartrate buffer at pH 5 was used to determine manganese peroxidase (MnP) activity. At 238 nm, manganese peroxidase was measured spectrophotometrically (Xu et al., 2018). The oxidation of 2,2′-azino-bis (3-ethylthiazoline-6-sulfonate) (ABTS) (2.5 mM) to its cation radical in 100 mM tartrate buffer at pH 5 was followed by dye-decolorizing peroxidase (DyP) activity. At 418 nm, dye-decolorizing peroxidase was measured spectrophotometrically (Salvachúa et al., 2013). Veratryl alcohol (2 mM) was used as a substrate for LiP during the oxidation of 0.21 mL of 50 mM sodium tartrate buffer at pH 2.5. At 310 nm, lignin peroxidase was measured. The enzymatic activity tests were all performed in the presence of 0.1 mM H_2O_2. All oxidative enzymatic activities were measured in units (U) per milliliter (i.e., one millimole of substrate oxidized per minute). The measured H_2O_2 was normalized in relation to the treatment values in terms of representation.

2.7. Statistical analysis

The normal data distribution and variance homogeneity were tested for each treatment and soil type. One-way ANOVA was used for cumulative gas sampling (CO_2). Using a repeated-measures ANOVA test, the enzyme activity, ROS production, and Fenton contribution were tested over a 40-day incubation period. The last three variables measured were plotted as a six-sample time average. Duncan's multiple range test was used for multiple comparison means because all ANOVA tests were significant at p 0.05. The RStudio software was used for all analyses (1.1.442).

3. Results

3.1. Soil properties

The soils studied are formed from a variety of parent materials, including Granitic (Nahuelbuta), Metamorphic (Alerce Costero), and Volcanic-allophanic (Puyehue); their textures range from sandy to clay. The pH ranged from 3.6 to 5.1, with organic C levels ranging from 9.2 ± 0.1 to 11.4% ± 0.3. Natural H_2O_2 levels in soil range between 25.6 ± 0.7 and 33.7 ± 0.5 μM g^{-1} soil (Nahuelbuta<Alerce Costero< Puyehue soils). Puyehue soil had the highest content of Al complexed with SOM (Al_p) (11 g kg^{-1} soil ±1.5), while Nahuelbuta soil had the lowest (0.7 g kg^{-1} soil ±0.1). The $Al_o + 1/2\ Fe_o > 2\%$, which indicates Andic properties <2, was found at higher levels of 3.8% in Puyehue soil. The Al_o symbol represents Al-oxides associated with amorphous structures, such as Alp with SOM. Puyehue soil had the highest value of 3.1 ± 0.2 g kg^{-1} soil. The Puyehue soil had the lowest CEC (5.3 cmol(+) kg^{-1}), while Alerce Costero soil had the highest (19.7 cmol(+) kg^{-1}). The total Fe content was determined by combining the soluble ferrous iron Fe(II) and ferric iron Fe(III) forms, which ranged between 8.4 ± 0.5 and 11.8 ± 0.5 g kg^{-1}. Alerce Costero soil had a higher total Fe content than other soils (Table 1).

3.2. CO_2 evolution

Over the course of 36 days, increasing patterns of CO_2 efflux were observed in all evaluated soils (Figures 1A–C). The highest values were found in Alerce Costero soil during anaerobic incubation of sterilized samples inoculated with WRF, at pH of 4.5 (217.45 mg C kg^{-1}) (Figure 1B). The lowest levels of C mineralization (82 mg C kg^{-1}) with the lowest pH 4 were found in Nahuelbuta soil (Figure 1A). Alerce Costero and Puyehue soils followed a similar pattern, with the highest CO_2 release occurring at the highest pH levels, 4.5 and 5.1, and the lowest at induced pH 2.5 (Figures 1B,C). Figure 1A depicts the inverse trends for Nahuelbuta soil. Furthermore, all the soils treated with WRF without Fenton, and soils treated without inoculum, showed a lower average rate values than the combined treatments (WRF + Fenton). Similarly, the lowest average rate of mineralization was observed in sterile soils treated with Fenton, followed by WRF without Fenton induction (Figures 1A,C).

3.3. Exo-enzyme activities

After 36 days of incubation, the activity of LiP, MnP, and DyP was measured. When compared to non-induced Fenton groups, all WRF

10.3389/fmicb.2023.1148750

TABLE 1 Characteristics of soil used in the study.

Analysis	Units	Nahuelbuta	Alerce Costero	Puyehue
SOC[a]	%	9.20 ± 0.1	9.7 ± 0.2	11.4 ± 0.3
Total *N*	%	0.5 ± 0.01	0.4 ± 0.00	0.6 ± 0.03
C:N ratio	Unitless	24.3	23.8	19.1
pH water	Unitless	3.6 ± 0.2	4.5 ± 0.2	5.1 ± 0.1
H_2O_2	μM g^{-1} soil	25.6 ± 0.7	28.0 ± 0.9	33.7 ± 0.5
Al_p[b]	g kg^{-1} soil	0.7 ± 0.1	5.7 ± 0.02	11.0 ± 1.5
Al_O[c]	g kg^{-1} soil	7 ± 0.02	0.73 ± 0.1	3.1 ± 0.2
$Al_o + 1/2\ Fe_o$	Unitless	1.25	1.85	3.8
Al Saturation	%	80.0	93.5	22.4
Total Fe	%	10.4 ± 0.3	11.8 ± 0.5	8.4 ± 0.5
Fe^{2+}	%	2.3 ± 0.5	5.8 ± 0.4	3.2 ± 0.2
Fe^{3+}	%	8.1 ± 0.3	6.0 ± 0.5	5.2 ± 0.3
CEC[d]	cmol(+)kg^{-1} soil	11.8	19.7	5.3
Parent materials	Unitless	Granitic	Metamorphic	Volcanic-allophanic
Clay type[e]		K	Q,I,K	Allophane-imogollite
Texture[f]		L	CL	SCL

[a]Soil organic carbon.
[b]Pyrophosphate extractable Al.
[c]Oxalate extractable Al.
[d]Effective cation exchange capacity.
[e]Q quartz, K kaolinite, I illite.
[f]SCL sandy clay loam, CL clay loam, L loam.

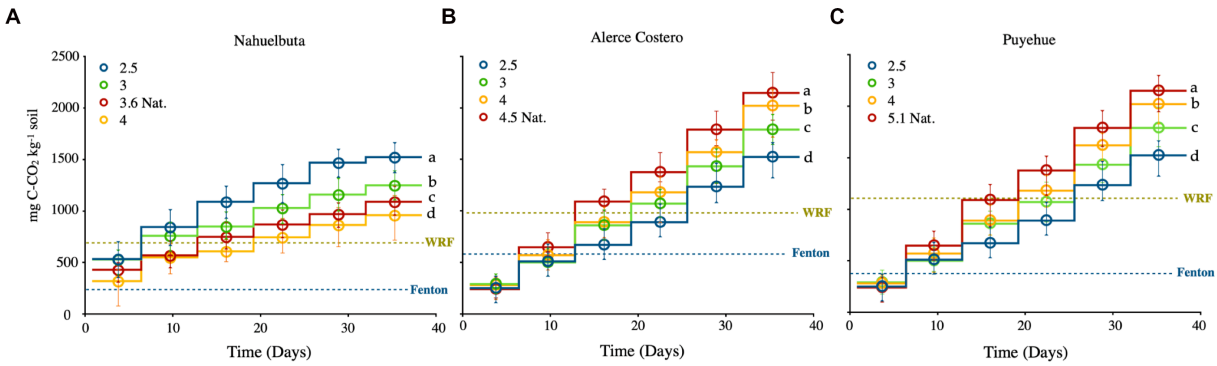

FIGURE 1
(A–C) CO_2 evolution from anaerobic sterilized soils inoculated with WRF and H_2O_2/Fe for Fenton reaction, derived from three temperate rain forest sites with varying pH and incubated for 40days at 12°C. The blue dotted lines represent the average rate of CO_2 released by the induced Fenton reaction in sterilized soils at natural pH, while the green dotted lines represent the average rate of CO_2 released by WRF at natural pH without the induction of the Fenton reaction. Significant differences ($p<0.05$) are indicated by different letters in each panel. The ladder graph depicts the total amount of CO_2 emitted between measurements.

plus induced-Fenton reactions increased proportionally to enzyme activity. The responses of enzyme activities to pH changes in the soils studied varied (Figure 2). Except for Puyehue soil, only the Nahuelbuta microcosm showed a decrease in activity as the pH increased, with the highest activity observed at pH 2.5 (Figures 2A,D,G). LiP, MnP, and DyP were one, two, and eight times higher, respectively, than at natural pH. The CO_2 released was distributed uniformly across the soil pH gradient. With the exception of Alerce Costero with LiP and Puyehue, the highest pH showed the lowest enzymatic activity and CO2 release after 36 days of incubation. LiP activity in Alerce Costero soil displayed a distinct pattern of activity when compared to MnP and DyP. The activity of the LiP increased as the pH increased from acidic to moderate acidic, with higher activity observed at pH (4.5) (Figure 2B). MnP and DyP, on the other hand, significantly reduced their activity from pH 2.5 to 4.5, while CO_2 increased at day 36 (Figures 2E,H). The pH variation in Puyehue soil was observed to have a non-linear distribution. Lip, MnP, and DyP activity were found to be lower in acidic conditions (pH 2.5), with the highest activity at pH 3 (Figures 2C,F,I), followed by a decrease in activity at natural pH (4.5).

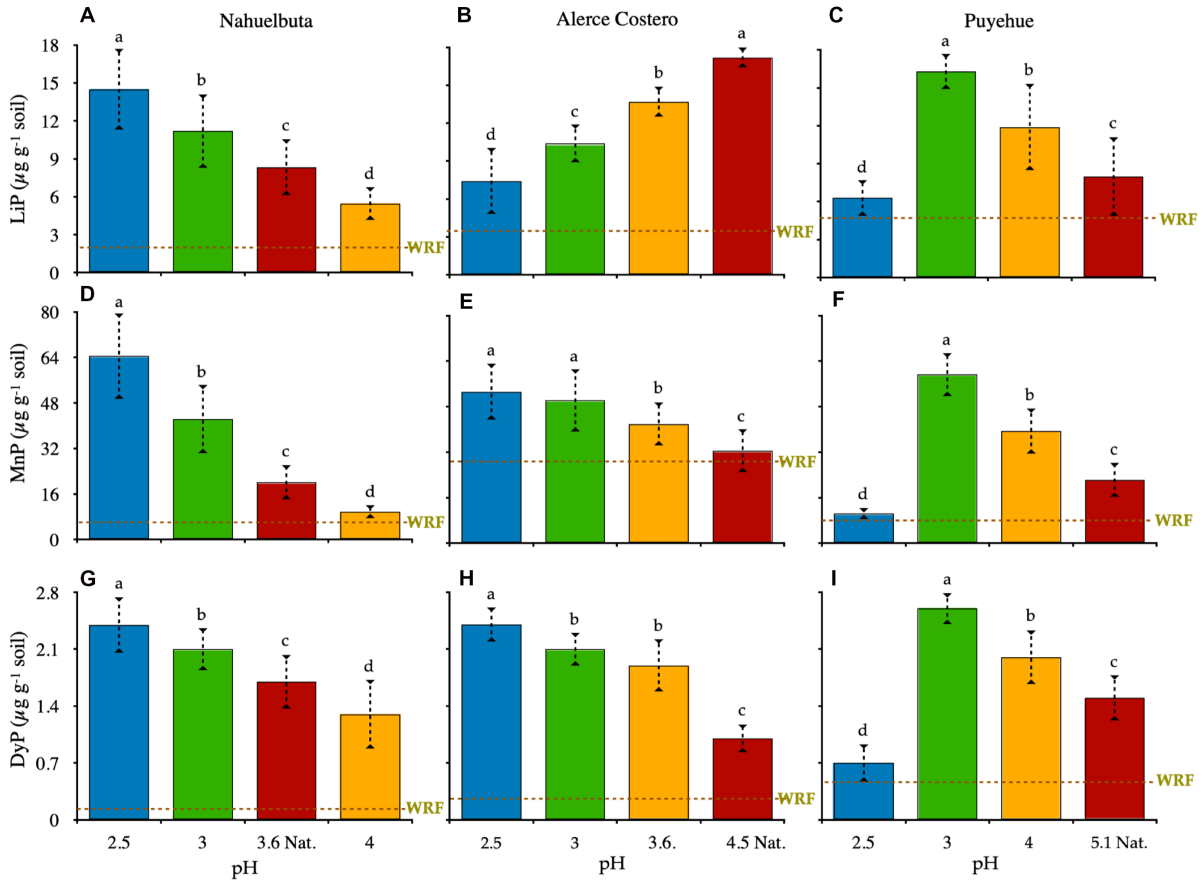

FIGURE 2
A–C: lignin peroxidase (LiP); **D–F**: manganese peroxidase (MnP); and **G–I**: dye-decolorizing peroxidase (DyP) in soils inoculated with WRF from three temperate forest soil sites at various pH levels. At natural pH, the green dotted lines represent the average rate of cumulative enzyme activity by WRF in the absence of the Fenton reaction. Within each panel, different letters indicate significant differences ($p<0.05$).

3.4. Effect of pH on *ROS* generation

pH had an effect on O_2•- production, and the variation was significant between treatments and soils, ranging from 0.5 to 1.3 μmol g^{-1} soil (Figures 3A,D,G). The highest values in Nahuelbuta soil were obtained at higher pH, in the Fenton + WRF group, and in the independent treatments (Figures 3A–C). This pattern was also observed in Alerce Costero soil, where pH 2.5 and 3 had the highest levels of O_2•-, decreasing to 4 and 4.5 (Figure 3A). In comparison to the other soils, the values in Puyehue soil were inverse to the trend (Figure 3G). The lowest levels of O_2•- were found in the most acidic values (2.5), but at pH 3, the maximum production was reached, and as the pH increased, the O_2•- content decreased (Figure 3G). As the pH changed, the production of H_2O_2 varied without a clear trend (Figures 3B,C,H). The highest value of 3.4 μmol g^{-1} of soil was discovered in Alerce Costero at a natural pH of 4.5 (Figure 3E). Puyehue had the lowest H_2O_2 production of 1.3 μmol g^{-1} soil and the lowest pH of 2.5 (Figure 3H). These values take into account the subtraction of the added H_2O_2 to initiate the Fenton H_2O_2/Fe(II) reaction (10,1 ratio). When compared to the other reactive oxygen species, the production of hydroxyl radicals (•OH) was the highest (ROS) (Figures 3C,F,I). Similar to H_2O_2 production, there was no discernible trend in •OH production, with the highest value of 4.3 μmol g^{-1} soil being recorded at the lowest pH 2.5 in Nahuelbuta (Figure 3C). The almost undetectable •OH 0.7 μmol g^{-1} soil was recorded in Puyehue with the lowest pH of 2.5 (Figure 3I). The WRF + Fenton treatment produced the highest total ROS, followed by Fenton and the WRF treatments with lower contributions (Figure 3). Furthermore, the cumulative production of ROS (the sum of the values of each ROS in all soils) was found to be lowest for O_2•-, followed by •OH, and H_2O_2 had the highest abundance.

3.5. H_2O_2 consumption

Figure 4 depicts the consumption of H_2O_2 by exoenzyme and Fenton reaction after 36 days of incubation due to their high oxidative content, allowing them to be used as a cofactor in catalysis and iron oxidation (Fenton). When WRF was added to Nahuelbuta soil, this increased H_2O_2 consumption between pH 2.5 and 3.6, but decreased at pH 4. The Fenton reaction, on the other hand, consumes more H_2O_2 at higher pH levels (pH 4) (Figure 4A). This was not the case with Alerce Costero soil. At moderate acidity pH

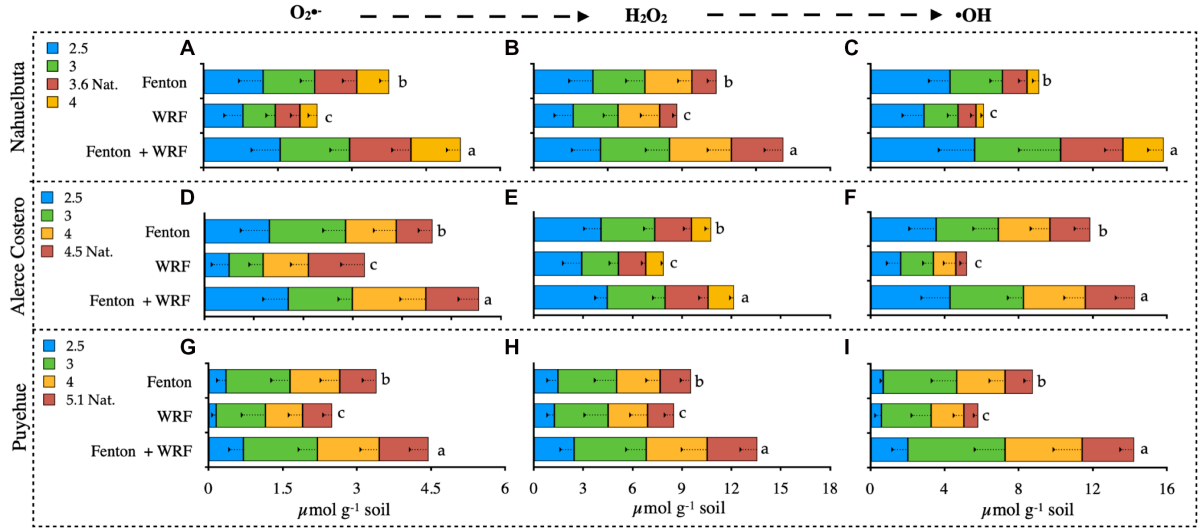

FIGURE 3
Detection of reactive oxygen species (ROS): superoxide anion **(A,D,G)**; hydrogen peroxide **(B,E,H)**; and hydroxyl radical **(C,F,I)** from soils inoculated with WRF from three temperate forest soil sites at different pHs. Significant differences ($p<0.05$) are indicated by different letters in each panel.

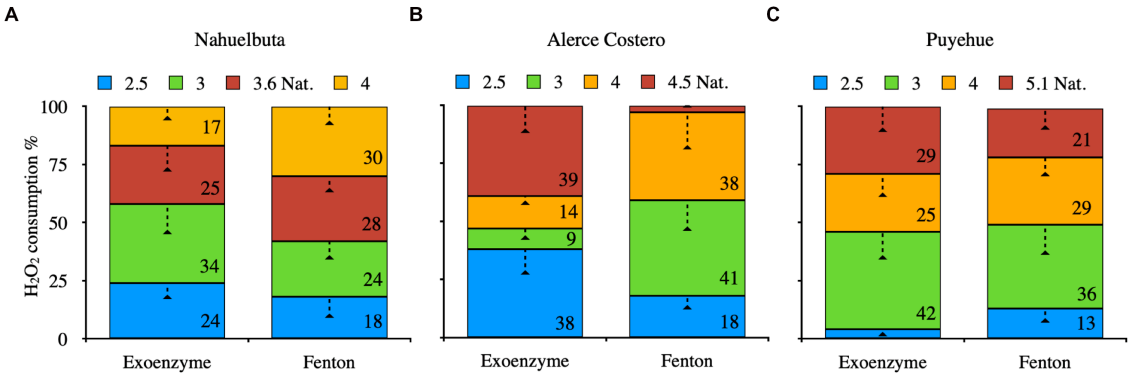

FIGURE 4
The average of exoenzyme activity or Fenton reaction from anaerobic sterilized soils inoculated with WRF from Nahuelbuta **(A)**, Alerce Costero **(B)**, and Puyehue **(C)** forest soil sites at different pH levels. Incubated for 36 days at 12°C. Significant differences ($p < 0.05$) are indicated by different letters in each panel.

4.5 and acid condition (2.5), the exoenzyme consumes more H_2O_2, whereas consumption is similar but significantly reduced at pH 3 and 4. The Fenton reaction, on the other hand, exhibits higher consumption values between pH 3 and 4, but lower consumption values between pH 4.5 and 2.5 (Figure 4B). At pH 3.6, similar consumption values were observed in both exoenzyme and Fenton reactions, but not at the other pH tested. When the pH is raised, exoenzymes consume the least. At pH 2.5, the Fenton reaction produced the lowest values (Figure 4C).

3.6. Relationships between variables measured

The consumption of CO_2 and H_2O_2 was found to have a positive and significant relationship (Figures 5A–C). CO_2 production in WRF-treated soils was strongly related to peroxide consumption ($p < 0.01$, $R2 > 0.85$). Puyehue soil had a lower CO_2 evolution trend associated with H_2O_2 consumption, but the tendency was lower in comparison to Alerce Costero soil, which had a higher CO_2 production and H_2O_2 consumption at pH 3, with a steeper slope (Figures 5B,C).

4. Discussion

The abiotic decomposition of SOM is driven by reactive oxygen species such as O_2•-, •OH, and H_2O_2, which occurs naturally even in the absence of enzymatic activity (Piccolo et al., 2018). H_2O_2 can be incorporated into soils via wet and dry atmospheric deposition (Petigara et al., 2002), intense solar radiation (Georgiou et al., 2015), oxidation of Fe (II) or reduced dissolved organic carbon (DOC) by

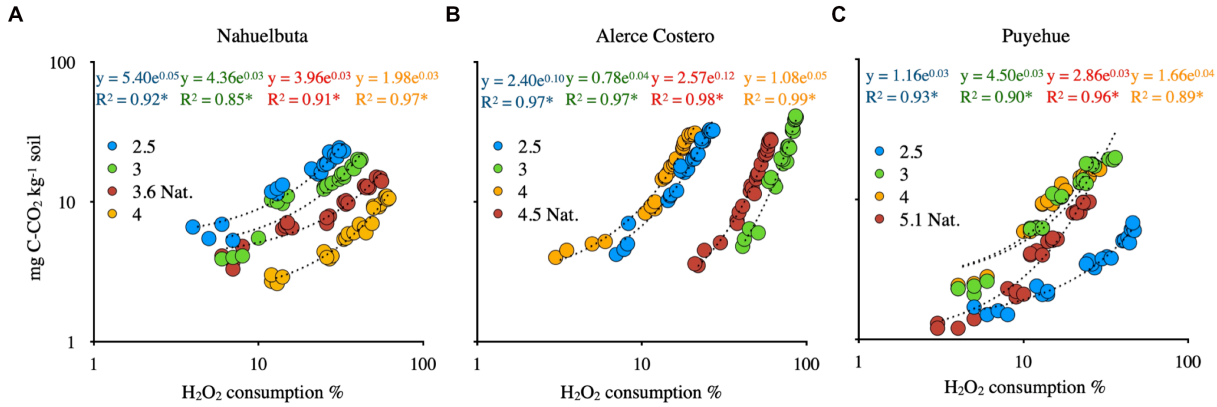

FIGURE 5
The relationships between CO_2 and H_2O_2 consumption in anaerobic sterilized soils inoculated with WRF from Nahuelbuta **(A)**, Alerce Costero **(B)** and Puyehue **(C)** forest soil sites at different pH levels. For 40 days, it was incubated at 12°C. All relationships are statistically significant at $p < 0.01$.

oxygen (Page et al., 2013; Trusiak et al., 2018), and biotic input via the release of various oxidative compounds by soil bacteria and fungi. The biotic or abiotic H_2O_2 input is critical in the decomposition of labile and recalcitrant SOM, increasing H_2O_2 concentration (Merino et al., 2020, 2021b). An excess of H_2O_2, on the other hand, causes competition for H_2O_2 between abiotic and biotic processes.

The WRF generates endogenous H_2O_2 that serves as a cofactor for many enzymes that control fungal biomass conversion and the activity of lignolytic enzymes (e.g., Mn-peroxidase, LiP-peroxidase, lytic polysaccharide monooxygenases), which can be driven in the absence of O_2 (Wong, 2009; Suryadi et al., 2022). Brown-rot fungi, which lack lignin peroxidases, may use the released H_2O_2 to drive the Fenton reaction, which is unique to these fungi (Arantes et al., 2012). As a result, competition can have a significant impact on the efficiency with which SOM is mineralized. Excess H_2O_2 may cause parallel (additive or synergistic) biotic and abiotic reactions, whereas fungi native production will compensate for the oxidant's substrate for the Fenton reaction if there is insufficient H_2O_2. This would have an antagonistic effect on SOM degradation efficiency.

Both biotic (Diaz et al., 2013; Shah et al., 2016) and abiotic (Garrido-Ramírez et al., 2010; Georgiou et al., 2015) factors influenced the level of H_2O_2 in soil. The pH of the soil influences both the biotic and abiotic response to oxidative processes, according to our findings. The biotic component is most sensitive to changes in pH, whereas Fenton-mediated oxidation increases H_2O_2 consumption and CO_2 efflux. When the pH was close to 5.1, the Alerce Costero and Puyehue soils showed similar higher CO_2 emission trends. The highest efflux was observed in Nahuelbuta soil at more extreme acidic pH levels (2.5). This could be attributed to the *Schizophyllum commune* strain, which grows well *in vitro* under acidic conditions, which could translate into increased enzymatic activity. Microbial activity regulates extracellular O_2•- concentrations in the soil environment (Diaz et al., 2016), which may affect soil H_2O_2 levels. The effect of pH treatment on WRF activity in the three soils studied was comparable to previous studies (Leff et al., 2015; Ling et al., 2016). Soil CO_2 emissions had a significant positive relationship with soil H_2O_2 consumption (Figure 5). Increased biodiversity may improve Fe mobilization and H_2O_2 decomposition in soils, according to these findings. This effect is closely related to soil functional selection, which includes nutritional and physical conditions that favor the establishment of specific microorganisms over others (Mimmo et al., 2014). Based on soil organic matter (SOM) availability and N content, previous research has shown that endemic microbiota can cause significant CO_2 flux and reactive oxygen species (ROS) production (Merino et al., 2021a).

Reactive oxygen species are known to play a critical role in the generation of CO_2 by WRF (Hammel et al., 2002), the soil CO_2 released was investigated using ROS as a factor. Given that H_2O_2 has long been used as an oxidant in soil degradation and SOM assessment, our discovery of a strong and linear relationship between CO_2 released and soil H_2O_2 concentrations was not surprising (Robinson, 1927). Previously, researchers discovered a strong positive linear correlation between CO_2 production and H_2O_2 concentrations in deciduous forest soils (Jugold et al., 2012). It is possible that different types of soil precursors will react differently to H_2O_2. More research on the specific precursors of abiotic CH_4 produced in soils should be conducted to determine how the precursors and ROS are likely to interact biochemically. However, we were unable to establish a clear relationship between H_2O_2 concentrations and the other ROS precursors, implying that the H_2O_2 levels used in this study were possibly too high and that other factors (e.g., soil Fe or Mn) had become limiting in the generation of ROS.

Our findings show that anaerobic soils produce a higher proportion of •OH in soils, and that Fe(II) is the primary electron donor allowing the synthesis of •OH and subsequent SOM decomposition, which results in CO_2 release in soils. •OH measurements during anaerobic incubation were consistent with previous research (Page et al., 2013; Minella et al., 2015). •OH generation in anaerobic and low-O_2 soil can also be supported by reducing conditions (i.e., high electron donating capacity and thus high concentrations of electron donors) present across a broad pH range (Page et al., 2013). The pH and oxygen levels in the studied soils were significantly lower (Lipson et al., 2012, 2013), and Fe(II) concentrations provided highly reducing conditions. •OH production from the oxidation of reduced components such as Fe(II) or reduced SOM can be significantly influenced by pH. •OH can also be produced by oxidizing Fe(II) at a pH close to neutral (Remucal and Sedlak, 2011). For example, oxidation of Fe(II) at pH 5 may result in the formation of ferryl iron (Fe(IV)) and •OH,

reducing the ratio of •OH generated per mol oxidized Fe(II) (Vermilyea and Voelker, 2009; Remucal and Sedlak, 2011). Other studies have revealed that at low pH (5), Fe(II) oxidation produces more •OH than Fe(IV) (Remucal and Sedlak, 2011). In contrast to Fe(II) oxidation, the effect of pH on the production of •OH from reduced DOC oxidation has not been studied. Aeschbacher et al. (2012) found that the oxidation of DOC to produce •OH is more favorable at high pH than at low pH, implying that this process occurs more frequently at higher pH.

5. Conclusion

This research investigated the impact of reactive oxygen species (ROS) on CO_2 efflux and enzymatic activity during long-term anaerobic incubation. Despite the fact that few studies have proven that H_2O_2 availability has an effect, our findings show that abiotic and biotic reactions using reactive oxygen species as a feed for both mechanisms have an antagonistic and synergistic effect on GHG emission. However, in all soils tested, ROS production significantly increased biotic and non-biotic CO_2 emissions. This implies that microorganisms and soil structure have an additional influence on C efflux, which is pH dependent. When bacterial microbiota undergoes redox fluctuations, WRF contributes more than 70% of GHG emissions (N_2O and CO_2), which is consistent with previous research conducted in the same forest region. According to the findings of this study, the mechanisms of microbial SOM oxidation are highly dependent on the stability and abundance of oxidant radical and non-radical compounds, as well as changes in soil pH.

Data availability statement

The datasets presented in this study can be found in online repositories. The names of the repository/repositories and accession number(s) can be found below: NCBI—OQ341229, OQ339139 + OQ341421.

Author contributions

CM-G and IJ-F: conceptualization, resources, writing—original draft preparation, and funding acquisition. CM-G: methodology, formal analysis, and project administration. IJ-F: investigation. FM-B: writing—review and editing. All authors contributed to the article and approved the submitted version.

Funding

This research was funded by FONDECYT Postdoctorado, grant number 3200758, and FONDECYT regular, grant number 1220716. The APC was partially funded by Universidad de La Frontera, grant number DI21-1003.

Conflict of interest

The authors declare that the research was conducted in the absence of any commercial or financial relationships that could be construed as a potential conflict of interest.

Publisher's note

All claims expressed in this article are solely those of the authors and do not necessarily represent those of their affiliated organizations, or those of the publisher, the editors and the reviewers. Any product that may be evaluated in this article, or claim that may be made by its manufacturer, is not guaranteed or endorsed by the publisher.

Supplementary material

The Supplementary material for this article can be found online at: https://www.frontiersin.org/articles/10.3389/fmicb.2023.1148750/full#supplementary-material

References

Abedini, A., Daud, A. R., Abdul Hamid, M. A., and Kamil Othman, N. (2014). Radiolytic formation of Fe3O4 nanoparticles: influence of radiation dose on structure and magnetic properties. *PLoS One* 9:e90055. doi: 10.1371/journal.pone.0090055

Aeschbacher, M., Graf, C., Schwarzenbach, R. P., and Sander, M. (2012). Antioxidant properties of humic substances. *Environ. Sci. Technol.* 46, 4916–4925. doi: 10.1021/es300039h

Arantes, V., Jellison, J., and Goodell, B. (2012). Peculiarities of brown-rot fungi and biochemical Fenton reaction with regard to their potential as a model for bioprocessing biomass. *Appl. Microbiol. Biotechnol.* 94, 323–338. doi: 10.1007/s00253-012-3954-y

Bank, T. L., Kukkadapu, R. K., Madden, A. S., Ginder-Vogel, M., Baldwin, M., and Jardine, P. (2008). Effects of gamma-sterilization on the physico-chemical properties of natural sediments. *Chem. Geol.* 251, 1–7. doi: 10.1016/j.chemgeo.2008.01.003

Becker, K. H., Brockmann, K. J., and Bechara, J. (1990). Production of hydrogen peroxide in forest air by reaction of ozone with terpenes. *Nature* 346, 256–258. doi: 10.1038/346256a0

Bernhard, N., Moskwa, L.-M., Schmidt, K., Oeser, R. A., Aburto, F., Bader, M. Y., et al. (2018). Pedogenic and microbial interrelations to regional climate and local topography: new insights from a climate gradient (arid to humid) along the coastal cordillera of Chile. *Catena* 170, 335–355. doi: 10.1016/j.catena.2018.06.018

Berns, A. E., Philipp, H., Narres, H.-D., Burauel, P., Vereecken, H., and Tappe, W. (2008). Effect of gamma-sterilization and autoclaving on soil organic matter structure as studied by solid state NMR, UV and fluorescence spectroscopy. *Eur. J. Soil Sci.* 59, 540–550. doi: 10.1111/j.1365-2389.2008.01016.x

Brown, M. E., Barros, T., and Chang, M. C. (2012). Identification and characterization of a multifunctional dye peroxidase from a lignin-reactive bacterium. *ACS Chem. Biol.* 7, 2074–2081. doi: 10.1021/cb300383y

Dalal, R. C., and Allen, D. E. (2008). Greenhouse gas fluxes from natural ecosystems. *Aust. J. Bot.* 56, 369–407. doi: 10.1071/BT07128

Diaz, J. M., Hansel, C. M., Apprill, A., Brighi, C., Zhang, T., Weber, L., et al. (2016). Species-specific control of external superoxide levels by the coral holobiont during a natural bleaching event. *Nat. Commun.* 7, 1–10. doi: 10.1038/ncomms13801

Diaz, J. M., Hansel, C. M., Voelker, B. M., Mendes, C. M., Andeer, P. F., and Zhang, T. (2013). Widespread production of extracellular superoxide by heterotrophic bacteria. *Science* 340, 1223–1226. doi: 10.1126/science.1237331

Dixon, R. K., Solomon, A., Brown, S., Houghton, R., Trexier, M., and Wisniewski, J. (1994). Carbon pools and flux of global forest ecosystems. *Science* 263, 185–190. doi: 10.1126/science.263.5144.185

Du, H.-Y., Yu, G.-H., Sun, F.-S., Usman, M., Goodman, B. A., Ran, W., et al. (2019). Iron minerals inhibit the growth of *Pseudomonas brassicacearum* J12 via a free-radical

mechanism: implications for soil carbon storage. *Biogeosciences* 16, 1433–1445. doi: 10.5194/bg-16-1433-2019

Garrido-Ramírez, E. G., Theng, B. K., and Mora, M. L. (2010). Clays and oxide minerals as catalysts and nanocatalysts in Fenton-like reactions—a review. *Appl. Clay Sci.* 47, 182–192. doi: 10.1016/j.clay.2009.11.044

Georgiou, C. D., Sun, H. J., McKay, C. P., Grintzalis, K., Papapostolou, I., Zisimopoulos, D., et al. (2015). Evidence for photochemical production of reactive oxygen species in desert soils. *Nat. Commun.* 6:7100. doi: 10.1038/ncomms8100

Greenwald, R. A. (2018). *Handbook Methods for Oxygen Radical Research* CRC Press. doi: 10.1201/9781351072922

Hammel, K., Kapich, A., Jensen, K., and Ryan, Z. (2002). Reactive oxygen species as agents of wood decay by fungi. *Enzym. Microb. Technol.* 30, 445–453. doi: 10.1016/S0141-0229(02)00011-X

Horisawa, S., Sakuma, Y., and Doi, S. (2013). Identification and species-typing of wood rotting fungi using melting curve analysis. *J. Wood Sci.* 59, 432–441. doi: 10.1007/s10086-013-1349-z

Jofré, I., Matus, F., Mendoza, D., Nájera, F., and Merino, C. (2021). Manganese-oxidizing Antarctic Bacteria (Mn-Oxb) release reactive oxygen species (ROS) as secondary Mn (II) oxidation mechanisms to avoid toxicity. *Biology* 10:1004. doi: 10.3390/biology10101004

Jugold, A., Althoff, F., Hurkuck, M., Greule, M., Lelieveld, J., and Keppler, F. (2012). Non-microbial methane formation in oxic soils. *Biogeosci. Discuss.* 9, 5291–5301. doi: 10.5194/bgd-9-11961-2012

Kakeshpour, T., Metaferia, B., Zare, R. N., and Bax, A. (2022). Quantitative detection of hydrogen peroxide in rain, air, exhaled breath, and biological fluids by NMR spectroscopy. *Proc. Natl. Acad. Sci.* 119:e2121542119. doi: 10.1073/pnas.2121542119

Köster, K., Köster, E., Kulmala, L., Berninger, F., and Pumpanen, J. (2017). Are the climatic factors combined with reindeer grazing affecting the soil CO2 emissions in subarctic boreal pine forest? *Catena* 149, 616–622. doi: 10.1016/j.catena.2016.06.011

Kuzyakov, Y. (2006). Sources of CO2 efflux from soil and review of partitioning methods. *Soil Biol. Biochem.* 38, 425–448. doi: 10.1016/j.soilbio.2005.08.020

Leff, J. W., Jones, S. E., Prober, S. M., Barberán, A., Borer, E. T., Firn, J. L., et al. (2015). Consistent responses of soil microbial communities to elevated nutrient inputs in grasslands across the globe. *Proc. Natl. Acad. Sci.* 112, 10967–10972. doi: 10.1073/pnas.1508382112

Lenhart, K., Bunge, M., Ratering, S., Neu, T. R., Schüttmann, I., Greule, M., et al. (2012). Evidence for methane production by saprotrophic fungi. *Nat. Commun.* 3, 1–8. doi: 10.1038/ncomms2049

Liang, C., and He, B. (2018). A titration method for determining individual oxidant concentration in the dual sodium persulfate and hydrogen peroxide oxidation system. *Chemosphere* 198, 297–302. doi: 10.1016/j.chemosphere.2018.01.115

Lin, Y., Campbell, A. N., Bhattacharyya, A., DiDonato, N., Thompson, A. M., Tfaily, M. M., et al. (2021). Differential effects of redox conditions on the decomposition of litter and soil organic matter. *Biogeochemistry* 154, 1–15. doi: 10.1007/s10533-021-00790-y

Ling, N., Zhu, C., Xue, C., Chen, H., Duan, Y., Peng, C., et al. (2016). Insight into how organic amendments can shape the soil microbiome in long-term field experiments as revealed by network analysis. *Soil Biol. Biochem.* 99, 137–149. doi: 10.1016/j.soilbio.2016.05.005

Lipson, D. A., Raab, T. K., Goria, D., and Zlamal, J. (2013). The contribution of Fe (III) and humic acid reduction to ecosystem respiration in drained thaw lake basins of the Arctic coastal plain. *Glob. Biogeochem. Cycles* 27, 399–409. doi: 10.1002/gbc.20038

Lipson, D. A., Zona, D., Raab, T., Bozzolo, F., Mauritz, M., and Oechel, W. (2012). Water-table height and microtopography control biogeochemical cycling in an Arctic coastal tundra ecosystem. *Biogeosciences* 9, 577–591. doi: 10.5194/bg-9-577-2012

Lovley, D. R., and Phillips, E. J. (1987). Rapid assay for microbially reducible ferric iron in aquatic sediments. *Appl. Environ. Microbiol.* 53, 1536–1540. doi: 10.1128/aem.53.7.1536-1540.1987

Luzio, W., Sadzawka, A., Besoain, E., and Lara, P. (2003). Influence of volcanic materials on red clay soil genesis. *R. C. Suelo Nutr. Veg.* 3, 37–52.

Merino, C., Jofré, I., and Matus, F. (2021a). Soil redox controls CO2, CH4 and N2O efflux from White-rot Fungi in temperate Forest ecosystems. *J. Fungi* 7:621. doi: 10.3390/jof7080621

Merino, C., Kuzyakov, Y., Godoy, K., Cornejo, P., and Matus, F. (2020). Synergy effect of peroxidase enzymes and Fenton reactions greatly increase the anaerobic oxidation of soil organic matter. *Sci. Rep.* 10:11289. doi: 10.1038/s41598-020-67953-z

Merino, C., Kuzyakov, Y., Godoy, K., Jofré, I., Nájera, F., and Matus, F. (2021b). Iron-reducing bacteria decompose lignin by electron transfer from soil organic matter. *Sci. Total Environ.* 761:143194. doi: 10.1016/j.scitotenv.2020.143194

Mimmo, T., Del Buono, D., Terzano, R., Tomasi, N., Vigani, G., Crecchio, C., et al. (2014). Rhizospheric organic compounds in the soil–microorganism–plant system: their role in iron availability. *Eur. J. Soil Sci.* 65, 629–642. doi: 10.1111/ejss.12158

Minella, M., De Laurentiis, E., Maurino, V., Minero, C., and Vione, D. (2015). Dark production of hydroxyl radicals by aeration of anoxic lake water. *Sci. Total Environ.* 527-528, 322–327. doi: 10.1016/j.scitotenv.2015.04.123

Naylor, D., McClure, R., and Jansson, J. (2022). Trends in microbial community composition and function by soil depth. *Microorganisms* 10:540. doi: 10.3390/microorganisms10030540

Neculman, R., Rumpel, C., Matus, F., Godoy, R., Steffens, M., and de la Luz Mora, M. (2013). Organic matter stabilization in two Andisols of contrasting age under temperate rain forest. *Biol. Fertil. Soils* 49, 681–689. doi: 10.1007/s00374-012-0758-2

Page, S., Kling, G., Sander, M., Harrold, K., Logan, J., McNeill, K., et al. (2013). Dark formation of hydroxyl radical in Arctic soil and surface waters. *Environ. Sci. Technol.* 47, 12860–12867. doi: 10.1021/es4033265

Petigara, B. R., Blough, N. V., and Mignerey, A. C. (2002). Mechanisms of hydrogen peroxide decomposition in soils. *Environ. Sci. Technol.* 36, 639–645. doi: 10.1021/es001726y

Piccolo, A., Spaccini, R., Cozzolino, V., Nuzzo, A., Drosos, M., Zavattaro, L., et al. (2018). Effective carbon sequestration in Italian agricultural soils by in situ polymerization of soil organic matter under biomimetic photocatalysis. *Land Degrad. Dev.* 29, 485–494. doi: 10.1002/ldr.2877

Raich, J. W., and Schlesinger, W. H. (1992). The global carbon dioxide flux in soil respiration and its relationship to vegetation and climate. *Tellus B* 44, 81–99. doi: 10.3402/tellusb.v44i2.15428

Remucal, C., and Sedlak, D. (2011). The role of iron coordination in the production of reactive oxidants from ferrous Iron oxidation by oxygen and hydrogen peroxide. *ACS Symp. Ser.* 1071, 177–197. doi: 10.1021/bk-2011-1071.ch009

Robinson, W. (1927). The determination of organic matter in soils by means of hydrogen peroxide. *J. Agric. Res.* 34, 339–356.

Sadzawka, A., Carrasco, M., Grez, R., Mora, M., Flores, H., and Neaman, A. (2006). *Métodos de análisis de suelos recomendados para los suelos de Chile. Revision 2006*. Instituto de Investigaciones Agropecuarias, Chile.

Salvachúa, D., Prieto, A., Martínez, Á. T., and Martínez, M. J. (2013). Characterization of a novel dye-decolorizing peroxidase (DyP)-type enzyme from Irpex lacteus and its application in enzymatic hydrolysis of wheat straw. *Appl. Environ. Microbiol.* 79, 4316–4324. doi: 10.1128/aem.00699-13

Schlesinger, W. H., and Andrews, J. A. (2000). Soil respiration and the global carbon cycle. *Biogeochemistry* 48, 7–20. doi: 10.1023/A:1006247623877

Shah, F., Nicolás, C., Bentzer, J., Ellström, M., Smits, M., Rineau, F., et al. (2016). Ectomycorrhizal fungi decompose soil organic matter using oxidative mechanisms adapted from saprotrophic ancestors. *New Phytol.* 209, 1705–1719. doi: 10.1111/nph.13722

Soil Survey Staff (2014). *Keys to Soil Taxonomy*, *12th Edn* Washington, DC: Natural Resources Conservation Service, United States Department of Agriculture. [Google Scholar].

Stookey, L. L. (1970). Ferrozine---a new spectrophotometric reagent for iron. *Anal. Chem.* 42, 779–781. doi: 10.1021/ac60289a016

Suryadi, H., Judono, J. J., Putri, M. R., Eclessia, A. D., Ulhaq, J. M., Agustina, D. N., et al. (2022). Biodelignification of lignocellulose using ligninolytic enzymes from white-rot fungi. *Heliyon* 8:e08865. doi: 10.1016/j.heliyon.2022.e08865

Sutherland, T., Sparks, C., Joseph, J., Wang, Z., Whitaker, G., Sham, T., et al. (2017). Effect of ferrous ion concentration on the kinetics of radiation-induced iron-oxide nanoparticle formation and growth. *Phys. Chem. Chem. Phys.* 19, 695–708. doi: 10.1039/C6CP05456K

Takahashi, Y., Katoh, S., Shikura, N., Tomoda, H., and Omura, S. (2003). Superoxide dismutase produced by soil bacteria increases bacterial colony growth from soil samples. *J. Gen. Appl. Microbiol.* 49, 263–266. doi: 10.2323/jgam.49.263

Trevors, J. T. (1996). Sterilization and inhibition of microbial activity in soil. *J. Microbiol. Methods* 26, 53–59. doi: 10.1016/0167-7012(96)00843-3

Trusiak, A., Treibergs, L. A., Kling, G. W., and Cory, R. M. (2018). The role of iron and reactive oxygen species in the production of CO2 in arctic soil waters. *Geochim. Cosmochim. Acta* 224, 80–95. doi: 10.1016/j.gca.2017.12.022

Van Reeuwijk, L. (2002). *Procedures for Soil Analysis*. Wageningen, The Netherlands. doi: 10.4236/aim.2018.87040

Velikova, V., Yordanov, I., and Edreva, A. (2000). Oxidative stress and some antioxidant systems in acid rain-treated bean plants: protective role of exogenous polyamines. *Plant Sci.* 151, 59–66. doi: 10.1016/S0168-9452(99)00197-1

Vermilyea, A., and Voelker, B. (2009). Photo-Fenton reaction at near neutral pH. *Environ. Sci. Technol.* 43, 6927–6933. doi: 10.1021/es900721x

Walsh, J. E., Fetterer, F., Scott Stewart, J., and Chapman, W. L. (2017). A database for depicting Arctic Sea ice variations back to 1850. *Geogr. Rev.* 107, 89–107. doi: 10.1111/j.1931-0846.2016.12195.x

White, T., Bruns, T., Lee, S., Taylor, J., Innis, M., Gelfand, D., et al. (1990). "Amplification and direct sequencing of fungal ribosomal RNA genes for Phylogenetics" in *PCR*

Protocols: A Guide to Methods and Applications. eds. M. A. Innis, D. H. Gelfand, J. J. Sninsky and T. J. White (New York: Academic Press), 315–322.

Willey, J. D., Kieber, R. J., and Lancaster, R. D. (1996). Coastal rainwater hydrogen peroxide: concentration and deposition. *J. Atmos. Chem.* 25, 149–165. doi: 10.1007/BF00053789

Wong, D. W. (2009). Structure and action mechanism of ligninolytic enzymes. *Appl. Biochem. Biotechnol.* 157, 174–209. doi: 10.1007/s12010-008-8279-z

Xu, Z., Qin, L., Cai, M., Hua, W., and Jin, M. (2018). Biodegradation of Kraft lignin by newly isolated *Klebsiella pneumoniae*, pseudomonas putida, and *Ochrobactrum tritici* strains. *Environ. Sci. Pollut. Res.* 25, 14171–14181. doi: 10.1007/s11356-018-1633-y

Xu, S., Reuter, T., Gilroyed, B., Tymensen, L., Hao, Y., Hao, X., et al. (2013). Microbial communities and greenhouse gas emissions associated with the biodegradation of specified risk material in compost. *Waste Manage. (New York)* 33, 1372–1380. doi: 10.1016/j.wasman.2013.01.036

10.3389/fmicb.2023.1148750

Glossary

ROS	reactive oxygen species
WRF	White Rot Fungi
O_2-	superoxide anion
H_2O_2	hydrogen peroxide
OH	hydroxyl radicals
SOM	soil organic matter
NxO	reactive nitrogen species
LiP	lignin peroxidase
MnP	manganese peroxidase
DyP	dye decolorizing peroxidase
GHG	green house gasses
Ah	first mineral horizon of soil
TOC	total organic carbon
CEC	cation exchange capacity
ITS	internal transcribed spacer
CFU	colony forming units
DOC	dissolved organic carbon

frontiers | Frontiers in Microbiology

TYPE Original Research
PUBLISHED 15 June 2023
DOI 10.3389/fmicb.2023.1165045

OPEN ACCESS

EDITED BY
Yu Luo,
Zhejiang University, China

REVIEWED BY
Qin Peng,
Chinese Academy of Sciences (CAS), China
Ying Wang,
Northwest A&F University, China

*CORRESPONDENCE
Kristina Ivashchenko
✉ ivashchenko.kv@gmail.com

RECEIVED 13 February 2023
ACCEPTED 25 May 2023
PUBLISHED 15 June 2023

CITATION
Sushko S, Ovsepyan L, Gavrichkova O, Yevdokimov I, Komarova A, Zhuravleva A, Blagodatsky S, Kadulin M and Ivashchenko K (2023) Contribution of microbial activity and vegetation cover to the spatial distribution of soil respiration in mountains. *Front. Microbiol.* 14:1165045. doi: 10.3389/fmicb.2023.1165045

Contribution of microbial activity and vegetation cover to the spatial distribution of soil respiration in mountains

Sofia Sushko[1,2], Lilit Ovsepyan[3], Olga Gavrichkova[4,5], Ilya Yevdokimov[6], Alexandra Komarova[1], Anna Zhuravleva[6], Sergey Blagodatsky[7], Maxim Kadulin[8] and Kristina Ivashchenko[1]*

[1]Laboratory of Carbon Monitoring in Terrestrial Ecosystems, Institute of Physicochemical and Biological Problems in Soil Science, Pushchino, Russia, [2]Department of Soil Physics, Physical Chemistry and Biophysics, Agrophysical Research Institute, Saint Petersburg, Russia, [3]Center for Isotope Biogeochemistry, University of Tyumen, Tyumen, Russia, [4]Research Institute on Terrestrial Ecosystems, National Research Council, Porano, Italy, [5]National Biodiversity Future Center, Palermo, Italy, [6]Laboratory of Soil Carbon and Nitrogen Cycles, Institute of Physicochemical and Biological Problems in Soil Science, Pushchino, Russia, [7]Terrestrial Ecology Group, Institute of Zoology, University of Cologne, Cologne, Germany, [8]Soil Science Faculty, Lomonosov Moscow State University, Moscow, Russia

The patterns of change in bioclimatic conditions determine the vegetation cover and soil properties along the altitudinal gradient. Together, these factors control the spatial variability of soil respiration (R_S) in mountainous areas. The underlying mechanisms, which are poorly understood, shape the resulting surface CO_2 flux in these ecosystems. We aimed to investigate the spatial variability of R_S and its drivers on the northeastern slope of the Northwest Caucasus Mountains, Russia (1,260–2,480ma.s.l.), in mixed, fir, and deciduous forests, as well as subalpine and alpine meadows. R_S was measured simultaneously in each ecosystem at 12 randomly distributed points using the closed static chamber technique. After the measurements, topsoil samples (0–10cm) were collected under each chamber (n=60). Several soil physicochemical, microbial, and vegetation indices were assessed as potential drivers of R_S. We tested two hypotheses: (i) the spatial variability of R_S is higher in forests than in grasslands; and (ii) the spatial variability of R_S in forests is mainly due to soil microbial activity, whereas in grasslands, it is mainly due to vegetation characteristics. Unexpectedly, R_S variability was lower in forests than in grasslands, ranging from 1.3–6.5 versus 3.4–12.7μmol CO_2 m^{-1} s^{-1}, respectively. Spatial variability of R_S in forests was related to microbial functioning through chitinase activity (50% explained variance), whereas in grasslands it was related to vegetation structure, namely graminoid abundance (27% explained variance). Apparently, the chitinase dependence of R_S variability in forests may be related to soil N limitation. This was confirmed by low N content and high C:N ratio compared to grassland soils. The greater sensitivity of grassland R_S to vegetation structure may be related to the essential root C allocation for some grasses. Thus, the first hypothesis concerning the higher spatial variability of R_S in forests than in grasslands was not confirmed, whereas the second hypothesis concerning the crucial role of soil microorganisms in forests and vegetation in grasslands as drivers of R_S spatial variability was confirmed.

KEYWORDS

soil CO_2 emission, altitudinal gradient, forest and grassland ecosystems, soil properties, plant community structure

1. Introduction

Soil respiration (R_S) is one of the major fluxes of the global carbon (C) cycle affecting atmospheric CO_2 concentrations. The process of R_S potentially provides feedback to global climate change due to the large amount of C currently stored in soil organic matter (SOM), otherwise known as soil organic carbon (SOC) (Reichstein et al., 2003; Frey et al., 2013). SOC accounts for approximately 1,500 Pg of total C unequally distributed in the uppermost meter of the global soil layer, representing the largest terrestrial C pool (Kutsch et al., 2010; Schaufler et al., 2010; Mayer et al., 2020). The ratio between SOC accumulation in terrestrial ecosystems and SOC loss as CO_2 efflux from soil determines whether an ecosystem serves as an atmospheric sink or source of C (Schlesinger and Andrews, 2000; Bolstad et al., 2004).

The processes and factors affecting R_S has become a heavily scrutinized topic in the international research community in the broad context of its efforts to mitigate long-term climate change (Bu et al., 2012; Leifeld et al., 2013). However, the extremely high temporal and spatial variability of R_S remains a challenge for the development of accurate regional and global models of the C cycle (Bond-Lamberty and Thomson, 2010). The temporal variation of the R_S process is studied worldwide and can be effectively predicted by the dynamics of soil temperature and moisture (Luo and Zhou, 2006; Xu and Shang, 2016; Hursh et al., 2017; He et al., 2023). However, much remains unclear about the spatial variation of R_S within different ecosystems, landscapes, and biomes, making it difficult to predict.

R_S composed of autotrophic (mainly root respiration) and heterotrophic components hampers the quantification of spatial drivers controlling the total CO_2 efflux from soil (Chen et al., 2017). The contribution of each of these components is characterized by high spatial heterogeneity (Subke et al., 2006). More specifically, the spatial variation of root respiration is affected by vegetation, i.e., by species composition, abundance of herbaceous species, and the corresponding density of fine roots in the upper soil layer (Rodeghiero and Cescatti, 2008). At the same time, changes in the microbial capacity to decompose SOM (enzymatic activity, basal respiration, microbial biomass abundance, etc.) from site to site determine the spatial distribution of heterotrophic respiration (Ananyeva et al., 2020). Consequently, the drivers of spatial distribution of different components of R_S are interdependent, and it is quite difficult to determine which of these components are key.

Mountain landscapes occupy almost 25% of the global surface area (Kapos et al., 2000) and accumulate significant amounts of SOM (Canedoli et al., 2020); consequently, their contribution to the global C cycle can be considerable (Hansson et al., 2021). As for regional models describing the C cycle in mountains, the contribution of R_S accounts for up to 21% of regional emissions estimates, exceeding even that of the C-rich soil of steppes (Kudeyarov et al., 2007). Nevertheless, there is a significant lack of data on R_S in mountainous areas (Kudeyarov and Kurganova, 2005; Liu et al., 2014). These shortcomings are related to difficulties in logistics and equipment delivery, unfavorable climatic conditions, and measurement features (Lin et al., 2017). For instance, when measuring R_S on mountain slopes, the correction factor on steepness should be applied (Xu and Shang, 2016). Therefore, researchers usually select a flat plot to determine R_S, resulting in a lack of data about mountain landscapes with steep slopes. Hence, an extension of the regional database is necessary for better understanding the spatial patterns of R_S in mountains and its drivers.

Most mountains (e.g., Himalayas, Alps, Caucasus) are covered with forests, which are replaced by grasslands at increased altitudes (Bardelli et al., 2017; Ahmad et al., 2020; Ivashchenko et al., 2021). Hence, the distribution patterns of R_S change at higher altitudes. A higher variation coefficient in forests than in grasslands has been shown due to the high heterogeneity of soil conditions caused by gaps in forest canopies (Rodeghiero and Cescatti, 2008; Katayama et al., 2009; Qi et al., 2010; Darenova et al., 2016; Shi et al., 2019). Besides, considering that the ratio of heterotrophic to autotrophic respiration in forests is mainly higher than in grasslands as reviewed by Hanson et al. (2000), it would be reasonable to assume a different contribution of microbial and vegetation properties to the spatial variations of R_S in these ecosystems. Despite a number of works having been conducted on the determination of drivers of spatial patterns of R_S in forests (Luan et al., 2012; Jiang et al., 2020), there is still a lack of clear understanding on how they are combined in different ecosystem types. Such assessments face the substantial challenge of organizing simultaneous measurements of R_S across various ecosystems to avoid the effect of temporal variability (Jiang et al., 2020). The spatial variability of R_S could be assayed using manipulation experiments or monitoring natural environmental gradients in the field. Manipulation experiments in controlled environments negatively affect the ability to predict system responses to changing factors and, accordingly, the capacity to effectively schedule and implement conservation actions (Pressey et al., 2007; Reside et al., 2017; Ettinger et al., 2019). Interpreting the data from monitoring experiments performed in natural environments is a more challenging issue; nonetheless, it is a promising alternative to manipulation experiments as more realistic assessments of R_S and its drivers could be achieved.

Thus, we developed an experimental design that allows for the mitigation of the effect of temporal variability via simultaneous measurements in various ecosystems along altitudinal gradient and only focused on spatial factors within forests and grasslands of the examined mountain slope. The following hypotheses were formulated:

i. The spatial variability of R_S in forests is higher than in grasslands due to the high heterogeneity of environmental conditions (e.g., temperature and litter thickness) caused by canopy gaps compared to open grasslands.
ii. The spatial variability of R_S in forests is attributable mainly to soil microbial activity, while spatial variability of R_S in grasslands is attributable mainly to vegetation properties, taking into account different contributions of heterotrophic and autotrophic components to this process for the two ecosystem types.

2. Materials and methods

2.1. Study area and experimental design

The study was conducted in the Northwest Caucasus Mountains (43°40'N; 40°47'E) in Karachay-Cherkess Republic, South Russia. The mountain slope-to-test was the northeastern exposure and covered five vegetation belts: mixed forest at 1,200–18,00 m a.s.l., fir forest at

1,800–2,040 m a.s.l., deciduous forest at 2,040–2,290 m a.s.l., subalpine meadow at 2,290–2,300 m a.s.l., and alpine meadow at 2,300–2,500 m a.s.l. (Figure 1). The soil types were Cambisols, Umbrisols, and Leptosols formed on non-alkaline bedrock. The mean annual air temperature ranged from 3.5 to 5.9°C (our data for years 2018–2021; Table 1) and annual precipitation ranged from 800 to 1,850 mm (the nearest meteorological stations were located at 1,313 m a.s.l. and 2,006 m a.s.l.). The dominant vegetation species along the studied slope are shown in Table 1.

In each vegetation belt, 12 plots of 0.5 × 0.5 m were randomly established as described by Ivashchenko et al. (2021). In total, there were 60 plots along a 1.2 km altitudinal gradient. R_S was measured simultaneously at all plots from 9:30 to 10:30 a.m. on August 11, 2018. This design was aimed at estimating the drivers of spatial variation of R_S without considering the causes of its temporal changes. The measurement time (day and hour) was chosen so that the primary drivers of temporal variability of R_S (i.e., plant phenology, soil temperature, and moisture) were close to representative throughout the altitudinal gradient. First, most plant species along the study slope reach their maximum phytomass and ripening stage in the first half of August. Second, on the eastern slope, there is enough light during the morning for photosynthesis, but there are still no large spatial fluctuations in soil temperature. On the measurement day, soil moisture across the slope was equally sufficient due to preceding rain events typical for the summer season at the location. Vegetation and soil physicochemical and microbial properties characterizing the sources, conditions, and mediators of CO_2 formation in soil were considered as potential drivers of spatial variability of R_S. In this case, only the upper 10-cm soil layer was taken into account, since (i) its microbial properties showed a close correlation with R_S for different soils and ecosystems (Sushko S. et al., 2019; Sushko S. V. et al., 2019),

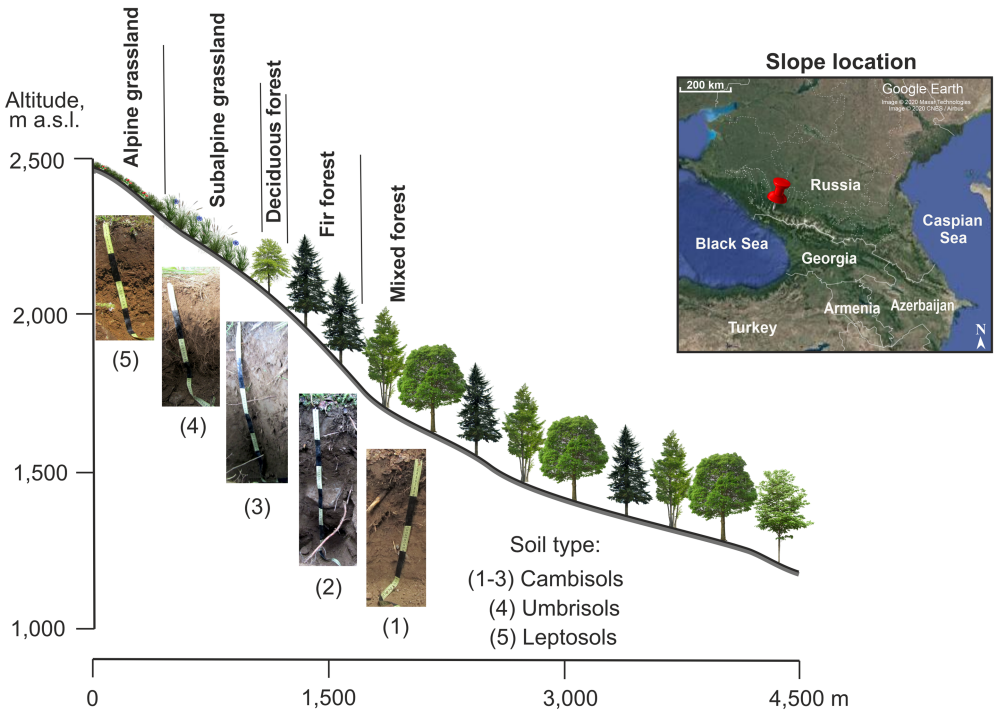

FIGURE 1
Scheme of the northeastern slope of Mt. Tkachiha (Northwest Caucasus, Karachay-Cherkess Republic, Russia).

TABLE 1 General characteristics of studied forest and grassland sites along the northeastern slope of Mt. Tkachiha.

Site	Altitude, m a.s.l.	Slope, °	MAT, °C		Dominant vegetation
			Air	Soil	
Forests					
mixed	1,260	7	5.9	NA	*Fagus orientalis, Abies nordmanniana, Picea orientalis*
fir	1,960	20	3.4	3.9	*Abies nordmanniana*
deciduous	2,060	26	4.1	3.6	*Acer trautvetteri, Sorbus aucuparia, Betula pendula*
Grasslands					
subalpine	2,240	9	4.8	4.0	*Calamagrostis arundinacea, Festuca ovina*
alpine	2,480	6	3.5	3.2	*Carex* sp., *Vaccinium vitis-idaea*

MAT, mean annual temperature for years 2018–2021; NA, not available.

and (ii) it provides main portion of surface CO_2 fluxes from moist soils (Wiaux et al., 2015).

Vegetation surveys to identify plant species and their projective cover for the herbaceous layer were carried out at each 0.5 × 0.5 m plot before R_S measurements. Simultaneously with the R_S measurement, soil temperature was recorded at a 10 cm depth using the Checktemp sensor (Hanna Instruments, Germany), after which a single composite sample per plot (mixing 5 cores with Ø 5 cm) was taken from the upper 0–10 cm layer, placed in a plastic bag, and transported to the lab. Fresh samples ($n = 60$) were immediately sieved through a 2 mm mesh to exclude roots, debris, stones, and homogenized them. A portion of each soil sample was used to determine its moisture by the gravimetric method (8 h, 105°C). The remained soil was used for microbial and chemical analysis. Subsamples for microbial analysis were stored at 4°C for up to 2 weeks after sampling.

2.2. Soil respiration

Soil respiration (R_S), i.e., CO_2 efflux from the soil surface, was measured by the closed static chamber technique. For this, non-transparent PVC chambers (Ø 15.5 cm, volume 1.8 L) were inserted into the soil to a depth of 2–3 cm (above-ground grass was preliminarily cut) perpendicular to the slope surface. Three air samples (20 ml) were taken from each chamber through a rubber stopper with a gas-tight syringe and analyzed with an infrared gas analyzer (SBA-5, PP system, USA). The first zero-time sample was collected immediately after installing the chamber, while the other two were collected at an interval of 3–5 min. The day before, preliminary measurements were performed with gas sampling at nine time points (0, 1, 2, 3, 4, 5, 10, 15, 20 min) to determine the period of initial linear increasing of CO_2 concentration inside the closed chamber at each site. It was found that 5 min is a representative time for all ecosystems during which the gas increases linearly (mean $R^2 = 0.98 \pm 0.03$). Additionally, we recorded atmospheric pressure along the altitudinal gradient simultaneously with R_S measurements using a meteorological barometer. The R_S rate (μmol CO_2 m^{-2} s^{-1}) was calculated according to the following equation:

$$R_S = \frac{VP}{RST} \times \frac{\partial C}{\partial t}, \quad (1)$$

where V is chamber volume (m^3), P is air chamber pressure (Pa), R is gas constant (8.314 m^3 Pa K^{-1} mol^{-1}), S is soil surface area (m^2), T is chamber air temperature (K), and $\partial C/\partial t$ is change of CO_2 concentration inside the chamber over time (μmol mol^{-1} s^{-1}). The final R_S rate was corrected for the surface slope angle in degrees (θ): $R_S/\cos\theta$ (Xu and Shang, 2016).

2.3. Soil and vegetation analysis

Soil total C and N contents were determined by the dry combustion method using a CHNS analyzer (Leco Corp., USA). Dissolved organic carbon (DOC) and dissolved total nitrogen (DTN) were determined in 0.05 M K_2SO_4 extracts (5 g soil: 20 mL solution) using a Shimadzu TOC-VCPN analyzer (Shimadzu Corp., Japan) (Makarov et al., 2015). The pH was measured in a soil:water suspension (1:2.5 ratio) with a conductivity Sartorius Basic Meter (Germany). Microbial biomass carbon (MBC) was measured by the substrate-induced respiration method (Anderson and Domsch, 1978; International Organization for Standardization, 1997). Basal respiration (BR) was measured as the rate of soil CO_2 release using gas chromatography (KrystaLLyuks-4,000 M; Meta-Chrom, Russia) (International Organization for Standardization, 2002). The MBC and BR values were determined under optimum hydrothermal conditions for the microorganisms: 22°C and 65% water holding capacity. Three hydrolytic C-and N-acquiring enzymes (β-D-glucosidase, chitinase, and leucine aminopeptidase) were measured using fluorogenic substrates (Marx et al., 2005; International Organization for Standardization/Technical Specification, 2019) as detailed by Ivashchenko et al. (2021). The soil samples for MBC, BR, and enzyme activities were pre-incubated at 22°C for 72 h (Loeppmann et al., 2016).

We chose characteristics of the herbaceous layer as a potential driving factor along the altitudinal gradient because: (i) it is a uniform ecological plant group for forest and grassland sites; (ii) despite a small contribution to overall forest biomass, this plant strata significantly affect N, P, K, and Mg cycles and mediate C dynamics at the ecosystem level (Gilliam, 2007). For each of the plots studied, the number of species (richness) and total projective coverage for graminoids and forbs were estimated (Ivashchenko et al., 2021). These functional plant groups were the most abundant and presented throughout the altitudinal gradient. In addition, the Shannon-Wiener plant diversity index (H_{plant}) for the herbaceous layer was calculated using the following equation:

$$H_{plant} = -\sum p_i \ln p_i \quad (2)$$

where p_i is the ratio of i species projective cover to total projective cover of all species per plot.

2.4. Statistical analysis

The spatial variability of the studied properties within forests and grasslands was quantified by the coefficient of variation (CV, %), calculated as the ratio of the standard deviation to the mean. Additionally, boxplots combined with dot plots were used to show the variability of R_S across the studied sites. The significance of differences in variables between two or more independent groups was tested by Welch's t-test or one-factor analysis of variance (ANOVA), respectively. Principal component analysis (PCA) was used to show variations and relationships between the studied environmental variables, as well as to illustrate the difference between forest and grassland sites. To reveal possible drivers of R_S spatial variability within forests and grasslands, we used forward stepwise regression and path analysis. First, significant factors within each group of variables (soil physicochemical, microbial, and vegetation) were identified by forward stepwise regression using permutation tests. Afterward, the causal relation between the identified predictors was examined using path analysis. The pre-analysis and preparation of data included (1) checking the normality of distribution with a histogram plot and Shapiro–Wilk's test, (2) log-transformation of some variables to achieve a normal distribution (i.e., C, N, C:N, DOC, BR, enzyme activity), and (3) centering and scaling to unit variance. All analyses and visualizations were performed in the R software system (version 4.1.2, RStudio Team, 2023) using the following packages: "ggplot2"

for boxplots (Wickham, 2016), "FactoMineR" (Lê et al., 2008) and "factoextra" (Kassambara and Mundt, 2020) for PCA, "packfor" for forward stepwise regression (Dray et al., 2016), and "lavaan" for path analysis (Rosseel, 2012).

TABLE 2 Topsoil (0–10cm) and vegetation (herbaceous layer) characteristics of forest and grassland sites along the studied mountain slope.

Variables	Forests (n=35)		Grasslands (n=24)	
	Mean±SE	CV, %	Mean±SE	CV, %
C, g kg^{-1}	73±4	30	162±11***	32
N, g kg^{-1}	5.1±0.2	28	13.1±0.8***	31
DOC, μg g^{-1}	127±6	29	206±8***	19
DTN, μg g^{-1}	59±6	63	95±11**	55
C:N	14.3±0.3	14	12.2±0.2***	8
pH	5.2±0.1	10	5.0±0.1	7
Temperature, °C	12.3±0.2	10	13.4±0.1***	5
WC, %	39±1	22	53±2**	20
MBC, μg C g^{-1}	1,883±97	30	4,475±247***	27
BR, μg C g^{-1} h^{-1}	2.57±0.18	42	3.62±0.27**	36
β-Glucosidase†	1.28±0.24	112	2.95±0.39***	64
Chitinase	2.96±0.68	137	7.18±1.53*	104
LAP[1]	6.71±1.11	98	0.27±0.05***	83
Coverage, %	18±2	73	94±2***	9
Graminoids, %	2±1	164	44±5***	56
Forbs, %	11±2	110	34±3***	47
Richness	5	54	7 **	27
H_{plant}	0.94±0.08	50	1.32±0.08**	31

Values present means±standard error (SE) with a coefficient of variation (CV); *$P \leq 0.05$; **0.01; ***0.001 for Welch's t-test. C, total carbon; N, total nitrogen; DOC, dissolved organic carbon; DTN, dissolved total nitrogen; WC, water content; MBC, microbial biomass carbon; BR, basal respiration; LAP, leucine aminopeptidase; Richness, number of species; H_{plant}, Shannon–Wiener diversity index. †Unit for enzyme activity is μmol MUF g^{-1} h^{-1} (β-glucosidase, chitinase) or μmol AMC g^{-1} h^{-1} (LAP).

3. Results

3.1. Environmental characteristics in forests and grasslands

As expected, soil environments essentially differed between mountain forests and grasslands (Table 2). Grasslands located at higher altitudes than forests accumulated more organic matter (in the C, N, DOC, DTN forms) in soils characterized by a lower C:N ratio. Under both types of vegetation, the soils were strongly acidic (pH 5.0–5.2). Soil temperature in forests varied noticeably higher than in grasslands; its average values were 14.1, 11.3, 11.6, 13.7, and 13.0°C for mixed, fir, deciduous forests, subalpine and alpine grasslands, respectively. Conversely, water content was more homogenous in forests than in grasslands, averaging 39.3, 38.8, 39.4, 45.3 and 61.2% for the above listed ecosystems, respectively. Among the physicochemical properties studied in forest and grassland soils, the DTN content showed the highest spatial variability (CV 55–63%).

Differences in contents of total and dissolved forms of C and N between the forest and grassland soils led to significant differences in their microbial properties. Basically, indices of microbial activity in grasslands exceeded those in forests, except for leucine aminopeptidase (LAP) activity. Among the soil microbial properties, the activity of enzymes had the highest spatial variation within both forests and grasslands (CV 64–137%).

The forest understory (18% projective coverage) was formed mostly by forbs (11%). By contrast, the projective coverage (>90%) of grasslands almost equally consisted of graminoids and forbs. As a result, the number of species and the homogeneity of their distribution within a plot (H_{plant}) were higher in grasslands than in forests. In general, the spatial variation of all of the vegetation properties studied was considerably higher in forests than in grasslands (CV 50–164% vs. 9–56%).

The PCA analysis for all measured characteristics showed a clear grouping of studied sites by vegetation type, i.e., forests and grasslands (Figures 2A,B). Among the soil physicochemical parameters, the organic matter (in the C, N, DOC, DTN forms) and water contents mostly differed between forest and grassland soils (allocation of points along axis 1; r^2=0.64–0.92) (Figure 2A). It is worth noting that the

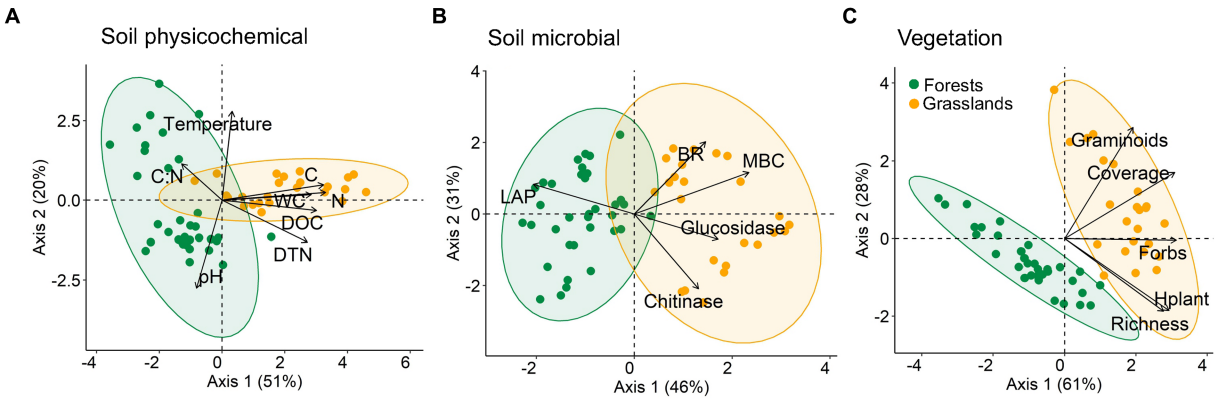

FIGURE 2
Principal component analysis (PCA) ordination triplot for soil physicochemical **(A)**, soil microbial **(B)**, and vegetation **(C)** characteristics of mountain forest and grassland sites. See variable abbreviations in Table 2.

10.3389/fmicb.2023.1165045

temperature and pH value of forest soils were characterized by extremely high variance (allocation of points along axis 2; $r^2 = 0.64–0.65$), while for grassland soils they were more homogeneous. Equally high variation for soil microbial parameters was found within both forests and grasslands (Figure 2B). At the same time, soils under these vegetation types were separately grouped along axis 1, mainly according to MBC content and LAP activity ($r^2 = 0.76$ and 0.59, respectively). In terms of herbaceous layer features, forest and grassland sites were clearly separated from each other mainly along axis 1, which is associated with variations in almost all of the studied characteristics (total and forbs projective coverage, number of species, H_{plant}; $r^2 = 0.60–0.76$) (Figure 2C).

3.2. Spatial variation of soil respiration and its possible drivers

The R_S rate in the forests was, on average, half of that in the grasslands, reaching 3.7 and 7.3 μmol CO_2 m^{-1} s^{-1}, respectively (Figure 3). Within forests, R_S increased significantly in the following order: fir < deciduous < mixed forests with average values of 3.0, 3.6 and 4.6 μmol CO_2 m^{-1} s^{-1}, respectively ($p < 0.001$ for one-way ANOVA). At the same time, R_S did not differ between subalpine and alpine grasslands with average values of 8.1 and 6.4 μmol CO_2 m^{-1} s^{-1}, respectively ($p = 0.09$ for Welch's *t*-test). In general, the spatial variation of R_S in forests was lower than that in grasslands (CV 28 and 33%, respectively).

Difference in R_S rate between forests and grasslands was associated with their divergence in soil (C, N, DOC, temperature, MBC and enzyme activities; $R^2 = 0.23–0.45$, $p \leq 0.001$) and vegetation properties (coverage and graminoid abundance; $R^2 = 0.49$ and 0.55, $p \leq 0.001$) (Supplementary Figure S1). Notably, the relationship with vegetation were stronger than with soil conditions, indicating its primary role in determining R_S rate across ecosystem types.

Stepwise regression analysis showed that R_S spatial variation in forests was best predicted by soil temperature, chitinase activity, and species richness of the herbaceous layer (explained variation 29–50%) (Table 3). The best predictors for grasslands included chitinase activity and graminoid abundance (explained variation 19 and 27%, respectively).

Subsequent path analysis was used to explore the direct or indirect effects of the identified predictors on R_S spatial variation. For forests, soil temperature was included in the path model both as (i) a direct factor, due to changing physical components of R_S, e.g., gas pressure and its diffusive transport throughout pore space, and (ii) an indirect factor, acting through the regulation of chitinase activity. The plant species richness was considered only as an indirect factor since it determines the quality of the organic substrate entering the soil (root exudates, above-and below-ground litter), which, in turn, can affect chitinase activity. In general, the path model explained 50% of R_S variation across forest sites (Figure 4A). In turn, soil temperature affected R_S indirectly through the regulation of chitinase activity. Plant species richness did not affect chitinase, showing only a strong negative correlation with temperature.

For grasslands, chitinase activity, graminoid abundance, and, additionally, C:N ratio as their linking factor (indicated on the base correlation among all variables; see Supplementary Table S1) were included in the path model. As a result, the proposed model explained 29% of the R_S variation in grasslands (Figure 4B). As expected, graminoids affected chitinase activity via changes in the soil C:N ratio. However, the significance of direct or indirect effects of graminoids and chitinase activity on R_S was not confirmed by the model despite its overall satisfactory goodness-of-fit. Nevertheless, the largest standardized path coefficient (0.41) was found for the direct effect of graminoids on R_S. This fact can likely explain the more pronounced effect of vegetation features on grassland R_S variability than soil characteristics associated with the microbial decomposition of SOM (e.g., chitinase activity).

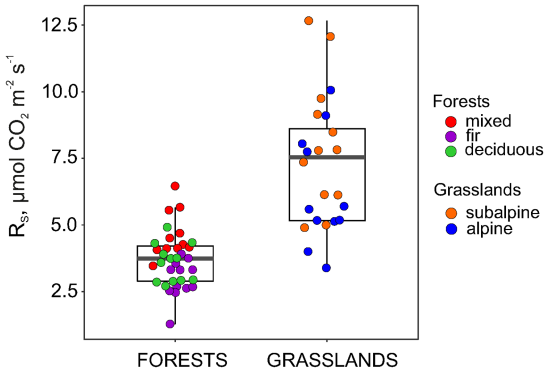

FIGURE 3
Soil respiration (R_S) for mountain forest and grassland sites along altitudinal gradient.

TABLE 3 Results of stepwise regression for *Rs* dependence on soil and vegetation characteristics in mountain forest and grassland sites.

Variables	Forests (*n*=35)		Grasslands (*n*=24)	
	R^2	*F*-value	R^2	*F*-value
C	0.01	0.81	0.02	0.47
N	0.02	1.31	0.01	0.34
DOC	0.00	0.14	0.00	0.01
DTN	0.03	2.31	0.08	1.99
C:N	0.02	1.37	0.11	2.62
pH	**0.07**	**5.03***	0.00	0.03
Temperature	**0.45**	**26.54*****	0.00	0.07
Water content	0.06	4.58	0.04	0.93
MBC	0.03	1.94	0.05	1.44
BR	0.01	0.74	0.07	1.89
β-Glucosidase	0.01	0.73	0.05	1.41
Chitinase	**0.50**	**32.72*****	**0.19**	**5.09***
LAP	0.05	3.37	0.04	1.30
Coverage	0.00	0.09	0.04	1.10
Graminoids	0.01	0.23	**0.27**	**8.19****
Forbs	0.02	0.71	0.01	0.29
Richness	**0.29**	**12.79***	0.01	0.57
Hplant	0.02	0.71	0.02	0.79

For each variable group, the analysis was performed separately. See variable abbreviations in Table 2. Bold indicates significant values at *$p \leq 0.05$; **0.01; ***0.001.

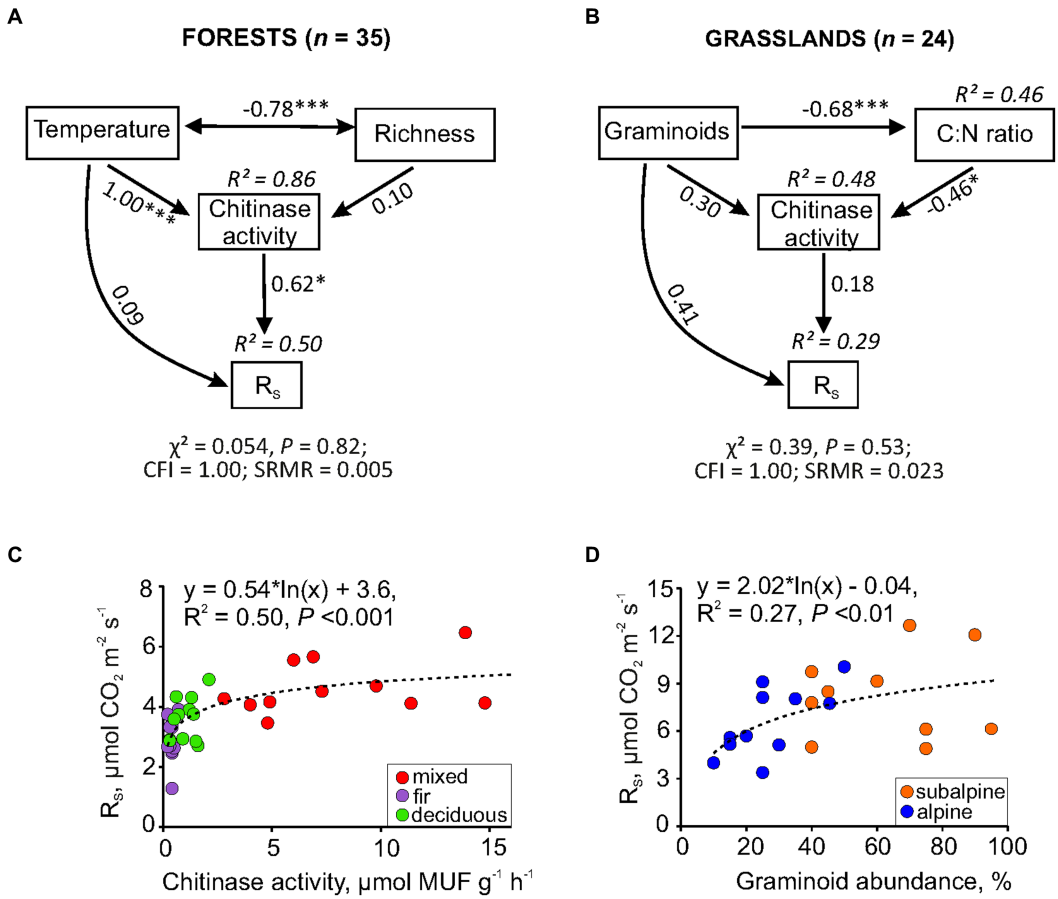

FIGURE 4
Path models and simple regression revealed the effects of soil (temperature, chitinase activity, C:N ratio) and vegetation factors (species richness, graminoid abundance) on R_S spatial variability in mountain forests **(A,C)** and grasslands **(B,D)**. In the path model, numbers within double-headed arrows are correlation coefficients between variables, numbers within one-way arrows are standardized path coefficients indicating the size effect of the causal relationship among variables (*$p \leq 0.05$; **0.01; ***0.001); CFI, comparative fit index; SRMR, standardized root mean square residual.

Summarizing the results of all of the analyses performed, one can conclude that the spatial changes in R_S within mountain forests were mainly driven by soil chitinase activity alone, while spatial changes in R_S in grasslands were associated with graminoid abundance. These relationships have been additionally demonstrated using a simple regression (Figures 4C,D).

4. Discussion

4.1. Spatial variability of soil respiration in mountain forests and meadows

Our results showed a higher R_S rate in grasslands than in forests, which is consistent with the earlier reported difference between these ecosystem types (Raich and Tufekciogul, 2000; Kao and Chang, 2009). Meanwhile, intra-ecosystem R_S variability was also higher in grasslands than in forests (Figure 3), which contradicts both the data reported for other mountain regions (Rodeghiero and Cescatti, 2008; Darenova et al., 2016) and our first hypothesis. On the one hand, this discrepancy can be attributed to the different time scales of measurements and, accordingly, different sources of R_S variation. Specifically, our data show only the spatial variation in R_S at individual time points without including its fluctuations during a season or year (i.e., combined spatio-temporal variability), unlike that in the above-mentioned studies. On the other hand, high altitude grasslands adopt accelerated photorespiration to complete growth and development within a short growing season (Streb and Cornic, 2012). Alpine species reach maximum photosynthetic capacity at a wide range of light intensity (i.e., 530–3,000 µmol photons m^{-2} s^{-1}) with a higher interspecific variation than in lowland plants (Korner and Diemer, 1987). This phenomenon, along with a species-specific time lag between photosynthesis and root-derived CO_2 efflux from soil (Kuzyakov and Gavrichkova, 2010), could have caused high spatial variability in R_S within grasslands in our study.

4.2. Drivers of spatial variability in soil respiration in mountain forests and meadows

In our study, the drivers of spatial variability in R_S were fundamentally different between forests and grasslands. In forests, both biotic and abiotic factors influenced the spatial variability of

R_S. A primary biotic driver was soil chitinase activity (Figure 4). The chitinase is one of the key enzymes of the C-and N-cycling, catalyzing degradation of chitin and peptidoglycan to carbohydrates and inorganic N available for soil microorganisms and plants (Andersson et al., 2004). With an increase in the availability of substrates for maintenance and growth of microorganisms and plants, their enzyme production would diminish, and vice versa (Allison et al., 2010). The relationship between chitinase activity and R_S in forests could be explained by soil N deficiency, which is confirmed by significantly low contents of total and dissolved N forms, as well as by a high C:N ratio (Table 2). At the same time, the N-related enzyme LAP did not affect R_S, unlike chitinase (Table 3). A reasonable explanation for this finding is that LAP catalyzes the hydrolysis of amino acids (Sinsabaugh et al., 2009), which is a less important source of N than amino sugars (i.e., chitin) contained in microbial necromass (Buckeridge et al., 2022). The main abiotic driver of the spatial variability in forest R_S was soil temperature, which acted indirectly through the regulation of chitinase (Figure 4). The lower temperatures stimulate microbial necromass accumulation that would decompose primarily with increase in temperature, in particular by the chitinase (Bai et al., 2016; Wang et al., 2021). Moreover, a dominant portion of microbial necromass in forest topsoil is represented by fungi, which is an essential source of chitin and other amino sugars (Ni et al., 2020; Wang et al., 2021). Accordingly, in our study, a strong relationship between temperature and chitinase was found at colder soil conditions in forests compared to grasslands (Table 2). Thus, chitinase activity and its dependence on biotic and abiotic factors is critically important considering the inter-relations between C-and N-cycling in forest soils.

In grasslands, spatial variability in R_S was related to vegetation structure, especially graminoid abundance, rather than chitinase activity (Table 3 and Figure 4). Overall, weaker relationships between potential drivers and R_S in grasslands unlike in forests can be attributed to the difference in the heterogeneity of the above-and below-ground vegetation structure, biomass, and C allocation. Below-ground C allocation of photosynthates in grasslands is high, especially for some graminoids (Liu et al., 2021), which can eventually cause a considerable fraction of autotrophic (root-derived) respiration in R_S (Hanson et al., 2000). Therefore, the relationship between R_S and graminoid abundance was the most pronounced in studied grasslands. An important role of the vegetation structure and functioning in spatial heterogeneity of R_S in grasslands was also confirmed by previous studies (e.g., Bahn et al., 2008; Fóti et al., 2016). At the same time, abiotic factors would be crucial for R_S changes at unfavorable temperature and water conditions, e.g., in cold and drought periods. Therefore, we can expect an enormous variation in the importance of a number of spatial drivers of R_S depending on season, as earlier reported by Shi and colleagues (Shi et al., 2020) for grassland ecosystems.

4.3. Prospects to study and forecast spatial variability of soil respiration

Monitoring R_S is a complicated task due to its high variability in space and time (Rodeghiero and Cescatti, 2008). The spatial variation coefficient of R_S can also be higher than that of R_S temporal variation (Rodeghiero and Cescatti, 2008; Jiang et al., 2020). Therefore, the optimization of R_S measurements to decrease uncertainties caused by spatial factors is an urgent matter. A sample size for R_S measurements could be optimized using multiple probability simulation (Rodeghiero and Cescatti, 2008). However, for such a model, comprehensive information on R_S spatial variability and its site-specific drivers is needed. Previous studies of R_S spatial variability were combined with examinations of its temporal dynamics (Martin and Bolstad, 2005; Kosugi et al., 2007; Luan et al., 2012; Jiang et al., 2020). Under such conditions, spatial and temporal variability are overlapped since the measurements for different plots by closed chamber methods take several hours to even several days (Jiang et al., 2020). Consequently, high temporal variability in R_S contributes to uncertainty in its spatial variability. The most accurate measurements are provided by long-term systems for multiplexed soil CO_2 flux measurements, which are able to evaluate both spatial and temporal flux variations without overlapping across a large footprint (LI-COR, 2023). However, this measurement system is expensive and difficult to install on steep slopes. In our study, we sought to minimize R_S temporal variability in mountain ecosystems, and thus focused on its spatial variability, which makes our research relatively novel for such kinds of field experiments. Simultaneous air sampling from closed chambers in five ecosystems took approximately 1 h and allowed for the analysis of CO_2 concentrations on the same day despite the time spent for climbing and descent. However, extrapolating our results in time should be performed with care because seasonal variability in R_S was not considered in the current set-up. Nevertheless, splitting the drivers for spatial patterns of R_S between forests and grasslands constitutes a useful integration for C-cycle models (Jackson et al., 2017). Moreover, projecting our results to the consequences of climate change allowed us to assay not only C turnover changes but also drivers of its spatial variability at treeline shifts in mountains; therefore, further research in this direction appears to be a promising endeavor (Chen et al., 2022).

5. Conclusion

This study provides a comprehensive analysis of vegetation and soil factors along the altitudinal gradients to identify potential drivers of R_S spatial variability. The results have shown principal differences in R_S spatial patterns and their drivers between forest and grassland ecosystems. A higher spatial variability of this process was found in grasslands than in forests, which contradicts our first hypothesis. Soil microbial activity (i.e., chitinase) contributed greatly to spatial variability of R_S in forests, while vegetation (graminoid abundance) was more considerable factors in grasslands, which fully confirmed our second hypothesis. These findings highlighted how CO_2 fluxes in mountain forest and grassland ecosystems are regulated by a number of biotic and abiotic factors, emphasizing the most probable mechanisms of mutual regulations of C-and N-cycles.

Data availability statement

The raw data supporting the conclusions of this article will be made available by the authors, without undue reservation.

Author contributions

SS and KI: conception of the study. SS, KI, LO, AK, MK, and AZ: field measurements and laboratory analysis. SS, KI, LO, OG, SB, and IY: data interpretation, result discussion, and writing original draft. All authors contributed to the article and approved the submitted version.

Funding

Analytical processing and modeling were supported by state assignment No. 122111000095–8. Data survey was supported by Russian Science Foundation No. 22–74-10124.

Acknowledgments

We thank Kristina Radchenko, Alexander Tronin, Evgeny Ivashchenko, Anton Rogovoy, and Elvira Shtain for helping in field measurements and soil sampling. We are grateful to Vadim Smirnov for the discussion of the soil sampling design, to Viacheslav Vasenev for sharing equipment, to Valentin Lopes de Gerenyu for analyzing total carbon and nitrogen in the soil samples. We also thank the staff of Caucasian State Nature Biosphere Reserve for allowing us to carry out our investigation and technical support.

Conflict of interest

The authors declare that the research was conducted in the absence of any commercial or financial relationships that could be construed as a potential conflict of interest.

Publisher's note

Supplementary material

The Supplementary material for this article can be found online at: https://www.frontiersin.org/articles/10.3389/fmicb.2023.1165045/full#supplementary-material

References

Ahmad, M., Uniyal, S. K., Batish, D. R., Singh, H. P., Jaryan, V., Rathee, S., et al. (2020). Patterns of plant communities along vertical gradient in Dhauladhar Mountains in lesser Himalayas in North-Western India. *Sci. Total Environ.* 716:136919. doi: 10.1016/j.scitotenv.2020.136919

Allison, S. D., Wallenstein, M. D., and Bradford, M. A. (2010). Soil-carbon response to warming dependent on microbial physiology. *Nat. Geosci.* 3, 336–340. doi: 10.1038/ngeo846

Ananyeva, N. D., Sushko, S. V., Ivashchenko, K. V., and Vasenev, V. I. (2020). Soil microbial respiration in subtaiga and forest-steppe ecosystems of European Russia: field and laboratory approaches. *Eurasian Soil Sci.* 53, 1492–1501. doi: 10.1134/S106422932010004X

Anderson, J. P. E., and Domsch, K. H. (1978). A physiological method for the quantitative measurement of microbial biomass in soils. *Soil Biol. Biochem.* 10, 215–221. doi: 10.1016/0038-0717(78)90099-8

Andersson, M., Kjøller, A., and Struwe, S. (2004). Microbial enzyme activities in leaf litter, humus and mineral soil layers of European forests. *Soil Biol. Biochem.* 36, 1527–1537. doi: 10.1016/j.soilbio.2004.07.018

Bahn, M., Rodeghiero, M., Anderson-Dunn, M., Dore, S., Gimeno, C., Drösler, M., et al. (2008). Soil respiration in European grasslands in relation to climate and assimilate supply. *Ecosystems* 11, 1352–1367. doi: 10.1007/s10021-008-9198-0

Bai, Y., Eijsink, V. G. H., Kielak, A. M., van Veen, J. A., and de Boer, W. (2016). Genomic comparison of chitinolytic enzyme systems from terrestrial and aquatic bacteria: comparison of bacterial chitinolytic systems. *Environ. Microbiol.* 18, 38–49. doi: 10.1111/1462-2920.12545

Bardelli, T., Gómez-Brandón, M., Ascher-Jenull, J., Fornasier, F., Arfaioli, P., Francioli, D., et al. (2017). Effects of slope exposure on soil physico-chemical and microbiological properties along an altitudinal climosequence in the Italian Alps. *Sci. Total Environ.* 575, 1041–1055. doi: 10.1016/j.scitotenv.2016.09.176

Bolstad, P. V., Davis, K. J., Martin, J., Cook, B. D., and Wang, W. (2004). Component and whole-system respiration fluxes in northern deciduous forests. *Tree Physiol.* 24, 493–504. doi: 10.1093/treephys/24.5.493

Bond-Lamberty, B., and Thomson, A. (2010). Temperature-associated increases in the global soil respiration record. *Nature* 464, 579–582. doi: 10.1038/nature08930

Bu, X., Ruan, H., Wang, L., Ma, W., Ding, J., and Yu, X. (2012). Soil organic matter in density fractions as related to vegetation changes along an altitude gradient in the Wuyi Mountains, southeastern China. *Appl. Soil Ecol.* 52, 42–47. doi: 10.1016/j.apsoil.2011.10.005

Buckeridge, K. M., Creamer, C., and Whitaker, J. (2022). Deconstructing the microbial necromass continuum to inform soil carbon sequestration. *Funct. Ecol.* 36, 1396–1410. doi: 10.1111/1365-2435.14014

Canedoli, C., Ferrè, C., Abu El Khair, D., Comolli, R., Liga, C., Mazzucchelli, F., et al. (2020). Evaluation of ecosystem services in a protected mountain area: soil organic carbon stock and biodiversity in alpine forests and grasslands. *Ecosyst. Serv.* 44:101135. doi: 10.1016/j.ecoser.2020.101135

Chen, W., Ding, H., Li, J., Chen, K., and Wang, H. (2022). Alpine treelines as ecological indicators of global climate change: who has studied? What has been studied? *Ecol. Inform.* 70:101691. doi: 10.1016/j.ecoinf.2022.101691

Chen, Z., Xu, Y., Fan, J., Yu, H., and Ding, W. (2017). Soil autotrophic and heterotrophic respiration in response to different N fertilization and environmental conditions from a cropland in Northeast China. *Soil Biol. Biochem.* 110, 103–115. doi: 10.1016/j.soilbio.2017.03.011

Darenova, E., Pavelka, M., and Macalkova, L. (2016). Spatial heterogeneity of CO_2 efflux and optimization of the number of measurement positions. *Eur. J. Soil Biol.* 75, 123–134. doi: 10.1016/j.ejsobi.2016.05.004

Dray, S., Legendre, P., and Blanchet, G. (2016). Packfor: Forward selection with permutation (Canoco p.46). R Package Version 0.0-8/r136. Available at: https://R-Forge.R-project.org/projects/sedar/

Ettinger, A. K., Chuine, I., Cook, B. I., Dukes, J. S., Ellison, A. M., Johnston, M. R., et al. (2019). How do climate change experiments alter plot-scale climate? *Ecol. Lett.* 22, 748–763. doi: 10.1111/ele.13223

Fóti, S., Balogh, J., Herbst, M., Papp, M., Koncz, P., Bartha, S., et al. (2016). Meta-analysis of field scale spatial variability of grassland soil CO_2 efflux: interaction of biotic and abiotic drivers. *Catena* 143, 78–89. doi: 10.1016/j.catena.2016.03.034

Frey, S. D., Lee, J., Melillo, J. M., and Six, J. (2013). The temperature response of soil microbial efficiency and its feedback to climate. *Nat. Clim. Chang.* 3, 395–398. doi: 10.1038/nclimate1796

Gilliam, F. S. (2007). The ecological significance of the herbaceous layer in temperate forest ecosystems. *Bioscience* 57, 845–858. doi: 10.1641/B571007

Hanson, P. J., Edwards, N. T., Garten, C. T., and Andrews, J. A. (2000). Separating root and soil microbial contributions to soil respiration: a review of methods and observations. *Biogeochemistry* 48, 115–146. doi: 10.1023/A:1006244819642

Hansson, A., Dargusch, P., and Shulmeister, J. (2021). A review of modern treeline migration, the factors controlling it and the implications for carbon storage. *J. Mt. Sci.* 18, 291–306. doi: 10.1007/s11629-020-6221-1

He, Y., Wang, Y., Jiang, Y., Yin, G., Cao, S., Liu, X., et al. (2023). Drivers of soil respiration and nitrogen mineralization change after litter management at a subtropical Chinese sweetgum tree plantation. *Soil Use Manag.* 39, 92–103. doi: 10.1111/sum.12823

Hursh, A., Ballantyne, A., Cooper, L., Maneta, M., Kimball, J., and Watts, J. (2017). The sensitivity of soil respiration to soil temperature, moisture, and carbon supply at the global scale. *Glob. Change Biol.* 23, 2090–2103. doi: 10.1111/gcb.13489

International Organization for Standardization (1997). *Soil quality – Determination of soil microbial biomass – Part 1: substrate-induced respiration method (ISO standard no. 14240–1:1997)*. Geneva: International Organization for Standardization.

International Organization for Standardization (2002). *Soil quality – Laboratory methods for determination of microbial soil respiration (ISO standard no. 16072:2002)*. Geneva: International Organization for Standardization.

International Organization for Standardization/Technical Specification (2019). *Soil quality – Measurement of enzyme activity patterns in soil samples using fluorogenic substrates in micro-well plates (ISO standard no. 22939:2019)*. Geneva: International Organization for Standardization.

Ivashchenko, K., Sushko, S., Selezneva, A., Ananyeva, N., Zhuravleva, A., Kudeyarov, V., et al. (2021). Soil microbial activity along an altitudinal gradient: vegetation as a main driver beyond topographic and edaphic factors. *Appl. Soil Ecol.* 168:104197. doi: 10.1016/j.apsoil.2021.104197

Jackson, R. B., Lajtha, K., Crow, S. E., Hugelius, G., Kramer, M. G., and Piñeiro, G. (2017). The ecology of soil carbon: pools, vulnerabilities, and biotic and abiotic controls. *Annu. Rev. Ecol. Evol. Syst.* 48, 419–445. doi: 10.1146/annurev-ecolsys-112414-054234

Jiang, Y., Zhang, B., Wang, W., Li, B., Wu, Z., and Chu, C. (2020). Topography and plant community structure contribute to spatial heterogeneity of soil respiration in a subtropical forest. *Sci. Total Environ.* 733:139287. doi: 10.1016/j.scitotenv.2020.139287

Kao, W. Y., and Chang, K. W. (2009). Soil CO_2 efflux from a mountainous forest-grassland ecosystem in Central Taiwan. *Bot. Stud.* 50, 337–342.

Kapos, V., Rhind, J., Edwards, M., Price, M. F., and Ravilious, C. (2000). "Developing a map of the world's mountain forests", in *Forests in sustainable mountain development: a state of knowledge report for 2000*. eds. M. F. Price and N. Butt (Wallingford: CABI Pub.), 4–9. doi: 10.1079/9780851994468.0004

Kassambara, A., and Mundt, F. (2020). Factoextra: extract and visualize the results of multivariate data analyses. R package version 1.0.7. Available at: http://www.sthda.com/english/rpkgs/factoextra

Katayama, A., Kume, T., Komatsu, H., Ohashi, M., Nakagawa, M., Yamashita, M., et al. (2009). Effect of forest structure on the spatial variation in soil respiration in a Bornean tropical rainforest. *Agric. For. Meteorol.* 149, 1666–1673. doi: 10.1016/j.agrformet.2009.05.007

Korner, C., and Diemer, M. (1987). In situ photosynthetic responses to light, temperature and carbon dioxide in herbaceous plants from low and high altitude. *Funct. Ecol.* 1:179. doi: 10.2307/2389420

Kosugi, Y., Mitani, T., Itoh, M., Noguchi, S., Tani, M., Matsuo, N., et al. (2007). Spatial and temporal variation in soil respiration in a southeast Asian tropical rainforest. *Agric. For. Meteorol.* 147, 35–47. doi: 10.1016/j.agrformet.2007.06.005

Kudeyarov, V., and Kurganova, I. (2005). Respiration of Russian soils: database analysis, long-term monitoring, and general estimates. *Eurasian Soil Sci.* 38, 983–992.

Kudeyarov, V. N., Zavarzin, G. A., Blagodatsky, S. A., Borisov, A. V., Voronin, P. U., Demkin, V. A., et al. (2007). *Pools and fluxes of carbon in terrestrial ecosystems of Russia*. Moscow: Nauka

Kutsch, W. L., Bahn, M., and Heinemeyer, A. (Eds.) (2010). *Soil carbon dynamics: an integrated methodology*. *1st* Edn. Cambridge: Cambridge University Press.

Kuzyakov, Y., and Gavrichkova, O. (2010). Time lag between photosynthesis and carbon dioxide efflux from soil: a review of mechanisms and controls. *Glob. Change Biol.* 16, 3386–3406. doi: 10.1111/j.1365-2486.2010.02179.x

Lê, S., Josse, J., and Husson, F. (2008). FactoMineR: An R package for multivariate analysis. *J. Stat. Softw.* 25, 1–18. doi: 10.18637/jss.v025.i01

Leifeld, J., Bassin, S., Conen, F., Hajdas, I., Egli, M., and Fuhrer, J. (2013). Control of soil pH on turnover of belowground organic matter in subalpine grassland. *Biogeochemistry* 112, 59–69. doi: 10.1007/s10533-011-9689-5

LI-COR (2023). Long-term systems. Available at: https://www.licor.com/env/products/soil_flux/long-term (Accessed October 03, 2019).

Lin, J. C., Mallia, D. V., Wu, D., and Stephens, B. B. (2017). How can mountaintop CO_2 observations be used to constrain regional carbon fluxes? *Atmospheric Chem. Phys.* 17, 5561–5581. doi: 10.5194/acp-17-5561-2017

Liu, Y., Xu, M., Li, G., Wang, M., Li, Z., and De Boeck, H. J. (2021). Changes of aboveground and belowground biomass allocation in four dominant grassland species across a precipitation gradient. *Front. Plant Sci.* 12:650802. doi: 10.3389/fpls.2021.650802

Liu, X. P., Zhang, W. J., Hu, C. S., and Tang, X. G. (2014). Soil greenhouse gas fluxes from different tree species on Taihang Mountain, North China. *Biogeosciences* 11, 1649–1666. doi: 10.5194/bg-11-1649-2014

Loeppmann, S., Semenov, M., Blagodatskaya, E., and Kuzyakov, Y. (2016). Substrate quality affects microbial-and enzyme activities in rooted soil. *J. Plant Nutr. Soil Sci.* 179, 39–47. doi: 10.1002/jpln.201400518

Luan, J., Liu, S., Zhu, X., Wang, J., and Liu, K. (2012). Roles of biotic and abiotic variables in determining spatial variation of soil respiration in secondary oak and planted pine forests. *Soil Biol. Biochem.* 44, 143–150. doi: 10.1016/j.soilbio.2011.08.012

Luo, Y., and Zhou, X. (2006). *Soil respiration and the environment*. Amsterdam; Boston: Elsevier Academic Press.

Makarov, M. I., Malysheva, T. I., Menyailo, O. V., Soudzilovskaia, N. A., Van Logtestijn, R. S. P., and Cornelissen, J. H. C. (2015). Effect of K_2SO_4 concentration on extractability and isotope signature (δ^{13} C and δ^{15} N) of soil C and N fractions: extractability, δ^{13} C and δ^{15} N of soil C and N fractions. *Eur. J. Soil Sci.* 66, 417–426. doi: 10.1111/ejss.12243

Martin, J. G., and Bolstad, P. V. (2005). Annual soil respiration in broadleaf forests of northern Wisconsin: influence of moisture and site biological, chemical, and physical characteristics. *Biogeochemistry* 73, 149–182. doi: 10.1007/s10533-004-5166-8

Marx, M.-C., Kandeler, E., Wood, M., Wermbter, N., and Jarvis, S. C. (2005). Exploring the enzymatic landscape: distribution and kinetics of hydrolytic enzymes in soil particle-size fractions. *Soil Biol. Biochem.* 37, 35–48. doi: 10.1016/j.soilbio.2004.05.024

Mayer, M., Prescott, C. E., Abaker, W. E. A., Augusto, L., Cécillon, L., Ferreira, G. W. D., et al. (2020). Tamm review: influence of forest management activities on soil organic carbon stocks: a knowledge synthesis. *For. Ecol. Manag.* 466:118127. doi: 10.1016/j.foreco.2020.118127

Ni, X., Liao, S., Tan, S., Peng, Y., Wang, D., Yue, K., et al. (2020). The vertical distribution and control of microbial necromass carbon in forest soils. *Glob. Ecol. Biogeogr.* 29, 1829–1839. doi: 10.1111/geb.13159

Pressey, R. L., Cabeza, M., Watts, M. E., Cowling, R. M., and Wilson, K. A. (2007). Conservation planning in a changing world. *Trends Ecol. Evol.* 22, 583–592. doi: 10.1016/j.tree.2007.10.001

Qi, Y. C., Dong, Y. S., Jin, Z., Peng, Q., Xiao, S. S., and He, Y. T. (2010). Spatial heterogeneity of soil nutrients and respiration in the desertified grasslands of inner Mongolia, China. *Pedosphere* 20, 655–665. doi: 10.1016/S1002-0160(10)60055-0

Raich, J. W., and Tufekciogul, A. (2000). Vegetation and soil respiration: correlations and controls. *Biogeochemistry* 48, 71–90. doi: 10.1023/A:1006112000616

Reichstein, M., Rey, A., Freibauer, A., Tenhunen, J., Valentini, R., Banza, J., et al. (2003). Modeling temporal and large-scale spatial variability of soil respiration from soil water availability, temperature and vegetation productivity indices. *Glob. Biogeochem. Cycles* 17, 15-1–15-15. doi: 10.1029/2003GB002035

Reside, A. E., Beher, J., Cosgrove, A. J., Evans, M. C., Seabrook, L., Silcock, J. L., et al. (2017). Ecological consequences of land clearing and policy reform in Queensland. *Pac. Conserv. Biol.* 23:219. doi: 10.1071/PC17001

Rodeghiero, M., and Cescatti, A. (2008). Spatial variability and optimal sampling strategy of soil respiration. *For. Ecol. Manag.* 255, 106–112. doi: 10.1016/j.foreco.2007.08.025

Rosseel, Y. (2012). Lavaan: An R package for structural equation modeling. *J. Stat. Softw.* 48, 1–36. doi: 10.18637/jss.v048.i02

RStudio Team (2023). RStudio: integrated development for R. RStudio, PBC, Boston, MA. Available at: http://www.rstudio.com/]

Schaufler, G., Kitzler, B., Schindlbacher, A., Skiba, U., Sutton, M. A., and Zechmeister-Boltenstern, S. (2010). Greenhouse gas emissions from European soils under different land use: effects of soil moisture and temperature. *Eur. J. Soil Sci.* 61, 683–696. doi: 10.1111/j.1365-2389.2010.01277.x

Schlesinger, W. H., and Andrews, J. A. (2000). Soil respiration and the global carbon cycle. *Biogeochemistry* 48, 7–20. doi: 10.1023/A:1006247623877

Shi, B., Hu, G., Henry, H. A. L., Stover, H. J., Sun, W., Xu, W., et al. (2020). Temporal changes in the spatial variability of soil respiration in a meadow steppe: the role of abiotic and biotic factors. *Agric. For. Meteorol.* 287:107958. doi: 10.1016/j.agrformet.2020.107958

Shi, B., Xu, W., Zhu, Y., Wang, C., Loik, M. E., and Sun, W. (2019). Heterogeneity of grassland soil respiration: antagonistic effects of grazing and nitrogen addition. *Agric. For. Meteorol.* 268, 215–223. doi: 10.1016/j.agrformet.2019.01.028

Sinsabaugh, R. L., Hill, B. H., and Follstad Shah, J. J. (2009). Ecoenzymatic stoichiometry of microbial organic nutrient acquisition in soil and sediment. *Nature* 462, 795–798. doi: 10.1038/nature08632

Streb, P., and Cornic, G. (2012). "Photosynthesis and antioxidative protection in alpine herbs" in *Plants in alpine regions*. ed. C. Lütz (Vienna: Springer Vienna), 75–97.

Subke, J. A., Inglima, I., and Francesca Cotrufo, M. (2006). Trends and methodological impacts in soil CO_2 efflux partitioning: a metaanalytical review. *Glob. Change Biol.* 12, 921–943. doi: 10.1111/j.1365-2486.2006.01117.x

Sushko, S. V., Ananyeva, N. D., Ivashchenko, K. V., and Kudeyarov, V. N. (2019). Soil CO_2 emission, microbial biomass, and basal respiration of Chernozems under different land uses. *Eurasian Soil Sci.* 52, 1091–1100. doi: 10.1134/S1064229319090096

Sushko, S., Ananyeva, N., Ivashchenko, K., Vasenev, V., and Kudeyarov, V. (2019). Soil CO_2 emission, microbial biomass, and microbial respiration of woody and grassy areas in Moscow (Russia). *J. Soils Sediments* 19, 3217–3225. doi: 10.1007/s11368-018-2151-8

Wang, B., An, S., Liang, C., Liu, Y., and Kuzyakov, Y. (2021). Microbial necromass as the source of soil organic carbon in global ecosystems. *Soil Biol. Biochem.* 162:108422. doi: 10.1016/j.soilbio.2021.108422

Wiaux, F., Vanclooster, M., and Van Oost, K. (2015). Vertical partitioning and controlling factors of gradient-based soil carbon dioxide fluxes in two contrasted soil profiles along a loamy hillslope. *Biogeosciences* 12, 4637–4649. doi: 10.5194/bg-12-4637-2015

Wickham, H. (2016). *Ggplot2: Elegant graphics for data analysis*. *2nd ed*. Cham: Springer International Publishing

Xu, M., and Shang, H. (2016). Contribution of soil respiration to the global carbon equation. *J. Plant Physiol.* 203, 16–28. doi: 10.1016/j.jplph.2016.08.007

frontiers | Frontiers in Microbiology

TYPE Original Research
PUBLISHED 07 July 2023
DOI 10.3389/fmicb.2023.1173748

OPEN ACCESS

EDITED BY
Ye Deng,
Chinese Academy of Sciences (CAS), China

REVIEWED BY
Zheng Gao,
Shandong Agricultural University, China
Ziyan Wei,
Chinese Academy of Sciences (CAS), China

*CORRESPONDENCE
Yongjun Liu
✉ Vincentliu2020@163.com
Zhenghua Liu
✉ liuzhenghua2017csu@163.com
Wenqiao Deng
✉ 23738320@qq.com

RECEIVED 25 February 2023
ACCEPTED 22 May 2023
PUBLISHED 07 July 2023

CITATION
Li L, Liu Y, Xiao Q, Xiao Z, Meng D, Yang Z, Deng W, Yin H and Liu Z (2023) Dissecting the HGT network of carbon metabolic genes in soil-borne microbiota.
Front. Microbiol. 14:1173748.
doi: 10.3389/fmicb.2023.1173748

Dissecting the HGT network of carbon metabolic genes in soil-borne microbiota

Liangzhi Li[1,2], Yongjun Liu[3]*, Qinzhi Xiao[4], Zhipeng Xiao[5], Delong Meng[1,2], Zhaoyue Yang[1,2], Wenqiao Deng[6]*, Huaqun Yin[1,2] and Zhenghua Liu[1,2]*

[1]School of Minerals Processing and Bioengineering, Central South University, Changsha, China, [2]Key Laboratory of Biometallurgy of Ministry of Education, Central South University, Changsha, China, [3]Hunan Tobacco Science Institute, Changsha, China, [4]Yongzhou Tobacco Company of Hunan Province, Yongzhou, China, [5]Hengyang Tobacco Company of Hunan Province, Hengyang, China, [6]Changsha Institute of Agricultural Science, Changsha, China

The microbiota inhabiting soil plays a significant role in essential life-supporting element cycles. Here, we investigated the occurrence of horizontal gene transfer (HGT) and established the HGT network of carbon metabolic genes in 764 soil-borne microbiota genomes. Our study sheds light on the crucial role of HGT components in microbiological diversification that could have far-reaching implications in understanding how these microbial communities adapt to changing environments, ultimately impacting agricultural practices. In the overall HGT network of carbon metabolic genes in soil-borne microbiota, a total of 6,770 nodes and 3,812 edges are present. Among these nodes, phyla Proteobacteria, Actinobacteriota, Bacteroidota, and Firmicutes are predominant. Regarding specific classes, Actinobacteria, Gammaproteobacteria, Alphaproteobacteria, Bacteroidia, Actinomycetia, Betaproteobacteria, and Clostridia are dominant. The Kyoto Encyclopedia of Genes and Genomes (KEGG) functional assignments of glycosyltransferase (18.5%), glycolysis/gluconeogenesis (8.8%), carbohydrate-related transporter (7.9%), fatty acid biosynthesis (6.5%), benzoate degradation (3.1%) and butanoate metabolism (3.0%) are primarily identified. Glycosyltransferase involved in cell wall biosynthesis, glycosylation, and primary/secondary metabolism (with 363 HGT entries), ranks first overwhelmingly in the list of most frequently identified carbon metabolic HGT enzymes, followed by pimeloyl-ACP methyl ester carboxylesterase, alcohol dehydrogenase, and 3-oxoacyl-ACP reductase. Such HGT events mainly occur in the peripheral functions of the carbon metabolic pathway instead of the core section. The inter-microbe HGT genetic traits in soil-borne microbiota genetic sequences that we recognized, as well as their involvement in the metabolism and regulation processes of carbon organic, suggest a pervasive and substantial effect of HGT on the evolution of microbes.

KEYWORDS

soil, microbiota, horizontal gene transfer, network, carbon metabolic gene

1. Introduction

Microorganisms are the foundation of the Earth's biosphere and play an integral and unique role in various ecological processes and functions, where they interact to form complex functional networks (Zhou et al., 2010). Soil is an important component of the global carbon cycle and is critical to climate change mitigation. Almost all life on Earth cannot leave the living soils, which emphasizes the significance of soil-borne microbiota for essential life-supporting processes (e.g., carbon and nitrogen cycling). The soil organic carbon (SOC) reservoir (about 1,500 Gt) is supposed to be greater than the sum of the carbon stocks in the air and global flora (about 560 Gt) (van Elsas, 2019; Jassey et al., 2022). Microorganisms have much higher growth rates and carbon turnover rates than plants. The size of the soil organic carbon pool depends to a large extent on microorganisms, as their growth and activity balance the accumulation of organic carbon and its release through the decomposition of plant die-offs. Soil-borne microbes control the kinetics of soil carbon transformation by converting carbon from plants, incorporating carbon resources to increase biomass, and breaking down terrestrial organic compounds. For instance, strong biological methane-oxidizing activities in agricultural soils can lead to the emissions of biogenic CO_2 linked to CH_4 oxidation by a large biodiversity of methanotrophs (Cappelletti et al., 2016). Globally, soil algae absorb about 3.6 Pg of carbon per year, which is 6.4% of annual terrestrial net primary productivity (NPP) and equivalent to 31% of global anthropogenic carbon emissions (Jassey et al., 2022). Soil-borne microflora is not only dynamic temporally but also varied geographically. As a result, fluctuations in the activities and quantity of the communities that constitute such soil-borne microflora are frequently seen (Fierer, 2017). The heterogeneity in soil-borne microbiota composition is primarily caused by the spatial heterogeneity of amounts and concentrations of, for example, nutrition, mineral resources, pH, and moisture in the soil mass (Fierer, 2017; van Elsas, 2019), as well as shaped by genetic recombination and gene-specific selection processes (Crits-Christoph et al., 2020). Besides, the carbon resource abundance and diversity in soil have been proven to correlate the ecological certainty during the bio-control of microbe-induced plant disease (Zhou et al., 2023).

Horizontal gene transfer (HGT), or the interchange of genetic material across phylogenetic clades, is thought to be an efficient strategy for dispersing reproductive fitness for prokaryotic and eukaryotic cells (Huang, 2013; Daubin and Szöllősi, 2016; Li et al., 2022). Employing transmitting mobile genetic elements (MGEs) like plasmids, viruses, transposons, and gene transfer agents (GTA, tailed phage-like entities capable of packing and transferring random pieces of the host genome) as well as by direct absorption and assimilation of naked DNA by homologous or unauthorized recombination, new genes are transferred through HGT (Thomas and Nielsen, 2005; Lang and Beatty, 2007). As a result, the origins of specific genes within a particular species can vary, and patterns of gene exchange between near and remotely affiliated lineages can be seen on various genomes (Gogarten et al., 2002; Koonin, 2005; Kunin et al., 2005). HGT is commonly described based on contradicting phylogenetic trees upon genomic comparison (Delsuc et al., 2005; Li et al., 2019). In recent decades, the evolution and HGT processes of genetic traits have been investigated in a variety of ecosystems, where multiple factors (e.g., environmental conditions, ancestral genome sizes) might have influenced the frequency of HGT during evolution (Huang, 2013; Daubin and Szöllősi, 2016; Li et al., 2022). Stable HGT flux induced under selection was also suggested to enhance microbial interplay's structural stability and thereby maintain microbial communities' equilibrium (Fan et al., 2018). For instance, it was reported that 9.6% of the genes within a prokaryotic genome were recently acquired on average (Kloesges et al., 2011), while in *E. coli* 18% of genes were recently acquired *via* HGT (Lawrence and Ochman, 2002), and in Rickettsiales 25% of core genes were recently transferred (Hernández-López et al., 2013).

Even though the terrestrial area is a continually fluctuating and difficult place (Fierer, 2017), factors like limited nutritional and ion intensities that endorse competency, clay deposits that sustain the perseverance of bacteriophages and naked DNA, and the capacity of subsoil microbes to aggregate for genetic exchange suggest that HGT processes could be performing in this globalized context. Consistently, the transmission of antibiotic-resistance genes in the soil *via* MGEs (e.g., bacteriophage) has been highlighted as a public concern (Gallo et al., 2019; Zhang et al., 2022). Besides, soil is stratified geographically and varied physiologically and biologically on various dimensions, which offers a unique habitat for microbiota of diverse background. Many agronomic factors, such as pH, saltiness, warmth, and humidity, influence the organization of the microbiota inside the complicated soil-borne biomass (Frindte et al., 2019). The microscopic society's shape and function in soils could also be influenced by temporal changes such as meteorological conditions, rhizosphere exudation, as well as other periodical supplies of plant organic matter (Zheng et al., 2019; Chernov and Zhelezova, 2020). In natural soil settings, the first investigative research on HGT among microorganisms was conducted in the 1970s (Weinberg and Stotzky, 1972; Graham and Istock, 1978). Since then, further investigations have employed fieldwork and microcosm experiments to evaluate ecological HGT (van Elsas et al., 2006). Plant-associated soils and biofilm communities are well-known hotspots for HGT due to the great genetic variety on such a restricted geographical level (Fan et al., 2018). It was found that the genetic factors in HGT are more abundant in the rhizosphere than in bulk soil, therefore HGT may aid in the development of rhizosphere competence (Vieira et al., 2020). Previous bipartite network analyses have provided evidence of genetic exchange, plasmid fusion and fission, exogenetic plasmid transfer, and environmental adaptation of the soil bacteria such as *Rhizobium* (Corel et al., 2018; Li L. et al., 2020; Li X. et al., 2020). In addition, plasmid transmission from transplanted *P. fluorescens* to native gram-negative rhizobacteria in soil has been proven to happen in natural settings (Balthazar et al., 2021).

Many terrestrial subterranean microbes have also been found to contain MGEs, and some of them have already shown conjugative activity in a lab environment or even in bulk soil. Solitary (Feng et al., 2007) or multiple (Brockman et al., 1989) plasmids could be present in subterranean isolates, with big plasmids that are more apt to own recombinant functionality seeming to predominate (Fredrickson et al., 1988). Microorganisms buried deeper underground have been shown to harbor extremely large (>150 kb) conjugative plasmids at a higher rate than microorganisms from shallower subsurface soils (Ogunseitan et al., 1987; Fredrickson et al., 1988). Degradative genetic determinants are commonly found in subsurface large plasmids, which significantly increase the host's metabolism adaptability (Romine et al., 1999; Basta et al., 2004). Elements similar to recombinases are also present in several accessible plasmids, implying

the possibility of incorporation and excision from the soil microbial genome (Romine et al., 1999). Among the sequenced soil subsoil genomes, *G. thermodenitrificans* was discovered to match 11 and 3% of its genetic makeup with *Bacillus* sp. and other Firmicutes, respectively. Around 2.7% of the genes in *G. thermodenitrificans* NG80-2 exclusively occur in distant relatives and may have undergone HGT. This includes two groups of proteins associated with nitrogen use that seem to have originated separately. The addition of such genes and the catabolic plasmid pLW1071 has significantly improved the metabolic adaptability in nutrient-poor conditions (Feng et al., 2007). Furthermore, the introduction of MGEs into synthesized microbial communities (SynComs) was considered an effective way for manipulating the microbial community for applicable purposes (e.g., carbon storage) (Song et al., 2014; Tsoi et al., 2019; de Lorenzo, 2022).

Yet, unlike simple bacterial mixes in a lab, the complexities of HGT mechanisms in wild areas, including the heavily heterogeneous populations, still need to be fully deciphered. *In situ* critical cellular events, additional chemical triggers for genetic exchange or absorption, and natural factors like cell-MGE interactions are examples of the complexities. In addition, there needs to be more focus on the environmental implications, such as how these HGT activities affect microbial communities' capacity to adapt to wild areas, and how these HGT mechanisms reflect the features of the particular ecosystem. Though there is a growing interest in elucidating the underlying microbial mechanisms driving soil carbon transformation, stabilization, and release processes, many unknowns remain. Nonetheless, many earlier studies mainly concentrated on HGT episodes of particular lineages and on significant issues such as adaption-associated processes (Li et al., 2019; Li L. et al., 2020; Li X. et al., 2020; Li et al., 2021). Regardless of these efforts, there is so much to be learned in a holistic mode about the quantity and effects of HGT-driven genetic makeup in soil-borne microbiota that can confer a variety of carbon assimilation and dissimilation functions (e.g., central carbon cycles, fatty acid biosynthesis). This poses significant challenges to understanding gene flow in terrestrial microbial communities. As a result, it remains to be seen whether there are inter-microbe HGT(s) that have promoted the development of soil-borne microbiota in a variety of conditions. If these HGT markers exist, how do they work to counteract environmental stressors, and how widely disseminated are these markers throughout the genetic material of soil-borne microbiota?

A variety of natural systems, including protein expression (Alon, 2007), biochemical processes (Pál et al., 2005), biomolecule interplay (Jeong et al., 2001), contradicting evolutionary indications (Huson and Bryant, 2006), and ecosystem dynamics (Rezende et al., 2007), are being modeled using network infrastructure (Proulx et al., 2005). In theory, the network is capable of better displaying the patterns of microbial genomic evolution (Doolittle and Bapteste, 2007). HGT networks are a distinctive form of sharing gene networks. They are intended to investigate trends in genetic dispersion brought on by HGT throughout ecological evolution.

Under this context, we performed BLASTP-driven screenings and HGT network constructions to discover and investigate potential inter-microbe HGT genes linked to carbon metabolism throughout genomic sequences of all accessible strains isolated from soils, followed by network constructions. Our results suggested that the HGT episodes may significantly contribute to genetic imports that contribute to the soil-borne microbiota's increased carbon metabolic versatility and adaptivity. Our knowledge of microbial interplay and the adaptable development of microbes to deal with various situations have therefore been enhanced as a result of this work. However, further experimental work is still necessary to evaluate the occurrence of HGT in the vast and unexplored environment of the terrestrial subsurface.

2. Results

2.1. Overall statues

We first queried and retrieved all the items in the public database (Genbank/IMG) with the keyword "soil" within the "biosample" or "habitat" regions. We then chose and downloaded from the public database (Genbank/IMG) the out-coming high-quality genomes of soil microbial isolates ($n = 764$, see Supplementary Table S1 for details at https://doi.org/10.6084/m9.figshare.22154828.v1) for downstream analyses. Putative microbial horizontally transferred genes (HTGs) in these genomes were identified employing the BLASTP-based IMGAP pipeline under default mode (Markowitz et al., 2010), which resulted in a total of 37,481 HTG entries, followed by manual pickup of HTGs that are related to carbon metabolism. These processes eventually produce a total of 4,554 HTG entries related to carbon metabolism, as listed in Supplementary Table S2 at https://doi.org/10.6084/m9.figshare.22154828.v1.

The significance of HGT to biological diversification could be better understood through a network study of gene patterns amongst genomes. A directed phylogenomic network can be built using HGT inference techniques that consider the provider and receptor of the lateral gene delivery event (Popa et al., 2011). Similar to the methods used in previous work (Beiko et al., 2005), we established the phylogenomic HGT networks of carbon metabolic genes in soil-borne microbiota using HGT occurrences predicted to examine the HGT component within microbiological diversification (Figure 1). A baseline species (tested genomes) evolutionary tree's exterior and internal nodes make up the HGT network's vertex. Between the nodes, edges in the network refer to alleged gene transfer occurrences. If a gene relative is transferred across the nodes through a suspected HGT episode, these nodes are interconnected in the HGT networks. The HGT network's edge weight is correlated with the amount of horizontally shared genes. Clusters are formed when specific subgroups of organisms have stronger connections among themselves than with other factions in the networks (Guimerà and Nunes Amaral, 2005; Gallos et al., 2007).

In the overall HGT network of carbon metabolic genes in soil-borne microbiota, a total of 6,770 nodes and 3,812 edges are present (Figure 1). Among the nodes, phyla Proteobacteria (34.65%), Actinobacteriota (26.68%), Bacteroidota (9.28%), and Firmicutes (7.89%) are predominant, followed by Cyanobacteria (1.54%) and Ascomycota (1.30%). Regarding specific classes, Actinobacteria (26.26%), Gammaproteobacteria (16.1%), Alphaproteobacteria (14.15%), Bacteroidia (7.42%), Actinomycetia (6%), Betaproteobacteria (4.08%), Clostridia (3.31%), and Bacili (3.25%) are dominant in the overall HGT network of carbon metabolic genes. The average path length (the average of the shortest route between any two nodes in the network) of the total HGT network is 1.55, indicating

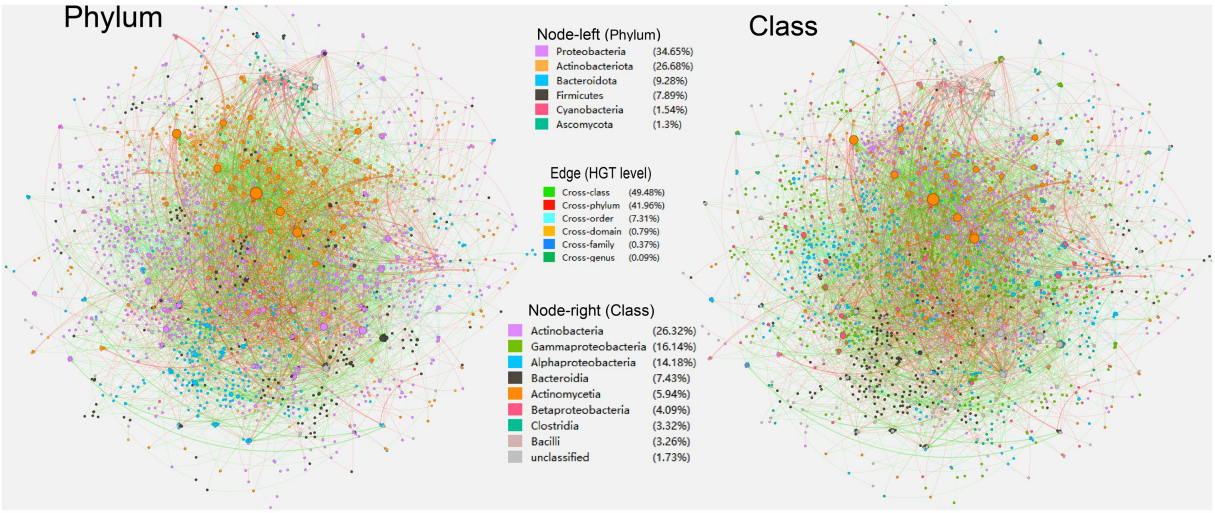

FIGURE 1
An overall directed horizontal gene transfer (HGT) network of carbon metabolic genes harbored by the soil-borne microbiota. Nodes represent genomes of species. The colors are marked according to the node's taxonomy (left, phylum; right, class). The edges represent HGT events and are directed from the donor to the recipient.

that the related carbon metabolic genes could be easily and rapidly transported through tested soil-borne microbiota. The HGT network's thickest (weight > = 5) edges are mainly formed by cross-domain HGT events from archaeal phylum Haloarchaea to Bacteria (26/36 entries, 74.3%), with HGT from *Methanosarcina acetivorans* C2A (Haloarchaea) to *Streptomyces yangpuensis* fd2-tb (Actinobacteriota) having the highest HGT frequency ($n = 14$) (see Supplementary Table S3 at https://doi.org/10.6084/m9.figshare.22154828.v1). The chimeric nature and high externalization rate (especially on carbohydrate biosynthesis genes) of Haloarchaea have been highlighted previously (Galagan et al., 2002; Nelson-Sathi et al., 2012; Garushyants et al., 2015).

In Kyoto Encyclopedia of Genes and Genomes (KEGG) functional assignments, glycosyltransferases (18.5%), glycolysis/gluconeogenesis (8.8%), carbohydrate-related transporters (7.9%), fatty acid biosynthesis (6.5%), benzoate degradation (3.1%), and butanoate metabolism (3.0%) are most frequently identified (Figure 2). These results suggest that soil-borne microbiota is involved in a range of carbon metabolic processes, particularly those related to the breakdown and transportation of carbohydrates and fatty acids. This may have important implications for soil health and ecosystem function.

We then used two classical network centralities, degree and betweenness, to examine what taxonomic groups are holding and shaping the HGT network (see Supplementary Tables S4, S5 at https://doi.org/10.6084/m9.figshare.22154828.v1). The most commonly used centrality measurement, degree, counts the edges that link a specific node. In a directed graph, the arrows are directional, pointing from one node (HGT donor) to another (HGT acceptor), so the number of arrows pointing to each node is its entry degree. In contrast, the number of arrows pointing away from this node is its outgoing degree. Of the top 30 nodes having the highest degree values (>25), class Actinomycetia occupies the most (43.2%) of these nodes (see Supplementary Table S4 at https://doi.org/10.6084/m9.figshare.22154828.v1), followed by classes Deltaproteobacteria (13.3%) and Betaproteobacteria (13.3%). In comparison, most other nodes (92.5%) in the overall HGT network of carbon metabolic genes in soil-borne microbiota display a degree value <5. In particular, the highest degree values in correspondent classes were seen in the genomes of *Kribbella soli* VKM Ac-2,540 (98, Actinomycetia), *Anaeromyxobacter* sp. Red232 (55, Deltaproteobacteria), *Paenibacillus piri* MS74 (41, Bacilli), *Pseudoduganella violaceinigra* DSM 15887(36, Betaproteobacteria), and *Pyrinomonas methylaliphatogenes* K22 (35, Blastocatellia).

Another centrality measurement, betweenness, measures how frequently a specific node is located on the shortest path possible between any pair of nodes within the network. Nodes with large betweenness centralities act as essential reservoirs or communicators for the common-good genetic codes. Of the top 30 nodes having the highest betweenness centrality values (>20) in the overall HGT network of carbon metabolic genes in soil-borne microbiota (see Supplementary Table S5 at https://doi.org/10.6084/m9.figshare.22154828.v1), class Actinomycetia also occupies most (60.0%) of these nodes, followed by class Deltaproteobacteria (10.0%). Primarily exhibiting the highest betweenness centrality values in correspondent classes are genomes of *Jiangella anatolica* GTF31 (558, Actinomycetia), *Pyrinomonas methylaliphatogenes* K22 (195.5, Blastocatellia), *Saccharicrinis fermentans* DSM 9555 (168, Bacteroidia), *Methylovulum miyakonense* HT12 (89, Gammaproteobacteria), and *Nitrosospira multiformis* ATCC 25196 (60.5, Betaproteobacteria). In comparison, most other nodes (98.2%) in the overall HGT network of carbon metabolic genes in soil-borne microbiota display a betweenness centrality value <5. On the other hand, nodes that display lower betweenness centralities either occupy peripheral positions in the network or form their linked constituents.

We further investigated the network's community composition by segmenting it into sub-network according to the major phyla present in the overall HGT network (Figure 3). The sub-networks were created by extracting corresponding taxonomic (e.g., Proteobacteria) nodes acting as HGT donors and acceptors, respectively, as well as extracting their direct edges (Figure 3A). The donor and acceptor sub-networks of the same phyla generally exhibited similar network properties in

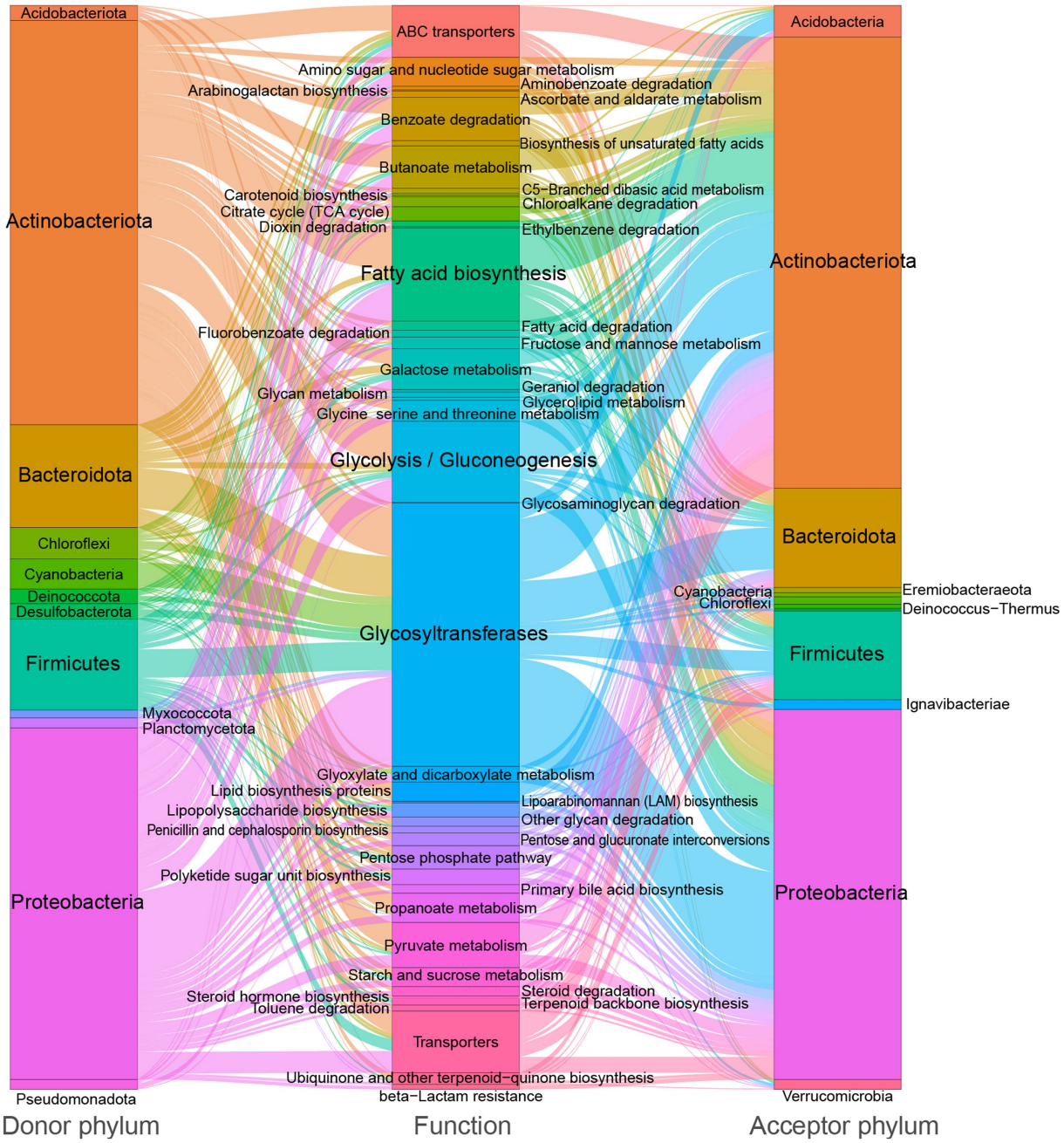

FIGURE 2
Sankey diagram showing the distribution of donor taxa, recipient taxa, and function categories of carbon metabolic genes within the soil-borne microbiota HGT network, with edge thickness and proportion indicating the relative frequency of transfer events.

comparison (Table 1). The same possesses for sub-network construction were applied to nodes of phyla Actinobacteria and Bacteroidota (Figures 3B,C).

In the sub-network that Proteobacteria members act as HGT donors (Figure 3A, left), Actinomycetia (4.51%) and Bacili (1.13%) are the most frequently observed classes outside the phyla Proteobacteria, indicating that classes Actinomycetia and Bacili are the major cross-phylum recipients of the genetic goods carried by Proteobacteria; whereas in the sub-network where Proteobacteria acting as HGT acceptor (Figure 3A, right), Actinobacteria (7.39%) and Bacteroidia (3.5%) are the most frequently observed classes outside the phyla Proteobacteria, suggesting that classes Actinobacteria and Bacteroidia are major cross-phylum donors of carbon metabolic genes to Proteobacteria.

Secondly, in the sub-network that Actinobacteriota members act as HGT donors (Figure 3B, left), Betaproteobacteria (1.61%), Deltaproteobacteria (1.44%), and Alphaproteobacteria (1.02%) the most frequently observed classes outside the phyla Actinobacteriota, indicating that these classes are the primary cross-phylum recipients of the genetic goods carried by Actinobacteriota; whereas in the sub-network where Actinobacteriota acting as HGT acceptor (Figure 3B, right), Alphaproteobacteria (7.16%), superior to

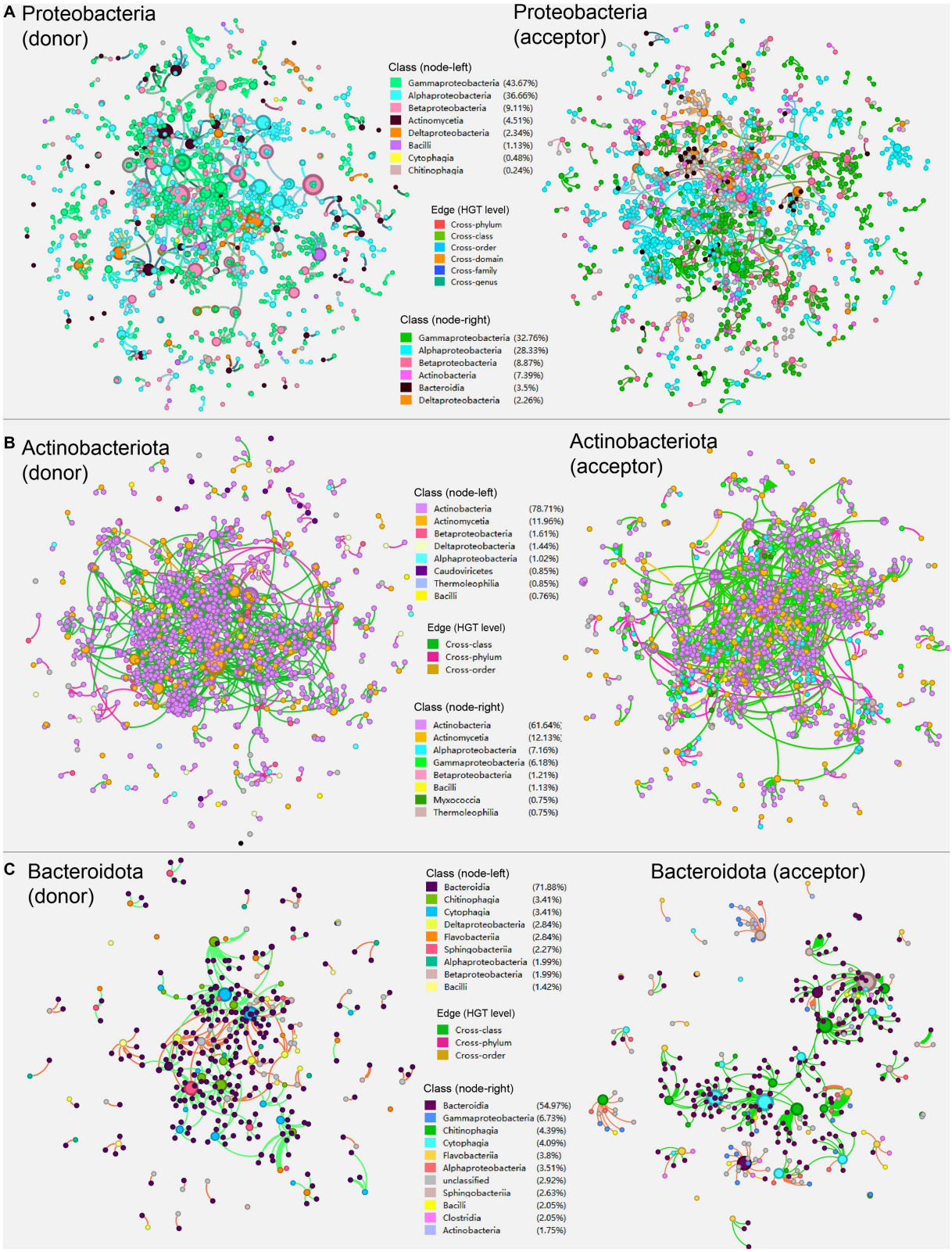

FIGURE 3
The sub-networks created by extracting corresponding taxonomic (e.g., Proteobacteria) nodes acting as HGT donors and acceptors, respectively, as well as extracting their direct edges according to the major phyla present in the overall HGT network: **(A)** Proteobacteria; **(B)** Actinobacteriota; **(C)** Bacteroidota. Nodes represent genomes of species. The edges represent HGT events and are directed from the donor to the recipient. The colors are marked according to the node's taxonomy.

10.3389/fmicb.2023.1173748

TABLE 1 Network properties of the overall and sub-networks of carbon metabolic HGT detected in soil-borne microbiota.

HGT Network	Node number	Edge number	Average degree	Average weighted degree	average clustering coefficient	Diameter	Connected components	Modularity	Average path length	Average eigenvector centrality
Overall	6,770	3,812	1.126	1.343	0.001	5	143	0.863	1.55	0.136
Proteobacteria (donor)	1,241	1,173	0.945	1.041	0.001	3	123	0.922	1.106	0.08096
Proteobacteria (acceptor)	1,286	1,261	0.981	1.083	0.001	3	86	0.915	1.144	0.0653
Actinobacteria (donor)	1,179	1,325	1.124	1.38	0.001	5	63	0.828	1.73	0.052857
Actinobacteria (acceptor)	1,327	1,499	1.13	1.381	0.001	5	40	0.845	1.761	0.0604
Bacteroidota (donor)	353	346	0.98	1.159	0.0001	2	36	0.847	1.042	0.0261
Bacteroidota (acceptor)	342	330	0.965	1.108	0.0001	2	23	0.888	1.057	0.02255

Gammaproteobacteria (6.18%), and Betaproteobacteria (1.21%), stands for the most frequently observed classes outside the phyla Actinobacteriota, which indicates that classes from Proteobacteria like Alphaproteobacteria are major cross-phylum donors of carbon metabolic genes to Actinobacteriota.

Lastly, in the sub-network where Bacteroidota members act as HGT donors (Figure 3C, left), Deltaproteobacteria (2.84%), Betaproteobacteria (1.99%), and Alphaproteobacteria (1.99%) are the most frequently observed classes outside the phyla Bacteroidota, indicating that these classes are the major cross-phylum recipients of the genetic goods carried by Bacteroidota; whereas in the sub-network where Bacteroidota acting as HGT acceptor (Figure 3C, right), Gammaproteobacteria (6.73%), Alphaproteobacteria (3.51%), and Bacilli (2.5%) are the most frequently observed classes outside the phyla Bacteroidota, suggesting that these classes are major cross-phylum donors of carbon metabolic genes to Bacteroidota.

Network properties such as the node number, edge number, average (weighted) degree, as well as average path length were higher in the "acceptor" network than in the "donor" one in the corresponding networks of Proteobacteria and Actinobacteria, respectively. While the connector component (number of subgraphs in which each pair of nodes is connected) shows the opposite trend (higher in the "acceptor"). Average eigenvector centralities (that measure the transitive influence of nodes) decline from the Proteobacteria network to that of Actinobacteria, and, finally, Bacteroidota. Other network properties like modularity (measuring the structural strength and density of a network community) show only slight variations among groups (Table 1).

2.2. Carbon metabolic functions

We further created sub-networks that extracted HGT events (edges) corresponding to specific carbon metabolic functions (e.g., core carbon metabolic pathway, fatty acid biosynthesis) and nodes acting as HGT donors and acceptors, respectively, as well as extracting their direct edges (Figure 4).

In the sub-network reflecting HGT episodes of core carbon metabolism (700 edges/genes, 882 nodes/genomes), genes attributed to pathways of glycolysis/gluconeogenesis (10.14%), butanoate metabolism (7.29%), pyruvate metabolism (7.29%), and galactose metabolism (7.00%) are predominant. Microbial classes Actinobacteria (27.66%), Gammaproteobacteria (13.83%), and Alphaproteobacteria (12.59%) are mostly seen (Figure 4A).

Alcohol dehydrogenase that metabolizes alcoholic substances (with 230 entries) is dominant in the current sub-network of core carbon metabolism (Figure 4A, marked with red rectangles) and ranks third in the list of most frequently identified carbon-metabolism-related horizontal transferred gene (HTG) from the soil-borne microbiota (see Supplementary Table S2 at https://doi.org/10.6084/m9.figshare.22154828.v1). Alcohol dehydrogenase exhibits a wide range of substrate specificity additionally, oxidizing mainly primary and secondary aliphatic alcohols when utilizingNAD^+ as a co-substrate. It is also able to reduce aldehydes and ketones (Tsigos et al., 1998). Accordingly, HGT of alcohol dehydrogenase genes from prokaryotes and unicellular eukaryotes was also reported previously (Espinosa and Paz-Y-Miño-C, 2012; McCarthy and Fitzpatrick, 2016).

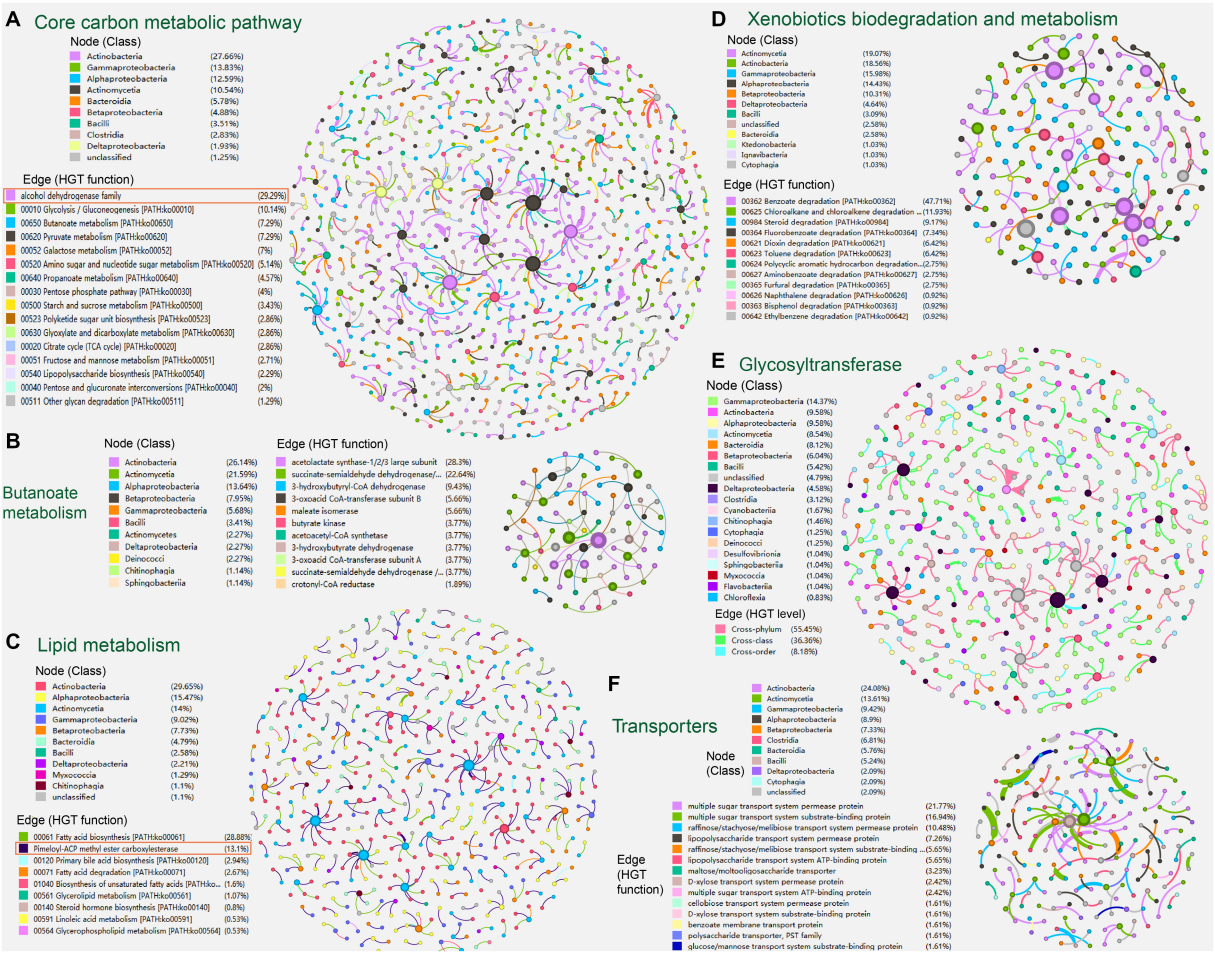

FIGURE 4
The sub-networks created by extracting HGT events (edges) corresponding to specific carbon metabolic functions: **(A)** core carbon metabolism; **(B)** butanoate metabolism; **(C)** lipid metabolism; **(D)** xenobiotics biodegradation and metabolism; **(E)** glycosyltransferase; **(F)** transport protein family. Nodes represent genomes of species. The edges represent HGT events and are directed from the donor to the recipient.

We further extracted the sub-networks of butanoate metabolism (53 edges, 88 nodes). In the sub-network, HGT genes encoding acetolactate synthase (28.3%), succinate-semialdehyde dehydrogenase (22.64%), and 3-hydroxybutyryl-CoA dehydrogenase (9.43%) are predominant. Microbial classes Actinobacteria (26.14%), Actinomycetia (21.59%), and Alphaproteobacteria (13.64%) are mostly seen (Figure 4B).

Likewise, in the sub-network reflecting HGT episodes of lipid metabolism (374 edges, 543 nodes), genes attributed to fatty acid biosynthesis (28.88%), primary bile acid biosynthesis (2.94%), and fatty acid degradation (2.67%) are predominant. Microbial classes Actinobacteria (29.65%), Alphaproteobacteria (15.47%), Actinomycetia (14.0%), Gammaproteobacteria (9.02%), and Betaproteobacteria (7.73%) are mostly seen at the same time (Figure 4C).

Unexpectedly, the pimeloyl-ACP methyl ester carboxylesterase (with 231 entries) is dominant in the current sub-network of lipid metabolism (Figure 4C, marked with red rectangles) and ranks second in the list of most frequently identified carbon-metabolism-related HTGs from the soil-borne microbiota (see Supplementary Table S2 at https://doi.org/10.6084/m9.figshare.22154828.v1). Pimeloyl-ACP methyl ester carboxylesterase catalyzes the hydrolysis of the ester bonds of pimeloyl-ACP esters that allow the synthesis of pimeloyl-ACP *via* the fatty acid synthetic pathway (Lin et al., 2010). Previous reports have also found pimeloyl-ACP methyl ester carboxylesterase located in MGEs, such as the plasmids of the psychrotolerant *Polaromonas* spp. isolated from Arctic and Antarctic glaciers (Ciok et al., 2018). It follows that 3-oxoacyl-ACP reductase (FabG) (with 74 entries) ranks third in the list of most frequently identified carbon-metabolism-related HTG from the soil-borne microbiota (see Supplementary Table S2 at https://doi.org/10.6084/m9.figshare.22154828.v1). FabG is the key enzyme directly responsible for the synthesis of 3-hydroxyacyl-ACPs in the fatty acid synthesis elongation cycle (Yu et al., 2019). As shown in previous studies, FabG has also been frequently observed in mobile genetic elements, like the plasmids of plant growth-promoting bacteria *Azospirillum brasilense* (Yu et al., 2019), and the plastid genomes of *Eustigmatophyte Algae* (Ševcíková et al., 2019).

Similarly, in the sub-network reflecting HGT episodes of xenobiotics biodegradation and metabolism (374 edges, 543 nodes), genes attributed to benzoate degradation (47.71%), chloroalkane/chloroalkene degradation (11.93%), steroid degradation (9.17%), fluorobenzoate degradation (7.34%), dioxin degradation (6.42%), and

toluene degradation (6.42%) are predominant. At the same time, microbial classes Actinomycetia (19.07%), Actinobacteria (18.56%), Gammaproteobacteria (15.98%), Alphaproteobacteria (14.43%), and Betaproteobacteria (10.31%) are mostly observed (Figure 4D).

Regarding specific protein families, glycosyltransferase family (with 363 HGT entries) ranks first overwhelmingly in the list of most frequently identified carbon-metabolism-related HGT enzymes from the soil-borne microbiota (see Supplementary Table S2 at https://doi.org/10.6084/m9.figshare.22154828.v1). While microbial classes Gammaproteobacteria (14.37%), Actinobacteria (9.58%), Alphaproteobacteria (9.58%), Actinomycetia (8.54%), Bacteroidia, (8.12%), Betaproteobacteria (6.04%), and Bacilli (5.42%) are mostly observed to encode glycosyltransferase (Figure 4E). Glycosyltransferase is capable of catalyzing the sequential transfer of glycosyl moieties to the undecaprenyl phosphate carrier lipid during the early steps of polysaccharide synthesis, as well as various other acceptors like proteins, nucleic acid, and secondary metabolites (Garrison-Schilling et al., 2014; Zhang et al., 2020). Glycosyltransferase complexes are known to be involved in cell wall biosynthesis, protein glycosylation, and primary and secondary metabolism in both microbes and plants (Chang et al., 2003; Harholt et al., 2012), whose vital roles in enhancing metabolic flexibility and adaptive advantages might have endorsed the frequent HGT-driven expansions of glycosyltransferase across microbial species. Bacterial and viral glycosyltransferases determine their surface chemistry, influencing the interplay with their hosts (Brew et al., 2010). Our finding is also in line with previous investigations, which have found glycosyltransferase in Rickettsial plasmids (El et al., 2016). Also, the vascular wilt fungus *Verticillium* acquired glycosyltransferase involved in the synthesis of extracellular glucans by HGT from Proteobacteria (Lacroix and Citovsky, 2016). Besides, glycosyltransferase operons acquired *via* HGT were found to modify the O-antigen in *Salmonella enterica* serovar Typhi (Kintz et al., 2017).

Transport protein families (124 edges, 191 nodes) of organic carbon compounds were also visualized by sub-network creation (Figure 4F). In the sub-network, genes attributed to multiple sugar transport system (38.71%), raffinose/stachyose/melibiose transport system (16.13%), and lipopolysaccharide transport system (12.91%) are predominant. At the same time, microbial classes Actinobacteria (24.08%), Actinomycetia (13.61%), Gammaproteobacteria (9.42%), Alphaproteobacteria (8.90%), Betaproteobacteria (7.33%), and Clostridia (6.81%) are mostly observed to encode the transporters.

Also, there are other specific carbon metabolic enzymes enriched in the HGT network (see Supplementary Table S2 at https://doi.org/10.6084/m9.figshare.22154828.v1), such as beta-lactamase family enzymes (159 entries) that degrade multiple metabolites (e.g., antibiotics) for the use of the substrates as nutrients or carbon sources (Graham et al., 2016; Crofts et al., 2018; Maatouk et al., 2022), catechol 2,3-dioxygenase-like lactoylglutathione lyase (54 entries,COG0346) that could enable the degradation of phenol or lignin (Hupert-Kocurek et al., 2012), 2-polyprenyl-6-methoxyphenol hydroxylase (53 entries,COG0654) involved in the aerobic degradation of aromatic compounds (Trias et al., 2017) as well as quinol monooxygenase YgiN (34 entries) related to aerobic redox and physiology. Mapping these HTGs of carbon metabolism onto the correspondent KEGG pathways showed that most HTGs locate on the fringe of the metabolic cycles, and the core carbon metabolic sections rarely transfer (see Supplementary Figures S1–S5 at https://doi.org/10.6084/m9.figshare.22154828.v1).

3. Discussion

An editorial in the journal Science has advocated that more thorough investigations be conducted into the appearance and mechanics of HGT episodes ("Why does lateral transfer occur in so many species and how?") (American Association for the Advancement of Science, 2005). We thoughtfully evaluated that the current study could have provided several suggestions for this subject.

A variety of soil-borne carbon-cycle HGT events of cross-class and even cross-phylum levels were discovered with considerably high transfer frequency (Figure 1). The constructed HGT networks demonstrate that genetic exchange across microbial genera is a significant contributor to microorganisms' biodiversity and adaptivity. The characteristic of a "small-world system" found in previous HGT networks was also observed in our study, which refers to a network that has a small diameter in terms of the number of nodes and a handful of strongly linked nodes that allow for flux to flow across the system (Proulx et al., 2005). A small-world architecture in the HGT network indicates that significantly advantageous genes that arise in any microbe could transcend taxonomic boundaries and stretch another microbe through a limited amount of HGT episodes, where genomes with high betweenness can act as a link between otherwise unconnected parts of the network and transfer genes to numerous other genomes in the ecosystem with a small number of genetic transactions. Similarly, a recent study also found that the HGT rate was increased in organisms with similar ecological distributions (Zhou et al., 2021). Besides, the observed variations in network properties (Table 1) may have multiple implications for HGT events, highlighting the importance of understanding network dynamics in studying HGT events (Kunin et al., 2005; Kloesges et al., 2011; Popa et al., 2011; Li L. et al., 2020; Li X. et al., 2020). For example, a higher number of nodes and edges in the "acceptor" network may indicate a greater potential for gene transfer due to more opportunities for contact between bacteria. Similarly, higher degrees or connector components may create more interconnectedness amongst bacterial populations and facilitate the spread of genetic material. On the other hand, a longer average path length between nodes in a network may reduce the likelihood of gene transfer, as the distance between two bacteria would be higher and the chance of interaction would be lower. Moreover, differences in eigenvector centralities among network groups may illustrate the presence of influential nodes--nodes with high centrality values that may play significant roles in mediating gene transfer. Modularity can also impact the strength and density of community structures within a network, potentially creating barriers or pathways for gene transfer.

The phylum Proteobacteria was the most abundant taxon in soil samples, accounting for an average of 30% of metagenomic sequences (Guo et al., 2018). In keeping with this, our study found that nodes of classes, including Actinobacteria as well as Proteobacteria classes, such as Alphaproteobacteria and Gammaproteobacteria are extensively present in our overall HGT network of carbon metabolism (Figure 1), implying that HGT is widespread during the evolution of species in these classes. However, the sampling density of sequenced microbial genomes might be biased toward Proteobacteria, since the predominance of Proteobacteria in the genome dataset might be responsible for the enormous rate of HGTs within this group. Previous studies have confirmed that Proteobacterial MGEs constitute the major connected component in the virulence network, and extensive gene sharing exists among Actinobacteria and Gammaproteobacteria (Tamminen et al.,

2012; Jiang et al., 2017). Previous studies have also validated experimentally the possibility of MGE-mediated HGT in soil samples, in which plasmids from the donor strains *Psudomonas putida* KT2440, *Escherichia coli* MG1655, and *Kluyvera* sp. can be transferred to a wide range of bacterial phyla from agricultural soils (Klümper et al., 2015), including (α–ε) Proteobacteria, Acidobacteria. Actinobacteria, Bacteroidetes, Firmicutes, Fusobacter, Gemmatimonadetes, Planctomyces, spirochaetes, Candidate division TM7, Verrucomicrobia as well as Eukaryote (Zhang et al., 2015).

Externalized genes carried by MGEs could act as containers for the shared genetic pool (Norman et al., 2009). In our study, uneven functional distributions of the externalized gene are also discovered, in which HTGs are mostly incorporated into the peripheral functions of the carbon metabolic pathway (e.g., nutrient transport and dispensable reaction). In contrast, the core metabolic sections (e.g., intermediate reactions and biomass production) of putative competent significance are mostly evolutionarily unvaried (see Supplementary Figures S1–S5 at https://doi.org/10.6084/m9.figshare.22154828.v1). Similar findings were also reported previously. For example, according to research on the horizontally gained genes within the *E. coli* metabolic pathways (Pál et al., 2005), HGT is more common among proteins engaged in the absorption and consumption of resources than those responsible for the generation of biomass, which suggested that their function influences the HGT probability of metabolic genes in the internal metabolic pathway. This uneven functional distribution could also be explained by the "complexity hypothesis" (Jain et al., 1999; Muller et al., 2018), which proposed that proteins in a complicated system, like ribosomal systems or core metabolic cycles, are specialized to work. Decreased adaptation of the microbial recipients will arise from an HGT incidence that leads to substituting such a gene with a less-suited counterpart. The proportional influence of functionality type and the number of interactive participants on HGT incidence was also investigated, demonstrating that the "complexity theory" still holds up in the genome-scale analyses (Cohen et al., 2011).

On the other hand, soil multi-functionality is affected by the environment and by microbial community composition and diversity (Zheng et al., 2019). Environmental factors in the soil also impact the HGT processes and lead to uneven distribution. The microbial HGT rate in soil relies on environmental stress variables like surface temperatures, pH (Rochelle et al., 1989), soil composition (Richaume et al., 1992), and wetness (Richaume et al., 1989). The gene-sharing network revealed strong correlations between gene connectivity and the trailed soil variables (Zhou et al., 2010). Besides, the persistence and transportation of genetically modified bacteria were impacted by fluidity in subsoil (Trevors et al., 1990). In terms of biological variables, the existence of fungi (Sengeløv et al., 2000), protozoa (Johannes Sørensen et al., 1999), and roundworms (Daane et al., 1996, 1997) could also impact sexual plasmid transmission in soil. Moreover, the generation of leachate and root elongation looked to be the main contributors to the incidence of HGT inside the rhizosphere (Mølbak et al., 2007). Transmission rates were roughly 10 times lower in the bean and cereal rhizospheres than in the control soils (Musovic et al., 2006). Lastly, the other key factor contributing to the rise in local MGE quantities and HGT incidence in this environment is the implementation of manure, pesticides, and antimicrobials to the land (Gotz and Smalla, 1997). Correspondently, various organic degradative genes were found mobilized among soil-borne microbiota *via* HGT in our study (Figure 4D), whose catabolic activities might be further applied for bio-remediation of polluted environments (Top et al., 2002; Nojiri et al., 2004). It is recently confirmed that genes of microalgal origin have conferred *Caenorhabditis elegans* the ability to degrade cyanogenic toxins (Wang et al., 2022). Previous studies also found that functional categories "biosynthesis and degradation of surface polysaccharides and lipopolysaccharides" and "DNA regulation and modification" tend to be enriched in the HGT entries. In consistence, we found glycosyltransferase in our study as the most abundant protein encoded by HTG related to carbon metabolism. The glycosyltransferase family was reported to be involved in the glycosylation and modifications of biomolecules, including the bases in DNA, which might alter the host's gene expression pattern (Iyer et al., 2013). Also, it was reported that glycosyltransferases were significantly enriched in horizontally transferred genes in the human gut, while soil microbiota has similar expansions of the glycosyltransferase repertoires as the gut (Lozupone et al., 2008). Another generally enriched functional category in the HGT profile is metabolite transporter (Cordero and Hogeweg, 2009; Paquola et al., 2018), which is also reflected by our results (Figure 4F).

In conclusion, the inter-microbe HGT genetic traits in soil-borne microbiota genetic sequences that we recognized through our assessments, as well as their involvement in carbon metabolism and resilience to various environmental stressors typically found in territory ecosystems, suggest a pervasive and substantial effect of HGT on the evolvement of microbes. Nevertheless, the information we have provided here is not thorough. The examples of inter-microbe HGT documented so far represent just the tip of a giant biological iceberg. Upcoming studies are expected to offer a more intriguing view of both the scope and the biological importance of HGT in microbes as increasing numbers of genomic data of higher quality are becoming accessible for yet more branches in the tree of life for microbes. Further work will be necessary to evaluate the occurrence of HGT in the vast, heterogeneous, and isolated environment of the terrestrial subsurface and to assess the full impact of gene transfer on terrestrial subsurface microbial evolution.

4. Materials and methods

We first queried and retrieved all the items in the public database (Genbank/IMG) with the keyword "soil" within the "biosample" or "habitat" regions. We have then chosen and downloaded from the public database (Genbank/IMG) the resultant high-quality 764 genomes of soil microbial isolates as listed in Supplementary Table S1 at https://doi.org/10.6084/m9.figshare.22154828.v1 for downstream analyses. The Integrated Microbial Genomes Annotation Pipeline (IMGAP) v.5.0 (Markowitz et al., 2010) under default mode was used to identify horizontally transferred genes (HTGs) in the genetic sequences of individual collected soil-borne microbiota, as conducted in previous studies (Li L. et al., 2020; Li X. et al., 2020; Li et al., 2021, 2022). It used the following criteria to determine which genes inside the trialed genomes were horizontally transferred from remote descendants: genes with the finest BLASTP matches (most significant bit scores) or over 90% of the best hits discovered beyond the phylogenetic clade of the trialed genome (i.e., from remote phylum, class, etc.) and with lower-scoring matches or no hits within the original phylogenetic clade of the trialed genome. The HTG sequences were annotated with the eggnog mapper v.2.0 (Huerta-Cepas et al., 2019). This resulted in a total of 37,481 HTG entries, followed by the pickup of HTGs that are related to carbon metabolism according to the Kyoto Encyclopedia of Genes and Genomes

(KEGG) classification. These processes eventually produce a total of 4,554 HTG entries related to carbon metabolism. We then used the Gephi network visualization package[1] for network visualization and exploration of carbon metabolism HTGs. Fruchterman Reingold and Openord layout approaches were used for network visualization in the Gephi. The graphical user interface of the KEGG pathway map color tool was applied for coloring map objects, including split-coloring and gradation[2].

Data availability statement

The original contributions presented in the study are included in the article/supplementary material, further inquiries can be directed to the corresponding authors.

Author contributions

LL and ZL conceived and designed the research. YL, QX, and ZX provided the computing sources. LL, DM, ZY, and HY analyzed the data. LL wrote the manuscript. All authors contributed to the article and approved the submitted version.

Funding

This research was supported by the key project of Science and Technology of Hunan Branch of China National Tobacco Corporation (CD2022KJ01, 2022431021240240, HN2021KJ05), Natural Science Foundation of Changsha (No. kq2202089), Fundamental Research Funds for the Central Universities of Central South University (No. 2022ZZTS0420), Hunan International Scientific and Technological Cooperation Base of Environmental Microbiome and Application (No. 2018WK4019), and key project of Science and Technology of China National Tobacco Corporation (No. 110202201004) (JY-04).

Acknowledgments

We are grateful for resources from the High-Performance Computing Center of Central South University.

Conflict of interest

YL, QX, and ZX were employed by Zhangjiajie Tobacco Company of Hunan Province.

The remaining authors declare that the research was conducted in the absence of any commercial or financial relationships that could be construed as a potential conflict of interest.

Publisher's note

1 https://gephi.org

2 https://www.kegg.jp/kegg/mapper/color.html

References

Alon, U. (2007). Network motifs: theory and experimental approaches. *Nat. Rev. Genet.* 8, 450–461. doi: 10.1038/nrg2102

American Association for the Advancement of Science (2005). So much more to know. *Science* 309, 78–102. doi: 10.1126/science.309.5731.78b

Balthazar, C., Joly, D. L., and Filion, M. (2021). Exploiting beneficial Pseudomonas spp. for Cannabis production. *Front. Virol.* 12:833172. doi: 10.3389/fmicb.2021.833172

Basta, T., Keck, A., Klein, J., and Stolz, A. (2004). Detection and characterization of conjugative degradative plasmids in xenobiotic-degrading sphingomonas strains. *J. Bacteriol.* 186, 3862–3872. doi: 10.1128/JB.186.12.3862-3872.2004

Beiko, R. G., Harlow, T. J., and Ragan, M. A. (2005). Highways of gene sharing in prokaryotes. *Proc. Natl. Acad. Sci.* 102, 14332–14337. doi: 10.1073/pnas.0504068102

Brew, K., Tumbale, P., and Acharya, K. R. (2010). Family 6 glycosyltransferases in vertebrates and bacteria: inactivation and horizontal gene transfer may enhance mutualism between vertebrates and bacteria. *J. Biol. Chem.* 285, 37121–37127. doi: 10.1074/jbc.R110.176248

Brockman, F. J., Denovan, B. A., Hicks, R. J., and Fredrickson, J. K. (1989). Isolation and characterization of quinoline-degrading bacteria from subsurface sediments. *Appl. Environ. Microbiol.* 55, 1029–1032. doi: 10.1128/aem.55.4.1029-1032.1989

Cappelletti, M., Ghezzi, D., Zannoni, D., Capaccioni, B., and Fedi, S. (2016). Diversity of methane-oxidizing Bacteria in soils from "hot lands of Medolla" (Italy) featured by anomalous high-temperatures and biogenic CO_2 emission. *Microbes Environ.* 31, 369–377. doi: 10.1264/jsme2.ME16087

Chang, R., Yeager, A. R., and Finney, N. S. (2003). Probing the mechanism of a fungal glycosyltransferase essential for cell wall biosynthesis. UDP-chitobiose is not a substrate for chitin synthase. *Org. Biomol. Chem.* 1, 39–41. doi: 10.1039/b208953j

Chernov, T. I., and Zhelezova, A. D. (2020). The dynamics of soil microbial communities on different timescales: a review. *Eurasian Soil Sci.* 53, 643–652. doi: 10.1134/S106422932005004X

Ciok, A., Budzik, K., Zdanowski, M. K., Gawor, J., Grzesiak, J., Decewicz, P., et al. (2018). Plasmids of psychrotolerant *Polaromonas* spp. isolated from arctic and Antarctic glaciers – diversity and role in adaptation to polar environments. *Front. Microbiol.* 9:1285. doi: 10.3389/fmicb.2018.01285

Cohen, O., Gophna, U., and Pupko, T. (2011). The complexity hypothesis revisited: connectivity rather than function constitutes a barrier to horizontal gene transfer. *Mol. Biol. Evol.* 28, 1481–1489. doi: 10.1093/molbev/msq333

Cordero, O. X., and Hogeweg, P. (2009). The impact of long-distance horizontal gene transfer on prokaryotic genome size. *Proc. Natl. Acad. Sci.* 106, 21748–21753. doi: 10.1073/pnas.0907584106

Corel, E., Méheust, R., Watson, A. K., McInerney, J. O., Lopez, P., and Bapteste, E. (2018). Bipartite network analysis of gene sharings in the microbial world. *Mol. Biol. Evol.* 35, 899–913. doi: 10.1093/molbev/msy001

Crits-Christoph, A., Olm, M. R., Diamond, S., Bouma-Gregson, K., and Banfield, J. F. (2020). Soil bacterial populations are shaped by recombination and gene-specific selection across a grassland meadow. *ISME J.* 14, 1834–1846. doi: 10.1038/s41396-020-0655-x

Crofts, T. S., Wang, B., Spivak, A., Gianoulis, T. A., Forsberg, K. J., Gibson, M. K., et al. (2018). Shared strategies for β-lactam catabolism in the soil microbiome. *Nat. Chem. Biol.* 14, 556–564. doi: 10.1038/s41589-018-0052-1

Daane, L. L., Molina, J. A., Berry, E. C., and Sadowsky, M. J. (1996). Influence of earthworm activity on gene transfer from *Pseudomonas fluorescens* to indigenous soil bacteria. *Appl. Environ. Microbiol.* 62, 515–521. doi: 10.1128/aem.62.2.515-521.1996

Daane, L. L., Molina, J., and Sadowsky, M. J. (1997). Plasmid transfer between spatially separated donor and recipient bacteria in earthworm-containing soil microcosms. *Appl. Environ. Microbiol.* 63, 679–686. doi: 10.1128/aem.63.2.679-686.1997

Daubin, V., and Szöllősi, G. J. (2016). Horizontal gene transfer and the history of life. *Cold Spring Harb. Perspect. Biol.* 8:a18036. doi: 10.1101/cshperspect.a018036

de Lorenzo, V. (2022). Environmental Galenics: large-scale fortification of extant microbiomes with engineered bioremediation agents. *Philos. Trans. R. Soc. Lond. Ser. B Biol. Sci.* 377:20210395. doi: 10.1098/rstb.2021.0395

Delsuc, F., Brinkmann, H., and Philippe, H. (2005). Phylogenomics and the reconstruction of the tree of life. *Nat. Rev. Genet.* 6, 361–375. doi: 10.1038/nrg1603

Doolittle, W. F., and Bapteste, E. (2007). Pattern pluralism and the tree of life hypothesis. *Proc. Natl. Acad. Sci. U. S. A.* 104, 2043–2049. doi: 10.1073/pnas.0610699104

El, K. K., Pontarotti, P., Raoult, D., and Fournier, P. E. (2016). Origin and evolution of rickettsial plasmids. *PLoS One* 11:e147492. doi: 10.1371/journal.pone.0147492

Espinosa, A., and Paz-Y-Miño-C, G. (2012). Discrimination, crypticity, and incipient taxa in entamoeba. *J. Eukaryot. Microbiol.* 59, 105–110. doi: 10.1111/j.1550-7408.2011.00606.x

Fan, Y., Xiao, Y., Momeni, B., and Liu, Y. (2018). Horizontal gene transfer can help maintain the equilibrium of microbial communities. *J. Theor. Biol.* 454, 53–59. doi: 10.1016/j.jtbi.2018.05.036

Feng, L., Wang, W., Cheng, J., Ren, Y., Zhao, G., Gao, C., et al. (2007). Genome and proteome of long-chain alkane degrading *Geobacillus thermodenitrificans* NG80-2 isolated from a deep-subsurface oil reservoir. *Proc. Natl. Acad. Sci. U. S. A.* 104, 5602–5607. doi: 10.1073/pnas.0609650104

Fierer, N. (2017). Embracing the unknown: disentangling the complexities of the soil microbiome. *Nat. Rev. Microbiol.* 15, 579–590. doi: 10.1038/nrmicro.2017.87

Fredrickson, J. K., Hicks, R. J., Li, S. W., and Brockman, F. J. (1988). Plasmid incidence in bacteria from deep subsurface sediments. *Appl. Environ. Microbiol.* 54, 2916–2923. doi: 10.1128/aem.54.12.2916-2923.1988

Frindte, K., Pape, R., Werner, K., Löffler, J., and Knief, C. (2019). Temperature and soil moisture control microbial community composition in an arctic–alpine ecosystem along elevational and micro-topographic gradients. *ISME J.* 13, 2031–2043. doi: 10.1038/s41396-019-0409-9

Galagan, J. E., Nusbaum, C., Roy, A., Endrizzi, M. G., Macdonald, P., FitzHugh, W., et al. (2002). The genome of *M. acetivorans* reveals extensive metabolic and physiological diversity. *Genome Res.* 12, 532–542. doi: 10.1101/gr.223902

Gallo, I., Furlan, J., Sanchez, D. G., and Stehling, E. G. (2019). Heavy metal resistance genes and plasmid-mediated quinolone resistance genes in *Arthrobacter* sp. isolated from Brazilian soils. *Antonie Van Leeuwenhoek* 112, 1553–1558. doi: 10.1007/s10482-019-01281-9

Gallos, L. K., Song, C., Havlin, S., and Makse, H. A. (2007). Scaling theory of transport in complex biological networks. *Proc. Natl. Acad. Sci.* 104, 7746–7751. doi: 10.1073/pnas.0700250104

Garrison-Schilling, K. L., Kaluskar, Z. M., Lambert, B., and Pettis, G. S. (2014). Genetic analysis and prevalence studies of the brp exopolysaccharide locus of *Vibrio vulnificus*. *PLoS One* 9:e100890. doi: 10.1371/journal.pone.0100890

Garushyants, S. K., Kazanov, M. D., and Gelfand, M. S. (2015). Horizontal gene transfer and genome evolution in Methanosarcina. *BMC Evol. Biol.* 15:102. doi: 10.1186/s12862-015-0393-2

Gogarten, J. P., Doolittle, W. F., and Lawrence, J. G. (2002). Prokaryotic evolution in light of gene transfer. *Mol. Biol. Evol.* 19, 2226–2238. doi: 10.1093/oxfordjournals.molbev.a004046

Gotz, A., and Smalla, K. (1997). Manure enhances plasmid mobilization and survival of *Pseudomonas putida* introduced into field soil. *Appl. Environ. Microbiol.* 63, 1980–1986. doi: 10.1128/aem.63.5.1980-1986.1997

Graham, J. B., and Istock, C. A. (1978). Genetic exchange in *Bacillus subtilis* in soil. *Mol. Gen. Genet. MGG* 166, 287–290. doi: 10.1007/BF00267620

Graham, D. W., Knapp, C. W., Christensen, B. T., McCluskey, S., and Dolfing, J. (2016). Appearance of β-lactam resistance genes in agricultural soils and clinical isolates over the 20th century. *Sci. Rep.* 6:21550. doi: 10.1038/srep21550

Guimerà, R., and Nunes Amaral, L. A. (2005). Functional cartography of complex metabolic networks. *Nature* 433, 895–900. doi: 10.1038/nature03288

Guo, X., Feng, J., Shi, Z., Zhou, X., Yuan, M., Tao, X., et al. (2018). Climate warming leads to divergent succession of grassland microbial communities. *Nat. Clim. Chang.* 8, 813–818. doi: 10.1038/s41558-018-0254-2

Harholt, J., Sørensen, I., Fangel, J., Roberts, A., Willats, W. G., Scheller, H. V., et al. (2012). The glycosyltransferase repertoire of the spikemoss *Selaginella moellendorffii* and a comparative study of its cell wall. *PLoS One* 7:e35846. doi: 10.1371/journal.pone.0035846

Hernández-López, A., Chabrol, O., Royer-Carenzi, M., Merhej, V., Pontarotti, P., and Raoult, D. (2013). To tree or not to tree? Genome-wide quantification of recombination and reticulate evolution during the diversification of strict intracellular bacteria. *Genome Biol. Evol.* 5, 2305–2317. doi: 10.1093/gbe/evt178

Huang, J. (2013). Horizontal gene transfer in eukaryotes: the weak-link model. *BioEssays* 35, 868–875. doi: 10.1002/bies.201300007

Huerta-Cepas, J., Szklarczyk, D., Heller, D., Hernández-Plaza, A., Forslund, S. K., Cook, H., et al. (2019). EggNOG 5.0: a hierarchical, functionally and phylogenetically annotated orthology resource based on 5090 organisms and 2502 viruses. *Nucleic Acids Res.* 47, D309–D314. doi: 10.1093/nar/gky1085

Hupert-Kocurek, K., Guzik, U., and Wojcieszyńska, D. (2012). Characterization of catechol 2,3-dioxygenase from *Planococcus* sp. strain S5 induced by high phenol concentration. *Acta Biochim. Pol.* 59, 345–351. doi: 10.18388/abp.2012_2119

Huson, D. H., and Bryant, D. (2006). Application of phylogenetic networks in evolutionary studies. *Mol. Biol. Evol.* 23, 254–267. doi: 10.1093/molbev/msj030

Iyer, L. M., Zhang, D., Burroughs, A. M., and Aravind, L. (2013). Computational identification of novel biochemical systems involved in oxidation, glycosylation and other complex modifications of bases in DNA. *Nucleic Acids Res.* 41, 7635–7655. doi: 10.1093/nar/gkt573

Jain, R., Rivera, M. C., and Lake, J. A. (1999). Horizontal gene transfer among genomes: the complexity hypothesis. *Proc. Natl. Acad. Sci. U. S. A.* 96, 3801–3806. doi: 10.1073/pnas.96.7.3801

Jassey, V. E. J., Walcker, R., Kardol, P., Geisen, S., Heger, T., Lamentowicz, M., et al. (2022). Contribution of soil algae to the global carbon cycle. *New Phytol.* 234, 64–76. doi: 10.1111/nph.17950

Jeong, H., Mason, S. P., Barabási, A. L., and Oltvai, Z. N. (2001). Lethality and centrality in protein networks. *Nature* 411, 41–42. doi: 10.1038/35075138

Jiang, X., Ellabaan, M., Charusanti, P., Munck, C., Blin, K., Tong, Y., et al. (2017). Dissemination of antibiotic resistance genes from antibiotic producers to pathogens. *Nat. Commun.* 8:15784. doi: 10.1038/ncomms15784

Johannes Sørensen, S., Schyberg, T., and Rønn, R. (1999). Predation by protozoa on *Escherichia coli* K12 in soil and transfer of resistance plasmid RP4 to indigenous bacteria in soil. *Appl. Soil Ecol.* 11, 79–90. doi: 10.1016/S0929-1393(98)00117-6

Kintz, E., Heiss, C., Black, I., Donohue, N., Brown, N., Davies, M. R., et al. (2017). *Salmonella enterica* Serovar Typhi lipopolysaccharide O-antigen modification impact on serum resistance and antibody recognition. *Infect. Immun.* 85. doi: 10.1128/IAI.01021-16

Kloesges, T., Popa, O., Martin, W., and Dagan, T. (2011). Networks of gene sharing among 329 proteobacterial genomes reveal differences in lateral gene transfer frequency at different phylogenetic depths. *Mol. Biol. Evol.* 28, 1057–1074. doi: 10.1093/molbev/msq297

Klümper, U., Riber, L., Dechesne, A., Sannazzarro, A., Hansen, L. H., Sørensen, S. J., et al. (2015). Broad host range plasmids can invade an unexpectedly diverse fraction of a soil bacterial community. *ISME J.* 9, 934–945. doi: 10.1038/ismej.2014.191

Koonin, E. V. (2005). Orthologs, paralogs, and evolutionary genomics. *Annu. Rev. Genet.* 39, 309–338. doi: 10.1146/annurev.genet.39.073003.114725

Kunin, V., Goldovsky, L., Darzentas, N., and Ouzounis, C. A. (2005). The net of life: reconstructing the microbial phylogenetic network. *Genome Res.* 15, 954–959. doi: 10.1101/gr.3666505

Lacroix, B., and Citovsky, V. (2016). Transfer of DNA from Bacteria to eukaryotes. *MBio* 7. doi: 10.1128/mBio.00863-16

Lang, A. S., and Beatty, J. T. (2007). Importance of widespread gene transfer agent genes in α-proteobacteria. *Trends Microbiol.* 15, 54–62. doi: 10.1016/j.tim.2006.12.001

Lawrence, J. G., and Ochman, H. (2002). Reconciling the many faces of lateral gene transfer. *Trends Microbiol.* 10, 1–4. doi: 10.1016/s0966-842x(01)02282-x

Li, L., Liu, Z., Meng, D., Liu, X., Li, X., Zhang, M., et al. (2019). Comparative genomic analysis reveals the distribution, organization, and evolution of metal resistance genes in the genus acidithiobacillus. *Appl. Environ. Microbiol.* 85, e2118–e2153. doi: 10.1128/AEM.02153-18

Li, L., Liu, Z., Zhang, M., Meng, D., Liu, X., Wang, P., et al. (2020). Insights into the metabolism and evolution of the genus *Acidiphilium*, a typical acidophile in acid mine drainage. *MSystems* 5, e820–e867. doi: 10.1128/mSystems.00867-20

Li, L., Liu, Z., Zhou, Z., Zhang, M., Meng, D., Liu, X., et al. (2021). Comparative genomics provides insights into the genetic diversity and evolution of the DPANN superphylum. *MSystems* 6, e0060221–e0060621. doi: 10.1128/mSystems.00602-21

Li, L., Peng, S., Wang, Z., Zhang, T., Li, H., Xiao, Y., et al. (2022). Genome mining reveals abiotic stress resistance genes in plant genomes acquired from microbes via HGT. *Front. Plant Sci.* 13:1025122. doi: 10.3389/fpls.2022.1025122

Li, X., Wang, H., Tong, W., Feng, L., Wang, L., Rahman, S. U., et al. (2020). Exploring the evolutionary dynamics of Rhizobium plasmids through bipartite network analysis. *Environ. Microbiol.* 22, 934–951. doi: 10.1111/1462-2920.14762

Lin, S., Hanson, R. E., and Cronan, J. E. (2010). Biotin synthesis begins by hijacking the fatty acid synthetic pathway. *Nat. Chem. Biol.* 6, 682–688. doi: 10.1038/nchembio.420

Lozupone, C. A., Hamady, M., Cantarel, B. L., Coutinho, P. M., Henrissat, B., Gordon, J. I., et al. (2008). The convergence of carbohydrate active gene repertoires in human gut microbes. *Proc. Natl. Acad. Sci. U. S. A.* 105, 15076–15081. doi: 10.1073/pnas.0807339105

Maatouk, M., Ibrahim, A., Pinault, L., Armstrong, N., Azza, S., Rolain, J. M., et al. (2022). New beta-lactamases in candidate phyla radiation: owning pleiotropic enzymes

is a smart paradigm for microorganisms with a reduced genome. *Int. J. Mol. Sci.* 23. doi: 10.3390/ijms23105446

Markowitz, V. M., Chen, I. A., Palaniappan, K., Chu, K., Szeto, E., Grechkin, Y., et al. (2010). The integrated microbial genomes system: an expanding comparative analysis resource. *Nucleic Acids Res.* 38, D382–D390. doi: 10.1093/nar/gkp887

McCarthy, C. G., and Fitzpatrick, D. A. (2016). Systematic search for evidence of interdomain horizontal gene transfer from prokaryotes to oomycete lineages. *MSphere* 1. doi: 10.1128/mSphere.00195-16

Mølbak, L., Molin, S., and Kroer, N. (2007). Root growth and exudate production define the frequency of horizontal plasmid transfer in the Rhizosphere. *FEMS Microbiol. Ecol.* 59, 167–176. doi: 10.1111/j.1574-6941.2006.00229.x

Muller, E. E. L., Faust, K., Widder, S., Herold, M., Martínez Arbas, S., and Wilmes, P. (2018). Using metabolic networks to resolve ecological properties of microbiomes. *Curr. Opin. Syst. Biol.* 8, 73–80. doi: 10.1016/j.coisb.2017.12.004

Musovic, S., Oregaard, G., Kroer, N., and Sørensen, S. J. (2006). Cultivation-independent examination of horizontal transfer and host range of an IncP-1 plasmid among gram-positive and gram-negative bacteria indigenous to the barley rhizosphere. *Appl. Environ. Microbiol.* 72, 6687–6692. doi: 10.1128/AEM.00013-06

Nelson-Sathi, S., Dagan, T., Landan, G., Janssen, A., Steel, M., McInerney, J. O., et al. (2012). Acquisition of 1,000 eubacterial genes physiologically transformed a methanogen at the origin of Haloarchaea. *Proc. Natl. Acad. Sci. U. S. A.* 109, 20537–20542. doi: 10.1073/pnas.1209119109

Nojiri, H., Shintani, M., and Omori, T. (2004). Divergence of mobile genetic elements involved in the distribution of xenobiotic-catabolic capacity. *Appl. Microbiol. Biotechnol.* 64, 154–174. doi: 10.1007/s00253-003-1509-y

Norman, A., Hansen, L. H., and Sørensen, S. J. (2009). Conjugative plasmids: vessels of the communal gene pool. *Philos. Trans. R. Soc. B Biol. Sci.* 364, 2275–2289. doi: 10.1098/rstb.2009.0037

Ogunseitan, O. A., Tedford, E. T., Pacia, D., Sirotkin, K. M., and Sayler, G. S. (1987). Distribution of plasmids in groundwater bacteria. *J. Ind. Microbiol.* 1, 311–317. doi: 10.1007/BF01569309

Pál, C., Papp, B., and Lercher, M. J. (2005). Adaptive evolution of bacterial metabolic networks by horizontal gene transfer. *Nat. Genet.* 37, 1372–1375. doi: 10.1038/ng1686

Paquola, A. C. M., Asif, H., Pereira, C. A. D. B., Feltes, B. C., Bonatto, D., Lima, W. C., et al. (2018). Horizontal gene transfer building prokaryote genomes: genes related to exchange between cell and environment are frequently transferred. *J. Mol. Evol.* 86, 190–203. doi: 10.1007/s00239-018-9836-x

Popa, O., Hazkani-Covo, E., Landan, G., Martin, W., and Dagan, T. (2011). Directed networks reveal genomic barriers and DNA repair bypasses to lateral gene transfer among prokaryotes. *Genome Res.* 21, 599–609. doi: 10.1101/gr.115592.110

Proulx, S. R., Promislow, D. E. L., and Phillips, P. C. (2005). Network thinking in ecology and evolution. *Trends Ecol. Evol.* 20, 345–353. doi: 10.1016/j.tree.2005.04.004

Rezende, E. L., Lavabre, J. E., Guimarães, P. R., Jordano, P., and Bascompte, J. (2007). Non-random coextinctions in phylogenetically structured mutualistic networks. *Nature* 448, 925–928. doi: 10.1038/nature05956

Richaume, A., Angle, J. S., and Sadowsky, M. J. (1989). Influence of soil variables on in situ plasmid transfer from *Escherichia coli* to *Rhizobium fredii*. *Appl. Environ. Microbiol.* 55, 1730–1734. doi: 10.1128/aem.55.7.1730-1734.1989

Richaume, A., Smit, E., Faurie, G., and van Elsas, J. D. (1992). Influence of soil type on the transfer of plasmid RP4p from *Pseudomonas fluorescens* to introduced recipient and to indigenous bacteria. *FEMS Microbiol. Lett.* 101, 281–291. doi: 10.1016/0378-1097(92)90825-9

Rochelle, P. A., Fry, J. C., and Day, M. J. (1989). Factors affecting conjugal transfer of plasmids encoding mercury resistance from pure cultures and mixed natural suspensions of epilithic bacteria. *J. Gen. Microbiol.* 135, 409–424. doi: 10.1099/00221287-135-2-409

Romine, M. F., Stillwell, L. C., Wong, K. K., Thurston, S. J., Sisk, E. C., Sensen, C., et al. (1999). Complete sequence of a 184-kilobase catabolic plasmid from *Sphingomonas aromaticivorans* F199. *J. Bacteriol.* 181, 1585–1602. doi: 10.1128/JB.181.5.1585-1602.1999

Sengeløv, G., Kowalchuk, G. A., and Sørensen, S. J. (2000). Influence of fungal-bacterial interactions on bacterial conjugation in the residuesphere. *FEMS Microbiol. Ecol.* 31, 39–45. doi: 10.1016/s0168-6496(99)00079-3

Ševcíková, T., Yurchenko, T., Fawley, K. P., Amaral, R., Strnad, H., Santos, L., et al. (2019). Plastid genomes and proteins illuminate the evolution of eustigmatophyte algae and their bacterial endosymbionts. *Genome Biol. Evol.* 11, 362–379. doi: 10.1093/gbe/evz004

Song, H., Ding, M., Jia, X., Ma, Q., and Yuan, Y. (2014). Synthetic microbial consortia: from systematic analysis to construction and applications. *Chem. Soc. Rev.* 43, 6954–6981. doi: 10.1039/C4CS00114A

Tamminen, M., Virta, M., Fani, R., and Fondi, M. (2012). Large-scale analysis of plasmid relationships through gene-sharing networks. *Mol. Biol. Evol.* 29, 1225–1240. doi: 10.1093/molbev/msr292

Thomas, C. M., and Nielsen, K. M. (2005). Mechanisms of, and barriers to, horizontal gene transfer between bacteria. *Nat. Rev. Microbiol.* 3, 711–721. doi: 10.1038/nrmicro1234

Top, E. M., Springael, D., and Boon, N. (2002). Catabolic mobile genetic elements and their potential use in bioaugmentation of polluted soils and waters. *FEMS Microbiol. Ecol.* 42, 199–208. doi: 10.1111/j.1574-6941.2002.tb01009.x

Trevors, J. T., van Elsas, J. D., van Overbeek, L. S., and Starodub, M. E. (1990). Transport of a genetically engineered *Pseudomonas fluorescens* strain through a soil microcosm. *Appl. Environ. Microbiol.* 56, 401–408. doi: 10.1128/aem.56.2.401-408.1990

Trias, R., Ménez, B., le Campion, P., Zivanovic, Y., Lecourt, L., Lecoeuvre, A., et al. (2017). High reactivity of deep biota under anthropogenic CO(2) injection into basalt. *Nat. Commun.* 8:1063. doi: 10.1038/s41467-017-01288-8

Tsigos, I., Velonia, K., Smonou, I., and Bouriotis, V. (1998). Purification and characterization of an alcohol dehydrogenase from the Antarctic psychrophile *Moraxella* sp. TAE123. *Eur. J. Biochem.* 254, 356–362. doi: 10.1046/j.1432-1327.1998.2540356.x

Tsoi, R., Dai, Z., and You, L. (2019). Emerging strategies for engineering microbial communities. *Biotechnol. Adv.* 37:107372. doi: 10.1016/j.biotechadv.2019.03.011

van Elsas, J. D. T. J. (2019). *Modern soil microbiology*. *3rd* Edn CRC Press.

van Elsas, J. D., Turner, S., and Trevors, J. T. (2006). "Bacterial conjugation in soil" in eds. P. Nannipieri and K. Smalla (Berlin, Heidelberg: Springer Berlin Heidelberg), 331–353.

Vieira, S., Sikorski, J., Dietz, S., Herz, K., Schrumpf, M., Bruelheide, H., et al. (2020). Drivers of the composition of active rhizosphere bacterial communities in temperate grasslands. *ISME J.* 14, 463–475. doi: 10.1038/s41396-019-0543-4

Wang, B., Pandey, T., Long, Y., Delgado-Rodriguez, S. E., Daugherty, M. D., and Ma, D. K. (2022). Co-opted genes of algal origin protect *C. elegans* against cyanogenic toxins. *Curr. Biol.* 32, 4941–4948.e3. doi: 10.1016/j.cub.2022.09.041

Weinberg, S. R., and Stotzky, G. (1972). Conjugation and genetic recombination of *Escherichia coli* in soil. *Soil Biol. Biochem.* 4, 171–180. doi: 10.1016/0038-0717(72)90008-9

Yu, Y., Ma, J., Guo, Q., Ma, J., and Wang, H. (2019). A novel 3-oxoacyl-ACP reductase (FabG3) is involved in the xanthomonadin biosynthesis of *Xanthomonas campestris* pv. Campestris. *Mol Plant Pathol* 20, 1696–1709. doi: 10.1111/mpp.12871

Zhang, Y., Guo, Y., Qiu, T., Gao, M., and Wang, X. (2022). Bacteriophages: underestimated vehicles of antibiotic resistance genes in the soil. *Front. Microbiol.* 13:936267. doi: 10.3389/fmicb.2022.936267

Zhang, M., Warmink, J., Pereira, E. S. M., Brons, J., Smalla, K., and van Elsas, J. D. (2015). IncP-1β plasmids are important carriers of fitness traits for Variovorax species in the Mycosphere—two novel plasmids, pHB44 and pBS64, with differential effects unveiled. *Microb. Ecol.* 70, 141–153. doi: 10.1007/s00248-014-0550-y

Zhang, P., Zhang, Z., Zhang, L., Wang, J., and Wu, C. (2020). Glycosyltransferase GT1 family: phylogenetic distribution, substrates coverage, and representative structural features. *Comput. Struct. Biotechnol. J.* 18, 1383–1390. doi: 10.1016/j.csbj.2020.06.003

Zheng, Q., Hu, Y., Zhang, S., Noll, L., Böckle, T., Dietrich, M., et al. (2019). Soil multifunctionality is affected by the soil environment and by microbial community composition and diversity. *Soil Biol. Biochem.* 136:107521. doi: 10.1016/j.soilbio.2019.107521

Zhou, H., Beltrán, J. F., and Brito, I. L. (2021). Functions predict horizontal gene transfer and the emergence of antibiotic resistance. *Sci. Adv.* 7:j5056:eabj5056. doi: 10.1126/sciadv.abj5056

Zhou, J., Deng, Y., Luo, F., He, Z., Tu, Q., and Zhi, X. (2010). Functional molecular ecological networks. *MBio* 1, e110–e169. doi: 10.1128/mBio.00169-10

Zhou, X., Liu, L., Zhao, J., Zhang, J., Cai, Z., and Huang, X. (2023). High carbon resource diversity enhances the certainty of successful plant pathogen and disease control. *New Phytol.* 237, 1333–1346. doi: 10.1111/nph.18582

frontiers | Frontiers in Microbiology

TYPE Original Research
PUBLISHED 14 August 2023
DOI 10.3389/fmicb.2023.1172862

OPEN ACCESS

EDITED BY
Mikhail Semenov,
Russian Academy of Agricultural Sciences, Russia

REVIEWED BY
Ilya Yevdokimov,
Russian Academy of Sciences, Russia
Chong Juan You,
Beijing Forestry University, China

*CORRESPONDENCE
Gregory M. Bonito
bonito@msu.edu

RECEIVED 23 February 2023
ACCEPTED 10 July 2023
PUBLISHED 14 August 2023

CITATION
Benucci GMN, Toosi ER, Yang F, Marsh TL, Bonito GM and Kravchenko A (2023) The microbiome structure of decomposing plant leaves in soil depends on plant species, soil pore sizes, and soil moisture content. *Front. Microbiol.* 14:1172862. doi: 10.3389/fmicb.2023.1172862

The microbiome structure of decomposing plant leaves in soil depends on plant species, soil pore sizes, and soil moisture content

Gian Maria Niccolò Benucci [1,2], Ehsan R. Toosi[1], Fan Yang[3], Terence L. Marsh[3], Gregory M. Bonito [1,2,3]* and Alexandra Kravchenko[1,2]

[1]Plant Soil and Microbial Sciences, Michigan State University, East Lansing, MI, United States, [2]Great Lakes Bioenergy Research Center, Michigan State University, East Lansing, MI, United States, [3]Microbiology and Molecular Genetics, Michigan State University, East Lansing, MI, United States

Microbial communities are known as the primary decomposers of all the carbon accumulated in the soil. However, how important soil structure and its conventional or organic management, moisture content, and how different plant species impact this process are less understood. To answer these questions, we generated a soil microcosm with decomposing corn and soy leaves, as well as soil adjacent to the leaves, and compared it to control samples. We then used high-throughput amplicon sequencing of the ITS and 16S rDNA regions to characterize these microbiomes. Leaf microbiomes were the least diverse and the most even in terms of OTU richness and abundance compared to near soil and far soil, especially in their bacterial component. Microbial composition was significantly and primarily affected by niche (leaves vs. soil) but also by soil management type and plant species in the fungal microbiome, while moisture content and pore sizes were more important drivers for the bacterial communities. The pore size effect was significantly dependent on moisture content, but only in the organic management type. Overall, our results refine our understanding of the decomposition of carbon residues in the soil and the factors that influence it, which are key for environmental sustainability and for evaluating changes in ecosystem functions.

KEYWORDS

soil microbiome, CONSTAX2, metabarcoding, ITS rDNA, 16S rDNA, detritusphere, soil pores, leaf litter

Introduction

Adding aboveground plant residues to the topsoil can increase soil fertility, improve hydraulic properties, enhance carbon sequestration, and reduce erosion (Miguez and Bollero, 2005; Scholberg et al., 2010). Sustainable agriculture management practices that involve residue additions include cover cropping, green manure cropping, and crop residue incorporation by tillage (Lal, 1997). Such practices are growing in popularity worldwide and are particularly important in organically based agriculture and in agricultural systems in developing countries. The benefits of incorporating plant residues stem from their decomposition within the soil, which provides soil carbon and nutrient inputs and is driven by microorganisms (Lehtinen et al., 2014; Liu et al., 2017).

Micro-environmental conditions within the soil matrix influence microbiome activity and composition (Chenu et al., 2001; Mummey and Stahl, 2004; Wolf et al., 2013). Soil pores are known to play a major role in shaping soil micro-environments (Kravchenko and Guber, 2017). They enable gas and liquid transport, impact microbial colonization of the soil matrix (Dechesne et al., 2003; Long and Or, 2009; Wang et al., 2013), and create physical barriers between microbial communities (Treves et al., 2003) that can either reduce or enhance accessibility to predators (Wright et al., 1995) and other stress factors (Harvey et al., 2021). Connectivity among the soil micro-environments, facilitated through liquid bridges, is a major driver of the diversity of microbial communities within the soil matrix (Tiedje et al., 2001; Long and Or, 2005; Carson et al., 2010). Accounting for the characteristics of the soil pore space in numerical modeling is necessary for understanding the mechanisms and drivers of microbial dynamics and activity (Golparvar et al., 2021). However, while significant attention has been given to the role of pore characteristics in influencing microorganisms in bulk soil, defined as the soil not affected by plant residues or live plant roots (Bickel and Or, 2020; Nunan et al., 2020; Xia et al., 2022), relatively less is known about how such characteristics contribute to microbiome dynamics around incorporated plant residues.

The soil in the immediate vicinity of decomposing plant residue is known as the detritusphere (Kögel-Knabner et al., 2023), and physical properties in this zone drive the rate of residue decomposition and the fate of decomposition products (Kravchenko et al., 2017; Kim et al., 2020). A greater abundance of large pores in the detritusphere stimulates decomposition and leads to greater quantities of residual carbon being fully decomposed into CO_2 and emitted into the atmosphere (Toosi et al., 2017). The prevalence of small pores stimulates the diffusion of decomposition products into the surrounding soil matrix, enriching it with new C inputs but also potentially stimulating microbial activity, thus priming the loss of native soil organic matter (Toosi et al., 2017).

In this study, we used microcosms to test the impact that soil pore size, moisture, and plant tissue quality have on fungal and bacterial dynamics and the incorporation of leaf litter residue into soil across space and time. We hypothesized that the decomposing residue itself would drive microbial community composition changes in the soil and that environmental conditions within the soil matrix, specifically the presence and size distribution of soil pores and the level of soil moisture, would define the composition of microbial communities on the decomposing residue and in the surrounding detritusphere. Assessment of the microbial community composition over a time course, i.e., at 7, 14, and 24 days, improves our ability to detect diversity patterns that with only one sampling time would not be possible to detect. It also provides insight into longer-term trends and factors involved in microbial turnover. We explored their role in microcosm systems from soils of contrasting long-term agricultural management histories, namely, conventional and organic row crop agriculture practices, and with residues (leaves) of two plant species common in conventional row crop agriculture, namely, corn [*Zea mays* (L.)] and soybean [*Glycine max* (L.)].

Materials and methods

Study design

A detailed description of the study site and the setup of the microcosm experiment is provided by Toosi et al. (2017); thus, here we only briefly highlight the key components of the experiment. The soil for the microcosms was collected from two contrasting agricultural management practices, namely, conventionally fertilized corn-soybean-wheat rotation (Conv) and biologically based corn-soybean-wheat rotation with winter cover crops (Bio), implemented since 1989 at the Long-Term Ecological Research site at Kellogg Biological Station, Michigan. During each 3-year rotation cycle (the Bio practice), the cover crop red clover (*Trifolium pratense* L.) is frost-seeded into winter wheat and then incorporated into the soil 10 months later prior to corn planting, and the cereal rye (*Secale cereale* L.) is planted after corn harvest and incorporated prior to soybean planting. The studied soil is Kalamazoo loam (fine-loamy, mixed, and mesic Typic Hapludalf) (Robertson and Hamilton, 2015).

The soil material dominated by large pores, referred to further on as the large pore soil, consisted of a 1–2 mm aggregate fraction obtained by sieving air-dried bulk soil. The soil material dominated by small pores, referred to further on as small pore soil, was created from a subset of the 1–2 mm fraction by crushing and sieving the soil to a 0.05–0.1 mm size range. Creating small pore material from the large-pore material in this study ensured maximum consistency between the inherent chemical and biological properties of the two materials; however, we are aware that the procedure could have potentially affected soil microorganisms (Powlson, 1980). X-ray-computed microtomography of the soil materials revealed that the large pore material had a substantial presence of $>30\,\mu m$ Ø pores, which represented the pore space in-between the 1 and 2 mm aggregates, and of $<2\,\mu m$ Ø pores from within the aggregates. The pores space of the small pore material was dominated by 5–$10\,\mu m$ Ø pores, with no $>30\,\mu m$ Ø pores present (Toosi et al., 2017). The microcosms were constructed so as to maintain the same bulk density of $1.1\,g\,cm^{-3}$, so both materials had the same 58% total porosity.

The treatment design for the incubation experiment consisted of the following factors: two agricultural management practices (Conv and Bio), two soil materials with contrasting pore size diameters (PSD: large and small pore materials), two soil moisture levels (18 and 28% volumetric water contents), two plant residue substrates (corn and soybean leaves), and no residue treatment (control). Since the colonization of a new substrate by soil microbiota is dynamic and therefore changes with time, we sampled the microcosms at three time points (7, 14, and 24 days after the start of the incubation). Three replicated microcosms were prepared for each treatment combination, for a total of 216 microcosms. Samples were processed as three experimental blocks in a randomized complete block design.

Each microcosm was 8 mm in diameter and 10 mm in length (Supplementary Figure S1) and contained a Ø7 mm dry leaf disk placed in-between two equal soil layers (0.45 g above and 0.45 g below the leaf). Microcosms were incubated at 20°C in the dark. At each sampling time, the microcosms were randomly assigned to the specific sampling time point, taken out of the incubation, and

10.3389/fmicb.2023.1172862

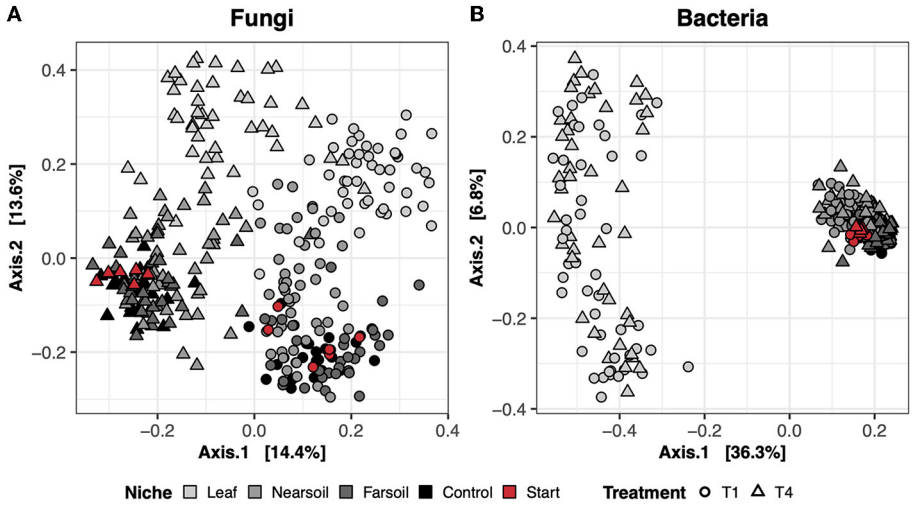

FIGURE 1
Principal Coordinate Analysis (PCoA) based on Bray-Curtis dissimilarity matrices of fungal **(A)** and bacterial **(B)** communities. Incubated samples that did not contain leaves are referred to as control (black), and dry samples of the soil materials used in the study (prior to incubation) are referred to as start (red).

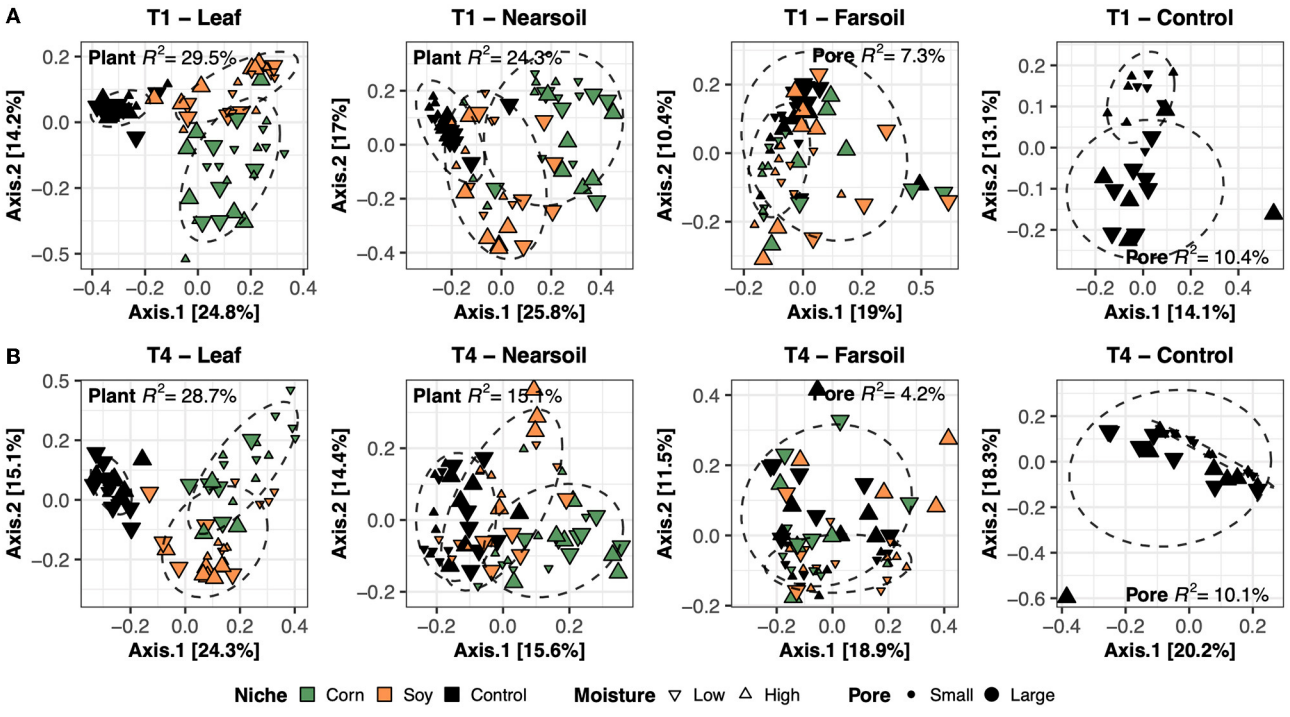

FIGURE 2
Principal Coordinate Analysis (PCoA) based on Bray-Curtis dissimilarity matrices of fungal microbiomes. PCoA of all samples grouped by treatment and niche: T1-leaf, T1-near soil, T1-far soil, and T1-control **(A)** and T4-leaf, T4-near soil, T4-far soil, and T4-control **(B)**. Sample points are coded according to plant (color), moisture (shape), and size (pore). Factors that explained the most variation in the data are reported, as are the R^2 and 75% confidence level ellipses assuming a normal distribution.

prepared for microbial analyses. Each control microcosm (without a plant leaf) was processed as a single sample. From each treatment microcosm with plant leaf, we procured three samples for microbial analysis, representing what we consider to be three ecological niches differing in quantity and quality of the nutrient sources available for the microorganisms. These consisted of the remains of the plant leaf itself, the soil layer at a 0–2 mm distance from the leaf, and the soil layer at a 3–5 mm distance from the leaf. The latter two samples are referred to as soil adjacent (near soil) to the leaf and soil non-adjacent (far soil) to the leaf, respectively. The samples were placed on ice immediately after cutting and then kept frozen at −80°C until further analysis. In addition,

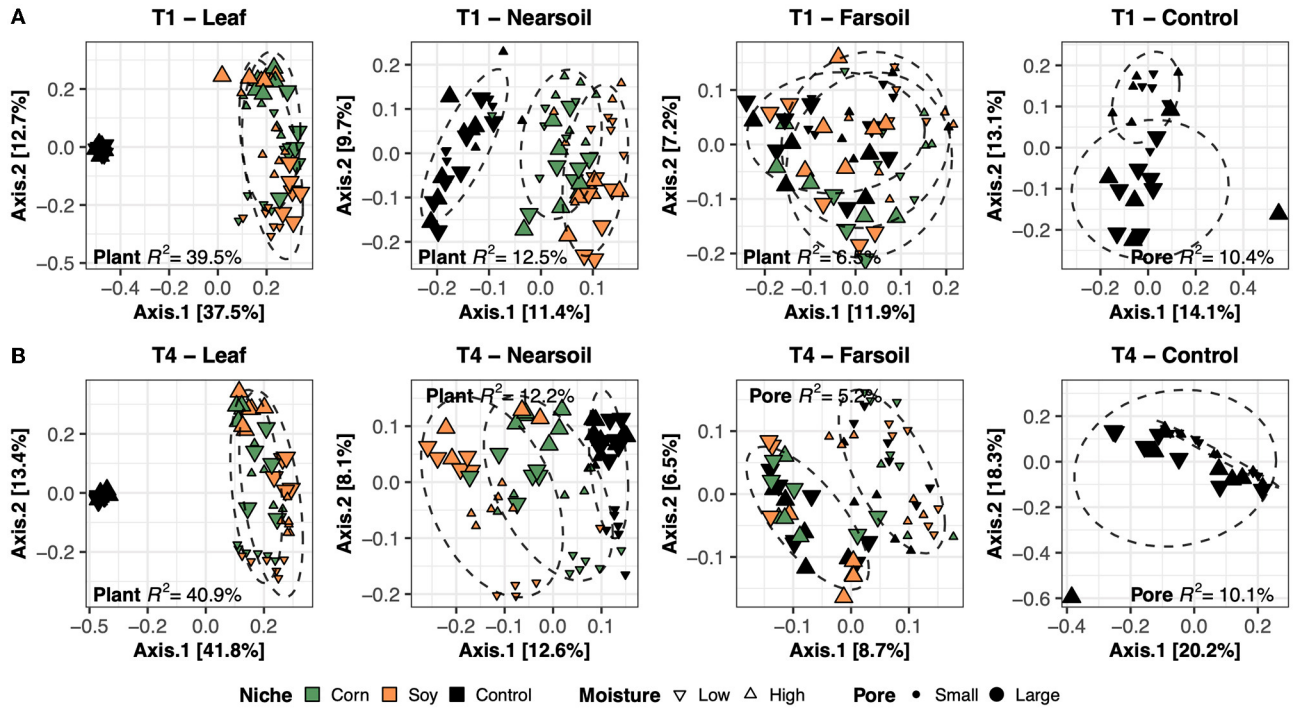

FIGURE 3
Principal Coordinate Analysis (PCoA) based on Bray-Curtis dissimilarity matrices of bacterial microbiomes. PCoA of all samples grouped by treatment and niche: T1-leaf, T1-near soil, T1-far soil, and T1-control **(A)** and T4-leaf, T4-near soil, T4-far soil, and T4-control **(B)**. Sample points are coded according to plant (color), moisture (shape), and size (Pore). Factors that explained the most variation in the data are reported, as are the R^2, and 75% confidence level ellipses assuming a normal distribution.

baseline microbial analyses were conducted in air-dry samples of large- and small-pore starting materials from conventional (T1) and organic (T4) managements that were not subjected to incubation.

This experiment was a component of a larger study that examined the effects of management practices, PSDs, soil moisture level, and plant leaf source (corn vs. soybean) on leaf decomposition, the emission of CO_2 and N_2O during incubations, the distribution of leaf decomposition products within the soil, and soil priming effects. The findings on these other components of the study have been published elsewhere (Kravchenko and Guber, 2017; Toosi et al., 2017) and thus provide auxiliary information for analyzing the data from the experiment described here.

DNA extraction, library preparation, and sequencing

DNA was extracted from soil samples with the MoBio Power Soil kit according to the vendor's protocol, with the exception that a Biospec Mini-Beadbeater-16 was used for cell disruption. Approximately 0.25–0.5 g of soil was extracted for each sample. Samples were shaken for 1.5 min at 25°C. DNA yield was quantitated with a Nanodrop Spectrophotometer. Total soil DNA was amplified and sequenced at the Michigan State University sequencing core facility. Briefly, to assess fungal communities, the ITS region was amplified using the primer sets ITS1F12 (5′-GAACCWGCGGARGGATCA) and ITS2 (5′-GCTGCGTTCTTCATCGATGC). Amplification products were run in the same manner as the V4 amplification products (below) but on a separate MiSeq v2 flow cell.

To assess prokaryote communities, the microbial 16S rRNA gene V4 regions were amplified using primer sets 515F (5′-GTGCCAGCMGCCGCGGTAA-3′) and 806R (5′-GGACTACHVGGGTWTCTAAT-3′) following the method described by Kozich et al. (2013). Amplicons of 16S rRNA gene V4 regions were pooled and run on a standard MiSeq v2 flow cell with a 500-cycle reagent kit (PE250). Base calling was done using the Illumina Real-Time Analysis (RTA) version 1.18.54, and the output of RTA was demultiplexed and converted to FastQ format using the Illumina Bcl2fastq version 1.8.4.

Fungal and prokaryotic sequence processing

Raw forward and reverse Illumina ITS reads were quality evaluated with FastQC (Andrews, 2010) and merged with PEAR (Zhang et al., 2014). Primers and adapters were removed with Cutadapt (Martin, 2011). Reads were quality filtered (Edgar and Flyvbjerg, 2015; Edgar, 2016), de-replicated, removed from singleton sequences, and clustered into operational taxonomic units (OTUs) based on 97% similarity using the UPARSE algorithm (Edgar, 2013). Taxonomy assignments were performed

in CONSTAX2 (Liber et al., 2021) using the UNITE sequence database (Kõljalg et al., 2013).

Raw forward and reverse Illumina 16S reads were processed as previously described (Rieke et al., 2018) with the following modifications. Briefly, we used Ribosomal Database Project (RDP) Paired-end Reads Assembler (Cole et al., 2014) to merge the primer-trimmed pair-ended reads to 250–280 bases and a minimal Q score of 25. Using BLAST, we confirmed that the assembled 16S rRNA gene V4 sequences shorter than 250 bases or longer than 280 bases were non-microbial. Vsearch (2.4.3, 64-bit) (Rognes et al., 2016) was used to remove chimeras *de novo*, followed by removing chimeras by reference using RDP 16S rRNA gene training set sequences (No. 15). High-quality and chimera-free sequences were then clustered at 97% sequence similarity by CD-HIT (4.6.1) (Fu et al., 2012). The taxonomy of each representative OTU sequence was identified using the RDP Classifier (Wang et al., 2007; Fu et al., 2012) with a confidence cutoff of 50% (-c 0.5). Finally, OTUs detected fewer than five times across all samples were removed.

Statistical modeling

For each marker gene (i.e., ITS and 16S), otu_table (McDonald et al., 2012), taxonomic classifications, representative OTU sequences, and metadata files were imported into the R statistical environment (R Core Team., 2023) and combined with the *phyloseq* package (McMurdie and Holmes, 2014). To standardize the sequencing depth across all samples, we rarefied all samples to the minimum sample size (i.e., 1,010 sequences for the fungi and 13,377 sequences for the prokaryotes) in the *phyloseq* R package (McMurdie and Holmes, 2013).

To explore differences in microbial community beta-diversity, we analyzed two components, namely, (i) community structure, defined as the difference in multivariate space between samples and sample groups and (ii) community dispersion, defined as multivariate variance within each sample group. Community structure was investigated using principal coordinate analysis (PCoA) of the Bray-Curtis distance matrix with the function "ordinate" in *phyloseq* (McMurdie and Holmes, 2014). A permutational multivariate analysis of variance (Permanova) was used to test differences among *a priori* defined sample groups (Anderson, 2001) with the function "adonis" in the *vegan* R package (Oksanen et al., 2019). To assess the amount of multivariate dispersions (Anderson et al., 2006) around centroids, we used the "betadisper" function in *vegan*. Statistical differences in dispersion were assessed through pairwise permutational ANOVA, using the "anova" function in the *car* R package, with 9,999 permutations. All *P*-values were corrected based on the Benjamini-Hochberg method (Benjamini and Hochberg, 1995).

To explore which bacterial genera will follow the decomposing residue vs. soil and the increasing vs. decreasing time trends, we first conducted a 3-way factorial ANOVA for the abundances of individual OTUs. To identify the leaf-dominating and soil-dominating genera, the ANOVA was followed by contrasts comparing the leaf with near soil and the leaf with far soil and a non-incubated control, tested simultaneously ($P < 0.01$). Then, the abundances of genera identified as either leaf- or soil-dominating were subjected to linear regression with time as the independent variable to identify those that exhibited a clear positive or negative linear trend ($P < 0.05$).

Alpha diversity, OTU richness, and Shannon diversity indexes were calculated in *vegan* with the "specnumber" and "diversity" functions of the *vegan* package (Oksanen et al., 2019). The Shannon index was standardized to 0–1 to allow for easier comparisons across groups, as previously explained (Benucci et al., 2022). Significant differences ($P \leq 0.05$) in alpha diversity were assessed by a Wilcoxon test, with P-values corrected with the Benjamini-Hochberg method (Benjamini and Hochberg, 1995). All graphs were plotted in the *ggplot2* (Wickham, 2016) and *ggpubr* (Kassambara, 2020) R packages. Minimal graphical adjustments to improve the figures' visibility were performed in *Inkscape* (Inkscape Project, 2020).

Results

Sequencing results

This study resulted from community data from 252 samples that yielded 2,193,913 (8,671.6 ± 6,448.2 mean reads and standard deviation per sample, respectively) ITS reads and 3,701,268 (14,629.52 ± 7,687.7) 16S reads in the otu_table after quality filtering. The data were rarefied at 1,010 reads per sample for ITS and 13,377 for 16S.

Beta diversity

In the dry control samples (i.e., the soil materials used in the study tested prior to incubation), the long-term history of contrasting agricultural management practices (T1 = conventional vs. T4 = organic) influenced both fungal and bacterial microbiomes (Supplementary Table S1). However, neither fungal nor bacterial communities differed between the large- and small-pore soil materials (Supplementary Table S1). In the study samples, the largest amount of variation in composition was present across different niches (i.e., leaf, near soil, and far soil), as hypothesized, which accounted for roughly 16% and 39% of the total variance in fungal and bacterial communities, respectively (Supplementary Table S1). Differences across niches and treatments are clear in the principal coordinate analysis (PCoA) ordination plots based on the Bray-Curtis dissimilarity of fungal (Figure 1A) and bacterial communities (Figure 1B), with clear clustering of samples along the first and second PCoA axes, respectively. Fungal communities were also more clearly impacted by soil treatment (T1 = conventional vs. T4 = organic), which explains nearly 11% of the variance, and, to a lesser extent, by plant species (i.e., corn or soy), pore size (i.e., small or large), and moisture content (i.e., low or high). Bacterial communities were also impacted by pore size (~2.5%), moisture content (~2%), treatment (~2%), and plant species (~1.5%), but these effects were hidden by the effect of niche. Significant interactions ($P \leq 0.05$, after Benjamini-Hochberg *P*-value correction), mainly involving niche and other factors, were also present, but, in general, the amount of variation explained was negligible (Supplementary Table S2).

TABLE 1 Permanova (Permutational Multivariate Analysis of Variance Using Distance Matrices) and Betadisper (Multivariate Homogeneity of Groups Dispersions) models on the subsetted fungal and bacterial datasets according to slice and treatment (leaf-T1, leaf-T4, near soil-T1, T1-control, near soil-T4, far soil-T1, far soil-T4, and T4-control).

Fungi	*Permanova*						*Betadisper*		
Group	Factor	Df	Sum.Sq	F	R^2	P.adj	Sum.Sq	F	P.adj
T1-Leaf	***Plant***	2	4.22612	14.90845	0.29459	**0.00080**	0.0132	0.5592	0.5743
T1-Leaf	*Pore*	1	0.44086	3.11042	0.03073	**0.01840**	0.0883	13.6263	**0.0004**
T1-Nearsoil	***Plant***	2	2.85516	11.13978	0.24329	**0.00080**	0.0233	1.7466	0.1824
T1-Nearsoil	*Pore*	1	0.44797	3.49560	0.03817	**0.00880**	0.0425	14.7884	**0.0003**
T1-Farsoil	***Pore***	1	0.74554	4.85338	0.07261	**0.00080**	0.3237	71.3412	**0.0000**
T1-Farsoil	*Moisture*	1	0.42277	2.75218	0.04118	**0.00800**	0.0063	0.5691	0.4537
T1-Control	***Pore***	1	0.32534	2.38360	0.10468	**0.00040**	0.0427	10.4906	**0.0041**
T4-Leaf	***Plant***	2	4.03977	15.91940	0.28679	**0.00080**	0.0507	2.0021	0.1436
T4-Leaf	*Pore*	1	0.92249	7.27047	0.06549	**0.00080**	0.0299	4.4552	**0.0387**
T4-Leaf	*Time*	2	0.81393	3.20743	0.05778	**0.00080**	0.0202	1.2462	0.2946
T4-Leaf	*Moisture*	1	0.55793	4.39724	0.03961	**0.00160**	0.0067	0.8304	0.3656
T4-Leaf	*Pore:Moisture*	1	0.37736	2.97408	0.02679	**0.02000**	-	-	-
T4-Nearsoil	***Plant***	2	1.60929	6.19018	0.15103	**0.00080**	0.0094	0.5129	0.6012
T4-Nearsoil	*Pore*	1	0.40427	3.11009	0.03794	**0.00160**	0.2103	36.0006	**0.0000**
T4-Nearsoil	*Moisture*	1	0.34383	2.64510	0.03227	**0.01120**	0.0066	0.7250	0.3976
T4-Farsoil	***Pore***	1	0.35941	2.63748	0.04163	**0.01440**	0.3542	56.6875	**0.0000**
T4-Farsoil	*Plant:Pore:Moisture*	1	0.40467	2.96966	0.04687	**0.00480**	-	-	-
T4-Control	***Pore***	1	0.30512	2.49281	0.10162	**0.01240**	0.1199	18.9037	**0.0003**
Bacteria									
Group	Factor	Df	Sum.Sq	F	R^2	P.adj	Sum.Sq	F	P.adj
T1-Leaf	***Plant***	2	7.99222	33.13792	0.39641	**0.00080**	0.2459	32.4638	**0.0000**
T1-Leaf	*Moisture*	1	1.69730	14.07491	0.08418	**0.00080**	0.0029	0.4915	0.4857
T1-Leaf	*Time*	2	1.22462	5.07759	0.06074	**0.00080**	0.0127	1.4587	0.2398
T1-Leaf	*Pore*	1	1.01912	8.45110	0.05055	**0.00080**	0.0002	0.0480	0.8273
T1-Nearsoil	***Plant***	2	0.96853	5.43286	0.12532	**0.00080**	0.0010	0.6545	0.5231
T1-Nearsoil	*Time*	2	0.53755	3.01534	0.06956	**0.00080**	0.0003	0.1776	0.8377
T1-Nearsoil	*Pore*	1	0.45416	5.09507	0.05877	**0.00080**	0.0018	2.0833	0.1536
T1-Nearsoil	*Moisture*	1	0.25621	2.87432	0.03315	**0.00080**	0.0012	1.7753	0.1873
T1-Farsoil	*Time*	2	0.52353	2.90084	0.08460	**0.00080**	0.0000	0.0285	0.9719
T1-Farsoil	***Plant***	2	0.40441	2.24080	0.06535	**0.00080**	0.0013	0.9940	0.3765
T1-Farsoil	*Pore*	1	0.36626	4.05886	0.05919	**0.00080**	0.0032	5.2212	**0.0261**
T1-Control	*Time*	2	0.36715	2.03374	0.16551	**0.00040**	0.0220	2.1863	0.1398
T1-Control	***Pore***	1	0.19382	2.14727	0.08737	**0.00960**	0.0427	10.4906	**0.0041**
T4-Leaf	***Plant***	2	7.65287	37.25758	0.40881	**0.00080**	0.2337	20.6704	**0.0000**
T4-Leaf	*Pore*	1	1.67765	16.33514	0.08962	**0.00080**	0.0187	3.0142	0.0873
T4-Leaf	*Time*	2	1.57711	7.67806	0.08425	**0.00080**	0.0400	5.0084	**0.0095**
T4-Leaf	*Moisture*	1	0.98904	9.63021	0.05283	**0.00080**	0.0010	0.3096	0.5799
T4-Leaf	*Pore:Moisture*	1	0.52480	5.10997	0.02803	**0.00720**	-	-	-

(Continued)

TABLE 1 (Continued)

Fungi	*Permanova*						*Betadisper*		
Group	Factor	Df	Sum.Sq	F	R^2	P.adj	Sum.Sq	F	P.adj
T4-Nearsoil	***Plant***	2	0.88452	5.07130	0.12185	**0.00080**	0.0012	0.7689	0.4678
T4-Nearsoil	*Pore*	1	0.39821	4.56619	0.05486	**0.00080**	0.0010	1.1113	0.2957
T4-Nearsoil	*Time*	2	0.32738	1.87699	0.04510	**0.00320**	0.0003	0.2050	0.8152
T4-Nearsoil	*Moisture*	1	0.25161	2.88516	0.03466	**0.00080**	0.0002	0.2241	0.6375
T4-Nearsoil	*Pore:Moisture*	1	0.19160	2.19708	0.02639	**0.00880**	-	-	-
T4-Farsoil	*Time*	2	0.34319	1.94229	0.05863	**0.00080**	0.0013	0.8474	0.4338
T4-Farsoil	***Pore***	1	0.30714	3.47648	0.05247	**0.00080**	0.0010	1.1832	0.2812
T4-Farsoil	*Plant*	2	0.29821	1.68774	0.05094	**0.00080**	0.0003	0.1571	0.8550
T4-Farsoil	*Moisture*	1	0.15576	1.76304	0.02661	**0.00960**	0.0000	0.0122	0.9124
T4-Farsoil	*Plant:Pore:Moisture*	1	0.14815	1.67689	0.02531	**0.01440**	-	-	-
T4-Control	*Time*	2	0.25182	1.49254	0.11267	**0.00240**	0.1105	4.4663	**0.0242**
T4-Control	***Pore***	1	0.19786	2.34541	0.08853	**0.00040**	0.1199	18.9037	**0.0003**
T4-Control	*Moisture*	1	0.16089	1.90716	0.07199	**0.00080**	0.0039	0.3283	0.5724

Time was treated as a fixed effect and included as a factor variable in the models (Time + Plant * Pore * Moisture, and Time + Pore * Moisture for just the control samples). The order of the factors was chosen to first remove variance from variables with the highest impact in the models and better investigate the remaining variables. Only factors with significant ($P \leq 0.05$) Benjamini-Hochberg-corrected P-values are displayed. Factor explaining the highest R^2 for each model and significant adjusted p-values are reported in bold.

To better evaluate the impacts of all the variables, the datasets were divided by niche and treatment into eight subsets composed of leaf-T1, leaf-T4, near soil-T1, near soil-T4, far soil-T1, far soil-T4, control-T1, and control-T4. The PCoA ordinations generated for each subset showed significantly different clusters of samples for both fungi (Figure 2) and bacteria (Figure 3), as supported by the Permanova tests.

Overall, the Permanova [$P \leq 0.05$, after Benjamini-Hochberg (BH) correction] results showed that plant species and pore size were the two main drivers of the communities in both T1 and T4 and for each studied niche. In particular, plant species were always the major driver of variation in the leaf and the near soil niches (and also in the far soil for the bacterial microbiome in T1), while pore sizes impacted the far soil (i.e., soil further away from the leaf) niches; control samples were impacted by pore sizes the most (Table 1). Microbiome variance attributed to plant species ranged from about 29% in the T1-leaf to 15% in the T4-near soil of the fungal microbiome and from about 40% in the T1-leaf to 5.1% in the T4-far soil of the bacterial microbiomes, with no substantial difference between T1 and T4. Microbiome variance attributed to pore sizes ranging from about 7.3% in T1-far soil (10.5% in the T1-control samples) to 3.1% in T1-leaf of the fungal microbiome and from about 8.9% in T4-leaf (8.8% in the T4-control samples) to 5% in T1-leaf of the bacterial microbiome, with, in general, higher variance in T4 compared to T1 if we do not consider the control samples. Moisture content was most important in shaping the bacterial rather than fungal microbiome. Significant effects were present in T1-far soil (4.1%), T4-leaf (3.9%), and T4-near soil (3.2%) in the fungal microbiomes, and T1-leaf (8.4%), T1-near soil (3.3%), T4-leaf (5.3%), T4-near soil (3.6%), T4-far soil (2.7%), and T4-control samples (7.2%) in the bacterial microbiomes.

The effect of time was the most important for the bacterial microbiome than the fungal microbiome, and significant pore:moisture and plant:pore:moisture interactions were also present in both fungal and bacterial communities, but only in T4 treatments, which represent the organic management type. Microbiomes clustered mainly according to plant and pore, as shown by the fungal (Figure 2) and bacterial (Figure 3) PCoA ordinations, as emphasized by 75% confidence ellipses.

Alpha diversity

Alpha diversity measurements were also impacted primarily by niche, followed by other factors both in fungal (Figure 4) and bacterial (Figure 5) microbiomes. The bar plots also showed that there were no substantial alpha diversity differences between the T1 and T4 treatments. In particular, OTU richness in the leaf was considerably lower than that of the soils and controls, but differences between near soil, far soil, and control soil were also present. In the leaf niche, there was a significant ($P \leq 0.05$ after BH correction) effect of pore size in the T1 sample of the fungal microbiome and a significant effect of moisture in both the T1 and T4 samples of the bacterial microbiomes. In the near soil niche, a higher richness was present in the small pores of T1 and T4 in fungi, but only in T1 in bacterial microbiomes. In the far soil niche, fungal microbiomes were affected by pore sizes in T1 and T4, but only in T1, a higher richness was detected for the bacterial microbiomes. The effect of pore sizes and moisture content was also significant in T1 and T4, respectively, but only in the fungal microbiome.

Regarding Shannon diversity, differences between niches were mostly limited to the leaves being different from soils and control samples. Additionally, Shannon diversity followed an opposite trend to richness, being higher in leaves (a more evenly abundant microbiome) and lower in soils, and this phenomenon was more evident in the bacterial (Supplementary Figure S3) than fungal

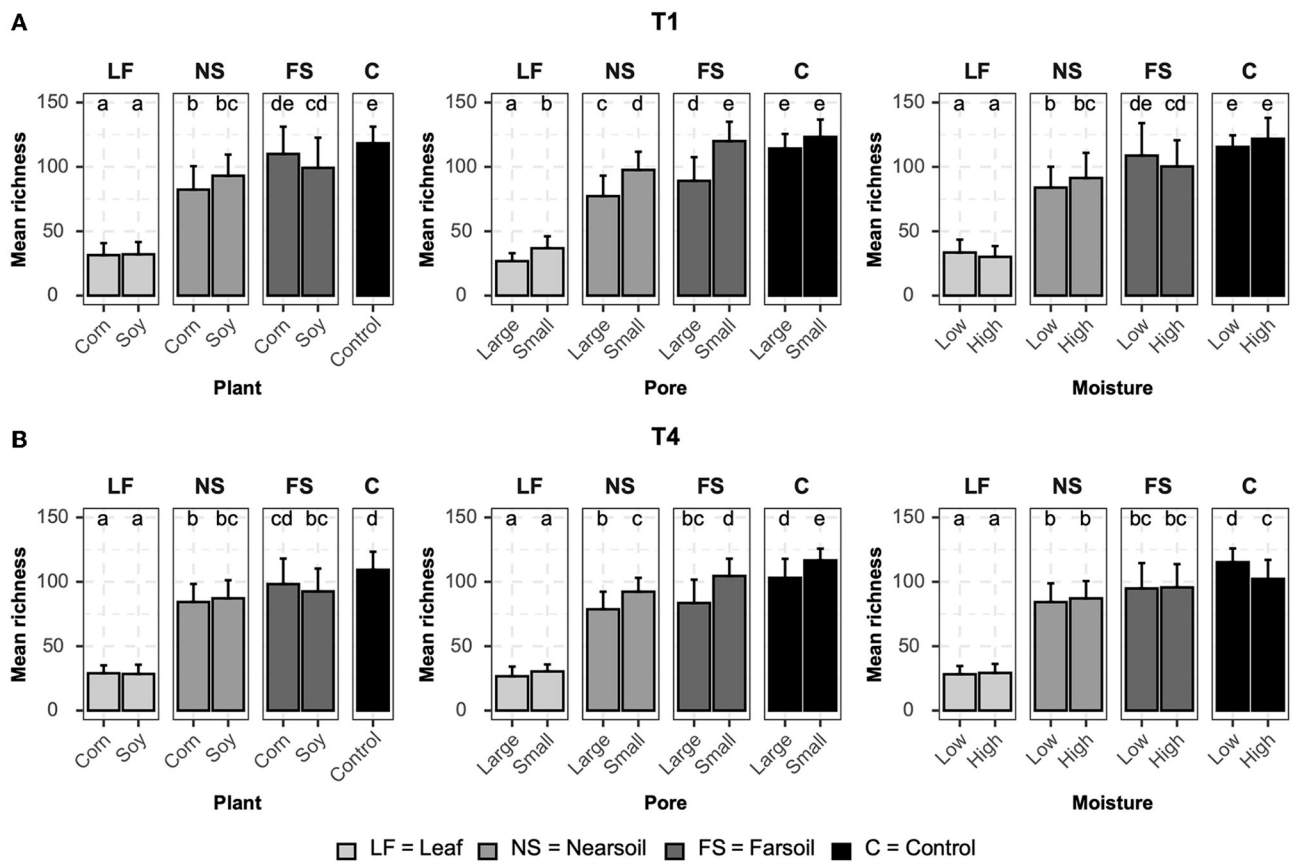

FIGURE 4
Bar plots showing significant differences ($P \leq 0.05$ after Benjamini-Hochberg correction) in mean observed species richness (±standard deviation) for fungal microbiomes in **(A)** conventional (T1) and **(B)** organic (T4) managament samples. Samples were grouped according to treatment, and statistical differences were calculated across niche factors (leaf, near soil, far soil, and control) using pairwise Wilcoxon tests.

(Supplementary Figure S4) microbiome. In particular, in the leaf niche, there was a significant ($P \leq 0.05$ after BH correction) effect of moisture in both T1 and T4 in the fungal microbiome, but Shannon diversity was higher for the T4 bacterial microbiome in soy, small, and low moisture samples. Shannon diversity was significantly higher in the T1 near soil niche for the fungi but also in soy, large pores, and low moisture for the bacterial microbiome in T1 samples. No other significant differences were present. Large pores and low moisture samples were more even in T1 and T4 far soil samples of the bacterial microbiomes, respectively.

Most abundant, variable, and significantly different OTUs across treatments

In Figure 6, the most abundant fungal (Figure 6A) and bacterial (Figure 6B) OTUs are reported, averaged across all samples, and those that showed the highest variation and had significantly different mean abundance ($P \leq 0.05$) after BH correction across the treatments. Some of these selected taxa showed different treatments. For example, FOTU85 (Xilariales) was higher in abundance in soy leaves and small pores, while present in small amounts in the control samples. FOTU58 (*Apodus* sp.) was instead significantly more abundant in corn leaves, but its abundance was not relevantly affected by other factors. Some OTUs were present and significantly different between factors in the in T1 treatment (e.g., FOTU545-*Mucor*), others only in the T4 treatment (e.g., FOTU100-*Podospora*). In the bacterial dataset, POTU25222-*Chitinophaga*, POTU27262-*Flavobacterium*, POTU24422-*Bdellovibrio*, and other unclassified bacteria were higher in soy samples with large pores and high moisture content in T1 samples. Other OTUs, such as unclassified Gammaproteobacteria, POTU6175-*Saccharibacillus*, and POTU12661-*Aureimonas*, were also higher in soy samples with large pores and high moisture content, but only in T1.

In the near soil samples, FOTU272-*Robillarda* showed a higher abundance in large pores, together with FOTU216-Pleosporales and FOTU366-*Ballistosporomyces* (Figure 7A). Unclassified Gammaproteobacteria were higher in abundance in soy, large pores, and high moisture in T1, while an unclassified OTU in the Alphaproteobacteria was higher in T4, in corn, large pores, and high moisture samples. In T1, the most abundant and variable OTUs were associated with soil, while in the T4 treatment, they were associated with corn. POTU12661-*Aureimonas* and POTU12354-*Asticcacaulis* were the only two prokaryotes with a higher abundance in small soil pores (Figure 7B).

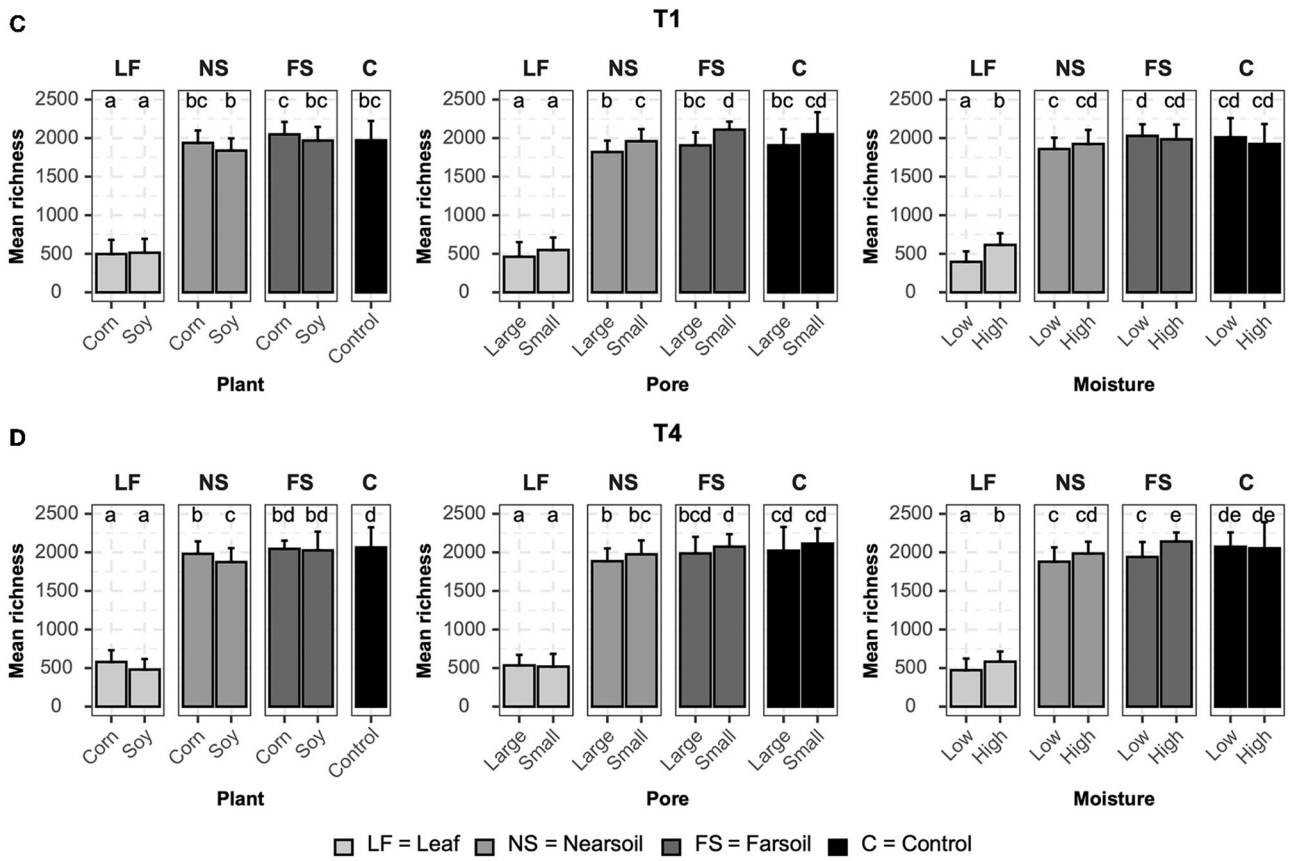

FIGURE 5
Bar plots showing significant differences ($P \leq 0.05$ after the Benjamini-Hochberg correction method) in the mean observed species richness (±standard deviation) for bacterial microbiomes in **(A)** conventional (T1) and **(B)** organic (T4) managament samples. Samples were grouped according to treatment, and statistical differences were calculated across niche factors (leaf, near soil, far soil, and control) using pairwise Wilcoxon tests.

In the far soil samples, some of the same OTUs present in the near soil samples were abundant and variable across groups. For example, FOTU545-*Mucor* (Figure 8A) was shown to be higher in corn with large pores and high moisture content, while FOTU358-Chaetothyriales (Figure 8B) was higher in soy with large pores and high moisture content; both were higher in T1 compared to T4, highlighting inherent differences between soil communities. In general, in T4, the most abundant OTUs that vary across factors were also present in the control samples, while in T1, they were absent.

Discussion

In this study, we tested the impact of the prevalence of soil pores of a certain size range, different soil moisture contents, and decomposition of plant tissue of different qualities on fungal and bacterial dynamics across space and time. We explored both the tissue itself and the surrounding detritusphere. We found that soils subjected to long-term differences in soil management practice, i.e., conventional vs. organic management, had the greatest influence on microbial community structure, likely the result of differences in plant diversity but also due to increases in soil organic matter in the organic management in these field soils (Syswerda et al., 2011). That is in agreement with observations by Epp Schmidt et al. (2022) on the soils from similar management practices, also after extended implementation. The microbial community in the long-term biologically based treatment showed greater microbial richness (Figure 3), consistent with a number of past reports (de Graaff et al., 2019).

As expected, the greatest contrast in microbial community composition was observed between the community on the decomposing residue and the communities of the surrounding soil. Leaf microbiomes were less species rich as compared to the adjacent soil (Figure 3), likely reflecting the special environment dominated by leaf decomposers, organisms that benefited from their necromass, and predators. The decomposing leaves, providing a carbon and nutrient supply, drive microbial functioning in the soil microenvironment (Figure 3).

As we reported in a companion study, decomposition rates and magnitudes substantially differed between microcosms with incubated corn vs. soybean leaves (Kravchenko et al., 2017). While >85% of the soybean residue was completely decomposed after 7 days of incubation, only 30–50% of the corn residue was decomposed by that time. However, surprisingly, the effect of plant species on the composition of the microbial community was relatively minor, especially for bacteria. Mortierellomycetes, a clade of fungi reportedly abundant in agricultural conventionally and

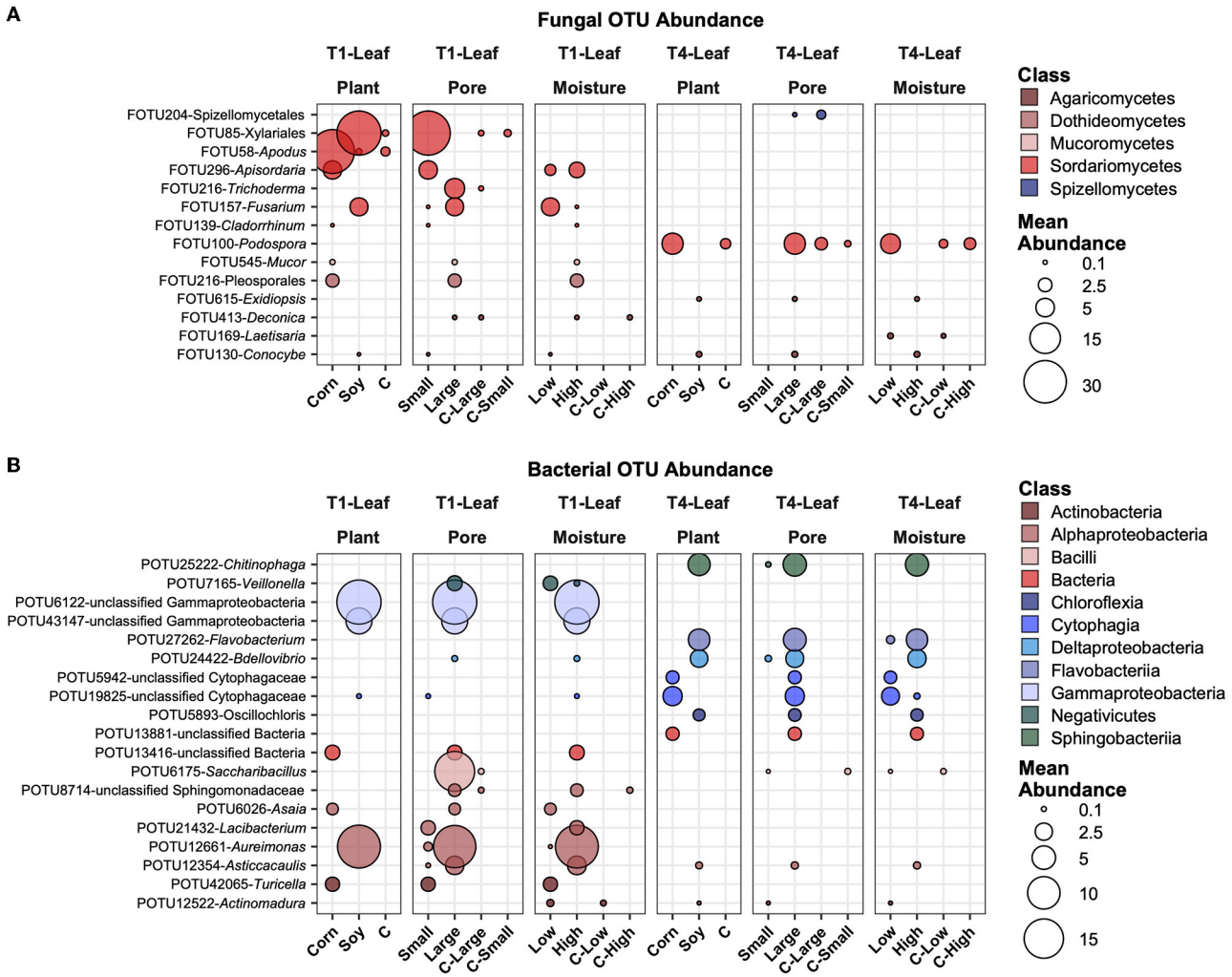

FIGURE 6
Top abundant, variable, and significantly different (pairwise Wilcoxon tests, $P \leq 0.05$ after Benjamini-Hochberg correction method) OTUs across T1 and T4 treatments in the fungal **(A)** and bacterial **(B)** microbiomes of the leaf. Point sizes represent the mean abundance across samples at a treatment level. Only significantly different OTUs among the top 25 were selected among the most variable (OTUs with a difference in abundance between treatment levels ≥ the 50 percentile of the coefficient of variation for that OTU across samples for the fungi and ≥ the 75 percentile for the bacteria) and are shown.

organically managed systems (Epp Schmidt et al., 2022; Benucci et al., 2023) and known to include soil saprotrophs as well as plant growth promoters (Põlme et al., 2020; Vandepol et al., 2022), had a greater abundance on soybean leaves than corn leaves. Agaricomycetes and Sordariomycetes groups, known to include large proportions of wood and litter saprotrophs (Põlme et al., 2020), were more abundant in corn than in soybean leaves.

We hypothesized that micro-environments within small pore-dominated soil, especially when accompanied by low soil moisture, would stimulate greater diversity of microbial communities. Smaller and less hydraulically connected pore spaces generate more fragmented microhabitats, shielding inhabitants from predation and competition (Tiedje et al., 2001; Wolf et al., 2013; Bickel and Or, 2020). This effect was expected to be more pronounced in bacteria than in fungi since hyphal growth was assumed to enable fungi to easily navigate and spread through the pore space, allowing them greater resistance to fluctuations in local environmental conditions (Barnard et al., 2013; Nunan et al., 2020). Our findings only partially supported this hypothesis (Figure 3). Greater bacterial diversity was indeed observed in small pore treatments than in large pore treatments, but it was statistically significant only in the soil of conventional agriculture and was only a numeric trend in organic management. However, a greater diversity of fungi was consistently observed in the soils of both management practices. The result suggests a greater than expected sensitivity of fungi to micro-environmental conditions, even at a few-cm spatial scale.

However, the association between soil moisture and microbial richness was either absent or the opposite of what we anticipated. Moisture did not influence fungal richness, and on decomposing residues and partially in the surrounding soil, greater richness was associated with higher moisture (Figure 3). It is possible that the lower moisture of the study limited many organisms and selected for those tolerant of drier conditions, while the optimal (field capacity) moisture of our high soil moisture treatment provided an

10.3389/fmicb.2023.1172862

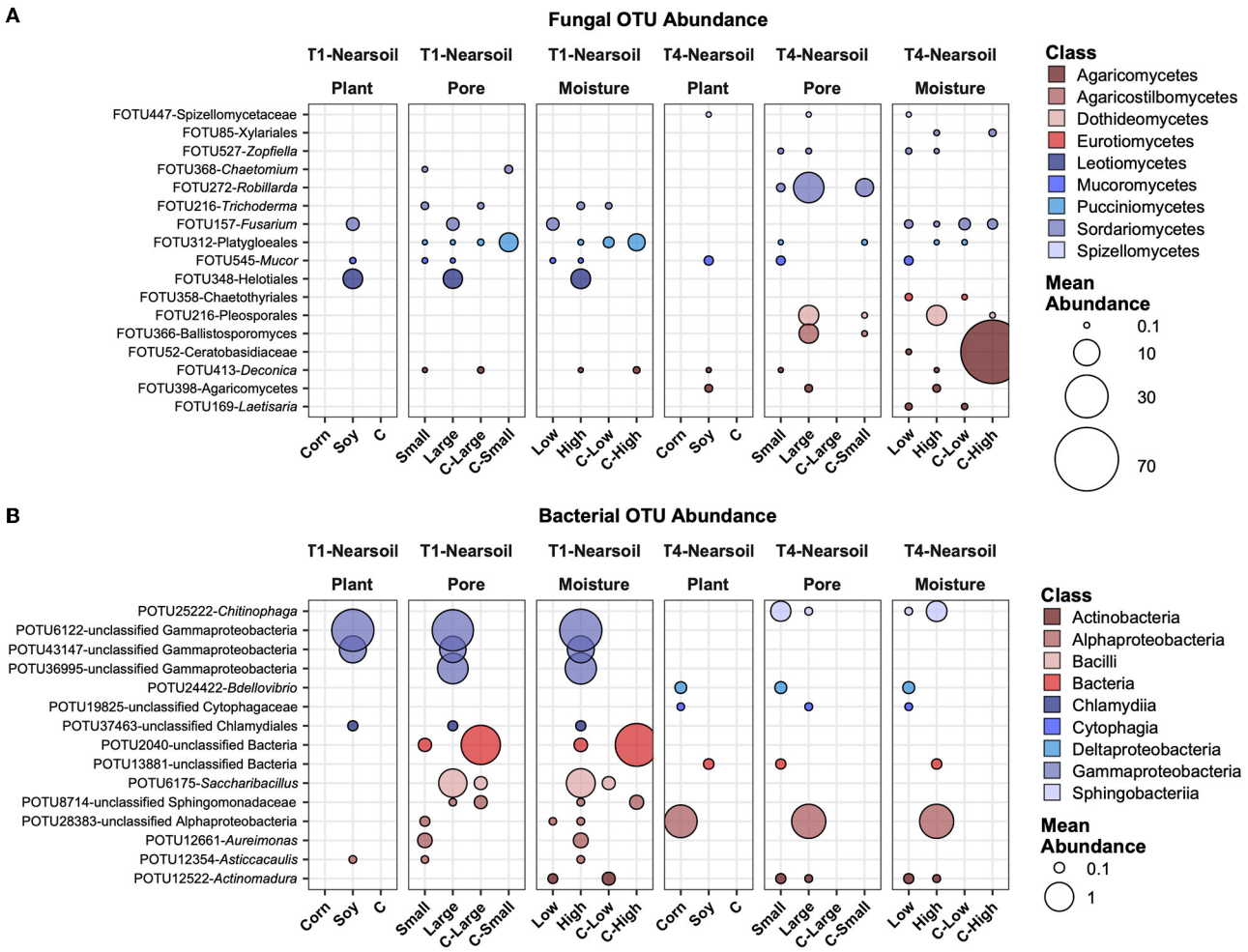

FIGURE 7
Top abundant, variable, and significantly different (pairwise Wilcoxon tests, $P \leq 0.05$ after Benjamini-Hochberg correction method) OTUs across T1 and T4 treatments in the fungal **(A)** and bacterial **(B)** microbiomes of the Nearsoil. Point sizes represent the mean abundance across samples at a treatment level. Only significantly different OTUs among the top 25 were selected among the most variable (OTUs with differences in abundance between treatment levels ≥ the 50 percentile of the coefficient of variation for that OTU across samples for the fungi and ≥ the 75 percentile for the bacteria) and are shown.

optimal growth environment. Indeed, the moisture corresponding to field capacity was reported as beneficial to bacterial diversity in both experimental works (Carson et al., 2010) and theoretical considerations (Bickel and Or, 2020).

Nevertheless, for several bacterial groups, the associations with pores were consistent with the associations with soil moisture levels, suggesting the contribution of general micro-environmental effects to the performance of these microorganisms during the experiment. Betaproteobacteria and Bacteriodetes were in greater abundance in both large-pore soils and at higher soil moisture (Figure 5). Gammaproteobacteria and Shingobacteria were in greater abundance in both small-pore soils and at lower soil moisture. Actinobacteria, a phylum known to be resistant to desiccation (Bardgett and Caruso, 2020), was also notably more abundant in both small-pore soils and at lower soil moisture. A number of Acidobacteria groups, which are usually described as oligotrophs resistant to harsh environments, were also in greater abundance in small pores, as were Anaerolinea. The higher abundance of Acidobacteria in the small pore treatment, with its lower oxygen supply, was expected. Consistent with our findings, Xia et al. (2022) reported a greater abundance of Actinobacteria in smaller pores and drier conditions and a greater abundance of Betaproteobacteria in large pores.

Conclusion

We reported here that decomposing leaves in the soil drive microbial activity and turnover over time. As we hypothesized, incubated fresh plant detritus was shown to harbor a reduced diversity but a more even microbiome composition compared to that of the adjacent communities in the soil and was the most important factor explaining fungal and bacterial microbiomes across space. We did not entirely expect to have such an important effect of management type (organic vs. conventional), which was also variable across the different niches, and impactful on the effect of pore size on both bacterial microbiomes. Soil pores and moisture content were influenced by both niche and management type and

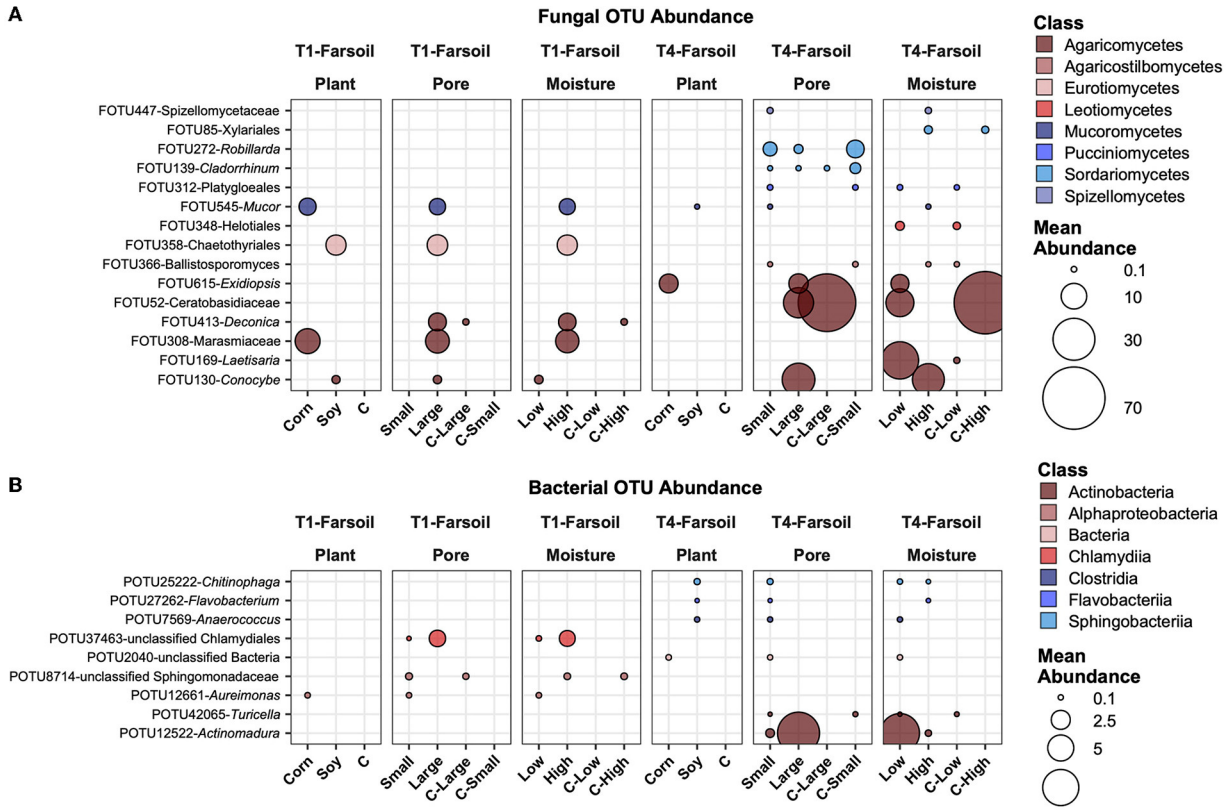

FIGURE 8
Top abundant, variable, and significantly different (pairwise Wilcoxon tests, $P \leq 0.05$ after Benjamini-Hochberg correction method) OTUs across T1 and T4 treatments in the fungal **(A)** and bacterial **(B)** microbiomes of the far soil. Point sizes represent the mean abundance across samples at a treatment level. Only significantly different OTUs among the top 25 were selected among the most variable (OTUs with a difference in abundance between treatment levels ≥ the 50 percentile of the coefficient of variation for that OTU across samples for the fungi and ≥ the 75 percentile for the bacteria) and are shown.

were important in shaping bacterial communities, which are known to rely on water films for dispersal and were more dynamic over time compared to fungi. In contrast, and as hypothesized, plant species had a greater effect on the fungal community composition over time. Together, these results contribute to our understanding of the decomposition of carbon residues in the soil and the factors that regulate the microbes that drive soil C and nutrient cycling.

Data availability statement

Raw ITS and 16S sequences .fastq reads were submitted to the Sequence Read Archive (Leinonen et al., 2011) under the bioproject number PRJNA938072. Data sets, and R code developed to analyze them, are accessible at: https://github.com/Gian77/Scientific-Papers-R-Code. Additional material associated with this article is also available in the Supplementary material.

Author contributions

GBe: performed the data analysis, created figures and tables, and wrote the manuscript. ET: conceived experimental approaches and carried out the research experiment and sampling. FY: processed samples and generated amplicon sequence data. TM: analyzed data and created figures and tables. GBo: wrote and edited the manuscript. AK: conceived experimental approaches and wrote and edited the manuscript. All authors contributed to the article and approved the submitted version.

Funding

This study was funded in part by the NSF LTER Program (DEB 1027253) at the Kellogg Biological Station, in part by the Great Lakes Bioenergy Research Center, U.S. Department of Energy, Office of Science, Office of Biological and Environmental Research under Award Number DE-SC0018409, and in part by Michigan State University AgBioResearch.

Conflict of interest

The authors declare that the research was conducted in the absence of any commercial or financial relationships that could be construed as a potential conflict of interest.

Publisher's note

All claims expressed in this article are solely those of the authors and do not necessarily represent those of

their affiliated organizations, or those of the publisher, the editors and the reviewers. Any product that may be evaluated in this article, or claim that may be made by its manufacturer, is not guaranteed or endorsed by the publisher.

Supplementary material

The Supplementary Material for this article can be found online at: https://www.frontiersin.org/articles/10.3389/fmicb.2023.1172862/full#supplementary-material

References

Anderson, M. J. (2001). A new method for non-parametric multivariate analysis of variance. *Aust. Ecol.* 26, 32–46. doi: 10.1111/j.1442-9993.2001.01070.pp.x

Anderson, M. J., Ellingsen, K. E., and McArdle, B. H. (2006). Multivariate dispersion as a measure of beta diversity. *Ecol. Lett.* 9, 683–693. doi: 10.1111/j.1461-0248.2006.00926.x

Andrews, S. (2010). *FastQC: A Quality Control Tool for High Throughput Sequence Data*. Available online at: http://www.bioinformatics.babraham.ac.uk/projects/fastqc

Bardgett, R. D., and Caruso, T. (2020). Soil microbial community responses to climate extremes: resistance, resilience and transitions to alternative states. *Philos. Trans. R. Soc. Lond. B Biol. Sci.* 375, 20190112. doi: 10.1098/rstb.2019.0112

Barnard, R. L., Osborne, C. A., and Firestone, M. K. (2013). Responses of soil bacterial and fungal communities to extreme desiccation and rewetting. *ISME J.* 7, 2229–2241. doi: 10.1038/ismej.2013.104

Benjamini, Y., and Hochberg, Y. (1995). Controlling the false discovery rate: a practical and powerful approach to multiple testing. *J.R. Stat. Soc.: Series B (Methodological)* 57, 289–300. doi: 10.1111/j.2517-6161.1995.tb02031.x

Benucci, G. M. N., Wang, X., Zhang, L., Bonito, G., and Yu, F. (2022). Yeast and lactic acid bacteria dominate the core microbiome of fermented "hairy" tofu (Mao tofu). *Diversity* 14, 207. doi: 10.3390/d14030207

Benucci, G. M. N., Beschoren da Costa, P., Wang, X., and Bonito, G. (2023). Stochastic and deterministic processes shape bioenergy crop microbiomes along a vertical soil niche. *Environ. Microbiol.* 25, 352–366. doi: 10.1111/1462-2920.16269

Bickel, S., and Or, D. (2020). Soil bacterial diversity mediated by microscale aqueous-phase processes across biomes. *Nat. Commun.* 11, 13966. doi: 10.1038/s41467-019-13966-w

Carson, J. K., Gonzalez-Quiñones, V., Murphy, D. V., Hinz, C., Shaw, J. A., and Gleeson, D. B. (2010). Low pore connectivity increases bacterial diversity in soil. *Appl. Environ. Microbiol.* 76, 3936–3942. doi: 10.1128/AEM.03085-09

Chenu, C., Hassink, J., and Bloem, J. (2001). Short-term changes in the spatial distribution of microorganisms in soil aggregates as affected by glucose addition. *Biol. Fertil. Soils* 34, 349–356. doi: 10.1007/s003740100419

Cole, J. R., Wang, Q., Fish, J. A., Chai, B., McGarrell, D. M., Sun, Y., et al. (2014). Ribosomal database project: data and tools for high throughput rRNA analysis. *Nucleic Acids Res.* 42, D633–D642. doi: 10.1093/nar/gkt1244

de Graaff, M.-A., Hornslein, N., Throop, H. L., Kardol, P., and van Diepen, L. T. A. (2019). "Chapter one - effects of agricultural intensification on soil biodiversity and implications for ecosystem functioning: a meta-analysis," in *Adv. Agron,* Sparks, D. L. (Cambridge: Academic Press), 1–44. doi: 10.1016/bs.agron.2019.01.001

Dechesne, A., Pallud, C., Debouzie, D., Flandrois, J. P., Vogel, T. M., Gaudet, J. P., et al. (2003). A novel method for characterizing the microscale 3D spatial distribution of bacteria in soil. *Soil Biol. Biochem.* 35, 1537–1546. doi: 10.1016/S0038-0717(03)00243-8

Edgar, R. (2016). *UCHIME2: Improved Chimera Prediction for Amplicon Sequencing*. Available online at: https://www.biorxiv.org/content/10.1101/074252v1#:~:text=Abstract,denoising%E2%80%9D)%20and%20other%20applications

Edgar, R. C. (2013). UPARSE: highly accurate OTU sequences from microbial amplicon reads. *Nat. Methods* 10, 996–998. doi: 10.1038/nmeth.2604

Edgar, R. C., and Flyvbjerg, H. (2015). Error filtering, pair assembly and error correction for next-generation sequencing reads. *Bioinformatics* 31, 3476–3482. doi: 10.1093/bioinformatics/btv401

Epp Schmidt, D., Dlott, G., Cavigelli, M., Yarwood, S., and Maul, J. E. (2022). Soil microbiomes in three farming systems more affected by depth than farming system. *Appl. Soil Ecol.* 173, 104396. doi: 10.1016/j.apsoil.2022.104396

Fu, L., Niu, B., Zhu, Z., Wu, S., and Li, W. (2012). CD-HIT: accelerated for clustering the next-generation sequencing data. *Bioinformatics* 28, 3150–3152. doi: 10.1093/bioinformatics/bts565

Golparvar, A., Kästner, M., and Thullner, M. (2021). Pore-scale modeling of microbial activity: what we have and what we need. *Vadose Zone J.* 20. doi: 10.1002/vzj2.20087

Harvey, H. J., Mitzakoff, A. M. T., Wildman, R. D., Mooney, S. J., and Avery, S. V. (2021). Microbial metal resistance within structured environments is inversely related to environmental pore size. *Appl. Environ. Microbiol.* 87, e0100521. doi: 10.1128/AEM.01005-21

Inkscape Project (2020). *Inkscape*. Available online at: https://inkscape.org (accessed April, 2023).

Kassambara, A. (2020). *ggpubr: "ggplot2" Based Publication Ready Plots. R package version 0.4.0.* Available online at: https://CRAN.R-project.org/package=ggpubr (accessed April, 2023).

Kim, K., Guber, A., Rivers, M., and Kravchenko, A. (2020). Contribution of decomposing plant roots to N2O emissions by water absorption. *Geoderma* 375, 114506. doi: 10.1016/j.geoderma.2020.114506

Kögel-Knabner, I., Wiesmeier, M., and Mayer, S. (2023). Mechanisms of soil organic carbon sequestration and implications for management. *Burleigh Dodds Series in Agricult. Sci.* 2, 36. doi: 10.19103/AS.2022.0106.02

Kõljalg, U., Nilsson, R. H., Abarenkov, K., Tedersoo, L., Taylor, A. F. S., Bahram, M., et al. (2013). Towards a unified paradigm for sequence-based identification of fungi. *Mol. Ecol.* 22, 5271–5277. doi: 10.1111/mec.12481

Kozich, J. J., Westcott, S. L., Baxter, N. T., Highlander, S. K., and Schloss, P. D. (2013). Development of a dual-index sequencing strategy and curation pipeline for analyzing amplicon sequence data on the MiSeq Illumina sequencing platform. *Appl. Environ. Microbiol.* 79, 5112–5120. doi: 10.1128/AEM.01043-13

Kravchenko, A. N., and Guber, A. K. (2017). Soil pores and their contributions to soil carbon processes. *Geoderma* 287, 31–39. doi: 10.1016/j.geoderma.2016.06.027

Kravchenko, A. N., Toosi, E. R., Guber, A. K., Ostrom, N. E., Yu, J., Azeem, K., et al. (2017). Hotspots of soil N2O emission enhanced through water absorption by plant residue. *Nat. Geosci.* 10, 496–500. doi: 10.1038/ngeo2963

Lal, R. (1997). Residue management, conservation tillage and soil restoration for mitigating greenhouse effect by CO2-enrichment. *Soil Tillage Res.* 43, 81–107. doi: 10.1016/S0167-1987(97)00036-6

Lehtinen, T., Schlatter, N., Baumgarten, A., Bechini, L., Krüger, J., Grignani, C., et al. (2014). Effect of crop residue incorporation on soil organic carbon and greenhouse gas emissions in European agricultural soils. *Soil Use Manage.* 30, 524–538. doi: 10.1111/sum.12151

Leinonen, R., Sugawara, H., Shumway, M., and International Nucleotide Sequence Database Collaboration (2011). The sequence read archive. *Nucleic Acids Res.* 39, D19–21. doi: 10.1093/nar/gkq1019

Liber, J., Bonito, G., and Benucci, G. M. N. (2021). CONSTAX2: Improved taxonomic classification of environmental DNA markers. *Bioinformatics* 37, 3941–3943. doi: 10.1093/bioinformatics/btab347

Liu, D. L., Zeleke, K. T., Wang, B., Macadam, I., Scott, F., and Martin, R. J. (2017). Crop residue incorporation can mitigate negative climate change impacts on crop yield and improve water use efficiency in a semiarid environment. *Eur. J. Agron.* 85, 51–68. doi: 10.1016/j.eja.2017.02.004

Long, T., and Or, D. (2005). Aquatic habitats and diffusion constraints affecting microbial coexistence in unsaturated porous media. *Water Resour. Res.* 41, 3796. doi: 10.1029/2004WR003796

Long, T., and Or, D. (2009). Dynamics of microbial growth and coexistence on variably saturated rough surfaces. *Microb. Ecol.* 58, 262–275. doi: 10.1007/s00248-009-9510-3

Martin, M. (2011). Cutadapt removes adapter sequences from high-throughput sequencing reads. *EMBnet J.* 17, 10. doi: 10.14806/ej.17.1.200

McDonald, D., Clemente, J. C., Kuczynski, J., Rideout, J. R., Stombaugh, J., Wendel, D., et al. (2012). The biological observation matrix (BIOM) format or: how I learned to stop worrying and love the ome-ome. *Gigascience* 1, 7. doi: 10.1186/2047-217X-1-7

McMurdie, P. J., and Holmes, S. (2013). phyloseq: an R package for reproducible interactive analysis and graphics of microbiome census data. *PLoS ONE.* 8, e61217. doi: 10.1371/journal.pone.0061217

McMurdie, P. J., and Holmes, S. (2014). Waste not, want not: why rarefying microbiome data is inadmissible. *PLoS Comput. Biol.* 10, e1003531. doi: 10.1371/journal.pcbi.1003531

Miguez, F. E., and Bollero, G. A. (2005). Review of corn yield response under winter cover cropping systems using meta-analytic methods. *Crop Sci.* 45, 2318–2329. doi: 10.2135/cropsci2005.0014

Mummey, D. L., and Stahl, P. D. (2004). Analysis of soil whole- and inner-microaggregate bacterial communities. *Microb.Ecol.*48, 41–50. doi: 10.1007/s00248-003-1000-4

Nunan, N., Schmidt, H., and Raynaud, X. (2020). The ecology of heterogeneity: soil bacterial communities and C dynamics. Philos. T. R. *Soc. B* 375, 20190249. doi: 10.1098/rstb.2019.0249

Oksanen, J., Blanchet, F. G., Friendly, M., Kindt, R., Legendre, P., McGlinn, D., et al. (2019). *vegan: Community Ecology Package, R package version 2.5-6.* Available online at: https://CRAN.R-project.org/package=vegan (accessed April, 2023).

Põlme, S., Abarenkov, K., Henrik Nilsson, R., Lindahl, B. D., Clemmensen, K. E., Kauserud, H., et al. (2020). FungalTraits: a user-friendly traits database of fungi and fungus-like stramenopiles. *Fungal Divers.* 105, 1–16. doi: 10.1007/s13225-020-00466-2

Powlson, D. S. (1980). The effects of grinding on microbial and non-microbial organic matter in soil. *J. Soil Sci.* 31, 77–85. doi: 10.1111/j.1365-2389.1980.tb02066.x

R Core Team. (2023). *R: A Language and Environment for Statistical Computing.* Vienna, Austria: R Foundation for Statistical Computing. Available online at: https://www.R-project.org/ (accessed April, 2023).

Rieke, E. L., Soupir, M. L., Moorman, T. B., Yang, F., and Howe, A. C. (2018). Temporal dynamics of bacterial communities in soil and leachate water after swine manure application. *Front. Microbiol.* 9, 3197. doi: 10.3389/fmicb.2018.03197

Robertson, G. P., and Hamilton, S. K. (2015). "Long-term ecological research at the Kellogg Biological Station LTER site.," in *The Ecology of Agricultural Landscapes: Long-Term Research on the Path to Sustainability,* 1, 32. Available online at: https://books.google.com/books?hl=en&lr=&id=WPBxBgAAQBAJ&oi=fnd&pg=PA1&dq=Long-term$+$ecological$+$research$+$in$+$agricultural$+$landscapes$+$at$+$the$+$Kellogg$+$Biological$+$Station$+$LTER$+$site$+$conceptual$+$and$+$experimental$+$framework&ots=45cabs3V7D&sig=jZl52DGI7gAVCG-JIa-bov2g7vQ (accessed April, 2023).

Rognes, T., Flouri, T., Nichols, B., Quince, C., and Mah,é, F. (2016). VSEARCH: a versatile open source tool for metagenomics. *PeerJ.* 4, e2584. doi: 10.7717/peerj.2584

Scholberg, J. M. S., Dogliotti, S., Leoni, C., Cherr, C. M., Zotarelli, L., and Rossing, W. A. H. (2010). "Cover crops for sustainable agrosystems in the Americas," in *Genetic Engineering, Biofertilisation, Soil Quality and Organic Farming*, Lichtfouse, E. (ed.). (Dordrecht: Springer Netherlands), 23–58. doi: 10.1007/978-90-481-8741-6_2

Syswerda, S. P., Corbin, A. T., Mokma, D. L., Kravchenko, A. N., and Robertson, G. P. (2011). Agricultural management and soil carbon storage in surface vs. Deep layers. *Soil Sci. Soc. Am. J.* 75, 92–101. doi: 10.2136/sssaj2009.0414

Tiedje, J. M., Cho, J. C., Murray, A., Treves, D., Xia, B., and Zhou, J. (2001). "Soil teeming with life: new frontiers for soil science," in *Sustainable Management of Soil Organic Matter* (UK: CABI Publishing), 393–425. doi: 10.1079/9780851994659.0393

Toosi, E. R., Kravchenko, A. N., Guber, A. K., and Rivers, M. L. (2017). Pore characteristics regulate priming and fate of carbon from plant residue. *Soil Biol. Biochem.* 113, 219–230. doi: 10.1016/j.soilbio.2017.06.014

Treves, D. S., Xia, B., Zhou, J., and Tiedje, J. M. (2003). A two-species test of the hypothesis that spatial isolation influences microbial diversity in soil. *Microb. Ecol.* 45, 20–28. doi: 10.1007/s00248-002-1044-x

Vandepol, N., Liber, J., Yocca, A., Matlock, J., Edger, P., and Bonito, G. (2022). Linnemannia elongata (Mortierellaceae) stimulates Arabidopsis thaliana aerial growth and responses to auxin, ethylene, and reactive oxygen species. *PLoS ONE.* 17, e0261908. doi: 10.1371/journal.pone.0261908

Wang, Q., Garrity, G. M., Tiedje, J. M., and Cole, J. R. (2007). Naive Bayesian classifier for rapid assignment of rRNA sequences into the new bacterial taxonomy. *Appl. Environ. Microbiol.* 73, 5261–5267. doi: 10.1128/AEM.00062-07

Wang, W., Kravchenko, A. N., Johnson, T., Srinivasan, S., Ananyeva, K. A., Smucker, A. J. M., et al. (2013). Intra-aggregate pore structures and escherichia coli distribution by water flow within and movement out of soil macroaggregates. *Vadose Zone J.* 1, 12. doi: 10.2136/vzj2013.01.0012

Wickham, H. (2016). *ggplot2: Elegant Graphics for Data Analysis*. New York: Springer-Verlag New York. Available online at: https://ggplot2.tidyverse.org (accessed April, 2023). doi: 10.1007/978-3-319-24277-4

Wolf, A. B., Vos, M., de Boer, W., and Kowalchuk, G. A. (2013). Impact of matric potential and pore size distribution on growth dynamics of filamentous and non-filamentous soil bacteria. *PLoS ONE.* 8, e83661. doi: 10.1371/journal.pone.0083661

Wright, D. A., Killham, K., Glover, L. A., and Prosser, J. I. (1995). Role of pore size location in determining bacterial activity during predation by protozoa in soil. *Appl. Environ. Microbiol.* 61, 3537–3543. doi: 10.1128/aem.61.10.3537-3543.1995

Xia, Q., Zheng, N., Heitman, J. L., and Shi, W. (2022). Soil pore size distribution shaped not only compositions but also networks of the soil microbial community. *Appl. Soil Ecol.* 170, 104273. doi: 10.1016/j.apsoil.2021.104273

Zhang, J., Kobert, K., Flouri, T., and Stamatakis, A. (2014). PEAR: a fast and accurate Illumina Paired-End reAd mergeR. *Bioinformatics* 30, 614–620. doi: 10.1093/bioinformatics/btt593

frontiers | Frontiers in Microbiology

TYPE Original Research
PUBLISHED 21 September 2023
DOI 10.3389/fmicb.2023.1163444

OPEN ACCESS

EDITED BY
Hui Li,
Institute of Applied Ecology, Chinese Academy of Sciences (CAS), China

REVIEWED BY
Xin Sui,
Heilongjiang University, China
Jianyong Wang,
Northeast Normal University, China

*CORRESPONDENCE
Fan Yang
✉ yangfan@iga.ac.cn
Zhichun Wang
✉ wangzhichun@iga.ac.cn

RECEIVED 10 February 2023
ACCEPTED 15 August 2023
PUBLISHED 21 September 2023

CITATION
Guo L, Tóth T, Yang F and Wang Z (2023) Effects of different types of vegetation cover on soil microorganisms and humus characteristics of soda-saline land in the Songnen Plain. *Front. Microbiol.* 14:1163444. doi: 10.3389/fmicb.2023.1163444

Effects of different types of vegetation cover on soil microorganisms and humus characteristics of soda-saline land in the Songnen Plain

Liangliang Guo[1,2], Tibor Tóth[3], Fan Yang[1]* and Zhichun Wang[1]*

[1]Northeast Institute of Geography and Agroecology, Chinese Academy of Sciences, Changchun, China, [2]University of Chinese Academy of Sciences, Beijing, China, [3]Centre for Agricultural Research, Institute for Soil Sciences, Budapest, Hungary

Introduction: In the soda-saline grasslands of the Songnen Plain, Jilin Province, China, the prohibition of grazing has led to significant changes in plant communities and soil properties. However, the intricate interplay between soil physical and chemical attributes, the soil microbial community, and their combined influence on soil humus composition remains poorly understood.

Methods: Our study aimed to evaluate the impact of natural vegetation restoration on soil properties, microbial community diversity, and composition in the soda-saline soil region of the Songnen Plain. We conducted assessments of soil physical and chemical properties, analyzed community diversity, and composition at a soil depth range of 0–20 cm. The study covered soils with dominant soda-saline vegetation species, including *Suaeda glauca* Bunge, *Puccinellia chinampoensis* Ohwi, *Chloris virgata* Swarta, *Phragmites australis* (Clay.), *Leymus chinensis* (Trin.), and Tzvelev. We compared these vegetated soils to bare land devoid of any plants.

Results: We found that soil organic content (SOC) in vegetation restoration areas was higher than in bare land, with SOC content varying between 3.64 and 11.15 g/kg in different vegetated areas. Notably, soil pH emerged as a pivotal factor, explaining 11.4% and 12.2% of the variance in soil bacteria and fungi, respectively. There were correlations between SOC content and the relative abundance of specific microbial groups, with Acidobacteria and Mortierella showing a positive correlation, while Actinobacteria, Gemmatimonadetes, and Ascomycota exhibited significant negative correlations with SOC.

Discussion: The disparities in SOC composition and content among the soda-saline vegetation types were primarily attributed to variations in pH. Consequently, reducing soil pH is identified as a critical step in the process of vegetation restoration in soda-saline land. Prohibiting grazing has the potential to increase soda-saline SOC content and enhance microbial diversity, with *Leymus chinensis* and *Phragmites australis* showing particularly promising results in terms of higher SOC carbon content and microbial diversity.

KEYWORDS

vegetation restoration, physical properties of soil, soil humus carbon component, soda-saline soil, soil microorganism

1. Introduction

The western part of the Songnen Plain is located in the northeast of China. It is one of the three major soda-saline soil regions in the world (Yang et al., 2016), with an area of 3.42×10^6 ha (Wang et al., 2003). $NaHCO_3$ and Na_2CO_3 are the main salts there, with soil pH mostly above 8.5, often ranging between 9.0 and 10.5, which is the characteristic pH value of severe soda-saline land (Chi et al., 2011). In the past, due to long-term salinization and human disturbances, the grassland in this region has suffered severe degradation, leading to a decline in soil productivity and almost no surface vegetation (Zhao et al., 2022). To restore the damaged ecosystem, a no-grazing policy has been implemented since 2002, allowing natural vegetation to regrow and restore soil quality and functionality. After years of regeneration, there has been an increase in vegetation cover, and a relatively stable natural ecology has been established through long-term succession. Additionally, diverse plant communities have emerged due to variations in microtopography, habitats, and degrees of degradation. Plants such as *Suaeda salsa*, *Puccinellia chinampoensis*, *Phragmites australis*, *Chloris virgata*, and *Leymus chinensis* exhibit a patchy distribution across plots with different levels of salinization (Figure 1).

The status and movement of soil water and salt determine the formation of different vegetation communities, while the change in soil salinity is influenced by various factors, such as climate conditions, surface and subsurface water, vegetation types, and field management. Vegetation growth also contributes to the accumulation of soil organic matter (SOM) (Mahmood et al., 1994). SOM is a mixture of special polymer compounds formed by animal and plant residues in the soil under the action of soil organisms (Kögel-Knabner, 2002). The main active components of SOM are humic substances (HS), which are produced by chemical activities in natural environments, including aquatic ecosystems, soils, and sediments, and have a major impact on biogeochemical processes (DiDonato et al., 2016; Zaiets and Poch, 2016). HS can be further classified into the groups of humic acid (HA), fulvic acid (FA), and humin (HM) (Kou et al., 2022). HA and FA are the most active components in soil HS and play important roles in enhancing soil aggregation, maintaining soil fertility, increasing soil buffering capacity, and regulating pH (Lehmann and Kleber, 2015). Different soil types have different HA/FA ratios (Klučáková, 2018; Ampong et al., 2022). At the same time, this ratio is related to soil fertility (Kononova, 2013). SOM belongs to the soil solid phase, and most of it combines with minerals to form organomineral complexes or microaggregates of different sizes. High soil salinity has a certain impact on the structure, composition, and characteristics of soil humus, which are closely related to the properties and fertility of the soil. Therefore, the study of the correlation between salinity and humus composition in soda-saline soil is of great theoretical and practical significance for the formation, regeneration, and decomposition of humus in soda-saline soil, revealing the migration and transmission mechanisms of substances between saline soil and vegetation types.

The soil microbiome plays a pivotal role in soil ecological processes (Hartmann and Six, 2022). Soil electrical conductivity and soil sodium ion content are the primary factors influencing the structure and composition of soil bacterial communities in soda-saline land (Wang S. et al., 2020). Notably, soil salinity not only significantly diminishes bacterial richness but also affects bacterial community composition (Guan et al., 2021). In a study by Chang et al. (2022), it was revealed that soda-saline soils covered with natural vegetation have positive effects on soil physicochemical properties and prokaryotic communities, as opposed to highly saline bare sodic spots. Generally, diverse plant communities create distinct soil environments, leading to shifts in soil microbial communities (Wang X. et al., 2020; Qiu et al., 2022). These alterations in microbial diversity and community composition undoubtedly influence the interplay between the microbiome and nutrient cycling, subsequently affecting plant growth in saline soils.

Conversely, certain fungi, such as mycorrhizae, possess the capacity to assist plants in resource acquisition and high salinity tolerance within stressful settings (Wang et al., 2019). Moreover, fungi collaborate with bacteria to uphold the stability of soil microbial networks and contribute to ecosystem functionalities (Li et al., 2022). Revegetation affects land productivity and the hydrological cycle and changes the structure and function of soil microbial communities and humus. Soil microorganisms and humus are the main components of soil organic carbon, and they play an important role in the soil carbon cycle and global carbon balance. However, there is still a lack of systematic research on the changes and mechanisms of soil microorganisms and humus in different stages of vegetation degradation in the Songnen Plain.

Based on the aforementioned considerations, we postulate that soils encompassing various plant communities exhibit distinct organic matter components and diminished salt stress. Consequently, the soil within diverse plant communities harbors greater microbial diversity functionality than the highly saline and alkaline barren soil patches. To scrutinize this conjecture, we studied the diversity and composition of both bacterial and fungal communities in soils beneath five halophytic communities within a soda-saline ecosystem. Our analysis encompassed the measurements of soil pH, electrical conductivity, salinity, organic matter composition, salt stress, and microbial functions. We quantified the ratio of soil bacteria to archaea and assessed fungal diversity and composition using advanced high-throughput sequencing techniques. Notably, we identified indicator taxa that exhibited a significant association with specific habitats. Primarily, the present study aimed to explore the impact of distinct vegetation types on organic matter composition and the interrelationship of microorganisms within soda-saline soils.

2. Materials and methods

2.1. Site description

The study area is situated in the Da'an Sodic Land Experimental Ecological Station (45°53′-47°8′N, 123°45′-124°42′E), located in the west of the Songnen Plain. It has an average elevation of 152 m and an annual average temperature of 3.6–4.4°C. The monthly average temperature stays above 0°C from April to October. Soda-saline meadow soil is the dominant soil type. Due to grazing before 2002, the experimental area has been exposed to heavy salinity for a long time, characterized by severe grassland degradation and low vegetation cover. Since early 2002, grazing has been prohibited on grasslands,

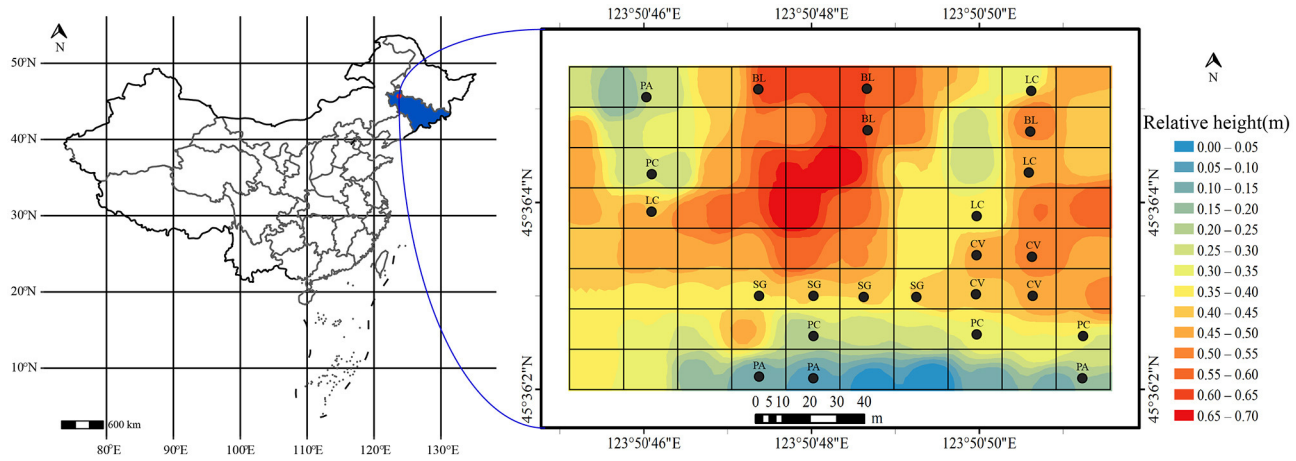

FIGURE 1
The location of the experiment and the distribution of sampling squares. BL, bare land without vegetation on the surface; CV, *Chloris virgata*; LC, *Leymus chinensis*; PA, *Phragmites australis*; PC, *Puccinellia chinampoensis*; SG, *Suaeda glauca*.

leading to a subsequent increase in vegetation coverage. Over the course of several years, through long-term succession, a relatively stable and natural ecological system has been established. Additionally, diverse plant communities arose as a result of variations in minor topography, habitat, and degree of degradation.

We divided the study site into 80 plots of 15 × 15 m each, which were randomly assigned to one of five treatments (Figure 1). The study site was 120 m wide (1.8×10^4 m^2). The following six vegetation communities were distinguished and sampled, I. Bare land (BL) without vegetation on the surface; II. *Chloris virgata* (CV); III. *Leymus chinensis* (LC); IV. *Phragmites australis* (PA); V. *Puccinellia chinampoensis* (PC); VI. *Suaeda glauca* (SG); see details in Supplementary Table S1.

2.2. Soil sampling

Soil samples were collected in September 2022, when vegetation matures. Plant residues were removed prior to sampling to avoid aboveground disturbance. Soil samples were collected using the five-point sampling method. Five cylindrical soil samples were randomly drilled in each square with a diameter of 5 cm and a depth of 20 cm. They were broken up and thoroughly mixed into a composite soil sample, with each square replicated four times. Finally, 24 mixed soil samples (6 vegetation variants × 4 replicates) were obtained. Shoots, roots, and gravel were manually removed from the soil samples. Soil samples were then passed through a 2-mm sieve and divided into three equal aliquots. The first one was air-dried at room temperature and used for physicochemical analysis; the second sample was immediately frozen at −80°C and used for microbiological analysis; and the third sample was also air-dried at room temperature but kept in a dark and dry place for backup purposes.

2.3. Soil analysis

Soil bulk density was measured using the ring knife method. The analysis and determination methods for soil humus and optical properties were adopted from the study by Dou (2010). Specific experimental operations were as follows: 5.00 g of oil passed through a 0.25-millimeter sieve was weighed into a low-speed centrifuge tube; 30 ml of distilled water was added and stirred evenly with a glass rod; the tube was then placed on a constant temperature water bath oscillator (70 ± 2°C, 145 r/min) for 1 h and centrifuged at a low speed of 3,500 r/min for 15 min. The supernatant was filtered into a 50-ml volumetric bottle with a quantitative filter paper, and the residue was washed once with 20 ml distilled water to obtain WSS (water-extracted organic matter). Moreover, 30 ml of lye mixed from 0.1 mol/L NaOH and $Na_4P_2O_7$ was added to the residue in the centrifugation tube, mixed evenly with a glass rod, and then extracted for 1 h by shaking on a constant temperature water bath oscillator (70 ± 2°C, 145 r/min). After the removal, it was centrifuged at 3,500 r/min for 15 min, filtered with a quantitative filter paper into a 50-ml volumetric bottle, and the residue was washed with 20-ml mixed lye, filtered into the volumetric bottle, and filled up with distilled water to a constant volume. The soluble solution is HE (extractable humus substance). Then, 30 ml of the HE solution was poured into a 50-ml Erlenmeyer flask, and 0.5 mol/L of H_2SO_4 solution was added to adjust the pH to 1.0–1.5. The acidified solution was incubated in a water bath at 60–70°C for 2 h and left to rest overnight. The following day, the solution was filtered with a quantitative filter paper, the precipitate was HA (humic acid), and the solution was FA (fulvic acid). The HA precipitate was washed three times with a 0.05-mol/L H_2SO_4 solution, and the solution was discarded. Finally, the HA precipitate was dissolved in a warm (60°C) 0.05-mol/L NaOH solution in a 50-ml volumetric bottle and finally dissolved in a 0.05-mol/L NaOH solution. The residue in the centrifuge tube was humin (HM), which was washed in distilled water three times. After centrifugation, the precipitate was dried, finely ground, and screened for determination. FA and HA

were measured using a Shimadzu TOC analyzer (TOC-L, CPH). Analysis of SOM and HM was performed using the K_2CrO_7-H_2SO_4 oxidation method (Walkley and Black, 1934).

The PQ value is an indicator of the degree of humification in the soil. It is commonly used to assess the maturity and stability of soil organic matter. The PQ value is calculated by dividing the content of humic acid (HA) by the sum of humic acid (HA) and fulvic acid (FA). A higher PQ value indicates a higher proportion of humic acid in the organic matter, indicating a higher degree of humification. The changes in PQ value can reflect the processes of organic matter formation and decomposition in the soil and the influence of environmental factors such as soil texture and vegetation type on organic matter. The calculation formula is as follows:

$$PQ = \frac{HA}{HA + FA} \quad (1)$$

A 1:5 soil-water ratio was used to extract and analyze water-soluble salts. pH, EC, Na^+, K^+, Ca^{2+}, Mg^{2+}, CO_3^{2-}, HCO_3^-, Cl^-, SO_4^{2-} and other major ion concentrations were determined. A conductivity meter was used to measure $EC_{1:5,}$ and a pH meter was used to measure soil $pH_{1:5}$. Na^+, K^+, $Ca^{2+,}$ and Mg^{2+} ion concentrations were determined using atomic absorption spectrophotometry, and CO_3^{2-} and HCO_3^- were determined using double indicator neutralization titration. Cl^- ions were determined using silver nitrate titration and SO_4^{2-} ions using barium sulfate turbidimetry.

The soil sodium adsorption ratio (SAR) is an indicator that measures the relative proportion between the content of sodium ion and the content of other ions, such as calcium and magnesium, in the soil. It can be used to assess the degree of soil salinization and alkalization. SAR is calculated using Equation 2 (Chi et al., 2011):

$$SAR = \frac{[Na^+]}{\sqrt{([Ca^{2+}] + [Mg^{2+}])/2}}, \quad (2)$$

where $[Na^+]$, $[Ca^{2+}]$, and $[Mg^{2+}]$ are the corresponding ion concentrations in $mmol_c/L$, and the unit of SAR is $(mmol_c/L)$.

Total alkalinity was calculated using the following formula:

$$\text{Total alkalinity} = CO_3^{2-} + HCO_3^- (mmol_c/L) \quad (3)$$

Mean weight diameter (MWD) stands for mean weight diameter, which is a measure of soil aggregate stability. Soil aggregates are groups of soil particles that are bound together by various forces. Soil aggregate stability indicates how well the aggregates resist breaking apart when exposed to external forces, such as water or wind erosion. Soil aggregate stability is important for soil structure, water infiltration, nutrient cycling, and plant growth. The wet sieving method was used to divide soil aggregates into four size fractions: (i) macroaggregates (>2.0 mm), (ii) small aggregates (0.25–2.0 mm), (iii) microaggregates (0.053–0.25 mm), and (iv) silt and clay (<0.053 mm). Approximately 100 g of air-dried soil moistened to field capacity after soaking was immersed in water over a sieve (2 mm, 1 mm, 0.25 mm, and 0.053 mm), oscillating at a frequency of 30 times per minute for 2 min with a vertical amplitude of 3 cm. Soil aggregates on the sieve were collected, dried at 50°C for 3 days, and weighed. Material passing through the 0.053-mm sieve was not collected but calculated by subtracting the remaining weight from the total 100 g.

The MWD was calculated using Equation 4:

$$MWD = \sum_{i=1}^{n} Xi\ Wi, \quad (4)$$

where Xi is the average diameter (mm) of sieved aggregates in any particle size range and Wi is the weight percentage (%) of aggregates in any particle size range, where i = 1, 2, …, 4 represent the aggregate size classes such as >2.0 mm, 0.25–2.0 mm, 0.053–0.25 mm, and <0.053 mm, respectively (Kemper and Rosenau, 1986).

2.4. Soil DNA extraction, PCR amplification, and Illumina sequencing

Nucleic acid was extracted using the OMEGA Soil DNA Kit (D5625-01) (Omega Bio-Tek, Norcross, GA, USA). For the extracted DNA, 0.8% agarose gel electrophoresis was carried out to determine the molecular size, and a UV spectrophotometer was used to quantify the DNA. In this analysis, the 16S rRNA gene was amplified by PCR using the primer pairs 341F (5′-barcode + CCTACGGGNGGCWGCAC-3′), 806R (5′-GGACTACHVGGGTWTCTAAT-3′). The ITS2 rDNA gene was amplified by PCR using the primer pairs ITS3-KYO2 (GATGAAGAACGYAGYRAA) and ITS4 (TCCTCCGCTTATTGATATGC). Later, 2×250-bp paired-end sequencing was performed on the Illumina NovaSeq machine using the NovaSeq 6000 SP Reagent Kit (500 cycles).

We implemented a complete pipeline using the DADA2 R package (Callahan et al., 2016) (version 1.14) to convert pair-ended fastq files from the sequencer to merged, denoised, chimera-free, and inferred sample sequences. Paired-end denoised reads were merged into raw Amplifier Sequence Variant (ASV) with a minimum overlap of 12 bp. Chimera sequences were identified and deleted by the UCHIME algorithm (Edgar et al., 2011). After the removal of chimeras, the denoised, chimera-free ASV sequences and their abundances were output. Finally, a naive Bayesian model with a confidence threshold value of 0.8 was used to classify the representative ASV sequences into different organisms using an RDP classifier (Wang et al., 2007) (version 2.2) based on the SILVA database (Pruesse et al., 2007) (version138.1) or the ITS2 UNITE (Unified System for the DNA-based fungal species linked to the classification) database (Ankenbrand et al., 2015) (version update_2015). We excluded chloroplasts, mitochondria, and rare ASVs (relative abundance <0.005%) of bacteria and archaea.

2.5. Statistical analysis

Differences in the physicochemical properties and the microbial characteristics of soil under different plant communities were compared using a one-way analysis of variance and LSD tests. To meet the statistical premise of homoscedasticity of data, the data were passed through Levene's test based on the

raw or log-transformed data before the ANOVA and LSD tests. The correlation between them was analyzed using Pearson correlation analysis. The R (4.1.3) "linkET" package (https://github.com/Hy4m/linkET) was used to plot heatmaps. The R "vegan" package was used to perform principal coordinate analysis (PCoA) to reveal differences in soil bacterial communities under different communities, and the Mantel test and redundancy analysis (RDA) were performed to investigate the relationship between environmental factors and bacterial and fungi community structure. Permutational multivariate analysis of variance (PERMANOVA) was performed on the Bray-Curtis distance using Adonis from the vegan package (https://github.com/vegandevs/vegan). Variance partitioning was analyzed using the varpart function from the vegan package to assess the relative effects of different plant community types, soil properties, and electrical conductivity on changes in community composition. Indicator species analysis was performed using the indicspecies package to identify taxa significantly associated with a given habitat at the ASV level (https://github.com/cran/indicspecies), and the significance of the association was evaluated at a false discovery rate (FDR) with a corrected p-value of <0.05 (Benjamini and Hochberg, 1995).

3. Results

3.1. Soil properties of different plant communities

Soil physical and chemical properties under the investigated plant communities differed significantly (Table 1). The pH, EC, SAR, total alkalinity, and bulk density of LC and PA were significantly lower than those of other plant communities. LC and PA significantly increased the MWD of the soil. The soil organic carbon content under different vegetation communities varied from 3.64 to 11.15 g/kg, and the soil organic carbon content of the LC community was the largest. The trend of water-soluble organic carbon (WSS) content differed from that of organic carbon, and the WSS content was higher in PA and BL. The largest constituent of organic matter was humin, and its content under LC was the highest. However, the humin content under PC was significantly higher than that under PA. Fulvic acid and humic acid contents were significantly different in under-investigated plant communities, and their content under LC was the highest. The PQ ratio, which indicates the degree of humification of soil organic matter, ranged from 0.53 to 0.63 among different plant communities. LC had the highest PQ ratio (0.63), indicating a higher degree of humification and a higher quality of humus, while PA had the lowest PQ ratio (0.53), indicating a lower degree of humification and a lower quality of humus.

3.2. Soil bacterial community composition and diversity

There are 36 phyla of bacterial communities in the soil of different plant communities, mainly composed of Proteobacteria (20.2%), Actinobacteria (12.84%), Bacteroidetes (11.96%), Acidobacteria (9.16%), Gemmatimonadetes (8.88%), Planctomycetes (8.87%), Firmicutes (5.73%), and Chloroflexi (5.15%). Eleven phyla of fungi were identified, with the most prevalent being Ascomycota (61.77%), Mortierellomycota (10.69%), and Basidiomycota (5.26%). Among bacteria, the relative abundance of Actinobacteria in LC, CV, and PA was significantly decreased and Acidobacteria was significantly increased in LC and PA community soils (Figure 2). In addition, Verrucomicrobia and Patescibacteria were increased in LC soil. The abundance of Bacteroidetes and Gemmatimonadetes was highest in SG soil. Most of the fungi belonged to Ascomycota, especially in SG and CV community soil samples. PA and LC communities promoted the abundance of Mortierellomycota, and BL provided the highest abundance of Mucoromycota out of all communities.

The 30 genera of bacterial and fungal communities were analyzed further to compare their relative abundance, indicator species status, and ecological functions in different plant communities. The relative abundance of the 30 most abundant genera accounted for 20.61% and 37.19% of bacterial and fungal abundance, respectively (Figure 3). Most of these genera (29 for bacteria and 29 for fungi) were also identified as indicator taxa. Abundant bacteria came from Proteobacteria, Planctomonas, Bacteroidetes, and Acidobacteria, belonging to *Halomonas*, *Nitrolancea,* and *Urania-1B-19_marine_sediment_group*. *Rhodopirellula* is a unique indicator genus of BL. Indicator species belong to the CV community, including *Pir4_lineage*, *Pseudomonas*, *Acinetobacter*, *Blastocatella*, *Stenotrophobacter*, and *Flavisolibacter*. LC has its own indicators: *Pirellula*, *RB41*, *Streptomyces*, *AKYG587,* and *Candidatus_Udaeobacter*. *Ralstonia*, *Bryobacter*, *Sphingomonas*, *Flavobacterium*, *Nitrospira*, *Terrimonas,* and *Subgroup_10* are indicator species belonging to the PA plant community. *Truepera*, *Anditalea*, *Pontibacter*, *Ilumatobacter*, *Azoarcus*, *Bacillus,* and *Luteolibacter* are the indicator species of PC. The abundant fungi come from Ascomycota, and the indicator species of the BL community include *Cercospora*, *Ascochyta*, *Cunninghamella*, *Candida,* and *Aspergillus*. *Periconia* is not an indicator species; the rest are indicator species of different plant communities.

In the soda-saline environment (Figure 4), among the bacteria, the diversity of PA was the highest, followed by LC, which was higher than that in other communities. In fungi, the diversity of LC was the highest, and the Shannon index of SG was significantly lower than that of the BL plant community. In addition, the observed species of the phylogenetic bacterial community of ASV, Fisher, Chao1, and ACE were positively correlated with the fungal community (Figure 5).

PCoA plots based on Bray-Curtis distances clearly showed that there were significant differences between fungal and bacterial soil microbial communities (Supplementary Table S2). In the case of bacteria, environmental factors explained 33.3% of the community variation, and for fungi, environmental factors explained 35.8% of the community variation. Variations in bacterial and fungal communities were mainly explained by pH. The SOC explained more variation for fungi (0.086 vs. 0.063) than bacteria (Figure 6).

3.3. Factors affecting soil organic matter in different plant communities

Pearson correlation analysis showed that Actinobacteria, Gemmatimonadetes, and Ascomycota were significantly

10.3389/fmicb.2023.1163444

TABLE 1 Soil chemical properties under different plant communities.

	BL	CV	SG	PC	PA	LC
WSS ($g \cdot kg^{-1}$)	0.17 ± 0.02^{b}	0.12 ± 0.01^{cd}	0.11 ± 0^{d}	0.11 ± 0.01^{d}	0.23 ± 0.02^{a}	0.13 ± 0.02^{c}
FA ($g \cdot kg^{-1}$)	0.19 ± 0.02^{f}	0.52 ± 0^{c}	0.44 ± 0^{d}	0.27 ± 0.03^{e}	1.11 ± 0.06^{b}	1.25 ± 0.04^{a}
HA ($g \cdot kg^{-1}$)	0.26 ± 0.02^{e}	0.65 ± 0.01^{c}	0.65 ± 0.02^{c}	0.36 ± 0.02^{d}	1.26 ± 0.17^{b}	2.13 ± 0.05^{a}
HM ($g \cdot kg^{-1}$)	2.98 ± 0.04^{e}	4.42 ± 0.23^{d}	5.68 ± 0.19^{c}	6.67 ± 0.18^{b}	5.71 ± 0.11^{c}	7.76 ± 0.19^{a}
SOC ($g \cdot kg^{-1}$)	3.64 ± 0.02^{e}	5.97 ± 0.06^{d}	7.04 ± 0.02^{c}	7.15 ± 0.05^{c}	8.24 ± 0.2^{b}	11.15 ± 0.29^{a}
PQ	0.57 ± 0.04^{bc}	0.56 ± 0.01^{bc}	0.6 ± 0.01^{ab}	0.57 ± 0.01^{bc}	0.53 ± 0.05^{c}	0.63 ± 0^{a}
pH	10.65 ± 0.05^{a}	10.42 ± 0.08^{b}	10.63 ± 0.03^{ab}	10.53 ± 0.06^{ab}	9.51 ± 0.13^{c}	9.39 ± 0.27^{c}
$EC_{1:5}$ ($dS \cdot m^{-1}$)	4.86 ± 0.84^{a}	0.87 ± 0.14^{c}	2.34 ± 0.46^{b}	1.19 ± 0.06^{c}	0.18 ± 0.04^{d}	0.18 ± 0.07^{d}
BD ($g \cdot cm^{-3}$)	1.55 ± 0.02^{a}	1.48 ± 0.04b	1.47 ± 0.03^{bc}	1.41 ± 0.05^{c}	1.33 ± 0.04^{d}	1.31 ± 0.05^{d}
Total alkalinity ($mmol_c L^{-1}$)	32.2 ± 8.84^{a}	6.85 ± 0.66^{cd}	17 ± 2.4^{b}	9.85 ± 1.09^{c}	2.3 ± 0.35^{d}	2.5 ± 0.35d
SAR ($mmol_c L^{-1}$)	28.5 ± 6.34^{a}	6.34 ± 1.37^{cd}	17.43 ± 2.23^{b}	8.19 ± 0.66^{c}	2.23 ± 0.63^{d}	2.39 ± 0.92^{d}
MWD	0.26 ± 0.01^{cd}	0.46 ± 0.03^{b}	0.19 ± 0.06^{d}	0.31 ± 0.05^{c}	0.61 ± 0.06^{a}	0.64 ± 0.04^{a}
Soil moisture content (%)	11.75 ± 2.22^{c}	14.00 ± 1.82^{c}	11.89 ± 1.44^{c}	26.01 ± 2.90^{a}	19.11 ± 1.19^{b}	23.45 ± 1.08^{a}

Values are the mean ± standard error ($n = 4$); the different letters in the same row indicate significant differences ($p < 0.05$) at different restoration types via the LSD test.
BL, bare land without vegetation on the surface; CV, *Chloris virgata*; LC, *Leymus chinensis*; PA, *Phragmites australis*; PC, *Puccinellia chinampoensis*; SG, *Suaeda glauca*; WSS, water extracted organic matter; FA, fulvic acid; HA, humic acid; HM, humin; SOC, soil organic carbon; EC, electrical conductivity; BD, bulk density; SAR, sodium adsorption ratio; and MWD, mean weight diameter.

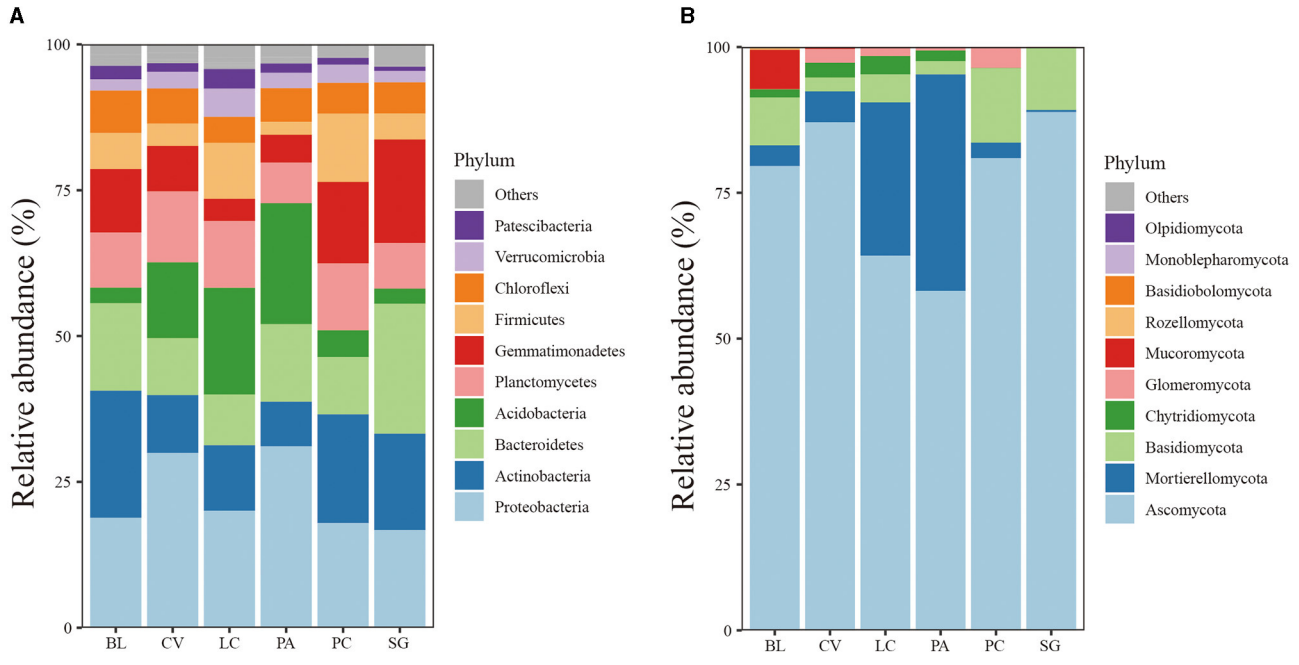

FIGURE 2
Relative abundances of the soil bacterial **(A)** and fungal communities **(B)** at the phylum level under the investigated plant communities.

negatively correlated with FA, HA, and SOC. Acidobacteria and Mortierellomycota were significantly positively correlated with WSS, FA, HA, and SOC ($p < 0.05$). Gemmatimonadetes and Ascomycota were significantly correlated with WSS (Table 2). Redundancy analysis showed that soil environmental factors and microorganisms accounted for 78.34% of the total variation in SOM components (Figure 7), and bacterial communities, pH, MWD, and fungi communities were the main factors affecting SOM components (Supplementary Figure S2).

10.3389/fmicb.2023.1163444

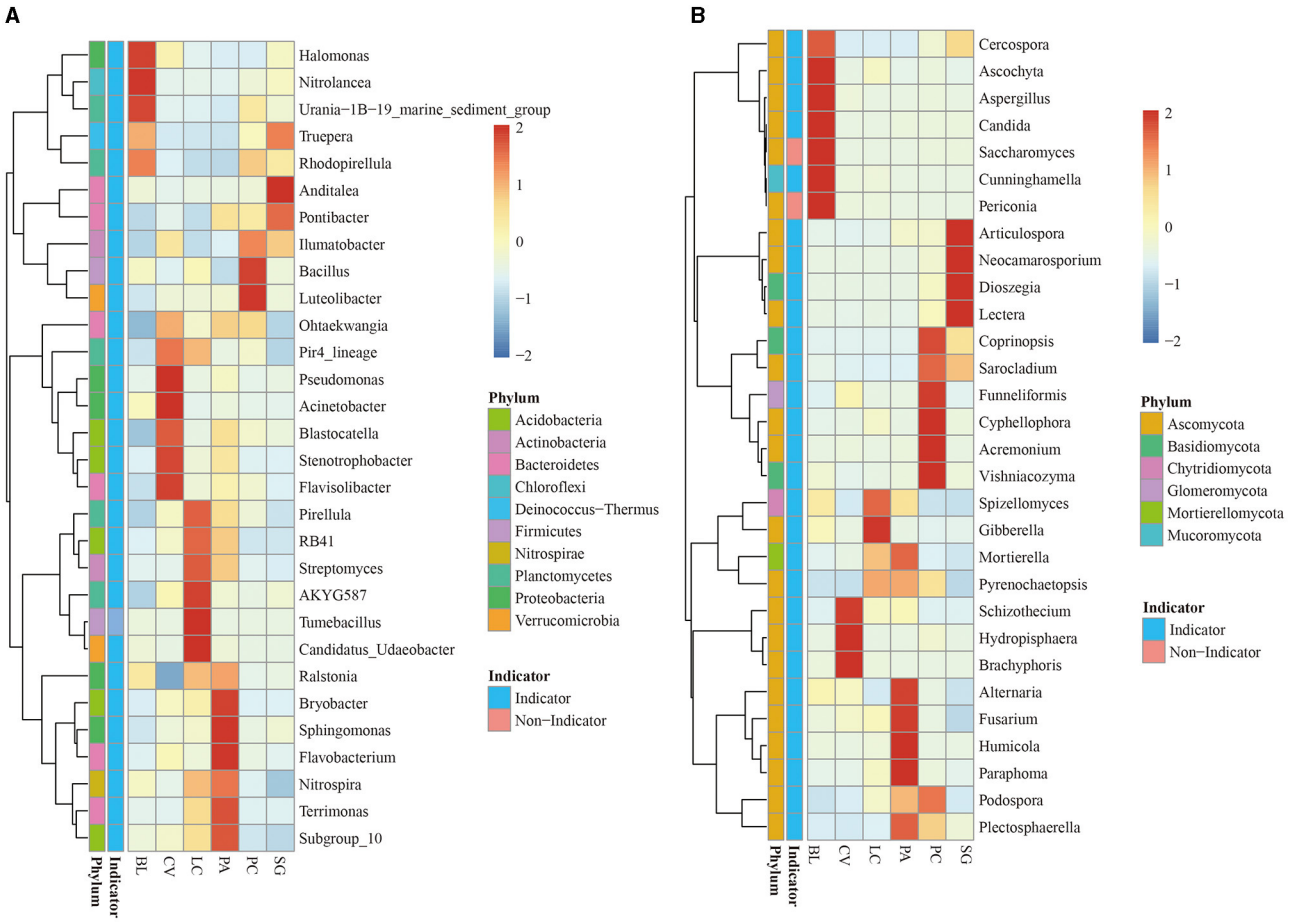

FIGURE 3
Distribution of the top 30 most abundant taxa (genus), their relative abundance, and indicator roles in the bacterial **(A)** and fungal **(B)** communities.

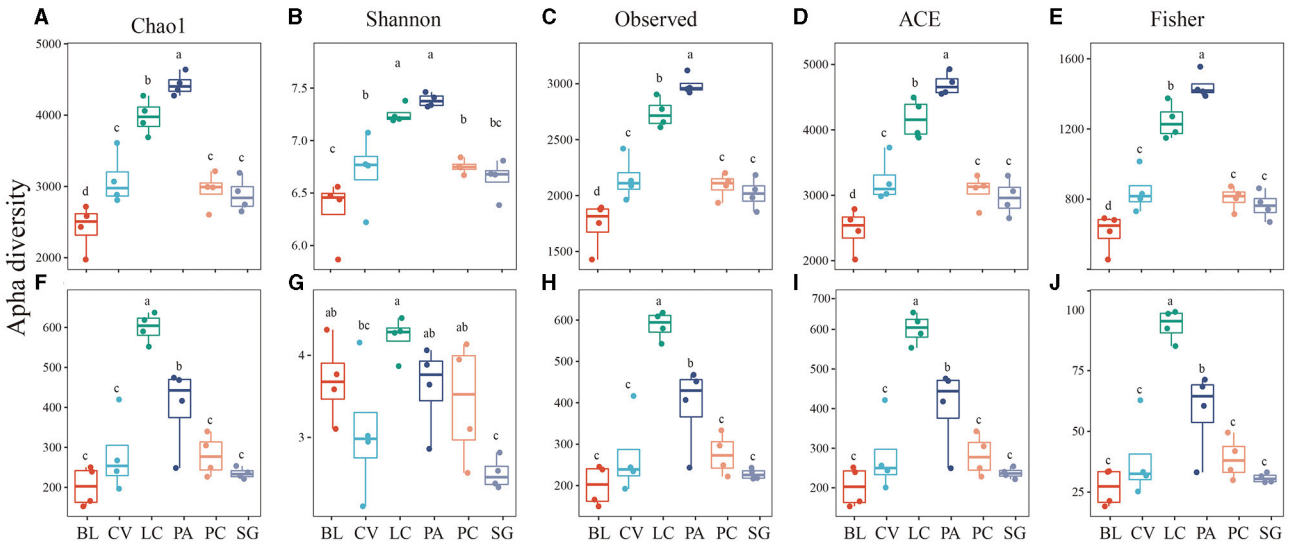

FIGURE 4
Alpha diversity of bacteria **(A–E)** and fungi **(F–J)** in different plant communities.

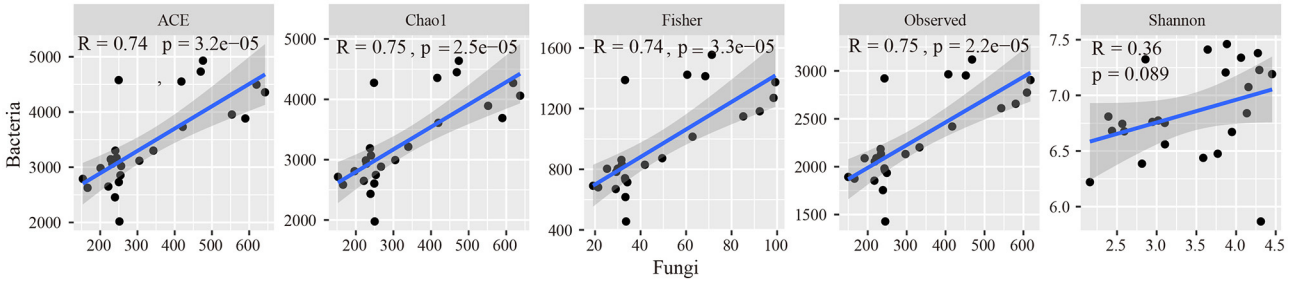

FIGURE 5
Relationships of bacterial alpha diversity to fungal diversity across different plant communities.

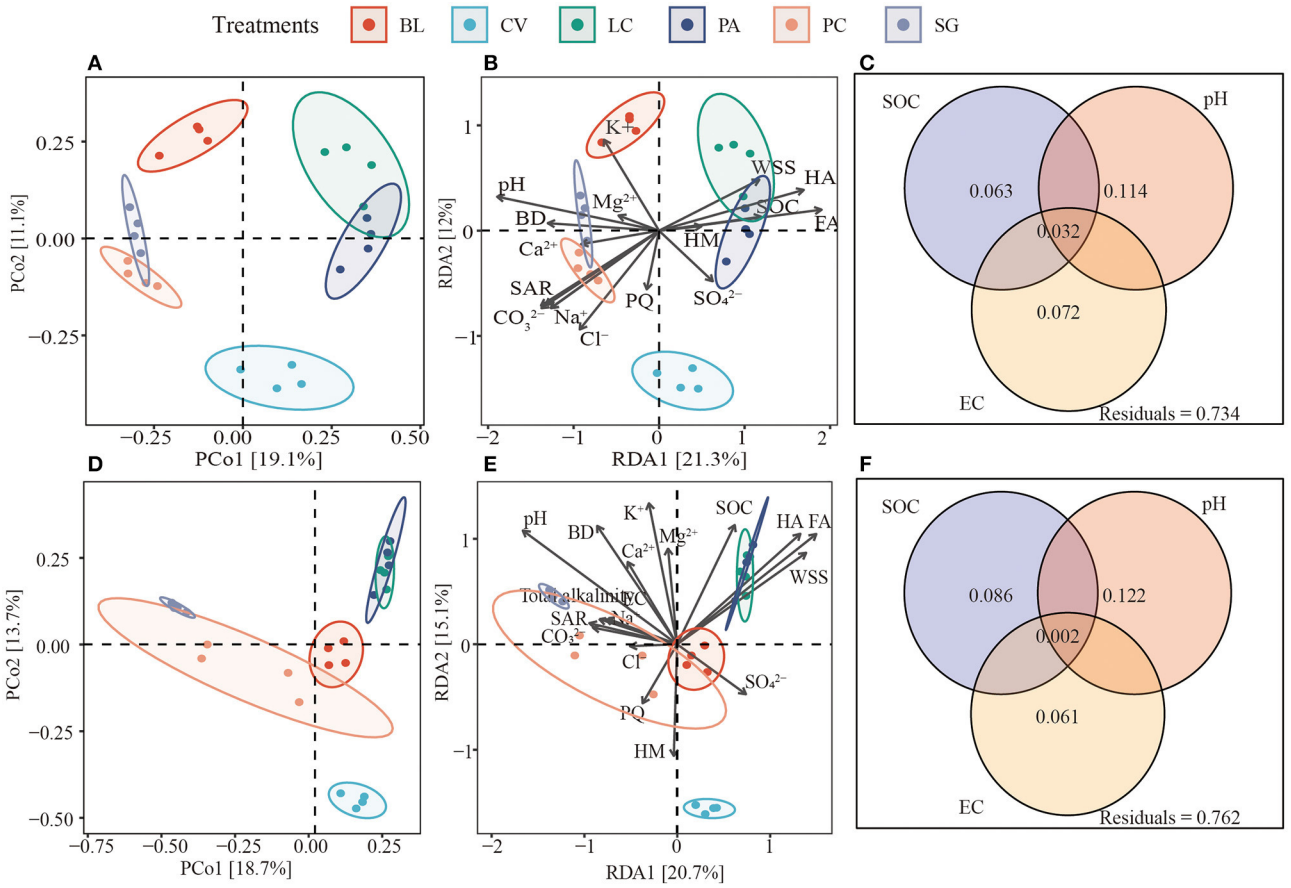

FIGURE 6
Differences in soil bacterial and fungal communities **(A, D)**. Redundancy analysis **(B, E)** shows bacterial and fungal communities and environmental factors between soils of different plant communities. **(C, F)** The contribution of soil organic matter (SOC), soil pH, and soil electrical conductivity (EC) to the composition of bacterial and fungal communities based on variance distribution analysis. BL, bare land without vegetation on the surface; CV, *Chloris virgata*; LC, *Leymus chinensis*; PA, *Phragmites australis*; PC, *Puccinellia chinampoensis*; SG, *Suaeda glauca*; WSS, water-soluble organic matter; FA, fulvic acid; HA, humic acid; HM, humin; SOC, soil organic carbon; EC, electrical conductivity; BD, bulk density; and SAR, sodium adsorption ratio.

4. Discussion

Studies have shown that vegetation has a certain resistance to soil salinity (Negrão et al., 2016; Ma et al., 2020; Han et al., 2021). Bare land has the highest soil salinity. Among vegetation types, the reduction of soil salinity was most obvious in PA and LC, which can be attributed to the elevated organic matter content and MWD of PA and LC. These factors facilitate microorganisms' enhanced diversity and activity, leading to the dissolution of soil $CaCO_3$.

As a result, Na^+ ions adsorbed on the surface of soda-saline soil are effectively replaced by Ca^{2+} ions, expediting the desalination process and improving the physical and chemical

TABLE 2 Correlations between soil microbial communities and soil humus.

	WSS (g/kg)	FA (g/kg)	HA (g/kg)	HM (g/kg)	SOC (g/kg)
Proteobacteria	0.280	0.247	0.104	−0.088	0.016
Actinobacteria	−0.292	−0.689**	−0.560**	−0.334	−0.520**
Bacteroidetes	0.061	−0.220	−0.262	−0.248	−0.249
Acidobacteria	0.474*	0.863**	0.760**	0.391	0.628**
Gemmatimonadetes	−0.441*	−0.664**	−0.601**	−0.182	−0.407*
Planctomycetes	−0.376	−0.065	0.031	0.075	0.054
Firmicutes	−0.273	−0.088	0.034	0.309	0.182
Chloroflexi	0.162	−0.390	−0.420*	−0.660**	−0.603**
Ascomycota	−0.482*	−0.564**	−0.504*	−0.279	−0.413*
Mortierellomycota	0.661**	0.835**	0.726**	0.374	0.605**
Basidiomycota	−0.320	−0.370	−0.313	0.029	−0.145

* and ** indicate significance at $0.01 < p < 0.05$ and $0.001 < p < 0.01$ respectively.
WSS, water-soluble organic matter; FA, fulvic acid; HA, humic acid; HM, humin; and SOC, soil organic carbon.

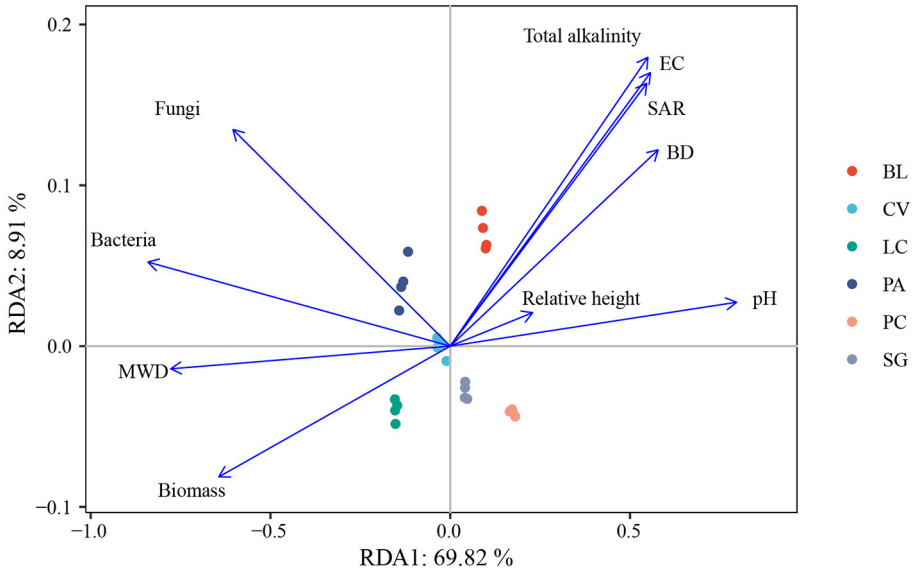

FIGURE 7
Ordination plots of redundancy analysis to identify the relationships among soil bacteria, fungal communities, environmental factors, and soil humus. BL, bare land without vegetation on the surface; CV, *Chloris virgata*; LC, *Leymus chinensis*; PA, *Phragmites australis*; PC, *Puccinellia chinampoensis*; SG, *Suaeda glauca*; EC, electrical conductivity; BD, bulk density; SAR, sodium adsorption ratio; and MWD, mean weight diameter.

properties of the soil (Qadir et al., 2007). Owing to the high pH of the soil and its high electrical conductivity, the rate of soil humification was affected, the accumulation of humus was reduced, and the conversion rate of FA to HA in the soil was also slow, resulting in a low PQ value (Zhao et al., 2019). With the regeneration of LC communities, biomass increases, which strengthens the arrangement of soil particles, further promotes the assembly of microaggregates into macroaggregates, and enhances soil structural stability with higher MWD, which helps keep organic matter from erosion and decomposition (Zhao et al., 2018; Feng et al., 2021). In our study, SOCs of different vegetation communities showed an obvious increasing trend from bare land to squares covered by adapted vegetation. Regarding the increase in soil HA and FA contents with increasing SOC content, the increase in SOC content under different vegetation types was also accompanied by higher MWD and higher proportions of HA and FA in SOM, indicating improved soil structure and humus quality. For different vegetation types, soil salinity and soil organic carbon content showed a significant negative correlation, and salinity had a small correlation with soil PQ value (Supplementary Figure S1). This showed that soil salinity under different plant communities affected the total soil organic carbon content. In the case of high salinity, soil organic carbon content was low. High salinity affects the growth of plants and reduces the return of organic residues to the soil, resulting in a decrease in soil organic matter.

Spontaneous vegetation regeneration significantly influences the diversity or richness of soil microbial communities (Liu et al., 2021). Chang et al. (2022) sequenced soil bacterial communities under different vegetation conditions and found that vegetation coverage can significantly increase bacterial ACE, Chao1, Shannon, and Simpson index communities. This is consistent with our findings that plant community reestablishment can enhance soil microbial diversity. Our results showed that Proteus, Acidobacteria, Actinomycetes, Bacteroidetes, and Monoas are the main bacterial species at all examined vegetated sites. In communities with higher SOC, such as LC and PA, the abundance of the Acidobacteria phylum is significantly increased. In addition, the abundance of the Actinomycetes phylum decreased, which is consistent with findings from previous studies and shows that these phyla are common and ubiquitous in soil (Dai et al., 2017). Acidobacteria harbor a broad library of carbohydrate-active enzymes that encode a wide range of carbohydrates and are involved in the breakdown, utilization, and biosynthesis of a wide variety of carbohydrates (Dedysh and Damsté, 2018). Acidobacteria play a beneficial role by selectively regulating the ecological processes of the host ecosystem. These bacteria provide two important ecological services, namely SOM decomposition and denitrification, to enhance carbon stability (Banerjee et al., 2018). These bacteria may enhance the key ecological process of soil carbon fixation. As members of Acidobacteria have been identified as the structural and functional cornerstone of the plant-soil microbiome and agricultural ecosystem (Kalam et al., 2020), studies have shown that Acidobacteria have a positive effect on plant root growth (da Rocha et al., 2010). Therefore, their existence can improve the performance and productivity of plants. Actinomycetes are K-strategy microorganisms resistant to stress (Bérard et al., 2015).

Most of the fungi belonged to Ascomycota. SG and CV significantly increased the abundance of Ascomycota. PA and LC plant communities increased the abundance of Mortierellomycota. BL significantly increased the relative abundance of Mucoromycota. It was reported in the literature that Ascomycetes were not adapted to grow in high-nutrient environments (Wu et al., 2019). Therefore, the increase in the relative abundance of Ascomycetes resulted from the higher salinity and lower organic matter content of SG and CV plant communities.

According to the redundancy analysis, the content and composition of soil organic matter varied significantly among different plant communities, which was mainly related to bacterial communities, pH, MWD, and fungal communities (Supplementary Figure S2). Among these factors, pH was the most important factor causing the difference in microbial communities (Figure 5). As the plant residues enter the soil, the differences in the microbial communities of plant communities lead to differences in the nature of soil organic matter produced by the decomposition of the residues (Kallenbach et al., 2016; Domeignoz-Horta et al., 2021). LC and PA plant communities can reduce soil pH, cause soil particles to aggregate (Wong et al., 2010), improve soil aggregation, protect soil organic matter from decomposition (Zhang et al., 2021), and change the soil microbial community, increasing soil organic matter content. This indicates that soil pH can indirectly affect the content and composition of soil organic matter by regulating soil microbial communities and soil aggregation ability, which shows that reducing soil pH is a key step in the process of restoring vegetation in soda-saline soil to increase soil carbon sequestration and fertility in the future.

5. Conclusion

During our soda-saline vegetation restoration tests, distinct plant communities exhibited the capacity to elevate SOC content and modify its composition compared to bare land. Concurrently, there was a noticeable enhancement in soil aggregation, bolstering plant productivity. Furthermore, these findings underscore the pivotal role of soil microbial communities in orchestrating organic matter alterations. An affirmative correlation was established between SOC content, Acidobacteria, and Mortierella, while Actinobacteria, Gemmatimonadetes, Ascomycota, and SOC content displayed significant negative correlations. Notably, pH emerged as a potent explanatory factor, accounting for 11.4% and 12.2% of the variability observed in soil bacteria and fungi, respectively. Hence, pH emerged as the primary driver behind microbial transformations. The observed disparities in SOC composition and content within soda-saline vegetation can primarily be attributed to variations in pH levels.

Consequently, reducing soil pH emerges as a pivotal step in the prospective process of vegetation restoration in soda-saline environments. The prohibition of grazing practices holds the potential to elevate soda-saline SOC content and foster microbial diversity. Among the spectrum of different vegetation types, *Leymus chinensis* and *Phragmites australis* stand out due to their heightened SOC carbon content and microbial diversity.

Data availability statement

The data presented in the study are deposited in the NCBI repository, accession number PRJNA935485 and PRJNA935506.

Author contributions

FY and LG conceived the research. LG performed the data analysis and wrote the manuscript. FY, ZW, and TT edited the manuscript. All authors reviewed and approved the manuscript, contributed to the article, and approved the submitted version.

Funding

This research was supported by the National Key Research and Development Plan (2022YFD1500501), the National Natural Science Foundation of China, Jilin Province (Nos. 41971066 and 2020ZKHT-03), and the Chinese Academy of Sciences S&T Cooperation high-tech industrialization special fund project (2022SYHZ0018).

Conflict of interest

The authors declare that the research was conducted in the absence of any commercial or financial relationships that could be construed as a potential conflict of interest.

Publisher's note

All claims expressed in this article are solely those of the authors and do not necessarily represent those of their affiliated organizations, or those of the publisher, the editors and the reviewers. Any product that may be evaluated in this article, or claim that may be made by its manufacturer, is not guaranteed or endorsed by the publisher.

Supplementary material

The Supplementary Material for this article can be found online at: https://www.frontiersin.org/articles/10.3389/fmicb.2023.1163444/full#supplementary-material

References

Ampong, K., Thilakaranthna, M. S., and Gorim, L. Y. (2022). Understanding the role of humic acids on crop performance and soil health. *Front. Agron.* 4, 848621. doi: 10.3389/fagro.2022.848621

Ankenbrand, M. J., Keller, A., Wolf, M., Schultz, J., and Förster, F. (2015). ITS2 database V: twice as much. *Mol. Biol. Evol.* 32, 3030–3032. doi: 10.1093/molbev/msv174

Banerjee, S., Schlaeppi, K., and van der Heijden, M. G. (2018). Keystone taxa as drivers of microbiome structure and functioning. *Nat. Rev. Microbiol.* 16, 567–576. doi: 10.1038/s41579-018-0024-1

Benjamini, Y., and Hochberg, Y. (1995). Controlling the false discovery rate: a practical and powerful approach to multiple testing. *J. Royal Statist. Soc. Series B* 57, 289–300. doi: 10.1111/j.2517-6161.1995.tb02031.x

Bérard, A., Sassi, M. B., Kaisermann, A., and Renault, P. (2015). Soil microbial community responses to heat wave components: drought and high temperature. *Clim. Res.* 66, 243–264. doi: 10.3354/cr01343

Callahan, B. J., McMurdie, P. J., Rosen, M. J., Han, A. W., Johnson, A. J. A., Holmes, S. P., et al. (2016). DADA2: High-resolution sample inference from Illumina amplicon data. *Nat. Methods* 13, 581–583. doi: 10.1038/nmeth.3869

Chang, C., Tian, L., Tian, Z., McLaughlin, N., and Tian, C. (2022). Change of soil microorganism communities under saline-sodic land degradation on the Songnen Plain in northeast China. *J. Plant Nutri. Soil Sci.* 185, 297–307. doi: 10.1002/jpln.202100230

Chi, C.-M., Zhao, C.-W., Sun, X.-J., and Wang, Z.-C. (2011). Estimating exchangeable sodium percentage from sodium adsorption ratio of salt-affected soil in the Songnen plain of northeast China. *Pedosphere* 21, 271–276. doi: 10.1016/S1002-0160(11)60127-6

da Rocha, U. N., van Elsas, J. D., and van Overbeek, L. S. (2010). Real-time PCR detection of Holophagae (Acidobacteria) and Verrucomicrobia subdivision 1 groups in bulk and leek (Allium porrum) rhizosphere soils. *J. Microbiol. Methods* 83, 141–148. doi: 10.1016/j.mimet.2010.08.003

Dai, H., Chen, Y., Yang, X., Cui, J., and Sui, P. (2017). The effect of different organic materials amendment on soil bacteria communities in barren sandy loam soil. *Environ. Sci. Pollut. Res.* 24, 24019–24028. doi: 10.1007/s11356-017-0031-1

Dedysh, S. N., and Damsté, J. S. S. (2018). Acidobacteria. *eLS* 4, 1–10. doi: 10.1002./9780470015902.a0027685

DiDonato, N., Chen, H., Waggoner, D., and Hatcher, P. G. (2016). Potential origin and formation for molecular components of humic acids in soils. *Geochim. Cosmochim. Acta* 178, 210–222. doi: 10.1016/j.gca.2016.01.013

Domeignoz-Horta, L. A., Shinfuku, M., Junier, P., Poirier, S., Verrecchia, E., Sebag, D., et al. (2021). Direct evidence for the role of microbial community composition in the formation of soil organic matter composition and persistence. *ISME Commun.* 1, 62. doi: 10.1038/s43705-021-00071-7

Dou, S. (2010). *Soil Organic Matter*. Beijing: Science Press.

Edgar, R. C., Haas, B. J., Clemente, J. C., Quince, C., and Knight, R. (2011). UCHIME improves sensitivity and speed of chimera detection. *Bioinformatics* 27, 2194–2200. doi: 10.1093/bioinformatics/btr381

Feng, H., Wang, S., Gao, Z., Pan, H., Zhuge, Y., Ren, X., et al. (2021). Aggregate stability and organic carbon stock under different land uses integrally regulated by binding agents and chemical properties in saline-sodic soils. *Land Degrad. Develop.* 32, 4151–4161. doi: 10.1002/ldr.4019

Guan, Y., Jiang, N., Wu, Y., Yang, Z., Bello, A., Yang, W., et al. (2021). Disentangling the role of salinity-sodicity in shaping soil microbiome along a natural saline-sodic gradient. *Sci. Total Environ.* 765, 142738. doi: 10.1016/j.scitotenv.2020.142738

Han, X., Qu, Y., Li, D., Qiu, Y., Yu, Y., Feng, Y., et al. (2021). Remediation of saline-sodic soil by plant microbial desalination cell. *Chemosphere* 277, 130275. doi: 10.1016/j.chemosphere.2021.130275

Hartmann, M., and Six, J. (2022). Soil structure and microbiome functions in agroecosystems. *Nat. Rev. Earth Environ.* 4, 4–18. doi: 10.1038/s43017-022-00366-w

Kalam, S., Basu, A., Ahmad, I., Sayyed, R. Z., El-Enshasy, H. A., Dailin, D. J., et al. (2020). Recent understanding of soil acidobacteria and their ecological significance: a critical review. *Front. Microbiol.* 11, 580024. doi: 10.3389/fmicb.2020.580024

Kallenbach, C. M., Frey, S. D., and Grandy, A. S. (2016). Direct evidence for microbial-derived soil organic matter formation and its ecophysiological controls. *Nat. Commun.* 7, 13630. doi: 10.1038/ncomms13630

Kemper, W. D., and Rosenau, R. C. (1986). Aggregate stability and size distribution. *Methods Soil Anal. Part 1 Phys. Mineral. Methods* 5, 425–442. doi: 10.2136/sssabookser5.1.2ed.c17

Klučáková, M. (2018). Size and charge evaluation of standard humic and fulvic acids as crucial factors to determine their environmental behavior and impact. *Front. Chem.* 6, 235. doi: 10.3389/fchem.2018.00235

Kögel-Knabner, I. (2002). The macromolecular organic composition of plant and microbial residues as inputs to soil organic matter. *Soil Biol. Biochem.* 34, 139–162. doi: 10.1016/S0038-0717(01)00158-4

Kononova, M. M. (2013). *Soil Organic Matter: Its Nature, Its Role in Soil Formation and in Soil Fertility*. Elsevier.

Kou, B., Hui, K., Miao, F., He, Y., Qu, C., Yuan, Y., et al. (2022). Differential responses of the properties of soil humic acid and fulvic acid to nitrogen addition in the North China Plain. *Environ. Res.* 214, 113980. doi: 10.1016/j.envres.2022.113980

Lehmann, J., and Kleber, M. (2015). The contentious nature of soil organic matter. *Nature* 528, 60–68. doi: 10.1038/nature16069

Li, J., Cui, L., Delgado-Baquerizo, M., Wang, J., Zhu, Y., Wang, R., et al. (2022). Fungi drive soil multifunctionality in the coastal salt marsh ecosystem. *Sci. Total Environ.* 818, 151673. doi: 10.1016/j.scitotenv.2021.151673

Liu, M., Li, X., Zhu, R., Chen, N., Ding, L., and Chen, C. (2021). Vegetation richness, species identity and soil nutrients drive the shifts in soil bacterial communities during restoration process. *Environ. Microbiol. Rep.* 13, 411–424. doi: 10.1111/1758-2229.12913

Ma, Y., Dias, M. C., and Freitas, H. (2020). Drought and salinity stress responses and microbe-induced tolerance in plants. *Front. Plant Sci.* 11, 591911. doi: 10.3389/fpls.2020.591911

Mahmood, K., Malik, K. A., Lodhi, M. A. K., and Sheikh, K. H. (1994). Soil–plant relationships in saline wastelands: vegetation, soils, and successional changes, during biological amelioration. *Environ. Conserv.* 21, 236–241. doi: 10.1017/S037689290003321X

Negrão, S., Schmöckel, S. M., and Tester, M. (2016). Evaluating physiological responses of plants to salinity stress. *Ann. Bot.* 119, 1–11. doi: 10.1093/aob/mcw191

Pruesse, E., Quast, C., Knittel, K., Fuchs, B. M., Ludwig, W., Peplies, J., et al. (2007). SILVA: a comprehensive online resource for quality checked and aligned ribosomal RNA sequence data compatible with ARB. *Nucleic Acids Res.* 35, 7188–7196. doi: 10.1093/nar/gkm864

Qadir, M., Oster, J. D., Schubert, S., Noble, A. D., and Sahrawat, K. L. (2007). Phytoremediation of sodic and saline-sodic soils. *Adv. Agron.* 96, 197–247. doi: 10.1016/S0065-2113(07)96006-X

Qiu, L., Kong, W., Zhu, H., Zhang, Q., Banerjee, S., Ishii, S., et al. (2022). Halophytes increase rhizosphere microbial diversity, network complexity and function in inland saline ecosystem. *Sci. Total Environ.* 831, 154944. doi: 10.1016/j.scitotenv.2022.154944

Walkley, A., and Black, I. A. (1934). An examination of the Degtjareff method for determining soil organic matter, and a proposed modification of the chromic acid titration method. *Soil Sci.* 37, 29–38. doi: 10.1097/00010694-193401000-00003

Wang, Q., Garrity, G. M., Tiedje, J. M., and Cole, J. R. (2007). Naive Bayesian classifier for rapid assignment of rRNA sequences into the new bacterial taxonomy. *Appl. Environ. Microbiol.* 73, 5261–5267. doi: 10.1128/AEM.00062-07

Wang, S., Luo, S., Zhou, X., Chang, C., Tian, L., Li, X., et al. (2019). Soil ameliorants alter physicochemical properties and fungal communities in saline-sodic soils of Northeast China. *Arch. Agron. Soil Sci.* 65, 1147–1159. doi: 10.1080/03650340.2018.1555707

Wang, S., Sun, L., Ling, N., Zhu, C., Chi, F., Li, W., et al. (2020). Exploring soil factors determining composition and structure of the bacterial communities in saline-alkali soils of Songnen Plain. *Front. Microbiol.* 10, 2902. doi: 10.3389/fmicb.2019.02902

Wang, X., Sun, R., Tian, Y., Guo, K., Sun, H., Liu, X., et al. (2020). Long-term phytoremediation of coastal saline soil reveals plant species-specific patterns of microbial community recruitment. *Msystems* 5, 10–1128. doi: 10.1128/mSystems.00741-19

Wang, Z. C., Li, Q. S., Li, X. J., Song, C. C., and Zhang, G. X. (2003). Sustainable agriculture development in saline-alkali soil area of Songnen Plain, Northeast China. *Chin. Geograph. Sci.* 13, 171–174. doi: 10.1007/s11769-003-0012-9

Wong, V. N., Greene, R. S. B., Dalal, R. C., and Murphy, B. W. (2010). Soil carbon dynamics in saline and sodic soils: a review. *Soil Use Manag.* 26, 2–11. doi: 10.1111/j.1475-200900251.x

Wu, S. H., Huang, B. H., Gao, J., Wang, S., and Liao, P. C. (2019). The effects of afforestation on soil bacterial communities in temperate grassland are modulated by soil chemical properties. *PeerJ* 7, e6147. doi: 10.7717/peerj.6147

Yang, F., An, F., Ma, H., Wang, Z., Zhou, X., Liu, Z., et al. (2016). Variations on soil salinity and sodicity and its driving factors analysis under microtopography in different hydrological conditions. *Water* 8, 227. doi: 10.3390/w8060227

Zaiets, O., and Poch, R. M. (2016). Micromorphology of organic matter and humus in Mediterranean mountain soils. *Geoderma* 272, 83–92. doi: 10.1016/j.geoderma.03006

Zhang, M., Dong, L., Wang, Y., Bai, X., Ma, Z., Yu, X., et al. (2021). The response of soil microbial communities to soil erodibility depends on the plant and soil properties in semiarid regions. *Land Degrad. Develop.* 32, 3180–3193. doi: 10.1002/ldr.3887

Zhao, F. Z., Fan, X. D., Ren, C. J., Zhang, L., Han, X. H., Yang, G. H., et al. (2018). Changes of the organic carbon content and stability of soil aggregates affected by soil bacterial community after afforestation. *Catena* 171, 622–631. doi: 10.1016/j.catena.08006

Zhao, X., Zhu, M., Guo, X., Wang, H., Sui, B., Zhao, L., et al. (2019). Organic carbon content and humus composition after application aluminum sulfate and rice straw to soda saline-alkaline soil. *Environ. Sci. Pollut. Res.* 26, 13746–13754. doi: 10.1007/s11356-018-2270-1

Zhao, Y., Wang, G., Zhao, M., Wang, M., and Jiang, M. (2022). Direct and indirect effects of soil salinization on soil seed banks in salinizing wetlands in the Songnen Plain, China. *Sci. Total Environ.* 819, 152035. doi: 10.1016/j.scitotenv.2021.152035

Frontiers in Microbiology

Explores the habitable world and the potential of microbial life

The largest and most cited microbiology journal which advances our understanding of the role microbes play in addressing global challenges such as healthcare, food security, and climate change.

Discover the latest Research Topics

See more →

Frontiers

Avenue du Tribunal-Fédéral 34
1005 Lausanne, Switzerland
frontiersin.org

Contact us

+41 (0)21 510 17 00
frontiersin.org/about/contact